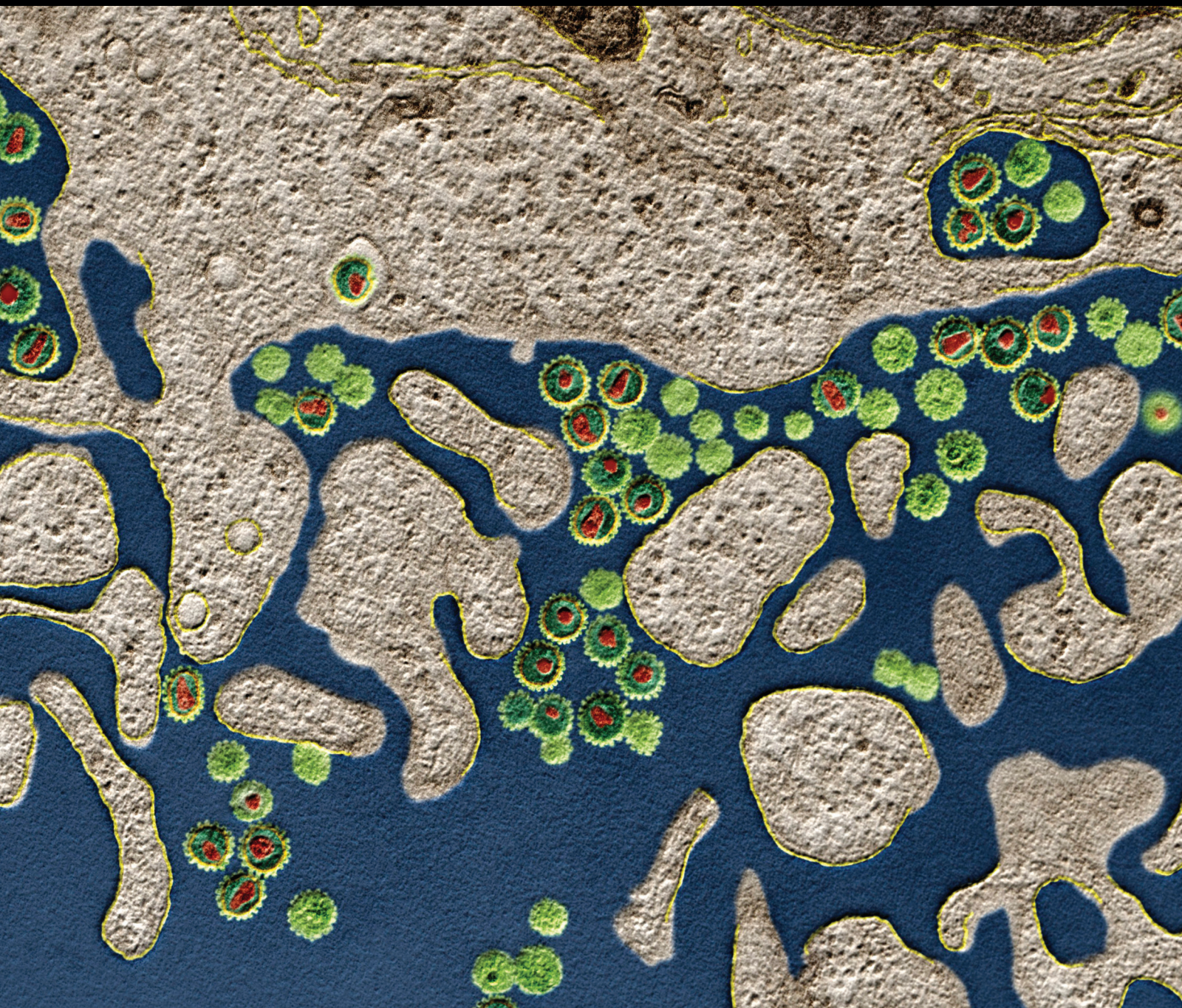


# Medical Plants and Immunological Regulation

Lead Guest Editor: Cheng Xiao

Guest Editors: Qingdong Guan, Yong Tan, Lifei Hou, and Wuxiang Xie





---

# **Medical Plants and Immunological Regulation**

Journal of Immunology Research

---

## **Medical Plants and Immunological Regulation**

Lead Guest Editor: Cheng Xiao

Guest Editors: Qingdong Guan, Yong Tan, Lifei Hou,  
and Wuxiang Xie



---

Copyright © 2018 Hindawi. All rights reserved.

This is a special issue published in "Journal of Immunology Research." All articles are open access articles distributed under the Creative Commons Attribution License, which permits unrestricted use, distribution, and reproduction in any medium, provided the original work is properly cited.

## Editorial Board

B. D. Akanmori, Congo  
Jagadeesh Bayry, France  
Kurt Blaser, Switzerland  
Eduardo F. Borba, Brazil  
Federico Bussolino, Italy  
Nitya G. Chakraborty, USA  
Cinzia Ciccacci, Italy  
Robert B. Clark, USA  
Mario Clerici, Italy  
Nathalie Cools, Belgium  
M. Victoria Delpino, Argentina  
Nejat K. Egilmez, USA  
Eyad Elkord, UK  
Steven E. Finkelstein, USA  
Maria Cristina Gagliardi, Italy  
Luca Gattinoni, USA  
Alvaro González, Spain  
Theresa Hautz, Austria  
Martin Holland, UK

Douglas C. Hooper, USA  
Eung-Jun Im, USA  
Hidetoshi Inoko, Japan  
Juraj Ivanyi, UK  
Ravirajsinh N. Jadeja, USA  
Peirong Jiao, China  
Taro Kawai, Japan  
Alexandre Keller, Brazil  
Hiroshi Kiyono, Japan  
Bogdan Kolarz, Poland  
Herbert K. Lyerly, USA  
Mahboobeh Mahdavinia, USA  
Giulia Marchetti, Italy  
Eiji Matsuura, Japan  
Chikao Morimoto, Japan  
Hiroshi Nakajima, Japan  
Paola Nistico, Italy  
Enrique Ortega, Mexico  
Patrice Petit, France

Isabella Quinti, Italy  
Eirini Rigopoulou, Greece  
Ilaria Roato, Italy  
Luigina Romani, Italy  
Aurelia Rughetti, Italy  
Francesca Santilli, Italy  
Takami Sato, USA  
Senthamil R. Selvan, USA  
Naohiro Seo, Japan  
Benoit Stijlemans, Belgium  
Jacek Tabarkiewicz, Poland  
Mizue Terai, USA  
Ban-Hock Toh, Australia  
Joseph F. Urban, USA  
Paulina Wlasiuk, Poland  
Baohui Xu, USA  
Xiao-Feng Yang, USA  
Maria Zervou, Greece  
Qiang Zhang, USA

## Contents

### **Medical Plants and Immunological Regulation**

Cheng Xiao , Qingdong Guan , Yong Tan , Lifei Hou , and Wuxiang Xie   
Editorial (2 pages), Article ID 9172096, Volume 2018 (2018)








### **Hei-Gu-Teng Zhuifenghuoluo Granule Modulates IL-12 Signal Pathway to Inhibit the Inflammatory Response in Rheumatoid Arthritis**

Kang Zheng , Zexu Chen, Wen Sun, Bin Liu , Danping Fan , Qingqing Guo , Hui Luo , Jiawen Shen, Li Li , Xiaojuan He , Shuang Kou, Xiaoya Li, Guoming Pang, Hongchuan Zhao , and Cheng Lu   
Research Article (10 pages), Article ID 8474867, Volume 2018 (2018)



### **The Role of Flavonoids in Inhibiting Th17 Responses in Inflammatory Arthritis**

Dimitra Kelepouri , Athanasios Mavropoulos , Dimitrios P. Bogdanos , and Lazaros I. Sakkas   
Review Article (11 pages), Article ID 9324357, Volume 2018 (2018)




### **Therapeutic Potential of Pien Tze Huang on Experimental Autoimmune Encephalomyelitis Rat**

Xuemei Qiu, Hui Luo , Xue Liu, Qingqing Guo , Kang Zheng , Danping Fan, Jiawen Shen, Cheng Lu , Xiaojuan He , Ge Zhang , and Aiping Lu   
Research Article (10 pages), Article ID 2952471, Volume 2018 (2018)

### ***Punica granatum* L. Leaf Extract Attenuates Lung Inflammation in Mice with Acute Lung Injury**

Aruanã Joaquim Matheus Costa Rodrigues Pinheiro, Jaciara Sá Gonçalves, Ádyla Wilenna Alves Dourado, Eduardo Martins de Sousa, Natilene Mesquita Brito, Lanna Karinny Silva, Marisa Cristina Aranha Batista, Joicy Cortez de Sá, Cinara Regina Aragão Vieira Monteiro, Elizabeth Soares Fernandes, Valério Monteiro-Neto , Lee Ann Campbell, Patrícia Maria Wiziack Zago, and Lidio Gonçalves Lima-Neto   
Research Article (11 pages), Article ID 6879183, Volume 2018 (2018)

### **Prevention and Treatment of Osteoporosis Using Chinese Medicinal Plants: Special Emphasis on Mechanisms of Immune Modulation**

Hongyan Zhao , Ning Zhao, Peng Zheng, Xiaohong Xu, Meijie Liu, Dan Luo, Huihui Xu , and Dahong Ju   
Review Article (11 pages), Article ID 6345857, Volume 2018 (2018)

### **Matrine Ameliorates Colorectal Cancer in Rats via Inhibition of HMGB1 Signaling and Downregulation of IL-6, TNF- $\alpha$ , and HMGB1**

Huizhen Fan , Chunyan Jiang, Baoyuan Zhong, Jianwen Sheng, Ting Chen, Qingqing Chen, Jingtao Li , and Hongchuan Zhao  
Research Article (8 pages), Article ID 5408324, Volume 2018 (2018)

### **Immunomodulatory Effect of Flavonoids of Blueberry (*Vaccinium corymbosum* L.) Leaves via the NF- $\kappa$ B Signal Pathway in LPS-Stimulated RAW 264.7 Cells**

Dazhi Shi, Mengyi Xu, Mengyue Ren, Enshan Pan, Chaohua Luo, Wei Zhang, and Qingfa Tang  
Research Article (7 pages), Article ID 5476903, Volume 2017 (2018)

**Neuroprotective Potential of Gentongping in Rat Model of Cervical Spondylotic Radiculopathy Targeting PPAR- $\gamma$  Pathway**

Wen Sun, Kang Zheng, Bin Liu, Danping Fan, Hui Luo, Xiaoyuan Qu, Li Li, Xiaojuan He, Jianfeng Yi, and Cheng Lu

Research Article (12 pages), Article ID 9152960, Volume 2017 (2018)

**New Insights into the Mechanisms of Chinese Herbal Products on Diabetes: A Focus on the “Bacteria-Mucosal Immunity-Inflammation-Diabetes” Axis**

Ze Zheng Gao, Qingwei Li, Xuemin Wu, Xuemin Zhao, Linhua Zhao, and Xiaolin Tong

Review Article (13 pages), Article ID 1813086, Volume 2017 (2018)

**Protective Effects of *Ophiocordyceps lanpingensis* on Glycerol-Induced Acute Renal Failure in Mice**

Yanyan Zhang, Yaxi Du, Hong Yu, Yongchun Zhou, and Feng Ge

Research Article (8 pages), Article ID 2012585, Volume 2017 (2018)

**Traditional Chinese Medicine Protects against Cytokine Production as the Potential Immunosuppressive Agents in Atherosclerosis**

Yan Ren, Wei Qiao, Dongliang Fu, Zhiwei Han, Wei Liu, Weijie Ye, and Zunjing Liu

Review Article (8 pages), Article ID 7424307, Volume 2017 (2018)

**Chinese Herbal Formula, Modified Danggui Buxue Tang, Attenuates Apoptosis of Hematopoietic Stem Cells in Immune-Mediated Aplastic Anemia Mouse Model**

Jingwei Zhou, Xue Li, Peiying Deng, Yi Wei, Juan Liu, Meng Chen, Yamei Xu, Dongmei Zhang,

Lingqun Zhu, Lixia Lou, Bin Dong, Qiushuo Jin, and Limin Chai

Research Article (12 pages), Article ID 9786972, Volume 2017 (2018)

**Mahuang Fuzi Xixin Decoction Attenuates Th1 and Th2 Responses in the Treatment of Ovalbumin-Induced Allergic Inflammation in a Rat Model of Allergic Rhinitis**

Mengyue Ren, Qingfa Tang, Feilong Chen, Xuefeng Xing, Yao Huang, and Xiaomei Tan

Research Article (12 pages), Article ID 8254324, Volume 2017 (2018)

**Ethyl Caffate Ameliorates Collagen-Induced Arthritis by Suppressing Th1 Immune Response**

Shikui Xu, Aixue Zuo, Zengjun Guo, and Chunping Wan

Research Article (11 pages), Article ID 7416792, Volume 2017 (2018)

## Editorial

# Medical Plants and Immunological Regulation

Cheng Xiao <sup>1</sup>, Qingdong Guan <sup>2</sup>, Yong Tan <sup>3</sup>, Lifei Hou <sup>4</sup>, and Wuxiang Xie <sup>5</sup>

<sup>1</sup>Institute of Clinical Medicine, China-Japan Friendship Hospital, Beijing 100029, China

<sup>2</sup>Cellular Therapy Laboratory, CancerCare Manitoba, Winnipeg, MB, Canada R3A 1R9

<sup>3</sup>Institute of Basic Research in Clinical Medicine, China Academy of Chinese Medical Sciences, Beijing 100700, China

<sup>4</sup>Program in Cellular and Molecular Medicine, Department of Pediatrics, Boston Children's Hospital, Harvard Medical School, Boston, MA 02115, USA

<sup>5</sup>Peking University Clinical Research Institute, Peking University Health Science Center, Beijing 100191, China

Correspondence should be addressed to Cheng Xiao; xc2002812@126.com and Yong Tan; tcmtanyong@126.com

Received 10 April 2018; Accepted 10 April 2018; Published 12 June 2018

Copyright © 2018 Cheng Xiao et al. This is an open access article distributed under the Creative Commons Attribution License, which permits unrestricted use, distribution, and reproduction in any medium, provided the original work is properly cited.

Immune regulation is crucial for the maintenance of immune system homeostasis. The abnormalities of immune regulation are involved in many diseases and disorders. Increasing studies show that medical plants, corresponding monomers, and formulas exert immunomodulatory effects, such as stimulatory effects on immune cells, immune organs, and cytokine production, as well as inhibitory effects on inflammation, allergy, and autoimmune disease. In this special issue, we present original research articles as well as review papers on medical plants and immunological regulation.

Plant monomers are major effective constituents of medical plants. Studies on monomers are greatly increased in recent years because they have specific molecular structure and are easier to be used in mechanism and molecule target research [1, 2]. The imbalance of T cell subsets plays an important role in rheumatoid arthritis (RA). IFN- $\gamma$  derived from Th1 cell predominates during the induction and acute phases of RA. S. Xu et al. investigated the antiarthritic potential of ethyl caffeate (ECF) isolated from *Elephantopus scaber* L. in collagen-induced arthritis (CIA) and found that ECF ameliorated CIA by suppressing Th1 response and IFN- $\gamma$  signaling pathway. Acute lung injury (ALI) is closely associated with the increased production of inflammatory mediators including cytokines (TNF- $\alpha$ , IL-1 $\beta$ , and IL-6), especially produced by alveolar macrophages and neutrophils. A. R. Pinheiro et al. assessed the anti-inflammatory potential of the ethyl acetate fraction (EAFPg) extracted from pomegranate leaf in a mouse model of LPS-induced acute

lung injury and proved that EAFPg could prevent inflammatory disorders in ALI. Matrine is a bioactive component extracted from *Sophora flavescens*. H. Fan et al. explored the therapeutic effect of matrine on CRC and found that matrine treated CRC via inhibition of HMGB1 signaling characterized by the downregulation of IL-6, TNF- $\alpha$ , and HMGB1.

The study on bioactive fraction is a hotspot of medical plant research [3]. Flavonoids from medical plants are considered as powerful immunomodulatory agents [4]. D. Kelepouri et al. reviewed the role of flavonoids in inhibiting Th17 responses in RA and experimental autoimmune arthritis. D. Shi et al. explored the immunomodulatory effect of flavonoids from blueberry leaves (FBL) in lipopolysaccharide- (LPS-) stimulated RAW 264.7 cells and found that the immune regulatory effects of FBL was through suppressing TNF via the NF- $\kappa$ B signal pathway. Besides, immunomodulatory activities of single medical plant were explored in this special issue. *Ophiocordyceps lanpingensis* (OL), a popular tonifying Chinese medical plant, has been used to treat renal inadequacy. Y. Zhang et al. investigated the protective effects of OL in acute renal failure (ARF) and found that OL could ameliorate renal dysfunction in glycerol-induced ARF in mice by inhibiting oxidative stress and enhancing IgG immune response.

Multitherbal formulas based on traditional Chinese medicine have been scientifically verified for use in complementary and alternative therapy for the diseases resulted



from abnormal immunomodulation, and they act on multiple targets and exert synergistic therapeutic efficacies [5, 6]. The clinical application of these formulas has attracted more and more scientific attentions. This special issue presented some studies which explored pharmacological mechanism of the formulas. Mahuang Fuzi Xixin decoction (MFXD), a famous Chinese formula, has been widely used in treating allergic rhinitis (AR). M. Ren et al. confirmed its therapeutic effect on allergic inflammation by regulating Th1 and Th2 immune responses in a rat model of OVA-induced AR. J. Zhou et al. investigated the effects of modified Danggui Buxue Tang (DGBX, a Chinese formula) on the regulation of the balance between proliferation and apoptosis of hematopoietic stem cells (HSCs) due to the aberrant immune response in a mouse model of aplastic anemia. The results indicated that DGBX could attenuate IFN- $\gamma$  production through interfering in SLAM/SAP signaling and distribution of T-bet in T cells, exert immunosuppressive effects by modulating the activation of the Stat/JAK/IRF-1 pathway, restrain cell apoptosis by intervening Fas-dependent pathway, and eventually attenuate immune-mediated destruction of HSCs. Pien Tze Huang (PZH), a classical Chinese patent formula, has been proved to have anti-inflammatory, neuroprotective, and immune regulatory effects. X. Qiu et al. investigated its therapeutic effects on experimental autoimmune encephalomyelitis (EAE) rats and found that PZH not only ameliorated the clinical severity of EAE rats but also remarkably reduced inflammatory cell infiltration in the central nervous system (CNS) of EAE rats, as well as significantly decreased the levels of IL-17A, IL-23, CCL3, and CCL5 in serum and the levels of p-P65 and p-STAT3 in the CNS. Gen Tong Ping (GTP) granule, another Chinese patent formula, has been widely used in curing cervical spondylotic radiculopathy (CSR). W. Sun et al. predicted the mechanism of GTP treating CSR using network pharmacology approach firstly and found that PPAR- $\gamma$  pathway might be involved in it. Then, the rat model of CSR induced by spinal cord injury (SCI) was used to verify the prediction. The results demonstrated that GTP modulated the PPAR- $\gamma$  pathway by inhibiting the immune inflammatory response and apoptosis as well as by protecting the cytoskeletal integrity of the spinal cord, ultimately played a neuroprotective role in CSR.

This special issue also presents constructive reviews about using medical plants to treat common and frequently occurring immune inflammatory diseases. Atherosclerosis is a chronic inflammatory disease caused by dyslipidemia and mediated by both innate and adaptive immune responses. Y. Ren et al. systematically reviewed medical plants that act as immunomodulatory agents of suppressive function on cytokine production in atherogenesis. The immune factors play important regulatory roles in the occurrence of osteoporosis. H. Zhao et al. provided a general overview on the immune regulation mechanisms of medical plants and corresponding monomers in the prevention and treatment of osteoporosis. Medical plants have been widely used to treat diabetes. Z. Gao et al. reviewed the pharmacological mechanisms of representative medical plants, monomers, and formulas treating diabetes and proposed that

these remedies improve glucose homeostasis through the “Bacteria-Mucosal Immunity-Inflammation-Diabetes” Axis. This axis was considered a “line” to string most antidiabetic agents together and might provide new perspectives and strategies for future research on diabetes and the development of hypoglycemic drugs.

Taken together, the articles in this special issue provide insights into medical plants and immunological regulation. In the future, an extensive investigation is required with respect to their precise mechanisms at the systemic, cellular, and molecular levels and extension to a large-scale clinical trial. Given the identified immunomodulatory effects of medical plants, it is interesting to design future therapeutic strategies for immune inflammatory diseases with a synergistic combination of medical plants and conventional therapies. We hope that researchers enjoy the articles of this special issue.

## Acknowledgments

We would like to thank the authors for their cutting-edge research data and thought-provoking reviews. We also express our gratitude to all the reviewers for their generously devoted time and highly valuable insights.




Cheng Xiao  
Qingdong Guan  
Yong Tan  
LIFEI Hou  
Wuxiang Xie

## References

- [1] M. Ganzer and S. Sturm, “Recent advances on HPLC/MS in medicinal plant analysis—an update covering 2011–2016,” *Journal of Pharmaceutical and Biomedical Analysis*, vol. 147, pp. 211–233, 2018.
- [2] M. L. Wu, Q. Li, J. Xu, and X. W. Li, “Complete chloroplast genome of the medicinal plant *Amomum compactum*: gene organization, comparative analysis, and phylogenetic relationships within Zingiberales,” *Chinese Medicine*, vol. 13, no. 1, p. 10, 2018.
- [3] H. H. Xiao, Y. Dai, M. S. Wong, and X. S. Yao, “Two new phenylpropanoids and one new sesquiterpenoid from the bioactive fraction of *Sambucus williamsii*,” *Journal of Asian Natural Products Research*, vol. 17, no. 6, pp. 625–632, 2015.
- [4] L. Wen, Y. Jiang, J. Yang, Y. Zhao, M. Tian, and B. Yang, “Structure, bioactivity, and synthesis of methylated flavonoids,” *Annals of the New York Academy of Sciences*, vol. 1398, no. 1, pp. 120–129, 2017.
- [5] W. Fan, P. Zheng, Y. Wang, P. Hao, J. Liu, and X. Zhao, “Analysis of immunostimulatory activity of polysaccharide extracted from Yu-Ping-Feng *in vitro* and *in vivo*,” *Biomedicine & Pharmacotherapy*, vol. 93, pp. 146–155, 2017.
- [6] F. Qin, J. Huang, X. Qiu, S. Hu, and X. Huang, “Quality control of modified xiaoyao san through the determination of 22 active components by ultra-performance liquid chromatography,” *Journal of AOAC International*, vol. 94, no. 6, pp. 1778–1784, 2011.

## Research Article

# Hei-Gu-Teng Zhuifenghuoluo Granule Modulates IL-12 Signal Pathway to Inhibit the Inflammatory Response in Rheumatoid Arthritis

Kang Zheng <sup>1,2</sup>, Zexu Chen,<sup>1,3</sup> Wen Sun,<sup>1,4</sup> Bin Liu <sup>1</sup>, Danping Fan <sup>1</sup>, Qingqing Guo <sup>1,2</sup>, Hui Luo <sup>1,5</sup>, Jiawen Shen,<sup>1,5</sup> Li Li <sup>1</sup>, Xiaojuan He <sup>1</sup>, Shuang Kou,<sup>1</sup> Xiaoya Li,<sup>6</sup> Guoming Pang,<sup>7</sup> Hongchuan Zhao <sup>8</sup> and Cheng Lu <sup>1</sup>

<sup>1</sup>Institute of Basic Research in Clinical Medicine, China Academy of Chinese Medical Sciences, Beijing 100700, China

<sup>2</sup>Institute for Advancing Translational Medicine in Bone & Joint Diseases, School of Chinese Medicine, Hong Kong Baptist University, Kowloon Tong 00852, Hong Kong

<sup>3</sup>College of the Second Clinical Medical, Guangzhou University of Chinese Medicine, Guangzhou 510000, China

<sup>4</sup>College of Chemical and Biological Engineering, Yichun University, Yichun 336000, China

<sup>5</sup>School of Life Science and Engineering, Southwest Jiaotong University, Chengdu 610000, China

<sup>6</sup>Chinese Academy of Medical Sciences/Peking Union Medical College, Beijing 100193, China

<sup>7</sup>Department of Diabetes, Kaifeng Hospital of TCM, Kaifeng 475000, China

<sup>8</sup>Department of Gastroenterology, China-Japan Friendship Hospital, Beijing 100029, China

Correspondence should be addressed to Hongchuan Zhao; zhaohongchuan2000@163.com and Cheng Lu; lv\_cheng0816@163.com

Received 26 October 2017; Revised 15 February 2018; Accepted 25 March 2018; Published 29 May 2018

Academic Editor: Lifei Hou

Copyright © 2018 Kang Zheng et al. This is an open access article distributed under the Creative Commons Attribution License, which permits unrestricted use, distribution, and reproduction in any medium, provided the original work is properly cited.

Rheumatoid arthritis (RA) is a type of chronic systemic inflammatory disease; it has a very complicated pathogenesis, and multiple pathological changes are implicated. Traditional Chinese medicine (TCM) like *Tripterygium wilfordii* Hook. F. or *Sinomenium acutum* (Thunb.) Rehd et Wils. has been extensively used for centuries in the treatment of arthritic diseases and been reported effective for relieving the severity of RA. Hei-Gu-Teng Zhuifenghuoluo granule (HGT) which contains *Periploca forrestii* Schltr., *Sinomenium acutum* (Thunb.) Rehd et Wils., and *Lysimachia paridiformis* Franch. var. *stenophylla* Franch. was a representative natural rattan herb formula for the treatment of RA in China, but the mechanism has not been elucidated. This study aimed at exploring the mechanism of HGT on RA using the bioinformatics analysis with *in vivo* and *in vitro* experiment validation. The potential action mechanism was first investigated by bioinformatics analysis via Ingenuity Pathway Analysis (IPA) software. After that, we use experimental validation such as collagen-induced arthritis (CIA) mice model *in vivo* and U937 cell model *in vitro*. The bioinformatics results suggested that HGT may have anti-inflammatory characteristic on RA and IL-12 signaling pathway could be the potential key trigger. *In vivo* experiments demonstrated that HGT ameliorated the symptoms in CIA mice and decreased the production of inflammatory cytokines in both mice ankle joints and serum. Furthermore, HGT effectively inhibited the activation of IL-12R and STAT4 on IL-12 signaling pathway. *In vitro* experiments showed that HGT inhibited the production of IL-12R and STAT4 induced by IL-12 in lipopolysaccharide- (LPS-) stimulated U937 cells. Moreover, IL-12R knockdown was able to interfere with the inhibition effects of HGT on the production of these cytokines. Our results confirmed the anti-inflammatory property of HGT, which was attributed to its inhibition on IL-12 signaling pathway.

## 1. Introduction

Rheumatoid arthritis (RA) which manifests as persistent and progressive joint destruction is a common chronic autoimmune disease with inflammation which leads to pain, stiffness, and the final result functional disability [1, 2]. Cartilage destruction, bone fusions and erosion, chronic granulation, and scar tissue result in the joints including hands and feet [3]. Traditional Chinese medicine (TCM) including herbals and herbal formulas or extracts, such as Qingfuguanjieshu, Wu Tou Tang, and extracts of the herb *Tripterygium wilfordii* Hook. F., is valid for alleviating the inflammation severity of RA by demonstration [4, 5]. Some natural rattan herbals can provide good therapeutic effect in RA such as *Tripterygium wilfordii* Hook. F. [6] and *Sinomenium acutum* (Thunb.) Rehd et Wils. [7]; their active compounds or underlying mechanisms have always been a research trend as their main bioactive ingredient pharmacological efficacy may account for analgesic and anti-inflammatory activities [8].

Hei-Gu-Teng Zhuifenghuoluo granule (HGT) was an antiarthritic Chinese herbal formula in China [9], which is identified as the over-the-counter (OTC) drug for treatment of arthritis by the Chinese State Food and Drug Administration (CFDA), composed of *Periploca forrestii* Schltr., *Sinomenium acutum* (Thunb.) Rehd et Wils., and *Lysimachia paridiformis* Franch. var. *stenophylla* Franch. Nowadays, investigators have not elucidated underlying molecular mechanism adequately.

Bioinformatics analysis technology, as a common way used for integrating multiple data, has become an essential way to help people understand organic life about biological relevant processes [10, 11]. Moreover, bioinformatics analysis method enables our required searching for the information of drugs, related genes, or proteins; constructs the interactional experimental system models; then makes underlying molecular interaction networks visualized. HGT consists of three herbals which were characterized by multicomponent and multitarget like other formulas. Based on abundantly existing databases, bioinformatics analysis can help better understand potential action mechanisms in the previous studies of our group [12, 13]. Therefore, in our study, we investigated the mechanism of HGT treatment on RA by bioinformatics analysis and *in vivo* and *in vitro* experimental validations.

## 2. Materials and Methods

**2.1. Analysis of Molecular Networks and Signaling Pathways of HGT and RA.** The human target proteins of HGT were found in PubChem platform (<https://pubchem.ncbi.nlm.nih.gov/>), and the key word was searched for in the PubChem Compound. The human target genes related with RA were found in the National Center for Biotechnology Information (NCBI) Gene database (<http://www.ncbi.nlm.nih.gov/gene>). "Rheumatoid arthritis" was used as a key word in Gene database searching. The obtained data were saved in an excel form for the next study [11, 13].

The human target protein and gene data acquired in the first step were imported into the IPA platform. The molecules being imputed to the IPA were termed "focus molecules." IPA

generated a set of networks based on different biofunctions. The molecules were showed as nodes, and the biological relationship between two nodes was showed as an edge (line). All edges were supported by at least one reference from a textbook, from the literature, or from canonical information stored in the IPKB. The nodes were showed with diverse shapes that represented the functional class of the gene product. The networks were sorted depending on the scores enumerated by IPA and represented the significance of the molecules for the network. The target protein networks of HGT and RA could be established. Some major information, such as top biological pathway network information, biological functions, canonical pathways, and other related bioanalytical information, was included. In order to study the mechanism of HGT on RA, the canonical pathway analysis in IPA was accomplished by using the compare module. In addition, IPA determined the significance of the association between the focus molecules and the canonical pathways using Fisher's exact test.

**2.2. Cell Culture and Viability Assay.** The human monocytic cell U937 (American Type Culture Collection, USA), as a classic cell model for RA research, was applied to the *in vitro* experiment [11]. They were placed in the fresh RPMI 1640 medium (GIBCO Chemical, USA) for 7-day cultivation at 37°C, accompanied by 10% FBS in it. For viability assay, the monocytic cells were planted at the surface of each well with an appropriate concentration of  $1.0 \times 10^5$  cells/mL in a 96-well plate, incubated with PMA (Sigma Aldrich Co., USA) at 37°C for stimulation. After 2-day stimulation, the cells were rinsed with PBS and then administrated with different concentrations of HGT (Beijing Handian Pharmaceutical Co., China) (0, 6.25, 12.5, 25, 50, 100, and 200 nM) for another 2 days. Then, 10  $\mu$ L of CCK-8 reagent (Dojindo Inc., Japan) was added and incubated for the last 3 h. The plate in an ELISA reader (Bio-Tek Instruments, USA) was placed, and the absorbance of each well at 450 nm was measured in the end.

**2.3. Cell Administration.** The U937 cells were planted at the surface of each well with a concentration of  $1.0 \times 10^6$  cells/mL in a 6-well plate and then treated with PMA for an incubation of 2 days at room temperature. After being rinsed with PBS for three times, the cells were harvested and then treated them or not with 100 ng/mL LPS (Sigma Aldrich Co., USA) for 2 h. Afterwards, the cells were administrated with a medium concentration (12.5 nM) of HGT for 2 days. At last, the supernatant and cells were collected for ELISA and western blot analysis, respectively.

### 2.4. Animals and Experimental Procedures

**2.4.1. Animals.** Twenty-eight male DBA/1 mice (18–22 g) were kept in an appropriate environment on a light/dark cycle for 7 days. The animal experiments were complied with the Research Ethics Committee of the Institute of Basic Research in Clinical Medicine, China Academy of Chinese Medical Sciences, China. All the mice were supplied by the Laboratory Animal Center of the Academy of Military Medical Sciences, China.

**2.4.2. Induction of Arthritis Model.** The mice collagen-induced arthritis (CIA) model was implemented on the basis of a previous study introduced by Smolen et al. [1]. Twenty-one mice were immunized through intradermal injection of 100  $\mu$ g bovine type II collagen (Chondrex, USA) into the base of the tail and meantime emulsified through supplementation with 100  $\mu$ L complete Freund's adjuvant (CFA) (Chondrex, USA). The day of the first immunization was determined on day 0 and the second immunization was on day 21; the animals received evaluation of severity degree two times every week. The degree was represented by the mean arthritic index on a 0–4 scale following the criterion below [2]: 0 = no swelling; 1 = slight swelling emerged on the foot and/or ankle; 2 = mild swelling emerged around the ankle and the tarsal; 3 = moderate swelling emerged around the ankle and the tarsal, accompanied by some erythema; and 4 = severe swelling emerged on the whole limb, accompanied by much erythema. Each limb was assessed, and the accumulated score was the final score. The mouse with a final score more than one score was judged to be a successful model.

**2.4.3. Administration.** On day 35, the CIA mice were randomly divided into three groups: model group, HGT group, and MTX group and the other 7 healthy mice as a normal group. In the HGT group and MTX group, the mice received oral administration once a day. The mice in the normal group and model group received the same volume of saline. All the animals were sacrificed after 35-day administration. The serum and ankle joints were collected and stored at  $-80^{\circ}\text{C}$  for the next studies.

**2.4.4. Histology and Immunohistochemistry.** The ankle joints were first put into 4% paraformaldehyde for 48 h fixation, then immersed in 10% EDTA for 1 month decalcification, and at last embedded in paraffin for the next experiments. The tissues of each mouse were sectioned to 7 pieces, with a thickness of 6  $\mu$ m. For histology examination, the sections were stained with hematoxylin and eosin (HE). Synovial inflammation was evaluated with a three-point scale ranging from 0 to 3 as previous research described by Guo et al. [5].

For immunohistochemistry, the sections of the ankle joints were first deparaffinized and rehydrated and incubated with polyclonal rabbit anti-IL-12 (Abcam, UK) in a humidity cabinet overnight at  $4^{\circ}\text{C}$ . Then, a secondary peroxidase antibody was supplemented and reacted for 2 h. Finally, the sections were treated with DAB substrate solution. Each section was imaged under a light microscope (Carl Zeiss, Germany).

**2.5. Enzyme-Linked Immunosorbent Assay (ELISA).** The levels of TNF- $\alpha$ , IL-1 $\beta$ , IL-4, IL-5, IL-6, IL-12, and IL-13 in cell culture supernatant and the levels of TNF- $\alpha$ , IL-1 $\beta$ , IL-6, and IL-12 in serum of the mice were measured by ELISA using unified ELISA kits (San Diego, USA) in the basis of the manufacturer's instructions.

**2.6. Real-Time PCR.** Frozen ankle tissues and monocytic cells were homogenized in nuclear lysis buffer (Trizol, Invitrogen, USA) for total RNA extraction, with a concentration of  $5 \times 10^6$  cells/mL. The lysate was collected and then centrifugated at room temperature with appropriate chloroform,

isopropanol, and 75% ethanol, respectively. Afterwards, the precipitate was harvested, and some RNase-free water was added. The reverse transcriptions were performed using QuantiTect Reverse Transcription Kit (Qiagen K.K., Japan). The expressions of these cytokine mRNAs were quantified by defining the levels of each cytokine mRNA, and the mRNA levels of TNF- $\alpha$ , IL-1 $\beta$ , IL-6, and IL-12 were quantified by 7500 real-time PCR system (Applied Biosystems, USA). The data were figured out by the  $\Delta\Delta\text{Ct}$  algorithm and were unified based on the expression of GAPDH.

**2.7. Western Blot Analysis.** Cytosolic extracts of the U937 cells administrated with HGT and the ankle joints were prepared and homogenized or lysed in RIPA lysis buffer. The level of IL-12R $\beta$ 1 and STAT4 was quantified with anti-IL-12R $\beta$ 1 (Abcam, UK) and anti-STAT4 (Abcam, UK) in the cytosolic fraction from ankle joint tissues. Protein concentrations were quantified by the assay kit (Biotime Biotechnology, China) and were unified based on the expression of GAPDH. The gray value of each protein band was calculated by ImageJ.

**2.8. Statistical Analysis.** GraphPad Prism 7.0 and Student's *t*-test were used for statistical analysis. All experimental results were represented as the mean  $\pm$  SD. *p* value less than 0.05 was judged as statistically significant.

### 3. Results

**3.1. Results of Bioinformatics Analysis.** Eight hundred and thirty-two genes related with RA were found from Gene database in NCBI. The top fifteen signaling pathways were focused on cellular immune response, cytokine signaling, humoral immune response, and intercellular and second-messenger signaling. Then, human target proteins of HGT were found from PubChem database. The details are shown in Table S1. After that, the molecular networks of HGT target proteins were obtained and shown in Figure 1(a), which included IL-12 signaling. We listed the top 12 shared signaling pathways of HGT and RA related to cell immune response (Figure 1(b)). Further comparative analysis showed that IL-12 signal pathway was measured to be the top one shared signaling pathway.

**3.2. Effect of HGT on Paw Swelling in CIA Mice.** After CIA establishment, paw swelling in immunized mice on about day 42 reduced accordingly. As illustrated in Figure 2, treatment with HGT significantly suppressed inflammation. HGT could conspicuously inhibit paw swelling from after treatment (Figure 2(a)); the arthritis scores treated with HGT and MTX were decreased (Figure 2(b)).

**3.3. Effect of HGT on Histopathological Changes in CIA Mice.** To evaluate inflammation induced by CIA, hematoxylin and eosin (H&E) staining was subsequently performed. As the results shown in Figure 3(a), there was no inflammatory cell infiltration in normal mice, but in CIA mice, there were clear slices exhibited. After treatment with HGT and MTX, inflammatory cell infiltration was noticeably decreased (Figure 3(b)).

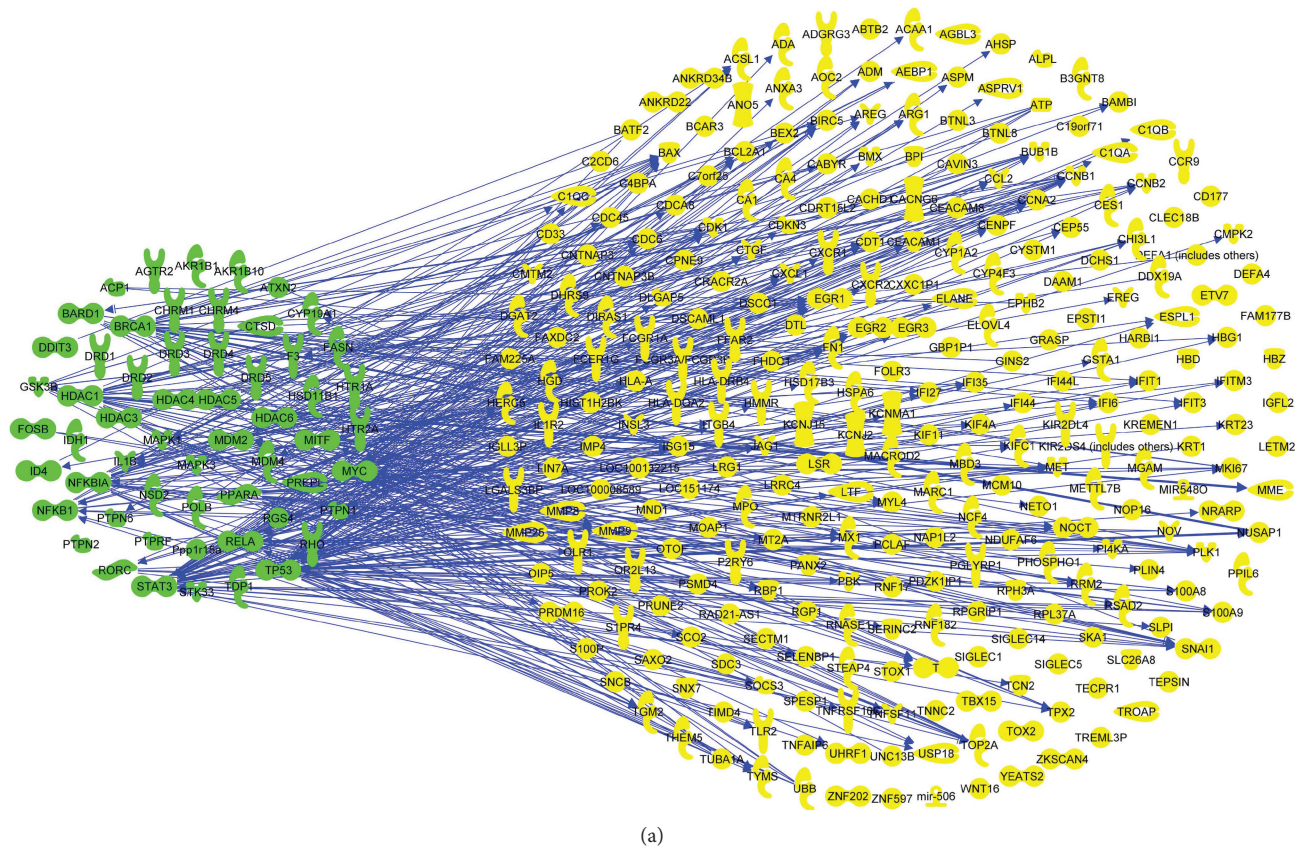


FIGURE 1: Bioinformatics analysis results. (a) The relationship between compound-related genes and RA disease-related genes; (b) shared signaling pathways between gene molecular networks related with rheumatoid arthritis (RA) and protein target molecular network of HGT performed using the Ingenuity Pathway Analysis (IPA) compare module. The signaling pathways of HGT were represented as dark blue, while the signaling pathways of RA were represented as light blue. The results showed that IL-12 signaling pathway was the top one shared signaling pathway.

3.4. Effect of HGT on Expression of Inflammatory Cytokines in Serum and CIA Mice Joints. As summarized in Figure 4, the expression of cytokines of TNF- $\alpha$  (Figure 4(a)), IL-1 $\beta$  (Figure 4(b)), and IL-6 (Figure 4(c)) in CIA mice serum was higher; HGT and MTX treatment both can significantly downregulate the levels. And then, the TNF- $\alpha$  mRNA

(Figure 4(d)), IL-1 $\beta$  mRNA (Figure 4(e)), and IL-6 mRNA (Figure 4(f)) expression in CIA mice treated with HGT and MTX could also significantly decrease.

3.5. The Effect of the Expression of IL-12 and STAT4 in CIA Mice. To observe the effect of HGT on production of IL-12

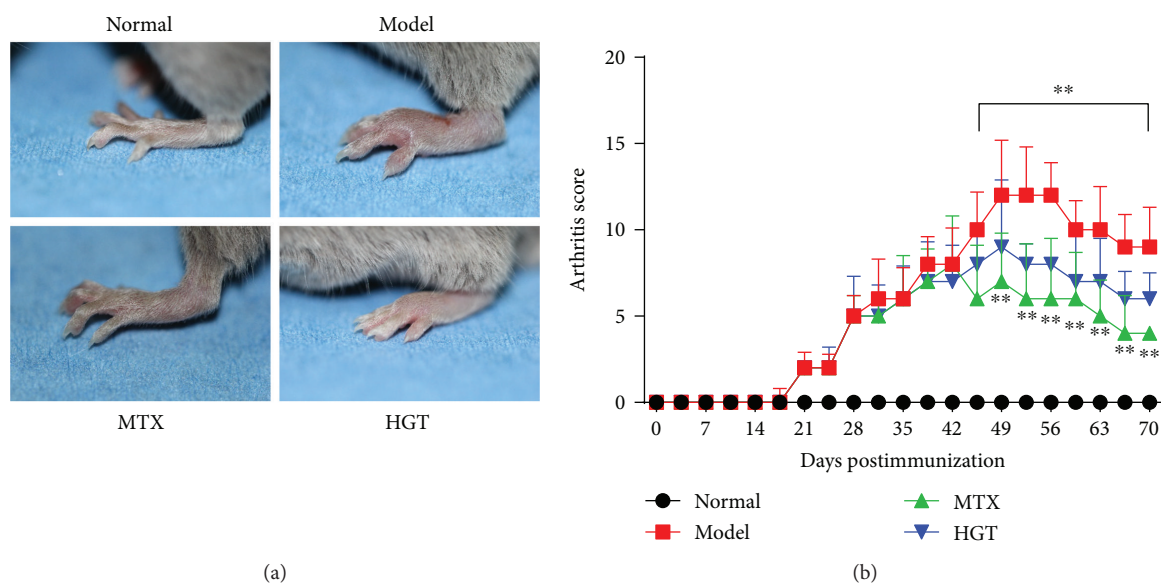


FIGURE 2: Effects of HGT on CIA mice. (a) The morphological characteristics of the representative of the CIA mice joint; (b) arthritic score in different days after the treatment of HGT; MTX represented the methotrexate group; HGT represented the HGT group. Data are represented as the mean  $\pm$  SD ( $n = 7$ ); \*\* $p < 0.01$ , comparison with model group.

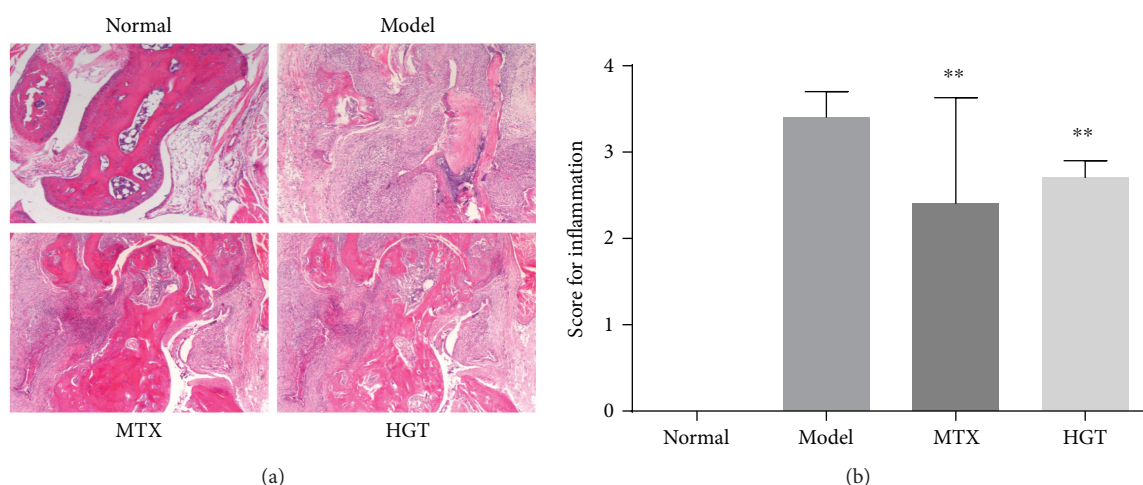


FIGURE 3: Effects of HGT on histopathological of CIA mice joints. (a) Histopathological characteristics of representative CIA mice joints; (b) inflammation score in the different group after treatment with HGT; MTX represented the methotrexate group, HGT represented the HGT group. Data are represented as the mean  $\pm$  SD ( $n = 7$ ); \*\* $p < 0.01$ , comparison with the model group.

and STAT4, we examined the expression of IL-12 and STAT4 in serum and ankle joints of CIA mice. The result indicated that HGT could decrease the production in both immunohistochemistry (Figure 5(a)) and serum (Figure 5(d)) and also mRNA expression (Figure 5(b)) in the ankle joints. Further, the protein levels of IL-12R $\beta$ 1 and STAT4 in mice ankle joints (Figure 5(c)) also markedly decreased after the treatment of HGT.

**3.6. Effects of HGT on Inflammatory Cytokine Expression in Cell Model.** U937 cells were first used to stimulate with LPS, and then IL-1 $\beta$ , TNF- $\alpha$ , and IL-6 were measured. The results showed that the TNF- $\alpha$  levels, IL-1 $\beta$  levels, and IL-6 levels in the supernatant of U937 cells treated with HGT were

inhibited both with ELISA measurement on secretion (Figures 6(a)–6(c)) and RT-PCR measurement of mRNA (Figures 6(d)–6(f)).

**3.7. Effects of Expression of Cytokines of HGT after IL-12R $\beta$ 1 Knockdown.** To determine the role in how the IL-12 signal pathway plays in the regulation of the effect HGT on LPS-induced inflammatory cytokine production, IL-12R $\beta$ 1 siRNA was used to knock down the expression of IL-12R $\beta$ 1. The results showed that IL-12 expression was significantly decreased in the U937 cells transfected with IL-12R $\beta$ 1 siRNA (Figure 7(a)). And also, the IL-12R $\beta$ 1 and STAT4 protein expression significantly decreased (Figure 7(b)). IL-12R $\beta$ 1 knockdown could decrease the levels of IFN- $\gamma$  (Figure 7(c))

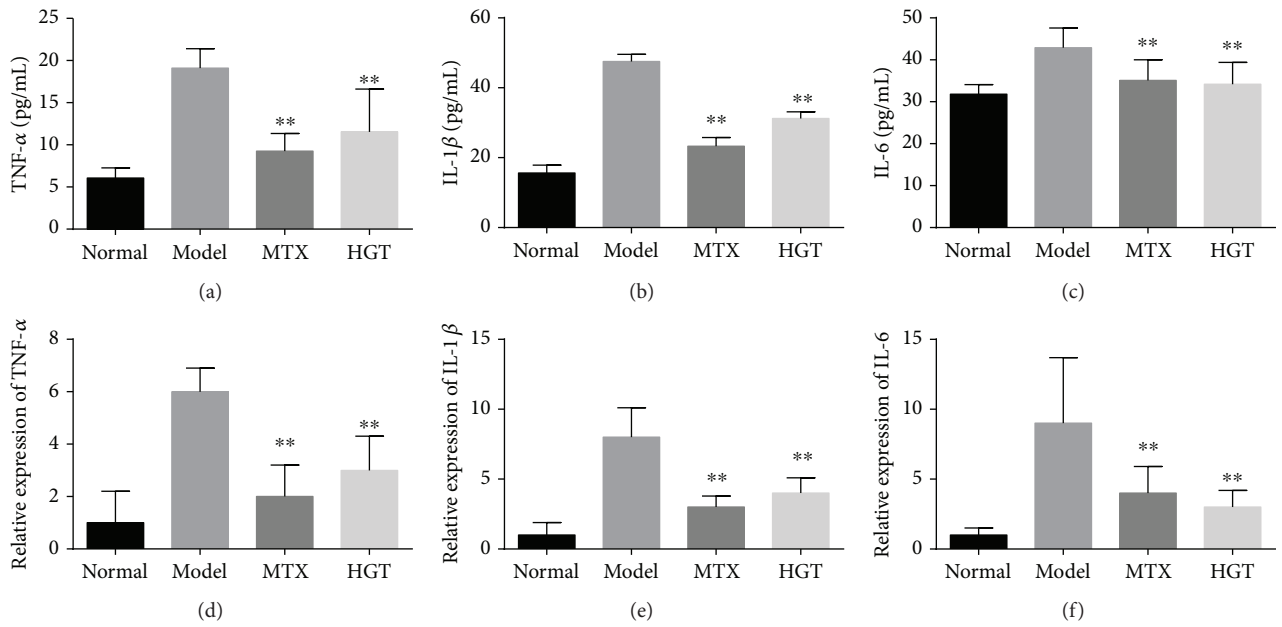


FIGURE 4: The effect of the expression of cytokines in mice. (a–c) IL-6, IL-1 $\beta$ , and TNF- $\alpha$  in the CIA mice with the treatment of HGT and also the mRNA expression in CIA mice joints with treatment. The data are represented as the mean  $\pm$  SD ( $n = 7$ ); \*\* $p < 0.01$ , when compared with the model group.

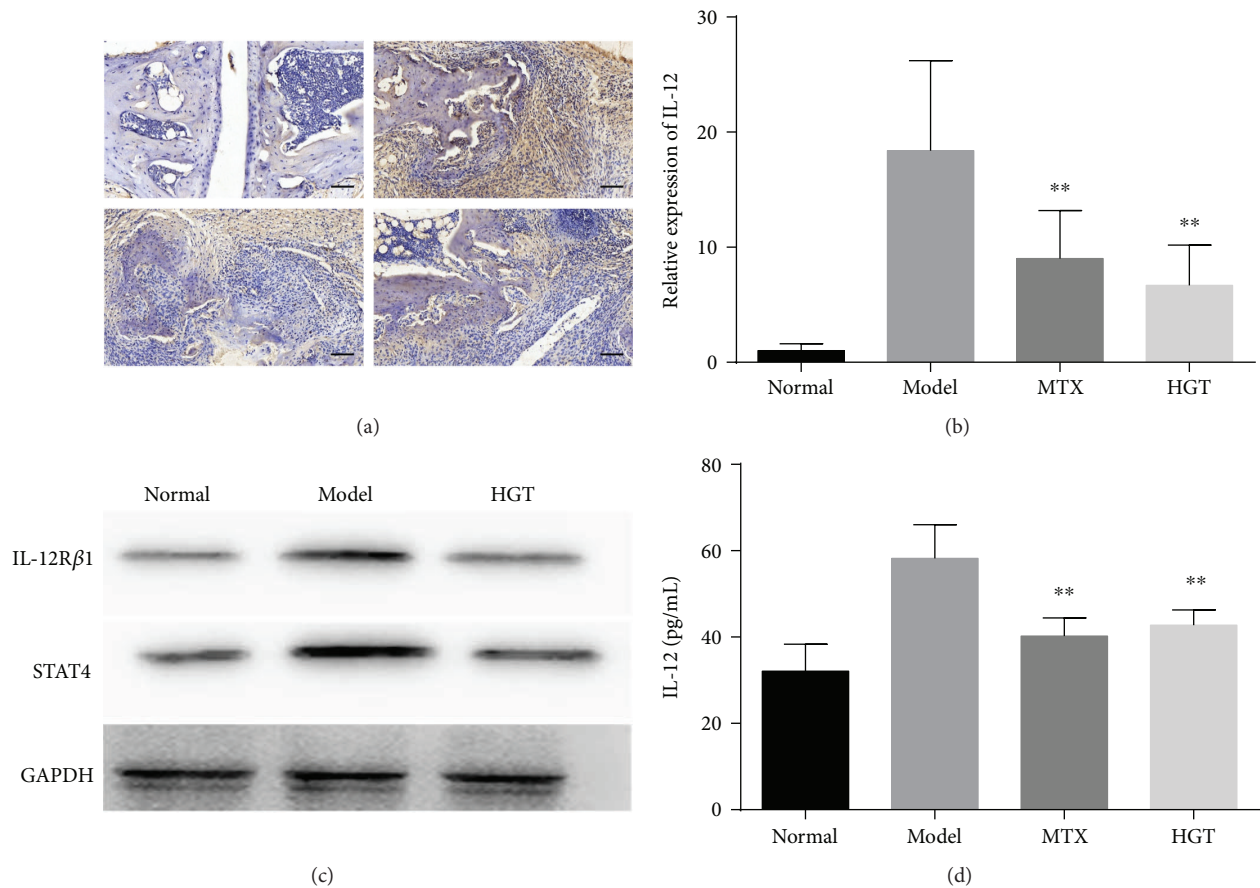


FIGURE 5: The effects of HGT on IL-12 and STAT4 expression in mice. (a) Immunohistochemistry of IL-12 in joints of mice with the treatment of HGT; (b) the levels of IL-12 mRNA in mouse joints after the treatment of HGT; (c) the expression of IL-12R $\beta$ 1 and STAT4 protein in CIA mice joints; (d) IL-12 in serum of CIA mice with the treatment of HGT. The data are represented as the mean  $\pm$  SD ( $n = 7$ ); \*\* $p < 0.01$ , when compared with the model group.

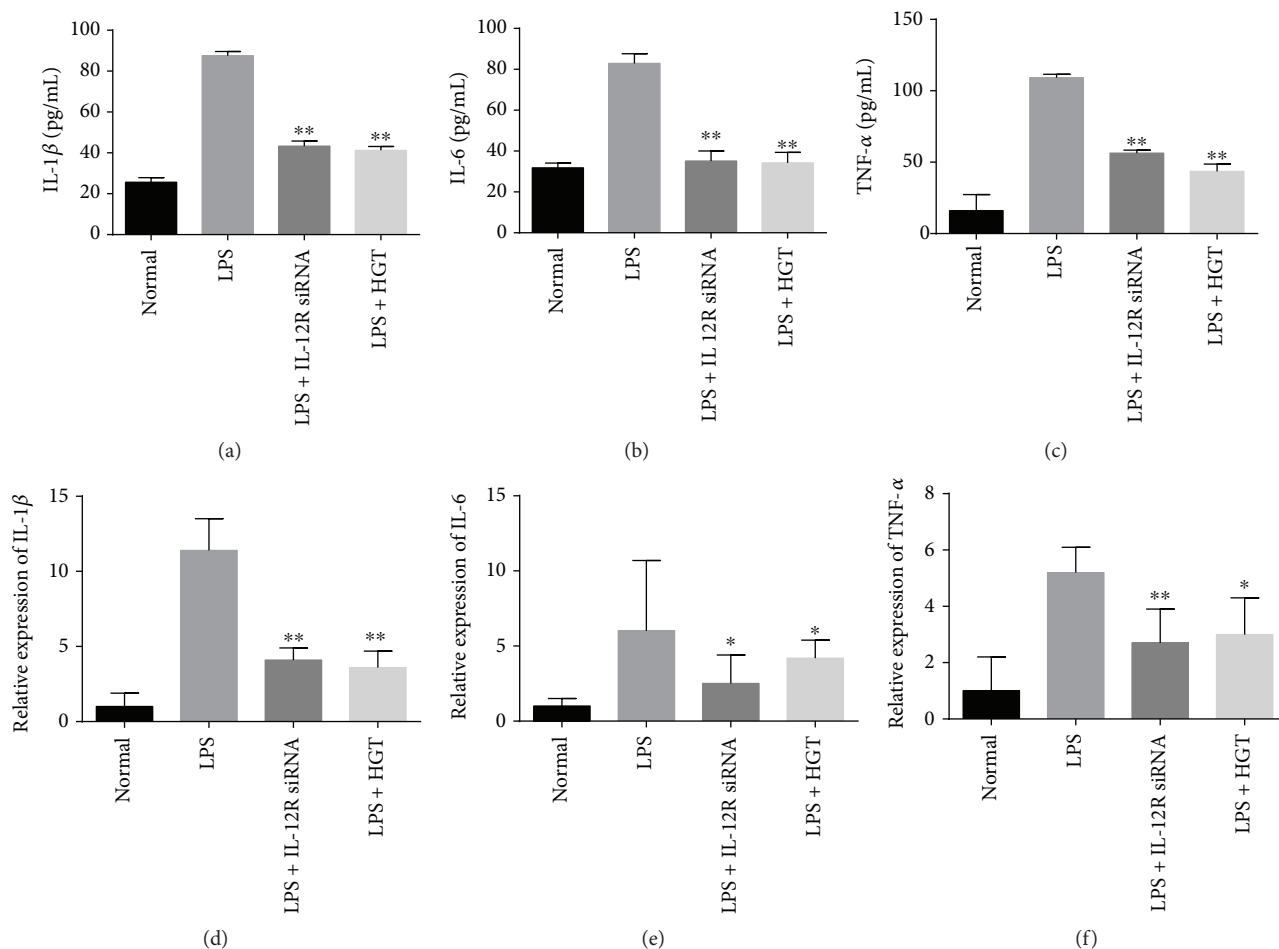


FIGURE 6: Effects of HGT on the expression of cytokines in U937 cells. (a–c) IL-6 levels, TNF- $\alpha$  levels, and IL-1 $\beta$  levels in LPS-induced U937 cells after the treatment of IL-12 siRNA and HGT; (d–f) IL-6, TNF- $\alpha$ , and IL-1 $\beta$  mRNA levels in LPS-induced U937 cells after treatment with IL-12 siRNA and HGT. The data are represented as the mean  $\pm$  SD ( $n = 7$ ); \* $p < 0.05$  and \*\* $p < 0.01$ , when compared with the LPS group.

and upregulate the levels of IL-4 (Figure 7(d)), IL-5 (Figure 7(e)), and IL-13 (Figure 7(f)). And also, no significant difference was found between the cells transfected with IL-12R $\beta$ 1 siRNA and the cells transfected with IL-12R $\beta$ 1 siRNA in the presence of HGT.

**3.8. Schematic Diagram Depicting How HGT Modulates the IL-12 Signaling Pathway to Inhibit the Inflammatory Response in Rheumatoid Arthritis.** By inhibiting IL-12R, Figure 8 shows how HGT could inhibit STAT4 and then inhibit the inflammation, meanwhile, decreasing TNF- $\alpha$  and IFN- $\gamma$ .

#### 4. Discussion

Traditional Chinese medicine (TCM) has been used for arthritic diseases in China for hundreds of years extensively. Hei-Gu-Teng Zhuifenghuoluo granule (HGT) composed of *Periploca forrestii* Schltr., *Sinomenium acutum* (Thunb.) Rehd et Wils., and *Lysimachia paridiformis* Franch. var. *stenophylla* Franch, was an antiarthritic Chinese herbal formula that was often used for treatment of

joint pain and RA by Chinese doctors. In this herbal formula, certain bioactive chemicals such as sinomenine and *Periploca forrestii* Schltr. saponin have been previously identified [10, 11]. Sinomenine is a natural alkaloid isolated from the roots of *Sinomenium acutum* (Thunb.) Rehd et Wils and a variety of bioactivities have been reported such as anti-inflammatory and antirheumatic. Based on these effects, sinomenine has been widely applied in clinical treatment of RA in China. The dry root or whole vine of *Sinomenium acutum* (Thunb.) Rehd et Wils. was effective in clinical prescription for the treatment of rheumatoid diseases. Saponins are the characteristic components and also the main active ingredients of *Periploca forrestii* Schltr. saponin which was extracted from *Periploca forrestii* Schltr. that could prophylactically treat autoimmune arthritis by controlling the systemic autoimmune responses, local inflammation, and bone destruction of the joints [12].

Nevertheless, the progress of RA is very complicated, so more and more mechanisms should be elucidated. Bioinformatics is a method which could provide important avenues in organic life for biological relevant processes. Therefore,



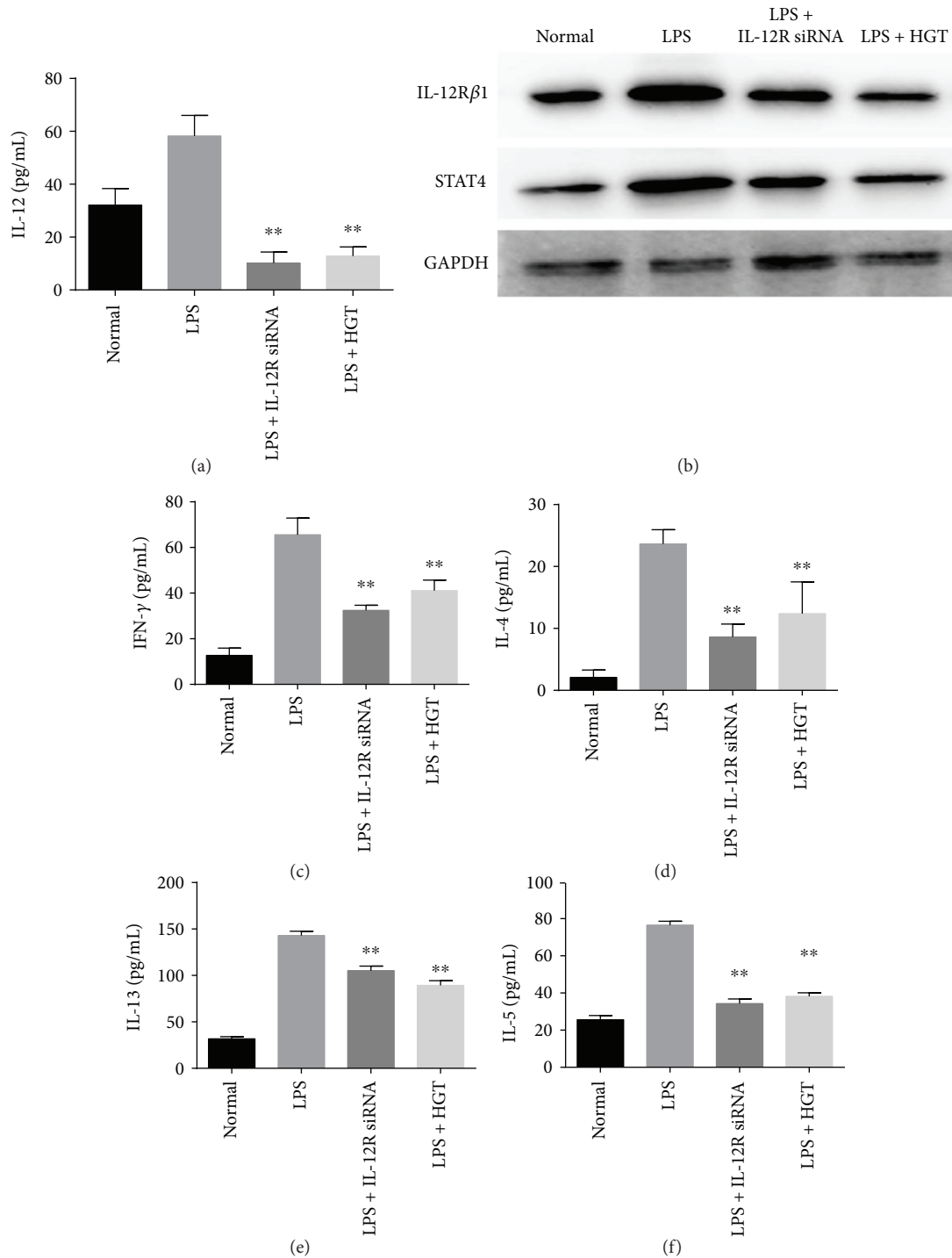


FIGURE 7: The effects of HGT on cytokine expression after IL-12Rβ1 knockdown. Firstly, the U937 cells were first treated with LPS and the other without LPS, and then all cells were transfected with IL-12Rβ1 siRNA. 48 h later, the U937 cells were then treated with HGT or without HGT for 48 h. (b) Western blot of the protein of IL-12Rβ1 and STAT4; (a, c, d, e, f) IL-12, IFN-γ, IL-4, IL-13, and IL-5 productions were determined by ELISA. The data are represented as the mean ± SD (n = 7); \*\*p < 0.01, when compared with the LPS group.

in order to investigate the potential mechanisms of HGT acting on RA, we employed an integrating network analysis of bioinformatics technology.

This bioinformatics analysis exposed that IL-12 signal pathway and IL-12 productions were related to RA and HGT, and this was consistent with some other previous

studies [8, 13]. And the other analysis also indicated that IL-12 signal pathway was involved in the signaling pathway of cytokine and cellular immune in RA. Interleukin-12 (IL-12) is a heterodimeric cytokine which is produced primarily by antigen-presenting cells [14, 15]. It has many immunoregulatory effects on T cells and natural killer (NK) cells [16].

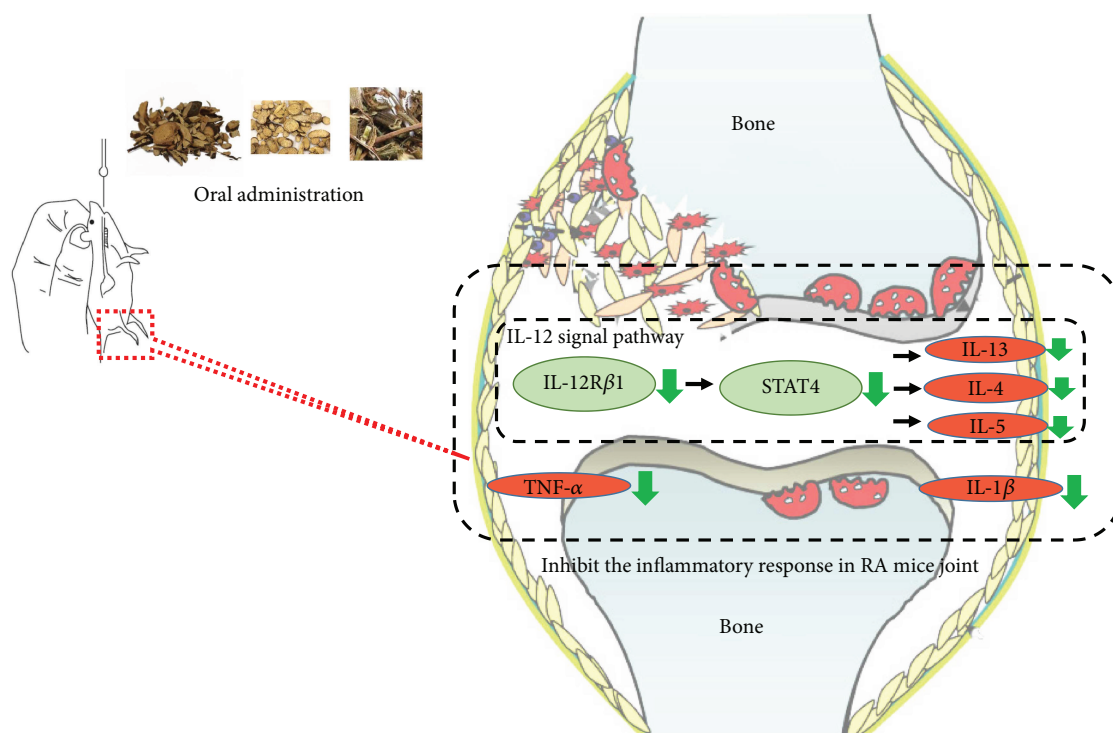


FIGURE 8: Schematic diagram depicting how HGT modulates the IL-12 signaling pathway to inhibit the inflammatory response in rheumatoid arthritis. By inhibiting IL-12R, HGT could inhibit STAT4 and then inhibit the inflammation, meanwhile, decreasing TNF- $\alpha$  and IFN- $\gamma$ .

In this experiment, we verify that IL-12 levels in serum and CIA mice joints were increased, and HGT could also decrease the IL-12 expression both in mRNA and protein. Then, our experiment showed that LPS increased the IL-12 mRNA and IL-12 protein and the inflammation framework of U937 cells. As IL-12 is required for the promotion of Th1 development as well as IFN- $\gamma$  expression [17, 18], IL-1 $\beta$ , IL-6, and TNF- $\alpha$  can be effected by STAT4. Our experiment showed both IL-12 knockdown and HGT could inhibit the production of IL-1 $\beta$ , TNF- $\alpha$ , and IL-6. And, the effects were retained after IL-12 knockdown, but there was no difference between cells transfected with IL-12 siRNA and cells transfected with IL-12 siRNA but treated with HGT simultaneously. IL-12R $\beta$ 1 plays an important role in IL-12 signaling pathway [19]. In this study, our bioinformatics analysis results showed that IL-12 signaling was involved in the inflammation regulation in HGT treatment of RA. STAT proteins like STAT1 or STAT4 are implicated in IL-12 signaling in T cells [20]. STAT4 is essential in mediating IL-12 function in T and NK cells [21, 22]. All major functions of IL-12 are abrogated in STAT4-deficient mice, including production of IFN- $\gamma$  and NK cell cytotoxic activity [23, 24]. This suggests that regulating the expression of STAT4 may also be an important control point in modulating IL-12 function in NK and T cells [25, 26]. Therefore, our results suggested that HGT might modulate IL-12/STAT4 signal pathway in inhibiting inflammatory response. In sum, we confirmed the anti-inflammatory property of HGT, which was attributed to its inhibition on IL-12 signaling. Our finding also suggested that we can search the target of TCM and the possible mechanisms.

## 5. Conclusions

In conclusion, we confirmed the anti-inflammatory property of HGT, which was attributed to its inhibition on IL-12 signaling. Our finding also suggested that we can search the target of TCM and the possible mechanisms. Meanwhile, the consensus between the results analyzed by bioinformatics method and previous studies suggesting bioinformatics analysis method was reliable.

## Disclosure

Cheng Lu and Hongchuan Zhao are the corresponding authors. Zexu Chen and Wen Sun are the co-first authors of this paper.

## Conflicts of Interest

The authors declare no conflict of interests.

## Authors' Contributions

Kang Zheng, Zexu Chen, and Wen Sun carried out most of the experimental work and drafted the manuscript. Bin Liu, Danping Fan, Xiaojuan He, and Li Li analyzed and interpreted the data. Qingqing Guo, Hui Luo, Jiawen Shen, and Guoming Pang assisted in the animal experiments and assays. Shuang Kou and Xiaoya Li helped in the revised version. Cheng Lu and Hongchuan Zhao designed this study and revised the manuscript. All authors read and approved

the final manuscript. Kang Zheng, Zexu Chen, and Wen Sun equally contributed to this work and are co-first author.

## Acknowledgments

This work was supported by the National Natural Science Foundation of China (Grant no. 81373773, 81673844) and China Academy of Chinese Medical Sciences (Z0552).

## Supplementary Materials

Table S1: human target proteins of HGT. (*Supplementary Materials*)

## References

- [1] J. S. Smolen, D. Aletaha, and I. B. McInnes, "Rheumatoid arthritis," *The Lancet*, vol. 388, no. 10055, pp. 2023–2038, 2016.
- [2] S. M. Atkinson, P. A. Usher, P. H. Kvist, H. Markholst, C. Haase, and A. Nansen, "Establishment and characterization of a sustained delayed-type hypersensitivity model with arthritic manifestations in C57BL/6J mice," *Arthritis Research & Therapy*, vol. 14, no. 3, p. R134, 2012.
- [3] U. Lathia, E. Ewara, and F. Nantel, "Impact of adherence to biological agents on health care resource utilization for patients over the age of 65 years with rheumatoid arthritis," *Patient Preference and Adherence*, vol. 11, pp. 1133–1142, 2017.
- [4] Y. F. Wong, H. Zhou, J. R. Wang, Y. Xie, H. X. Xu, and L. Liu, "Anti-inflammatory and analgesic effects and molecular mechanisms of JCICM-6, a purified extract derived from an anti-arthritic Chinese herbal formula," *Phytomedicine*, vol. 15, no. 6-7, pp. 416–426, 2008.
- [5] Q. Guo, K. Zheng, D. Fan et al., "Wu-Tou decoction in rheumatoid arthritis: integrating network pharmacology and in vivo pharmacological evaluation," *Frontiers in Pharmacology*, vol. 8, p. 230, 2017.
- [6] P. Lipsky and X. Tao, "A potential new treatment for rheumatoid arthritis:thunder god vine," *Seminars in Arthritis & Rheumatism*, vol. 26, no. 5, pp. 713–723, 1997.
- [7] Y. Li, J. Wang, Y. Xiao et al., "A systems pharmacology approach to investigate the mechanisms of action of *Semen Strychni* and *Tripterygium wilfordii* Hook F for treatment of rheumatoid arthritis," *Journal of Ethnopharmacology*, vol. 175, pp. 301–314, 2015.
- [8] J. Chen, X. Wang, Y.-g. Qu et al., "Analgesic and anti-inflammatory activity and pharmacokinetics of alkaloids from seeds of *Strychnos nux-vomica* after transdermal administration: effect of changes in alkaloid composition," *Journal of Ethnopharmacology*, vol. 139, no. 1, pp. 181–188, 2012.
- [9] J. F. Luo, Z. K. Hu, K. Deng et al., "The pharmacological effects and mechanism of Heiguteng Zhuifenghuoluo capsule in anti-rheumatoid arthritis disease," *Medical Science Journal of Central South China*, vol. 44, no. 2, 2017.
- [10] S. E. Calvano, W. Xiao, D. R. Richards et al., "A network-based analysis of systemic inflammation in humans," *Nature*, vol. 437, no. 7061, pp. 1032–1037, 2005.
- [11] D. Fan, X. He, Y. Bian et al., "Triptolide modulates TREM-1 signal pathway to inhibit the inflammatory response in rheumatoid arthritis," *International Journal of Molecular Sciences*, vol. 17, no. 4, p. 498, 2016.
- [12] X. Niu, C. Lu, C. Xiao et al., "The crosstalk of pathways involved in immune response maybe the shared molecular basis of rheumatoid arthritis and type 2 diabetes," *PLoS One*, vol. 10, no. 8, article e0134990, 2015.
- [13] B. Zhang, X. Wang, and S. Li, "An integrative platform of TCM network pharmacology and its application on a herbal formula, *Qing-Luo-Yin*," *Evidence-Based Complementary and Alternative Medicine*, vol. 2013, Article ID 456747, 12 pages, 2013.
- [14] B. Pulendran, H. Tang, and S. Manicassamy, "Programming dendritic cells to induce T<sub>H</sub>2 and tolerogenic responses," *Nature Immunology*, vol. 11, no. 8, pp. 647–655, 2010.
- [15] M. W. L. Teng, E. P. Bowman, J. J. McElwee et al., "IL-12 and IL-23 cytokines: from discovery to targeted therapies for immune-mediated inflammatory diseases," *Nature Medicine*, vol. 21, no. 7, pp. 719–729, 2015.
- [16] A. D'Andrea, M. Rengaraju, N. M. Valiante et al., "Production of natural killer cell stimulatory factor (interleukin 12) by peripheral blood mononuclear cells," *Journal of Experimental Medicine*, vol. 176, no. 5, pp. 1387–1398, 1992.
- [17] C. Heufler, F. Koch, U. Stanzl et al., "Interleukin-12 is produced by dendritic cells and mediates T helper 1 development as well as interferon- $\gamma$  production by T helper 1 cells," *European Journal of Immunology*, vol. 26, no. 3, pp. 659–668, 1996.
- [18] G. Trinchieri, "Proinflammatory and immunoregulatory functions of interleukin-12," *International Reviews of Immunology*, vol. 16, no. 3-4, pp. 365–396, 1998.
- [19] M. J. Brunda, "Interleukin-12," *Journal of Leukocyte Biology*, vol. 55, no. 2, pp. 280–288, 1994.
- [20] R. A. Seder and W. E. Paul, "Acquisition of lymphokine-producing phenotype by CD4<sup>+</sup> T cells," *Annual Review of Immunology*, vol. 12, no. 1, pp. 635–673, 1994.
- [21] J. Zou, D. H. Presky, C. Y. Wu, and U. Gubler, "Differential associations between the cytoplasmic regions of the interleukin-12 receptor subunits  $\beta$ 1 and  $\beta$ 2 and JAK kinases," *Journal of Biological Chemistry*, vol. 272, no. 9, pp. 6073–6077, 1997.
- [22] D. H. Presky, H. Yang, L. J. Minetti et al., "A functional interleukin 12 receptor complex is composed of two  $\beta$ -type cytokine receptor subunits," *Proceedings of the National Academy of Sciences of the United States of America*, vol. 93, no. 24, pp. 14002–14007, 1996.
- [23] C. M. Bacon, E. F. Petricoin, J. R. Ortaldo et al., "Interleukin 12 induces tyrosine phosphorylation and activation of STAT4 in human lymphocytes," *Proceedings of the National Academy of Sciences of the United States of America*, vol. 92, no. 16, pp. 7307–7311, 1995.
- [24] H.-J. Ahn, M. Tomura, W.-G. Yu et al., "Requirement for distinct Janus kinases and STAT proteins in T cell proliferation versus IFN- $\gamma$  production following IL-12 stimulation," *The Journal of Immunology*, vol. 161, no. 11, pp. 5893–5900, 1998.
- [25] W. E. Thierfelder, J. M. van Deursen, K. Yamamoto et al., "Requirement for Stat4 in interleukin-12-mediated responses of natural killer and T cells," *Nature*, vol. 382, no. 6587, pp. 171–174, 1996.
- [26] M. H. Kaplan, Y. L. Sun, T. Hoey, and M. J. Grusby, "Impaired IL-12 responses and enhanced development of Th2 cells in Stat4-deficient mice," *Nature*, vol. 382, no. 6587, pp. 174–177, 1996.

## Review Article

# The Role of Flavonoids in Inhibiting Th17 Responses in Inflammatory Arthritis

Dimitra Kelepouri <sup>1</sup>, Athanasios Mavropoulos <sup>1</sup>, Dimitrios P. Bogdanos <sup>1,2</sup>,  
and Lazaros I. Sakkas <sup>1</sup>

<sup>1</sup>Department of Rheumatology and Clinical Immunology, Faculty of Medicine, School of Health Sciences, University of Thessaly, 40500 Larissa, Greece

<sup>2</sup>Division of Liver Transplantation and Mucosal Biology, King's College London School of Medicine, Denmark Hill Campus, London SE5 9RS, UK

Correspondence should be addressed to Dimitrios P. Bogdanos; bogdanos@med.uth.gr

Received 23 October 2017; Accepted 3 January 2018; Published 5 March 2018

Academic Editor: Lifei Hou

Copyright © 2018 Dimitra Kelepouri et al. This is an open access article distributed under the Creative Commons Attribution License, which permits unrestricted use, distribution, and reproduction in any medium, provided the original work is properly cited.

Flavonoids have been considered powerful anti-inflammatory agents, and their exact immunomodulatory action as therapeutic agents in autoimmune diseases has started to emerge. Their role in the manipulation of immunoregulation is less understood. Several studies attempted to investigate the role of various flavonoids mainly in experimental models of autoimmune diseases, especially in the context of their potential effect on the increase of regulatory T cells (Tregs) and their ability to stimulate an overexpression of anti-inflammatory cytokines, in particular that of IL-10. The emergence of IL-17, a cytokine largely produced by Th17 cells, as a powerful proinflammatory stimulus which attenuates the induction of Tregs has prompted a series of studies investigating the role of flavonoids on Th17 cells in experimental models as well as human autoimmune diseases. This review thoroughly discusses accumulated data on the role of flavonoids on Th17 in rheumatoid arthritis and experimental autoimmune arthritis.

## 1. Introduction

Rheumatoid arthritis (RA) is the prototype of inflammatory chronic polyarthritis and is characterized by infiltration of T cells, B cells, macrophages, and fibroblasts in the synovial membrane, culminating in joint destruction and loss of function [1, 2]. The serological hallmark of the disease is the presence of high-titre rheumatoid factor (RF) and anticitrullinated peptide/antigen antibodies (ACPAs) [3–5].

## 2. The Role of Th17 Immune Response in RA Pathogenesis

The etiology of RA remains elusive; however, it is well recognized that CD4 T cells play a critical role in its pathogenesis as they heavily infiltrate the synovial membrane during RA synovitis [6]. This “T cell-centric theory” of RA pathogenesis has been challenged in the recent years as CD4 T cell

depletion therapy failed to improve RA in clinical trials and the lack of T helper 1- (Th1-) related cytokines paradoxically exacerbated arthritis in some animal models (the “Th1 paradox”). As a result, a new proposition emerged where the key mediators of RA are the proinflammatory cytokines derived from macrophages and fibroblast-like synoviocytes, like TNF- $\alpha$ , IL-1, and IL-6 [7]. This resulted in the successful application of “anticytokine therapy,” such as the anti-TNF- $\alpha$  therapy or the anti-IL-6 therapy, which has revolutionized current RA treatment [8].

From 2005 onwards, the discovery of Th17 cells added significant insight into how T cells participate in the initiation and perpetuation of RA [9, 10]. This led to the proposal of a new “Th17 cell-centric theory” and revived the interest on CD4 T cells, which were found to produce IL-17 in the RA synovium. Elegant studies in animal models (see below) revealed that Th17 cells are a lineage of CD4 T cells distinct from classical Th1 or Th2 cells and play significant roles in

autoimmune and inflammatory diseases [11]. The Th17 cells express the master transcription factor ROR $\gamma$ t, are differentiated *in vitro* by TGF- $\beta$  and IL-6, and can expand in the presence of IL-23, IL-1, and TNF- $\alpha$  [12]. Th17 differentiation may be cross-regulated by Th1, and, hence, the deficiency of Th1 cytokines led to the excessive differentiation of Th17 cells and paradoxically exacerbated RA in the animal models [13]. The advent of Th17 cells shed significant light in understanding the pathogenesis of RA.

Th17 cells are potent mediators of arthritis, which coordinate tissue inflammation, cartilage damage, and bone erosion. The arthritogenic potential of Th17 cells is mainly due to the pleiotropic effects of IL-17A (IL-17), which is produced by Th17 cells and acts on a variety of cells that constitute the synovial tissue [14, 15]. IL-17 synergistically enhances the production of TNF- $\alpha$ , IL-1, and IL-6 by macrophages and synovial fibroblasts. Additionally, IL-17 recruits neutrophils to the site of inflammation and promotes osteoclast differentiation, which leads to bone erosion and cartilage destruction. Two other cytokines produced by Th17 cells, IL-22 and IL-21, can alter the glycosylation of autoantibodies and grant them with inflammatory properties [16]. Th17 cells exhibit plasticity, that is, can shift to Th17/Th1 cells (producing both IL-17 and IFN- $\gamma$ ) and to Th1 cells (producing IFN- $\gamma$ , so-called nonclassic Th1 cells) [17, 18]. These Th17-derived Th1 cells (transdifferentiated, nonclassic Th1 cells) appear to be more pathogenic than Th17 cells [19].

The activation of highly inflammatory Th17 cells is controlled under physiological conditions by regulatory T cells (Tregs) in order to prevent the development of autoimmune diseases [20, 21]. Tregs express the master transcription factor Foxp3 and upregulate the expression of CD25 and CTLA-4 on their surfaces in order to suppress the activation of effector CD4 T cells in a cell contact-dependent manner. There are two types of Tregs: naturally occurring Tregs (nTregs), which are derived from the thymus, and induced Tregs (iTregs), which are induced to differentiate from naïve T cells in the periphery and express the potent immunomodulatory cytokine IL-10 [22].

### 3. Animal Models of Experimental Arthritis and Th17 Cells

Most work on experimental models of inflammatory arthritis has been performed using type II collagen-induced arthritis (CIA) mice, SKG mice, and TNF- $\alpha$  transgenic mice [23–26]. These studies confirm the significant role of IL-17 in inflammatory arthritis.

**3.1. Type II Collagen-Induced Arthritis Mice.** Genetically susceptible strains of mice, such as C57BL/6 and DBA/1 mice, when injected with type II collagen in complete Freund's adjuvant, induced synovitis and erosion that histologically resembled RA [27, 28].

Sera of these mice contain antibodies against type II collagen, which can induce arthritis in other mice (CAIA, anti-type II collagen antibody-induced arthritis). IL-23-driven CD4 T cells, but not IL-12-driven Th1 cells, are the key mediators of CIA. The IL-23-driven CD4 T cells secreted

IL-17 (Th17 cells) [29, 30]. Th17 cells contributed not only to joint inflammation but also to osteoclast differentiation and bone destruction.

**3.2. SKG Mice.** These mice are generated on a BALB/c genetic background and spontaneously develop autoimmune arthritis that resembles human RA [24, 31]. Similar to CIA, SKG arthritis is dependent on proinflammatory cytokines such as IL-6 and particularly IL-17 [32–35]. SKG CD4 T cells that were deficient in IL-17 failed to induce arthritis upon adoptive transfer into RAG2-deficient mice, while the induction of arthritis was accelerated by the transfer of IFN- $\gamma$ -deficient CD4 T cells [35].

**3.3. K/BxN Mice.** These mice express both the T cell receptor (TCR) transgene KRN and the MHC class II molecule A(g7) (K/BxN mice) and develop severe inflammatory arthritis [15, 36–38].

**3.4. TNF- $\alpha$  Transgenic Mice.** DBA/1 mice expressing a human TNF- $\alpha$  transgene develop a severe form of erosive arthritis [39–41]. Although anti-IL-17 therapy had only minor effects on joint inflammation induced by TNF- $\alpha$ , it effectively reduced bone erosion in TNF- $\alpha$  transgenic mice [42, 43]. This result suggested that although arthritis in TNF- $\alpha$  transgenic mice can develop in a T cell-independent manner, IL-17 may also contribute to bone destruction, which is mediated by TNF- $\alpha$  [44].

**3.5. gp130 F759/F759 Knock-In Mice.** Glycoprotein 130 (gp130) mediates signal transduction by IL-6 family cytokines such as IL-6, IL-27, and IL-35, through the signal transducer and activator of transcription 3 (STAT3) and/or Src homology region 2 domain-containing phosphatase 2 (SHP2) signaling. In this mouse model [45], Th17 cells are expanded as IL-6/gp130 signaling promotes Th17 differentiation [46].

**3.6. IL-1 Receptor-Antagonist Knockout Mice.** IL-1RA-deficient mice on a BALB/c background spontaneously developed chronic inflammatory polyarthritis [47, 48]. Overexpression of IL-1 leads to expansion of Th17 cells. As a result, the expression of IL-17 or IL-23 is greatly enhanced in IL-1RA KO mice, whereas arthritis development is inhibited during IL-17 deficiency or IL-23 blockade [49–51].

Studies of the impact of novel treatment/regimen, including diet complements, are usually studied in animal models, such as those mentioned above, the great majority of those conducted using the CIA model. Elegant reviews have been published discussing the current animal models of RA which summarize the pros and cons of each model as well as the role played by Th17 in the induction and perpetuation of inflammatory arthritis [11] (Table 1).

## 4. Flavonoids: An Overview

By the term *flavonoids*, we refer to a broad class of compounds that are defined by color (pigment). Literally, the term originates from the Latin word *flavus*, which means yellow. Flavonoids are a group of secondary plant metabolites

TABLE 1: Main features of animal models of rheumatoid arthritis regarding proinflammatory cytokines, including IL-17.

Animal models	IL-17	IL-23	IFN- $\gamma$	TNF- $\alpha$	IL-6	References
CIA mice	+	+	++	+++	++	[27, 29, 30, 105]
SKG mice	++	++	+	+	+	[32–35]
K/BxN mice	++	+/-	++	+	+/-	[15, 37, 38]
TNF- $\alpha$ transgenic mice	+	+	+	+++	+	[39, 40, 43, 44]
gp130 F759/F759 knock-in mice	++	+	+	+	++	[45, 46]
IL-1 RA knockout mice	++	++	+	+	+	[47, 49–51]

\*Low expression, \*\*moderate expression, and \*\*\*high expression.

present in the diet with cholesterol-lowering, antioxidant, and other health-beneficial biological activities [52–54]. They are also commonly found in seeds, nuts, grains, and spices and in some beverages, such as wine, tea, and beer [55].

Chemically, flavonoids are polyphenols conjugated to sugars (as a glycosylated form) although some can exist as free aglycones. The basic flavonoid structure is the flavan nucleus consisting of a 15-carbon skeleton arranged in two phenyl rings bound by a three-carbon bridge commonly encircled by oxygen, then forming three rings (Figure 1) [56]. The main classes of flavonoids are flavonols, flavones, flavanones, flavanols, isoflavones, and anthocyanidins [57].

Traditional Chinese medicine used over the last 3000 years to treat, manage, or prevent human diseases has largely been based on the beneficial role of natural bioactive compounds from herbs containing flavonoids [58]. A typical example is that of licorice, also called Gancao in China, derived from the dried roots and rhizomes of the *Glycyrrhiza* species, which is used to treat diabetes, tuberculosis, and other inflammatory disorders not only in China but also in Korea, Japan, and India [59]. Licorice is probably the most frequently used herbal medicine worldwide, as Gancao appears in over 50% of traditional Chinese medicine prescriptions and confectionery products [60]. The large number of natural compounds containing flavonoids and the wide range of cell signaling pathways involved make it extremely difficult to simplify the anti-inflammatory role of flavonoids in various inflammatory diseases. Such studies are elegantly reviewed elsewhere [61].

The anti-inflammatory activity of flavonoids is exerted through various mechanisms, mostly shared by most flavonoid compounds, and these largely include the direct or indirect inhibition of proinflammatory cytokines through the immunomodulation of key inflammatory signaling cascades, the diminished recruitment of proinflammatory cell subsets, their increased antioxidant properties, and their beneficial effect on immunoregulatory functions.

Recent evidence has suggested that flavonoids can be potential modifiers of innate and adaptive immunity [62–64]. Immune system impairment accounts for the increased risk of infections, inflammatory chronic disease, and autoimmunity. Flavonoids and polyphenols can target multiple inflammatory components and reinforce anti-inflammatory mechanisms with antioxidant potential [52, 54, 65]. Certain flavonoids, namely, quercetin, apigenin, and luteolin, reduce cytokine expression and secretion [66]. In this regard, flavonoids may have therapeutic potential

in the treatment of inflammation-related diseases as cytokine modulators. TLR suppression, PI3K/Akt inhibition, IKK/MAPK inhibition, mTORC1 inhibition, NF- $\kappa$ B, and JAK/STAT inhibition have been attributed as targets of flavonoid-mediated suppression of inflammation [67–69].

Although the immunomodulatory potential of flavonoids has been investigated to some extent, an established effect of these compounds in clinical trials has been controversial [70]. This is due to the diversity in their subclasses, as well as the unresolved problems related to the purity and the selected doses of these compounds. Nevertheless, current research in animal models and preclinical studies are promising and warrant further investigation of these compounds. However, very little is known about the impact of flavonoids on Th17-related immune modulation and their potential effect on autoimmune rheumatic disorders, such as RA. Some principal nutraceuticals that can modify the Th17 immune response and have shown some effects in animal models of RA are illustrated in Table 2.

**4.1. Oroxylin A.** Oroxylin A is one of the many flavonoid glycosides extracted from the plant *Scutellaria baicalensis radix* and the *Oroxylum indicum* tree bark but the only O-methylated flavone [71, 72]. Methylation provides flavonoids with increased metabolic stability and delays their hepatic metabolism. It also improves their intestinal absorption, ensuring better bioavailability.

In mice with induced arthritis, oroxylin A inhibited the production of inflammatory cytokines IL-1 $\beta$ , IL-6, TNF- $\alpha$ , and IL-17. TNF- $\alpha$ -induced p38 MAPK, ERK1/2, and NF- $\kappa$ B signaling pathways were also suppressed [73, 74]. Oroxylin A also increased the production of Tregs and reduced Th17 cells in the lymph nodes draining arthritis joints in mice with CIA [73] (Table 2). Oroxylin A suppressed the secretion of IL-1 $\beta$  and IL-6 from TNF- $\alpha$ -stimulated fibroblast-like synovial cells from RA patients. In TNF- $\alpha$ -stimulated RA fibroblast-like synovial cells, it also suppressed p38 MAPK and ERK-1/2 and prevented the nuclear translocation of NF- $\kappa$ B p65 [73].

Oroxylin A inhibits NO, cytokines, chemokines, and growth factors in induced macrophages via the calcium-STAT pathway and exerts an anti-inflammatory activity on lipopolysaccharide-induced mouse macrophages via Nrf2/ARE activation [75]. Inhibition of lipopolysaccharide-induced iNOS and COX-2 gene expression was also mediated via suppression of NF- $\kappa$ B [76].

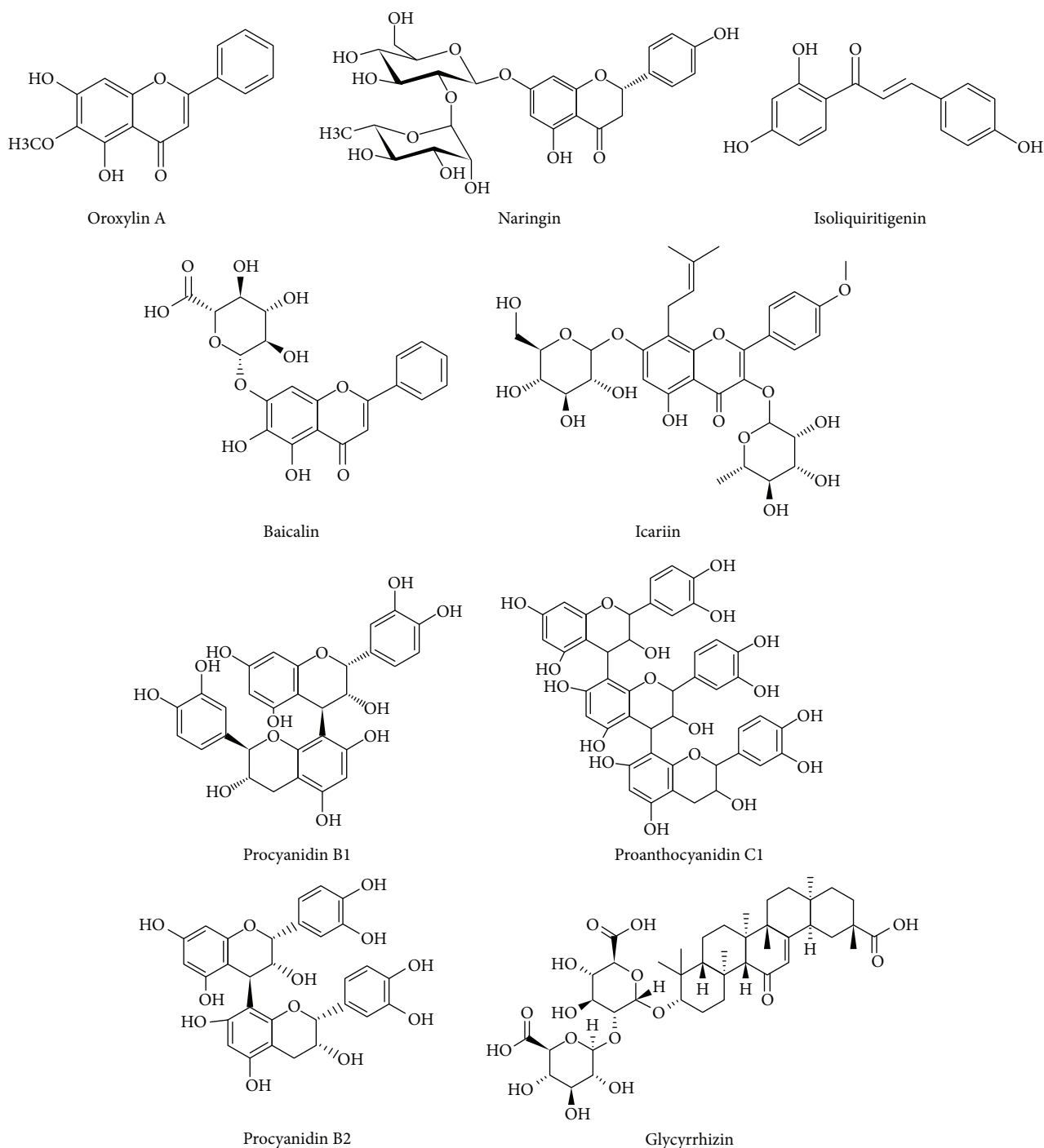


FIGURE 1: Chemical structures of principal flavonoids discussed in relation to their role on Th17 in rheumatoid arthritis and its experimental models.

**4.2. Baicalin.** Baicalin is a flavonoid compound isolated from the dry root of *Scutellaria baicalensis* Georgi (Huang-Qin), a medicinal plant. Baicalin is a flavone glycoside, glycosylated in the 7-position, glucuronide of baicalein. Baicalin inhibits Th17 cell differentiation *in vitro* and upregulates Foxp3<sup>+</sup> Tregs [77]. It also inhibits Th17 cell differentiation *in vivo* in lupus-prone MRL/lpr mice [77]. Baicalin reduced splenic Th17 cells and ameliorated murine adjuvant-induced arthritis without affecting Tregs. Furthermore, it significantly

blocked IL-17-stimulated synoviocyte gene expression of ICAM-1, VCAM1, IL-6, and TNF- $\alpha$  [78]. Baicalin blocked CIA in rats and inhibited the secretion of IL-1 $\beta$  and TNF- $\alpha$  in rat synovium [79]. Baicalin also prevented Th1 and Th17 cell differentiation via STAT/NF- $\kappa$ B signaling pathways and ameliorated clinical disease severity in experimental autoimmune encephalomyelitis (EAE) [80]. Furthermore, it suppressed Th17 development by upregulating the suppressor of cytokine signaling 3 (SOCS3) [80].

TABLE 2: Main features and findings of studies investigating the role of flavonoids in Th17 cells in animal models of rheumatoid arthritis.

Flavonoid name	Year of study	Experimental model	Administration and dosage	Biological finding	Clinical finding	References
Oroxylin A	2016	In male mice DBA/1 with type II collagen-induced arthritis	10 mg/kg oroxylin A for 10 days intraperitoneal	Increase of Tregs and reduction of Th17	Significant decline in arthritis and histological damage	[73]
Baicalin	2013	In male mice C57BL/6 (B6) with adjuvant-induced arthritis	100 mg/kg baicalin intraperitoneal for 7 days	Inhibition of splenic Th17 cells expansion <i>in vivo</i> . Inhibition of IL-17 inflammation in synovioocytes	Alleviation of inflammatory joint injury in mice with adjuvant-induced arthritis	[78]
Icariin	2014	In male mice C57BL/6 (B6) with type II collagen-induced arthritis	Oral dose of 25 mg/kg with icariin for 20 days	Decrease of Th17 cells and repression of IL-17 production	Suppression of inflammatory arthritis dependent on IL-17 production	[84]
Condensed tannins from apples	2015	In mice DBA/1 with type II collagen-induced arthritis	5–7 mL 1% w/v oral administration of ACT per day for 2 weeks	Reduction of IL-17 expression. Downregulation of Th17 development. Increase of Treg production	Delay in rheumatoid arthritis development in mice	[91]
Anthocyanins from black soybean seed	2015	In mice DBA/1 with type II collagen-induced arthritis	60 mg/kg oral administration of AEBs dissolved in saline for 7 weeks	Reduction of IL-17-expressing T cells. Inhibition of Th17 cell differentiation and Th17 cell differentiation-associated genes	Antiarthritic effects: decrease in incidence of arthritis, histological inflammation, cartilage scores, and oxidative stress	[104]
Grape seed proanthocyanidins	2011	In male mice DBA/1J with type II collagen-induced arthritis	300 mg/kg GSPE 3 times a week for 2 weeks	Repression of IL-17 in Th cells. Inhibition of Th17 cells. Induction of Foxp3 Treg cells. Inhibition of Th17-associated gene expression in human Th17 cells	Inhibition of the activity of autoimmune arthritis. Attenuation of the symptoms of collagen-induced arthritis	[94]
Grape seed proanthocyanidins	2013	In BALB/c female adult mice	25, 50, 100 mg/kg oral administration of GSPE once a day for 2 weeks	Increase of Foxp3 <sup>+</sup> Treg cells and reduction of Th17 cells. Upregulation of Th2 cells. Induction of Th17/Treg rebalance	Antiarthritic activity. Protection of GSPE against arthritis. Significant reduction in paw edema in mice	[95]



UP446, a composition consisting primarily of baicalin from *Scutellaria baicalensis* Georgi and catechin from the heartwoods of *Acacia catechu*, has been previously shown to reduce the production of eicosanoids and leukotrienes through dual inhibition of COX and lipo-oxygenase (LOX) enzymes and to decrease mRNA and protein levels of IL-1 $\beta$ , IL-6, and TNF- $\alpha$ , suggesting a potential benefit of UP446 in alleviating symptoms of RA and support further assessment of this botanical composition in patients with RA [81].

A combination of flavonoids from the *Scutellaria* root has been found to inhibit PGE2 production more potently than individual flavonoids do. The synergistic effect of the flavonoid mixture of baicalin and oroxylin A reflected a broad action in inhibiting multiple steps in the NF- $\kappa$ B signaling pathway [71].

**4.3. Icariin.** Icariin is a prenylated flavonol glycoside, a subclass of flavonoids. Prenylated flavonoids occur when the flavonoid ring is substituted by prenyl groups. This provides them a stronger adherence to cell membranes and enhances lipophilicity. From the various flavonoid glycosides of the genus *Epimedium*, icariin is the most metabolically active constituent and is obtained from the aerial part of the plant [82]. The difference between flavonols and flavones (oroxylin, baicalin) is that the former possess a hydroxyl group in the 3 position and can be regarded as 3-hydroxyflavones.

Icariin can suppress cartilage and bone degradation in mice with CIA [83]. It appears that icariin can exert its effects through a profound reduction of Th17 cells and IL-17 production, through inhibition of the STAT3 pathway [84]. Icariin inhibited the progression of the disease in a dose-dependent manner.

The effect of icariin on CIA is not unexpected. It has been reported that icariin has antiosteoporotic, anti-inflammatory, and antidepressant-like activities [85]. Its role on Th17/Treg balance was also reported in airway inflammation of an ovalbumin- (OVA-) induced murine asthma model [86]. Icariin decreased the inflammatory cells infiltrating the peribronchial tissues and mucus hyperproduction. This was associated with reduction in CD4<sup>+</sup>ROR $\gamma$ t<sup>+</sup> T cells and increase in CD4<sup>+</sup>Foxp3<sup>+</sup> T cells in bronchial-alveolar lavage fluid (BALF). Furthermore, icariin caused a significant reduction in IL-6, IL-17, and TGF- $\beta$  levels in BALF. Also, icariin inhibited Th1 and Th17 cell differentiation and ameliorated EAE [87]. Finally, in mice with dextran sulfate sodium-induced colitis, icariin attenuated disease and inhibited the activation of STAT1 and STAT3, transcription factors of Th1 and Th17, respectively [88].

**4.4. Procyanidins B1, B2, and C1 from Apples.** Apples contain high concentrations of phytochemicals, phenolic compounds, and condensed tannins, including procyanidins B1, B2, and C1 [89]. Procyanidins are members of the proanthocyanidin (or condensed tannins) class of flavonoids. In fact, the most common subclass of proanthocyanidins are procyanidins, which are made of elementary flavan-3-ol (epi)catechin units.

Procyanidin B2 (PCB2) inhibits the production of proinflammatory cytokines in macrophages. PCB2 gallates inhibited the activation and proliferation of T cells after stimulation with anti-CD3 mAb and reduced the production of interferon- (IFN-)  $\gamma$ , IL-12p40, and IL-17 in splenocytes, but not IL-10 production [90]. DBA1/J mice with CIA fed with apple-condensed tannins exhibited a significant delay in the appearance of arthritic symptoms. Apple-condensed tannins reduced the production of the proinflammatory IL-17 and IFN- $\gamma$  cytokines [91].

**4.5. Grape Seed Proanthocyanidins.** Proanthocyanidins are polyphenolic compounds that can be found in the plant physiology of several plant species, mainly concentrated in tree barks and outer skins of seeds. Proanthocyanidins, commonly referred to as condensed tannins, are a class of flavanols, which belong to a larger group of polyphenolic compounds. Grape seed contains many polyphenolic compounds that have potential health-promoting benefits and is one of the richest sources of proanthocyanidins [92].

Grape seed proanthocyanidin extract (GSPE) treatment, in a dose-dependent manner, significantly reduced the severity of CIA and reduced the numbers of IL-17- and TNF- $\alpha$ -producing cells in the arthritic tissue and the spontaneous production of IL-17 and TNF- $\alpha$  by splenocytes. Furthermore, GSPE suppressed osteoclastogenesis *in vitro* in a dose-dependent manner [93]. GSPE from *Vitis vinifera* has potent antiarthritic effects on CIA by modifying the T cell homeostasis. Treg cells, which are important inhibitors of inflammation and mediators of self-tolerance, are deficient in RA. Park et al. showed that grape seed proanthocyanidins induce the development of Foxp3<sup>+</sup> Tregs [94]. GSPE-treated mice had significantly increased CD4<sup>+</sup>CD25<sup>+</sup>Foxp3<sup>+</sup> Tregs *in vivo*. The concomitant suppression of IL-17 production and the enhancement of Foxp3 expression by the GSPE in T cells of joints and splenocytes was associated with alleviation of established CIA. Furthermore, GSPE induced Foxp3<sup>+</sup> Tregs and suppressed IL-17-, IL-21-, and IL-22-producing T cells in human T cell culture, and this was associated with the abrogation of STAT3 [94]. In another study, Ahmad et al. demonstrated that the administration of GSPE in mice with adjuvant-induced arthritis alleviated arthritis, and this was associated with an increase in Foxp3<sup>+</sup> Tregs and decrease in Th17 and Th1 cells in peripheral blood and a decrease in IL-17A, IFN- $\gamma$ , and TNF- $\alpha$  in the arthritic tissue [95].

In other models, proanthocyanidins from the bark of *Metasequoia glyptostroboides* (MGEB) ameliorated allergic contact dermatitis through direct inhibition of T cell activation and Th1/Th17 responses. More specifically, the anti-inflammatory activity of MGEB was evaluated using 2,4-dinitrofluorobenzene- (DNFB-) induced allergic contact dermatitis (ACD) in mice [96]. MGEB inhibited Con A-induced proliferation and the expression of cell surface CD69 and CD25 in T cells *in vitro*. MGEB also significantly decreased the production of Th1/Th17 cytokines (IL-2, IFN- $\gamma$ , and IL-17) in activated T cells.

**4.6. Licorice.** Licorice is the root of *Glycyrrhiza glabra*, a medicinal plant famous for its sweet flavor. The licorice plant

is perennial, native to southern Europe and parts of Asia, such as India. It is known as a potent medicine, effective against peptic ulcer, constipation, cough, and viral infection. The various pharmacological properties of licorice are attributed to triterpene saponins, such as glycyrrhizin, and flavonoids, such as liquiritin, isoliquiritin, and their aglycones. The plant's roots contain significant amounts of phenolic and flavonoid compounds.

Guo et al. showed that two flavonoids isolated from licorice, isoliquiritigenin and naringenin, have the capacity to increase the number of Tregs [97]. They can also promote Treg cell differentiation and enhance Treg cell function. Naringenin can promote Treg cell differentiation, as an aryl hydrocarbon agonist expressed in both Th17 and Treg cells, whereas isoliquiritigenin cannot. Licorice Gly1 promoted Treg differentiation *in vitro* [97]. In addition, licorice decreased the production of IL-2, an inflammatory cytokine produced by Th1 cells that promotes T cell proliferation and survival.

The ability of licorice-related flavonoids to exert anti-inflammatory responses through the inhibition of Th17 cells is well established in other models of autoimmune diseases. Glycyrrhizin, a component of Chinese medicine licorice root, has the ability to inhibit the functions of high-mobility group box 1 (HMGB1). Glycyrrhizin treatment of TNBS-induced murine colitis model decreased the production of proinflammatory mediators HMGB1, IFN- $\gamma$ , IL-6, TNF- $\alpha$ , and IL-17. Furthermore, glycyrrhizin regulated the responses of dendritic cells (DCs) and macrophages and suppressed the proliferation of Th17 cells [98].

Naringenin is a flavanone glycoside found in grapes and citrus fruits (*Citrus paradisi*). The bitter flavor of grapefruit is attributed to this particular flavanone. Two rhamnose units are attached to its aglycon portion, naringenin, at the 7-carbon position. Both naringenin and naringin are strong antioxidants, with naringin being more potent. Both flavonoids block several inflammatory pathways, inhibiting inflammation and reducing oxidative stress [99]. Naringin is moderately soluble in water. Of interest, gut microflora breaks down naringin to its aglycon naringenin, which is then absorbed from the gut. In mice, naringenin reduced inflammatory pain by blocking the NF- $\kappa$ B pathway. It also interferes with enzymatic activity in the intestines and, thus, with the breakdown of certain drugs. Drugs affected by naringin are calcium channel blockers, estrogen, sedatives, medications for high blood pressure, and cholesterol-lowering drugs. No data currently exist on the role of this compound on experimental or human arthritis in relation to Th17/Treg imbalance.

Isoliquiritigenin (ISL) is a flavonoid with a chalcone structure. It shows various biologic properties, including anti-inflammatory and antioxidative actions, as well as vasorelaxant and estrogenic effects. Of relevance, chalcones are considered to be important intermediates in flavonoids' synthesis. Their biological activities include those that are anti-allergic, antiangiogenesis, and antitumor growth. At the cellular level, ISL inhibits various steps of angiogenesis, including VEGF-induced endothelial cell proliferation, tube formation, migration, and aortic ring sprout formation. ISL

suppresses adipose tissue inflammation by affecting the paracrine loop containing saturated fatty acids and TNF- $\alpha$  in cocultures on adipocytes and macrophages [100] through inhibition of NF- $\kappa$ B activation.

Whether ISL exerts any anti-inflammatory effect on RA or experimental arthritis remains unclear. Licochalcone A., derived from *Glycyrrhiza inflata*, reduced the clinical severity of EAE mice and inhibited IFN- $\gamma$ , IL-17, and TNF- $\alpha$  production in peritoneal cells [101].

*Glycine max*, commonly known as soybean in North America or soya bean, is a species of legume native in Asia. Soybean is a valuable and popular crop globally and is used to produce a variety of products such as soy paste, soybean sprouts, soy curd, soy milk, tofu, and oil.

Isoflavones and anthocyanins, both of which are beneficial for human health, are found in soybean. Several major anthocyanins (cyanidin-3-glucoside, delphinidin 3-glucoside, and petunidin 3-glucoside) have been isolated from the seed coat of black soybeans. The effect of soya bean in RA via Th17 inhibition has not been thoroughly studied so far.

**4.7. Anthocyanins.** Anthocyanins are water-soluble members of the flavonoid group, which, depending on their pH, may appear red, purple, or blue. Food plants rich in anthocyanins include the blueberry, raspberry, black rice, and black soybean [102]. Anthocyanin is a representative antioxidant of the flavonoid family found in plants [57].

Black soybean seed coats are an excellent source of anthocyanin. Anthocyanins are synthesized via the phenylpropanoid pathway and can be found in all parts of the plant, including leaves, stems, roots, flowers, and fruits. Anthocyanins are derived from anthocyanidins by adding sugars. Anthocyanins are very unstable compared to other flavonoids, particularly at neutral or alkaline pH. They are detected mainly as unmetabolized glycosides in plasma and in urine, rather than as aglycones.

Anthocyanins can interfere with and inhibit the process of carcinogenesis; thus, they are often described as natural antioxidants. The chemical structure of flavonoids is also important in determining their bioactive properties [103].

Min et al. described the potent antiarthritic activity of anthocyanins from black soybeans *in vivo* [104]. Anthocyanins extracted from black soybeans (AEBS) exerted therapeutic effects in a RA mouse model both *in vivo* and *in vitro* and in humans *in vitro*. AEBS decreased Th17 cells both *in vitro* and *in vivo* and inhibited the expression of proinflammatory cytokines (TNF- $\alpha$ , IL-6, IL-17, IL-21) in mice with CIA by blocking the NF- $\kappa$ B pathway. Finally, osteoclastogenesis was suppressed by AEBS in both DBA/1J mice and human cells *in vitro*.

## 5. Conclusion

In autoimmune arthritis, inflammatory Th17 cells producing IL-17 are inversely associated with anti-inflammatory regulatory T cells (Tregs). Flavonoids encompass various compounds present in traditional medicines, long used as therapeutic agents in autoimmune inflammatory diseases.

The anti-inflammatory properties of flavonoids are increasingly elucidated *in vitro* and in animal models of arthritis, as flavonoids have been shown to inhibit cyclooxygenase, to reduce the production of inflammatory cytokines, to suppress p38 MAPK, to inhibit Th17 cells, and to increase Tregs.

## Abbreviations

ACPA: Anticitrullinated peptide/antigen antibodies  
 CIA: Collagen-induced arthritis  
 GSPE: Grape seed proanthocyanidin extract  
 iTregs: Induced regulatory T cells  
 nTregs: Naturally occurring Tregs  
 RA: Rheumatoid arthritis  
 RF: Rheumatoid factor  
 Th: T helper cells.

## Conflicts of Interest

The authors declare that they have no conflicts of interest.

## Authors' Contributions

Dimitra Kelepouri and Athanasios Mavropoulos have gone through the bibliography and wrote a significant part of the first draft; Dimitrios P. Bogdanos had the original idea and supervised the search of the literature, rewritten the manuscript, and shaped its final version; and Lazaros I. Sakkas has corrected and rewrote a significant part of the manuscript and critically discussed its scientific context. All authors read and approved the final version of the submitted article.

## References

- [1] L. I. Sakkas, P. F. Chen, and C. D. Platsoucas, "T-cell antigen receptors in rheumatoid arthritis," *Immunologic Research*, vol. 13, no. 2-3, pp. 117-138, 1994.
- [2] L. I. Sakkas, N. A. Johanson, C. R. Scanzello, and C. D. Platsoucas, "Interleukin-12 is expressed by infiltrating macrophages and synovial lining cells in rheumatoid arthritis and osteoarthritis," *Cellular Immunology*, vol. 188, no. 2, pp. 105-110, 1998.
- [3] L. I. Sakkas, D. P. Bogdanos, C. Katsiari, and C. D. Platsoucas, "Anti-citrullinated peptides as autoantigens in rheumatoid arthritis—relevance to treatment," *Autoimmunity Reviews*, vol. 13, no. 11, pp. 1114-1120, 2014.
- [4] I. Alexiou, A. Germenis, A. Koutroumpas, A. Kontogianni, K. Theodoridou, and L. I. Sakkas, "Anti-cyclic citrullinated peptide-2 (CCP2) autoantibodies and extra-articular manifestations in Greek patients with rheumatoid arthritis," *Clinical Rheumatology*, vol. 27, no. 4, pp. 511-513, 2008.
- [5] I. Alexiou, A. Germenis, A. Ziogas, K. Theodoridou, and L. I. Sakkas, "Diagnostic value of anti-cyclic citrullinated peptide antibodies in Greek patients with rheumatoid arthritis," *BMC Musculoskeletal Disorders*, vol. 8, no. 1, p. 37, 2007.
- [6] C. Fournier, "Where do T cells stand in rheumatoid arthritis?," *Joint, Bone, Spine*, vol. 72, no. 6, pp. 527-532, 2005.
- [7] K. Schinnerling, J. C. Aguillon, D. Catalan, and L. Soto, "The role of interleukin-6 signalling and its therapeutic blockage in skewing the T cell balance in rheumatoid arthritis," *Clinical & Experimental Immunology*, vol. 189, no. 1, pp. 12-20, 2017.
- [8] O. Aravena, B. Pesce, L. Soto et al., "Anti-TNF therapy in patients with rheumatoid arthritis decreases Th1 and Th17 cell populations and expands IFN- $\gamma$ -producing NK cell and regulatory T cell subsets," *Immunobiology*, vol. 216, no. 12, pp. 1256-1263, 2011.
- [9] G. Azizi, F. Jadidi-Niaragh, and A. Mirshafiey, "Th17 cells in immunopathogenesis and treatment of rheumatoid arthritis," *International Journal of Rheumatic Diseases*, vol. 16, no. 3, pp. 243-253, 2013.
- [10] J. Miao, K. Zhang, M. Lv et al., "Circulating Th17 and Th1 cells expressing CD161 are associated with disease activity in rheumatoid arthritis," *Scandinavian Journal of Rheumatology*, vol. 43, no. 3, pp. 194-201, 2014.
- [11] M. Hashimoto, "Th17 in animal models of rheumatoid arthritis," *Journal of Clinical Medicine*, vol. 6, no. 7, 2017.
- [12] D. S. E. Zaky and E. M. A. El-Nahrery, "Role of interleukin-23 as a biomarker in rheumatoid arthritis patients and its correlation with disease activity," *International Immunopharmacology*, vol. 31, pp. 105-108, 2016.
- [13] R. Kugyelka, Z. Kohl, K. Olasz et al., "Enigma of IL-17 and Th17 cells in rheumatoid arthritis and in autoimmune animal models of arthritis," *Mediators of Inflammation*, vol. 2016, Article ID 6145810, 11 pages, 2016.
- [14] T. Kuwabara, F. Ishikawa, M. Kondo, and T. Kakiuchi, "The role of IL-17 and related cytokines in inflammatory autoimmune diseases," *Mediators of Inflammation*, vol. 2017, Article ID 3908061, 11 pages, 2017.
- [15] J. P. Jacobs, H. J. Wu, C. Benoist, and D. Mathis, "IL-17-producing T cells can augment autoantibody-induced arthritis," *Proceedings of the National Academy of Sciences of the United States of America*, vol. 106, no. 51, pp. 21789-21794, 2009.
- [16] D. M. Roeleveld and M. I. Koenders, "The role of the Th17 cytokines IL-17 and IL-22 in rheumatoid arthritis pathogenesis and developments in cytokine immunotherapy," *Cytokine*, vol. 74, no. 1, pp. 101-107, 2015.
- [17] F. Annunziato, L. Cosmi, V. Santarlasci et al., "Phenotypic and functional features of human Th17 cells," *Journal of Experimental Medicine*, vol. 204, no. 8, pp. 1849-1861, 2007.
- [18] L. Cosmi, R. Cimaz, L. Maggi et al., "Evidence of the transient nature of the Th17 phenotype of CD4+CD161+ T cells in the synovial fluid of patients with juvenile idiopathic arthritis," *Arthritis & Rheumatism*, vol. 63, no. 8, pp. 2504-2515, 2011.
- [19] S. Kotake, T. Yago, T. Kobashigawa, and Y. Nanke, "The plasticity of Th17 cells in the pathogenesis of rheumatoid arthritis," *Journal of Clinical Medicine*, vol. 6, no. 7, 2017.
- [20] K. Nistala and L. R. Wedderburn, "Th17 and regulatory T cells: rebalancing pro- and anti-inflammatory forces in autoimmune arthritis," *Rheumatology*, vol. 48, no. 6, pp. 602-606, 2009.
- [21] T. Morita, Y. Shima, J. B. Wing, S. Sakaguchi, A. Ogata, and A. Kumanogoh, "The proportion of regulatory T cells in patients with rheumatoid arthritis: a meta-analysis," *PLoS One*, vol. 11, no. 9, article e0162306, 2016.
- [22] J. Fessler, A. Felber, C. Duftner, and C. Dejaco, "Therapeutic potential of regulatory T cells in autoimmune disorders," *BioDrugs*, vol. 27, no. 4, pp. 281-291, 2013.
- [23] D. L. Asquith, A. M. Miller, I. B. McInnes, and F. Y. Liew, "Animal models of rheumatoid arthritis," *European Journal of Immunology*, vol. 39, no. 8, pp. 2040-2044, 2009.
- [24] K. K. Keller, L. M. Lindgaard, L. Wogensen et al., "SKG arthritis as a model for evaluating therapies in rheumatoid

- arthritis with special focus on bone changes," *Rheumatology International*, vol. 33, no. 5, pp. 1127–1133, 2013.
- [25] M. Hashimoto, K. Hirota, H. Yoshitomi et al., "Complement drives Th17 cell differentiation and triggers autoimmune arthritis," *Journal of Experimental Medicine*, vol. 207, no. 6, pp. 1135–1143, 2010.
- [26] J. Keffer, L. Probert, H. Cazlaris et al., "Transgenic mice expressing human tumour necrosis factor: a predictive genetic model of arthritis," *The EMBO Journal*, vol. 10, no. 13, pp. 4025–4031, 1991.
- [27] J. J. Inglis, G. Criado, M. Medghalchi et al., "Collagen-induced arthritis in C57BL/6 mice is associated with a robust and sustained T-cell response to type II collagen," *Arthritis Research & Therapy*, vol. 9, no. 5, p. R113, 2007.
- [28] J. J. Inglis, E. Simelyte, F. E. McCann, G. Criado, and R. O. Williams, "Protocol for the induction of arthritis in C57BL/6 mice," *Nature Protocols*, vol. 3, no. 4, pp. 612–618, 2008.
- [29] E. Lubberts, M. I. Koenders, B. Oppers-Walgreen et al., "Treatment with a neutralizing anti-murine interleukin-17 antibody after the onset of collagen-induced arthritis reduces joint inflammation, cartilage destruction, and bone erosion," *Arthritis & Rheumatism*, vol. 50, no. 2, pp. 650–659, 2004.
- [30] Y. Ito, T. Usui, S. Kobayashi et al., "Gamma/delta T cells are the predominant source of interleukin-17 in affected joints in collagen-induced arthritis, but not in rheumatoid arthritis," *Arthritis & Rheumatism*, vol. 60, no. 8, pp. 2294–2303, 2009.
- [31] R. C. Keith, J. L. Powers, E. F. Redente et al., "A novel model of rheumatoid arthritis-associated interstitial lung disease in SKG mice," *Experimental Lung Research*, vol. 38, no. 2, pp. 55–66, 2012.
- [32] H. Jeong, E. K. Bae, H. Kim et al., "Estrogen attenuates the spondyloarthritis manifestations of the SKG arthritis model," *Arthritis Research & Therapy*, vol. 19, no. 1, p. 198, 2017.
- [33] K. Rothe, N. Raulien, G. Kohler, M. Pierer, D. Quandt, and U. Wagner, "Autoimmune arthritis induces paired immunoglobulin-like receptor B expression on CD4<sup>+</sup> T cells from SKG mice," *European Journal of Immunology*, vol. 47, no. 9, pp. 1457–1467, 2017.
- [34] H. Benham, L. M. Rehaume, S. Z. Hasnain et al., "Interleukin-23 mediates the intestinal response to microbial  $\beta$ -1,3-glucan and the development of spondyloarthritis pathology in SKG mice," *Arthritis & Rheumatology*, vol. 66, no. 7, pp. 1755–1767, 2014.
- [35] K. Hirota, M. Hashimoto, H. Yoshitomi et al., "T cell self-reactivity forms a cytokine milieu for spontaneous development of IL-17<sup>+</sup> Th cells that cause autoimmune arthritis," *Journal of Experimental Medicine*, vol. 204, no. 1, pp. 41–47, 2007.
- [36] P. Monach, K. Hattori, H. Huang et al., "The K/BxN mouse model of inflammatory arthritis," *Methods in Molecular Medicine*, vol. 136, pp. 269–282, 2007.
- [37] W. S. Cho, E. Jang, H. Y. Kim, and J. Youn, "Interleukin 17-expressing innate synovial cells drive K/BxN serum-induced arthritis," *Immune Network*, vol. 16, no. 6, pp. 366–372, 2016.
- [38] A. D. Christensen, C. Haase, A. D. Cook, and J. A. Hamilton, "K/BxN serum-transfer arthritis as a model for human inflammatory arthritis," *Frontiers in Immunology*, vol. 7, p. 213, 2016.
- [39] P. Li and E. M. Schwarz, "The TNF- $\alpha$  transgenic mouse model of inflammatory arthritis," *Springer Seminars in Immunopathology*, vol. 25, no. 1, pp. 19–33, 2003.
- [40] D. M. Butler, A. M. Malfait, L. J. Mason et al., "DBA/1 mice expressing the human TNF-alpha transgene develop a severe, erosive arthritis: characterization of the cytokine cascade and cellular composition," *The Journal of Immunology*, vol. 159, pp. 2867–2876, 1997.
- [41] M. Pasparakis, L. Alexopoulou, V. Episkopou, and G. Kollias, "Immune and inflammatory responses in TNF alpha-deficient mice: a critical requirement for TNF alpha in the formation of primary B cell follicles, follicular dendritic cell networks and germinal centers, and in the maturation of the humoral immune response," *Journal of Experimental Medicine*, vol. 184, no. 4, pp. 1397–1411, 1996.
- [42] L. G. Pinto, T. M. Cunha, S. M. Vieira et al., "IL-17 mediates articular hypernociception in antigen-induced arthritis in mice," *Pain*, vol. 148, no. 2, pp. 247–256, 2010.
- [43] K. Zwerina, M. Koenders, A. Hueber et al., "Anti IL-17A therapy inhibits bone loss in TNF- $\alpha$ -mediated murine arthritis by modulation of the T-cell balance," *European Journal of Immunology*, vol. 42, no. 2, pp. 413–423, 2012.
- [44] K. A. Charles, H. Kulbe, R. Soper et al., "The tumor-promoting actions of TNF- $\alpha$  involve TNFR1 and IL-17 in ovarian cancer in mice and humans," *The Journal of Clinical Investigation*, vol. 119, no. 10, pp. 3011–3023, 2009.
- [45] S. Itoh, N. Udagawa, N. Takahashi et al., "A critical role for interleukin-6 family-mediated Stat3 activation in osteoblast differentiation and bone formation," *Bone*, vol. 39, no. 3, pp. 505–512, 2006.
- [46] H. Ogura, M. Murakami, Y. Okuyama et al., "Interleukin-17 promotes autoimmunity by triggering a positive-feedback loop via interleukin-6 induction," *Immunity*, vol. 29, no. 4, pp. 628–636, 2008.
- [47] R. Horai, S. Saijo, H. Tanioka et al., "Development of chronic inflammatory arthropathy resembling rheumatoid arthritis in interleukin 1 receptor antagonist-deficient mice," *Journal of Experimental Medicine*, vol. 191, no. 2, pp. 313–320, 2000.
- [48] M. Kotani, K. Hirata, S. Ogawa et al., "CD28-dependent differentiation into the effector/memory phenotype is essential for induction of arthritis in interleukin-1 receptor antagonist-deficient mice," *Arthritis & Rheumatism*, vol. 54, no. 2, pp. 473–481, 2006.
- [49] M. I. Koenders, I. Devesa, R. J. Marijnissen et al., "Interleukin-1 drives pathogenic Th17 cells during spontaneous arthritis in interleukin-1 receptor antagonist-deficient mice," *Arthritis & Rheumatism*, vol. 58, no. 11, pp. 3461–3470, 2008.
- [50] S. Nakae, S. Saijo, R. Horai, K. Sudo, S. Mori, and Y. Iwakura, "IL-17 production from activated T cells is required for the spontaneous development of destructive arthritis in mice deficient in IL-1 receptor antagonist," *Proceedings of the National Academy of Sciences of the United States of America*, vol. 100, no. 10, pp. 5986–5990, 2003.
- [51] M. Nishihara, H. Ogura, N. Ueda et al., "IL-6-gp130-STAT3 in T cells directs the development of IL-17<sup>+</sup> Th with a minimum effect on that of Treg in the steady state," *International Immunology*, vol. 19, no. 6, pp. 695–702, 2007.
- [52] P. G. Pietta, "Flavonoids as antioxidants," *Journal of Natural Products*, vol. 63, no. 7, pp. 1035–1042, 2000.
- [53] Z. P. Xiao, Z. Y. Peng, M. J. Peng, W. B. Yan, Y. Z. Ouyang, and H. L. Zhu, "Flavonoids health benefits and their

- molecular mechanism," *Mini-Reviews in Medicinal Chemistry*, vol. 11, no. 2, pp. 169–177, 2011.
- [54] D. E. Stevenson, J. M. Cooney, D. J. Jensen et al., "Comparison of enzymically glucuronidated flavonoids with flavonoid aglycones in an in vitro cellular model of oxidative stress protection," *In Vitro Cellular & Developmental Biology - Animal*, vol. 44, no. 3-4, pp. 73–80, 2008.
- [55] G. L. Hostetler, R. A. Ralston, and S. J. Schwartz, "Flavones: food sources, bioavailability, metabolism, and bioactivity," *Advances in Nutrition: An International Review Journal*, vol. 8, no. 3, pp. 423–435, 2017.
- [56] E. Corradini, P. Foglia, P. Giansanti, R. Gubbiotti, R. Samperi, and A. Lagana, "Flavonoids: chemical properties and analytical methodologies of identification and quantitation in foods and plants," *Natural Product Research*, vol. 25, no. 5, pp. 469–495, 2011.
- [57] M. A. Lila, "Anthocyanins and human health: an in vitro investigative approach," *Journal of Biomedicine and Biotechnology*, vol. 2004, no. 5, pp. 306–313, 2004.
- [58] Q. Wang, W. Song, X. Qiao et al., "Simultaneous quantification of 50 bioactive compounds of the traditional Chinese medicine formula Gegen-Qinlian decoction using ultra-high performance liquid chromatography coupled with tandem mass spectrometry," *Journal of Chromatography. A*, vol. 1454, pp. 15–25, 2016.
- [59] Y. Fu, J. Chen, Y. J. Li, Y. F. Zheng, and P. Li, "Antioxidant and anti-inflammatory activities of six flavonoids separated from licorice," *Food Chemistry*, vol. 141, no. 2, pp. 1063–1071, 2013.
- [60] Y. Mao, L. Peng, A. Kang et al., "Influence of Jiegeng on pharmacokinetic properties of flavonoids and saponins in Gancao," *Molecules*, vol. 22, no. 10, 2017.
- [61] H. Hosseinzadeh and M. Nassiri-Asl, "Pharmacological effects of *Glycyrrhiza* spp. and its bioactive constituents: update and review," *Phytotherapy Research*, vol. 29, no. 12, pp. 1868–1886, 2015.
- [62] J. M. Monk, T. Y. Hou, and R. S. Chapkin, "Recent advances in the field of nutritional immunology," *Expert Review of Clinical Immunology*, vol. 7, no. 6, pp. 747–749, 2011.
- [63] A. Salaritabar, B. Darvishi, F. Hadjiakhoondi et al., "Therapeutic potential of flavonoids in inflammatory bowel disease: a comprehensive review," *World Journal of Gastroenterology*, vol. 23, no. 28, pp. 5097–5114, 2017.
- [64] M. Burkard, C. Leischner, U. M. Lauer, C. Busch, S. Venturelli, and J. Frank, "Dietary flavonoids and modulation of natural killer cells: implications in malignant and viral diseases," *The Journal of Nutritional Biochemistry*, vol. 46, pp. 1–12, 2017.
- [65] A. Chu, "Antagonism by bioactive polyphenols against inflammation: a systematic view," *Inflammation & Allergy - Drug Targets*, vol. 13, no. 1, pp. 34–64, 2014.
- [66] Y. Li, J. Yao, C. Han et al., "Quercetin, inflammation and immunity," *Nutrients*, vol. 8, no. 3, p. 167, 2016.
- [67] M. Indra, S. Karyono, R. Ratnawati, and S. G. Malik, "Quercetin suppresses inflammation by reducing ERK1/2 phosphorylation and NF kappa B activation in leptin-induced human umbilical vein endothelial cells (HUVECs)," *BMC Research Notes*, vol. 6, no. 1, p. 275, 2013.
- [68] J. Y. Jhun, S. J. Moon, B. Y. Yoon et al., "Grape seed proanthocyanidin extract-mediated regulation of STAT3 proteins contributes to Treg differentiation and attenuates inflammation in a murine model of obesity-associated arthritis," *PLoS One*, vol. 8, no. 11, article e78843, 2013.
- [69] F. Pérez-Cano, M. Massot-Cladera, M. Rodríguez-Lagunas, and M. Castell, "Flavonoids affect host-microbiota crosstalk through TLR modulation," *Antioxidants*, vol. 3, no. 4, pp. 649–670, 2014.
- [70] A. Smeriglio, A. Calderaro, M. Denaro, G. Lagana, and E. Bellocco, "Effects of isolated isoflavones intake on health," *Current Medicinal Chemistry*, vol. 24, 2017.
- [71] T. Shimizu, N. Shibuya, Y. Narukawa, N. Oshima, N. Hada, and F. Kiuchi, "Synergistic effect of baicalein, wogonin and oroxylin A mixture: multistep inhibition of the NF- $\kappa$ B signaling pathway contributes to an anti-inflammatory effect of Scutellaria root flavonoids," *Journal of Natural Medicines*, vol. 72, no. 1, pp. 181–191, 2018.
- [72] L. Lu, Q. Guo, and L. Zhao, "Overview of oroxylin A: a promising flavonoid compound," *Phytotherapy Research*, vol. 30, no. 11, pp. 1765–1774, 2016.
- [73] Y.-I. Wang, J.-m. Gao, and L.-Z. Xing, "Therapeutic potential of oroxylin A in rheumatoid arthritis," *International Immunopharmacology*, vol. 40, pp. 294–299, 2016.
- [74] J. Y. Lee and W. Park, "Anti-inflammatory effects of oroxylin A on RAW 264.7 mouse macrophages induced with polyinosinic-polycytidylic acid," *Experimental and Therapeutic Medicine*, vol. 12, no. 1, pp. 151–156, 2016.
- [75] M. Ye, Q. Wang, W. Zhang, Z. Li, Y. Wang, and R. Hu, "Oroxylin A exerts anti-inflammatory activity on lipopolysaccharide-induced mouse macrophage via Nrf2/ARE activation," *Biochemistry and Cell Biology*, vol. 92, no. 5, pp. 337–348, 2014.
- [76] Y.-C. Chen, L.-L. Yang, and T. J.-F. Lee, "Oroxylin A inhibition of lipopolysaccharide-induced iNOS and COX-2 gene expression via suppression of nuclear factor- $\kappa$ B activation," *Biochemical Pharmacology*, vol. 59, no. 11, pp. 1445–1457, 2000.
- [77] J. Yang, X. Yang, Y. Chu, and M. Li, "Identification of baicalin as an immunoregulatory compound by controlling T<sub>H</sub>17 cell differentiation," *PLoS One*, vol. 6, no. 2, article e17164, 2011.
- [78] X. Yang, J. Yang, and H. Zou, "Baicalin inhibits IL-17-mediated joint inflammation in murine adjuvant-induced arthritis," *Clinical and Developmental Immunology*, vol. 2013, Article ID 268065, 8 pages, 2013.
- [79] H. Z. Wang, H. H. Wang, S. S. Huang et al., "Inhibitory effect of baicalin on collagen-induced arthritis in rats through the nuclear factor- $\kappa$ B pathway," *The Journal of Pharmacology and Experimental Therapeutics*, vol. 350, no. 2, pp. 435–443, 2014.
- [80] Y. Zhang, X. Li, B. Ciric et al., "Therapeutic effect of baicalin on experimental autoimmune encephalomyelitis is mediated by SOCS3 regulatory pathway," *Scientific Reports*, vol. 5, no. 1, 2015no. 1, article 17407, 2015.
- [81] M. Yimam, M. Pantier, L. Brownell, and Q. Jia, "UP446, analgesic and anti-inflammatory botanical composition," *Pharmacognosy Research*, vol. 5, no. 3, pp. 139–145, 2013.
- [82] H. Ma, X. He, Y. Yang, M. Li, D. Hao, and Z. Jia, "The genus *Epimedium*: an ethnopharmacological and phytochemical review," *Journal of Ethnopharmacology*, vol. 134, no. 3, pp. 519–541, 2011.
- [83] R. Feng, L. Feng, Z. Yuan et al., "Icariin protects against glucocorticoid-induced osteoporosis in vitro and prevents glucocorticoid-induced osteocyte apoptosis in vivo," *Cell Biochemistry and Biophysics*, vol. 67, no. 1, pp. 189–197, 2013.

- [84] L. Chi, W. Gao, X. Shu, and X. Lu, "A natural flavonoid glucoside, icariin, regulates Th17 and alleviates rheumatoid arthritis in a murine model," *Mediators of Inflammation*, vol. 2014, Article ID 392062, 10 pages, 2014.
- [85] B. Liu, C. Xu, X. Wu et al., "Icariin exerts an antidepressant effect in an unpredictable chronic mild stress model of depression in rats and is associated with the regulation of hippocampal neuroinflammation," *Neuroscience*, vol. 294, pp. 193–205, 2015.
- [86] Y. Wei, B. Liu, J. Sun et al., "Regulation of Th17/Treg function contributes to the attenuation of chronic airway inflammation by icariin in ovalbumin-induced murine asthma model," *Immunobiology*, vol. 220, no. 6, pp. 789–797, 2015.
- [87] R. Shen, W. Deng, C. Li, and G. Zeng, "A natural flavonoid glucoside icariin inhibits Th1 and Th17 cell differentiation and ameliorates experimental autoimmune encephalomyelitis," *International Immunopharmacology*, vol. 24, no. 2, pp. 224–231, 2015.
- [88] F. Tao, C. Qian, W. Guo, Q. Luo, Q. Xu, and Y. Sun, "Inhibition of Th1/Th17 responses via suppression of STAT1 and STAT3 activation contributes to the amelioration of murine experimental colitis by a natural flavonoid glucoside icariin," *Biochemical Pharmacology*, vol. 85, no. 6, pp. 798–807, 2013.
- [89] T. Shoji, M. Mutsuga, T. Nakamura, T. Kanda, H. Akiyama, and Y. Goda, "Isolation and structural elucidation of some procyanidins from apple by low-temperature nuclear magnetic resonance," *Journal of Agricultural and Food Chemistry*, vol. 51, no. 13, pp. 3806–3813, 2003.
- [90] S. Tanaka, K. Furuya, K. Yamamoto et al., "Procyanidin B2 gallates inhibit IFN- $\gamma$  and IL-17 production in T cells by suppressing T-bet and ROR $\gamma$ t expression," *International Immunopharmacology*, vol. 44, pp. 87–96, 2017.
- [91] K. Nakamura, H. Matsuoka, S. Nakashima, T. Kanda, T. Nishimaki-Mogami, and H. Akiyama, "Oral administration of apple condensed tannins delays rheumatoid arthritis development in mice via downregulation of T helper 17 (Th17) cell responses," *Molecular Nutrition & Food Research*, vol. 59, no. 7, pp. 1406–1410, 2015.
- [92] Z. Ma and H. Zhang, "Phytochemical constituents, health benefits, and industrial applications of grape seeds: a mini-review," *Antioxidants*, vol. 6, no. 3, 2017.
- [93] M. L. Cho, Y. J. Heo, M. K. Park et al., "Grape seed proanthocyanidin extract (GSPE) attenuates collagen-induced arthritis," *Immunology Letters*, vol. 124, no. 2, pp. 102–110, 2009.
- [94] M. K. Park, J. S. Park, M. L. Cho et al., "Grape seed proanthocyanidin extract (GSPE) differentially regulates Foxp3<sup>+</sup> regulatory and IL-17<sup>+</sup> pathogenic T cell in autoimmune arthritis," *Immunology Letters*, vol. 135, no. 1-2, pp. 50–58, 2011.
- [95] S. F. Ahmad, K. M. A. Zoheir, H. E. Abdel-Hamied et al., "Grape seed proanthocyanidin extract has potent antiarthritic effects on collagen-induced arthritis by modifying the T cell balance," *International Immunopharmacology*, vol. 17, no. 1, pp. 79–87, 2013.
- [96] F. Chen, X. Ye, Y. Yang et al., "Proanthocyanidins from the bark of *Metasequoia glyptostroboides* ameliorate allergic contact dermatitis through directly inhibiting T cells activation and Th1/Th17 responses," *Phytomedicine*, vol. 22, no. 4, pp. 510–515, 2015.
- [97] A. Guo, D. He, H.-B. Xu, C.-A. Geng, and J. Zhao, "Promotion of regulatory T cell induction by immunomodulatory herbal medicine licorice and its two constituents," *Scientific Reports*, vol. 5, no. 1, article 14046, 2015.
- [98] X. Chen, D. Fang, L. Li et al., "Glycyrrhizin ameliorates experimental colitis through attenuating interleukin-17-producing T cell responses via regulating antigen-presenting cells," *Immunologic Research*, vol. 65, no. 3, pp. 666–680, 2017.
- [99] M. A. Alam, N. Subhan, M. M. Rahman, S. J. Uddin, H. M. Reza, and S. D. Sarker, "Effect of citrus flavonoids, naringin and naringenin, on metabolic syndrome and their mechanisms of action," *Advances in Nutrition: An International Review Journal*, vol. 5, no. 4, pp. 404–417, 2014.
- [100] Y. Watanabe, Y. Nagai, H. Honda et al., "Isoliquiritigenin attenuates adipose tissue inflammation *in vitro* and adipose tissue fibrosis through inhibition of innate immune responses in mice," *Scientific Reports*, vol. 6, no. 1, article 23097, 2016.
- [101] L. B. A. Fontes, D. dos Santos Dias, L. S. A. de Carvalho et al., "Immunomodulatory effects of licochalcone A on experimental autoimmune encephalomyelitis," *Journal of Pharmacy and Pharmacology*, vol. 66, no. 6, pp. 886–894, 2014.
- [102] D. Esposito, A. Chen, M. H. Grace, S. Komarnytsky, and M. A. Lila, "Inhibitory effects of wild blueberry anthocyanins and other flavonoids on biomarkers of acute and chronic inflammation *in vitro*," *Journal of Agricultural and Food Chemistry*, vol. 62, no. 29, pp. 7022–7028, 2014.
- [103] A. Smeriglio, D. Barreca, E. Bellocco, and D. Trombetta, "Chemistry, pharmacology and health benefits of anthocyanins," *Phytotherapy Research*, vol. 30, no. 8, pp. 1265–1286, 2016.
- [104] H. K. Min, S. M. Kim, S. Y. Baek et al., "Anthocyanin extracted from black soybean seed coats prevents autoimmune arthritis by suppressing the development of Th17 cells and synthesis of proinflammatory cytokines by such cells, via inhibition of NF- $\kappa$ B," *PLoS One*, vol. 10, no. 11, article e0138201, 2015.
- [105] A. Mussener, M. J. Litton, E. Lindroos, and L. Klareskog, "Cytokine production in synovial tissue of mice with collagen-induced arthritis (CIA)," *Clinical & Experimental Immunology*, vol. 107, no. 3, pp. 485–493, 1997.

## Research Article

# Therapeutic Potential of Pien Tze Huang on Experimental Autoimmune Encephalomyelitis Rat

Xuemei Qiu,<sup>1,2</sup> Hui Luo ,<sup>1,2</sup> Xue Liu,<sup>1,2</sup> Qingqing Guo ,<sup>1,3</sup> Kang Zheng ,<sup>1,3</sup> Danping Fan,<sup>1</sup> Jiawen Shen,<sup>1,2</sup> Cheng Lu ,<sup>1</sup> Xiaojuan He ,<sup>1,3</sup> Ge Zhang ,<sup>3</sup> and Aiping Lu <sup>3</sup>

<sup>1</sup>Institute of Basic Research in Clinical Medicine, China Academy of Chinese Medical Sciences, Beijing 100700, China

<sup>2</sup>School of Life Science and Engineering, Southwest Jiaotong University, Chengdu 611756, China

<sup>3</sup>Law Sau Fai Institute for Advancing Translational Medicine in Bone & Joint Diseases, School of Chinese Medicine, Hong Kong Baptist University, Kowloon Tong, Hong Kong

Correspondence should be addressed to Xiaojuan He; hxj19@126.com, Ge Zhang; zhangge@hkbu.edu.hk, and Aiping Lu; aipinglu@hkbu.edu.hk

Received 8 September 2017; Accepted 31 December 2017; Published 27 February 2018

Academic Editor: Lifei Hou

Copyright © 2018 Xuemei Qiu et al. This is an open access article distributed under the Creative Commons Attribution License, which permits unrestricted use, distribution, and reproduction in any medium, provided the original work is properly cited.

Multiple sclerosis (MS) is a chronic inflammatory demyelinating disease of the central nervous system (CNS). There is still lack of commercially viable treatment currently. Pien Tze Huang (PZH), a traditional Chinese medicine, has been proved to have anti-inflammatory, neuroprotective, and immunoregulatory effects. This study investigated the possible therapeutic effects of PZH on experimental autoimmune encephalomyelitis (EAE) rats, a classic animal model of MS. Male Lewis rats were immunized with myelin basic protein (MBP) peptide to establish an EAE model and then treated with three doses of PZH. Clinical symptoms, organ coefficient, histopathological features, levels of proinflammatory cytokines, and chemokines as well as MBP and Olig2 were analyzed. The results indicated that PZH ameliorated the clinical severity of EAE rats. It also remarkably reduced inflammatory cell infiltration in the CNS of EAE rats. Furthermore, the levels of IL-17A, IL-23, CCL3, and CCL5 in serum and the CNS were significantly decreased; the p-P65 and p-STAT3 levels were also downregulated in the CNS, while MBP and Olig2 in the CNS of EAE rats had a distinct improvement after PZH treatment. In addition, PZH has no obvious toxicity at the concentration of 0.486 g/kg/d. This study demonstrated that PZH could be used to treat MS.

## 1. Introduction

Multiple sclerosis (MS) is the most frequent chronic inflammatory autoimmune neurodegenerative disorder of the central nervous system (CNS) with the hallmarks of focal demyelination and inflammatory cell infiltration in the brain and the spinal cord [1]. It is a debilitating disease with high disability and recurrence rates, endangering over one million people worldwide [2]. The etiology and pathogenesis of MS are still complicated and elusive [3]. Cytokines play essential roles in mediating and regulating the inflammatory response in the CNS during MS. A key player is interleukin- (IL-) 17 which was thought to modulate neuroinflammatory and demyelinating process [4, 5]. Suppression of IL-17 signaling could alleviate EAE [6]. In addition, increasing evidence

demonstrates that IL-23 induces IL-17 expression and allow the crucial role of the IL-23/IL17 pathway in MS to be recognized [7, 8]. Besides proinflammatory cytokines, some chemokines also play important roles in inflammatory process by mediating immune cells trafficking across the blood-brain barrier and modulating their transfer to lesion sites [9].

At present, the treatment of MS is limited to chemically synthesized drugs and several biological reagents, such as IFN- $\beta$ , glatiramer acetate, and natalizumab [10], which are not always effective and are often associated with severe side effects [11]. Thus, the identification of more effective and safe agents is urgently required.

Pien Tze Huang (PZH), a well-known traditional Chinese formulation, has been widely used in various inflammatory

diseases. Its main ingredients such as musk, calculus bovis (Niu Huang or ox's gallstone), Shedan (snake's gall), and *Notoginseng Radix et Rhizoma* (Tianqi or Sanqi) have been shown to exert anti-inflammatory, immunoregulatory, and neuroprotective functions [12–14]. Emerging evidences demonstrated that PZH could affect the expression of several inflammation-related factors. It showed a regulatory effect on NF- $\kappa$ B which is closely related to the expression of inflammatory factors [15]. And it could also inhibit STAT3 signaling which plays important roles in the pathogenesis of MS/EAE [16, 17]. Moreover, recent studies showed that ginsenoside Rg1 and Rd, the main active ingredients in *Notoginseng Radix et Rhizoma*, exerted a good effect on the EAE model [18, 19].

Considering these findings, we hypothesized that PZH might be used for MS treatment. Experimental autoimmune encephalomyelitis (EAE) is the most commonly used experimental model for MS. Guinea pig myelin basic protein- (MBP-) induced EAE in rats showed severe CNS inflammation, which is usually used for the study of acute CNS inflammation [20, 21]. Therefore, in the present study, we used the EAE rat model to investigate the potential therapeutic effects of PZH on MS. An earlier version of this work was presented as an abstract at the 15th Meeting of the Consortium for Globalization of Chinese Medicine (CGCM), 2016. We further investigated the therapeutic effects and explore the action mechanism of PZH on EAE rat in the present study.

## 2. Materials and Methods

**2.1. Animals.** Male Lewis rats (8–10 weeks old) weighing between 250 g and 300 g used in this study were purchased from Beijing Vital River Laboratories (Beijing, China). They were housed in a room maintained at a 12-hour light/dark cycle (temperature 22–25°C and relative humidity 40–60%). All rats had access to food pellets and filtered water ad libitum and were given one week to adapt to the new environment. All protocols used here received approval from the Ethical Animal Care and Use Committee in China Academy of Chinese Medical Sciences and Hong Kong Baptist University.

**2.2. Induction of EAE.** An active EAE model was established following a published protocol [22]. Male Lewis rats were inoculated subcutaneously (sc) in the pad of the left hind paw with 100  $\mu$ L antigenic emulsion containing equal volumes of saline with 20  $\mu$ g of guinea pig myelin basic protein (MBP) (Sigma-Aldrich, St. Louis, MO) and complete Freund's adjuvant (CFA) (Chondrex, Redmond, WA, USA) with *Mycobacterium tuberculosis* (2 mg/mL). Daily weight was recorded, and clinical signs were evaluated, using the following 5-grade scale [23]: 0, no clinical signs; 1, limp tail; 2, hind leg weakness; 3, paraplegia and incontinence; 4, quadriplegia; and 5, moribundity or death.

**2.3. Treatment.** Pien Tze Huang (PZH) was produced by Zhangzhou Pien Tze Huang Pharmaceutical Co. Ltd. (Zhangzhou, China; FDA approval no. Z35020243). Stock

solution of PZH was prepared by dissolving the PZH powder in saline, and the sample was fully blended again prior to use. Six groups were set up including the normal group, model group, prednisone acetate (PA) group (5 mg/kg/d), PZH low dose (PZH-L) group (0.054 g/kg/d), PZH middle dose (PZH-M) group (0.162 g/kg/d, equal to the clinical dose), and PZH high dose (PZH-H) group (0.486 g/kg/d). Rats for the drug groups were given daily different drugs for three weeks from day 10 (at the disease onset) after immunization, while the same volume of normal saline was given to rats for normal and model groups daily. All agents were intragastrically administered in a volume of 1 mL/100 g. After treatment, the heart, liver, spleen, lungs, and kidneys were removed and weighed for organ coefficients after washing off the blood. The sera were collected for ELISA analysis and blood biochemical determination. The whole brain and spinal cord were separated for hematoxylin-eosin (H&E) and immunohistochemical (IHC) analysis.

**2.4. Histopathology.** The brain and spinal cord were dissected after fixed in 10% neutral formalin for 48 h and embedded in paraffin after being embathed successively with different gradient ethanol and xylene. The paraffin sections of 6  $\mu$ m thick were obtained for H&E staining. The sections were observed with a LEICA DFC300 FX (Leica Microsystems Ltd.).

**2.5. Immunohistochemistry.** The sections (6  $\mu$ m thick) were dewaxed and hydrated by xylene and a graded series of alcohols after being incubated at 60°C for one hour. Heat-induced epitope retrieval was done in sodium citrate buffer. The activity of endogenous peroxidase was quenched with 3% hydrogen peroxide ( $H_2O_2$ ). Sections were firstly incubated with antibodies against IL-17 (dilution 1:1500, Bioss, Beijing, China), IL-23 (dilution 1:1000, Bioss, Beijing, China), CCL3 (dilution 1:1000, Bioss, Beijing, China), CCL5 (dilution 1:1000, Santa Cruz Biotechnology, Dallas, Texas, USA), NF- $\kappa$ B p65 (phospho S276) (dilution 1:1000, Abcam, Cambridge, UK), p-STAT3 (dilution 1:50, Cell Signaling Technology, Danvers, MA, USA), oligodendrocyte transcription factor (Olig2) (rabbit monoclonal antibody, dilution 1:200, Abcam, Cambridge, UK, 1:1000), or MBP (rabbit monoclonal antibody, dilution 1:1000, Cell Signaling Technology Inc., Danvers, MA, USA) overnight at 4°C, followed by incubation with Signal Stain<sup>®</sup> Boost IHC Detection Reagent (HRP, Rabbit) (Cell Signaling Technology, Danvers, MA, USA) according to the instructions from the manufacturers. The final color was detected using DAB Kit (ZSGB-BIO, Beijing, China) according to the manufacturer's instructions and counterstained with hematoxylin (Leagene, Beijing, China). PBS buffer was used instead of primary antibody as negative control. Images were captured at  $\times 200$  magnification by a LEICA DM6000B with a LEICA DFC300 FX (Leica Microsystems Ltd., Solms, Germany). Integral optical density (IOD) values of each image were calculated with an "Image-Pro Plus 6.0" software (Media Cybernetics, Rockville, MD, USA) [24].

**2.6. ELISA.** Commercial kits for IL-17A (eBioscience, San Diego, CA, USA), IL-23 (eBioscience, San Diego, CA,



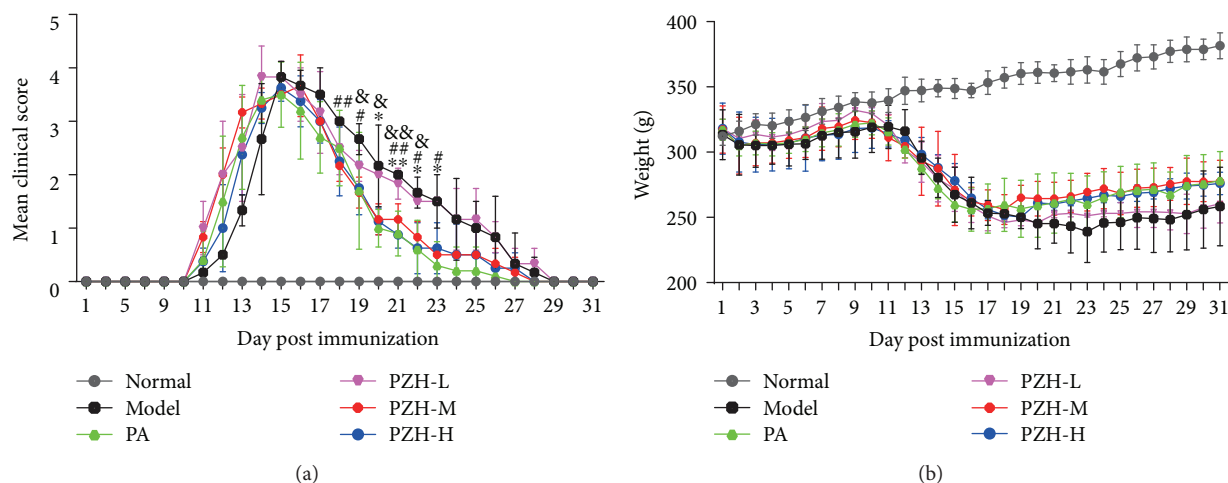


FIGURE 1: PZH ameliorated clinical symptoms of EAE rats. (a) Time course changes of the mean clinical score in rats from the respective group. (b) Time course changes of body weight in rats from the respective group. Results are shown as mean  $\pm$  SD. \* $P < 0.05$  and \*\* $P < 0.01$ ; PA group versus model group. # $P < 0.05$  and ## $P < 0.01$ ; PZH-M group versus model group. & $P < 0.05$  and && $P < 0.01$ ; PZH-H group versus model group.

USA), CCL3 (USCN LIFE, Wuhan, China), and CCL5 (USCN LIFE, Wuhan, China) were used for measuring the concentration of cytokines in the serum of rats. The assays were performed following the manufacturer's protocol.

**2.7. Blood Biochemical Determination.** For the detection of hematological biochemical parameters, alanine aminotransferase (ALT), aspartate aminotransferase (AST), creatinine (CREA), and UREA nitrogen (UREA) were tested with blood biochemical commercial kits by a Japan's Hitachi 7160 automatic biochemical analyzer.

**2.8. Statistical Analysis.** Statistical analyses were performed by using SPSS 18.0 software. The experimental values were presented as the means  $\pm$  SD. Comparisons of numerical data between the two groups were performed by Student's *t*-tests. Differences in the mean values of various groups were analyzed by using ANOVA. The *p* value  $< 0.05$  was considered significant.

### 3. Results

**3.1. PZH Ameliorated Clinical Symptoms of EAE Rats.** To examine the effect of PZH on an acute EAE model, PZH was orally administered to rats daily on day 10 post immunization. As shown in Figure 1(a), PZH effectively reduced the clinical score in remission phase, especially in the PZH-M and PZH-H groups. In addition, PZH slightly increased body weight compared with the model group, although there was no significant difference between the PZH group and the model group (Figure 1(b)). Interestingly, PZH exerted a similar effect to PA in terms of ameliorating clinical symptoms and increasing body weight, and there was no significant difference between the two groups.

**3.2. PZH Ameliorated CNS Inflammation in EAE Rats.** To explore the anti-inflammatory effect of PZH in EAE rats,

we observed the inflammation changes in different parts of the CNS including the brain, brainstem, and spinal cord by H&E staining. As shown in Figure 2, compared with the normal group, the model group showed significant vascular cuff-like changes and diffused inflammatory cell infiltration among the above three tissues. PZH treatment can dramatically reduce the degree of inflammatory lesions in the brain, brainstem, and spinal cord, which was a coincidence with the PA treatment.

**3.3. PZH Reduced Proinflammatory Cytokine and Chemokine Production in the CNS of EAE Rats.** Proinflammatory cytokines such as IL-23/IL-17 axis and chemokines play important roles in MS inflammation progression. To further investigate the anti-inflammatory effect of PZH in EAE rats, we therefore detected IL-17A, IL-23, CCL3, and CCL5 levels in the spinal cord of EAE rats. As shown in Figure 3, compared with the normal group, the levels of IL-17A, IL-23, CCL3, and CCL5 in the spinal cord of EAE rats were remarkably increased. PZH-M and PZH-H treatment could significantly decrease the levels of these factors.

**3.4. PZH Decreased Proinflammatory Cytokine and Chemokine Expression in Serum of EAE Rats.** To observe whether the levels of IL-17A, IL-23, CCL3, and CCL5 in the serum of EAE rats had also changed, we performed ELISA analysis. As shown in Figure 4, the levels of IL-17A, IL-23, CCL3, and CCL5 were significantly increased in the model group compared with the normal group, whereas PZH could remarkably decrease these proinflammatory cytokine and chemokine levels in the serum of EAE rats, especially in the PZH-M and PZH-H groups.

**3.5. PZH Downregulated NF- $\kappa$ B and STAT3 in CNS of EAE Rats.** To further investigate the anti-inflammatory mechanism of PZH, we detected the levels of p-P65 and p-STAT3 in the spinal cord of EAE rats by immunohistochemistry.

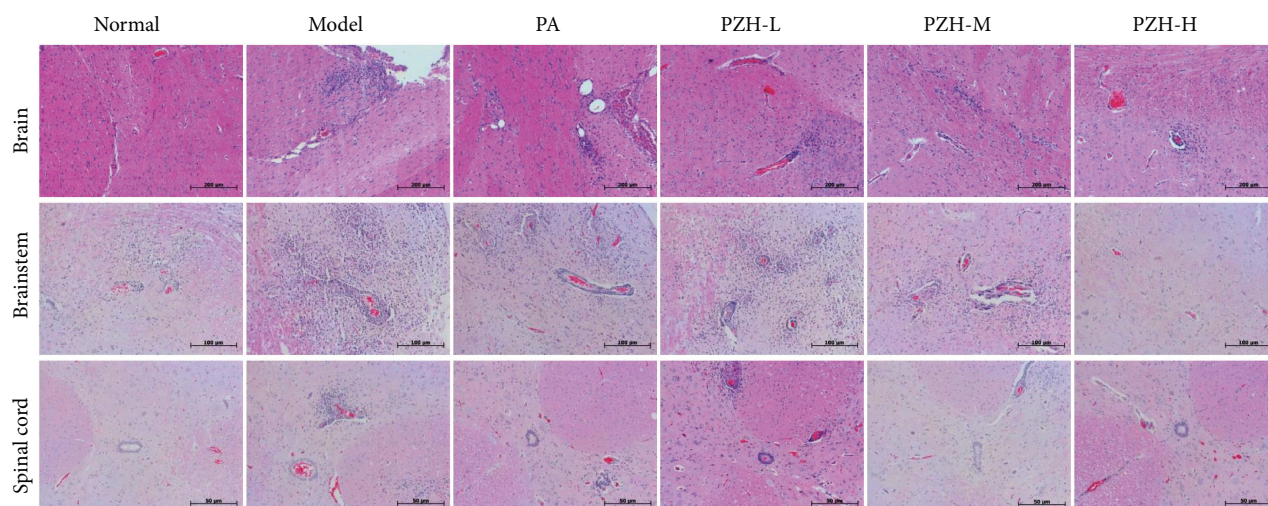


FIGURE 2: PZH ameliorated CNS inflammation in EAE rats. Rats were sacrificed at day 31, and the brain, brainstem, and spinal cord were harvested. Inflammation of the brain, brainstem, and spinal cord was analyzed by H&E staining.

The results in Figure 5 showed that p-P65 and p-STAT3 levels were remarkably increased compared with those in normal rats. PZH treatment could significantly decrease their levels, in particular of the PZH-M and PZH-H groups.

**3.6. PZH Increased the Expression of Olig2 and MBP in EAE Rats.** Because demyelination plays a crucial role in the course of disease, we wonder whether PZH has the potential in inhibiting demyelination. We then detected the levels of Olig2 and MBP in the CNS of EAE rats, two important proteins in the process of myelination of nerves. As shown in Figure 6, while the levels of Olig2 and MBP in the brain were significantly decreased in the model group compared with the normal group, PZH treatment could remarkably increase the Olig2 and MBP levels. It is worth noting that PZH may have a better effect than PA.

**3.7. PZH Had No Significant Toxicity in EAE Rats.** To investigate whether PZH had toxicity in EAE rats, organ coefficients as well as hepatotoxicity and nephrotoxicity were detected. As shown in Figure 7(a), organ coefficients of the heart, liver, spleen, lung, and kidney in the PZH group have no significant difference compared with the normal group. Further, as shown in Figures 7(b)–7(d), PZH treatment did not significantly change the levels of ALT and AST. Moreover, the levels of CREA and UREA in the PZH group had no obvious change either.

## 4. Discussion

MS is the prototypical inflammatory demyelinating disease of the CNS. EAE is regarded as a good model for studying MS mechanisms and developing drugs [25, 26]. It can be induced in a multitude of species and strains [20]. Rats of the inbred Lewis strain are commonly used due to its high susceptibility to EAE [27]. Lewis rats develop a monophasic EAE disease course associated with an acute onset and a spontaneous recovery, which bears resemblance to the

relapse of clinical signs seen in MS. This allows the investigation of one complete episode of symptom exacerbation and remission and therefore makes this animal model a frequently utilized tool for investigating immunological and pathological characteristics of MS [28, 29]. In this study, the disease in rats became clinically evident on day 10 after immunization, and neurological signs peak on day 15 followed by complete recovery by day 28, which was consistent with previous reports [30]. According to our data, PZH effectively reduced the clinical score on remission phase in EAE rats. Moreover, it remarkably inhibited the vascular cuff-like changes and diffused inflammatory cell infiltration in the brain, brainstem, and spinal cord. Collectively, PZH exerted an obvious therapeutic effect on EAE rats.

The IL-23/IL-17 axis performs important functions in MS pathogenesis. IL-23 is predominantly secreted from activated macrophages/microglia and dendritic cells [31], driving polarization of Th17 cells, which is characterized by the production of IL-17, IL-6, and tumor necrosis factor [32]. This type of shift facilitates CNS inflammation and the development of EAE. Consistent with this, IL-23 and IL-17 in the serum and CNS have been reported to serve an important role in the pathology and immunotherapy of MS [33]. In the present study, we found that PZH effectively reduced the levels of IL-17A and IL-23 in the serum and CNS of EAE rats. Furthermore, chemokines such as CCL3 and CCL5, which are already identified to be involved in MS and EAE, are responsible for the recruitment of leukocytes to the sites of inflammation [34, 35]. In the present study, our data firstly showed that PZH significantly decreased the levels of CCL3 and CCL5 in the serum and CNS of EAE rats, suggesting that PZH may prevent inflammatory cell recruitment so as to alleviate the CNS inflammation.

In order to further explore the action mechanism of PZH remitting CNS inflammation, we detected the levels of p-STAT3 and p-P65 in the CNS of EAE rats by immunohistochemistry. As reported in previous literatures,

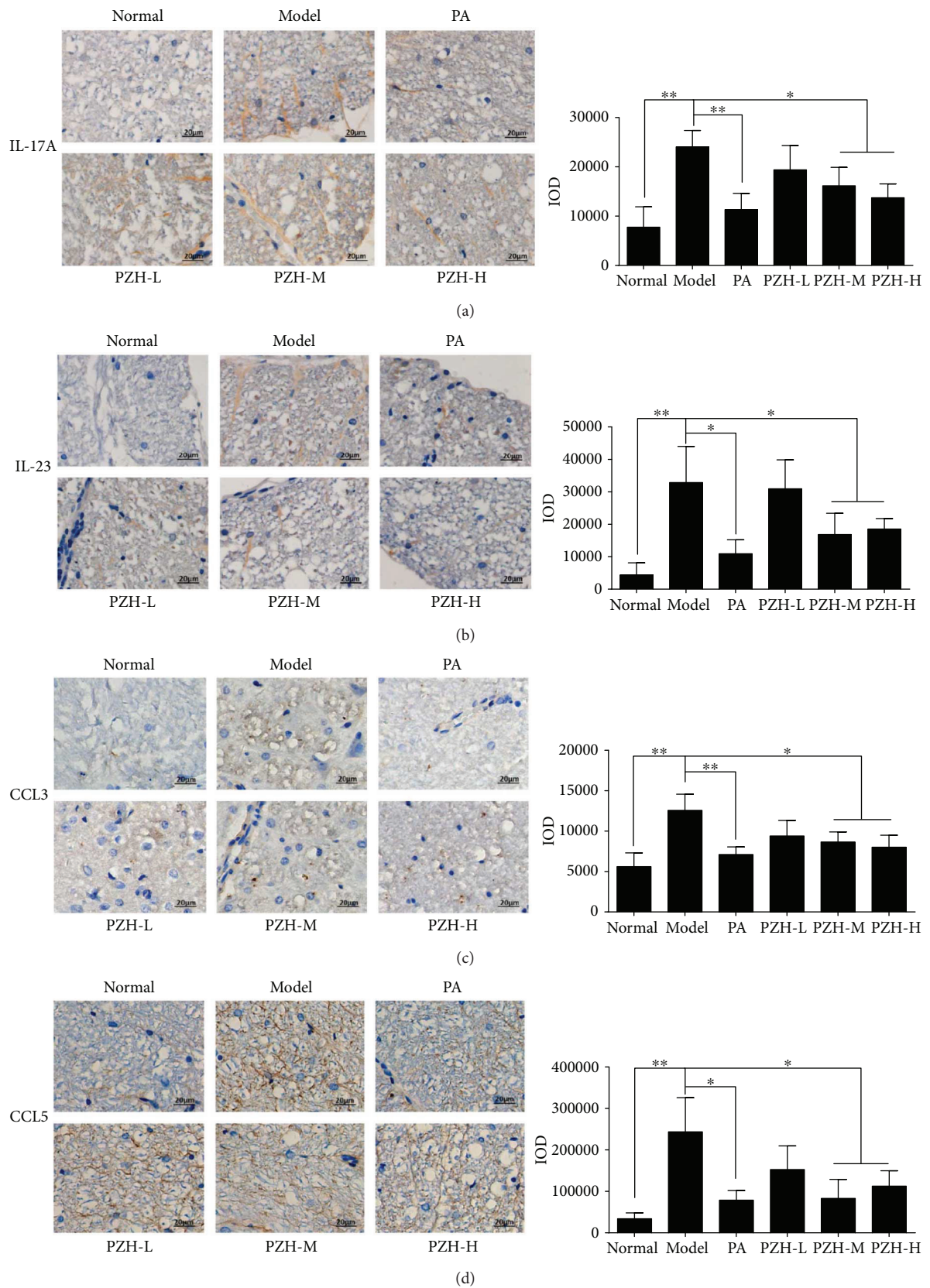


FIGURE 3: PZH decreased the levels of IL-23, IL-17A, CCL3, and CCL5 in the CNS of EAE rats. Representative immunohistochemistry images (left) and IOD means (right) of IL-23 (a), IL-17A (b), CCL3 (c), and CCL5 (d) in the spinal cord of rats from each group. Original magnification 200x. All data were shown as the mean  $\pm$  SD. \* $P < 0.05$  and \*\* $P < 0.01$ .

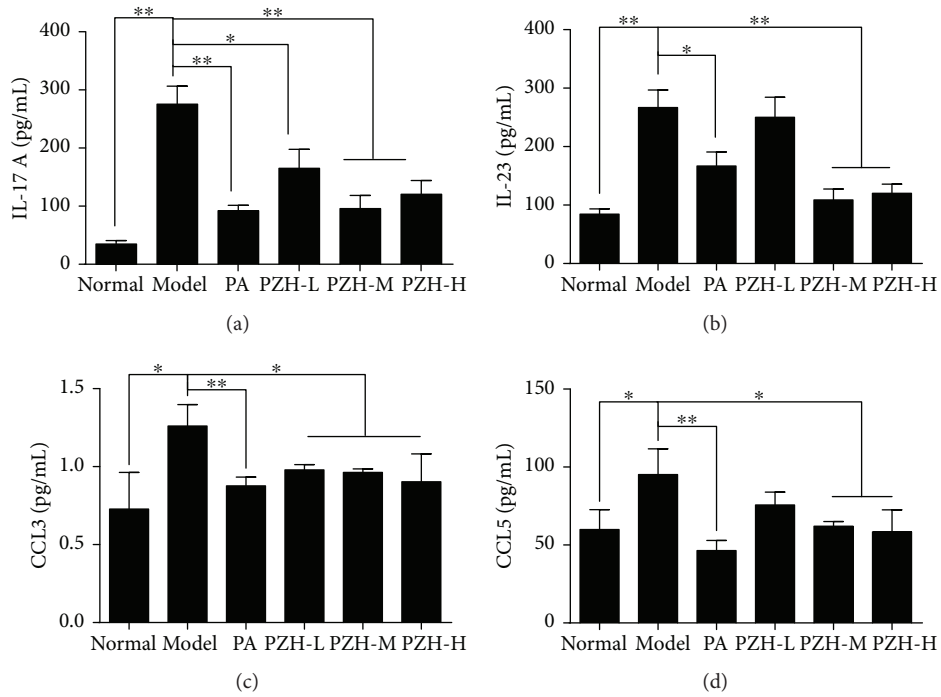


FIGURE 4: PZH reduced proinflammatory cytokine and chemokine expression in serum of EAE rats. Rats were sacrificed, and the serum was collected for ELISA analysis. The levels of IL-17A (a), IL-23 (b), CCL3 (c), and CCL5 (d) were shown, respectively. Data are shown as the mean  $\pm$  SD. \*  $P < 0.05$  and \*\*  $P < 0.01$ .

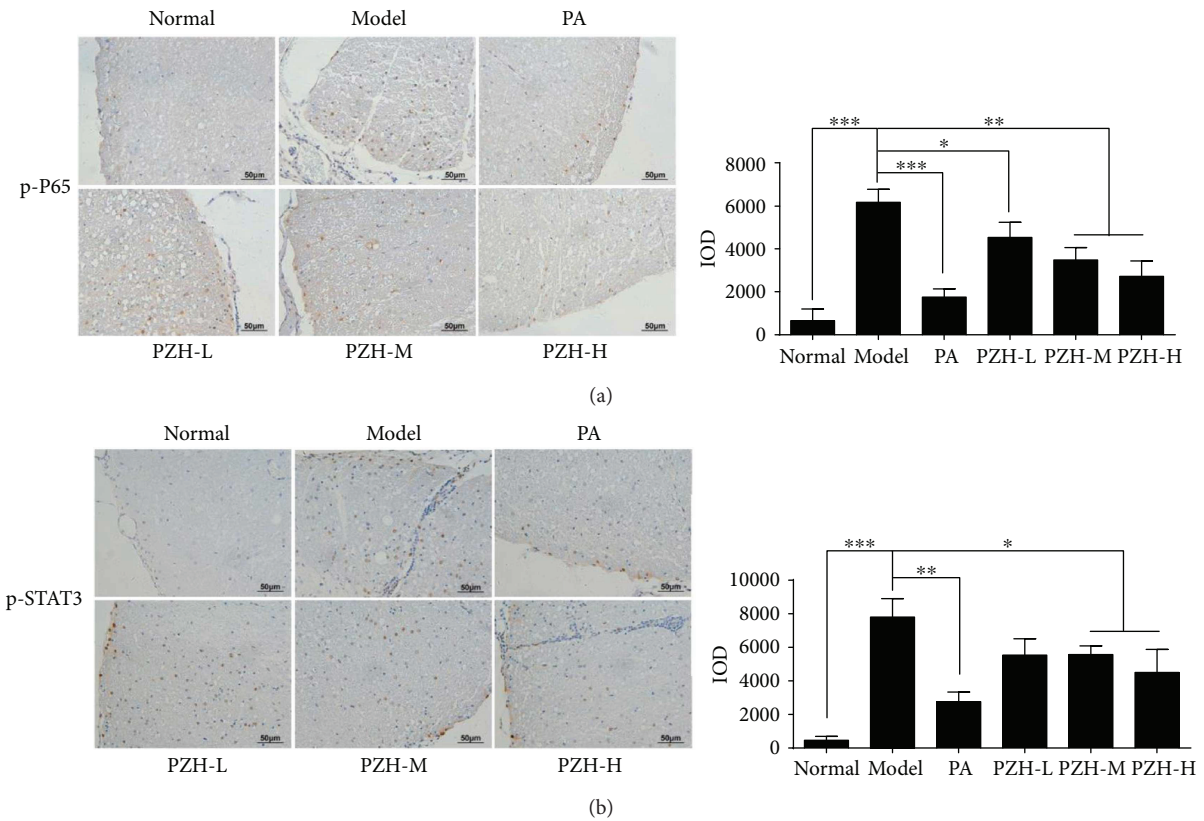


FIGURE 5: PZH downregulated the levels of p-P65 and p-STAT3 in the CNS of EAE rats. Representative immunohistochemistry images (left) and IOD means (right) of p-P65 (a) and p-STAT3 (b) in the spinal cord of rats from each group. Original magnification 200x. All data were shown as the mean  $\pm$  SD. \*  $P < 0.05$ , \*\*  $P < 0.01$ , and \*\*\*  $P < 0.001$ .

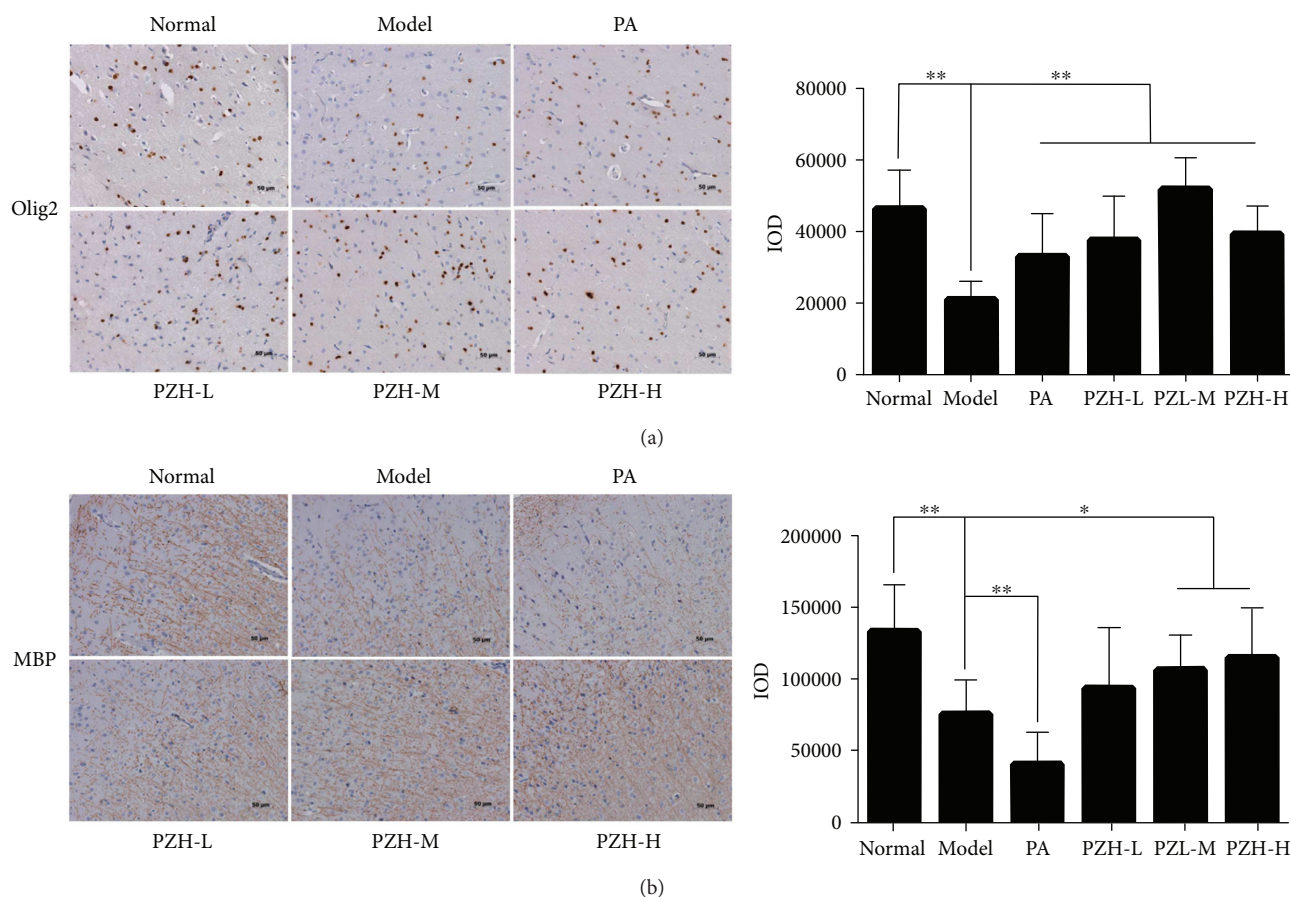


FIGURE 6: PZH increased the expression of Olig2 and MBP in EAE rats. Representative immunohistochemistry images (left) and IOD means (right) of Olig2 (a) and MBP (b) in the brain of rats from each group. Original magnification 200x. All data were shown as the mean  $\pm$  SD. \* $P < 0.05$  and \*\* $P < 0.01$ .

STAT3 signaling and NF- $\kappa$ B signaling are both proinflammatory pathways that can facilitate the expression of cytokines and chemokines [36, 37]. The severity of EAE can be alleviated by inhibiting the phosphorylation of STAT3 and/or NF- $\kappa$ B [38, 39]. In addition, PZH was reported to suppress STAT3 signaling and NF- $\kappa$ B signaling in other diseases [15, 16]. Similarly, we proved that PZH could also modulate these two pathways in EAE rats. To be more specific, the levels of p-STAT3 and p-P65 in the CNS of EAE rats were significantly reduced by PZH. Thus, it can be concluded that PZH inhibits the CNS inflammation in EAE rats through downregulating the STAT3 pathway and NF- $\kappa$ B pathway.

Besides the inflammation in the CNS, demyelination is also the typical characteristics in MS. Interestingly, several studies have indicated that PZH had a neuroprotective effect [40, 41], which makes us speculate whether it also exerts the similar effect in EAE rats. Unfortunately, due to the slight demyelination in an MBP-induced rat model [20], we did not find marked remyelination in PZH-treated EAE rats (data not shown). Therefore, we further detected the changes of MBP and Olig2, two important indicators to the detection of myelin loss and regeneration, in PZH-treated EAE rats. MBP, the second most abundant protein in the central nervous system myelin, is important in the process of

myelination of nerves and has already been used as the index of active demyelination [42, 43]. Olig2, restrictedly expressed in the CNS, is well known for promoting oligodendrocyte differentiation [44, 45]. Increasing evidence showed that inducible expression of Olig2 could enhance myelination and remyelination in the CNS [46]. In the present study, we indicated that PZH treatment obviously promoted the expression of MBP and Olig2 in the CNS of EAE rats, implying that PZH could facilitate the remyelination. Certainly, more EAE animal models with typical demyelination should be used to further confirm PZH's function in neural repair.

It is well known that drug safety is a key point to discover and develop new drugs, and drug safety plays a decisive role in the application of a certain drug [47]. Taking this into account, we evaluated the safety of PZH in the treatment of EAE rats. Organ coefficient is a nonspecific indicator, which can reflect the toxic effects on a target organ [48, 49]. In the present study, we found that PZH treatment did not change the organ coefficient of the heart, liver, spleen, lung, and kidney. To further confirm the safety of PZH, the levels of functional indicators of ALT and AST for the liver as well as CREA and UREA for the kidney were detected in the serum of EAE rats. Consistent with the results of organ

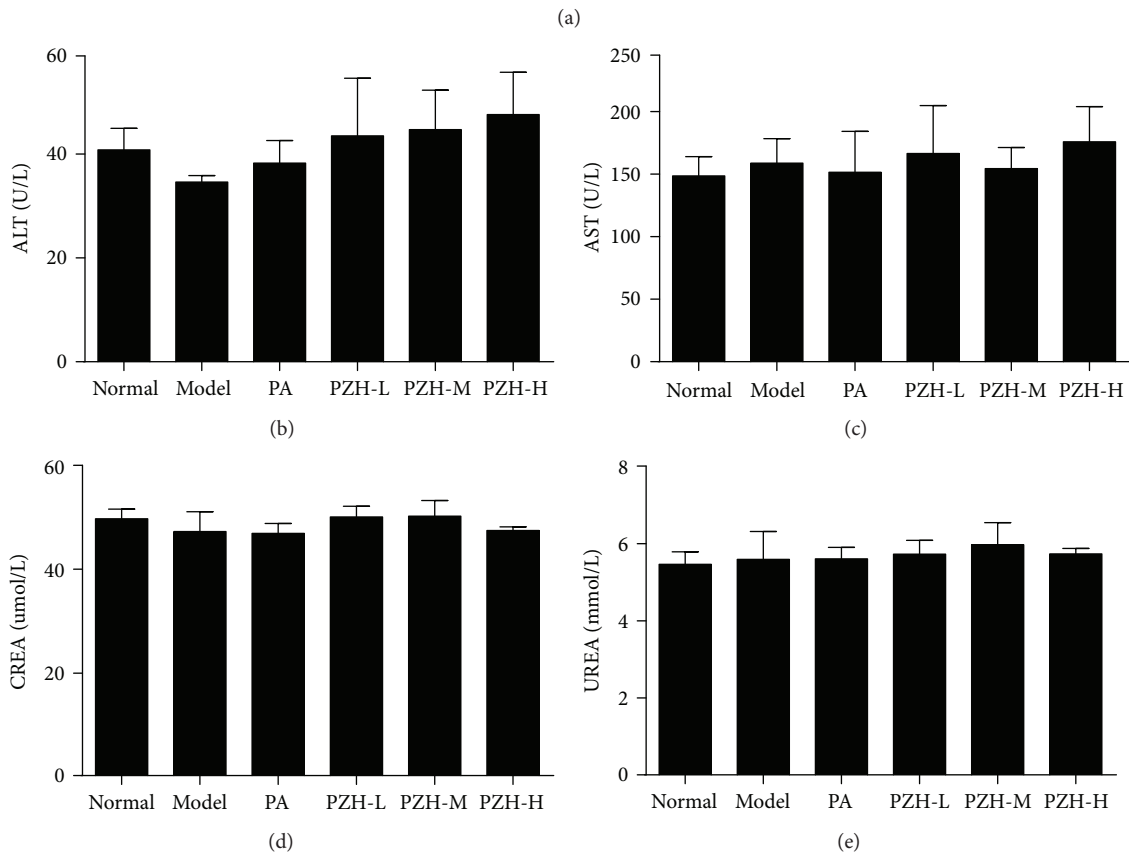
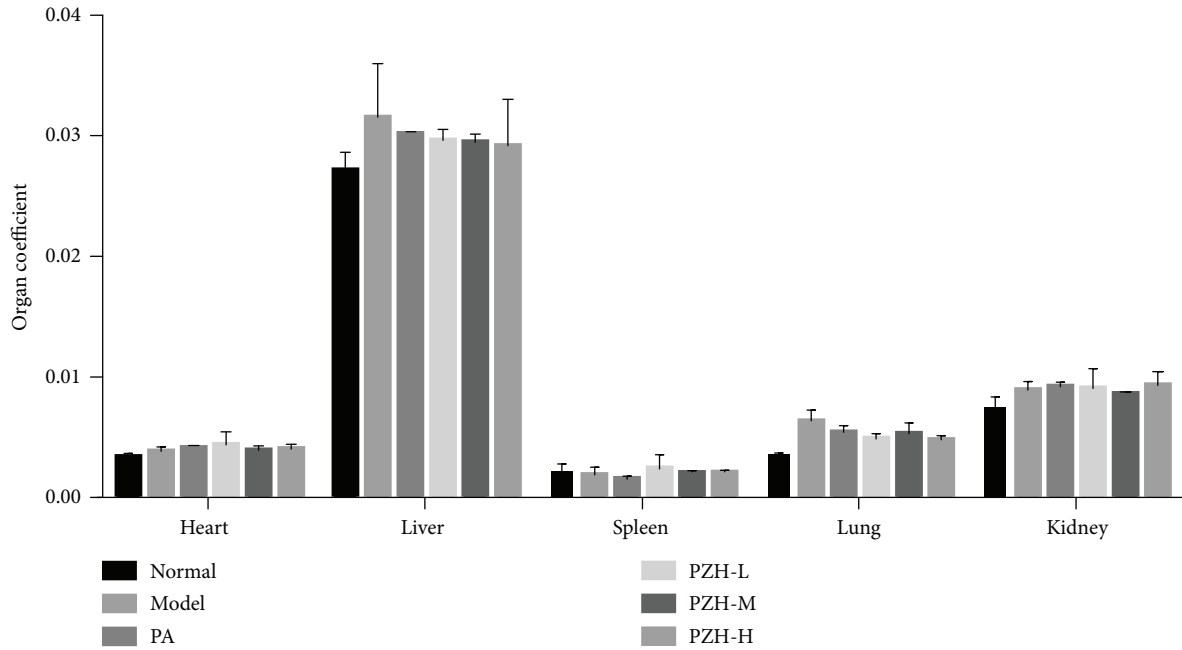


FIGURE 7: PZH has no significant toxicity in EAE rats. (a) The organ coefficient of several organs from the respective group was detected. The levels of ALT (b) and AST (c) for hepatotoxicity as well as CREA (d) and UREA (e) for nephrotoxicity were shown, respectively.

coefficient, PZH did not show significant liver and kidney functional impairment.

In conclusion, this study demonstrated that PZH exerted a good therapeutic effect on an acute model of EAE rats,

which was partly through relieving the infiltration of inflammatory cells in the CNS, suppressing the production of proinflammatory cytokines and chemokines, as well as promoting the expression of Olig2 and MBP.

## Conflicts of Interest

The authors declare that there are no competing interests.

## Authors' Contributions

Xuemei Qiu and Hui Luo performed the major research in equal contribution. Xue Liu, Qingqing Guo, Kang Zheng, Danping Fan, Jiawen Shen, and Cheng Lu provided the technical support. Xiaojuan He designed the study and revised the manuscript. Ge Zhang and Aiping Lu supervised the whole study.

## Acknowledgments

This research is supported by the Hong Kong Innovation and Technology Fund (UIM/310) and the Fundamental Research Funds for the Central Public Welfare Research Institutes (Z0551).

## References



- [1] M. Rangachari and V. K. Kuchroo, "Using EAE to better understand principles of immune function and autoimmune pathology," *Journal of Autoimmunity*, vol. 45, pp. 31–39, 2013.
- [2] H. F. McFarland and R. Martin, "Multiple sclerosis: a complicated picture of autoimmunity," *Nature Immunology*, vol. 8, no. 9, pp. 913–919, 2007.
- [3] C. A. Dendrou, L. Fugger, and M. A. Friese, "Immunopathology of multiple sclerosis," *Nature Reviews Immunology*, vol. 15, no. 9, pp. 545–558, 2015.
- [4] J. Zimmermann, M. Krauthausen, M. J. Hofer, M. T. Heneka, I. L. Campbell, and M. Müller, "CNS-targeted production of IL-17A induces glial activation, microvascular pathology and enhances the neuroinflammatory response to systemic endotoxemia," *PLoS One*, vol. 8, no. 2, article e57307, 2013.
- [5] Y. Komiyama, S. Nakae, T. Matsuki et al., "IL-17 plays an important role in the development of experimental autoimmune encephalomyelitis," *The Journal of Immunology*, vol. 177, no. 1, pp. 566–573, 2006.
- [6] Z. Kang, C. Z. Altuntas, M. F. Gulen et al., "Astrocyte-restricted ablation of interleukin-17-induced Act1-mediated signaling ameliorates autoimmune encephalomyelitis," *Immunity*, vol. 32, no. 3, pp. 414–425, 2010.
- [7] M. Kunz and S. M. Ibrahim, "Cytokines and cytokine profiles in human autoimmune diseases and animal models of autoimmunity," *Mediators of Inflammation*, vol. 2009, Article ID 979258, 20 pages, 2009.
- [8] T. Touil, D. Fitzgerald, G. X. Zhang, A. M. Rostami, and B. Gran, "Pathophysiology of interleukin-23 in experimental autoimmune encephalomyelitis," *Drug News & Perspectives*, vol. 19, no. 2, pp. 77–83, 2006.
- [9] A. Szczucinski and J. Losy, "Chemokines and chemokine receptors in multiple sclerosis. Potential targets for new therapies," *Acta Neurologica Scandinavica*, vol. 115, no. 3, pp. 137–146, 2007.
- [10] V. Bhise and S. Dhib-Jalbut, "Further understanding of the immunopathology of multiple sclerosis: impact on future treatments," *Expert Review of Clinical Immunology*, vol. 12, no. 10, pp. 1069–1089, 2016.
- [11] D. M. Wingerchuk and J. L. Carter, "Multiple sclerosis: current and emerging disease-modifying therapies and treatment strategies," *Mayo Clinic Proceedings*, vol. 89, no. 2, pp. 225–240, 2014.
- [12] G. Wei, D. F. Chen, X. P. Lai et al., "Muscone exerts neuroprotection in an experimental model of stroke via inhibition of the fas pathway," *Natural Product Communications*, vol. 7, no. 8, pp. 1069–1074, 2012.
- [13] T. B. Ng, "Pharmacological activity of sanchi ginseng (*Panax notoginseng*)," *The Journal of Pharmacy and Pharmacology*, vol. 58, no. 8, pp. 1007–1019, 2006.
- [14] Q. Q. Liang, M. Zhang, Q. Zhou, Q. Shi, and Y. J. Wang, "Muscone protects vertebral end-plate degeneration by anti-inflammatory property," *Clinical Orthopaedics and Related Research*, vol. 468, no. 6, pp. 1600–1610, 2010.
- [15] K. K. H. Lee, W. H. Kwong, F. t. Chau, D. T. Yew, and W. Y. Chan, "Pien Tze Huang protects the liver against carbon tetrachloride-induced damage," *Pharmacology and Toxicology*, vol. 91, no. 4, pp. 185–192, 2002.
- [16] A. Shen, Y. Chen, F. Hong et al., "Pien Tze Huang suppresses IL-6-inducible STAT3 activation in human colon carcinoma cells through induction of SOCS3," *Oncology Reports*, vol. 28, no. 6, pp. 2125–2130, 2012.
- [17] Q. Zhuang, F. Hong, A. Shen et al., "Pien Tze Huang inhibits tumor cell proliferation and promotes apoptosis via suppressing the STAT3 pathway in a colorectal cancer mouse model," *International Journal of Oncology*, vol. 40, no. 5, pp. 1569–1574, 2012.
- [18] M. J. Lee, M. Jang, J. Choi et al., "Korean red ginseng and ginsenoside-Rb1/-Rg1 alleviate experimental autoimmune encephalomyelitis by suppressing Th1 and Th17 cells and upregulating regulatory T cells," *Molecular Neurobiology*, vol. 53, no. 3, pp. 1977–2002, 2016.
- [19] D. Zhu, M. Liu, Y. Yang et al., "Ginsenoside Rd ameliorates experimental autoimmune encephalomyelitis in C57BL/6 mice," *Journal of Neuroscience Research*, vol. 92, no. 9, pp. 1217–1226, 2014.
- [20] C. S. Constantinescu, N. Farooqi, K. O'Brien, and B. Gran, "Experimental autoimmune encephalomyelitis (EAE) as a model for multiple sclerosis (MS)," *British Journal of Pharmacology*, vol. 164, no. 4, pp. 1079–1106, 2011.
- [21] H. Lassmann and M. Bradl, "Multiple sclerosis: experimental models and reality," *Acta Neuropathologica*, vol. 133, no. 2, pp. 223–244, 2017.
- [22] M. J. Noga, A. Dane, S. Shi et al., "Metabolomics of cerebrospinal fluid reveals changes in the central nervous system metabolism in a rat model of multiple sclerosis," *Metabolomics*, vol. 8, no. 2, pp. 253–263, 2012.
- [23] K. Kasarekło, R. Gadamski, P. Piotrowski, K. Kurzepa, B. Kwiatkowska-Patzer, and A. W. Lipkowski, "Effect of oral administration of pig spinal cord hydrolysate on clinical and histopathological symptoms of experimental allergic encephalomyelitis in rats," *Folia Neuropathologica*, vol. 53, no. 2, pp. 128–138, 2015.
- [24] R. Dong, F. Li, S. Qin et al., "Dataset on inflammatory proteins expressions and sialic acid levels in apolipoprotein E-deficient mice with administration of N-acetylneuraminic acid and/or quercetin," *Data in Brief*, vol. 8, pp. 613–617, 2016.
- [25] M. Basler, S. Mundt, T. Muchamuel et al., "Inhibition of the immunoproteasome ameliorates experimental autoimmune

- encephalomyelitis," *EMBO Molecular Medicine*, vol. 6, no. 2, pp. 226–238, 2014.
- [26] Y. Liu, A. T. Holdbrooks, P. de Sarno et al., "Therapeutic efficacy of suppressing the Jak/STAT pathway in multiple models of experimental autoimmune encephalomyelitis," *The Journal of Immunology*, vol. 192, no. 1, pp. 59–72, 2014.
- [27] R. H. Swanborg and J. A. Stepaniak, "Experimental autoimmune encephalomyelitis in the rat," in *Current Protocols in Immunology*, John Wiley & Sons, Inc., 2001.
- [28] G. Kim, K. Kohyama, N. Tanuma, H. Arimito, and Y. Matsumoto, "Persistent expression of experimental autoimmune encephalomyelitis (EAE)-specific Vbeta8.2 TCR spectratype in the central nervous system of rats with chronic relapsing EAE," *The Journal of Immunology*, vol. 161, no. 12, pp. 6993–6998, 1998.
- [29] K. Schaecher, A. Rocchini, J. Dinkins, D. D. Matzelle, and N. L. Banik, "Calpain expression and infiltration of activated T cells in experimental allergic encephalomyelitis over time: increased calpain activity begins with onset of disease," *Journal of Neuroimmunology*, vol. 129, no. 1-2, pp. 1–9, 2002.
- [30] R. Gold, C. Linington, and H. Lassmann, "Understanding pathogenesis and therapy of multiple sclerosis via animal models: 70 years of merits and culprits in experimental autoimmune encephalomyelitis research," *Brain*, vol. 129, no. 8, pp. 1953–1971, 2006.
- [31] Y. Li, N. Chu, A. Hu, B. Gran, A. Rostami, and G. X. Zhang, "Increased IL-23p19 expression in multiple sclerosis lesions and its induction in microglia," *Brain*, vol. 130, no. 2, pp. 490–501, 2007.
- [32] C. L. Langrish, Y. Chen, W. M. Blumenschein et al., "IL-23 drives a pathogenic T cell population that induces autoimmune inflammation," *Journal of Experimental Medicine*, vol. 201, no. 2, pp. 233–240, 2005.
- [33] D. W. Luchtman, E. Ellwardt, C. Larochele, and F. Zipp, "IL-17 and related cytokines involved in the pathology and immunotherapy of multiple sclerosis: current and future developments," *Cytokine & Growth Factor Reviews*, vol. 25, no. 4, pp. 403–413, 2014.
- [34] A. C. dos Santos, M. M. Barsante, R. M. Esteves Arantes, C. C. A. Bernard, M. M. Teixeira, and J. Carvalho-Tavares, "CCL2 and CCL5 mediate leukocyte adhesion in experimental autoimmune encephalomyelitis—an intravital microscopy study," *Journal of Neuroimmunology*, vol. 162, no. 1-2, pp. 122–129, 2005.
- [35] A. R. Glabinski, V. K. Tuohy, and R. M. Ransohoff, "Expression of chemokines rantes, MIP-1 $\alpha$  and GRO- $\alpha$  correlates with inflammation in acute experimental autoimmune encephalomyelitis," *Neuroimmunomodulation*, vol. 5, no. 3-4, pp. 166–171, 1998.
- [36] E. J. Hillmer, H. Zhang, H. S. Li, and S. S. Watowich, "STAT3 signaling in immunity," *Cytokine & Growth Factor Reviews*, vol. 31, pp. 1–15, 2016.
- [37] H. Yi, Y. Bai, X. Zhu et al., "IL-17A induces MIP-1 $\alpha$  expression in primary astrocytes via Src/MAPK/PI3K/NF- $\kappa$ B pathways: implications for multiple sclerosis," *Journal of Neuroimmune Pharmacology*, vol. 9, no. 5, pp. 629–641, 2014.
- [38] B. C. Dillingham, S. M. Knobloch, G. M. Many et al., "VBP15, a novel anti-inflammatory, is effective at reducing the severity of murine experimental autoimmune encephalomyelitis," *Cellular and Molecular Neurobiology*, vol. 35, no. 3, pp. 377–387, 2015.
- [39] H. Hou, J. Miao, R. Cao et al., "Rapamycin ameliorates experimental autoimmune encephalomyelitis by suppressing the mTOR-STAT3 pathway," *Neurochemical Research*, vol. 42, no. 10, pp. 2831–2840, 2017.
- [40] L. Lü, M. S. M. Wai, D. T. Yew, and Y. T. Mak, "Pien Tze Huang, a composite Chinese traditional herbal extract, affects survival of neuroblastoma cells," *The International Journal of Neuroscience*, vol. 119, no. 2, pp. 255–262, 2009.
- [41] L. Zhang, W. Lam, L. Lü et al., "Protective effects and potential mechanisms of Pien Tze Huang on cerebral chronic ischemia and hypertensive stroke," *Chinese Medicine*, vol. 5, no. 1, p. 35, 2010.
- [42] J. M. Boggs, "Myelin basic protein: a multifunctional protein," *Cellular and Molecular Life Sciences*, vol. 63, no. 17, pp. 1945–1961, 2006.
- [43] J. Matias-Guiu, J. M. Martinez-Vazquez, A. Ruibal, and A. Codina, "Cerebrospinal fluid levels of myelin basic protein and creatin kinase BB as index of active demyelination," *Acta Neurologica Scandinavica*, vol. 73, no. 2, pp. 203–207, 1986.
- [44] Q. Zhou, G. Choi, and D. J. Anderson, "The bHLH transcription factor Olig2 promotes oligodendrocyte differentiation in collaboration with Nkx2.2," *Neuron*, vol. 31, no. 5, pp. 791–807, 2001.
- [45] S. Z. Wang, J. Dulin, H. Wu et al., "An oligodendrocyte-specific zinc-finger transcription regulator cooperates with Olig2 to promote oligodendrocyte differentiation," *Development*, vol. 133, no. 17, pp. 3389–3398, 2006.
- [46] C. L. Maire, A. Wegener, C. Kerninon, and B. Nait Oumesmar, "Gain-of-function of Olig transcription factors enhances oligodendrogenesis and myelination," *Stem Cells*, vol. 28, no. 9, pp. 1611–1622, 2010.
- [47] M. N. Trame, K. Biliouris, L. J. Lesko, and J. T. Mettetal, "Systems pharmacology to predict drug safety in drug development," *European Journal of Pharmaceutical Sciences*, vol. 94, pp. 93–95, 2016.
- [48] J. Xu, H. Shi, M. Ruth et al., "Acute toxicity of intravenously administered titanium dioxide nanoparticles in mice," *PLoS One*, vol. 8, no. 8, article e70618, 2013.
- [49] R. Zhang, L. Zhang, D. Jiang et al., "Mouse organ coefficient and abnormal sperm rate analysis with exposure to tap water and source water in Nanjing reach of Yangtze River," *Ecotoxicology*, vol. 23, no. 4, pp. 641–646, 2014.



## Research Article

# ***Punica granatum* L. Leaf Extract Attenuates Lung Inflammation in Mice with Acute Lung Injury**

**Aruanã Joaquim Matheus Costa Rodrigues Pinheiro,<sup>1,2,3</sup> Jaciara Sá Gonçalves,<sup>1</sup> Ádylla Wilenna Alves Dourado,<sup>1</sup> Eduardo Martins de Sousa,<sup>1</sup> Natilene Mesquita Brito,<sup>4</sup> Lanna Karinny Silva,<sup>4</sup> Marisa Cristina Aranha Batista,<sup>5</sup> Joicy Cortez de Sá,<sup>6</sup> Cinara Regina Aragão Vieira Monteiro,<sup>1,7</sup> Elizabeth Soares Fernandes,<sup>1</sup> Valério Monteiro-Neto <sup>1,7</sup> Lee Ann Campbell,<sup>8</sup> Patrícia Maria Wiziack Zago,<sup>9</sup> and Lidio Gonçalves Lima-Neto <sup>1,2</sup>**

<sup>1</sup>Programa de Pós-Graduação, Universidade CEUMA, São Luís, MA, Brazil

<sup>2</sup>Programa de Pós-Graduação da Rede BIONORTE, Universidade Federal do Amazonas, Manaus, AM, Brazil

<sup>3</sup>Departamento de Farmácia, Faculdade Pitágoras, São Luís, MA, Brazil

<sup>4</sup>Laboratório de Estudos Ambientais, Instituto Federal do Maranhão, São Luís, MA, Brazil

<sup>5</sup>Laboratório de Farmacognosia I, Universidade Federal do Maranhão, São Luís, MA, Brazil

<sup>6</sup>Departamento de Medicina, Universidade CEUMA, São Luís, MA, Brazil

<sup>7</sup>Centro de Ciências Biológicas e da Saúde, Universidade Federal do Maranhão, São Luís, MA, Brazil

<sup>8</sup>Department of Global Health, University of Washington, Seattle, WA, USA

<sup>9</sup>Departamento de Odontologia, Universidade CEUMA, São Luís, MA, Brazil

Correspondence should be addressed to Lidio Gonçalves Lima-Neto; [lidio.neto@outlook.com](mailto:lidio.neto@outlook.com)

Received 25 August 2017; Revised 10 December 2017; Accepted 18 December 2017; Published 20 February 2018

Academic Editor: Yong Tan

Copyright © 2018 Aruanã Joaquim Matheus Costa Rodrigues Pinheiro et al. This is an open access article distributed under the Creative Commons Attribution License, which permits unrestricted use, distribution, and reproduction in any medium, provided the original work is properly cited.

The hydroalcoholic extract of *Punica granatum* (pomegranate) leaves was previously demonstrated to be anti-inflammatory in a rat model of lipopolysaccharide- (LPS-) induced acute peritonitis. Here, we investigated the anti-inflammatory effects of the ethyl acetate fraction obtained from the pomegranate leaf hydroalcoholic extract (EAFPg) on the LPS-induced acute lung injury (ALI) mouse model. Male Swiss mice received either EAFPg at different doses or dexamethasone (per os) prior to LPS intranasal instillation. Vehicle-treated mice were used as controls. Animals were culled at 4 h after LPS challenge, and the bronchoalveolar lavage fluid (BALF) and lung samples were collected for analysis. EAFPg and kaempferol effects on NO and cytokine production by LPS-stimulated RAW 264.7 macrophages were also investigated. Pretreatment with EAFPg (100–300 mg/kg) markedly reduced cell accumulation (specially neutrophils) and collagen deposition in the lungs of ALI mice. The same animals presented with reduced lung and BALF TNF- $\alpha$  and IL-1 $\beta$  expression in comparison with vehicle controls ( $p < 0.05$ ). Additionally, incubation with either EAFPg or kaempferol (100  $\mu$ g/ml) reduced NO production and cytokine gene expression in cultured LPS-treated RAW 264.7 macrophages. Overall, these results demonstrate that the prophylactic treatment with EAFPg attenuates acute lung inflammation. We suggest this fraction may be useful in treating ALI.

## 1. Introduction

Acute lung injury (ALI) is a clinical condition that causes disruption of the lung endothelial tissue and epithelial barrier and loss of lung function [1, 2]. ALI incidence remains high,

and it is associated with high rates of mortality and morbidity worldwide, especially in developing countries [3]. ALI is characterized by intense transepithelial leukocyte infiltration, exudate accumulation in the lungs, loss of integrity of the alveolar-capillary membrane, and tissue damage [4]. This

response has been suggested to be due to the increased production of inflammatory mediators including cytokines (TNF- $\alpha$ , IL-1 $\beta$ , and IL-6), especially by alveolar macrophages and neutrophils [5].

*Punica granatum* L. (pomegranate) has been shown to possess wound healing, antimicrobial, antioxidant, and anti-inflammatory properties [6–8]. Especially due to its anti-inflammatory activities, pomegranate is traditionally used to treat infections. In this context, we recently demonstrated that the leaf hydroalcoholic extract obtained from pomegranate is anti-inflammatory as it inhibits TNF- $\alpha$  production and decreases neutrophil migration in a rat model of lipopolysaccharide- (LPS-) induced acute peritonitis [8]. Furthermore, Haseeb et al. showed that the pomegranate fruit extract attenuates IL-6 production, reactive oxygen species, IL-1 $\beta$ -mediated phosphorylation of the inhibitor of nuclear factor kappa-B kinase subunit beta (IKK $\beta$ ), expression of IKK $\beta$  mRNA, degradation of I $\kappa$ B $\alpha$ , and the activation and nuclear translocation of NF- $\kappa$ B/p65 in human chondrocytes [9].

To date, pomegranate effects on acute lung inflammation have not been yet investigated. Here, we assessed the anti-inflammatory potential of the ethyl acetate fraction (EAFPg) obtained from a pomegranate leaf hydroalcoholic extract in a mouse model of LPS-induced acute lung injury.

## 2. Material and Methods

**2.1. Plant Material and Preparation of EAFPg.** Fresh leaves of *Punica granatum* L. were collected at the Ático Seabra Herbarium of the Universidade Federal do Maranhão in Sao Luis, Maranhão, Brazil [8], and a voucher specimen was deposited (voucher number 01002). The leaf hydroalcoholic extract was prepared, and the EAFPg was obtained as previously described [8].

**2.2. HPLC-DAD-ESI-IT/MS Analysis.** The chemical constituents of EAFPg were analyzed in a high-performance liquid chromatography (HPLC) system (LC-10AD, Shimadzu) equipped with a photodiode array detector coupled to an Esquire 3000 Plus ion trap mass spectrometer (Bruker Daltonics, Bremen, Germany), using electrospray ionization (ESI) as previously described [10]. Separation was performed using a Phenomenex Kinetex C-18 column (250  $\times$  4.6 mm, 5  $\mu$ m; Torrance, CA, USA). The column oven was maintained at room temperature. The HPLC was set up with an elution gradient as follows: 0–2 min, 5% B; 2–10 min, 5–25% B; 10–20 min, 25–40% B; 20–30 min, 40–50% B; 30–40 min, 50–60% B; and 40–50 min, 70–100% B. Acetic acid (2%) in Milli-Q water was used as mobile phase A, and methanol was used as mobile phase B. The injection volume consisted of 25  $\mu$ l of the reconstituted sample at 5 mg/ml, with a flow rate of 0.6 ml/min. Detection was achieved in a diode array detector (DAD) at 200–500 nm and with direct mass spectrometry/mass spectrometry, a method in negative electrospray (-ESI) mode with a detector voltage maintained at 4.0 kV, ion source at 40 V, and capillary temperature at 320°C. The nebulizing gas was nitrogen (N<sub>2</sub>) flowing at 7 ml/min, a sheath gas provided at a pressure of 27 psi, while helium was used as the collision gas. Analyses were carried

out using full-scan mass spectra and data-dependent MS<sup>2</sup> scans from *m/z* 100 to 2000. The compounds were identified on the basis of their molecular ion mass fragmentation. The obtained mass spectrum was compared with that of the literature.

### 2.3. In Vivo Assays

**2.3.1. Animals.** Sixty-six nonfasted male outbred Swiss mice (20–30 g) were used. Mice were obtained from the animal facility of Universidade CEUMA (UNICEUMA) and were kept in a climatically controlled environment (room temperature of 22  $\pm$  2°C and humidity of around 60%) under 12:12 h light-dark cycle (lights on 07:00 a.m.). All procedures were approved by the Ethics Committee of UNICEUMA (April 24, 2014; #107/2014) and carried out in accordance with the Brazilian Society for Animal Welfare (SBCAL).

**2.3.2. Induction of LPS-Induced ALI and Pharmacological Treatments.** Animals were randomly distributed into six groups (*n* = 6/group) for lung analysis and five groups (*n* = 6/group) for bronchoalveolar lavage fluid (BALF) analysis. Mice received a single oral administration (p.o.) of vehicle (saline, 10 ml/kg), EAFPg (30–300 mg/kg), or dexamethasone (5 mg/kg) 30 min prior to LPS challenge. ALI was induced by a single intranasal (i.n.) instillation of LPS (30,000 EU in 50  $\mu$ l/animal and 25  $\mu$ l/narine). Vehicle-treated mice were used as controls. Four hours after the challenge, mice were culled by anesthetic overdose with ketamine (120 mg/kg, i.p.) and xylazine (10 mg/kg, i.p.), and the bronchoalveolar lavage fluid (BALF) was collected. For this, the trachea of each mouse was cannulated and the alveoli were washed three times with 0.5 ml of ice-cold phosphate buffered saline (PBS) containing 0.5% sodium citrate. An aliquot of the BALF was separated and used for quantification of leukocyte counts and the rest centrifuged at 400  $\times$ g for 10 min at 4°C. The supernatant was immediately frozen and stored at –80°C for further analysis. In a separate series of experiments, the lungs were collected from animals that did not undergo BALF collection and were processed for histological analysis.

**2.3.3. Total and Differential Leukocyte Counts in BALF Samples.** Total cell counts were performed in a Neubauer chamber and microscope (Zeiss Axio Imager Z2 upright microscope, Carl Zeiss, Göttingen, Germany) after diluting an aliquot of the BALF with Türk solution (1:20). Another aliquot (50  $\mu$ l) was used for differential cell counts. For this, the slides were stained with May-Grünwald Giemsa and then analyzed by microscopy in an immersion objective. A minimum of 200 leukocytes was considered. Two independent researchers performed blinded analyses; if there was discordance, a third researcher performed the analysis.

**2.3.4. RT-qPCR Assays in the Lung Tissue.** TNF- $\alpha$ , IL-6, IL1- $\beta$ , and IL-10 mRNA expression in lung samples was determined by RT-qPCR. Total RNA was extracted by using a RNeasy Mini Kit (Qiagen, Hilden, Germany) according to the manufacturer's instructions in a QIAcube automatic DNA extractor (Qiagen, Hilden, Germany). Samples were

treated with DNase (Qiagen, Hilden, Germany) and then reverse-transcribed using 200 U of SuperScript II reverse transcriptase (Thermo Fisher Scientific) to obtain cDNA. The qPCR assays were carried out in 96-well plates using a double-stranded DNA dye (GoTaq® real-time PCR Master Mix from Promega) in a QuantStudio™ 6 flex real-time PCR instrument as previously described. GAPDH mRNA was used as an endogenous reference gene. mRNA relative expression was calculated using the  $2^{-\Delta\Delta C_t}$  method [11]. Results represent the mean values obtained from two independent experiments, with assays performed in triplicate.

**2.3.5. Cytokine Levels in BALF Samples.** BALF TNF- $\alpha$  and IL-10 protein levels were analyzed in enzyme-linked immunosorbent assay kits according to the manufacturer's instructions (R&D Systems). Sample readings for each cytokine were compared with those of a standard curve (0–800 pg/ml). Results are expressed as protein levels in pg/ml. All experiments were performed in triplicate.

**2.3.6. Albumin Levels in BALF Samples.** Albumin levels in BALF samples were measured by the Bradford method using the standard Quick Start Bradford Protein Assay Kit from Bio-Rad (Hercules, California) according to the manufacturer's instructions. Albumin was measured as it is an indicator of plasma extravasation. Absorbance was measured in an automated spectrophotometer at 650 nm. Readings obtained were compared with those of a standard curve of albumin (0–2.0 mg/ml). Results are expressed as mg of albumin per ml of BALF. All experiments were performed in triplicate.

**2.3.7. Histological Analysis.** The collected lungs were fixed in 10% neutral formalin for 24 h and then embedded in paraffin. After deparaffinization and dehydration as previously described [10], sections (4  $\mu$ m) were stained with hematoxylin and eosin or Masson's trichrome and analyzed by microscopy under 100x and 400x magnification. The density of leukocytes/unit area (130  $\mu$ m<sup>2</sup>) was determined by counting the number of cells on the integrating eyepiece that fell into areas of the bronchioli and distal lung parenchyma using the ImageJ Program. Using the same program, the collagen area was measured also in areas of the bronchioli and distal lung parenchyma. All measurements were performed in ten random sections of 130  $\mu$ m<sup>2</sup> per animal at 200x (for collagen area) and 400x magnification (for leukocyte count), and the researcher who performed the analysis was unaware of the experimental group designation. Two independent researchers performed blinded analyses; if there was discordance, a third researcher performed the analysis.

## 2.4. In Vitro Assays

**2.4.1. RAW 264.7 Macrophage Culture and Pharmacological Treatments.** RAW 264.7 cells were cultured and maintained in DMEM medium (Thermo Fisher Scientific, Waltham, Massachusetts, USA) containing 10% fetal bovine serum and 1% antibiotic solution—1000 U/ml penicillin G and 100 U/ml streptomycin sulfate (Thermo Fisher Scientific, Waltham, Massachusetts, USA). Cells ( $1 \times 10^5$  cells/well)

were treated with EAFPg (50–100  $\mu$ g/ml), kaempferol (25–100  $\mu$ g/ml), or dexamethasone (2–4  $\mu$ g/ml) and stimulated with LPS (10  $\mu$ g/ml; 30,000 EU/well/100  $\mu$ l; Sigma, St. Louis, MI, USA), at noncytotoxic concentrations. Then, cells were incubated for 48 h at 37°C and 5% CO<sub>2</sub>. Vehicle (1% DMSO in PBS) treated cells were used as controls.

**2.4.2. RT-qPCR Assays in RAW 264.7 Murine Macrophages.** TNF- $\alpha$ , IL-6, IL1- $\beta$ , and IL-10 mRNA expression was evaluated in RAW 264.7 cells by RT-qPCR as described in Section 2.3.4.

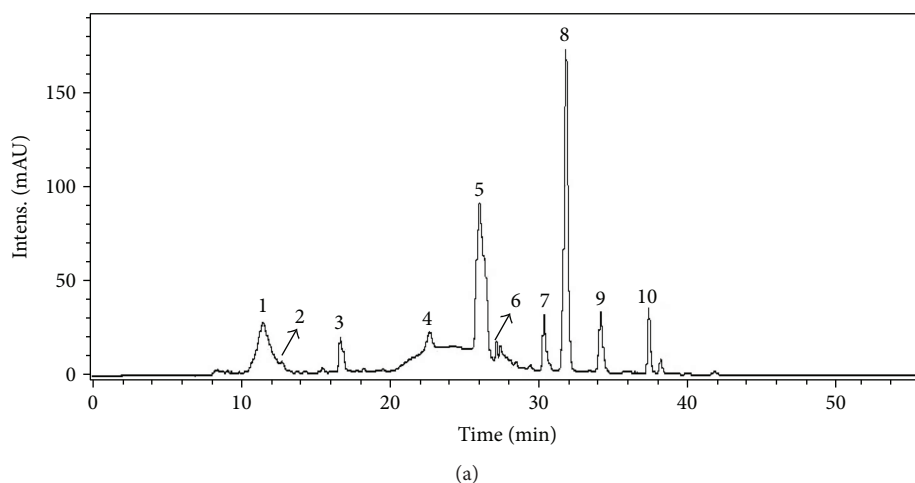
**2.4.3. NO Levels in Cell Culture Supernatants.** The production of NO was determined by measuring nitrite as previously described [7]. Briefly, cell supernatants were incubated with an equal volume of a Griess reagent (Sigma, St. Louis, MI, USA), and the absorbance was determined at 540 nm and compared with that obtained from a NO<sub>2</sub> standard curve (0–300  $\mu$ M). Results are expressed as  $\mu$ M of NO<sub>2</sub>.

**2.5. Statistical Analysis.** Data are expressed as mean  $\pm$  standard deviation (SD). Differences between groups were analyzed by one-way analysis of variance (ANOVA), followed by the Newman-Keuls multiple comparison test. Percentages of inhibition were calculated as the mean of the inhibitions obtained for each individual experiment. *p* values < 0.05 were considered statistically significant.

## 3. Results

**3.1. Phytochemical Analysis of EAFPg.** Figure 1 shows the HPLC analytical plot for EAFPg at 327 nm (a) and the detected components (b). These included punicalin (peak 1; retention time: 11.2 min), ellagic acid derivative (peak 2; retention time: 12.3 min), galloyl-HHDP-glucose (peak 3; retention time: 17.4 min), castalagin derivative (peaks 4 and 5; retention times: 23.6 and 26.6 min, resp.), granatin B (peak 6; retention time: 26.7 min), ellagic acid rhamnoside (peak 7; retention time: 32.2 min), kaempferol-3-O-glucoside (peak 8; retention time: 32.7 min), kaempferol derivative (peak 9; retention time: 34.9 min), and kaempferol-arabinoside (peak 10; retention time: 38.3 min).

**3.2. EAFPg Reduces Leukocyte Accumulation and Collagen Deposition into the Lungs of Mice with ALI.** Figures 2 and 3 show the effects of EAFPg (30–300 mg/kg) and dexamethasone (5 mg/kg) on the lung tissue of mice with LPS-induced ALI. Animals with ALI exhibited an intense inflammatory cell influx surrounding the bronchi (Figure 2(b)). The same mice also presented multifocal areas of collagen deposition (Figure 3(b)) in comparison with those which received i.n. saline (Figure 3(a)). LPS-induced pathological changes were not affected by the pretreatment with EAFPg at 30 mg/kg. On the other hand, pretreatment with EAFPg at 100–300 mg/kg markedly reduced the collagen deposition with leukocyte infiltration, with respect to LPS mice treated with vehicle (Figures 2(d), 2(e), 3(d), and 3(e)). Animals pretreated with dexamethasone also displayed attenuated lung inflammation (Figures 2(f) and 3(f)). In addition, EAFPg



ID peak	RT (min)	Compound	[M-H] <sup>-</sup>	MS <sup>n</sup> fragments
1	11.2	Punicalin	781	633
2	12.3	Ellagic acid derivate	799	781, 479, 301
3	17.4	Galloyl-HHDP-glucose	633	479, 301
4	23.6	Castalagin derivative	965	933
5	26.6	Castalagin derivative	965	—
6	26.7	Granatin B	951	933, 300
7	32.2	Ellagic acid rhamnoside	447	352, 262, 146
8	32.7	Kaempferol-3-O-glucoside	447	301
9	34.9	Kaempferol derivative	447	285
10	38.3	Kaempferol-arabinside	417	285

(b)

FIGURE 1: HPLC/DAD chromatogram of the acetyl acetate extract of pomegranate leaves (EAFPg) monitored at 327 nm (a). Structure of constituents identified by HPLC-DAD-ESI-IT/MS (b). ID: identification; RT: retention time; MS: mass spectrometer.

(100–300 mg/kg) and dexamethasone markedly diminished the numbers of leukocytes in the bronchial area ( $12.0 \pm 1.0$ ,  $13.0 \pm 1.0$ , and  $10.3 \pm 1.5$  leukocytes/ $130 \mu\text{m}^2$ , resp.) (Figure 2(g)) and in the alveolar parenchyma area ( $109.7 \pm 4.7$ ,  $66.3 \pm 2.5$ , and  $41.3 \pm 1.5$  leukocytes/ $130 \mu\text{m}^2$ , resp.) when compared with those of the vehicle-treated ALI mice ( $83.3 \pm 1.5$  leukocytes/ $130 \mu\text{m}^2$  and  $384.3 \pm 3.5$  leukocytes/ $130 \mu\text{m}^2$ ). Moreover, EAFPg (100–300 mg/kg) and dexamethasone markedly reduced the bronchial ( $7.5\% \pm 0.6\%$ ,  $7.0\% \pm 0.1\%$ , and  $6.7\% \pm 0.3\%$ , resp.; Figure 2(g)) and the alveolar parenchyma collagen deposition ( $3.7\% \pm 0.5\%$ ,  $3.3\% \pm 0.7\%$ , and  $2.2\% \pm 0.2\%$ , resp.) when compared with that of the ALI control group ( $33.3\% \pm 10.8\%$  and  $11.9\% \pm 2.7\%$ , resp.).

**3.3. EAFPg Reduces TNF- $\alpha$  and IL-1 $\beta$  but Not IL-6 mRNA Expression in the Lungs.** LPS instillation significantly increased TNF- $\alpha$ , IL-1 $\beta$ , and IL-6 mRNA expression in the lungs (Figures 4(a)–4(c)). When tested at 30 mg/kg, EAFPg did not affect TNF- $\alpha$ , IL-1 $\beta$ , and IL-6 mRNA expression. On the other hand, 100 and 300 mg/kg EAFPg

significantly downregulated lung TNF- $\alpha$  and IL-1 $\beta$  but not IL-6 expression in mice with ALI. Likewise, dexamethasone treatment significantly inhibited the expression of all evaluated cytokines, and the effects of the dexamethasone were significantly higher than those observed for EAFPg.

**3.4. Plasma Extravasation and BALF TNF- $\alpha$  Levels Are Reduced in Mice with ALI Treated with EAFPg.** Albumin and TNF- $\alpha$  protein levels were augmented in BALF samples obtained from mice with ALI (Figures 5(a) and 5(c)) while IL-10 was reduced (Figure 5(b)). On the other hand, IL-10 was reduced in the BALF from the same animals. Both EAFPg (100 mg/kg) and dexamethasone diminished the levels of TNF- $\alpha$  ( $219.8 \pm 6.4$  pg/ml) and albumin ( $120.6 \pm 42.8$  pg/ml) in the BALF when compared with those of LPS-challenged mice pretreated with vehicle ( $397 \pm 109.6$  and  $228.6 \pm 41.6$  pg/ml, resp.; Figures 5(a) and 5(c)). No effects were observed for either EAFPg or dexamethasone on IL-10 levels in the tested doses (Figure 5(b)).

**3.5. EAFPg Prevents Leukocyte Accumulation into the Alveoli.** Mice with LPS-induced ALI had increased numbers of total

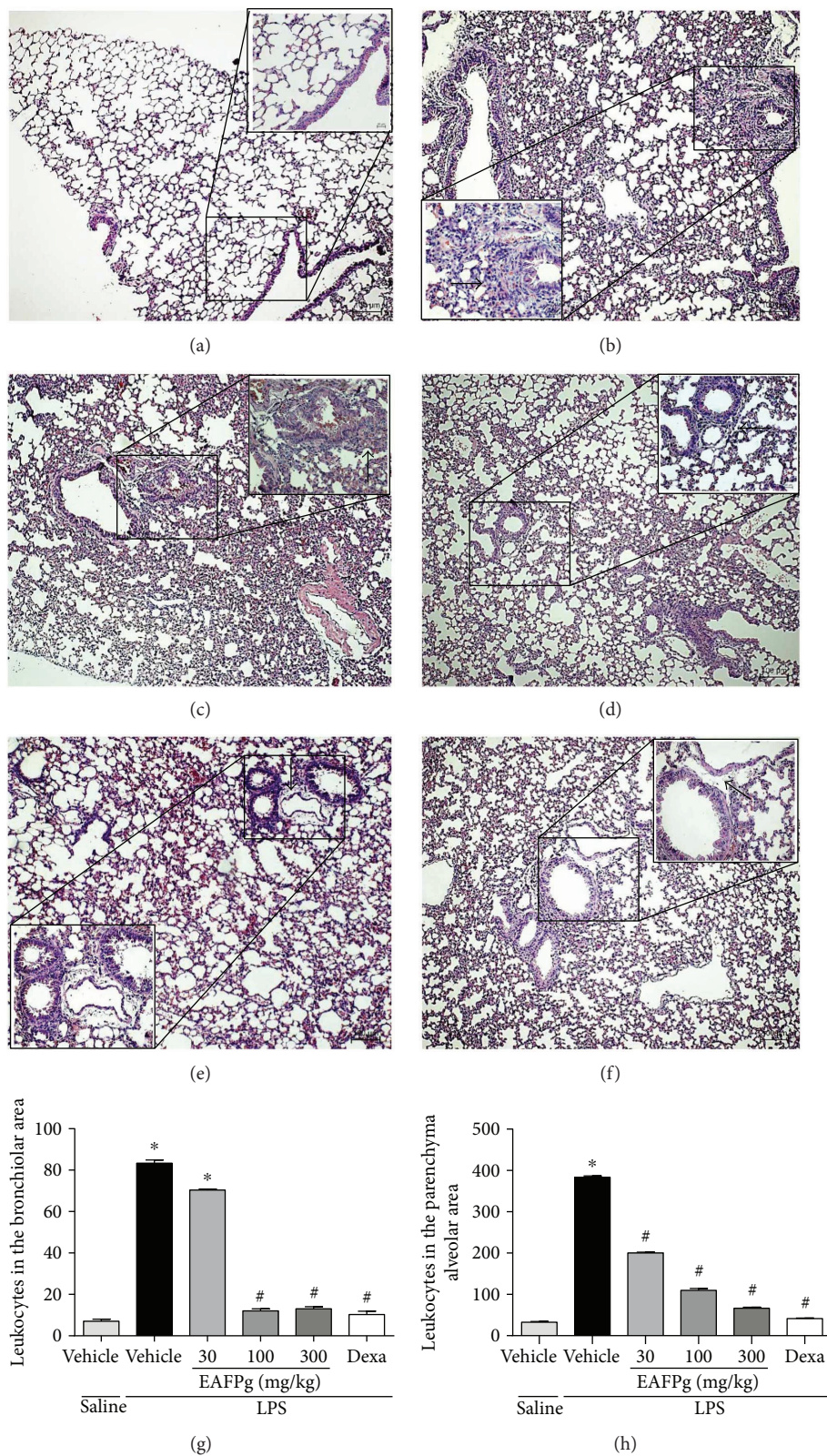


FIGURE 2: Effect of the pretreatment with EAFPg on leukocyte accumulation into the lungs obtained from mice treated with saline (a), LPS (b), 30 mg/kg EAFPg plus LPS (c), 100 mg/kg EAFPg plus LPS (d), 300 mg/kg EAFPg plus LPS (e), or 5 mg/kg dexamethasone plus LPS (f). Leukocyte counts in the bronchial (g) and alveolar parenchyma areas (h). Data is expressed as mean ± SD. Significances were calculated by one-way ANOVA followed by the Newman-Keuls multiple comparison test analysis. \* $p < 0.05$  differs from saline-treated mice; # $p < 0.05$  differs from vehicle-treated LPS-stimulated mice. Bronchiolar inflammatory cell infiltrates are shown as black arrows. Sections ( $4 \mu\text{m}$ ) were stained with hematoxylin and eosin. Magnification of 100x and 400x.

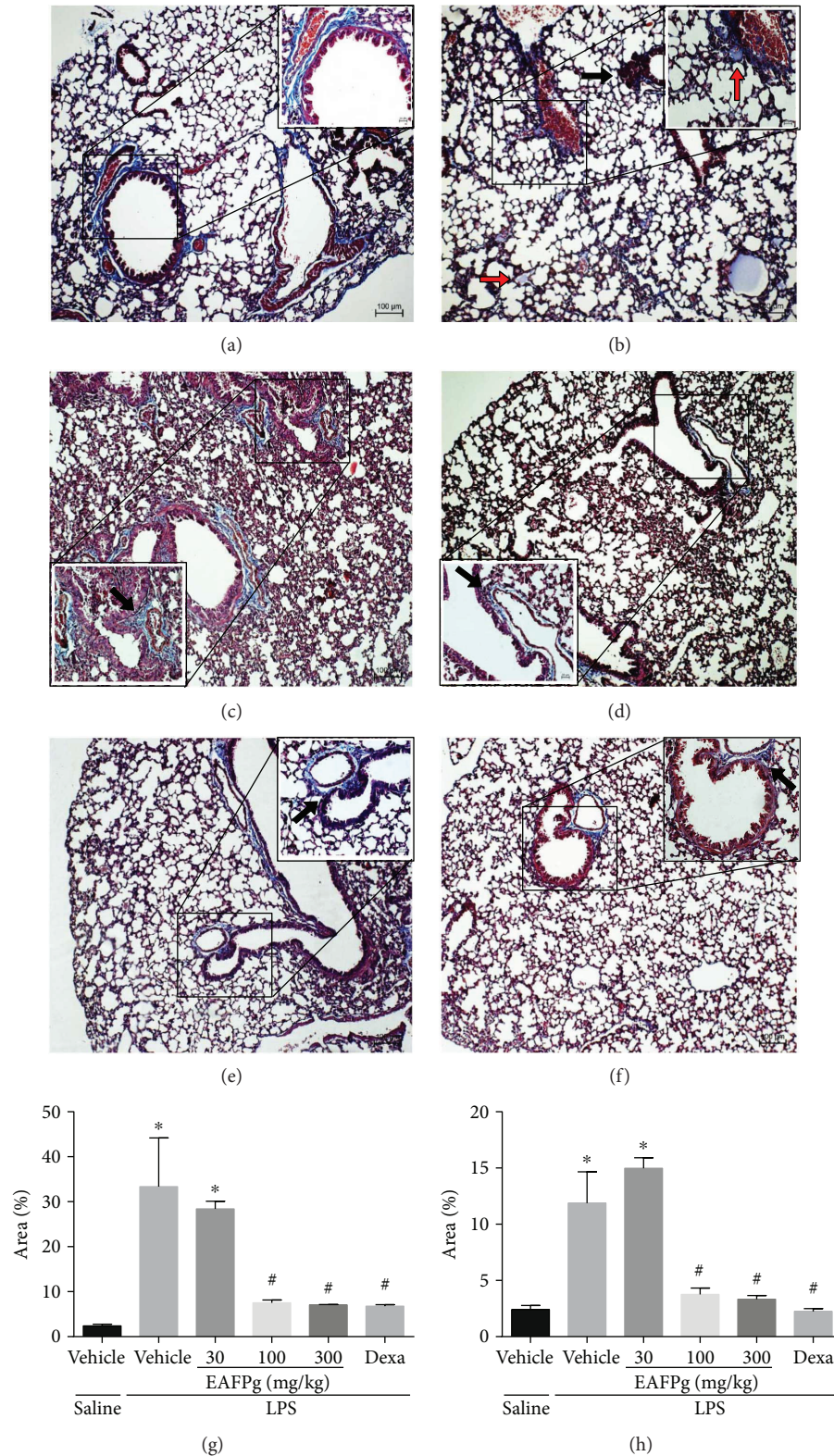


FIGURE 3: Effect of the pretreatment with EAFPg and dexamethasone on the collagen deposition in lung samples obtained from mice treated with saline (a), LPS (b), 30 mg/kg EAFPg plus LPS (c), 100 mg/kg EAFPg plus LPS (d), 300 mg/kg EAFPg plus LPS (e), or 5 mg/kg dexamethasone plus LPS (f). Quantitative analysis of the collagen area (percentage area) in the bronchial (g) and alveolar parenchyma areas (h). Data is expressed as mean  $\pm$  SD. Significances were calculated by one-way ANOVA followed by the Newman-Keuls multiple comparison test analysis. \* $p < 0.05$  differs from saline-treated mice; # $p < 0.05$  differs from vehicle-treated LPS-stimulated mice. Collagen areas with leukocyte infiltration are shown as red arrows. Sections (4  $\mu$ m) were stained with Masson's trichrome. Magnification of 100x and 400x.

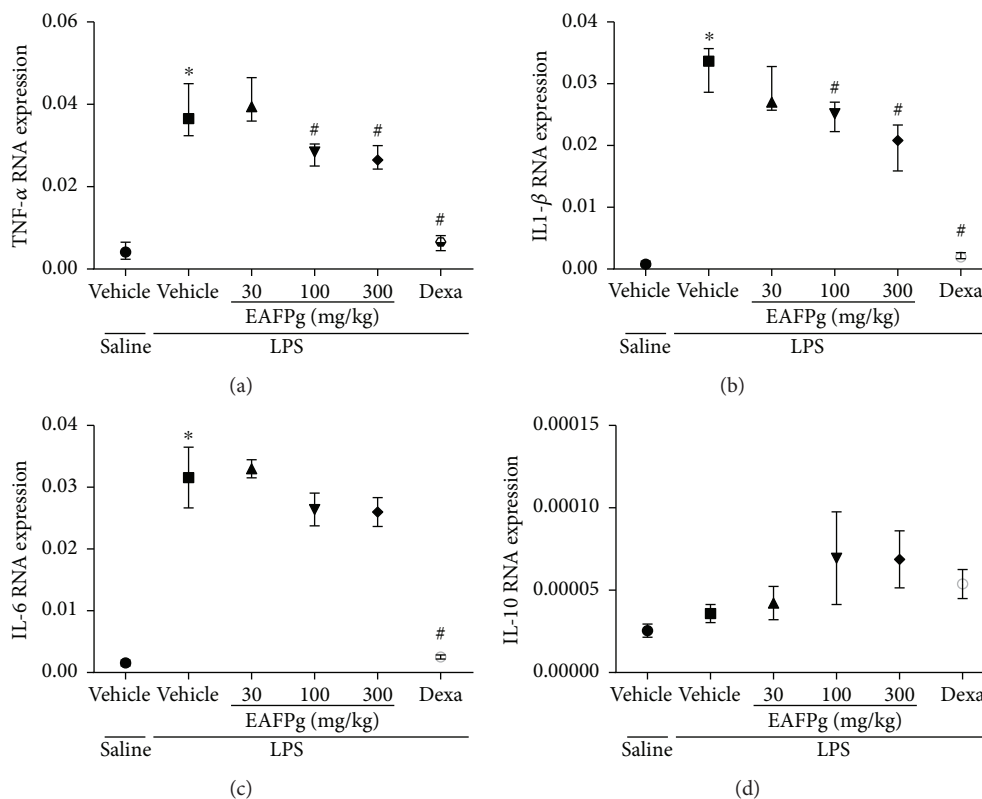


FIGURE 4: Effects of the pretreatment with EAFPg on TNF- $\alpha$  (a), IL-1 $\beta$  (b), IL-6 (c), and IL-10 gene expression in the lungs of the animals divided into six groups. Animals were randomly distributed into six groups ( $n = 6/\text{group}$ ). Mice received in the prophylactic scheme EAFPg (30 mg/kg, 100 mg/kg, and 300 mg/kg, p.o.), dexamethasone (DEXA, 5 mg/kg, p.o.), or vehicle (PBS, p.o.). The values are presented as the median and interquartile range. Significances were calculated by one-way ANOVA followed by the Newman-Keuls multiple comparison test analysis. Groups versus nonpretreated saline-injected mice (\* $p < 0.05$ ) and versus nonpretreated LPS-installed mice (# $p < 0.05$ ).

and differential leukocytes in their BALF in comparison with the saline group (Figures 6(a), 6(b), and 6(c)). In contrast, EAFPg- (100 mg/kg) pretreated mice with ALI had significantly lower numbers of leukocytes ( $35,814 \pm 12,005$  cells/ $\text{mm}^3$ ) in their BALF in comparison with vehicle-treated mice ( $58,733 \pm 13,629$  cells/ $\text{mm}^3$ ,  $p < 0.0001$ , see Figure 6(a)). A similar effect was noted for LPS-challenged mice pretreated with dexamethasone (Figure 6(a)). In addition, the number of neutrophils was significantly reduced in LPS-challenged mice pretreated with 100 mg/kg of EAFPg ( $32,878 \pm 11,116$  cells/ $\text{mm}^3$ ) when compared with vehicle-treated mice ( $54,813 \pm 12,678$  cells/ $\text{mm}^3$ ,  $p < 0.0001$ , see Figure 6(b)). No differences were observed in the number of macrophages between groups (Figure 6(c)).

**3.6. EAFPg, Kaempferol, and Dexamethasone Reduce Cytokine mRNA Expression in Cultured RAW 264.7 Macrophages.** IL-1 $\beta$ , IL-6, and IL-10 mRNA levels were downregulated by EAFPg (100  $\mu\text{g}/\text{ml}$ ), kaempferol (25–100  $\mu\text{g}/\text{ml}$ ), and dexamethasone (2–4  $\mu\text{g}/\text{ml}$ ) in macrophages activated by LPS (Figures 7(a), 7(b), and 7(c)).

**3.7. EAFPg and Kaempferol Reduce NO Release by Macrophages.** NO production was reduced in LPS-activated

macrophages incubated with EAFPg (100  $\mu\text{g}/\text{ml}$ ) and kaempferol (25–100  $\mu\text{g}/\text{ml}$ ) (Figures 8(a) and 8(b), resp.).

## 4. Discussion

Extracts prepared from pomegranate peels and seeds were described previously to possess anti-inflammatory properties [12, 13]. However, very little is known about the effects of pomegranate leaf extracts or fractions on inflammation. We recently demonstrated that the pomegranate leaf hydroalcoholic extract attenuates LPS-induced peritonitis by decreasing the accumulation of leukocytes and the release of proinflammatory mediators in the peritoneum [8]. We now show that EAFPg protects mice from ALI by reducing lung inflammation.

The phytochemical analysis of EAFPg demonstrated the presence of kaempferol, ellagic acid derivative, and other bioactive molecules, a similar composition to that previously observed for the leaf hydroalcoholic extract [8]. Chen et al. [14] showed that kaempferol significantly blocks LPS-induced activation of mitogen-activated protein kinases (MAPKs) and nuclear factor-kappa B (NF- $\kappa$ B). In addition, Cornelio Favarin et al. demonstrated that ellagic acid reduces cyclooxygenase-2- (COX-2-) induced exacerbation of inflammation, vascular permeability changes,

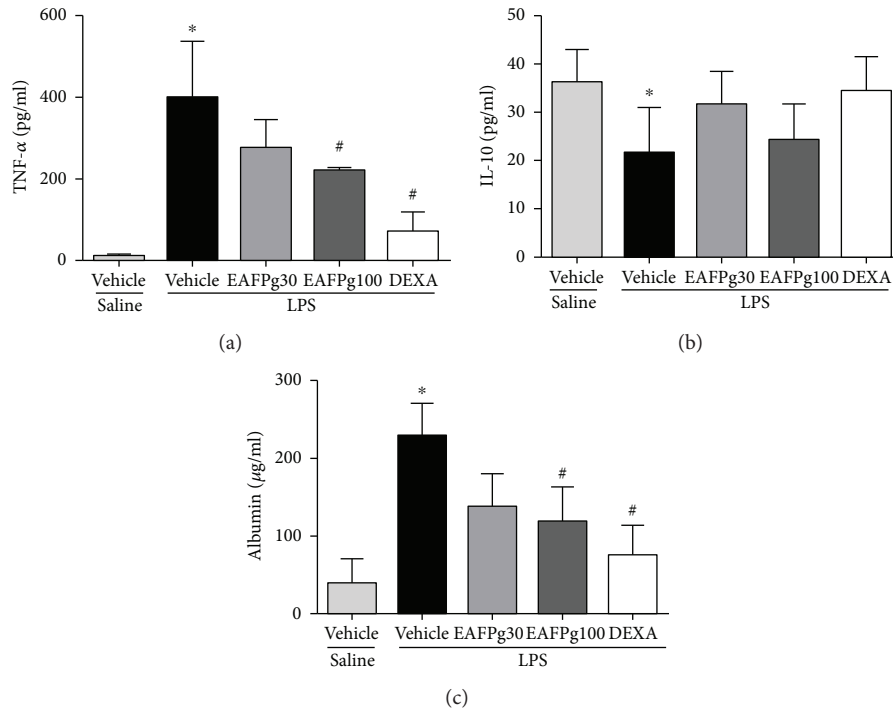


FIGURE 5: Effects of the pretreatment with EAFPg on TNF- $\alpha$  (a), IL-10 (b), and albumin (c) levels in BALF of the animals divided into six groups. Animals were randomly distributed into five groups ( $n = 6/\text{group}$ ). Mice received in the prophylactic scheme EAFPg (30 mg/kg and 100 mg/kg, p.o.), dexamethasone (DEXA, 5 mg/kg, p.o.), or vehicle (PBS, p.o.). The values are presented as the mean  $\pm$  SD. Significances were calculated by one-way ANOVA followed by the Newman-Keuls multiple comparison test analysis versus nonpretreated saline-injected mice ( $*p < 0.05$ ) and versus nonpretreated LPS-installed mice ( $\#p < 0.05$ ).

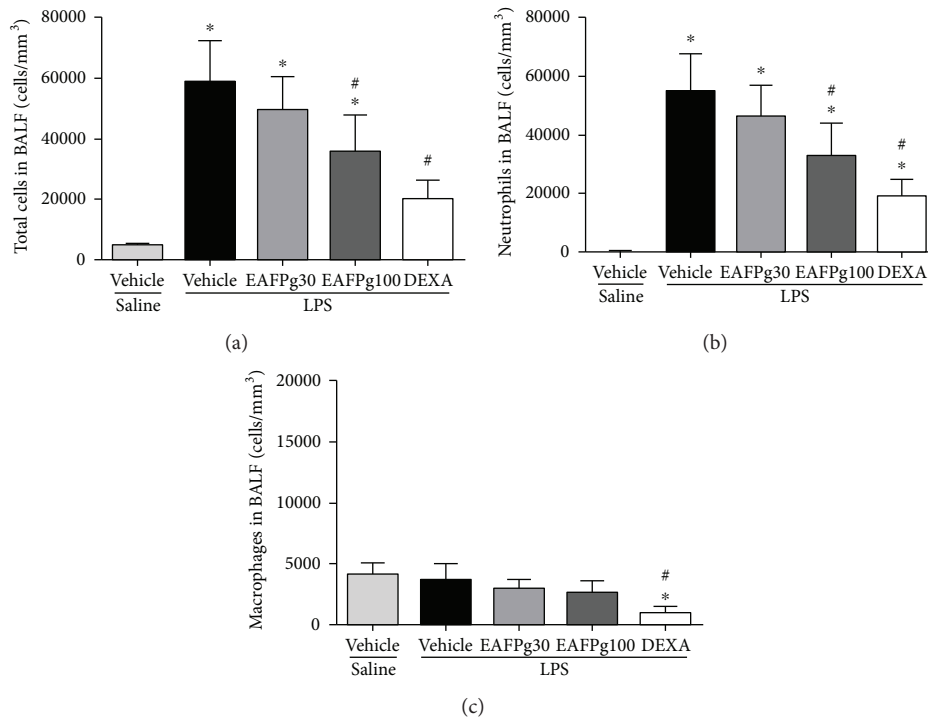


FIGURE 6: Effects of the pretreatment with EAFPg on the numbers of total leukocytes (a), neutrophils (b), or macrophages (c) in BALF and total leukocytes in the lungs. Animals were randomly distributed into five groups ( $n = 6/\text{group}$ ). Mice received in the prophylactic scheme EAFPg (30 mg/kg and 100 mg/kg, p.o.), dexamethasone (DEXA, 10 mg/kg, p.o.), or vehicle (PBS, p.o.). The values are presented as the mean  $\pm$  SD. Significances were calculated by one-way ANOVA followed by the Newman-Keuls multiple comparison test analysis versus nonpretreated saline-injected mice ( $*p < 0.05$ ) and versus nonpretreated LPS-installed mice ( $\#p < 0.05$ ).



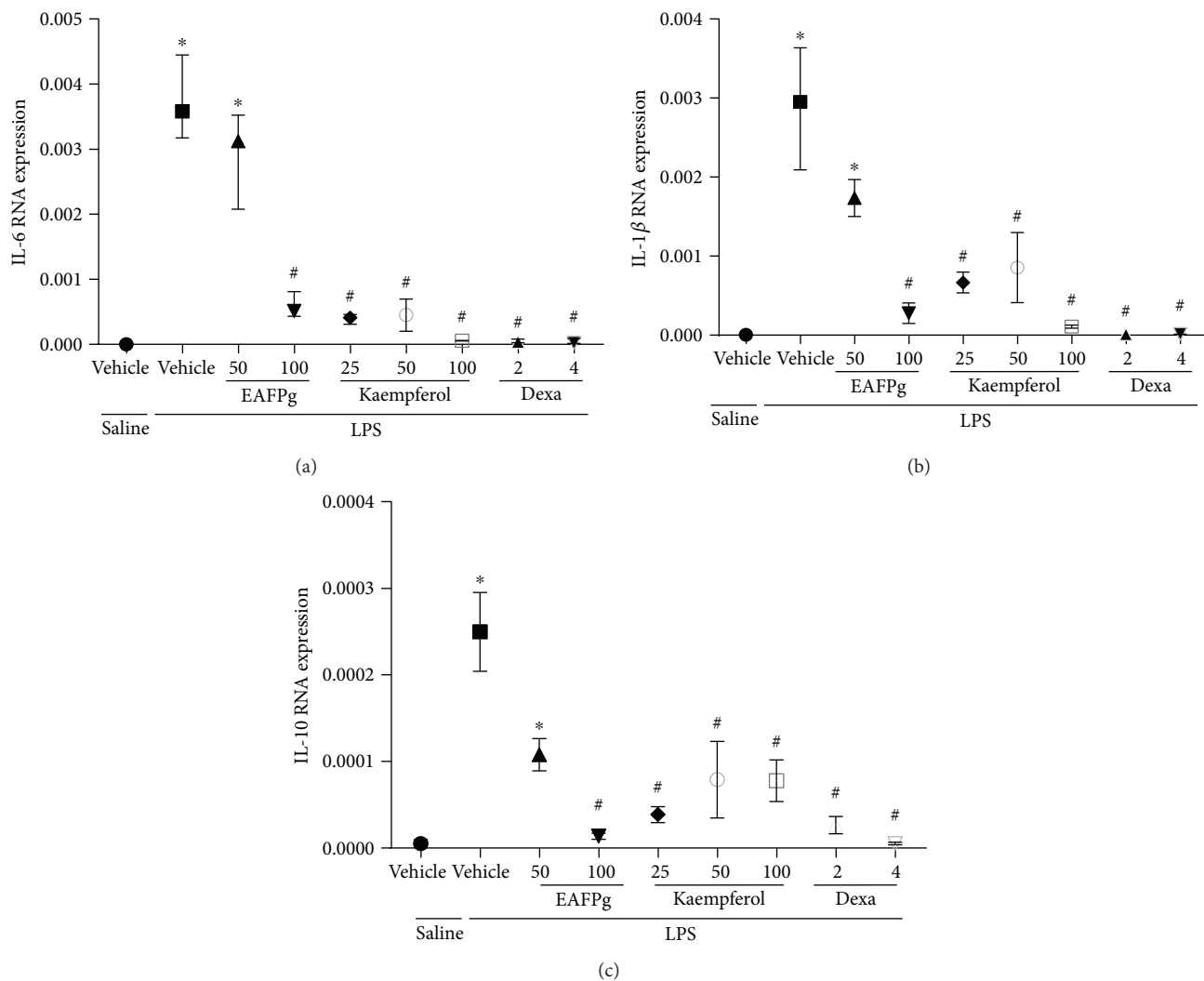


FIGURE 7: Effect of the pretreatment with EAFPg (50–100  $\mu\text{g/ml}$ ) or kaempferol (25–100  $\mu\text{g/ml}$ ) on IL-6 (a), IL-1 $\beta$  (b), and IL-10 (c) mRNA expression in RAW 264.7 macrophages. Data is expressed as mean  $\pm$  SD. Significances were calculated by one-way ANOVA followed by the Newman-Keuls multiple comparison test analysis. \* $p < 0.05$  differs from saline-treated cells; # $p < 0.05$  differs from vehicle-treated LPS-stimulated cells.

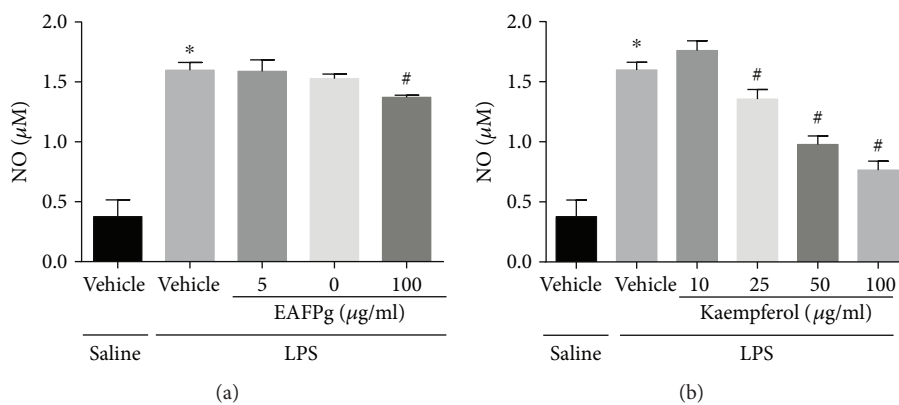


FIGURE 8: Effect of the pretreatment with EAFPg (50–100  $\mu\text{g/ml}$ ) (a) or kaempferol (25–100  $\mu\text{g/ml}$ ) (b) on NO release by RAW 264.7 macrophages. Data is expressed as mean  $\pm$  SD. Significances were calculated by one-way ANOVA followed by the Newman-Keuls multiple comparison test analysis. \* $p < 0.05$  differs from saline-treated cells; # $p < 0.05$  differs from vehicle-treated LPS-stimulated cells.

and neutrophil recruitment to the BALF of mice with ALI induced by acid [15]. However, kaempferol was found to be the major compound in EAFPg. Thus, we hypothesized that EAFPg is anti-inflammatory probably due to the content of kaempferol in its composition.

In patients with ALI, one of the main pathological changes observed in their lungs is an intense inflammatory infiltrate as a consequence of the increased permeability of the alveolar-capillary barrier and epithelial damage. In our study, it was observed that EAFPg suppresses lung inflammation and collagen deposition in the airways of mice intranasally challenged with LPS. Corroborating these findings, de Oliveira et al. [10] showed that the crude extract obtained from pomegranate leaves inhibits the pathological changes induced by ovalbumin in the lung tissue.

The inflammatory infiltrate observed in ALI results from intense and persistent inflammation. Initially, the inflammation is provoked by lung-resident macrophages that activate intracellular mediators after interacting with pathogen-associated molecular patterns, such as LPS. It was not observed that increased migration of monocyte-derived macrophages to the lung suggested that 4 hours is not enough for its migration. Large amounts of cytokines were primarily produced and released by lung-resident macrophages in response to LPS [16]. Therefore, to further evaluate the effects of the EAFPg on lung inflammation, we measured the inflammatory markers TNF- $\alpha$ , IL1- $\beta$ , and IL-6. We found that the pretreatment with EAFPg reduces the gene expression of these mediators in the lung tissue. TNF- $\alpha$  protein levels were also attenuated in the same mice. Additionally, cytokine mRNA expression was potently attenuated in LPS-stimulated macrophages treated with EAFPg or kaempferol. It was previously demonstrated that the hydroalcoholic extract from pomegranate leaves reduces TNF- $\alpha$  mRNA expression in peritoneal leukocytes obtained from rats with LPS-induced peritonitis [8].

TNF- $\alpha$  induces the expression of adhesion molecules on endothelial cells, thus contributing to neutrophil migration. In ALI, neutrophils are the first cells to be recruited into the lungs [17]. In the present study, we demonstrated that EAFPg reduces neutrophil migration into the alveoli. Accordingly, Bachoual et al. [18] showed that an aqueous extract of *P. granatum* peel inhibits neutrophil-mediated myeloperoxidase activity and attenuates LPS-induced lung inflammation in mice. In addition, Marques et al. [8] showed that the numbers of peritoneal leukocytes, especially neutrophils, are reduced in hydroalcoholic extract-treated rats with acute peritonitis.

Taken together, our data demonstrate that EAFPg may be used as food supplements, like tea, to prevent inflammatory disorders in which neutrophils play an essential role, such as ALI. However, further studies are necessary in order to address the effects of EAFPg in later time points of ALI.

## Conflicts of Interest

The authors declare that there is no commercial or financial relationship that could be construed as a potential conflict of interest.

## Authors' Contributions

Aruanã Joaquim Matheus Costa Rodrigues Pinheiro, Eduardo Martins de Sousa, Cinara Regina Aragão Vieira Monteiro, Valério Monteiro-Neto, Patrícia Maria Wiziack Zago, and Lidio Gonçalves Lima-Neto contributed to the conception and the design of the work. Aruanã Joaquim Matheus Costa Rodrigues Pinheiro, Jaciara Sá Gonçalves, Natilene Mesquita Brito, Lanna Karinny Silva, Ádylla Wilenna Alves Dourado, Elizabeth Soares Fernandes, and Lidio Gonçalves Lima-Neto contributed to the data acquisition and performed the experiments. Joicy Cortez de Sá, Marisa Cristina Aranha Batista, Elizabeth Soares Fernandes, Valério Monteiro-Neto, Lee Ann Campbell, and Lidio Gonçalves Lima-Neto wrote the manuscript. Aruanã Joaquim Matheus Costa Rodrigues Pinheiro, Natilene Mesquita Brito, Lanna Karinny Silva, and Marisa Cristina Aranha Batista characterized the pomegranate leaf extract. Aruanã Joaquim Matheus Costa Rodrigues Pinheiro, Jaciara Sá Gonçalves, Ádylla Wilenna Alves Dourado, Eduardo Martins de Sousa, Natilene Mesquita Brito, Lanna Karinny Silva, Marisa Cristina Aranha Batista, Joicy Cortez de Sá, Cinara Regina Aragão Vieira Monteiro, Elizabeth Soares Fernandes, Valério Monteiro-Neto, Lee Ann Campbell, and Lidio Gonçalves Lima-Neto critically revised the manuscript for important intellectual content and gave the final approval of the version to be published.

## Acknowledgments

This work was supported by the Fundação de Amparo à Pesquisa e ao Desenvolvimento Científico e Tecnológico do Maranhão (FAPEMA, Brazil; no. 00516-14) and Coordenação de Aperfeiçoamento de Pessoal de Nível Superior (CAPES, Brazil; no. 3325/2013).

## References

- [1] S. Sarwar, Z. S. Lin, C. F. Ku et al., "Protective effect of dihydro-resveratrol against lung injury in rats with cerulein-induced acute pancreatitis," *Planta Medica*, vol. 81, no. S 01, pp. S1-S381, 2016.
- [2] R. Tanaka, Y. Ishima, Y. Enoki et al., "Therapeutic impact of human serum albumin-thioredoxin fusion protein on influenza virus-induced lung injury mice," *Frontiers in Immunology*, vol. 5, p. 561, 2014.
- [3] S. K. Sahetya, E. C. Goligher, and R. G. Brower, "Fifty years of research in ARDS. Setting positive end-expiratory pressure in the acute respiratory distress syndrome," *American Journal of Respiratory and Critical Care Medicine*, vol. 195, no. 11, pp. 1429-1438, 2017.
- [4] T. R. Ramalho, M. T. Oliveira, A. L. Lima, C. R. Bezerra-Santos, and M. R. Piuvezam, "Gamma-terpinene modulates acute inflammatory response in mice," *Planta Medica*, vol. 81, no. 14, pp. 1248-1254, 2015.
- [5] M. I. Bittencourt-Mernak, N. M. Pinheiro, F. P. Santana et al., "Prophylactic and therapeutic treatment with the flavonone sakuranetin ameliorates LPS-induced acute lung injury," *American Journal of Physiology Lung Cellular and Molecular Physiology*, vol. 312, no. 2, pp. L217-L230, 2016.

- [6] E. P. Lansky and R. A. Newman, "Punica granatum (pomegranate) and its potential for prevention and treatment of inflammation and cancer," *Journal of Ethnopharmacology*, vol. 109, no. 2, pp. 177–206, 2007.
- [7] M. K. Reddy, S. K. Gupta, M. R. Jacob, S. I. Khan, and D. Ferreira, "Antioxidant, antimalarial and antimicrobial activities of tannin-rich fractions, ellagitannins and phenolic acids from *Punica granatum* L.," *Planta Medica*, vol. 73, no. 5, pp. 461–467, 2007.
- [8] L. C. Marques, A. J. Pinheiro, J. G. Araujo et al., "Anti-inflammatory effects of a pomegranate leaf extract in LPS-induced peritonitis," *Planta Medica*, vol. 82, no. 17, pp. 1463–1467, 2016.
- [9] A. Haseeb, N. M. Khan, O. S. Ashruf, and T. M. Haqqi, "A polyphenol-rich pomegranate fruit extract suppresses NF- $\kappa$ B and IL-6 expression by blocking the activation of IKK $\beta$  and NIK in primary human chondrocytes," *Phytotherapy Research*, vol. 31, no. 5, pp. 778–782, 2017.
- [10] J. F. de Oliveira, D. V. Garreto, M. C. da Silva et al., "Therapeutic potential of biodegradable microparticles containing *Punica granatum* L. (pomegranate) in murine model of asthma," *Inflammation Research*, vol. 62, no. 11, pp. 971–980, 2013.
- [11] L. G. Lima-Neto, R. D. Hirata, A. D. Luchessi et al., "Chlamydia pneumonia and increased TLR4 gene expression in leukocytes are associated with acute myocardial infarction," *Journal of Biological Regulators and Homeostatic Agents*, vol. 28, no. 3, pp. 449–460, 2014.
- [12] J. Mo, P. Panichayupakaranant, N. Kaewnopparat, A. Nitruangjaras, and W. Reanmongkol, "Topical anti-inflammatory and analgesic activities of standardized pomegranate rind extract in comparison with its marker compound ellagic acid in vivo," *Journal of Ethnopharmacology*, vol. 148, no. 3, pp. 901–908, 2013.
- [13] T. Ismail, P. Sestili, and S. Akhtar, "Pomegranate peel and fruit extracts: a review of potential anti-inflammatory and anti-infective effects," *Journal of Ethnopharmacology*, vol. 143, no. 2, pp. 397–405, 2012.
- [14] X. Chen, X. Yang, T. Liu et al., "Kaempferol regulates MAPKs and NF- $\kappa$ B signaling pathways to attenuate LPS-induced acute lung injury in mice," *International Immunopharmacology*, vol. 14, no. 2, pp. 209–216, 2012.
- [15] D. Cornelio Favarin, M. Martins Teixeira, E. Lemos de Andrade et al., "Anti-inflammatory effects of ellagic acid on acute lung injury induced by acid in mice," *Mediators of Inflammation*, vol. 2013, Article ID 164202, 13 pages, 2013.
- [16] J. M. Nicholls, L. L. Poon, K. C. Lee et al., "Lung pathology of fatal severe acute respiratory syndrome," *The Lancet*, vol. 361, no. 9371, pp. 1773–1778, 2003.
- [17] R. Jose, A. Williams, M. Sulikowski, D. Brealey, J. Brown, and R. Chambers, "Regulation of neutrophilic inflammation in lung injury induced by community-acquired pneumonia," *The Lancet*, vol. 385, article S52, Supplement 1, 2015.
- [18] R. Bachoual, W. Talmoudi, T. Boussetta, F. Braut, and J. El-Benna, "An aqueous pomegranate peel extract inhibits neutrophil myeloperoxidase in vitro and attenuates lung inflammation in mice," *Food and Chemical Toxicology*, vol. 49, no. 6, pp. 1224–1228, 2011.

## Review Article

# Prevention and Treatment of Osteoporosis Using Chinese Medicinal Plants: Special Emphasis on Mechanisms of Immune Modulation

Hongyan Zhao <sup>1,2</sup>, Ning Zhao,<sup>3</sup> Peng Zheng,<sup>4</sup> Xiaohong Xu,<sup>5</sup> Meijie Liu,<sup>1,2</sup> Dan Luo,<sup>6</sup> Huihui Xu <sup>1</sup> and Dahong Ju <sup>1,2</sup>

<sup>1</sup>Experimental Research Center, China Academy of Chinese Medical Sciences, Beijing 100700, China

<sup>2</sup>Institute of Basic Theory for Chinese Medicine, China Academy of Chinese Medical Science, Beijing 100700, China

<sup>3</sup>Institute of Clinical Basic Medicine, China Academy of Chinese Medical Sciences, Beijing 100700, China

<sup>4</sup>Jilin Provincial Hospital of Traditional Chinese Medicine, Changchun University of Chinese Medicine, Changchun 130021, China

<sup>5</sup>Changchun University of Chinese Medicine, Changchun 130117, China

<sup>6</sup>Traditional Chinese Medicine Hospital of Changping District, Beijing 102200, China

Correspondence should be addressed to Dahong Ju; [judahong@126.com](mailto:judahong@126.com)

Received 24 August 2017; Revised 5 November 2017; Accepted 6 December 2017; Published 20 February 2018

Academic Editor: Wuxiang Xie

Copyright © 2018 Hongyan Zhao et al. This is an open access article distributed under the Creative Commons Attribution License, which permits unrestricted use, distribution, and reproduction in any medium, provided the original work is properly cited.

Numerous studies have examined the pathogenesis of osteoporosis. The causes of osteoporosis include endocrine factors, nutritional status, genetic factors, physical factors, and immune factors. Recent osteoimmunology studies demonstrated that the immune system and immune factors play important regulatory roles in the occurrence of osteoporosis, and people should pay more attention to the relationship between immunity and osteoporosis. Immune and bone cells are located in the bone marrow and share numerous regulatory molecules, signaling molecules, and transcription factors. Abnormal activation of the immune system alters the balance between osteoblasts and osteoclasts, which results in an imbalance of bone remodeling and osteoporosis. The incidence of osteoporosis is also increasing with the aging of China's population, and traditional Chinese medicine has played a vital role in the prevention and treatment of osteoporosis for centuries. Chinese medicinal plants possess unique advantages in the regulation of the immune system and the relationships between osteoporosis and the immune system. In this review, we provide a general overview of Chinese medicinal plants in the prevention and treatment of osteoporosis, focusing on immunological aspects.

## 1. Introduction

Osteoporosis is a systemic skeletal disease characterized by a decrease in bone mass and microstructural degradation, which may increase bone fragility and fracture danger and consequently cause serious complications [1]. The etiology of osteoporosis is primarily concentrated in endocrine and metabolic disorders. However, osteoimmunology demonstrated that the immune system and immune factors may be involved in the development of osteoporosis and play important regulatory roles [2, 3]. The microenvironment created by bone cells provides conditions for development of the immune system, which regulates bone metabolism via B cells,

T cells, dendritic cells, and many cytokines [2–5]. Abnormal activation of the immune system alters the balance between osteoblasts and osteoclasts, which results in an imbalance in bone remodeling and causes osteoporosis [6–8].

Osteoporosis seriously affects human health, and there is no safe and effective method to restore lost bone. However, Chinese medicinal plants reduce bone loss and treat osteoporosis [9, 10]. Chinese medicinal plants possess unique advantages in the regulation of the immune system [11–18] and alter the relationships between osteoporosis and the immune system [3, 4, 7]. This review summarizes the progress of Chinese medicinal plants in the prevention and treatment of osteoporosis, focusing on the immunological aspects.

## 2. Immune System and Osteoporosis

The immune system is an important regulator of bone turnover. Therefore, the relationship between the immune system and bone is generally defined as “osteimmunology.” Osteoimmunology is a new interdisciplinary research field that focuses on the interactions between the immune system and bone at the anatomical, vascular, cellular, and molecular levels [19–21]. Osteoimmunology provides new pathogenetic and clinical interpretations for osteoporosis [6]. Many signaling factors and cytokines are involved in this field [22]. However, osteoprotegerin (OPG)/the receptor activator of nuclear factor- $\kappa$ B (RANK)/RANKL signaling is a key vinculum that is essential for osteoclastogenesis and immune regulation [4, 23]. Proinflammatory cytokines, such as tumor necrosis factor- (TNF-)  $\alpha$ , interleukin- (IL-) 1, and IL-17, also play pivotal roles in osteoimmunology [24]. Therefore, abnormalities of the immune system may cause bone diseases, such as osteoporosis and inflammatory bone loss [25]. Balancing the immune response promotes the formation of bone tissue, so as to improve osteoporosis.

**2.1. RANK/RANKL/OPG Signaling Pathway.** A functional imbalance between osteoblasts and osteoclasts causes osteoporosis. As a hallmark of osteoporosis, the increased activation of osteoclasts results in the progressive loss of bone mass and an increased susceptibility to bone fractures. RANKL is a TNF family cytokine that is primarily expressed by osteoblasts and also secreted by bone marrow stromal cells (BMSCs), preosteoblasts, osteocytes, fibroblasts, and cells of the immune system, including antigen-stimulated T cells and mature dendritic cells. Osteoclast differentiation is initiated via the binding of RANKL to RANK [26]. RANKL-RANK interaction activates the master transcription factor for osteoclastogenesis; nuclear factor of activated T cells, cytoplasmic 1 (NFATc1); tartrate-resistant acid phosphatase; calcitonin receptor; and cathepsin K [27]. OPG is produced by osteoblasts, BMSCs, B cells, and dendritic cells, is a soluble decoy receptor for RANKL, and prevents RANKL from binding to RANK on the surface of osteoclastic lineage cells [28, 29]. The relative ratio of RANKL to OPG is the critical determinant and the final step in the regulation of osteoclast biology and bone resorption. Therefore, dysregulation of the immune system may affect bone remodeling, and the immune system regulates bone metabolism primarily via the RANK/RANKL/OPG signaling pathway [30–33]. Various osteotropic hormones, cytokines, and drugs modulate the RANKL-to-OPG ratio [32, 34, 35].

### 2.2. Immune Cell

**2.2.1. T Cells.** The primary pathological process of osteoporosis is the imbalance of bone resorption and bone formation during bone remodeling. T cells regulate bone cells and hematopoiesis in the immune system, and these cells secrete inflammatory factors and Wnt ligands to promote bone formation and absorption [2, 3, 36]. T cells also regulate the dynamic balance of metabolism between bone mesenchymal cells and osteoblasts via CD40 ligands and costimulatory

molecules [37]. However, the stimulating and inhibiting effects of T cells are related to their subsets, cytokines, and local factors.

T cells may be generally classified as effector-cytotoxic T cells (CD8<sup>+</sup> cells) and T helper (Th) cells (CD4<sup>+</sup> cells). CD4<sup>+</sup> T cells develop into diverse Th cell subsets on activation and expansion and secrete signature cytokine profiles and mediate distinct effector functions [38]. T cells were divided into Th1 or Th2 cells depending on the cytokines produced, with Th1 producing IFN- $\gamma$  and IL-2 and Th2 producing primarily IL-4/IL-5/IL-10, until recently. Regulatory T cells (Tregs, CD4<sup>+</sup>CD25<sup>+</sup>Foxp3<sup>+</sup>) exhibit immune suppressive effects in the immune system, regulate bone remodeling, and are closely linked to skeletal-related disease, such as osteoporosis and rheumatoid arthritis (RA) [39, 40]. Tregs suppress osteoclastogenesis via the production of transforming growth factor- (TGF-)  $\beta$ , IL-10, and IL-4 [41, 42] and also regulate osteoclast differentiation via the cytotoxic T lymphocyte antigen (CTLA-4) [43, 44].

A third subset of IL-17-producing effector Th cells, called Th17 cells, was more recently discovered and characterized. Th17 cells play an important role in the pathogenesis of osteoporosis and directly produce high levels of IL-17, RANKL, and TNF to promote the formation and activation of osteoclasts [38, 45, 46]. Th17 cell populations and IL-17 levels were obviously increased in an osteoporosis model of ovariectomized (OVX) animals. Transcription factors related to Th17 cell differentiation are highly expressed [47]. IL-17 significantly promotes the production of RANKL, IL-6, and TNF, which promote bone resorption via upregulation of osteoclast formation [48, 49]. Th17 cells are responsible for regulating osteoclastogenesis, especially in autoimmune arthritis.

**2.2.2. B Cells.** The role of B cells in osteoimmunological interactions has been a matter of great concern. To our knowledge, B cells are active regulators of the RANK/RANKL/OPG system [23]. Bone-forming osteoblasts and BMSCs have historically been considered an important source of OPG under conditions of physiological bone remodeling. However, some studies demonstrated that B cells and plasma cells in the bone microenvironment are significant sources of OPG [50–52], which is a neutralizing soluble decoy receptor that competes with RANKL, thus blocking the binding of RANKL and RANK, which eliminates the effect of RANKL on osteoclasts [53]. However, other studies also demonstrated that activated B cells contributed to joint destruction via RANKL expression [54–57]. Xu et al. further demonstrated that mechanistic target of rapamycin complex 1 activation-stimulated RANKL expression in B cells sufficiently induced bone loss and osteoporosis [58].

**2.3. Cytokines.** A variety of cytokines are involved in the pathogenic process of osteoporosis. Recent studies showed that women with low bone mineral density (BMD) exhibited a proresorptive cytokine bias [59]. The proresorptive cytokines TNF, IL-6, IL-12, and IL-17 were higher in women with low BMD compared to women with normal BMD, and the antiresorptive cytokines IL-4, IL-10, and IL-23 were lower

in peripheral blood mononuclear cells (PBMCs). Estrogen decrease after menopause exerts the same stimulating effect, which increases osteoclastic activity via IL-1, IL-6, and TNF- $\alpha$  [60, 61]. IL-1 is a very important cytokine in osteoimmunological processes, and it acts as the primary stimulus of osteoclast-activating factor. TNF- $\alpha$  and IL-6 possess the same bone resorbing stimulating activity, and these three cytokines increase the osteoclast response to RANKL, which leads to osteolysis. OPG/RANK/RANKL signaling is the most important vinculum for osteoclastogenesis, and most cytokines exert effects via this pathway. RANKL and macrophage colony-stimulating factor (M-CSF) are the minimal necessary cytokines required for osteoclast formation [61]. M-CSF induces the proliferation and differentiation of osteoclast precursors and improves the survival of mature osteoclasts. Other inflammatory cytokines, such as IL-4, IL-10, IL-12, IL-13, IL-18, and interferon- $\gamma$ , strongly inhibit osteoclastogenesis and reduce bone loss [62–65].

**2.4. Autoimmune Diseases.** Autoimmune diseases, such as RA, ankylosing spondylitis (AS), systemic lupus erythematosus, and acquired immune deficiency syndrome, involve the damage to joints and bone. RA is characterized by synovial inflammation that results in severe juxta-articular bone erosions and systemic osteoporosis. Previous research showed a greater risk of osteoporotic fractures in RA patients across all age groups, sex, and various anatomic sites compared to non-RA patients [66]. Lower BMD of the lumbar spine and hip was reported in AS patients compared to a control group [67], and 21% of AS patients exhibited osteoporotic vertebral compression fractures, which was 5 times greater than the control population [68].

Associations between osteoclast and proinflammatory cytokines may partially explain the cause of osteoporosis in autoimmune diseases. Active immune cells at sites of inflammation produce proinflammatory and osteoclastogenic cytokines, which lead to bone erosions and peri-inflammatory and systemic bone loss. Proinflammatory cytokines, such as TNF- $\alpha$ , IL-1, IL-6, and IL-17, are higher in RA patients, which increase RANKL expression and cause bone loss [69]. Peri-inflammatory bone formation is impaired, which results in nonhealing of erosions and a local vicious circle of inflammation between synovitis, osteitis, and local bone loss.

### 3. Immunoregulation Mechanisms of Chinese Medicinal Plants in the Prevention and Treatment of Osteoporosis

Many plants in China are used for the prevention and treatment of bone and joint diseases, such as bone pain, osteoporosis, osteoarthritis, and RA. Compounds consisting primarily of these plants, such as Liuwei Dihuang pills (LWDHP) and Zuo-Gui-Wan (ZGW), play important roles in clinical treatment. Many studies investigated the important role in prevention and treatment of osteoporosis [70], and rapid progress has been made in delineating the mechanisms. Therefore, we discuss and summarize the

mechanism of some representative Chinese medicinal plants and compounds, especially immunoregulation (Table 1).

#### 3.1. Chinese Medical Plants and Its Monomer

**3.1.1. *Sinomenium acutum* (Thunb.) Rehd. et Wils. and SIN.** *Sinomenium acutum* (Thunb.) Rehd. et Wils. has been used as a natural drug to treat rheumatic diseases in China for centuries. SIN was isolated from the root and stem of *Sinomenium acutum* (Thunb.) Rehd. et Wils. in the 1920s [71], and it exhibited good anti-inflammatory and immunoregulatory properties [72].

Liu et al. [73] found that SIN significantly inhibited [ $^3$ H]-thymidine incorporation into mouse spleen cells activated with concanavalin A. The Th1-specific transcription factor T-bet is selectively expressed in Th1 cells and plays an important role in the development of Th1 cells via initiation of Th1 genetic processes and inhibition of the synthesis of Th2 cytokines. GATA-3 is a Th2 cell-specific transcription factor that is directly involved in the regulation of the differentiation of T lymphocytes, induces the generation of Th2 cells, eosinophil differentiation, and the regulation of eosinophil and natural killer cells; GATA-3 also inhibits the CD8 $^+$  T lymph cell differentiation and maturation. One clinical trial demonstrated that SIN decreased the expression of T-bet mRNA and IFN- $\gamma$  and regulated the ratio of T-bet and GATA-3 and Th1/Th2 cytokine balance in mesangial proliferative nephritis [74]. The novel derivatives of SIN directly inhibited Th17 cell differentiation and alleviated the inflammatory symptoms of experimental autoimmune encephalomyelitis [75].

SIN is widely used in the treatment of inflammatory diseases, especially RA. SIN significantly improved arthritis in rats via inhibition of synovial fibroblast proliferation and anti-type II collagen antibody levels [76, 77] and regulation of Th1/Th2 and the ratio of MMPs and their endogenous inhibitors, called TIMPs [77, 78]. Recent studies demonstrated that SIN modulated bone metabolism via suppression of osteoclastogenesis and related transduction signals. Li et al. demonstrated that SIN suppressed osteoclast formation and bone loss via modulation of RANKL signaling pathways [79] and Zhou et al. [80] revealed that SIN was a proinflammatory mediator that regulated the immunosuppressive effects of marrow stromal cells and inhibited osteoclast differentiation via inhibition of the PGE $_2$ -induced OPG/RANKL ratio. Further studies revealed that SIN inhibited the activation and relative gene expression of NF- $\kappa$ B, AP-1, and NFAT and downregulated phosphorylation of MAPK p38 in osteoclastogenesis via reduction of Toll-like receptor 4/TRAF6 expression [81]. Therefore, SIN may be a promising agent for the treatment of osteoporosis.

**3.1.2. *Davallia mariesii* Moore ex Bak. and Naringin.** Naringin is widely distributed in various types of plants, and it is a major component extracted from the Chinese medicinal herb *Davallia mariesii* Moore ex Bak. This herb exhibits inhibitory effects on inflammatory responses and bone destruction and anabolic effects on bone in clinical treatment. The experimental results confirmed that naringin inhibited

TABLE 1: Chinese medicinal plant targets involved in immunoregulation effects.

Chinese medicinal plants or compounds	Pharmacological effects	Target factors	Action	Model	Reference
SIN	Immunoregulation	T-bet/GATA-3	T-bet/GATA-3 ratio ↓ from PBMCs, IFN- $\gamma$ in the serum ↓	MsPGN	[74]
1032 (a derivative of SIN)	Inflammatory reaction	IL-17	IL-17, IL-6, TNF- $\alpha$ ↓, I $\kappa$ B $\alpha$ ↑, suppression of Th17	Encephalomyelitis/dendritic cells	[75]
SIN	Immunoregulation	MMPs/TIMPs	Synovial fibroblast proliferation, anti-type II collagen antibodies, IL-1 $\beta$ , IL-6, IL-5, TGF- $\beta$ ↓, the ratio of MMPs/TIMPs ↓	Arthritis rats	[76-78]
SIN	Inflammatory reaction	TLR4/TRAF6	TNF- $\alpha$ , TLR4, TRAF6, Fra-1, MMP-9, NF- $\kappa$ B, AP-1, NFAT, MAPK p38 ↓	Lipopolysaccharide-induced osteoclastogenesis and osteolysis	[81]
Naringin	Inflammatory reaction	Inflammatory cells	Inflammatory cells, high-mobility group box-1 ↓	Arthritis mice	[82]
Icaritin	Immunoregulation	TRAF6	NFATc1, TRAF6 ↓	O VX rat/RAW 264.7 mouse monocyte cell line/human PBMC	[98]
<i>Eucommia ulmoides</i>	Inflammatory reaction	Inflammatory cytokines	TNF- $\alpha$ , IL17, IL-1 $\beta$ ↓, IL-10 ↑	Arthritis rats	[107]
<i>Eucommia ulmoides</i>	Inflammatory reaction	PI3K/Akt, inflammatory cytokines	IL-1 $\beta$ , IL-6, MMP-3, phosphorylated MAPKs, PI3K/Akt, GSK-3 $\beta$ , NF- $\kappa$ B ↓, Nrf2, HO-1 ↑	Osteoarthritis rats/LPS-stimulated BV-2 microglial cells	[108, 109]
<i>Quercetin</i>	Inflammatory reaction	NF- $\kappa$ B	IL-6, IL-1 $\alpha$ ↓, IL-3, IL-4 ↑	RAW 264.7 cells	[112]
LWDHP	Immunoregulation	Inflammatory cytokines	IL-2 ↓, interferon- $\gamma$ , IL-4, IL-10 ↑	Adjuvant arthritis rats	[129]
ZGW	Immunoregulation	Th17/Treg	IL-6, ROR $\gamma$ t ↓, Foxp3 ↑	Estrogen-deficient mice	[133]

Sinomenine (SIN); mesangial proliferative glomerulonephritis (MsPGN); matrix metalloproteinases (MMPs); tissue inhibitors of metalloproteinases (TIMPs); tumor necrosis factor receptor associated-factor 6 (TRAF6); Fos-related antigen-1 (Fra-1); activator protein-1 (AP-1); nuclear factor of activated T cells (NFAT) c1; mitogen-activated protein kinases (MAPK); lipopolysaccharide (LPS); Toll-like receptor 4 (TLR4); phosphoinositide-3 kinase (PI3K); nuclear factor- $\kappa$ B (NF- $\kappa$ B); glycogen synthase kinase-3 $\beta$  (GSK-3 $\beta$ ); nuclear factor erythroid 2-related factor 2 (Nrf2); heme oxygenase-1 (HO-1), related orphan receptor gamma t (ROR $\gamma$ t).

inflammation via reduction of inflammatory cytokine and NF- $\kappa$ B expression [82].

Naringin exhibited some therapeutic effects on osteoporosis in animal experiments. Naringin inhibited tartrate-resistant acid phosphatase activity, decreased RANKL expression, inhibited osteoclast activity, reduced bone loss, and decreased BMD, which altered bone resorption. Further study demonstrated that naringin inhibited osteoclast activity via inhibition of RANK-mediated NF- $\kappa$ B and extracellular regulated protein kinase signaling [83]. Naringin increased osteoblast proliferation by increasing BMP-2 expression via PI3K, Akt, c-Fos/c-Jun, and the AP-1 pathway [84]. Wong et al. and Pang et al. also found that naringin increased osteopontin and osteoprotegerin expression and osteocalcin [85, 86]. Naringin promoted the osteogenic differentiation of BMSCs by upregulating Foxc2 expression via the IHH signaling pathway [87].

**3.1.3. *Epimedium davidii* Franch., Icariin, and Icaritin.** *Epimedium davidii* Franch. has been used for centuries to treat osteoporosis, based on the function of “strengthening” bones. Icariin is the primary active flavonoid glucoside isolated from *Epimedium davidii* Franch., and it is highly related to the therapeutic effects of this herb. However, its bone-strengthening activity attracted much more attention in recent years. Icariin enhances antiosteoporotic activity by initiating osteoblastic differentiation and mineralization, inhibiting adipogenesis, preventing osteoclast differentiation, and inducing apoptosis of osteoclasts, which decrease bone resorption and bone loss [88–92]. Liu et al.’s research indicated that icariin suppressed the differentiation of mesenchymal stem cells into adipocytes via inhibition of peroxisome proliferator-activated receptor gamma, CCAAT/enhancer binding protein  $\alpha$ , fatty acid-binding protein 4 mRNA, N1ICD, and jagged1 protein expression and increasing Notch2 mRNA in OVX rats, which improved osteoporosis [93]. Further research indicated that icariin also promoted bone fracture healing in OVX osteoporotic rats [94, 95]. Icariin could increase the proliferation and matrix mineralization of osteoblasts and promote NO synthesis. Further study showed that with icariin treatment, the BMP-2, SMAD4, Cbfa1/Runx2, and OPG gene expressions were upregulated; the RANKL gene expression was however downregulated. This effect may contribute to its action on the induction of osteoblast proliferation and differentiation, resulting in bone formation [96]. Liang’s results also indicated that icariin could promote bone formation via the BMP-2/Smad4 signal pathway in hFOB 1.19 cells then promote bone formation [97].

Icaritin, an internal metabolite of icariin, possesses similar function with icariin. Icaritin inhibited osteoclast formation via the downregulation of TRAF6 and coordinated inhibition of NF- $\kappa$ B, MAPK/AP-1, and reactive oxygen species signaling pathways to reduce NFATc1 expression and activity in vitro and in an OVX rat [98]. Wu et al. and Sheng et al. indicated that icaritin enhanced the osteogenic differentiation of derived mesenchymal stem cells and human adipose tissue-derived stem cells by increasing the protein levels of BMPs, Runx2, and osteocalcin [99] and inhibiting

adipogenesis of marrow mesenchymal stem cells via suppression of glycogen synthase kinase-3 $\beta$  and peroxisome proliferator-activated receptor gamma [100].

**3.1.4. *Eucommia ulmoides* and Quercetin.** *Eucommia ulmoides* is a kidney-tonifying herbal medicine in China with a long history for treatment of bone and joint diseases, such as osteoporosis, osteoarthritis, and RA. *Eucommia ulmoides* and its extracts participate in bone metabolism via activation of osteoblasts to facilitate osteogenesis and suppression of osteoclast activity to inhibit osteolysis [101]. In vivo studies showed that extracts of *Eucommia ulmoides* improve bone biomechanical quality via modification of BMD and trabecular microarchitecture in OVX rats [102–105]. In vitro evidence suggests that extracts of *Eucommia ulmoides* could induce primary osteoblastic cell proliferation and differentiation and inhibit osteoclastogenesis via an increase in OPG and decrease in RANKL expression [106].

An ethanol extract of *Eucommia ulmoides* relieved arthritis degradation via inhibition of the key proinflammatory cytokines TNF- $\alpha$ , IL17, and IL-1 $\beta$  and increases the anti-inflammatory effects of IL-10 [107]. The PI3K/Akt pathway may play an important role in this process. *Eucommia ulmoides* also inhibited the progression of osteoarthritis via inhibition of the PI3K/Akt pathway to reduce inflammatory cytokines, bone destruction, and bone loss [108, 109].

The flavonol glycoside quercetin was isolated from the leaves of *Eucommia ulmoides*, and its structure was identified using NMR and ESIMS analyses [110]. Quercetin exhibited soluble epoxide hydrolase inhibitory activity and anti-inflammatory properties, partially because of its capacity to downmodulate the NF- $\kappa$ B signal transduction pathway [111–114]. Quercetin suppressed osteoclastogenesis in vitro and prevented bone loss in OVX mice in vivo [115, 116]. Yamaguchi and Weitzmann found that quercetin potently suppressed osteoclastogenesis and RANKL-induced NF- $\kappa$ B activation in osteoclast precursors [117]. Guo et al. also found that quercetin inhibited RANK, TRAF6, and COX-2 expression, induced apoptosis, and inhibited bone resorptive activity in LPS-induced mature osteoclasts. Quercetin promoted the apoptotic signaling pathway, including increasing the phosphorylation of p38-MAPK, c-Jun N-terminal kinases/stress-activated protein kinases (JNK/SAPK), and Bax and inhibited Bcl-2 expression [118]. Some studies demonstrated that quercetin exerted a stimulatory effect on bone formation and reversed the inhibition of osteoblast differentiation induced by LPS via MAPK signaling in vitro [119, 120].

**3.1.5. Other Chinese Medicinal Plants and Monomers.** Many Chinese medicinal plants and monomers effectively treat osteoporosis. Echinacoside is isolated from *Cistanche tubulosa* (Schrenk) R. Wight stems, and it exhibited notable antiosteoporotic effects in an OVX rat model of osteoporosis and enhanced bone regeneration in MC3T3-E1 cells in vitro [121]. *Radix Dipsaci* has long been used as an antiosteoporotic drug. *Radix Dipsaci* total saponins are the main active ingredient of *Radix Dipsaci*, and this component effectively suppressed the loss of bone mass in OVX rats [122]. *Achyranthes bidentata* Blume. improved bone biomechanical



quality via modifications of BMD6 and trabecular microarchitecture, which prevented OVX-induced osteoporosis in rats [123]. *Achyranthes bidentata* Blume. and *Panax notoginseng* saponin are the main active components of *Panax notoginseng* that prevent OVX-induced osteoporosis via enhancement of BMD, bone strength, and prevention of the deterioration of trabecular microarchitecture in OVX osteoporosis rats [124]. Diarylheptanoid from *Curcuma comosa* Roxb. decreased NFATc1 and c-Fos expression via the MAPK pathway and inhibited RANKL-induced osteoclast differentiation [125]. The natural compound *Polygonatum sibiricum* polysaccharide promoted osteoblastic differentiation and mineralization via the ERK/GSK-3 $\beta$ / $\beta$ -catenin signaling pathways [126]. These studies provide a therapeutic approach for the use of Chinese plants in the prevention of osteoporosis.

### 3.2. Compound Recipes of Medicinal Plants

**3.2.1. LWDHP.** As a classic formula of traditional Chinese medicine, LWDHP has been used to prevent and treat various diseases with characteristic features of kidney yin deficiency in China for more than 1000 years. LWDHP is widely prescribed as therapy or adjuvant therapy for various diseases, such as menopause, osteoporosis, and diabetes. LWDHP exhibits a wide range of pharmacological effects via regulation of the balance of the neuroendocrine immunomodulation network [127].

LWDHP exhibits bidirectional regulation to the immune system. LWDHP exerted its pharmacological action via immunomodulation rather than immunosuppression, which differs from Cy and CsA [128]. Jian et al. demonstrated that LWDHP significantly inhibited the mRNA expression of IL-1 (Th1 cytokines) and promoted the expression of IFN- $\gamma$  (Th1 cytokines), IL-4 (Th2 cytokines), and IL-10 (Th2 cytokines) in splenocytes of AA rats. These results indicated that LWDHP enhanced the function of splenic Th cells via restoration of Th1 and Th2 cytokine levels and modulation of the balance of the Th1/Th2 [129]. LWDHP also significantly improved the function of T and B lymphocytes in aging mice and corrected the imbalance of CD4<sup>+</sup>/CD8<sup>+</sup> T cells in the spleen.

The mechanism of LWDHP treatment of osteoporosis is also related to its immunomodulatory function. The JAK/STAT signaling pathway plays a vital role in bone metabolism. LWDHP regulates immune function by increasing the expression of the immune-related gene cardiotrophin-like cytokine factor 1 and activation of the JAK/STAT signaling pathway to treat postmenopausal osteoporosis with kidney yin deficiency [130]. Xia et al. suggested that LWDHP could alleviate osteoporosis partially via a significant enhancement in the levels of Lrp-5,  $\beta$ -catenin, Runx2, and Osx, which were involved in the canonical Wnt/ $\beta$ -catenin signaling pathway of osteoblasts, in osteoporosis model induced by ovariectomy and in vitro experiments [131].

**3.2.2. ZGW.** The ZGW is another classical traditional Chinese medicine (TCM) herbal prescription for tonifying kidney

yin. This prescription was recorded in *Jing yue Quan shu*, which is a famous TCM book, in 1624 A.D.

Our results showed that the ZGW significantly increased the expression levels of Wnt1, low-density lipoprotein receptor-related protein 5, and beta-catenin proteins in osteoblasts and BMSCs of glucocorticoid-induced osteoporosis rats after eight weeks of administration [132]. These results indicated that the ZGW prevented and treated osteoporosis, and the Wnt signal transduction pathway played an important role in this progress. The Th17/Treg paradigm plays a vital role in the regulation of bone metabolism. Lai et al. found that the ratio of Th17 and Treg shifted to Th17 in estrogen-deficient OVX and aged mice. Treatment with ZGW markedly enhanced BMD, decreased IL-6 and ROR $\gamma$ t expression, and significantly increased the level of Foxp3. These results indicated that the ZGW could prevent bone loss, and the mechanism was a Th17/Treg paradigm that skewed towards Treg [133].

## 4. Conclusion

Many studies investigate the pathogenesis of osteoporosis, and the immunological regulation of osteoporosis is a new research hotspot that provides a new mechanism of the pathogenesis of osteoporosis. Immune and bone cells exist together in the microenvironment of bone cavities, and these cells share a variety of regulatory molecules. Many cytokines in bone metabolism play a very important role in the proliferation, differentiation, and activation of osteoclasts and osteoblasts. However, the specific mechanisms of these cytokines have not reached an indisputable conclusion, and the role of many cytokines in the process of bone metabolism is not clear.

The clinical efficacy of Chinese medicinal plants has shown their advantages in the treatment of osteoporosis. An increasing number of studies demonstrated that these plants play an important role in the treatment of osteoporosis by regulating the immune system, but more research is required. Notably, the mechanism of action of traditional Chinese medicine is not a single pathway, but it is multiroute and multitargeted. Therefore, its regulation of the immune system cannot be the only mechanism for the treatment of osteoporosis. Our continued improvement in understanding of the immunoregulatory mechanisms of osteoporosis will further elucidate the immunoregulatory mechanism of Chinese medicine for the treatment of osteoporosis.

## Conflicts of Interest

The authors declare no conflicts of interest.

## Authors' Contributions

Hongyan Zhao, Ning Zhao, and Dahong Ju participated in the design. Hongyan Zhao, Ning Zhao, Peng Zheng, Xiaohong Xu, Meijie Liu, Dan Luo, and Huihui Xu wrote the manuscript. Dahong Ju edited the manuscript. All of the authors approved the manuscript. Hongyan Zhao and Ning Zhao contributed equally to this work.

## Funding

This work was supported by the National Natural Science Foundation of China (Grant nos. 81373773, 81573845, 81673841, and 81673844).

## References

- [1] J. P. van den Bergh, T. A. van Geel, and P. P. Geusens, "Osteoporosis, frailty and fracture: implications for case finding and therapy," *Nature Reviews Rheumatology*, vol. 8, no. 3, pp. 163–172, 2012.
- [2] A. Limmer and D. C. Wirtz, "Osteoimmunology: influence of the immune system on bone regeneration and consumption," *Zeitschrift für Orthopädie und Unfallchirurgie*, vol. 155, no. 03, pp. 273–280, 2017.
- [3] M. N. Weitzmann and I. Oforokun, "Physiological and pathophysiological bone turnover—role of the immune system," *Nature Reviews Endocrinology*, vol. 12, no. 9, pp. 518–532, 2016.
- [4] A. Bozec and M. M. Zaiss, "T regulatory cells in bone remodelling," *Current Osteoporosis Reports*, vol. 15, no. 3, pp. 121–125, 2017.
- [5] L. Zhao, L. Huang, and X. Zhang, "Osteoimmunology: memorandum for rheumatologists," *Science China. Life Sciences*, vol. 59, no. 12, pp. 1241–1258, 2016.
- [6] H. Takayanagi, "Osteoimmunology and the effects of the immune system on bone," *Nature Reviews Rheumatology*, vol. 5, no. 12, pp. 667–676, 2009.
- [7] M. M. Guerrini and H. Takayanagi, "The immune system, bone and RANKL," *Archives of Biochemistry and Biophysics*, vol. 561, pp. 118–123, 2014.
- [8] T. Nakashima and H. Takayanagi, "Osteoimmunology: crosstalk between the immune and bone systems," *Journal of Clinical Immunology*, vol. 29, no. 5, pp. 555–567, 2009.
- [9] Z. Q. Wang, J. L. Li, Y. L. Sun et al., "Chinese herbal medicine for osteoporosis: a systematic review of randomized controlled trials," *Evidence-based Complementary and Alternative Medicine*, vol. 2013, Article ID 356260, 11 pages, 2013.
- [10] J. B. He, M. H. Chen, and D. K. Lin, "New insights into the tonifying k' in herbs and formulas for the treatment of osteoporosis," *Archives of Osteoporosis*, vol. 12, no. 1, p. 14, 2017.
- [11] L. Tong and K. D. Moudgil, "*Celastrus aculeatus* Merr. suppresses the induction and progression of autoimmune arthritis by modulating immune response to heat-shock protein 65," *Arthritis Research & Therapy*, vol. 9, no. 4, article R70, 2007.
- [12] A. Ma, Y. Yang, Q. Wang, Y. Wang, J. Wen, and Y. Zhang, "Antiinflammatory effects of oxymatrine on rheumatoid arthritis in rats via regulating the imbalance between Treg and Th17 cells," *Molecular Medicine Reports*, vol. 15, no. 6, pp. 3615–3622, 2017.
- [13] T. Chen, S. Yuan, X. N. Wan et al., "Chinese herb cinobufagin-reduced cancer pain is associated with increased peripheral opioids by invaded CD<sup>3/4/8</sup> lymphocytes," *Oncotarget*, vol. 8, no. 7, pp. 11425–11441, 2017.
- [14] S. Y. Park, S. J. Jung, K. C. Ha et al., "Anti-inflammatory effects of *Cordyceps* mycelium (*Paecilomyces hepiali*, CBG-CS-2) in Raw264.7 murine macrophages," *Oriental Pharmacy and Experimental Medicine*, vol. 15, no. 1, pp. 7–12, 2015.
- [15] C. Xiao, L. Zhao, Z. Liu et al., "The effect of triptolide on CD4+ and CD8+ cells in the Peyer's patch of DA rats with collagen induced arthritis," *Natural Product Research*, vol. 23, no. 18, pp. 1699–1706, 2009.
- [16] L. J. Ho and J. H. Lai, "Chinese herbs as immunomodulators and potential disease-modifying antirheumatic drugs in autoimmune disorders," *Current Drug Metabolism*, vol. 5, no. 2, pp. 181–192, 2004.
- [17] K. Asano, J. Matsuishi, Y. Yu, T. Kasahara, and T. Hisamitsu, "Suppressive effects of *Tripterygium wilfordii* Hook f., a traditional Chinese medicine, on collagen arthritis in mice," *Immunopharmacology*, vol. 39, no. 2, pp. 117–126, 1998.
- [18] A. F. Tawfik, S. J. Bishop, A. Ayalp, and F. S. el-Feraly, "Effects of artemisinin, dihydroartemisinin and arteether on immune responses of normal mice," *International Journal of Immunopharmacology*, vol. 12, no. 4, pp. 385–389, 1990.
- [19] H. Takayanagi, "Osteoimmunology: shared mechanisms and crosstalk between the immune and bone systems," *Nature Reviews Immunology*, vol. 7, no. 4, pp. 292–304, 2007.
- [20] M. B. Greenblatt and J. H. Shim, "Osteoimmunology: a brief introduction," *Immune Network*, vol. 13, no. 4, pp. 111–115, 2013.
- [21] H. Takayanagi, "Osteoimmunology in 2014: two-faced immunology—from osteogenesis to bone resorption," *Nature Reviews Rheumatology*, vol. 11, no. 2, pp. 74–76, 2015.
- [22] W. J. Boyle, W. S. Simonet, and D. L. Lacey, "Osteoclast differentiation and activation," *Nature*, vol. 423, no. 6937, pp. 337–342, 2003.
- [23] M. C. Walsh and Y. Choi, "Biology of the RANKL-RANK-OPG system in immunity, bone, and beyond," *Frontiers in Immunology*, vol. 5, p. 511, 2014.
- [24] L. Ginaldi and M. De Martinis, "Osteoimmunology and beyond," *Current Medicinal Chemistry*, vol. 23, no. 33, pp. 3754–3774, 2016.
- [25] G. Mori, P. D'Amelio, R. Faccio, and G. Brunetti, "The interplay between the bone and the immune system," *Clinical and Developmental Immunology*, vol. 2013, Article ID 720504, 16 pages, 2013.
- [26] T. Ikeda, M. Utsuyama, and K. Hirokawa, "Expression profiles of receptor activator of nuclear factor  $\kappa$ B ligand, receptor activator of nuclear factor  $\kappa$ B, and osteoprotegerin messenger RNA in aged and ovariectomized rat bones," *Journal of Bone and Mineral Research*, vol. 16, no. 8, pp. 1416–1425, 2001.
- [27] J. H. Kim and N. Kim, "Regulation of NFATc1 in osteoclast differentiation," *Journal of Bone Metabolism*, vol. 21, no. 4, pp. 233–241, 2014.
- [28] D. L. Lacey, E. Timms, H. L. Tan et al., "Osteoprotegerin ligand is a cytokine that regulates osteoclast differentiation and activation," *Cell*, vol. 93, no. 2, pp. 165–176, 1998.
- [29] W. S. Simonet, D. L. Lacey, C. R. Dunstan et al., "Osteoprotegerin: a novel secreted protein involved in the regulation of bone density," *Cell*, vol. 89, no. 2, pp. 309–319, 1997.
- [30] H. Wolski, K. Drews, A. Bogacz et al., "The RANKL/RANK/OPG signal trail: significance of genetic polymorphisms in the etiology of postmenopausal osteoporosis," *Ginekologia Polska*, vol. 87, no. 5, pp. 347–352, 2016.
- [31] N. A. Hamdy, "Targeting the RANK/RANKL/OPG signaling pathway: a novel approach in the management of osteoporosis," *Current Opinion in Investigational Drugs*, vol. 8, no. 4, pp. 299–303, 2007.

- [32] L. C. Hofbauer, C. A. Kuhne, and V. Viereck, "The OPG/RANKL/RANK system in metabolic bone diseases," *Journal of Musculoskeletal & Neuronal Interactions*, vol. 4, no. 3, pp. 268–275, 2004.
- [33] M. N. Weitzmann, "The role of inflammatory cytokines, the RANKL/OPG axis, and the immunoskeletal interface in physiological bone turnover and osteoporosis," *Scientifica*, vol. 2013, Article ID 125705, 29 pages, 2013.
- [34] S. Khosla, "Minireview: the OPG/RANKL/RANK system," *Endocrinology*, vol. 142, no. 12, pp. 5050–5055, 2001.
- [35] F. Xu, Y. Dong, X. Huang et al., "Pioglitazone affects the OPG/RANKL/RANK system and increase osteoclastogenesis," *Molecular Medicine Reports*, vol. 14, no. 3, pp. 2289–2296, 2016.
- [36] K. Okamoto and H. Takayanagi, "Regulation of bone by the adaptive immune system in arthritis," *Arthritis Research & Therapy*, vol. 13, no. 3, p. 219, 2011.
- [37] J. Y. Li, H. Tawfeek, B. Bedi et al., "Ovariectomy deregulates osteoblast and osteoclast formation through the T-cell receptor CD40 ligand," *Proceedings of the National Academy of Sciences of the United States of America*, vol. 108, no. 2, pp. 768–773, 2011.
- [38] K. Sato, A. Suematsu, K. Okamoto et al., "Th17 functions as an osteoclastogenic helper T cell subset that links T cell activation and bone destruction," *The Journal of Experimental Medicine*, vol. 203, no. 12, pp. 2673–2682, 2006.
- [39] M. M. Zaiss, R. Axmann, J. Zwerina et al., "Treg cells suppress osteoclast formation: a new link between the immune system and bone," *Arthritis & Rheumatism*, vol. 56, no. 12, pp. 4104–4112, 2007.
- [40] M. M. Zaiss, B. Frey, A. Hess et al., "Regulatory T cells protect from local and systemic bone destruction in arthritis," *The Journal of Immunology*, vol. 184, no. 12, pp. 7238–7246, 2010.
- [41] S. Y. Lee, Y. O. Jung, J. G. Ryu et al., "Intravenous immunoglobulin attenuates experimental autoimmune arthritis by inducing reciprocal regulation of Th17 and Treg cells in an interleukin-10-dependent manner," *Arthritis & Rheumatology*, vol. 66, no. 7, pp. 1768–1778, 2014.
- [42] H. Xu, H. Zhao, C. Lu et al., "Triptolide inhibits osteoclast differentiation and bone resorption *in vitro* via enhancing the production of IL-10 and TGF- $\beta$ 1 by regulatory T cells," *Mediators of Inflammation*, vol. 2016, Article ID 8048170, 10 pages, 2016.
- [43] K. Wing, Y. Onishi, P. Prieto-Martin et al., "CTLA-4 control over Foxp3<sup>+</sup> regulatory T cell function," *Science*, vol. 322, no. 5899, pp. 271–275, 2008.
- [44] R. Axmann, S. Herman, M. Zaiss et al., "CTLA-4 directly inhibits osteoclast formation," *Annals of the Rheumatic Diseases*, vol. 67, no. 11, pp. 1603–1609, 2008.
- [45] J. Pene, S. Chevalier, L. Preisser et al., "Chronically inflamed human tissues are infiltrated by highly differentiated Th17 lymphocytes," *The Journal of Immunology*, vol. 180, no. 11, pp. 7423–7430, 2008.
- [46] H. Takayanagi, "New immune connections in osteoclast formation," *Annals of the New York Academy of Sciences*, vol. 1192, no. 1, pp. 117–123, 2010.
- [47] A. M. Tyagi, K. Srivastava, M. N. Mansoori, R. Trivedi, N. Chattopadhyay, and D. Singh, "Estrogen deficiency induces the differentiation of IL-17 secreting Th17 cells: a new candidate in the pathogenesis of osteoporosis," *PLoS One*, vol. 7, no. 9, article e44552, 2012.
- [48] E. Romas, M. T. Gillespie, and T. J. Martin, "Involvement of receptor activator of NF $\kappa$ B ligand and tumor necrosis factor- $\alpha$  in bone destruction in rheumatoid arthritis," *Bone*, vol. 30, no. 2, pp. 340–346, 2002.
- [49] N. Takegahara, H. Kim, H. Mizuno et al., "Involvement of receptor activator of nuclear factor- $\kappa$ B ligand (RANKL)-induced incomplete cytokinesis in the polyploidization of osteoclasts," *The Journal of Biological Chemistry*, vol. 291, no. 7, pp. 3439–3454, 2016.
- [50] Y. Li, G. Toraldo, A. Li et al., "B cells and T cells are critical for the preservation of bone homeostasis and attainment of peak bone mass *in vivo*," *Blood*, vol. 109, no. 9, pp. 3839–3848, 2007.
- [51] T. J. Yun, P. M. Chaudhary, G. L. Shu et al., "OPG/FDCR-1, a TNF receptor family member, is expressed in lymphoid cells and is up-regulated by ligating CD40," *Journal of Immunology*, vol. 161, no. 11, pp. 6113–6121, 1998.
- [52] K. Titanji, A. Vunnavu, A. N. Sheth et al., "Dysregulated B cell expression of RANKL and OPG correlates with loss of bone mineral density in HIV infection," *PLoS Pathogens*, vol. 10, no. 11, article e1004497, 2014.
- [53] Y. Y. Kong, H. Yoshida, I. Sarosi et al., "OPGL is a key regulator of osteoclastogenesis, lymphocyte development and lymph-node organogenesis," *Nature*, vol. 397, no. 6717, pp. 315–323, 1999.
- [54] G. R. Ehrhardt, A. Hijikata, H. Kitamura, O. Ohara, J. Y. Wang, and M. D. Cooper, "Discriminating gene expression profiles of memory B cell subpopulations," *The Journal of Experimental Medicine*, vol. 205, no. 8, pp. 1807–1817, 2008.
- [55] K. Amara, E. Clay, L. Yeo et al., "B cells expressing the IgA receptor FcRL4 participate in the autoimmune response in patients with rheumatoid arthritis," *Journal of Autoimmunity*, vol. 81, pp. 34–43, 2017.
- [56] A. I. Pesce Viglietti, P. C. Arriola Benitez, G. H. Giambartolomei, and M. V. Delpino, "*Brucella abortus*-infected B cells induce osteoclastogenesis," *Microbes and Infection*, vol. 18, no. 9, pp. 529–535, 2016.
- [57] C. R. Jarry, E. F. Martinez, D. C. Peruzzo et al., "Expression of SOFAT by T- and B-lineage cells may contribute to bone loss," *Molecular Medicine Reports*, vol. 13, no. 5, pp. 4252–4258, 2016.
- [58] S. Xu, Y. Zhang, B. Liu et al., "Activation of mTORC1 in B lymphocytes promotes osteoclast formation via regulation of  $\beta$ -catenin and RANKL/OPG," *Journal of Bone and Mineral Research*, vol. 31, no. 7, pp. 1320–1333, 2016.
- [59] F. Azizieh, R. Raghupathy, D. Shehab, K. Al-Jarallah, and R. Gupta, "Cytokine profiles in osteoporosis suggest a proresorptive bias," *Menopause*, vol. 24, no. 9, pp. 1057–1064, 2017.
- [60] G. Eghbali-Fatourehchi, S. Khosla, A. Sanyal, W. J. Boyle, D. L. Lacey, and B. L. Riggs, "Role of RANK ligand in mediating increased bone resorption in early postmenopausal women," *The Journal of Clinical Investigation*, vol. 111, no. 8, pp. 1221–1230, 2003.
- [61] L. C. Hofbauer, S. Khosla, C. R. Dunstan, D. L. Lacey, W. J. Boyle, and B. L. Riggs, "The roles of osteoprotegerin and osteoprotegerin ligand in the paracrine regulation of bone resorption," *Journal of Bone and Mineral Research*, vol. 15, no. 1, pp. 2–12, 2000.
- [62] S. Wei, M. W. Wang, S. L. Teitelbaum, and F. P. Ross, "Interleukin-4 reversibly inhibits osteoclastogenesis via inhibition

- of NF- $\kappa$ B and mitogen-activated protein kinase signaling," *The Journal of Biological Chemistry*, vol. 277, no. 8, pp. 6622–6630, 2002.
- [63] J. M. Owens, A. C. Gallagher, and T. J. Chambers, "IL-10 modulates formation of osteoclasts in murine hemopoietic cultures," *Journal of Immunology*, vol. 157, no. 2, pp. 936–940, 1996.
- [64] Y. Morita, H. Kitaura, M. Yoshimatsu et al., "IL-18 inhibits TNF- $\alpha$ -induced osteoclastogenesis possibly via a T cell-independent mechanism in synergy with IL-12 in vivo," *Calcified Tissue International*, vol. 86, no. 3, pp. 242–248, 2010.
- [65] N. J. Horwood, J. Elliott, T. J. Martin, and M. T. Gillespie, "IL-12 alone and in synergy with IL-18 inhibits osteoclast formation in vitro," *The Journal of Immunology*, vol. 166, no. 8, pp. 4915–4921, 2001.
- [66] S. Y. Kim, S. Schneeweiss, J. Liu et al., "Risk of osteoporotic fracture in a large population-based cohort of patients with rheumatoid arthritis," *Arthritis Research & Therapy*, vol. 12, no. 4, p. R154, 2010.
- [67] B. Mermerci Başkan, Y. Pekin Doğan, F. Sivas, H. Bodur, and K. Ozoran, "The relation between osteoporosis and vitamin D levels and disease activity in ankylosing spondylitis," *Rheumatology International*, vol. 30, no. 3, pp. 375–381, 2010.
- [68] N. Davey-Ranasinghe and A. Deodhar, "Osteoporosis and vertebral fractures in ankylosing spondylitis," *Current Opinion in Rheumatology*, vol. 25, no. 4, pp. 509–516, 2013.
- [69] S. M. Jung, K. W. Kim, C. W. Yang, S. H. Park, and J. H. Ju, "Cytokine-mediated bone destruction in rheumatoid arthritis," *Journal of Immunology Research*, vol. 2014, Article ID 263625, 15 pages, 2014.
- [70] P. Rufus, N. Mohamed, and A. N. Shuid, "Beneficial effects of traditional Chinese medicine on the treatment of osteoporosis on ovariectomized rat models," *Current Drug Targets*, vol. 14, no. 14, pp. 1689–1693, 2013.
- [71] H. Yamasaki, "Pharmacology of sinomenine, an anti-rheumatic alkaloid from *Sinomenium acutum*," *Acta Medica Okayama*, vol. 30, no. 1, pp. 1–20, 1976.
- [72] Q. Wang and X. K. Li, "Immunosuppressive and anti-inflammatory activities of sinomenine," *International Immunopharmacology*, vol. 11, no. 3, pp. 373–376, 2011.
- [73] L. Liu, K. Resch, and V. Kaever, "Inhibition of lymphocyte proliferation by the anti-arthritis drug sinomenine," *International Journal of Immunopharmacology*, vol. 16, no. 8, pp. 685–691, 1994.
- [74] Y. Cheng, J. Zhang, W. Hou et al., "Immunoregulatory effects of sinomenine on the T-bet/GATA-3 ratio and Th1/Th2 cytokine balance in the treatment of mesangial proliferative nephritis," *International Immunopharmacology*, vol. 9, no. 7-8, pp. 894–899, 2009.
- [75] L. C. Yan, E. G. Bi, Y. T. Lou et al., "Novel sinomenine derivative 1032 improves immune suppression in experimental autoimmune encephalomyelitis," *Biochemical and Biophysical Research Communications*, vol. 391, no. 1, pp. 1093–1098, 2010.
- [76] L. Liu, E. Buchner, D. Beitz et al., "Amelioration of rat experimental arthritides by treatment with the alkaloid sinomenine," *International Journal of Immunopharmacology*, vol. 18, no. 10, pp. 529–543, 1996.
- [77] H. Feng, K. Yamaki, H. Takano, K. Inoue, R. Yanagisawa, and S. Yoshino, "Effect of sinomenine on collagen-induced arthritis in mice," *Autoimmunity*, vol. 40, no. 7, pp. 532–539, 2009.
- [78] H. Zhou, Y. F. Wong, J. Wang, X. Cai, and L. Liu, "Sinomenine ameliorates arthritis via MMPs, TIMPs, and cytokines in rats," *Biochemical and Biophysical Research Communications*, vol. 376, no. 2, pp. 352–357, 2008.
- [79] X. Li, L. He, Y. Hu et al., "Sinomenine suppresses osteoclast formation and *Mycobacterium tuberculosis* H37Ra-induced bone loss by modulating RANKL signaling pathways," *PLoS One*, vol. 8, no. 9, article e74274, 2013.
- [80] B. Zhou, X. Lu, Z. Tang et al., "Influence of sinomenine upon mesenchymal stem cells in osteoclastogenesis," *Biomedicine & Pharmacotherapy*, vol. 90, pp. 835–841, 2017.
- [81] L. He, H. Duan, X. Li et al., "Sinomenine down-regulates TLR4/TRAF6 expression and attenuates lipopolysaccharide-induced osteoclastogenesis and osteolysis," *European Journal of Pharmacology*, vol. 779, pp. 66–79, 2016.
- [82] K. Kawaguchi, H. Maruyama, R. Hasunuma, and Y. Kumazawa, "Suppression of inflammatory responses after onset of collagen-induced arthritis in mice by oral administration of the *Citrus flavanone* naringin," *Immunopharmacology and Immunotoxicology*, vol. 33, no. 4, pp. 723–729, 2011.
- [83] E. S. Ang, X. Yang, H. Chen, Q. Liu, M. H. Zheng, and J. Xu, "Naringin abrogates osteoclastogenesis and bone resorption via the inhibition of RANKL-induced NF- $\kappa$ B and ERK activation," *FEBS Letters*, vol. 585, no. 17, pp. 2755–2762, 2011.
- [84] J. B. Wu, Y. C. Fong, H. Y. Tsai, Y. F. Chen, M. Tsuzuki, and C. H. Tang, "Naringin-induced bone morphogenetic protein-2 expression via PI3K, Akt, c-Fos/c-Jun and AP-1 pathway in osteoblasts," *European Journal of Pharmacology*, vol. 588, no. 2-3, pp. 333–341, 2008.
- [85] K. C. Wong, W. Y. Pang, X. L. Wang et al., "*Drynaria fortunei*-derived total flavonoid fraction and isolated compounds exert oestrogen-like protective effects in bone," *The British Journal of Nutrition*, vol. 110, no. 3, pp. 475–485, 2013.
- [86] W. Y. Pang, X. L. Wang, S. K. Mok et al., "Naringin improves bone properties in ovariectomized mice and exerts oestrogen-like activities in rat osteoblast-like (UMR-106) cells," *British Journal of Pharmacology*, vol. 159, no. 8, pp. 1693–1703, 2010.
- [87] F. X. Lin, S. X. Du, D. Z. Liu et al., "Naringin promotes osteogenic differentiation of bone marrow stromal cells by up-regulating Foxc2 expression via the IHH signaling pathway," *American Journal of Translational Research*, vol. 8, no. 11, pp. 5098–5107, 2016.
- [88] J. H. Xu, M. Yao, J. Ye et al., "Bone mass improved effect of icariin for postmenopausal osteoporosis in ovariectomy-induced rats: a meta-analysis and systematic review," *Meno-pause*, vol. 23, no. 10, pp. 1152–1157, 2016.
- [89] L. Xue, Y. Jiang, T. Han et al., "Comparative proteomic and metabolomic analysis reveal the antiosteoporotic molecular mechanism of icariin from *Epimedium brevicornu maxim*," *Journal of Ethnopharmacology*, vol. 192, pp. 370–381, 2016.
- [90] G. Chen, C. Wang, J. Wang et al., "Antiosteoporotic effect of icariin in ovariectomized rats is mediated via the Wnt/ $\beta$ -catenin pathway," *Experimental and Therapeutic Medicine*, vol. 12, no. 1, pp. 279–287, 2016.
- [91] S. Qin, W. Zhou, S. Liu, P. Chen, and H. Wu, "Icariin stimulates the proliferation of rat bone mesenchymal stem cells via ERK and p38 MAPK signaling," *International Journal of Clinical and Experimental Medicine*, vol. 8, no. 5, pp. 7125–7133, 2015.

- [92] G. W. Li, Z. Xu, S. X. Chang, H. Nian, X. Y. Wang, and L. D. Qin, "Icariin prevents ovariectomy-induced bone loss and lowers marrow adipogenesis," *Menopause*, vol. 21, no. 9, pp. 1007–1016, 2014.
- [93] H. Liu, Y. Xiong, X. Zhu et al., "Icariin improves osteoporosis, inhibits the expression of PPAR $\gamma$ , C/EBP $\alpha$ , FABP4 mRNA, N1ICD and jagged1 proteins, and increases Notch2 mRNA in ovariectomized rats," *Experimental and Therapeutic Medicine*, vol. 13, no. 4, pp. 1360–1368, 2017.
- [94] H. Cao, Y. Zhang, W. Qian et al., "Effect of icariin on fracture healing in an ovariectomized rat model of osteoporosis," *Experimental and Therapeutic Medicine*, vol. 13, no. 5, pp. 2399–2404, 2017.
- [95] Y. Wu, L. Cao, L. Xia et al., "Evaluation of osteogenesis and angiogenesis of icariin in local controlled release and systemic delivery for calvarial defect in ovariectomized rats," *Scientific Reports*, vol. 7, no. 1, article 5077, 2017.
- [96] T. P. Hsieh, S. Y. Sheu, J. S. Sun, M. H. Chen, and M. H. Liu, "Icariin isolated from *Epimedium pubescens* regulates osteoblasts anabolism through BMP-2, SMAD4, and Cbfa1 expression," *Phytomedicine*, vol. 17, no. 6, pp. 414–423, 2010.
- [97] W. Liang, M. Lin, X. Li et al., "Icariin promotes bone formation via the BMP-2/Smad4 signal transduction pathway in the hFOB 1.19 human osteoblastic cell line," *International Journal of Molecular Medicine*, vol. 30, no. 4, pp. 889–895, 2012.
- [98] E. M. Tan, L. Li, I. R. Indran, N. Chew, and E. L. Yong, "TRAF6 mediates suppression of osteoclastogenesis and prevention of ovariectomy-induced bone loss by a novel prenyl-flavonoid," *Journal of Bone and Mineral Research*, vol. 32, no. 4, pp. 846–860, 2017.
- [99] T. Wu, T. Shu, L. Kang et al., "Icariin, a novel plant-derived osteoinductive agent, enhances the osteogenic differentiation of human bone marrow- and human adipose tissue-derived mesenchymal stem cells," *International Journal of Molecular Medicine*, vol. 39, no. 4, pp. 984–992, 2017.
- [100] H. Sheng, X. F. Rui, C. J. Sheng et al., "A novel semisynthetic molecule icaritin stimulates osteogenic differentiation and inhibits adipogenesis of mesenchymal stem cells," *International Journal of Medical Sciences*, vol. 10, no. 6, pp. 782–789, 2013.
- [101] H. Ha, J. Ho, S. Shin et al., "Effects of *Eucommia* Cortex on osteoblast-like cell proliferation and osteoclast inhibition," *Archives of Pharmacal Research*, vol. 26, no. 11, pp. 929–936, 2003.
- [102] R. Zhang, Z. G. Liu, C. Li et al., "Du-Zhong (*Eucommia ulmoides* Oliv.) cortex extract prevent OVX-induced osteoporosis in rats," *Bone*, vol. 45, no. 3, pp. 553–559, 2009.
- [103] Y. Li, M. J. Wang, S. Li et al., "Effect of total glycosides from *Eucommia ulmoides* seed on bone microarchitecture in rats," *Phytotherapy Research*, vol. 25, no. 12, pp. 1895–1897, 2011.
- [104] W. Zhang, T. Fujikawa, K. Mizuno et al., "Eucommia leaf extract (ELE) prevents OVX-induced osteoporosis and obesity in rats," *The American Journal of Chinese Medicine*, vol. 40, no. 04, pp. 735–752, 2012.
- [105] X. L. Tan, Y. H. Zhang, J. P. Cai, L. H. Zhu, W. J. Ge, and X. Zhang, "5-(Hydroxymethyl)-2-furaldehyde inhibits adipogenic and enhances osteogenic differentiation of rat bone mesenchymal stem cells," *Natural Product Communications*, vol. 9, no. 4, pp. 529–532, 2014.
- [106] R. Zhang, Y. L. Pan, S. J. Hu, X. H. Kong, W. Juan, and Q. B. Mei, "Effects of total lignans from *Eucommia ulmoides* barks prevent bone loss in vivo and in vitro," *Journal of Ethnopharmacology*, vol. 155, no. 1, pp. 104–112, 2014.
- [107] J. Y. Wang, Y. Yuan, X. J. Chen et al., "Extract from *Eucommia ulmoides* Oliv. ameliorates arthritis via regulation of inflammation, synovocyte proliferation and osteoclastogenesis in vitro and in vivo," *Journal of Ethnopharmacology*, vol. 194, pp. 609–616, 2016.
- [108] G. P. Xie, N. Jiang, S. N. Wang et al., "*Eucommia ulmoides* Oliv. bark aqueous extract inhibits osteoarthritis in a rat model of osteoarthritis," *Journal of Ethnopharmacology*, vol. 162, pp. 148–154, 2015.
- [109] S. H. Kwon, S. X. Ma, J. Y. Hwang et al., "The anti-inflammatory activity of *Eucommia ulmoides* Oliv. bark. involves NF- $\kappa$ B suppression and Nrf2-dependent HO-1 induction in BV-2 microglial cells," *Biomolecules & Therapeutics*, vol. 24, no. 3, pp. 268–282, 2016.
- [110] X. Dai, Q. Huang, B. Zhou, Z. Gong, Z. Liu, and S. Shi, "Preparative isolation and purification of seven main antioxidants from *Eucommia ulmoides* Oliv. (Du-zhong) leaves using HSCCC guided by DPPH-HPLC experiment," *Food Chemistry*, vol. 139, no. 1–4, pp. 563–570, 2013.
- [111] M. M. Bai, W. Shi, J. M. Tian et al., "Soluble epoxide hydrolase inhibitory and anti-inflammatory components from the leaves of *Eucommia ulmoides* Oliver (Duzhong)," *Journal of Agricultural and Food Chemistry*, vol. 63, no. 8, pp. 2198–2205, 2015.
- [112] T. Oliveira, C. A. Figueiredo, C. Brito et al., "Allium cepa L. and quercetin inhibit RANKL/porphyromonas gingivalis LPS-induced osteoclastogenesis by downregulating NF- $\kappa$ B signaling pathway," *Evidence-Based Complementary and Alternative Medicine*, vol. 2015, Article ID 704781, 11 pages, 2015.
- [113] K. S. Shim, H. Ha, T. Kim, C. J. Lee, and J. Y. Ma, "*Orostachys japonicus* suppresses osteoclast differentiation by inhibiting NFATc1 expression," *The American Journal of Chinese Medicine*, vol. 43, no. 05, pp. 1013–1030, 2015.
- [114] A. Wattel, S. Kamel, C. Prouillet et al., "Flavonoid quercetin decreases osteoclastic differentiation induced by RANKL via a mechanism involving NF  $\kappa$ B and AP-1," *Journal of Cellular Biochemistry*, vol. 92, no. 2, pp. 285–295, 2004.
- [115] M. Tsuji, H. Yamamoto, T. Sato et al., "Dietary quercetin inhibits bone loss without effect on the uterus in ovariectomized mice," *Journal of Bone and Mineral Metabolism*, vol. 27, no. 6, pp. 673–681, 2009.
- [116] J. T. Woo, H. Nakagawa, M. Notoya et al., "Quercetin suppresses bone resorption by inhibiting the differentiation and activation of osteoclasts," *Biological and Pharmaceutical Bulletin*, vol. 27, no. 4, pp. 504–509, 2004.
- [117] M. Yamaguchi and M. Weitzmann, "Quercetin, a potent suppressor of NF- $\kappa$ B and Smad activation in osteoblasts," *International Journal of Molecular Medicine*, vol. 28, no. 4, pp. 521–525, 2011.
- [118] C. Guo, G. Q. Hou, X. D. Li et al., "Quercetin triggers apoptosis of lipopolysaccharide (LPS)-induced osteoclasts and inhibits bone resorption in RAW264.7 cells," *Cellular Physiology and Biochemistry*, vol. 30, no. 1, pp. 123–136, 2012.
- [119] M. Yamaguchi, R. Hamamoto, S. Uchiyama, and K. Ishiyama, "Effects of flavonoid on calcium content in femoral tissue culture and parathyroid hormone-stimulated

- osteoclastogenesis in bone marrow culture in vitro,” *Molecular and Cellular Biochemistry*, vol. 303, no. 1-2, pp. 83–88, 2007.
- [120] X. C. Wang, N. J. Zhao, C. Guo, J. T. Chen, J. L. Song, and L. Gao, “Quercetin reversed lipopolysaccharide-induced inhibition of osteoblast differentiation through the mitogen-activated protein kinase pathway in MC3T3-E1 cells,” *Molecular Medicine Reports*, vol. 10, no. 6, pp. 3320–3326, 2014.
- [121] F. Li, X. Yang, Y. Yang et al., “Antiosteoporotic activity of echinacoside in ovariectomized rats,” *Phytomedicine*, vol. 20, no. 6, pp. 549–557, 2013.
- [122] Y. B. Niu, Y. H. Li, X. H. Kong et al., “The beneficial effect of *Radix Dipsaci* total saponins on bone metabolism in vitro and in vivo and the possible mechanisms of action,” *Osteoporosis International*, vol. 23, no. 11, pp. 2649–2660, 2012.
- [123] R. Zhang, S. J. Hu, C. Li, F. Zhang, H. Q. Gan, and Q. B. Mei, “*Achyranthes bidentata* root extract prevent OVX-induced osteoporosis in rats,” *Journal of Ethnopharmacology*, vol. 139, no. 1, pp. 12–18, 2012.
- [124] Y. Shen, Y. Q. Li, S. P. Li, L. Ma, L. J. Ding, and H. Ji, “Alleviation of ovariectomy-induced osteoporosis in rats by *Panax notoginseng* saponins,” *Journal of Natural Medicines*, vol. 64, no. 3, pp. 336–345, 2010.
- [125] S. Chawalitpong, N. Sornkaew, A. Suksamrarn, and T. Palaga, “Diarylheptanoid from *Curcuma comosa* Roxb. suppresses RANKL-induced osteoclast differentiation by decreasing NFATc1 and c-Fos expression via MAPK pathway,” *European Journal of Pharmacology*, vol. 788, pp. 351–359, 2016.
- [126] X. Peng, J. He, J. Zhao et al., “Polygonatum sibiricum polysaccharide promotes osteoblastic differentiation through the ERK/GSK-3 $\beta$ / $\beta$ -catenin signaling pathway *in vitro*,” *Rejuvenation Research*, 2017.
- [127] W. Zhou, X. Cheng, and Y. Zhang, “Effect of Liuwei Dihuang decoction, a traditional Chinese medicinal prescription, on the neuroendocrine immunomodulation network,” *Pharmacology & Therapeutics*, vol. 162, pp. 170–178, 2016.
- [128] F. Jian, Z. Yongxiang, and R. Xiangbin, “Effect of Liuwei Dihuang decoction, a traditional Chinese medicinal tonic prescription, on the immune function of adjuvant arthritis rats,” *Pharmacology and Clinics of Chinese Materia Medica*, vol. 1, pp. 3–5, 2001.
- [129] F. Jian, Z. Yongxiang, and R. Xiangbin, “Effect of Liuwei Dihuang decoction on the cytokine expression in splenocytes in AA rats,” *China Journal of Chinese Materia Medica*, vol. 2, pp. 56–59, 2001.
- [130] J. R. Ge, L. H. Xie, J. Chen et al., “Liuwei Dihuang pill (六味地黄丸) treats postmenopausal osteoporosis with Shen (kidney) yin deficiency via Janus kinase/signal transducer and activator of transcription signal pathway by up-regulating cardiotrophin-like cytokine factor 1 expression,” *Chinese Journal of Integrative Medicine*, 2016.
- [131] B. Xia, B. Xu, Y. Sun et al., “The effects of Liuwei Dihuang on canonical Wnt/ $\beta$ -catenin signaling pathway in osteoporosis,” *Journal of Ethnopharmacology*, vol. 153, no. 1, pp. 133–141, 2014.
- [132] M. J. Liu, L. I. Yan, J. H. Pan et al., “Effects of zuogui pill (左归丸) on Wnt signal transduction in rats with glucocorticoid-induced osteoporosis,” *Journal of Traditional Chinese Medicine*, vol. 31, no. 2, pp. 98–102, 2011.
- [133] N. Lai, Z. Zhang, B. Wang et al., “Regulatory effect of traditional Chinese medicinal formula Zuo-Gui-Wan on the Th17/Treg paradigm in mice with bone loss induced by estrogen deficiency,” *Journal of Ethnopharmacology*, vol. 166, pp. 228–239, 2015.

## Research Article

# Matrine Ameliorates Colorectal Cancer in Rats via Inhibition of HMGB1 Signaling and Downregulation of IL-6, TNF- $\alpha$ , and HMGB1

Huizhen Fan <sup>1</sup>, Chunyan Jiang,<sup>2</sup> Baoyuan Zhong,<sup>3</sup> Jianwen Sheng,<sup>1</sup> Ting Chen,<sup>1</sup> Qingqing Chen,<sup>1</sup> Jingtao Li <sup>4</sup> and Hongchuan Zhao<sup>4</sup>

<sup>1</sup>Department of Gastroenterology, The People's Hospital of Yichun City, Yichun, China

<sup>2</sup>Department of Dermatology, Beijing Hospital of Traditional Chinese Medicine, Beijing, China

<sup>3</sup>Department of General Surgery, First Affiliated Hospital of Gannan Medical College, Ganzhou, China

<sup>4</sup>Department of Gastroenterology, China-Japan Friendship Hospital, Beijing, China

Correspondence should be addressed to Huizhen Fan; fanfany@163.com and Jingtao Li; lijingtao1106@126.com

Received 27 July 2017; Revised 9 October 2017; Accepted 12 November 2017; Published 10 January 2018

Academic Editor: Qingdong Guan

Copyright © 2018 Huizhen Fan et al. This is an open access article distributed under the Creative Commons Attribution License, which permits unrestricted use, distribution, and reproduction in any medium, provided the original work is properly cited.

*Matrine* may be protective against colorectal cancer (CRC), but how it may work is unclear. Thus, we explored the underlying mechanisms of *matrine* in CRC. *Matrine*-related proteins and CRC-related genes and therapeutic targets of *matrine* in CRC were predicted using a network pharmacology approach. Five targets, including interleukin 6 (IL-6), the 26S proteasome, tumor necrosis factor alpha (TNF- $\alpha$ ), transforming growth factor beta 1 (TGF- $\beta$ 1) and p53, and corresponding high-mobility group box 1 (HMGB1) signaling and T helper cell differentiation were thought to be associated with *matrine*'s mechanism. Expression of predicted serum targets were verified in a 1,2-dimethylhydrazine dihydrochloride-induced CRC model rats that were treated with *matrine* (ip) for 18 weeks. Data show that *matrine* suppressed CRC growth and decreased previously elevated expression of IL-6, TNF- $\alpha$ , p53, and HMGB1. *Matrine* may have had a therapeutic effect on CRC via inhibition of HMGB1 signaling, and this occurred through downregulation of IL-6, TNF- $\alpha$ , and HMGB1.

## 1. Introduction

Colorectal cancer (CRC) is a malignant colon or rectal tumor and the third most common type of cancer, accounting for ~10% of all cancer cases and ~715,000 premature deaths annually [1, 2]. Conservative drug treatment, directed toward improving the quality of life and symptoms, is an important component of CRC therapy. Chinese herbal medicine has been used as an adjuvant treatment for CRC, but few reports describe mechanistic data for these compounds [3–5]. *Matrine* is a bioactive component extracted from *Sophora flavescens*, and a few studies have suggested that it may have anticancer activity and may be used as an adjuvant treatment for CRC [6–8]. How *matrine* exerts an effect, however, is not clear.

Network pharmacology uses systems pharmacology to help researchers to understand drug mechanisms of action [9]. Network pharmacology approaches have been used for drug discovery and design, and the development of biomarkers for disease detection [9, 10]. In Chinese medicine, the approach has been used to elucidate mechanisms of bioactive components of some Chinese herbs [11, 12]. Thus, we suggest that we can understand how *matrine* effects CRC using a predicted component-target network [13].

Using predicted targets of *matrine* for treating CRC and a network pharmacology approach, we treated 1,2-dimethylhydrazine dihydrochloride- (DMH-) induced CRC rats with *matrine* and measured target expression in serum to better understand how *matrine* may be applied clinically.

## 2. Materials and Methods

**2.1. Matrine-Related Proteins.** PubChem (<http://pubchem.ncbi.nlm.nih.gov/>) was searched for matrine-related proteins (until November 16, 2015). Because the proteins could be cross-referenced to other National Center for Biotechnology Information (NCBI) databases, the proteins that were tested in bioassays were collected [12]. Nineteen matrine-related proteins were included in the study (Supplementary Table 1).

**2.2. CRC-Related Genes.** CRC-related genes were searched in the NCBI Gene database (<http://www.ncbi.nlm.nih.gov/gene>) using the key words “colorectal cancer” (until November 16, 2015) [12]. Thirty-five CRC-related genes were included in the study (Supplementary Table 2).

**2.3. Network Pharmacological Analysis Using Ingenuity Pathways Analysis.** CRC-related genes and matrine-related proteins were uploaded into the Ingenuity Pathways Analysis Platform (IPA, <http://www.ingenuity.com>), which enabled the discovery, visualization, and exploration of molecular interactions to identify the biological mechanisms, pathways, and functions most relevant to genes or proteins of interest. The “core analysis” platform in the IPA was used to assess the uploaded genes and proteins. Scores were negative base 10 logarithms of Fisher’s exact test  $p$  value in the pathway analysis. Significance values for biological functions were assigned to each network by determining  $p$  values for gene enrichment in the network by comparing these data with the Ingenuity Pathway Knowledge Base [14].

**2.4. Matrine Solution and Reagents.** The matrine ampule (5 ml, 80 mg) was purchased from Baiyunshan Pharmaceutical Co. Ltd. (Guangzhou, China; batch number 20151203), and it was diluted with 10% glucose solution. DMH was purchased from Puzhen Biological Technology Co. Ltd. (Shanghai, China; CAS 306-37-6). ELISA kits used in this study included rat interleukin 6 (IL-6), tumor necrosis factor alpha (TNF- $\alpha$ ), high-mobility group box 1 (HMGB1) and transforming growth factor beta 1 (TGF- $\beta$ 1) ELISA kits (Enzyme-Linked Biotechnology Co. Ltd., Shanghai, China), a rat 26S proteasome ELISA kit (Bio-Medical Assay Co. Ltd., Beijing, China), and a rat tumor protein p53 (p53) ELISA kit (BD Biosciences, CA).

**2.5. Experimental Rats, Modeling, and Grouping.** A total of 32 male Wistar rats (80–100 g; license number SCXK 2016-007) were obtained from the Experimental Animal Center of the Beijing Capital University of Medical Sciences (China). All rats were housed in a temperature-, humidity-, and light-controlled environment, and food and tap water were provided ad libitum. The light-dark cycle was 12 hours (light phase from 06:00 to 18:00). All rats were acclimated in their cages for seven days prior to any experiments. The rodent license for the laboratory (number SYXK 11-00-0039) was issued by the Science and Technology Ministry of China. A colorectal carcinogenesis model was induced in rats using DMH once per week (30 mg/kg, sc) for 18 weeks [15]. Four experimental groups ( $n = 8/\text{group}$ ) were established as

follows: healthy controls; CRC model controls; and CRC model rats given low (LM) or high (HM) doses of matrine. All animal experimentation was performed under the Prevention of Cruelty to Animals Act (1986) of China and the NIH Guidelines for the Care and Use of Laboratory Animals (USA).

**2.6. Treatment Schedule.** Matrine doses used in the rats were equivalent to clinically relevant human adult doses based on an established formula for human-rat drug conversion. After all rats were acclimatized and grouped, the LM and HM groups received 15 and 30 mg/kg (ip) injections of matrine solution, every three days for 18 weeks. Meanwhile, all rats except for controls underwent colorectal carcinogenesis induction with DMH. Rats were observed daily, and at the end of the experiment, rats were sacrificed and their peripheral blood and colons were collected for analysis.

**2.7. ELISA.** To determine whether matrine administration affected expression of predicted target proteins (IL-6, 26S proteasome, TNF- $\alpha$ , TGF- $\beta$ 1, p53, and HMGB1) in the serum, protein expression was measured using commercial rat ELISA kits according to the manufacturer’s instructions.

**2.8. Statistical Analysis.** Experimental results were expressed as the means  $\pm$  SD. Statistical differences were analyzed by one-way ANOVA using SPSS Statistics 23. All statistical tests and corresponding  $p$  values were two sided, and  $p < 0.05$  was considered statistically significant.

## 3. Results

**3.1. Diseases or Disorders Associated with Matrine-Related Proteins.** Based on IPA analysis, matrine-related proteins were significantly associated with 22 diseases or disorders (Figure 1). The top five diseases or disorders, in order, were cancer, inflammatory responses, gastrointestinal disease, hepatic system disease, and infectious diseases. These data suggest that matrine may be a candidate treatment for cancer.

**3.2. Networks Associated with Matrine-Related Proteins.** Two matrine molecular networks were established based on matrine-related proteins. As shown in Figure 2(a), some molecules in the network were linked to specific functions, including T helper (Th) cell differentiation, cytokine communication between immune cells, and crosstalk between dendritic cells and natural killer cells. Figure 2(b) describes other specific functions. IPA data show that overall functions of both networks included cell-to-cell signaling and interaction, inflammatory responses, cellular growth and proliferation, and free radical scavenging. Thus, matrine may assist with immune regulation and anti-inflammatory responses.

**3.3. Networks Associated with CRC-Related Genes.** Two CRC networks were established based on CRC-related genes. Figure 3(a) shows that molecules were linked to specific functions, such as CRC metastasis and the molecular mechanisms of cancer. Additionally, polyamine regulation in colon cancer was a functional characteristic of the



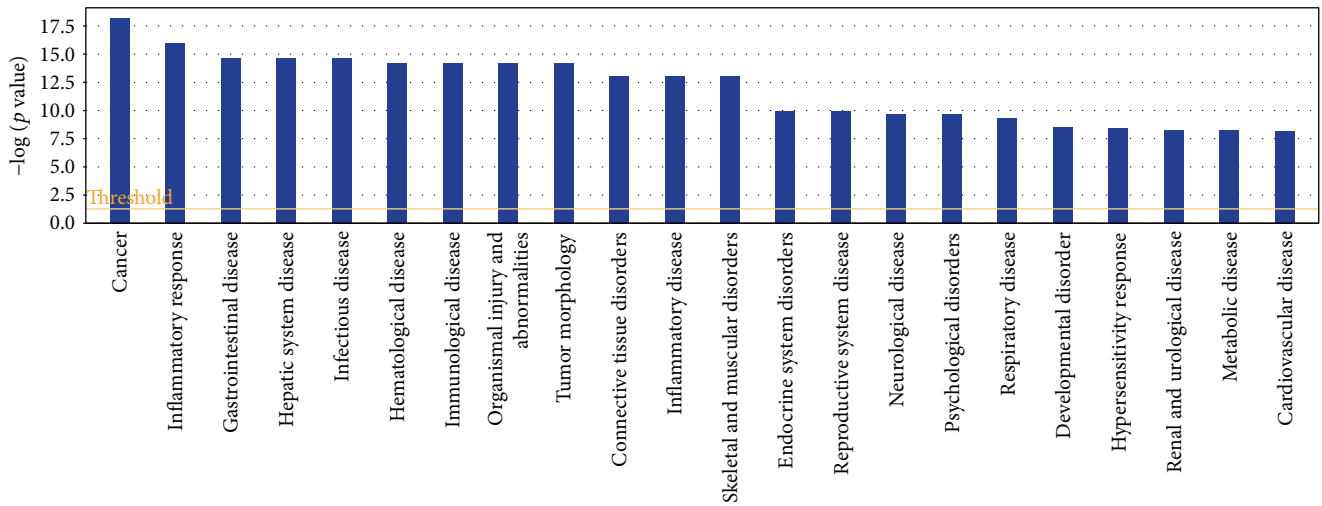


FIGURE 1: Diseases or disorders associated with matrine-related proteins. Statistical significance gradually decreases from left to right.

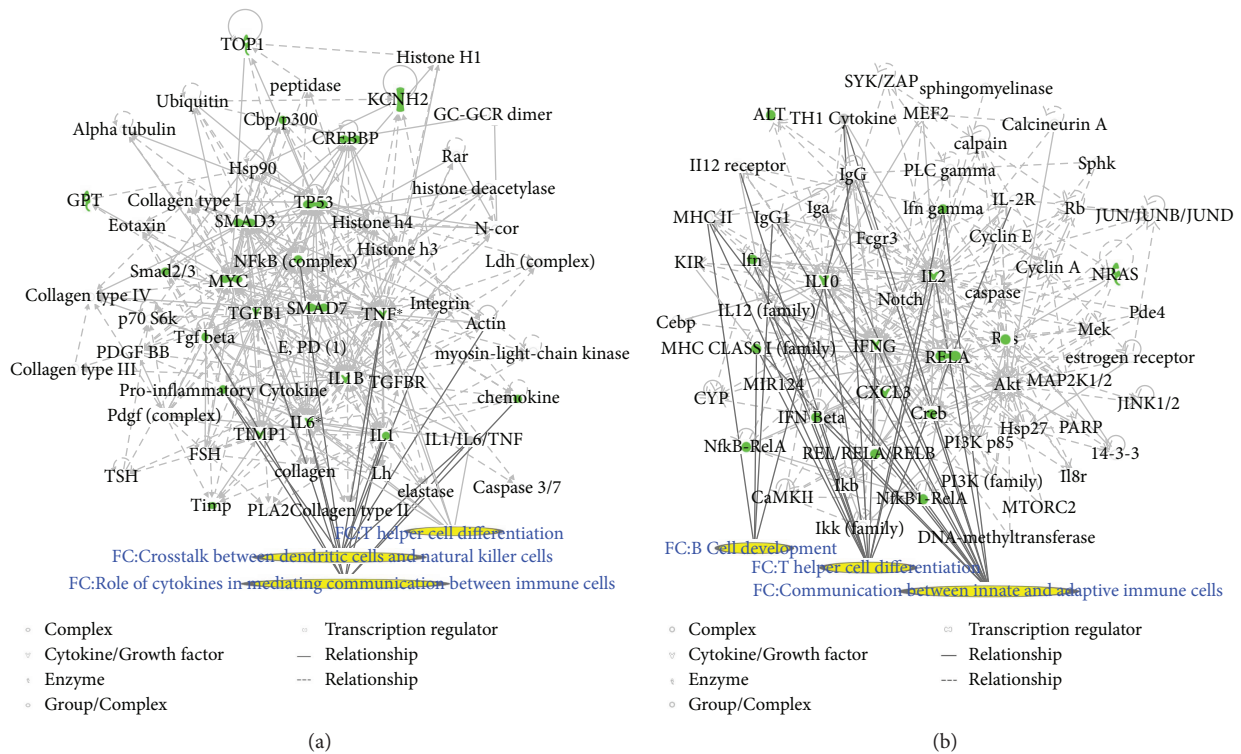


FIGURE 2: *Matrine* molecular networks. In each network, molecules are nodes, and a biological relationship between two nodes is represented by a line. Solid lines between molecules indicate a direct physical relationship between molecules, whereas dotted lines represent indirect functional relationships. Green symbols represent *matrine*-related proteins. Yellow symbols indicate the functional characteristics of the networks.

CRC networks (Figure 3(b)). Two CRC networks were associated with inflammatory and gastrointestinal diseases and organismal injury and abnormalities. This reflects the pathogenesis of CRC.

3.4. *Merging of the Matrine and CRC Networks.* To predict targets of *matrine* intervention in CRC, *matrine* and CRC networks were compared, network dimensions were reduced, and the networks were merged with the IPA. As shown in

Figure 4(a), five molecules, including IL-6, 26S proteasome, TNF- $\alpha$ , TGF- $\beta$ 1, and TP53, were identified as common linked molecules relevant to both *matrine* and CRC networks. According to the Ingenuity Knowledge Database, HMGB1 signaling was the most significantly related pathway for IL-6, TNF- $\alpha$ , and TGF- $\beta$ 1, and Th cell differentiation was the most significantly relevant function for these proteins. IL-6, TNF- $\alpha$ , and TGF- $\beta$ 1 were involved in HMGB1 signaling (Figure 4(b)). Thus, these five highly linked molecules and

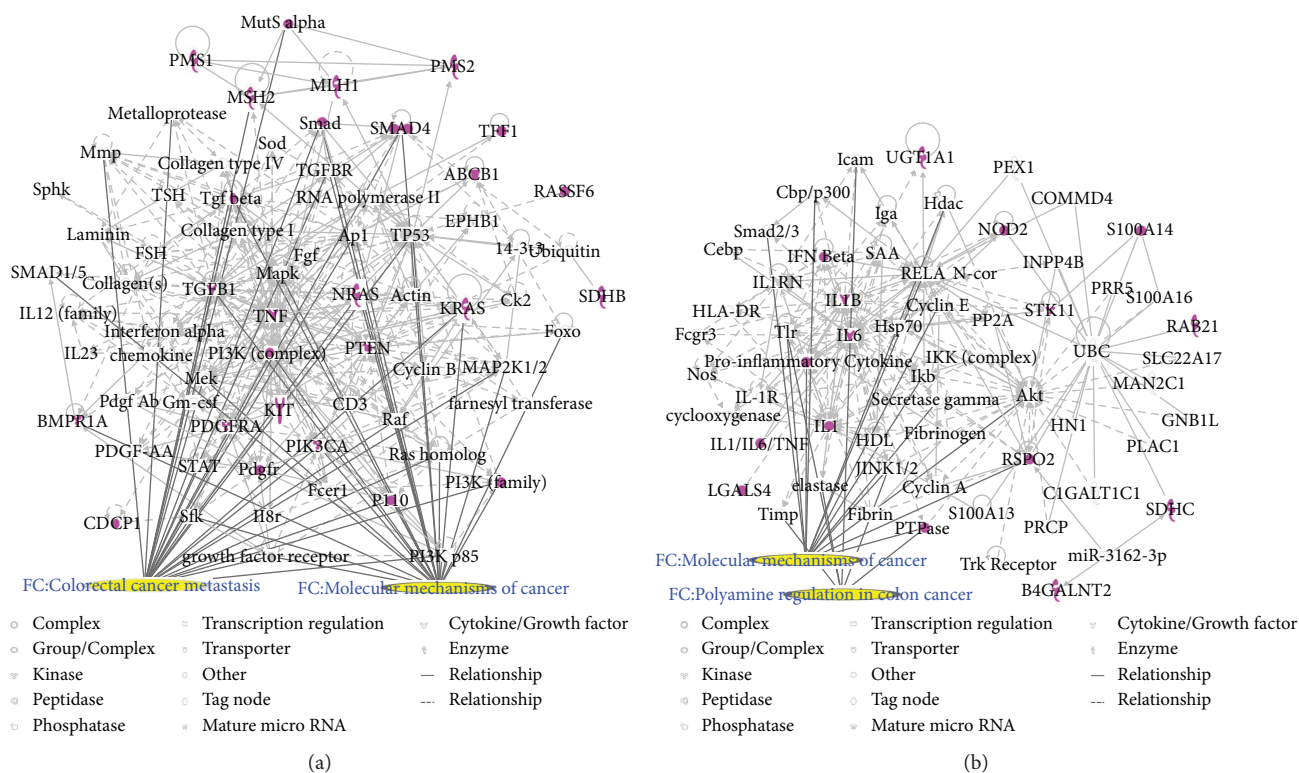


FIGURE 3: CRC molecular networks. In each network, molecules are nodes, and a biological relationship between two nodes is represented by a line. Solid lines between molecules indicate a direct physical relationship between molecules, whereas dotted lines represent indirect functional relationships. Purple symbols represent CRC-related genes. Yellow symbols indicate the functional characteristics of the networks.

HMGB1 signaling were likely associated with the mechanism of matrine for treating CRC, and they may be potential target proteins of matrine.

**3.5. Inhibitory Effect of Matrine on CRC Growth.** Tumor number, weight, and size for each rat were recorded to evaluate antitumor effects of matrine. Table 1 shows that compared to the model group, tumors in matrine-treated groups decreased. Additionally, tumor number, weight, and size in matrine-treated groups were fewer, and the HM group had the best outcome.

**3.6. Effect of Matrine on Expression of Predicted Target Proteins.** IL-6, TNF- $\alpha$ , HMGB1, and p53 were increased in the model group compared to the controls. Figure 5 shows that after matrine treatment, IL-6 and HMGB1 in the HM group decreased, and p53 in the LM group decreased. TNF- $\alpha$  decreased in both matrine-treated groups. The decrease in TNF- $\alpha$  in the HM group was more significant than that in the LM group. No significant differences were found among groups with respect to 26S proteasome and TGF- $\beta$ 1.

## 4. Discussion

CRC is a leading cause of cancer-related deaths worldwide, and studies suggest that matrine may have antitumor effects and could have potential for treating CRC. However, how this occurs is not clear. A network pharmacology approach

to understand mechanistic aspects of drugs may offer novel approaches for studying new compounds. We studied the effect of matrine on rats with CRC using this network pharmacology approach, and we observed that matrine significantly suppressed CRC growth; this was associated with dysregulation of specific proteins (IL-6, TNF- $\alpha$ , HMGB1, and p53) and a corresponding pathway (HMGB1 signaling) and a function (Th cell differentiation). To our knowledge, this study is the first report about the anti-CRC mechanism of matrine using network pharmacology.

IL-6 is mainly secreted by T cells and macrophages to stimulate an immune response and cause inflammation. IL-6 is critical for tumor microenvironment regulation and may be a key regulator during colorectal tumorigenesis via regulation of tumor-promoting inflammation [16–18]. Patients with advanced/metastatic cancer had high IL-6 [19, 20], and IL-6 expression was significantly elevated in CRC tissues compared to noncancerous tissues and was associated with invasiveness and lymph node metastasis [21]. Anti-IL-6 therapy was initially developed for treating autoimmune diseases, but the role of IL-6 in chronic inflammation suggests that IL-6 blockade may be feasible for cancer treatment [22, 23]. TNF- $\alpha$  is a cell signaling protein involved in systemic inflammation produced chiefly by activated macrophages. TNF- $\alpha$  plays a pivotal role in malignant cellular proliferation, angiogenesis, tissue invasion, and metastasis in CRC [24]. A previous study demonstrated that serum TNF- $\alpha$  may contribute to CRC susceptibility,

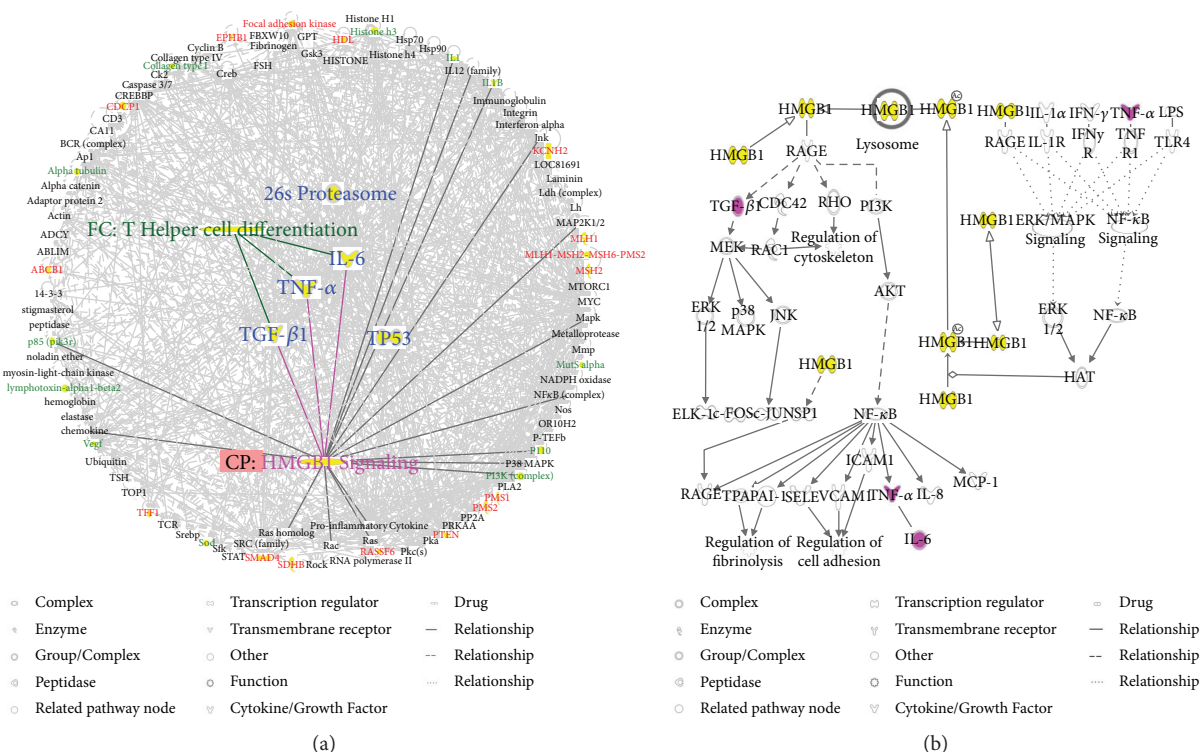


FIGURE 4: Common highly linked molecules and their most significantly related signaling pathways and functions in the “matrine-CRC” merged network. In the network, molecules are nodes, and biological relationships between two nodes are represented by lines. Solid lines between molecules show a direct physical relationship, whereas dotted lines show indirect functional relationships. (a) The five blue molecules in the center of the network represent common highly linked molecules. Red molecules represent CRC-related genes, and green molecules represent matrine-related proteins in the surrounding area of the network. In the Ingenuity Knowledge Database, “CP” is an abbreviation for “canonical pathway,” which represents a signaling pathway related to the highly linked molecules. “FC” is an abbreviation for “functional characteristic,” which represents functions related to the highly linked molecules. (b) Purple symbols represent highly linked molecules, and yellow symbols represent the molecules in the HMGB1 signaling pathway.

TABLE 1: CRC in different groups (mean ± SD).

Groups (n)	Incidence (%)	Number	Weight (g)	Size (cm <sup>3</sup> )
Control (8)	0	0	0	0
Model (8)	100	2.63 ± 0.74	0.89 ± 0.86	1.09 ± 0.65
LM (8)	87.5	2.25 ± 0.71	0.17 ± 0.21*	0.45 ± 0.50*
HM (8)	75.0	1.50 ± 0.76**	0.15 ± 0.17*	0.28 ± 0.27**

Note: matrine-administered groups compared to the model group. \*P < 0.05, \*\*P < 0.01.

and anti-TNF therapy was considered for CRC treatment [25]. In this study, matrine reduced elevated IL-6 and TNF-α in CRC, which was consistent with previous studies. TGF-β1 is a protein secreted by most immune cells, and it contributes to immune system control and performs cellular functions, including control of cell growth, proliferation, differentiation, and apoptosis [26]. A study showed that TGF-β1 promoted CRC immune escape [27]. TGF-β1 was increased in peripheral blood of CRC patients and may be associated with tumor size and location [28, 29]. Matrine did not affect TGF-β1 expression.

IL-6, TNF-α, and TGF-β1 are involved in HMGB1 signaling. HMGB1 is secreted by immune cells such as

macrophages, monocytes, and dendritic cells, and it acts as a cytokine mediator of inflammation [30–33]. HMGB1 signals through the receptor for advanced glycation end-products (RAGE), a multiligand receptor of the immunoglobulin superfamily. Cell activation by HMGB1 causes release of pro-inflammatory cytokines such as IL-6, TNF-α, and TGF-β1 [34]. HMGB1 is key to cancer development, progression, and metastasis because it activates cancer cells, enhances tumor angiogenesis, and suppresses host anticancer immunity [35]. HMGB1 targeting has been identified as a potential therapeutic strategy against cancer development, progression, and in particular, metastasis [36]. We found that along with decreased IL-6 and TNF-α, matrine inhibited increases

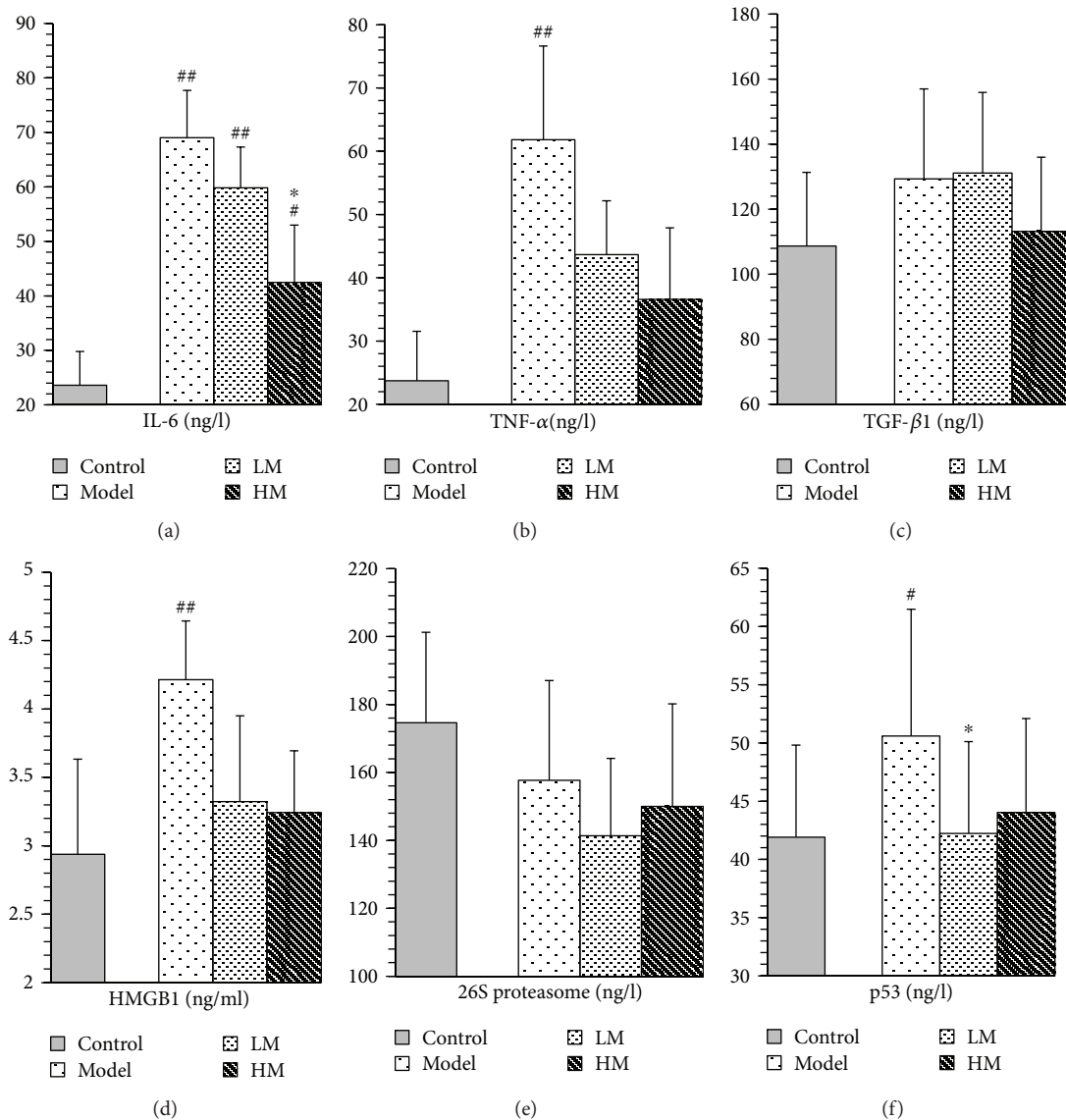


FIGURE 5: Expression of predicted target proteins in control, model and matrine-treated groups. Model, LM, and HM versus control, respectively: # $P < 0.05$  and ## $P < 0.01$ . LM and HM versus model, respectively: \* $P < 0.05$ .

in HMGB1 in CRC, suggesting that HMGB1 and HMGB1 signaling may be relevant targets for CRC treatment.

p53 is a protein encoded by the TP53 gene, which is the most frequently mutated gene in human cancers and is a key to preventing cancer formation [37, 38]. TP53 was thought to be a potential predictive biomarker for CRC development and it has been used in the targeted therapy of CRC [39–41]. Matrine decreased expression of p53 in CRC, suggesting that targeting p53 might explain how matrine affects CRC. Proteasomes are critical to the function of the adaptive immune system by regulating expression of proinflammatory cytokine TNF- $\alpha$  [42]. Increased proteasome was correlated with autoimmune disease activity [43]. Proteasome inhibitors were effective against tumors in cell culture, inducing apoptosis by disrupting regulated degradation of pro-growth cell cycle proteins [44]. Targeting the proteasome may thus be promising for treating

CRC [45, 46]. Our data suggest that targeting the 26S proteasome may explain how matrine affects CRC.

## 5. Conclusion

Inhibition of HMGB1 signaling characterized by abnormal expression of specific proteins (IL-6, TNF- $\alpha$ , and HMGB1) relevant to Th cell differentiation was likely the underlying mechanism of CRC treatment by matrine. This finding might facilitate the identification of new targets for CRC treatment as well as offer information for novel targets and purported mechanisms for Chinese herbal medicine.

## Conflicts of Interest

All authors declared no competing interests regarding the publication of this paper.

## Authors' Contributions

Huizhen Fan, Jingtao Li, and Hongchuan Zhao conceptualized and designed the experiments. Chunyan Jiang, Baoyuan Zhong, Jianwen Sheng, Ting Chen, and Qingqing Chen performed the experiments. Chunyan Jiang, Baoyuan Zhong, Ting Chen, Qingqing Chen, and Jianwen Sheng analyzed the data. Huizhen Fan, Jingtao Li, and Hongchuan Zhao contributed the reagents/materials/analysis tools. Chunyan Jiang, Huizhen Fan, and Jingtao Li wrote the paper. Huizhen Fan, Chunyan Jiang, and Baoyuan Zhong contributed equally to this work.

## Acknowledgments

This study was supported by the National Science Foundation of China (no. 81360606), the China Scholarship Council fund (no. 201609110029), the China-Japan Friendship Hospital Research funding (no. 2016-1-MS-5), and the National High Technology Research and Development Program of China (863 programs) (no. 2014AA020801).

## Supplementary Materials

Table S1: Matrine-related proteins. Table S2: CRC-related genes. (*Supplementary Materials*)

## References

- [1] D. Cunningham, W. Atkin, H. J. Lenz et al., "Colorectal cancer," *The Lancet*, vol. 375, no. 9719, pp. 1030–1047, 2010.
- [2] R. Lozano, M. Naghavi, K. Foreman et al., "Global and regional mortality from 235 causes of death for 20 age groups in 1990 and 2010: a systematic analysis for the Global Burden of Disease Study 2010," *The Lancet*, vol. 380, no. 9859, pp. 2095–2128, 2012.
- [3] T. H. Lin, H. R. Yen, J. H. Chiang, M. F. Sun, H. H. Chang, and S. T. Huang, "The use of Chinese herbal medicine as an adjuvant therapy to reduce incidence of chronic hepatitis in colon cancer patients: a Taiwanese population-based cohort study," *Journal of Ethnopharmacology*, vol. 202, pp. 225–233, 2017.
- [4] T. J. Chien, C. Y. Liu, R. H. Lu, C. W. Kuo, Y. C. Lin, and C. H. Hsu, "Therapeutic efficacy of traditional Chinese medicine, "Kuan-Sin-Yin", in patients undergoing chemotherapy for advanced colon cancer - a controlled trial," *Complementary Therapies in Medicine*, vol. 29, pp. 204–212, 2016.
- [5] T. H. Chao, P. K. Fu, C. H. Chang et al., "Prescription patterns of Chinese herbal products for post-surgery colon cancer patients in Taiwan," *Journal of Ethnopharmacology*, vol. 155, no. 1, pp. 702–708, 2014.
- [6] L. Wu, G. Wang, J. Wei et al., "Matrine derivative YF-18 inhibits lung cancer cell proliferation and migration through down-regulating Skp2," *Oncotarget*, vol. 8, no. 7, pp. 11729–11738, 2017.
- [7] X. Zhang and H. Yu, "Matrine inhibits diethylnitrosamine-induced HCC proliferation in rats through inducing apoptosis via p53, Bax-dependent caspase-3 activation pathway and down-regulating MLCK overexpression," *Iranian Journal of Pharmaceutical Research*, vol. 15, no. 2, pp. 491–499, 2016.
- [8] L. Ge, Y. f. Wang, J. h. Tian et al., "Network meta-analysis of Chinese herb injections combined with FOLFOX chemotherapy in the treatment of advanced colorectal cancer," *Journal of Clinical Pharmacy and Therapeutics*, vol. 41, no. 4, pp. 383–391, 2016.
- [9] W. Zhang, Y. Bai, Y. Wang, and W. Xiao, "Polypharmacology in drug discovery: a review from systems pharmacology perspective," *Current Pharmaceutical Design*, vol. 22, no. 21, pp. 3171–3181, 2016.
- [10] S. Y. Chan and J. Loscalzo, "The emerging paradigm of network medicine in the study of human disease," *Circulation Research*, vol. 111, no. 3, pp. 359–374, 2012.
- [11] J. Li, C. Lu, M. Jiang et al., "Traditional Chinese medicine-based network pharmacology could lead to new multicomponent drug discovery," *Evidence-Based Complementary and Alternative Medicine*, vol. 2012, Article ID 149762, 11 pages, 2012.
- [12] N. Zhao, J. Li, L. Li et al., "Molecular network-based analysis of guizhi-shaoyao-zhimu decoction, a TCM herbal formula, for treatment of diabetic peripheral neuropathy," *Acta Pharmacologica Sinica*, vol. 36, no. 6, pp. 716–723, 2015.
- [13] S. Zhao and S. Li, "Network-based relating pharmacological and genomic spaces for drug target identification," *PLoS One*, vol. 5, no. 7, article e11764, 2010.
- [14] Y. Tan, Q. Qi, C. Lu et al., "Cytokine imbalance as a common mechanism in both psoriasis and rheumatoid arthritis," *Mediators of Inflammation*, vol. 2017, Article ID 2405291, 13 pages, 2017.
- [15] L. Tanwar, H. Piplani, and S. Sanyal, "Anti-proliferative and apoptotic effects of etoricoxib, a selective COX-2 inhibitor, on 1,2-dimethylhydrazine dihydrochloride-induced colon carcinogenesis," *Asian Pacific Journal of Cancer Prevention*, vol. 11, no. 5, pp. 1329–1333, 2010.
- [16] J. Li, H. Y. Mo, G. Xiong et al., "Tumor microenvironment macrophage inhibitory factor directs the accumulation of interleukin-17-producing tumor-infiltrating lymphocytes and predicts favorable survival in nasopharyngeal carcinoma patients," *The Journal of Biological Chemistry*, vol. 287, no. 42, pp. 35484–35495, 2012.
- [17] M. Z. Bandy, H. M. Balkhi, A. S. Sameer, N. A. Chowdri, and E. Haq, "Strong association of interleukin-6–174G/C promoter single nucleotide polymorphism with a decreased risk of colorectal cancer in ethnic Kashmiri population: a case control study," *Tumour Biology*, vol. 39, no. 3, 2017.
- [18] J. Han, Q. Xi, Q. Meng et al., "Interleukin-6 promotes tumor progression in colitis-associated colorectal cancer through HIF-1 $\alpha$  regulation," *Oncology Letters*, vol. 12, no. 6, pp. 4665–4670, 2016.
- [19] P. Smith, A. Hobisch, D. Lin, Z. Culig, and E. Keller, "Interleukin-6 and prostate cancer progression," *Cytokine & Growth Factor Reviews*, vol. 12, no. 1, pp. 33–40, 2001.
- [20] G. Bellone, C. Smirne, F. A. Mauri et al., "Cytokine expression profile in human pancreatic carcinoma cells and in surgical specimens: implications for survival," *Cancer Immunology, Immunotherapy*, vol. 55, no. 6, pp. 684–698, 2006.
- [21] J. Zeng, Z. H. Tang, S. Liu, and S. S. Guo, "Clinicopathological significance of overexpression of interleukin-6 in colorectal cancer," *World Journal of Gastroenterology*, vol. 23, no. 10, pp. 1780–1786, 2017.
- [22] K. V. Korneev, K. S. N. Atretkhany, M. S. Drutskaya, S. I. Grivennikov, D. V. Kuprash, and S. A. Nedospasov, "TLR-

- signaling and proinflammatory cytokines as drivers of tumorigenesis," *Cytokine*, vol. 89, pp. 127–135, 2017.
- [23] D. Anestakis, S. Petanidis, S. Kalyvas et al., "Mechanisms and applications of interleukins in cancer immunotherapy," *International Journal of Molecular Sciences*, vol. 16, no. 1, pp. 1691–1710, 2015.
- [24] M. Z. Banday, H. M. Balkhi, Z. Hamid, A. S. Sameer, N. A. Chowdri, and E. Haq, "Tumor necrosis factor- $\alpha$  (TNF- $\alpha$ )-308G/A promoter polymorphism in colorectal cancer in ethnic Kashmiri population—a case control study in a detailed perspective," *Meta Gene*, vol. 9, pp. 128–136, 2016.
- [25] I. A. Gutierrez-Hurtado, A. M. Puebla-Pérez, J. I. Delgado-Saucedo et al., "Association between TNF- $\alpha$ -308G>A and -238G>A gene polymorphisms and TNF- $\alpha$  serum levels in Mexican colorectal cancer patients," *Genetics and Molecular Research*, vol. 15, no. 2, 2016.
- [26] J. J. Letterio and A. B. Roberts, "Regulation of immune responses by TGF- $\beta$ ," *Annual Review of Immunology*, vol. 16, no. 1, pp. 137–161, 1998.
- [27] X. Zhou, Y. Mao, J. Zhu et al., "TGF- $\beta$ 1 promotes colorectal cancer immune escape by elevating B7-H3 and B7-H4 via the miR-155/miR-143 axis," *Oncotarget*, vol. 7, no. 41, pp. 67196–67211, 2016.
- [28] N. S. Stanilov, L. Miteva, G. Cirovski, and S. A. Stanilova, "Increased transforming growth factor  $\beta$  and interleukin 10 transcripts in peripheral blood mononuclear cells of colorectal cancer patients," *Contemporary Oncology*, vol. 20, no. 6, pp. 458–462, 2016.
- [29] J. Ma, H. M. Gao, X. Hua, Z. Y. Lu, and H. C. Gao, "Role of TGF- $\beta$ 1 in human colorectal cancer and effects after cantharidinate intervention," *Asian Pacific Journal of Cancer Prevention*, vol. 15, no. 9, pp. 4045–4048, 2014.
- [30] J. R. Klune, R. Dhupar, J. Cardinal, T. R. Billiar, and A. Tsung, "HMGB1: endogenous danger signaling," *Molecular Medicine*, vol. 14, no. 7-8, pp. 476–484, 2008.
- [31] H. Wang, O. Bloom, M. Zhang et al., "HMG-1 as a late mediator of endotoxin lethality in mice," *Science*, vol. 285, no. 5425, pp. 248–251, 1999.
- [32] H. Yang, H. S. Hreggvidsdottir, K. Palmblad et al., "A critical cysteine is required for HMGB1 binding to Toll-like receptor 4 and activation of macrophage cytokine release," *Proceedings of the National Academy of Sciences of the United States of America*, vol. 107, no. 26, pp. 11942–11947, 2010.
- [33] H. Yang and K. J. Tracey, "Targeting HMGB1 in inflammation," *Biochimica et Biophysica Acta (BBA) - Gene Regulatory Mechanisms*, vol. 1799, no. 1-2, pp. 149–156, 2010.
- [34] <https://reports.ingenuity.com/rs/report/cpathway?id=ING%3A41lxf>.
- [35] M. T. Lotze and R. A. DeMarco, "Dealing with death: HMGB1 as a novel target for cancer therapy," *Current Opinion in Investigational Drugs*, vol. 4, no. 12, pp. 1405–1409, 2003.
- [36] H. Ohmori, Y. Luo, and H. Kuniyasu, "Non-histone nuclear factor HMGB1 as a therapeutic target in colorectal cancer," *Expert Opinion on Therapeutic Targets*, vol. 15, no. 2, pp. 183–193, 2011.
- [37] S. Surget, M. P. Khoury, and J. C. Bourdon, "Uncovering the role of p53 splice variants in human malignancy: a clinical perspective," *OncoTargets and Therapy*, vol. 7, pp. 57–68, 2013.
- [38] M. Hollstein, D. Sidransky, B. Vogelstein, and C. Harris, "p53 mutations in human cancers," *Science*, vol. 253, no. 5015, pp. 49–53, 1991.
- [39] M. Skerenova, E. Halašová, T. Matáková et al., "Low variability and stable frequency of common haplotypes of the TP53 gene region in colorectal cancer patients in a Slovak population," *Anticancer Research*, vol. 37, no. 4, pp. 1901–1907, 2017.
- [40] Y. Liu, X. Zhang, C. Han et al., "TP53 loss creates therapeutic vulnerability in colorectal cancer," *Nature*, vol. 520, no. 7549, pp. 697–701, 2015.
- [41] L. Du, J. J. Kim, J. Shen, B. Chen, and N. Dai, "KRAS and TP53 mutations in inflammatory bowel disease-associated colorectal cancer: a meta-analysis," *Oncotarget*, vol. 8, no. 13, pp. 22175–22186, 2017.
- [42] M. Karin and M. Delhase, "The I $\kappa$ B kinase (IKK) and NF- $\kappa$ B: key elements of proinflammatory signalling," *Seminars in Immunology*, vol. 12, no. 1, pp. 85–98, 2000.
- [43] J. Wang and M. A. Maldonado, "The ubiquitin-proteasome system and its role in inflammatory and autoimmune diseases," *Cellular & Molecular Immunology*, vol. 3, no. 4, pp. 255–261, 2006.
- [44] J. Adams, V. J. Palombella, E. A. Sausville et al., "Proteasome inhibitors: a novel class of potent and effective antitumor agents," *Cancer Research*, vol. 59, no. 11, pp. 2615–2622, 1999.
- [45] L. Yang, J. Wan, S. Xiao et al., "BH3 mimetic ABT-737 sensitizes colorectal cancer cells to ixazomib through MCL-1 down-regulation and autophagy inhibition," *American Journal of Cancer Research*, vol. 6, no. 6, pp. 1345–1357, 2016.
- [46] T. Wu, W. Chen, Y. Zhong et al., "Nuclear export of ubiquitinated proteins determines the sensitivity of colorectal cancer to proteasome inhibitor," *Molecular Cancer Therapeutics*, vol. 16, no. 4, pp. 717–728, 2017.

## Research Article

# Immunomodulatory Effect of Flavonoids of Blueberry (*Vaccinium corymbosum* L.) Leaves via the NF- $\kappa$ B Signal Pathway in LPS-Stimulated RAW 264.7 Cells

Dazhi Shi,<sup>1,2</sup> Mengyi Xu,<sup>1,2</sup> Mengyue Ren,<sup>1,2</sup> Enshan Pan,<sup>1</sup> Chao-hua Luo,<sup>1</sup> Wei Zhang,<sup>3</sup> and Qingfa Tang<sup>1,2</sup>

<sup>1</sup>School of Traditional Chinese Medicine, Southern Medical University, Guangzhou 510515, China

<sup>2</sup>Guangdong Provincial Key Laboratory of Chinese Medicine Pharmaceutics, Southern Medical University, Guangzhou 510515, China

<sup>3</sup>State Key Laboratory of Quality Research in Chinese Medicines, Macau Institute for Applied Research in Medicine and Health, Macau University of Science and Technology, Taipa, Macau

Correspondence should be addressed to Wei Zhang; [wzhang@must.edu.mo](mailto:wzhang@must.edu.mo) and Qingfa Tang; [tangqf96@163.com](mailto:tangqf96@163.com)

Received 24 August 2017; Accepted 13 November 2017; Published 27 December 2017

Academic Editor: Lifei Hou

Copyright © 2017 Dazhi Shi et al. This is an open access article distributed under the Creative Commons Attribution License, which permits unrestricted use, distribution, and reproduction in any medium, provided the original work is properly cited.

**Objective.** This study aimed to explore the immunoregulatory effect of flavonoids of blueberry (*Vaccinium corymbosum* L.) leaves (FBL). **Methods.** The flavonoids of blueberry leaves were prepared with 70% ethanol and were identified by ultraperformance liquid chromatography/quadrupole-time-of-flight mass spectrometry (UPLC/Q-ToF-MS). The immunoregulatory effect and possible regulatory mechanisms of FBL were investigated in lipopolysaccharide- (LPS-) induced RAW 264.7 cells. **Results.** According to the results of UPLC/Q-ToF-MS, nine flavonoids of blueberry leaves were identified. FBL showed a significant reduction in the production of TNF- $\alpha$  in LPS-stimulated RAW 264.7 cells. FBL significantly decreased the expression of NF- $\kappa$ B p65 and P-NF- $\kappa$ B p65 in LPS-induced RAW 264.7 cells in a dose-dependent manner. **Conclusion.** Our study showed the immunoregulatory effect of FBL through the suppression of TNF- $\alpha$  via the NF- $\kappa$ B signal pathway.

## 1. Introduction

Immunoregulation refers to the regulation of the immune system, such as stimulation, expression, amplification, or inhibition of any portion or stage of the immune response [1]. Inflammation is also part of the immunoregulation. Among various immune-related cells, macrophages not only phagocytose a variety of pathogenic microorganism, apoptotic cells, and tumor cells but also play important roles in the innate and adaptive immune responses [2]. Once infected with activation factors, macrophages release various inflammatory cytokines, including tumor necrosis factor-alpha (TNF- $\alpha$ ), interleukin-1beta (IL-1 $\beta$ ), and interleukin-6 (IL-6) [3]. These cytokines subsequently promote the activation and production of macrophages, then lead to macrophage infiltration and induce a local inflammatory response [4].

Many studies of the molecular mechanism of inflammation have shown that the nuclear factor-kappa B (NF- $\kappa$ B) signal pathways [5–8], which are closely related to macrophages' growth and proliferation, play an important role in the molecular mechanism of inflammation. p65 is one of the subunits of the NF- $\kappa$ B transcription factor protein family [9]. The heterodimers of p65 and p50 play a major role in the NF- $\kappa$ B signal pathway. p65 is associated with DNA binding, dimerization, transcriptional activation, and nuclear translocation [9, 10]. The phosphorylation of I $\kappa$ Bs in stimulating cells by an inducer could lead to activating the NF- $\kappa$ B signal pathway. Then, NF- $\kappa$ B signal pathway activation would lead to transducing a signal from the cell surface to the nucleus [11].

Blueberry, also named cranberry, is perennial deciduous or evergreen shrubs of *Vaccinium corymbosum* L. [12]. A growing number of studies found that blueberry possesses

several bioactivities such as antioxidation, free radical scavenging, anticancer, and lowering of blood pressure, plasma lipid, and blood glucose [13–16]. It has been widely used as health care products around the world. Blueberry leaves mainly contain phenylpropanoid and flavonoids [17], such as rutin, quercetin, kaempferol, and cyanidin-3-O-glu, which are similar to those of the fruits [18]. However, there are few studies about the bioactivities of blueberry leaves [8, 19].

In the present study, the chemical components of FBL were analyzed and identified by UPLC/Q-ToF-MS. Moreover, TNF- $\alpha$  was measured by ELISA, and NF- $\kappa$ B p65 and P-NF- $\kappa$ B p65 in LPS-induced RAW 264.7 cells were examined by Western blot. This study showed that FBL were a potential immune-adjusting reagent of the medicinal plant.

## 2. Materials and Methods

**2.1. Chemicals and Materials.** Indometacin tablets were obtained from Linfen Qilin Pharmaceutical Co. Ltd. (Shanxi, China). Dulbecco's modified Eagle's medium (DMEM) and fetal bovine serum (FBS) were obtained from Gibco (CA, USA). LPS and 3-(4,5-dimethyl-2-thiazolyl)-2,5-diphenyl-2-H-tetrazolium bromide (MTT) were purchased from Sigma-Aldrich Chemical (St. Louis, MO, USA). The enzyme-linked immunosorbent assay (ELISA) transcriptase kits for TNF- $\alpha$  were purchased from CUSABIO (Wuhan, China). The primary antibodies anti-NF- $\kappa$ B p65 antibody and anti-P-NF- $\kappa$ B p65 antibody were purchased from Abcam (Cambridge Science Park, UK). Peroxidase-labeled rabbit anti-mouse, sheep anti-rabbit immunoglobulin, and an enhanced chemiluminescence (ECL) detection system were obtained from Amersham (Arlington Heights, IL, USA). All other chemicals were purchased from Sigma-Aldrich Chemical. The dried leaves of blueberry were purchased from Jiagsu, China.

**2.2. Preparation of FBL.** The dried leaves of blueberry (20 kg) were first extracted for three times with 95% ethanol. The obtained extract was separated by macroporous resin D101. The 70% ethanol product was prepared into lyophilized FBL powder (17.0 g).

**2.3. UPLC/Q-ToF-MS Analysis of FBL.** Lyophilized FBL powder (0.01 g) was dissolved in 1 mL 3% DMSO (*v/v*). The FBL solution was solubilized by ultrasonic treatment for 5 min. Then, it was centrifuged at 15,000 rpm for 10 min. The supernatant was filtered through a 0.22  $\mu$ m syringe filter to be the stock solution of FBL. 50  $\mu$ L of the stock solution was transferred to a 1.5 mL tube, and 950  $\mu$ L of distilled water was added. The resulting solution was injected into the UPLC system for qualitative analysis.

The FBL sample was analyzed with the Waters Xevo G2 Q-ToF/UPLC system. Chromatographic separation was performed on a reversed-phase stationary phase (Agilent ZORBAX SB-Aq C18 column: 100 mm  $\times$  2.1 mm, 3.5  $\mu$ m) with an injection volume of 3  $\mu$ L. The mobile phase consisted of acetonitrile (A) and 0.1% formic acid (B) with a flow rate of 0.4 mL/min at 30°C. The gradient program was set as follows: 15% to 25% A at 0.0–20.0 min and 25% to 37% A

at 20.0–22.0 min. The interface between UPLC and Q-ToF was the ESI source with the electrospray inlet operated in the negative mode. The column effluent was introduced into Q-ToF. Detection of the ions was performed in the full-scan mode. Data acquisition range (*m/z*) is 150 to 1000. Ion source parameters were as follows: capillary voltage: 3200 V, cone hole voltage: 30 V, ion source temperature: 100°C, desolvent temperature: 350°C, volume flow rate of atomization gas (N<sub>2</sub>): 60 L/h, volume flow rate of desolvent gas (N<sub>2</sub>): 600 L/h, and collision energy (CE): 20 to 50 V. The analytical data were processed by the Masslynx software.

**2.4. Cell Lines and Cell Culture.** The murine macrophage cell line RAW 264.7 cells were obtained from the Institute of Biochemistry and Cell Biology (Shanghai, China). Cells were cultured in DMEM with 10% FBS, penicillin (100 U/mL), and streptomycin (100  $\mu$ g/mL) in a humidified atmosphere with 5% CO<sub>2</sub> at 37°C.

**2.5. Determination of Cell Viability.** Cell viability was measured by the MTT assay. RAW 264.7 cells were seeded at a density of  $5 \times 10^5$  cells/mL in 96-well plates. Then, various concentrations of test samples were treated for 3 h, and cells were continued to stimulate with 1  $\mu$ g/mL LPS for 24 h. Subsequently, MTT solution was given a final concentration of 0.5 mg/mL with incubation for 4 h at 37°C. After formazan was fully dissolved in DMSO, the absorption values were measured at 570 nm (reference, 630 nm) on a microplate reader. The cell viability in the control group (cells were treated by LPS) was set as 100%.

**2.6. Determination of FBL Treatment Duration.** RAW 264.7 cells were seeded at a density of  $5 \times 10^5$  cells/mL in 96-well plates. Then, cells were divided into 4 groups which were respectively treated with 62.50  $\mu$ g/mL FBL solution for 3 h, 6 h, 12 h, and 24 h. Cells were continued to stimulate with 1  $\mu$ g/mL LPS for 24 h. Cell viability was measured by the MTT assay as mentioned in Section 2.5. The control group (treated without FBL and LPS) and model group (only treated with LPS) were treated in parallel.

**2.7. Determination of TNF- $\alpha$  by ELISA.** RAW 264.7 cells were divided into the positive group, high-dose FBL group, middle-dose FBL group, and low-dose FBL group, which were treated with 44.70 mg/mL indometacin solution and 62.50, 15.62, and 3.91  $\mu$ g/mL FBL solution dissolved in DMEM for 6 h, respectively, and continued to stimulate with 1  $\mu$ g/mL LPS for 24 h. RAW 264.7 cells in the model group were just stimulated with 1  $\mu$ g/mL LPS for 24 h without the 6 h of pretreatment. RAW 264.7 cells in the control group were treated with neither LPS nor FBL. The supernatant was collected and mixed with the same volume of Griess reagent for 15 minutes at room temperature in the dark. The level of TNF- $\alpha$  in cultured media was determined by selective ELISA kits according to the manufacturer's instructions. The absorbance was detected on a microplate reader.

**2.8. Western Blot Analysis.** The macrophages in the above six groups were collected and resuspended in RIPA lysis buffer for 20 min at 4°C. The protein concentrations of NF- $\kappa$ B p65



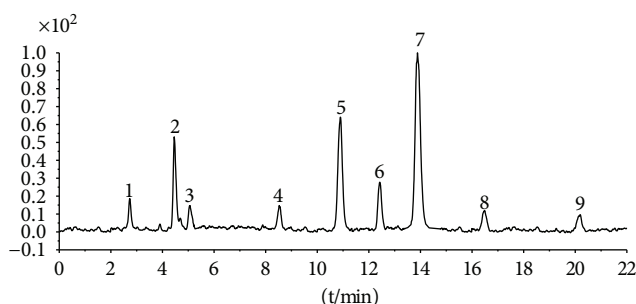


FIGURE 1: Total ion chromatogram of FBL in a negative mode. Peak attribution: myricetin (1), rutin (2), myricetin-3'-rhamnoside (3), toxicarisoflavone (4), 3,3',4',5,7-pentahydroxy-6-(4-hydroxybenzyl)-flavanone (5), iridin (6), quercetin (7), cyanidin-3-(6'-malonylglucoside) (8), and kaempferol (9).

and P-NF- $\kappa$ B p65 in the cell lysate were determined using a DC Protein Assay. Equal amounts of protein from each sample were separated by sodium dodecyl sulfate polyacrylamide gel electrophoresis (SDS-PAGE) at 80 V for 30 min and then at 120 V for 90 min and transferred onto the nitrocellulose membrane. The membranes were then incubated overnight at 4°C with the corresponding primary antibodies, followed by incubation with the appropriate secondary antibodies conjugated to horseradish peroxidase at room temperature for 2 hours. The ECL detection system was used to monitor the immune-reactive bands.

**2.9. Statistical Analysis.** All data are presented as mean  $\pm$  SD. The data were analyzed by the unpaired *t*-test. All statistical analyses were performed using SPSS 16.0 software (SPSS, Chicago, IL, USA), and a value of  $P < 0.05$  was accepted as statistically significant. All figures reflect the data obtained from at least three independent experiments.

### 3. Results

**3.1. Identification of the Main Constituents in FBL.** The major components of FBL were perfectly analyzed by a developed chromatographic method. The total ion chromatogram of FBL detected with UPLC/Q-ToF-MS in a negative mode was shown in Figure 1. The nine main constituents were detected as shown in Table 1. Nine peaks were identified as myricetin (1), rutin (2), myricetin-3'-rhamnoside (3), toxicarisoflavone (4), 3,3',4',5,7-pentahydroxy-6-(4-hydroxybenzyl)-flavanone (5), iridin (6), quercetin (7), cyanidin-3-(6'-malonylglucoside) (8), and kaempferol (9), respectively.

**3.2. Effects of FBL on Cell Viability.** The viability of RAW 264.7 cells treated with FBL solutions was shown in Table 2. The results showed that the cell viability decreased significantly at 125.00  $\mu$ g/mL and higher FBL concentrations ( $P < 0.01$ ), but there was no difference among 62.50, 31.25, 15.63, 7.81, and 3.91  $\mu$ g/mL groups. Therefore, 62.50  $\mu$ g/mL FBL was set as the high-dose group and then 15.63 and 3.91  $\mu$ g/mL FBL as the middle-dose and low-dose groups, respectively.

**3.3. FBL Treatment Duration of RAW 264.7 Cells.** Cell viability was determined via the MTT assay (Figure 2). The cell viability of model groups compared with control groups of different FBL treatment durations significantly increased ( $P < 0.01$ ). However, the cell viability of the FBL group compared with model groups decreased significantly among 6, 12, and 24 h FBL treatment duration groups ( $P < 0.01$ ). These data indicated RAW 264.7 cells treated with FBL for 6 h inhibited cell proliferation effectively.

**3.4. Effects of FBL on TNF- $\alpha$  Levels.** The levels of TNF- $\alpha$  in the culture media were measured by ELISA. As presented in Figure 3, the concentrations of TNF- $\alpha$  in the model group were increased significantly compared with those in the control group ( $P < 0.01$ ). The levels of TNF- $\alpha$  in the positive group were significantly decreased compared to those in the model group ( $P < 0.05$ ). The levels of TNF- $\alpha$  in the medium-dose FBL and high-dose FBL groups were significantly decreased compared to those in the model group ( $P < 0.05$ ). The levels of TNF- $\alpha$  in the high-dose FBL and low-dose FBL groups were significantly different compared to those in the medium-dose FBL group ( $P < 0.01$ ). These data indicated FBL negatively regulated the production of TNF- $\alpha$  at the transcriptional and translational levels in LPS-induced RAW 264.7 cells in a concentration-dependent manner.

**3.5. Effects of FBL on the Expression of NF- $\kappa$ B p65 and P-NF- $\kappa$ B p65.** To identify whether FBL mediates its anti-inflammatory activities by modulating NF- $\kappa$ B activation, the expression of NF- $\kappa$ B p65 and P-NF- $\kappa$ B p65 in LPS-activated macrophages treated with FBL was examined by Western blot (Figure 4). The level of NF- $\kappa$ B p65 and P-NF- $\kappa$ B p65 proteins in the model group was increased significantly compared with that in the control group ( $P < 0.01$ ). The level of NF- $\kappa$ B p65 and P-NF- $\kappa$ B p65 proteins of the positive group was decreased significantly compared to that in the model group ( $P < 0.01$ ). The concentrations of NF- $\kappa$ B p65 and P-NF- $\kappa$ B p65 of the middle- and high-dose groups were decreased significantly compared to those of the model group ( $P < 0.05$ ). These findings indicated that the anti-inflammatory action of FBL is at least partially due to the inhibition of NF- $\kappa$ B-dependent gene transcription.

### 4. Discussion

In this experiment, different columns and mobile phase conditions were tested and the appropriate chromatographic condition was obtained. Furthermore, the Q-ToF and MS conditions were determined after several attempts. The negative mode was selected because of better graphs and data compared. The parameters capillary voltage, collision energies, and ion source temperature were determined after multiple trials. The flavonoids of blueberry leaf (FBL) extract were identified by UPLC/Q-ToF-MS, mainly containing myricetin (1), rutin (2), myricetin-3'-rhamnoside (3), toxicarisoflavone (4), 3,3',4',5,7-pentahydroxy-6-(4-hydroxybenzyl)-flavanone (5), iridin (6), quercetin (7), cyanidin-3-(6'-malonylglucoside) (8), and kaempferol (9). The constituents were identified on the basis of references

TABLE 1: Identification of nine constituents of FBL by UPLC/Q-TOF-MS.

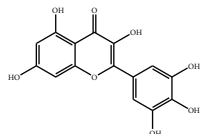
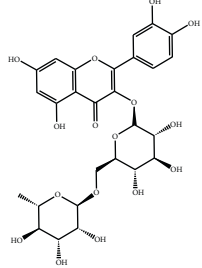
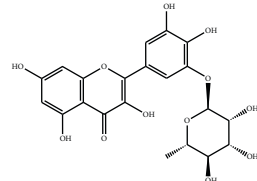
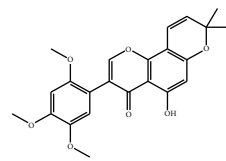
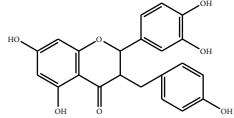
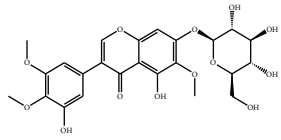
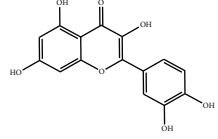
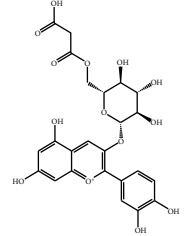
Number	R <sub>T</sub> /min	Constituents	Elemental composition	MS <sup>1</sup> /MS <sup>2</sup> (m/z)	Chemical structures
1	2.7	Myricetin	C <sub>15</sub> H <sub>10</sub> O <sub>8</sub>	317.0391 [M-H] <sup>-</sup> 179.0031, 151.0121, 109.0338	
2	4.5	Rutin	C <sub>27</sub> H <sub>30</sub> O <sub>16</sub>	609.1937 [M-H] <sup>-</sup> 301.0345, 300.0273	
3	5.2	Myricetin-3'-rhamnoside	C <sub>21</sub> H <sub>20</sub> O <sub>12</sub>	463.0771 [M-H] <sup>-</sup> 301.0293, 151.0093	
4	8.5	Toxicarisoflavone	C <sub>23</sub> H <sub>22</sub> O <sub>7</sub>	409.1559 [M-H] <sup>-</sup> 179.0310, 161.0223	
5	10.9	3,3',4',5,7-Pentahydroxy-6-(4-hydroxybenzyl)-flavanone	C <sub>22</sub> H <sub>18</sub> O <sub>8</sub>	409.1484 [M-H] <sup>-</sup> 179.0357, 135.0451	
6	12.4	Iridin	C <sub>24</sub> H <sub>26</sub> O <sub>13</sub>	521.1553 [M-H] <sup>-</sup> 359.1210, 315.1213, 297.1056, 163.0369	
7	13.2	Quercetin	C <sub>15</sub> H <sub>10</sub> O <sub>7</sub>	301.0283 [M-H] <sup>-</sup> 178.9975, 151.0028	
8	16.4	Cyanidin-3-(6'-malonyl-glucoside)	C <sub>24</sub> H <sub>23</sub> O <sub>14</sub>	533.1048 [M-H] <sup>-</sup> 357.0873, 301.0362	

TABLE 1: Continued.

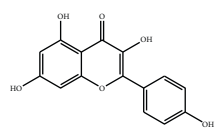
Number	R <sub>T</sub> /min	Constituents	Elemental composition	MS <sup>1</sup> /MS <sup>2</sup> (m/z)	Chemical structures
9	20.2	Kaempferol	C <sub>15</sub> H <sub>10</sub> O <sub>6</sub>	285.0196 [M-H] <sup>-</sup> 159.0665, 93.0676	

TABLE 2: Effects of FBL on the viability of RAW 264.7 cells.

FBL (μg/mL)	500.00	250.00	125.00	62.50	31.25	15.63	7.81	3.91
Cell viability (%) (X ± S)	74.80 ± 4.59**	83.15 ± 1.76**	88.75 ± 1.78**	101.50 ± 1.97	100.84 ± 4.32	101.05 ± 3.68	100.58 ± 2.76	100.33 ± 3.45

Control groups were treated only with 1 μg/mL LPS; the cell viability in the control group (cells were treated by LPS) was set as 100%. FBL groups were treated with 1 μg/mL LPS and different concentrations of FBL. \*\**P* < 0.01 versus control group treated with only LPS.

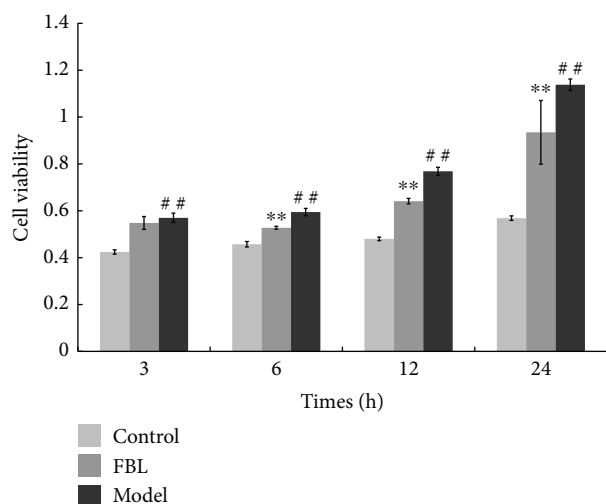


FIGURE 2: FBL treatment duration of RAW 264.7 cells. Control groups were treated without LPS and FBL, model groups were treated with only 1 μg/mL LPS, and FBL groups were treated with 1 μg/mL LPS and 62.50 μg/mL FBL. \*\**P* < 0.01: FBL group versus model group during the same treating time. ##*P* < 0.01: model group versus control group during the same treating time.

and mass spectrometry data, and several constituents were identified based on the reference standards.

The macrophage-based innate immune response plays an important role in congenital immune response. LPS-stimulated RAW 264.7 murine macrophage cells are generally considered a suitable model to study the immunomodulatory and anti-inflammatory effects of drugs [20]. In this study, the LPS-stimulated RAW 264.7 cell was prepared as an inflammation model. Not only the levels of TNF-α but also those of IL-6 were determined. After being stimulated with LPS, RAW 264.7 cells induced and released inflammatory factors IL-6 and TNF-α rapidly. The level of IL-6 showed no difference among the three FBL dose groups compared to

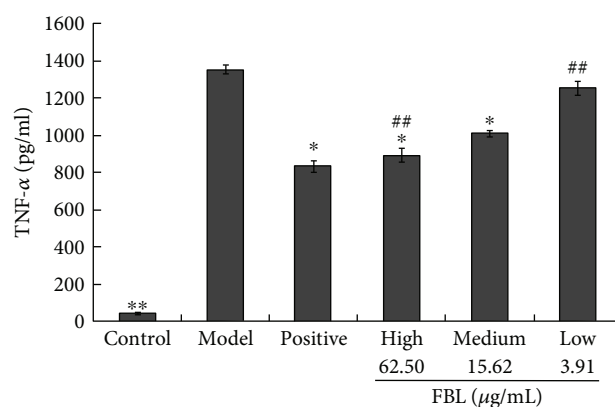


FIGURE 3: Effects of FBL on TNF-α levels in LPS-stimulated RAW 264.7 cells. Control group treated without LPS and FBL; model group treated with only 1 μg/mL LPS for 24 h; positive group treated with 44.70 mg/mL indometacin for 6 h and 1 μg/mL LPS for 24 h; and FBL groups treated with 62.50, 15.62, and 3.91 μg/mL FBL for 6 h, respectively, and 1 μg/mL LPS for 24 h. \**P* < 0.05 and \*\**P* < 0.01 versus control group. ##*P* < 0.01 versus medium-dose FBL group.

the model group. This illustrated that FBL had no effects on IL-6, which is related to the STAT signal pathway [21]. The results of TNF-α indicated that FBL could regulate in a concentration-dependent manner. Referenced to the studies of the NF-κB signal pathway, the production of cytokine TNF-α could activate the NF-κB signal pathway. Thus, the following experiment was designed to focus on the NF-κB signal pathway.

It has been reported that the nuclear transcription factor NF-κB is involved in the transcriptional regulation of a variety of cytokines and inflammatory mediators [22], which can specifically bind to a specific site of gene promoters and enhancer sequences to promote transcription and expression [23]. NF-κB p65 located in the cytoplasm would be inactivated after binding to its inhibitor IκB [24]. When it is subjected to external stimuli (such as LPS), IκBα

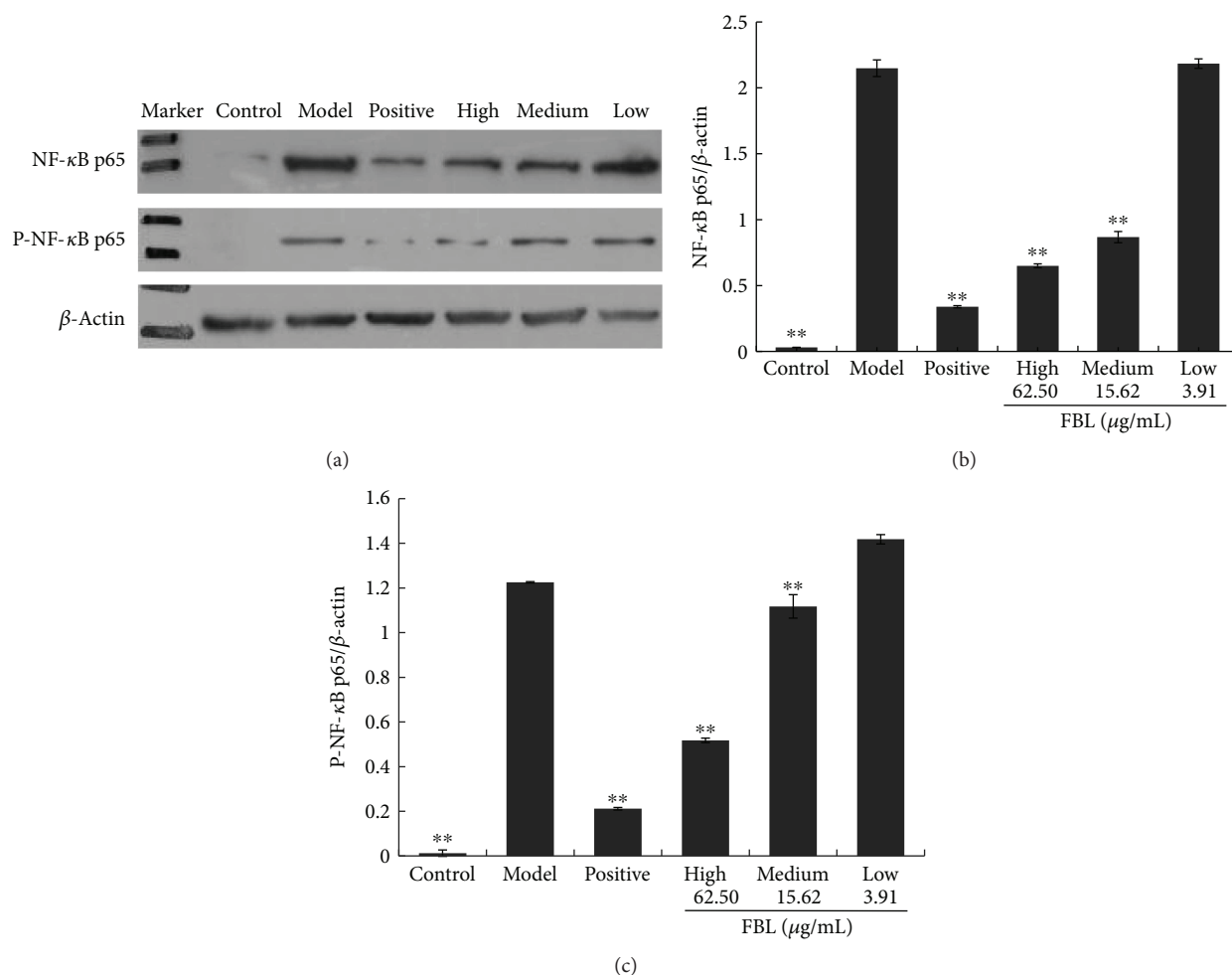


FIGURE 4: Effects of FBL on the expressions of NF-κB p65 and P-NF-κB p65 in LPS-stimulated RAW 264.7 cells. Control group treated without LPS and FBL; model group treated with only 1 μg/mL LPS for 24 h; positive group treated with 44.70 mg/mL indometacin for 6 h and 1 μg/mL LPS for 24 h; and FBL groups treated with 62.50, 15.62, and 3.91 μg/mL FBL for 6 h, respectively, and 1 μg/mL LPS for 24 h. (a) The picture of NF-κB p65, P-NF-κB p65, and β-actin; (b) the ratio of NF-κB p65 to β-actin; and (c) the ratio of P-NF-κB p65 to β-actin. \*\* $P < 0.01$  versus model group.

phosphorylates, degrades, and dissociates from the NF-κB/IκBα complex [25, 26]. The activated NF-κB p65 following the translocation into the cell nucleus combines with the target gene promoter or enhancer [27]. It continued to rapidly induce the synthesis and transcription of target gene mRNA. In our study, the level of NF-κB pathway protein p65 and its phosphorylated protein P-p65 was decreased in the high- and middle-dose groups compared to the model group. The result indicated that the FBL could inhibit the transcription of the NF-κB-dependent gene. It also illustrated that the anti-inflammatory of FBL is partially caused by inhibition of NF-κB-dependent gene transcription.

## 5. Conclusion

In summary, nine flavonoids of blueberry leaves were identified by UPLC/Q-ToF-MS which are similar to those of the blueberry fruit. The FBL could significantly reduce the expression and release of TNF-α in LPS-induced RAW 264.7 cells in a dose-dependent manner. Furthermore, the results of p65

and P-p65 suggested that FBL inhibits inflammation-related factor expression by suppressing the NF-κB signal pathway. Our findings provided some reference for the further development and utilization of the blueberry plant.

## Conflicts of Interest

The authors declare that they have no conflict of interest on this manuscript.

## Authors' Contributions

Dazhi Shi and Mengyi Xu contributed equally to this work.

## Acknowledgments

This work was supported by a grant from the National Natural Science Foundation of China (no. 81202431), the Natural Science Foundation of Guangdong Province

(no. 2015A030313282), and the Macao Science and Technology Development Fund (FDCT) (006/2015/A1).

## References

- [1] W. N. Abood, I. Fahmi, M. A. Abdulla, and S. Ismail, "Immunomodulatory effect of an isolated fraction from *Tinospora crispa* on intracellular expression of INF-gamma, IL-6 and IL-8," *BMC Complementary and Alternative Medicine*, vol. 205, no. 14, pp. 1–12, 2014.
- [2] X. Liu, J. Xie, S. Jia et al., "Immunomodulatory effects of an acetylated *Cyclocarya paliurus* polysaccharide on murine macrophages RAW264.7," *International Journal of Biological Macromolecules*, vol. 98, pp. 576–581, 2017.
- [3] N. Moazzezy, M. Oloomi, and S. Bouzari, "Effect of Shiga toxin and its subunits on cytokine induction in different cell lines," *International Journal of Molecular and Cellular Medicine*, vol. 2, no. 3, pp. 108–117, 2014.
- [4] Y. H. Huang, H. M. Wang, Z. Y. Cai, F. Y. Xu, and X. Y. Zhou, "Lipoxin A4 inhibits NF- $\kappa$ B activation and cell cycle progression in RAW264.7 cells," *Inflammation*, vol. 37, no. 4, pp. 1084–1090, 2014.
- [5] X. Li, J. Shen, Y. Jiang et al., "Anti-inflammatory effects of chloranthalactone B in LPS-stimulated RAW264.7 cells," *International Journal of Molecular Sciences*, vol. 17, no. 11, p. 1938, 2016.
- [6] K. Qing, B. Khuntirat, C. Mah et al., "Adeno-associated virus type 2-mediated gene transfer: correlation of tyrosine phosphorylation of the cellular single-stranded D sequence-binding protein with transgene expression in human cells in vitro and murine tissues in vivo," *Journal of Virology*, vol. 2, no. 72, pp. 1593–1599, 1998.
- [7] H. Chu, Q. Tang, H. Huang, W. Hao, and X. Wei, "Grape-seed proanthocyanidins inhibit the lipopolysaccharide-induced inflammatory mediator expression in RAW264.7 macrophages by suppressing MAPK and NF- $\kappa$ B signal pathways," *Environmental Toxicology and Pharmacology*, vol. 41, pp. 159–166, 2016.
- [8] D. Zhao, N. Su, Z. Hongyan, L. Yang, T. Huo, and C. Wang, "Isolation and quantification of flavonoids in blueberry leaves by microemulsion liquid chromatography," *Food Science*, vol. 36, no. 14, pp. 91–95, 2015.
- [9] Z. Q. Wei, L. Yan, J. G. Deng, and J. Deng, "Mangiferin protects rats against chronic bronchitis via regulating NF- $\kappa$ B (P65) and I $\kappa$ B $\alpha$  expression in mononuclear cells," *Acta Pharmaceutica Sinica*, vol. 49, no. 05, pp. 596–601, 2014.
- [10] C. Liu, H. Zhang, P. Cheng, and F. Zhou, "Expression of pre-B-cell colony enhancing factor and its influence on the expression of PBEF, TNF- $\alpha$ , IL-1 $\beta$  and NF- $\kappa$ B p65 in pulmonary tissues of rats with ARDS," *Journal of Chongqing Medical University*, vol. 39, no. 09, pp. 1226–1230, 2014.
- [11] A. Kumar, Y. Takada, A. M. Boriek, and B. B. Aggarwal, "Nuclear factor- $\kappa$ B: its role in health and disease," *Journal of Molecular Medicine*, vol. 82, no. 7, pp. 434–448, 2004.
- [12] L. Yingchang and M. Xianjun, "Studies on antioxidant activity of flavonoids from leaves of blueberry," *Acta Nutrimenta Sinica*, vol. 30, no. 04, pp. 427–429, 2008.
- [13] W. Xu, Q. Zhou, Y. Yao et al., "Inhibitory effect of Gardenblue blueberry (*Vaccinium ashei* Reade) anthocyanin extracts on lipopolysaccharide-stimulated inflammatory response in RAW 264.7 cells," *Journal of Zhejiang University Science B*, vol. 17, no. 6, pp. 425–436, 2016.
- [14] C. Wan, T. Yuan, A. L. Cirello, and N. P. Seeram, "Antioxidant and  $\alpha$ -glucosidase inhibitory phenolics isolated from highbush blueberry flowers," *Food Chemistry*, vol. 135, no. 3, pp. 1929–1937, 2012.
- [15] A. Brambilla, R. Lo Scalzo, G. Bertolo, and D. Torreggiani, "Steam-blanching highbush blueberry (*Vaccinium corymbosum* L.) juice: phenolic profile and antioxidant capacity in relation to cultivar selection," *Journal of Agricultural and Food Chemistry*, vol. 56, no. 8, pp. 2643–2648, 2008.
- [16] K. Nagao, K. Higa, B. Shirouchi et al., "Effect of *Vaccinium ashei* reade leaves on lipid metabolism in Otsuka Long-Evans Tokushima fatty rats," *Bioscience, Biotechnology, and Biochemistry*, vol. 6, no. 72, pp. 1619–1622, 2008.
- [17] L. Wei and W. Chun-peng, "Research progresses on blueberry of phytochemical constituents and activities in recently ten years," *The Food Industry*, vol. 36, no. 10, pp. 233–237, 2015.
- [18] S. Moze, T. Polak, L. Gasperlin et al., "Phenolics in Slovenian bilberries (*Vaccinium myrtillus* L.) and blueberries (*Vaccinium corymbosum* L.)," *Journal of Agricultural and Food Chemistry*, vol. 59, no. 13, pp. 6998–7004, 2011.
- [19] D. Zhao, N. Su, L. Yang, H. Zheng, T. Huo, and C. Wang, "In vitro anti-inflammatory effect of total flavonoids from blueberry leaves," *Food Science*, vol. 36, no. 17, pp. 231–235, 2015.
- [20] M. Mendis, E. Leclerc, and S. Simsek, "Arabinosylated hydrolyzates as immunomodulators in lipopolysaccharide-induced RAW264.7 macrophages," *Food & Function*, vol. 7, no. 7, pp. 3039–3045, 2016.
- [21] T. Venkatesan, Y. Choi, J. Lee, and Y. K. Kim, "Pinus densiflora needle supercritical fluid extract suppresses the expression of pro-inflammatory mediators iNOS, IL-6 and IL-1  $\beta$ , and activation of inflammatory STAT1 and STAT3 signaling proteins in bacterial lipopolysaccharide-challenged murine macrophages," *DARU Journal of Pharmaceutical Sciences*, vol. 25, no. 1, pp. 18–27.
- [22] Y. J. Kim, J. Deok, S. Kim et al., "Anti-inflammatory effect of Piper attenuatum methanol extract in LPS-stimulated inflammatory responses," *Evidence-based Complementary and Alternative Medicine*, vol. 2017, Article ID 4606459, 10 pages, 2017.
- [23] F. Chen, V. Castranova, X. Shi, and L. M. Demers, "New insights into the role of nuclear factor- $\kappa$ B, a ubiquitous transcription factor in the initiation of diseases," *Clinical Chemistry*, vol. 1, no. 45, pp. 7–17, 1999.
- [24] S. T. Tang, H. Su, Q. Zhang et al., "Sitagliptin inhibits endothelin-1 expression in the aortic endothelium of rats with streptozotocin-induced diabetes by suppressing the nuclear factor- $\kappa$ B/I $\kappa$ B $\alpha$  system through the activation of AMP-activated protein kinase," *International Journal of Molecular Medicine*, vol. 37, no. 6, pp. 1558–1566, 2016.
- [25] T. Peng, W. Zhou, F. Guo et al., "Centrosomal protein 55 activates NF- $\kappa$ B signalling and promotes pancreatic cancer cells aggressiveness," *Scientific Reports*, vol. 7, no. 1, p. 5925, 2017.
- [26] M. L. Schmitz and P. A. Baeuerle, "Multi-step activation of NF- $\kappa$ B/Rel transcription factors," *Immunobiology*, vol. 193, no. 2–4, pp. 116–127, 1995.
- [27] G. Ji, R. Chen, and J. Zheng, "Macrophage activation by polysaccharides from *Atractylodes macrocephala* Koidz through the nuclear factor- $\kappa$ B pathway," *Pharmaceutical Biology*, vol. 53, no. 4, pp. 512–517, 2015.

## Research Article

# Neuroprotective Potential of Gentongping in Rat Model of Cervical Spondylotic Radiculopathy Targeting PPAR- $\gamma$ Pathway

Wen Sun,<sup>1,2</sup> Kang Zheng,<sup>2</sup> Bin Liu,<sup>2</sup> Danping Fan,<sup>2</sup> Hui Luo,<sup>2,3</sup> Xiaoyuan Qu,<sup>4</sup> Li Li,<sup>2</sup> Xiaojuan He,<sup>2</sup> Jianfeng Yi,<sup>1</sup> and Cheng Lu<sup>2</sup>

<sup>1</sup>College of Chemical and Biological Engineering, Yichun University, Yichun 336000, China

<sup>2</sup>Institute of Basic Research in Clinical Medicine, China Academy of Chinese Medical Sciences, Beijing 100700, China

<sup>3</sup>School of Life Science and Engineering, Southwest Jiaotong University, Chengdu 610000, China

<sup>4</sup>Beijing Yjheal Medical Research Center, Beijing 100100, China

Correspondence should be addressed to Jianfeng Yi; 906165468@qq.com and Cheng Lu; lv\_cheng0816@163.com

Received 2 May 2017; Revised 15 July 2017; Accepted 25 July 2017; Published 5 November 2017

Academic Editor: Qingdong Guan

Copyright © 2017 Wen Sun et al. This is an open access article distributed under the Creative Commons Attribution License, which permits unrestricted use, distribution, and reproduction in any medium, provided the original work is properly cited.

Cervical spondylotic radiculopathy (CSR) is the most general form of spinal degenerative disease and is characterized by pain and numbness of the neck and arm. Gentongping (GTP) granule, as a classical Chinese patent medicine, has been widely used in curing CSR, whereas the underlying mechanism remains unclear. Therefore, the aim of this study is to explore the pharmacological mechanisms of GTP on CSR. The rat model of CSR was induced by spinal cord injury (SCI). Our results showed that GTP could significantly alleviate spontaneous pain as well as ameliorate gait. The HE staining and Western blot results showed that GTP could increase the quantity of motoneuron and enhance the activation of peroxisome proliferator-activated receptor gamma (PPAR- $\gamma$ ) in the spinal cord tissues. Meanwhile, immunofluorescence staining analysis indicated that GTP could reduce the expression of TNF- $\alpha$  in the spinal cord tissues. Furthermore, the protein level of Bax was decreased whereas the protein levels of Bcl-2 and NF200 were increased after the GTP treatment. These findings demonstrated that GTP might modulate the PPAR- $\gamma$  pathway by inhibiting the inflammatory response and apoptosis as well as by protecting the cytoskeletal integrity of the spinal cord, ultimately play a neuroprotective role in CSR.

## 1. Introduction

Cervical spondylotic radiculopathy (CSR) is one of the most general form of spinal degenerative disease [1]. The clinical manifestations of CSR focus on pain and numbness of the neck and arm as well as restricted neck movement, which greatly impact the patient's life and work [2]. The orthopedic of TCM theory holds that both the static system and the dynamic system are critical in maintaining normal position and function of the cervical spine. The imbalance of both static and dynamic forces can result in a degeneration of posterior column stability and then lead to rapid degeneration of the cervical intervertebral discs, thus causing a series of syndromes distributed along the spinal nerve roots [3, 4]. However, poor understanding of the pathobiology of CSR has limited the therapeutic progression of neurological

dysfunction [5]. The strategies currently approved for treatment of CSR include operative treatment and nonoperative treatment categories (including drugs, traction, physical therapy, functional exercise, etc.) [6, 7], in which Chinese herbal medicine therapy has occupied an important position [8–10].

*Gentongping* (GTP) granule is a classic traditional Chinese medicine (TCM) granule refined from several Chinese herbal medicines, such as *Radix Paeoniae Alba*, *Radix Puerariae*, *Carthamus tinctorius*, and so forth. It is widely produced in China in accordance with the China Pharmacopoeia standard of quality control and generally used for the treatment of cervical and lumbar spine disease [11, 12]. In preparation technology studies, Zhu et al. obtained a high-efficiency formulation [13]. High-performance liquid chromatography (HPLC) was also

repeatedly used in the determination of principal component analysis of GTP [14, 15]. For pharmacodynamic evaluation, Chen et al. and Peng et al. observed the therapeutic efficacy in improving the symptoms and signs of patients with cervical spondylosis radiculopathy [16, 17]. Although the herb product has been applied generally, the scientific basis of GTP treatment on CSR remains unclear.

Network pharmacology, a novel research field that elaborates the potential mechanisms of biological systems by analyzing diverse biological networks, may have the capacities to address the relationship between complex Chinese herbal medicine and disease [18]. According to our previous studies [19–21], we have obtained structural information of the composite compounds of each ingredient in GTP from TCM Database@Taiwan [22] (<http://tcm.cmu.edu.tw/>), which is currently the largest noncommercial TCM database worldwide. In total, we collected the structural information of 15 compounds for *Raidix Paeoniae Alba*, 22 compounds for *Radix Puerariae*, and 23 compounds for *Carthamus tinctorius*. We found that Galuteolin was the main component of *Raidix Paeoniae Alba* and arachidic acid was the main component of *Radix Puerariae* and *Carthamus tinctorius*. According to the PubChem database [23] (<https://pubchem.ncbi.nlm.nih.gov/>), we searched for an important protein peroxisome proliferator-activated receptor gamma (PPAR- $\gamma$ ), which was the target protein of arachidic acid (Supplementary Table 1 available online at <https://doi.org/10.1155/2017/9152960>). PPAR- $\gamma$  and its downstream molecules are involved in nociception [24]. PPAR- $\gamma$  coactivator, a cluster of nuclear transcriptional coactivators, plays an important role in several metabolism procedures including mitochondrial biogenesis, thermogenesis, respiration, insulin secretion, and gluconeogenesis, as well as the regulation of inflammation [25, 26]. The PPAR- $\gamma$  agonists have potential therapeutic actions on nervous disorders, including neuropathic pain, and have been regarded as promising therapeutic strategies for spinal cord injury patients [27, 28]. Thus, we speculated that the PPAR- $\gamma$  pathway might be involved in the GTP treatment of CSR for effective neuropathic pain relief.

Spinal cord injury (SCI) results in a gradually amplified necrotic area of cavitation, due to secondary neuronal death accelerated by acute inflammation, edema, apoptosis, and glial scarring [29–31]. Previous studies have shown that the rat model of SCI is a clinically relevant model [32]. Therefore, the purpose of this study was to implement the SCI model to investigate the basic therapeutic mechanism of GTP on CSR concerning the PPAR- $\gamma$  pathway.

## 2. Materials and Methods

**2.1. Animals.** Forty male Sprague-Dawley (SD) rats with mean weights of 190–210 g were obtained from Beijing Vital River Laboratory Animal Technology Co. Ltd. (China). The animals were maintained in a specific pathogen-free environment at an appropriate temperature and humidity and were allowed free access to standard rodent chow and water. Body weight was recorded once every three days. Before surgery, the rats were kept in the cages for 7 days for adaptation to

the environment and the exercise [33]. The rodent license of the laboratory (number SYXK-2010-0032) was issued by the National Science and Technology Ministry of China. Animal care and experimental protocols complied with the Research Ethics Committee of 163 Institute of Basic Theory of Chinese Medicine, China Academy of Chinese Medical Sciences.

**2.2. Spinal Cord Compression Model.** Male SD rats were anesthetized with intraperitoneal injection of 10% chloral hydrate (0.30 mL/100 g). Then, the surgical area was shaved and disinfected with 75% ethanol and betadine [5]. A 3.5 cm midline incision was incised at the C4-T1 area in nuchal, and the skin and superficial muscles were retracted, followed by the exposure of the C4-C6 laminae. The cervical laminae were identified by counting from T1. After that, ligamentum flavum of C5-C6 and C6-C7 were resected, the periosteum of C6 lamina was removed, and then a nylon suture measuring 15 mm long with a 0.5 mm diameter was implanted underneath the C6 lamina. The dura mater underneath was carefully separated from the lamina to avoid a tear and cerebral spinal fluid (CSF) leak. In the animals assigned to the sham operation group, the implantation passed through the dorsal epidural space [34]. Multilayer tissue closure was then performed [5]. After recovery on a heating pad, the rats were housed in individual cages and given food and water ad libitum.

**2.3. Drug Preparation and Administration.** After one week of SCI operation, all rats received drug administration. The drug concentrations and administration profiles were implemented based on the specification and kinetic properties. The treatment group was administered with GTP (Beijing Handian Pharmaceutical Co. Ltd., China) at a concentration of 0.32 g/100 g dissolved in saline solution. The positive control group was administered with fenbid (Glaxo Smith Kline Investment Co. Ltd., China) at a concentration of 4 mg/100 g dissolved in saline solution. The normal group, sham group, and model group were all given with saline with the same volume [35]. All rats were administered once a day for 5 weeks before sacrificed.

**2.4. Neurobehavioral Assessments.** Animals received a neurobehavioral test on the seventh day after the SCI operation. The rats were placed in an observation box. The duration of left forepaw leaving from the bottom was recorded over 15 min divided by 3 times, and the degree of spontaneous pain was evaluated by the duration. Meanwhile, the postures of rest and walk were monitored. The concrete process for evaluating gait was executed according to the previous study performed by Kawakami et al. and Dubuisson and Dennis [36, 37], and the rating scale was recorded as follows: 1 = normal gait without forepaw deformity; 2 = normal gait with a marked forepaw deformity such as flexed and/or inverted paw or slight gait instability with a paw drop when walking; and 3 = severe gait instability with motor paresis of the ipsilateral left forepaw. The assessment was implemented once a week for a period of 6 weeks.

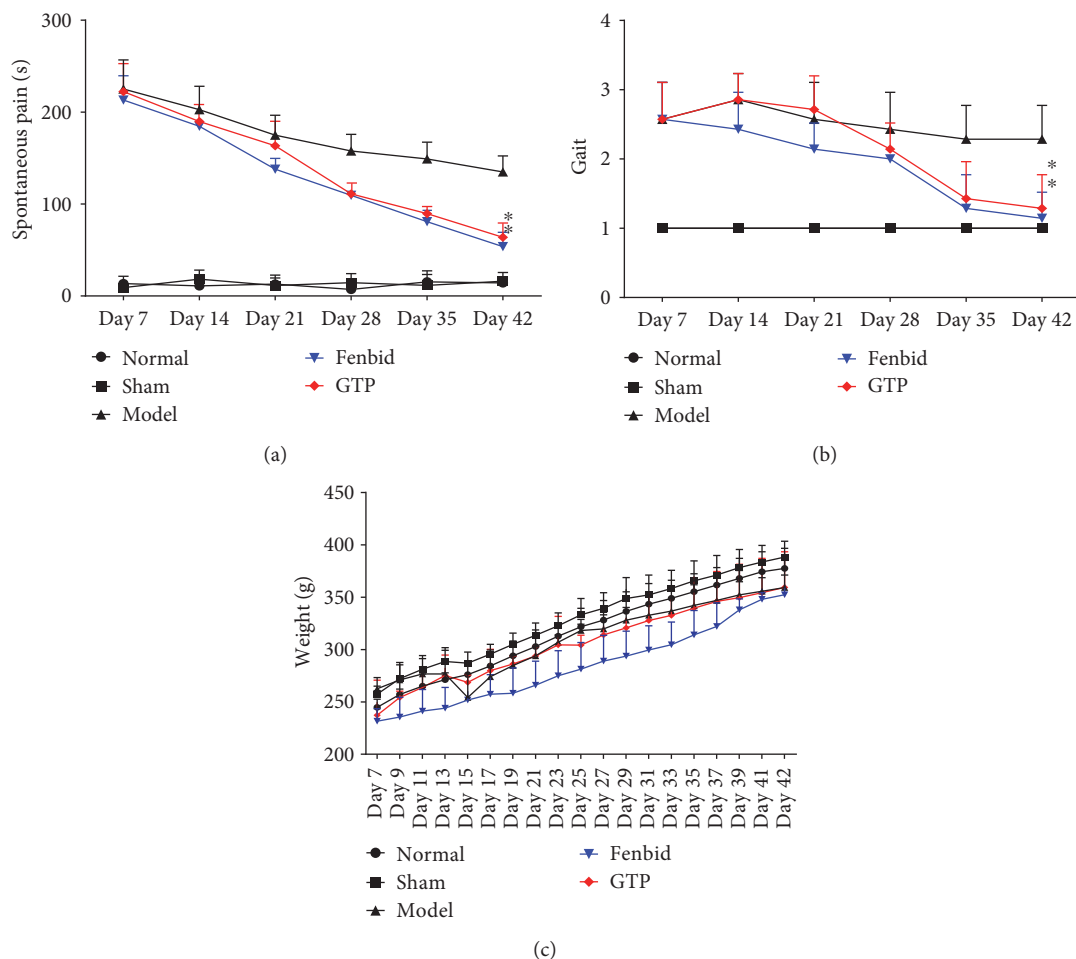


FIGURE 1: Effects of GTP on locomotor recovery and weight in rats. (a) Spontaneous pain. (b) Gait. (c) Weight. Compared to the model group, GTP treatment significantly reduced the duration of spontaneous pain ( $P < 0.05$ ). The data are expressed as the mean  $\pm$  SD,  $n = 8$ . \* $P < 0.05$  versus model group.

**2.5. Electrophysiology.** At 6 weeks postsurgery, sensory-evoked potentials (SEPs) were recorded in each group. The rats were immobilized on a stereotaxic board in a prone position. After removing interlaminar ligaments between C5 and C6, two pairs of steel needle electrodes were positioned, respectively, at C6 ganglion and Erb's point for recording evoked potentials. Another pair of steel needle electrodes was inserted into the median nerve of the left forepaw as stimulating electrodes. A constant current stimulus of 0.1 ms in duration and 3.5 mA in intensity was applied at a rate of 2 Hz. At a bandwidth of 10–3000 Hz, a total of 800 SEPs were averaged and replicated. The evoked potential amplitudes were measured as the voltage difference from the peak of the first positive peak (P1) to the peak of the first negative peak (N1) [5].

**2.6. Histopathology.** The specimens were immersed into 4% paraformaldehyde in 1x phosphate-buffered saline (4% PFA) and stored at 4°C for fixation. After being fixed for 48 h, they were removed and placed in fresh fixative. Fixed tissue samples were disposed of paraffin embedding and dehydration routinely. A total of 5 serial cross sections

with thickness of 5  $\mu$ m were obtained from each rat and processed with hematoxylin and eosin (HE) staining. The images were obtained using a light microscope (Carl Zeiss, Germany). Motoneurons were identified by the presence of large nuclei and Nissl bodies, which densely stained in the cytoplasm [38]. All sections were evaluated morphologically by the same pathologist who was blinded to each group.

**2.7. Western Blot Analysis.** Cytosolic extracts were prepared as described previously [39], with slight modifications. Briefly, 2 cm tissue segments containing the lesion from each rat were processed. The level of PPAR- $\gamma$ , TNF- $\alpha$ , Bax, Bcl-2, and NF200 was quantified in the cytosolic fraction from spinal cord tissue. Protein concentration was determined with the assay kit (Biotime Biotechnology, China). Proteins were separated electrophoretically and transferred to nitrocellulose membranes. Membranes were blocked with 5% (w/v) nonfat dried milk in buffered saline for 45 minutes at room temperature and subsequently probed with the following specific antibodies: anti-PPAR- $\gamma$  (1:1000, v/v, Abcam, UK), anti-TNF- $\alpha$  (1:1000, v/v, Abcam, UK), anti-Bcl-2 (1:500,



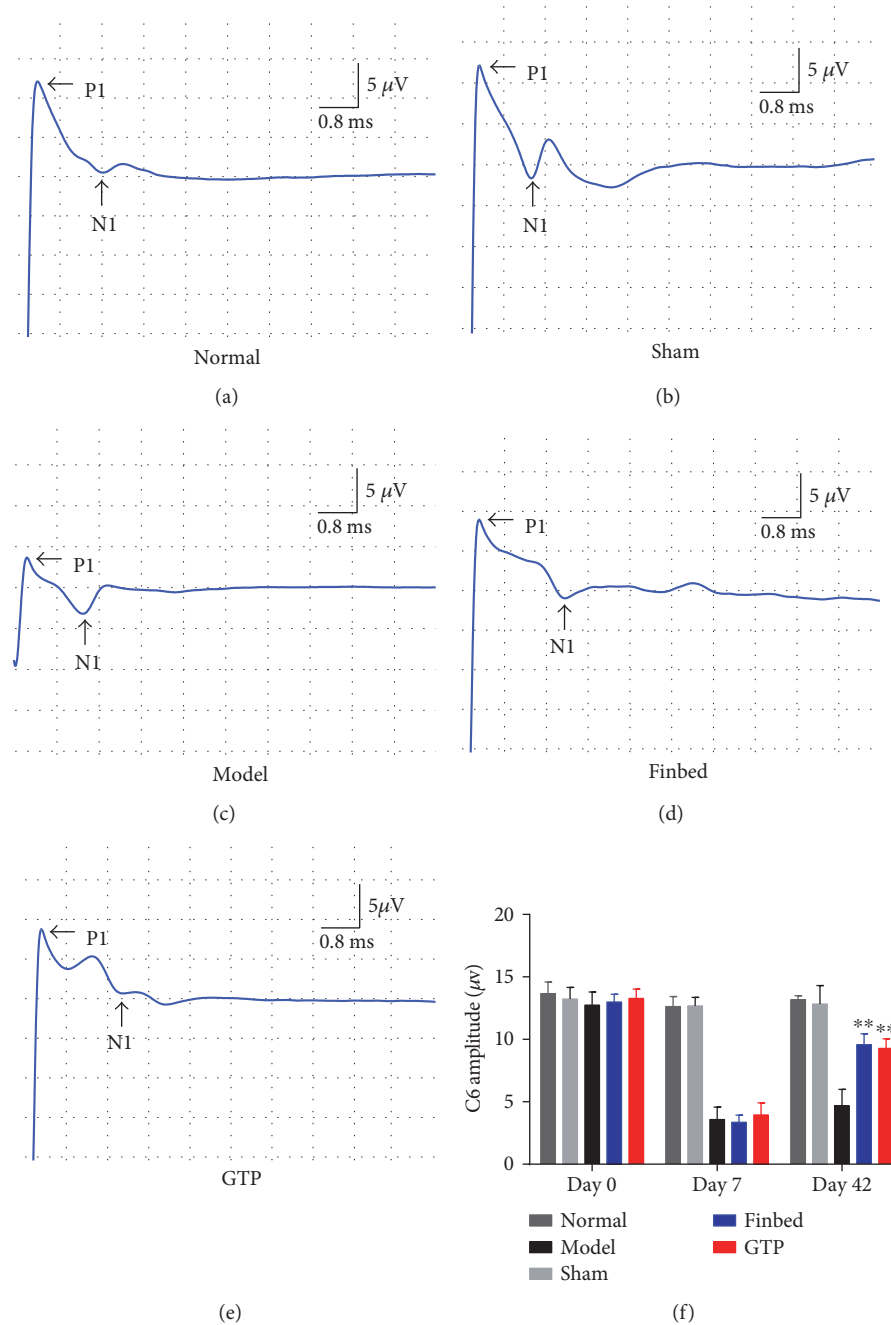


FIGURE 2: Effects of GTP on somatosensory-evoked potentials (SEPs) after SCI in rats. (a, b, c, d, e) The electrophysiological detection at C6 ganglion. The evoked potential amplitudes were measured as the voltage difference from the peak of the first positive peak (P1) to the peak of the negative peak (N1). (f) The GTP group had significantly higher peak amplitude than the model group ( $P < 0.01$ ). The data are expressed as the mean  $\pm$  SD,  $n = 8$ . \*\*\* $P < 0.01$  versus model group.

$v/v$ , Abcam, UK), anti-Bax (1:2000,  $v/v$ , Abcam, UK), and anti-NF200 (1:500,  $v/v$ , Abcam, UK) in  $1 \times$  TBST, 5%  $w/v$  bovine serum albumin (BSA) at  $4^{\circ}\text{C}$  overnight. Membranes were incubated with peroxidase-conjugated goat anti-rabbit IgG (1:2000,  $v/v$ , ZSGB Bio. Co. Ltd., Beijing, China) secondary antibody for 2 h at room temperature [40].

To ascertain if Western blots were loaded with equal amounts of protein lysates, they were also incubated in the presence of the antibody anti-GAPDH protein (1:1000,

$v/v$ , Abcam, UK). Signals were detected with the chemiluminescence detection system (Thermo Fisher Scientific Inc., USA), according to the manufacturer's instructions [40]. Gel-Pro Plus Analyzer software (Media Cybernetics) was used for integrated optical density (OD) analysis [35].

**2.8. Immunofluorescence.** Tissue samples were deparaffinized and rehydrated, and after boiling in 0.1 M citrate buffer for 1 min, detection of TNF- $\alpha$  and GFAP was carried out. In

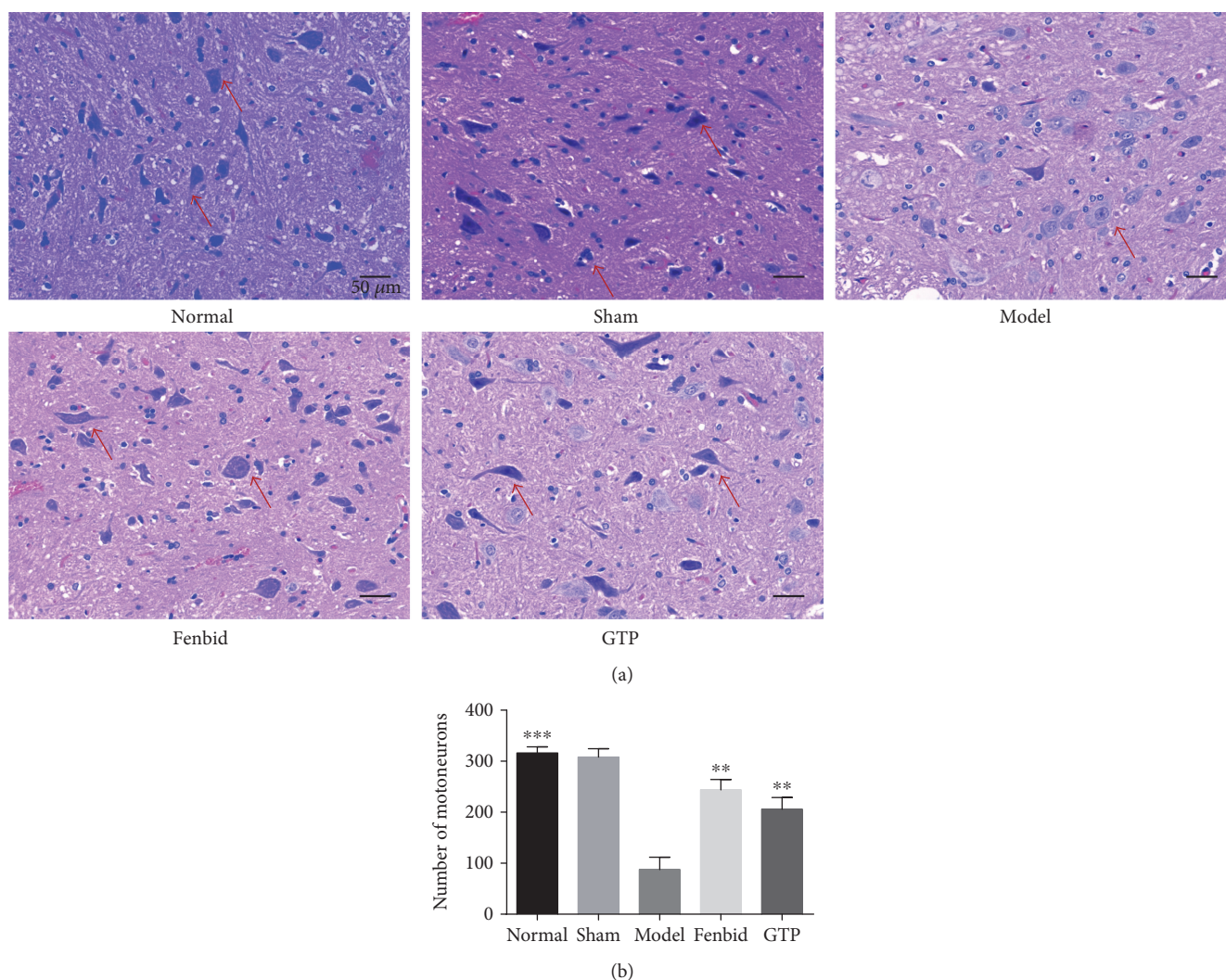


FIGURE 3: Effect of GTP on histological alterations of the spinal cord tissues. (a) HE staining (200x) of the spinal cord tissues. In the normal group, the motoneuron nuclei were densely blue stained, while in the model group, the motoneuron nuclei were stained light blue. (b) In the model group, the number of motoneurons was dramatically decreased compared to the normal group ( $P < 0.001$ ). In GTP group, the number of motoneurons was significantly increased compared to the model group ( $P < 0.01$ ). The data are expressed as the mean  $\pm$  SD,  $n = 8$ . \*\* $P < 0.01$  and \*\*\* $P < 0.001$  versus model group.

order to minimize nonspecific adsorption, the sections were incubated in 1% ( $v/v$ ) bovine serum albumin in PBS for 25 min and then incubated with polyclonal rabbit anti-TNF- $\alpha$  (1:100,  $v/v$ , Abcam, UK) and goat monoclonal anti-GFAP (1:1000;  $v/v$ , Abcam, UK) antibody in a humidity cabinet overnight at 4°C. Using PBS, the sections were washed three times for 15 min, followed by incubating with anti-rabbit Alexa Fluor-488 antibody (1:200,  $v/v$ , Santa Cruz, USA) and anti-goat Alexa Fluor-594 antibody (1:200,  $v/v$ , Santa Cruz, USA) secondary antibody for 2 h at room temperature. For nuclear staining, 1  $\mu\text{g}/\text{mL}$  DAPI in PBS was added and then rinsed for three times again. Fluorescence quenching agent was added to maintain fluorescence sensitization. All images were captured at a magnification of 200x on a fluorescence microscope (Carl Zeiss, Germany) [40].

**2.9. TUNEL Staining.** To determine the ability of GTP treatment on preventing apoptotic cell death after SCI, terminal deoxynucleotidyl transferase-mediated dUTP nick end labeling (TUNEL) was performed with the in situ cell death detection kit, POD (Roche Applied Science, USA). In order to block endogenous peroxidase activity, the sections were immersed in 3%  $\text{H}_2\text{O}_2$  for 15 min in the dark. Sections were permeated with proteinase K solution (20  $\mu\text{g}/\text{mL}$  in 10 mM Tris/HCl, pH 7.5) at 37°C for 15 min and then rinsed in phosphate-buffered saline (PBS) for three times, followed by application of TUNEL reaction mixture in a humidified chamber at 37°C for 1 h. To label apoptotic cells, the sections were then incubated for 30 min at 37°C with converter-POD. The sections were rinsed in PBS, treated with DAB substrate solution, and washed again with PBS. The negative control was incubated in Label Solution without terminal transferase,

and as a positive control, DNase I recombinant was added 10 min prior to labeling procedures to induce DNA strand breaks. Each section was imaged under a light microscope (Carl Zeiss, Germany), and the quantity of TUNEL positive cells was counted [35].

**2.10. Enzyme-Linked Immunosorbent Assay (ELISA).** The level of TNF- $\alpha$  in the serum of rats was measured by ELISA using a commercial ELISA kit (Abcam, Germany) according to the manufacturer's instructions [41] (Supplementary Figure 1).

**2.11. Statistical Analysis.** All data are represented as the mean  $\pm$  SD. Statistical differences were analyzed by Student's *t*-test for paired data with GraphPad Prism 7 software (USA).  $P < 0.05$  was considered as statistically significant.

### 3. Results

**3.1. Effects of GTP on Locomotor Recovery and Weight in Rats.** The scores of spontaneous pain and gait were assessed by Kawakami et al. and Dubuisson and Dennis. In the last week, the scores of spontaneous pain showed a significant decrease in the GTP group compared to the model group ( $P < 0.05$ , Figure 1(a)); meanwhile, the gait score of the GTP group showed an obvious decrease compared to the model group ( $P < 0.05$ , Figure 1(b)). The body weights of all groups were not significantly different.

**3.2. Effect of GTP on Somatosensory-Evoked Potentials (SEPs) in Rats.** Changes of axonal function were examined using electrophysiology detection [35]. SEP amplitude was significantly higher in the GTP group than in the model group ( $P < 0.01$ , Figure 2(f)). Peak latencies were not significantly different among groups.

**3.3. Effect of GTP on Histological Alterations of the Spinal Cord Tissues.** HE staining was applied to analyze histopathological alterations. The number of motoneurons in the chronic compression site reduced progressively. In the normal group, a portion of motoneurons were observed with condensed nuclei and darkly stained cytoplasm, and no histopathological changes were observed (Figure 3(a)). In the model group, motoneurons appeared as irregular morphologies and the number of motoneurons was significantly decreased compared to the normal group ( $P < 0.01$ , Figure 3(b)). The treatment of GTP markedly improved the pathological conditions.

**3.4. Effects of GTP on PPAR- $\gamma$  Expression in Spinal Cord Tissues.** To determine whether the expression of PPAR- $\gamma$  is associated with the protective effects of GTP against SCI-induced neurotoxicity, the protein levels of PPAR- $\gamma$  were determined by Western blot analysis (Figure 4(a)). The level of PPAR- $\gamma$  in the model group was markedly lower compared to the normal group ( $P < 0.01$ , Figure 4(b)), and the expression of PPAR- $\gamma$  was obviously increased when the rats were treated with GTP ( $P < 0.05$ , Figure 4(b)).

**3.5. Effects of GTP on TNF- $\alpha$  Expression in Spinal Cord Tissues.** The protein content of TNF- $\alpha$  in the spinal cord of

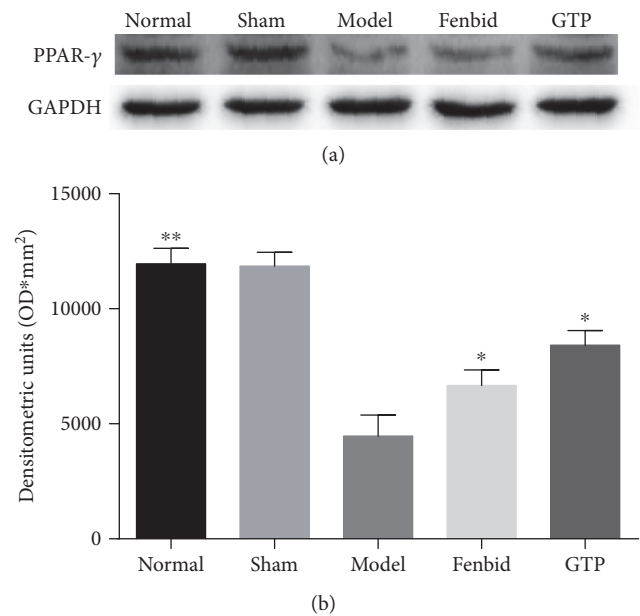


**FIGURE 4: Effects of GTP on PPAR- $\gamma$  expression in spinal cord tissues.** The detection of PPAR- $\gamma$  level in spinal cord tissues was assayed by Western blot analysis. The level of PPAR- $\gamma$  in the model group was markedly lower compared to the normal group ( $P < 0.01$ ). The level of PPAR- $\gamma$  was obviously increased in the GTP group ( $P < 0.05$ ). The data are expressed as the mean  $\pm$  SD,  $n = 8$ . \* $P < 0.05$  and \*\* $P < 0.01$  versus model group.

the rats was detected by Western blot. The rats in the model group had a higher TNF- $\alpha$  protein level compared with the rats in the normal group ( $P < 0.05$ , Figures 5(a) and 5(b)). By contrast, treatment with GTP significantly reduced the TNF- $\alpha$  protein level in contrast with SCI alone ( $P < 0.05$ , Figures 5(a) and 5(b)). Our data thus indicate that GTP inhibits TNF- $\alpha$  protein expression in the injured spinal cord.

Moreover, in order to confirm astrogliosis and TNF- $\alpha$  expression and to localize TNF- $\alpha$  to certain cell types, we implemented immunofluorescence staining. Spinal cord tissues were double stained with antibodies against TNF- $\alpha$  (green) and GFAP (red) (Figure 5(c)). The results revealed increased astrogliosis (GFAP<sup>+</sup> cells) in SCI rat such as activation of the microglia. The expression of TNF- $\alpha$  protein was notably increased in SCI-treated rats ( $P < 0.05$ , Figure 5(d)), while GFAP immunoreactivity and microglia activation were reduced ( $P < 0.05$ , Figure 5(e)). The yellow spots represented the colocalization between GFAP and TNF- $\alpha$ .

**3.6. Effects of GTP on Intrinsic Apoptosis.** The detection of Bcl-2 and Bax levels in spinal cord tissues with Western blot analysis (Figure 6(a)). The expression of Bcl-2 in the GTP group was obviously higher than in the model group (Figure 6(b)). A substantial increase in Bax expression was also found in spinal cord tissues from SCI; GTP treatment significantly attenuated Bax level in the spinal cord (Figure 6(c)).

Apoptotic cells emerged throughout the white and gray matter of the spinal cord. SCI-induced apoptosis in the spinal cord was detected by TUNEL staining. In the normal group,

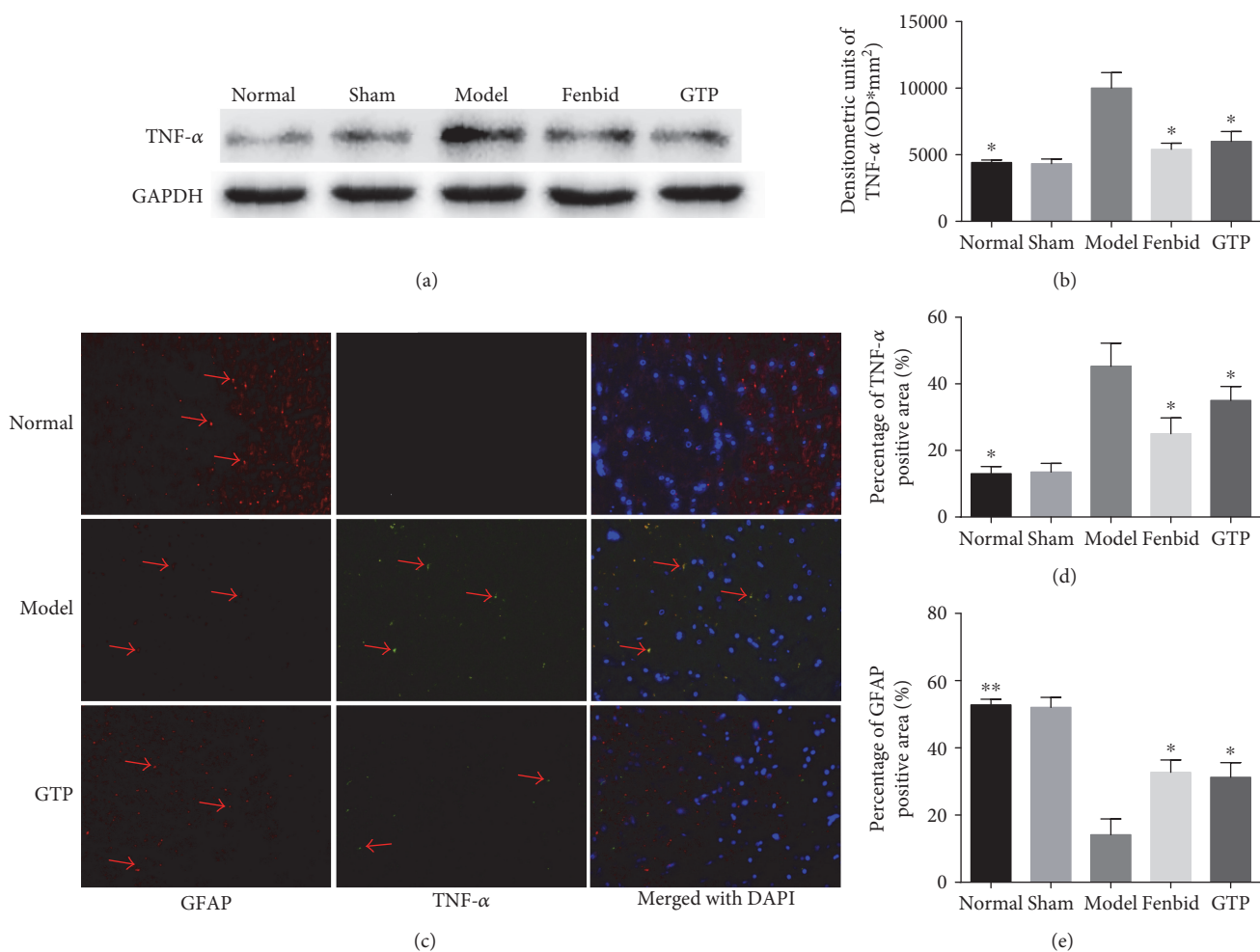


FIGURE 5: Effects of GTP on TNF- $\alpha$  expression in spinal cord tissues. (a, b) The detection of TNF- $\alpha$  level in spinal cord tissues was assayed by Western blot analysis. (c) Representative photomicrographs showing immunofluorescence staining of TNF- $\alpha$  (green), GFAP (red), and merging of the photographs (200x). (d, e) Statistical analysis of the TNF- $\alpha$ - and GFAP-positive staining areas. In the model group, the expression of TNF- $\alpha$  was obviously increased ( $P < 0.05$ ) and GFAP was decreased compared to the normal group ( $P < 0.01$ ). In the GTP group, the expression of TNF- $\alpha$  was obviously decreased ( $P < 0.05$ ) and GFAP was increased compared with the model group ( $P < 0.05$ ). The data are expressed as the mean  $\pm$  SD,  $n = 8$ . \* $P < 0.05$  and \*\* $P < 0.01$  versus model group.

there was almost no TUNEL-positive cell, and the neurons presented with a normal morphology (Figure 6(d)). In the model group, the number of TUNEL-positive cells was significantly increased when compared to the normal group ( $P < 0.01$ , Figure 6(e)). However, GTP treatment markedly reduced the number of TUNEL-positive cells in contrast with the model group ( $P < 0.05$ , Figure 6(e)).

**3.7. Effect of GTP on Cytoskeletal Integrity of Axons.** In this study, the cytoskeletal integrity of the cervical (C6) spinal cord was assessed. Homogenates of 8 mm of the spinal cord around the lesion epicenter were utilized for Western blot analysis to detect the cytoskeletal protein neurofilament 200 (NF200). It has been elaborated that after SCI, calcium-mediated excitotoxicity leads to the attenuation of NF200 [42]. Compared with the normal group, the expression of NF200 in the GTP treatment group was mildly lower, but far higher than in the model group ( $P < 0.05$ , Figure 7).

## 4. Discussion

Cervical spondylotic radiculopathy is one of the most common type of cervical degenerative disease. In recent years, many studies have confirmed that nonoperative therapy has more evident effects than operative therapy on the optimized scheme of CSR [6, 7]. Spinal cord injury, as the most common cause of CSR, has a high prevalence and a profound impact on patients and on society as a whole [40]. In the current study, a compression material was used to result in a progressive injury in rats, which then produced neurological deficits and ultimately formed a clinically relevant model [5]. This model is critical for screening neuroprotective agent and determining their mechanisms for the development of therapy.

*Gentongping* granule is one of the classical herbal products for treating CSR [16]. Many long-term clinical trials have reported that this medicine exerts admirable neuroprotective effects on CSR patients [11, 16, 17]. However, few pharmacological studies have been carried out on the specific

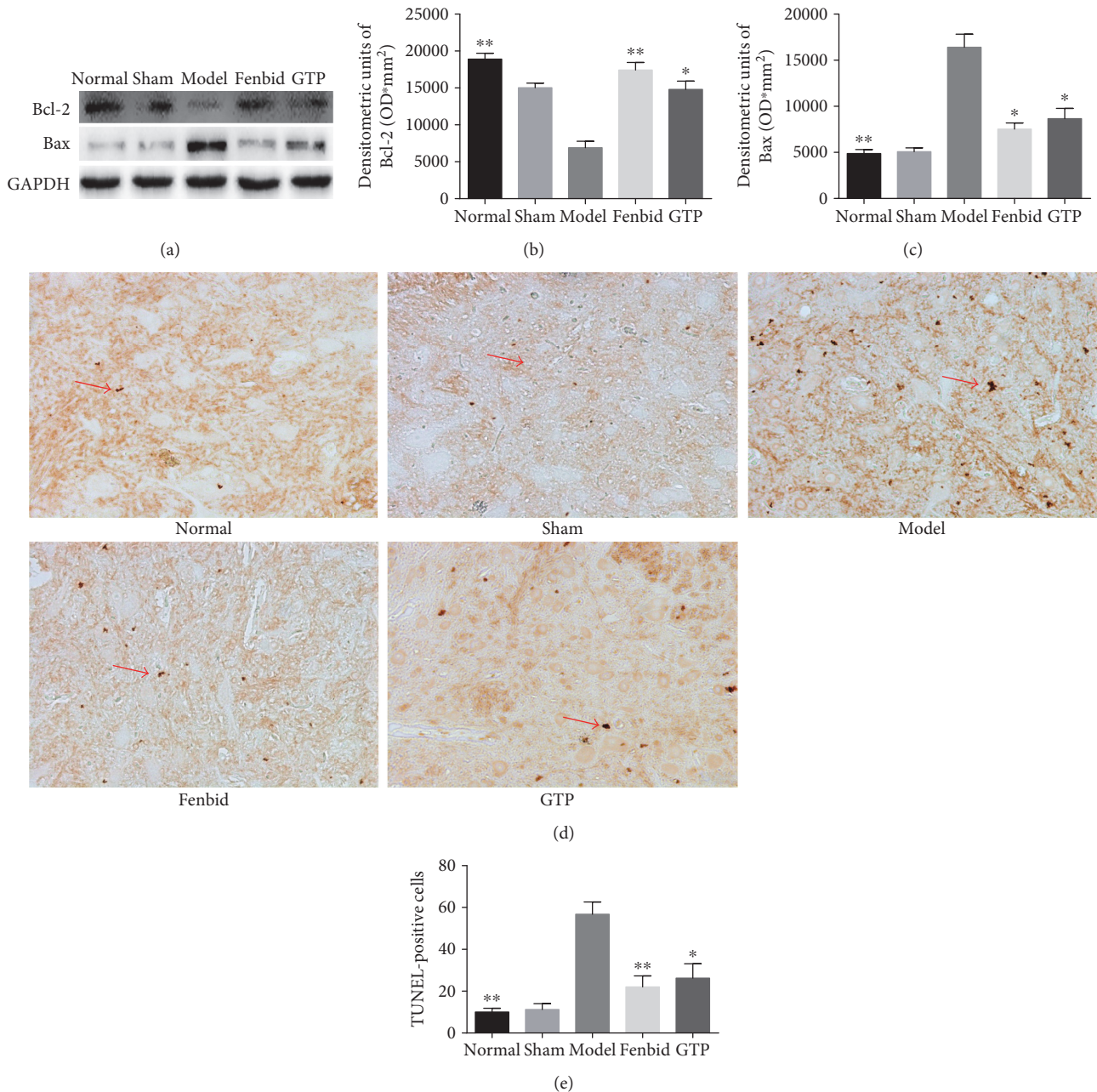


FIGURE 6: Effects of GTP on intrinsic apoptosis. (a) The detection of Bcl-2 and Bax levels in spinal cord tissues with Western blot analysis. In the model group, the expression of Bax was significantly increased ( $P < 0.01$ ) and Bcl-2 was decreased compared with the normal group ( $P < 0.01$ ). In the GTP group, the expression of Bax was obviously decreased ( $P < 0.05$ ) and Bcl-2 was increased compared with the model group ( $P < 0.05$ ). (d) TUNEL (200x) staining of the spinal cord tissues. (e) In the GTP group, the number of TUNEL-positive cells was obviously decreased compared to the model group. The data are expressed as the mean  $\pm$  SD,  $n = 8$ . \* $P < 0.05$  and \*\* $P < 0.01$  versus model group.

mechanism. This study demonstrated that GTP improved behavioral function and somatosensory-evoked potentials, such as amelioration of gait and amplitude. Behavioral assessment is a prevalent method for accessing the degree of neural injury [36, 37]. In the present study, compared with the normal group, the rank of spontaneous pain and gait exhibited an obvious deterioration in the model group. Moreover, behavioral scores were significantly different between the GTP group and the model group. Based on

the powerful spinal cord self-healing action, the behavioral function of rodents following SCI gradually recovered in the late stage of the experiment. However, the animal models in this study were sacrificed once behavioral assessment demonstrated a significant difference between the GTP group and the model group, and the effect of the self-healing could be ignored. Therefore, in the present study, GTP restored the behavioral function, indicating a satisfactory improvement on neuropathic pain.

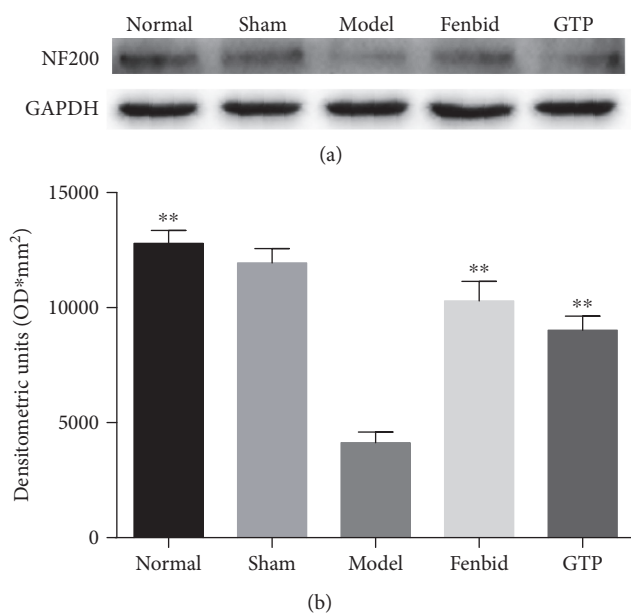


FIGURE 7: Effect of GTP on the cytoskeletal integrity of axons. (a) The detection of NF200 level in spinal cord tissues was assayed by Western blot analysis. (b) In the model group, the expression of NF200 was significantly decreased compared with the normal group ( $P < 0.01$ ). In the GTP group, the expression of NF200 was significantly increased compared with the model group ( $P < 0.01$ ). The data are expressed as the mean  $\pm$  SD,  $n = 8$ . \*\* $P < 0.01$  versus model group.

Hematoxylin and eosin staining was used to determine whether spinal cord neurons underwent pathological changes. In normal neuronal nuclei, there are numerous Nissl bodies that are associated with the nutritional condition of neurons, and the quantity of Nissl bodies are often used to indicate the neural state [43]. The smaller the quantity is, the more severe the injury becomes. In extremely serious pathological conditions, few Nissl bodies could even be observed [44]. In the present study, spinal cord tissues stained with HE exhibited densely dark blue nuclei in the normal group, while in the model group, it exhibited a light blue staining in nuclei, which meant that the Nissl bodies which existed in neuronal nuclei were shrunken. For the GTP group, we found that the color was deepened, which demonstrated a restored neuronal number in the spinal cord, indicating that neuronal function was retained.

Peroxisome proliferator-activated receptor gamma, one of PPAR superfamily members, has been observed in multiple immunocytes, such as monocytes, macrophages, and lymphocytes [45]. In this regard, we performed a Western blot analysis to determine the PPAR- $\gamma$  level in the spinal cord. We found that the expression of PPAR- $\gamma$  markedly decreased in the model group, whereas in the GTP group, the expression was significantly increased. In recent years, many researchers have indicated that PPAR- $\gamma$ -mediated mechanisms directly or indirectly favor the neuroprotective events [46]. The neuroprotection could also be abolished by a PPAR- $\gamma$  antagonist [47]. Furthermore, growing evidence confirmed that there are intimate associations

between PPAR- $\gamma$  and SCI in neuroprotection [29, 31]. Using database retrieval, we also found that PPAR- $\gamma$  was a common target protein of *Radix Puerariae* and *Carthamus tinctorius*, which are two critical components of GTP. The results indicated that GTP might exert its therapeutic action on PPAR- $\gamma$ .

Recent studies suggest that neuroimmune activation involving the activation of neurons and the releasing of inflammatory mediators contributes to neuropathic pain [48]. The expression of proinflammatory cytokines, such as TNF- $\alpha$ , has been well demonstrated in regulating the precise cellular events including activating astrocytes in SCI [40]. PPAR- $\gamma$ , being highly expressed in immunocytes, such as monocytes, macrophages, and lymphocytes [45], holds a pivotal role in adjusting inflammatory responses by regulating the activity of TNF- $\alpha$  in neuroprotective events [49, 50]. Furthermore, PPAR- $\gamma$  agonists curtail the inflammatory cytokines expressed in SCI models, indicating that the prevention of inflammation is a contributing factor to neuroprotection [31]. This study exhibited that TNF- $\alpha$  level in the model group was substantially augmented compared with the GTP group. In immunofluorescence staining, we applied GFAP, a specific marker of astrocyte, to confirm the specific cell type in which TNF- $\alpha$  existed. The images further determined that the inflammatory cytokine was activated exactly in neurons. As a consequence, the evidences suggested a therapeutic potential in neuroinflammatory disorders that might be attributed to a PPAR- $\gamma$ -involved mechanism. Recently, reduction of GFAP has been reported in major neuropathic disease [51]. Evidence showed that the inhibition of the astrocyte reaction and astrogliosis may be linked to the reduction of neuronal damage [52], which is considered as a physical barrier for neuron regeneration. Moreover, in our future studies, consideration of the expression of GFAP could be very appreciable.

Additionally, several researchers have suggested that the neuronal injury induced by SCI may be intimately associated with the activation of apoptotic proteins, such as antiapoptotic protein B-cell lymphoma 2 (Bcl-2) and proapoptotic protein Bcl-2-associated X (Bax) [53]. In our study, GTP was shown to have an antiapoptotic effect via increasing Bcl-2 and decreasing Bax expression in the spinal cord. In accordance, the rodents in the model group were shown to have increased Bax expression and decreased Bcl-2 expression in the spinal cord, while in the GTP group, the expressions of the two apoptotic proteins were reversed, which demonstrated that the apoptotic case was attenuated after GTP administration. This outcome was further verified by the TUNEL assay, presented as a large quantity of TUNEL-positive cells in the model group, while the number significantly decreased in the GTP group. As a previous study exposed, PPAR- $\gamma$  agonists contribute to the expression of Bcl-2 in various neurons and might facilitate cellular survival. In addition, the contribution was prevented by PPAR- $\gamma$  antagonist [53]. Based on this evidence, we inferred that GTP could exert antiapoptotic action through mediating PPAR- $\gamma$ . Interestingly, previous research showed that apoptotic proteins could be attributed to the production of pro-inflammatory cytokines; meanwhile, increased inflammatory

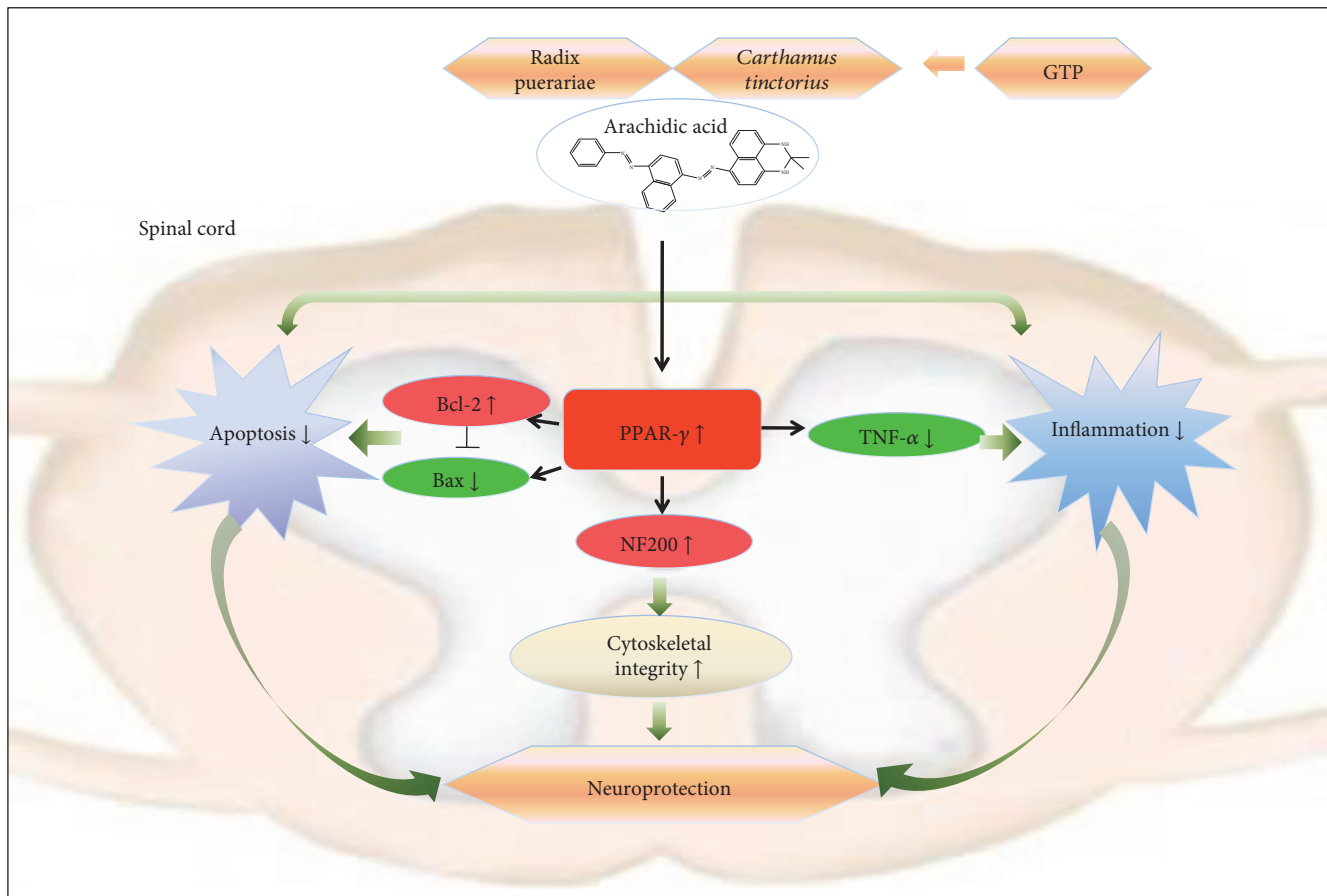


FIGURE 8: Schematic diagram depicting how GTP modulates the PPAR- $\gamma$  pathway to play a neuroprotection role in CSR. As indicated, arachidic acid is the common component of Radix Puerariae and *Carthamus tinctorius*. By directly activating PPAR- $\gamma$ , GTP could inhibit inflammation and apoptosis by decreasing TNF- $\alpha$  and Bax and increasing Bcl-2, respectively. Meanwhile, by aggrandizing NF200, GTP could improve the cytoskeletal integrity.

cytokines lead to apoptosis in a positive feedback regulation way [54].

We also studied the cytoskeletal integrity of neurons, by observing the expression of neurofilament protein (NF200) in the spinal cord. NF200 is an essential component of the neuronal and axonal cytoskeleton and is extremely important in the maintenance of neuronal functions following SCI [55]. The degradation of NF200 in axons suggested a certain degree of cytoskeletal breakdown in SCI [35]. This study determined the level of NF200 through quantity analysis. As demonstrated, the level of NF200 in the GTP group was distinctly higher compared with the model group, indicating that GTP treatment had a satisfactory improvement on cytoskeletal integrity. Due to upregulation of PPAR- $\gamma$  facilitating the remodeling of cytoskeletal integrity [56], our results showed a potential association between GTP and cytoskeletal integrity. The result was also consistent with the abovementioned alterations of motoneurons. Meanwhile, the results strongly reinforced the idea that the cytoskeletal integrity of the spinal cord could supply neuronal nutrients [55]. It was also shown that even a small number of surviving axons may bring about dramatic improvement in functional outcomes [57].

Nevertheless, there are a number of limitations to the present study. The present model is based on chronic compression of the spinal cord; however, it was unlikely to fully reflect the progressive nature of human disease. Further research into the mechanisms of GTP on the secondary effect on regeneration following SCI is required.

## 5. Conclusions

In conclusion, our experiment pointed to the neuroprotective effect of GTP. We demonstrated that GTP promoted motor function recovery and decreased neuropathic pain after SCI. A protective effect of GTP could be due in part to curtailing inflammation and antiapoptosis while promoting neuron regeneration. The potential mechanisms might be modulated by activating PPAR- $\gamma$  and subsequently inhibiting the expression of TNF- $\alpha$  and Bax as well as enhancing the expression of Bcl-2 and NF200 (summarized mechanistic pathways are represented in Figure 8).

## Conflicts of Interest

The authors declare no conflict of interests.

## Authors' Contributions

Wen Sun and Kang Zheng made equal contributions to this work. Jianfeng Yi and Cheng Lu contributed equally.

## Acknowledgments

This work was supported by Beijing Nova Project no. xx2014B073.

## References

- [1] Y. Tanaka, S. Kokubun, T. Sato, and H. Ozawa, "Cervical roots as origin of pain in the neck or scapular regions," *Spine*, vol. 31, no. 17, pp. E568–E573, 2006.
- [2] F. Yang, W. X. Li, Z. Liu, and L. Liu, "Balance chiropractic therapy for cervical spondylotic radiculopathy: study protocol for a randomized controlled trial," *Trials*, vol. 17, no. 1, p. 513, 2016.
- [3] A. I. Binder, "Cervical spondylosis and neck pain," *BMJ*, vol. 334, no. 7592, pp. 527–531, 2007.
- [4] J. S. Anderson, A. W. Hsu, and A. N. Vasavada, "Morphology, architecture, and biomechanics of human cervical multifidus," *Spine*, vol. 30, no. 4, pp. E86–E91, 2005.
- [5] S. K. Karadimas, E. Moon, W. R. Yu et al., "A novel experimental model of cervical spondylotic myelopathy (CSM) to facilitate translational research," *Neurobiology of Disease*, vol. 54, pp. 43–58, 2013.
- [6] L. A. Liu, S. Zhang, H. Wang, and L. Tang, "Acupuncture combined with moxibustion plaster for nerve-root type cervical spondylosis," *Zhongguo Zhen Jiu*, vol. 36, no. 2, pp. 139–143, 2016.
- [7] J. W. Zhou, Z. Y. Jiang, R. B. Ye et al., "Controlled study on treatment of cervical spondylopathy of the nerve root type with acupuncture, moxibustion and massage as main," *Zhongguo Zhen Jiu*, vol. 26, no. 8, pp. 537–543, 2006.
- [8] L. Hui, W. Mei-ping, and C. Jun, "Clinical observation on combined Chinese medicine therapy for the treatment of cervical spondylotic radiculopathy," *Shanghai Journal of Traditional Chinese Medicine*, vol. 1, pp. 59–61, 2015.
- [9] K. Trinh, X. Cui, and Y. J. Wang, "Chinese herbal medicine for chronic neck pain due to cervical degenerative disc disease," *Spine*, vol. 35, no. 24, pp. 2121–2127, 2010.
- [10] J. X. Li, C. J. Xiang, and X. Q. Liu, "Clinical study on analgesic mechanism of bitongxiao in treating neck pain due to cervical spondylitis," *Zhongguo Zhong Xi Yi Jie He Za Zhi*, vol. 21, no. 7, pp. 516–518, 2001.
- [11] J. Cai, J. Luo, and Z. Tongfei, "Clinical observation of 45 cases of Gentongping for the treatment of cervical spondylotic radiculopathy," *Chinese Journal of Traditional Medical Science and Technology*, vol. 239, 2007.
- [12] L. Zhigang, L. Wei, J. Wang, and S. Weizhong, "Clinical observation of Gentongping treatment for lumbar hyperosteoegeny," *Journal of Henan University*, vol. 28, no. 1, pp. 70–71, 2009.
- [13] S. F. Zhu, J. H. Ren, W. Tang et al., "Preparation process of Gentongping dropping pills," *Chinese Traditional and Herbal Drugs*, vol. 42, pp. 2020–2022, 2011.
- [14] T. Wang, X. Guo, and Z. Jingping, "Quantitative analysis of paeoniflorin in Gentongping by high-performance liquid chromatography method," *China Journal of Chinese Materia Medica*, vol. 22, no. 2, pp. 35–36, 1997.
- [15] X. Chen, L. Zhang, and Z. Anqing, "Quantitative analysis of puerarin and paeoniflorin by high-performance liquid chromatography method," *Chinese Herbal Medicines*, vol. 28, no. 1, pp. 22–23, 1997.
- [16] X. Y. Chen, W. Jia, M. J. Liu, X. Q. Meng, Y. D. Ma, and L. L. Wang, "Observation on therapeutic effect of digital acupoint pressure for treatment of the nerve root type of cervical spondylosis," *Zhongguo Zhen Jiu*, vol. 29, no. 8, pp. 659–662, 2009.
- [17] D. Q. Peng, Y. X. Dong, and Y. X. Liu, "Effect of He's Santong method of acupuncture for treatment of cervical spondylosis of nerve-root type," *Journal of Traditional Chinese Medicine*, vol. 50, no. 3, pp. 231–234, 2009.
- [18] Y. Zhang, X. Mao, Q. Guo et al., "Pathway of PPAR-gamma coactivators in thermogenesis: a pivotal traditional Chinese medicine-associated target for individualized treatment of rheumatoid arthritis," *Oncotarget*, vol. 7, no. 13, pp. 15885–15900, 2016.
- [19] B. He, C. Lu, G. Zheng et al., "Combination therapeutics in complex diseases," *Journal of Cellular and Molecular Medicine*, vol. 20, no. 12, pp. 2231–2240, 2016.
- [20] G. Chen, C. Lu, Q. Zha et al., "A network-based analysis of traditional Chinese medicine cold and hot patterns in rheumatoid arthritis," *Complementary Therapies in Medicine*, vol. 20, no. 1–2, pp. 23–30, 2012.
- [21] B. He, C. Lu, M. L. Wang et al., "Drug discovery in traditional Chinese medicine: from herbal fufang to combinatory drugs," *Science*, vol. 350, pp. S74–S76, 2015.
- [22] C. Y. C. Chen, "TCM database@Taiwan: the world's largest traditional Chinese medicine database for drug screening in silico," *PLoS One*, vol. 6, p. 5, 2011.
- [23] S. Kim, P. A. Thiessen, E. E. Bolton et al., "PubChem substance and compound databases," *Nucleic Acids Research*, vol. 44, no. D1, pp. D1202–D1213, 2016.
- [24] T. Maeda and S. Kishioka, "Chapter 13 PPAR and pain," *International Review of Neurobiology*, vol. 85, pp. 165–177, 2009.
- [25] Y. Hatazawa, M. Tadaishi, Y. Nagaike et al., "PGC-1 $\alpha$ -mediated branched-chain amino acid metabolism in the skeletal muscle," *PLoS One*, vol. 9, no. 3, article e91006, 2014.
- [26] A. P. Russell, "PGC-1 $\alpha$  and exercise: important partners in combating insulin resistance," *Current Diabetes Reviews*, vol. 1, no. 2, pp. 175–181, 2005.
- [27] S. B. Churi, O. S. Abdel-Aleem, K. K. Tumber, H. Scuder-Porter, and B. K. Taylor, "Intrathecal rosiglitazone acts at peroxisome proliferator-activated receptor- $\gamma$  to rapidly inhibit neuropathic pain in rats," *The Journal of Pain*, vol. 9, no. 7, pp. 639–649, 2008.
- [28] H. Kim, J. Hwang, S. Park et al., "A peroxisome proliferator-activated receptor gamma agonist attenuates neurological deficits following spinal cord ischemia in rats," *Journal of Vascular Surgery*, vol. 59, no. 4, pp. 1084–1089, 2014.
- [29] D. M. McTigue, R. Tripathi, P. Wei, and A. T. Lash, "The PPAR gamma agonist Pioglitazone improves anatomical and locomotor recovery after rodent spinal cord injury," *Experimental Neurology*, vol. 205, no. 2, pp. 396–406, 2007.
- [30] T. B. Jones, E. E. McDaniel, and P. G. Popovich, "Inflammatory-mediated injury and repair in the traumatically injured spinal cord," *Current Pharmaceutical Design*, vol. 11, no. 10, pp. 1223–1236, 2005.
- [31] S. W. Park, J. H. Yi, G. Miranpuri et al., "Thiazolidinedione class of peroxisome proliferator-activated receptor  $\gamma$  agonists prevents neuronal damage, motor dysfunction, myelin loss,



- neuropathic pain, and inflammation after spinal cord injury in adult rats," *Journal of Pharmacology and Experimental Therapeutics*, vol. 320, no. 3, pp. 1002–1012, 2007.
- [32] J. Lee, K. Satkunendrarajah, and M. G. Fehlings, "Development and characterization of a novel rat model of cervical spondylotic myelopathy: the impact of chronic cord compression on clinical, neuroanatomical, and neurophysiological outcomes," *Journal of Neurotrauma*, vol. 29, no. 5, pp. 1012–1027, 2012.
- [33] S. Yamamoto, R. Kurokawa, and P. Kim, "Cilostazol, a selective type III phosphodiesterase inhibitor: prevention of cervical myelopathy in a rat chronic compression model," *Journal of Neurosurgery: Spine*, vol. 20, no. 1, pp. 93–101, 2014.
- [34] R. S. Dhillon, J. Parker, Y. A. Syed et al., "Axonal plasticity underpins the functional recovery following surgical decompression in a rat model of cervical spondylotic myelopathy," *Acta Neuropathologica Communications*, vol. 4, no. 1, p. 89, 2016.
- [35] Y. Wu, K. Satkunendrarajah, Y. Teng, D. S. L. Chow, J. Buttigieg, and M. G. Fehlings, "Delayed post-injury administration of riluzole is neuroprotective in a preclinical rodent model of cervical spinal cord injury," *Journal of Neurotrauma*, vol. 30, no. 6, pp. 441–452, 2013.
- [36] M. Kawakami, J. N. Weinstein, K. F. Spratt et al., "Immunohistochemical and quantitative demonstrations of pain induced by lumbar nerve root irritation of the rat," *Spine*, vol. 19, no. 16, pp. 1780–1794, 1994.
- [37] D. Dubuisson and S. G. Dennis, "The formalin test: a quantitative study of the analgesic effects of morphine, meperidine, and brain stem stimulation in rats and cats," *Pain*, vol. 4, no. 2, pp. 161–174, 1977.
- [38] P. Kim, T. Haisa, T. Kawamoto, T. Kirino, and S. Wakai, "Delayed myelopathy induced by chronic compression in the rat spinal cord," *Annals of Neurology*, vol. 55, no. 4, pp. 503–511, 2004.
- [39] J. R. Bethea, M. Castro, R. W. Keane, T. T. Lee, W. D. Dietrich, and R. P. Yeziarski, "Traumatic spinal cord injury induces nuclear factor- $\kappa$ B activation," *Journal of Neuroscience*, vol. 18, no. 9, pp. 3251–3260, 1998.
- [40] I. Paterniti, D. Impellizzeri, R. Di Paola et al., "Docosahexaenoic acid attenuates the early inflammatory response following spinal cord injury in mice: in-vivo and in-vitro studies," *Journal of Neuroinflammation*, vol. 11, p. 6, 2014.
- [41] X. H. Li, Y. Y. Deng, F. Li, J. S. Shi, and Q. H. Gong, "Neuroprotective effects of sodium hydrosulfide against  $\beta$ -amyloid-induced neurotoxicity," *International Journal of Molecular Medicine*, vol. 38, no. 4, pp. 1152–1160, 2016.
- [42] P. A. Schumacher, J. H. Eubanks, and M. G. Fehlings, "Increased calpain I-mediated proteolysis, and preferential loss of dephosphorylated NF200, following traumatic spinal cord injury," *Neuroscience*, vol. 91, no. 2, pp. 733–744, 1999.
- [43] R. Gupta, M. Singh, and A. Sharma, "Neuroprotective effect of antioxidants on ischaemia and reperfusion-induced cerebral injury," *Pharmacological Research*, vol. 48, no. 2, pp. 209–215, 2003.
- [44] L. Wu, T. Yang, C. Yang et al., "Delayed neurological deterioration after surgery for intraspinal meningiomas: ischemia-reperfusion injury in a rat model," *Oncology Letters*, vol. 10, no. 4, pp. 2087–2094, 2015.
- [45] O. Braissant, F. Foufelle, C. Scotto, M. Dauca, and W. Wahli, "Differential expression of peroxisome proliferator-activated receptors (PPARs): tissue distribution of PPAR-alpha, -beta, and -gamma in the adult rat," *Endocrinology*, vol. 137, no. 1, pp. 354–366, 1996.
- [46] X. R. Zhao, N. Gonzales, and J. Aronowski, "Pleiotropic role of PPAR $\gamma$  in intracerebral hemorrhage: an intricate system involving Nrf2, RXR, and NF- $\kappa$ B," *CNS Neuroscience & Therapeutics*, vol. 21, no. 4, pp. 357–366, 2015.
- [47] K. M. Fuenzalida, M. C. Aguilera, D. G. Piderit et al., "Peroxisome proliferator-activated receptor  $\gamma$  is a novel target of the nerve growth factor signaling pathway in PC12 cells," *Journal of Biological Chemistry*, vol. 280, no. 10, pp. 9604–9609, 2005.
- [48] G. Moalem and D. J. Tracey, "Immune and inflammatory mechanisms in neuropathic pain," *Brain Research Reviews*, vol. 51, no. 2, pp. 240–264, 2006.
- [49] I. M. Verma, "Nuclear factor (NF)- $\kappa$ B proteins: therapeutic targets," *Annals of the Rheumatic Diseases*, vol. 63, Supplement 2, pp. ii57–ii61, 2004.
- [50] Q. Han, Q. Yuan, X. Meng, J. Huo, Y. Bao, and G. Xie, "6-Shogaol attenuates LPS-induced inflammation in BV2 microglia cells by activating PPAR- $\gamma$ ," *Oncotarget*, vol. 8, no. 26, pp. 42001–42006, 2017.
- [51] J. A. Cobb, K. O'Neill, J. Milner et al., "Density of GFAP-immunoreactive astrocytes is decreased in left hippocampi in major depressive disorder," *Neuroscience*, vol. 316, pp. 209–220, 2016.
- [52] E. Acaz-Fonseca, R. Sanchez-Gonzalez, I. Azcoitia, M. A. Arevalo, and L. M. Garcia-Segura, "Role of astrocytes in the neuroprotective actions of 17 $\beta$ -estradiol and selective estrogen receptor modulators," *Molecular and Cellular Endocrinology*, vol. 389, no. 1–2, pp. 48–57, 2014.
- [53] K. Fuenzalida, R. Quintanilla, P. Ramos et al., "Peroxisome proliferator-activated receptor  $\gamma$  up-regulates the Bcl-2 anti-apoptotic protein in neurons and induces mitochondrial stabilization and protection against oxidative stress and apoptosis," *Journal of Biological Chemistry*, vol. 282, no. 51, pp. 37006–37015, 2007.
- [54] A. M. Mahmoud, O. E. Hussein, W. G. Hozayen, and S. M. Abd El-Twab, "Methotrexate hepatotoxicity is associated with oxidative stress, and down-regulation of PPAR $\gamma$  and Nrf2: protective effect of 18 $\beta$ -Glycyrrhetic acid," *Chemico-Biological Interactions*, vol. 270, pp. 59–72, 2017.
- [55] N. Kimura, T. Kumamoto, H. Ueyama, H. Horinouchi, and E. Ohama, "Role of proteasomes in the formation of neurofilamentous inclusions in spinal motor neurons of aluminum-treated rabbits," *Neuropathology*, vol. 27, no. 6, pp. 522–530, 2007.
- [56] N. R. Labriola and E. M. Darling, "Temporal heterogeneity in single-cell gene expression and mechanical properties during adipogenic differentiation," *Journal of Biomechanics*, vol. 48, no. 6, pp. 1058–1066, 2015.
- [57] M. G. Fehlings and C. H. Tator, "The relationships among the severity of spinal cord injury, residual neurological function, axon counts, and counts of retrogradely labeled neurons after experimental spinal cord injury," *Experimental Neurology*, vol. 132, no. 2, pp. 220–228, 1995.

## Review Article

# New Insights into the Mechanisms of Chinese Herbal Products on Diabetes: A Focus on the “Bacteria-Mucosal Immunity-Inflammation-Diabetes” Axis

Ze Zheng Gao,<sup>1</sup> Qingwei Li,<sup>1</sup> Xuemin Wu,<sup>2</sup> Xuemin Zhao,<sup>1</sup> Linhua Zhao,<sup>3</sup> and Xiaolin Tong<sup>1,2</sup>

<sup>1</sup>Department of Endocrinology, Guang'anmen Hospital, China Academy of Chinese Medical Sciences, Beijing 100054, China

<sup>2</sup>Shenzhen Hospital, Guangzhou University of Chinese Medicine, Guangzhou 518034, China

<sup>3</sup>Laboratory of Molecular Biology, Guang'anmen Hospital, China Academy of Chinese Medical Sciences, Beijing 100053, China

Correspondence should be addressed to Linhua Zhao; melonzhao@163.com and Xiaolin Tong; tongxiaolin@vip.163.com

Received 4 May 2017; Revised 27 June 2017; Accepted 25 July 2017; Published 15 October 2017

Academic Editor: Cheng Xiao

Copyright © 2017 Ze Zheng Gao et al. This is an open access article distributed under the Creative Commons Attribution License, which permits unrestricted use, distribution, and reproduction in any medium, provided the original work is properly cited.

Diabetes, especially type 2, has been rapidly increasing all over the world. Although many drugs have been developed and used to treat diabetes, side effects and long-term efficacy are of great challenge. Therefore, natural health product and dietary supplements have been of increasing interest alternatively. In this regard, Chinese herbs and herbal products have been considered a rich resource of product development. Although increasing evidence has been produced from various scientific studies, the mechanisms of action are lacking. Here, we have proposed that many herbal monomers and formulae improve glucose homeostasis and diabetes through the BMID axis; B represents gut microbiota, M means mucosal immunity, I represents inflammation, and D represents diabetes. Chinese herbs have been traditionally used to treat diabetes, with minimal side and toxic effects. Here, we reviewed monomers such as berberine, ginsenoside, *M. charantia* extract, and curcumin and herbal formulae such as Gegen Qinlian Decoction, Danggui Liu Huang Decoction, and Huanglian Wendan Decoction. This review was intended to provide new perspectives and strategies for future diabetes research and product.

## 1. Introduction

In July 2015, the International Diabetes Federation (IDF) released the seventh edition of “IDF diabetes map,” which showed that China had approximately 1.096 million diabetes cases in 2015, ranking the highest in the world. According to the current development trend, the number of diabetes cases in China is projected to reach 150.7 million in 2040. The incidence of diabetes is estimated to increase by 69% in developing countries and 20% in developed countries from 2010 to 2030. Thus, schemes in preventing and treating diabetes are warranted. Currently, Chinese herbs for the prevention and treatment of diabetes and its minimal complications are considered advantageous, and a large number of evidence-based clinical studies have confirmed these effects [1–7].

Modern medical technology provides a new way and direction for the prevention and treatment of diabetes. Chinese herbs have been historically and traditionally used

in the treatment of diabetes, which dates back to the Qin dynasty (221 to 207 BC). Globalization and progress in medical science rejuvenate the ancient Chinese herbs, and an increasing number of studies have shown that various specific monomers and Chinese formulae can be used in the prevention and treatment of diabetes through the “Bacteria-Mucosal Immunity-Inflammation-Diabetes” axis (BMID axis). We retrieved the literature and screened out more than 40 relevant Chinese herbs and its derivatives that have been used to treat diabetes regulating multiple targets. We have chosen some of them which have been widely studied and characterized, including monomers and prescriptions. The specific monomers include berberine, *M. charantia* extract, ginsenoside, and curcumin, and prescriptions include Gegen Qinlian Decoction (GGQLD), Danggui Liu Huang Decoction (DGLHD), and Huanglian Wendan Decoction (HLWDD). Here, we attempt to explore the possible mechanisms of action of these in diabetic treatment from

the perspective of immunology and provide potentially novel therapeutic strategies that may improve clinical treatment on diabetes.

## 2. New Insights into Diabetes: “Bacteria-Mucosal Immunity-Inflammation-Diabetes” Axis

The gut microbiota represents a microbial community located in the intestine, composed of over a trillion microorganisms with hundreds of species, which play an important role in digestion and intestinal mucosal immunity. There is increasing evidence that confirms that the changes in gut microbiota are associated with insulin resistance and diabetes.

*2.1. Diabetes Is Associated with Imbalance of Gut Microbiota.* In mice and humans, there are two main bacterial phyla, Bacteroidetes and Firmicutes, which are found in the gut through metagenomic analysis [8]. The normal mice keep a relative balance among these two bacterial phyla, but the bacterial phylum Firmicutes is increased in obese mice observably [9]. A study has shown that a high-fat diet (HFD) can reduce the number of *Bifidobacterium* species (spp.), resulting in the development of endotoxemia and diabetes; an oligosaccharide-rich diet increases the number of *Bifidobacterium* species (spp.) and subsequently reduces the level of inflammation and improves glucose intolerance [10]. The metagenomic analysis revealed that patients with type 2 diabetes had moderate levels of gut microbiota dysbiosis, characterized by the decrease in the abundance of some universal butyrate-producing bacteria and the increase in the abundance of some bacteria which reduce sulfate and antioxidant stress [11]. A human study showed that the number of *Faecalibacterium prausnitzii*, which was associated with the production of short-chain fatty acids and butyrate, is increased [12]. Gut microbiota of diabetic patients and mice changed significantly, indicating that reversing this change may reduce the incidence of insulin resistance and diabetes.

*2.2. Disorder of Mucosal Immunity Leads to Diabetes.* Gut microbiota affects insulin resistance and type 2 diabetes mellitus (T2DM) by altering the intestinal epithelial barrier and intestinal mucosal immunity. The main function of the intestinal epithelial barrier is to limit intestinal contents such as water, chyme, and gut microbiota and also to regulate immune responses. The epithelial barrier needs a continuous epithelial cell layer, and the tight junctions are the major characteristic. The tight junctions consist of a complex network of transmembrane proteins, cytoplasmic proteins, and regulatory proteins. There are two pathways: “pore” and “leak”. The “pore” pathway is a high-capacity, size-selective, and charge-selective route, and the “leak” pathway refers to a low-capacity pathway that has limited selectivity [13]. In HFD-induced mice, intestinal bacteria or bacterial products cause the elevation of tumor necrosis factor (TNF) and interleukin- (IL-) 13. These inflammatory factors increase transcription and activity of the myosin light-chain

kinase (MLCK) and IL-13-dependent claudin-2 and subsequently increase permeability of “pore” and “leak” pathways and the pass of lipopolysaccharide (LPS) [14–16]. This change leads to an increase in chronic inflammation in the liver, fat, and other tissues and other metabolic diseases. In addition to the intestinal bacterial products, the gut microbiota can also directly pass the intestinal barrier and translocate to the pancreatic lymph nodes, activate NOD-like receptors 2 (NOD2), and contribute to diabetes [17].

The intestinal mucosal immunity is the most important line of defense against intestinal infection through the functions of goblet cells, intestinal epithelial cells (IEC), innate lymphoid cells (ILC), and other rapid responsive immune cells, such as macrophages and neutrophils. The goblet cells and IEC can produce antimicrobial peptides (AMPs) and mucin to prevent pathogens from penetrating the intestine [18]. IEC can secrete anti-inflammatory mediators such as IL-25, IL-33, and transforming growth factor- $\beta$  (TGF- $\beta$ ). These mediators can influence micro-associated molecular patterns (MAMPs) by binding to Toll-like receptors 5 (TLR5) and NOD2. ILC inhibits the body’s chronic low-level inflammation through the secretion of IL-22, IL-17A, IL-17F, and so forth [19]. HFD can reduce the diversity and alter the distribution balance of gut microbiota and thus reduce the production of mucin and other antimicrobial factors. Invasive bacteria and the associated products alter the intestinal mucosal immunity, and that contributes to the development of T2DM [20].

*2.3. Inflammation Affects Diabetes through Multiple Pathways.* The alternation of intestinal mucosal immunity and increased production of inflammatory factors have been considered to be linked to the development of T2DM. The pathophysiological processes are proposed to mainly include three pathways: (1) The nuclear factor kappa-B (NF- $\kappa$ B) pathway are activated by the inhibitor of nuclear factor kappa-B kinase (IKK) and proinflammatory cytokines such as TNF- $\alpha$ , IL-1, and IL-6. The activated IKK and proinflammatory cytokines phosphorylate the inhibitor of NF- $\kappa$ B (I $\kappa$ B). When I $\kappa$ B is phosphorylated, I $\kappa$ B and NF- $\kappa$ B are dissociated, resulting in NF- $\kappa$ B degradation. Then, NF- $\kappa$ B enters the nucleus, thereby mediating the expression of a variety of inflammatory genes [21, 22]. (2) IKK regulates insulin receptor substrate serine/threonine phosphorylation, interfering with normal tyrosine phosphorylation and weakening the insulin signal transduction. IKK is currently considered the link between inflammation and insulin resistance (IR). TNF- $\alpha$  and free fatty acid (FFA) activate Jun N-terminal kinase (JNK) and product insulin receptor substrate number 307 serine, which interferes with the insulin signal transduction via the IR/IRS/PI3K pathway. (3) The SOCS family of the cytokine signaling factor (SOCS) pathway mediates cytokine-induced IR. SOCS-1, SOCS-3, and SOCS-6 are involved, which predominantly inhibit the phosphorylation of IRS1 and IRS2 tyrosine residues and accelerate the degradation of IRS1 and IRS2 [23, 24].

*2.4. “Bacteria-Mucosal Immunity-Inflammation-Diabetes” Axis.* It has been shown that gut microbiota affects the

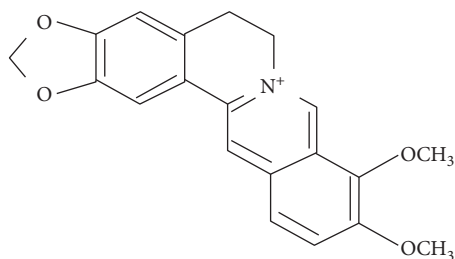


FIGURE 1: Molecular structure of berberine.

intestinal epithelial barrier and intestinal mucosal immunity, alters the level of inflammation, and influences insulin resistance and diabetes. This potential pathogenesis of diabetes is referred to as the “BMID” axis, “B” represents gut microbiota, “M” represents mucosal immunity, “I” represents inflammation, and of course, “D” represents diabetes. This axis is like a “line” to string most antidiabetic agents together and may provide new perspectives and strategies for future research on diabetes and the development of hypoglycemic drugs.

### 3. Herbal Monomers

Herbal monomers are major effective constituents of Chinese herbs. Studies on monomers are increasing in recent years, because they have specific molecular structure and are easier to be used in mechanism research and observing effective targets of Chinese herbs. Here, we screened out five representative monomers to find out their different functions based on the BMID axis. They have been widely researched and applied in treating diabetes for a long time.

**3.1. Berberine.** *Rhizoma coptidis* has been used for centuries in traditional Chinese medicine (TCM) as an antipyretic and alexipharmacons, and its main active component is berberine (BBR, Figure 1) [25]. BBR is an isoquinoline and found in many plants of the berberidaceae family. Recent studies have shown that BBR and its derivatives possess a variety of disease-fighting activities, they regulate the immune system, inhibit inflammation, and reduce insulin resistance [26, 27], and they have an anticancer effect likewise; it was reported that BBR inhibits the progression of pancreatic, colon, and breast cancer [28–31].

**3.1.1. Effect of BBR on Diabetes.** Insulin resistance (IR) is a metabolic state in which insulin inefficiently regulates the tissue and cell for their uptake and utilization of glucose. Nod-like receptor family pyrin domain containing 3 (NLRP3) contributes to obesity-induced inflammation and insulin resistance [32]. A recent study showed that BBR inhibited saturated fatty acid palmitate- (PA-) induced activation of NLRP3 and release of interleukin-1 $\beta$  (IL-1 $\beta$ ) in macrophages by activating AMPK-dependent autophagy, thus reducing inflammation and insulin resistance [26]. An animal study showed that BBR reduced blood TNF- $\alpha$ , IL-6, and MCP-1 levels of JNK and IKK $\beta$  phosphorylation in obese mice fed with a high-fat diet, as well as indicated that BBR improves

insulin resistance possibly through inhibiting the activation of macrophages in adipose tissue [33].

**3.1.2. Effect of BBR on Gut Microbiota and Intestinal Mucosal Immunity.** Intestinal barrier integrity and immune tolerance are associated with the pathogenesis of diabetes. Defects in the integrity of the mucosal barriers and leakage of the gut microbiome can contribute to the low-grade inflammation of tissues, which is well known to be associated with glucose metabolism in the muscle, liver, and adipose tissue and causes glucose intolerance and T2DM [17, 34]. Recent studies have shown that BBR imparts beneficial effects on the immune cells of the intestinal immune system and influences the expression of intestinal immune factors. It also inhibits the expression of IL-1 $\beta$ , IL-4, IL-10, MIF, and TNF- $\alpha$  mRNA and reduces the low-grade inflammation [35].

Intestinal microflora is an important factor in mediating the development of obesity-related metabolic disorders (including type 2 diabetes). The current results suggest that BBR can regulate the intestinal microflora, restore the intestinal barrier, reduce metabolic endotoxemia and systemic inflammation, and improve gut peptide levels in high-fat diet-fed rats; it indicates that BBR is possibly an effective agent for the treatment of obesity and diabetes [36]. A study showed that BBR improved metabolic disorders induced by high-fat diets by modulating the gut-intestinal-brain axis, including changes in the distribution and diversity of microbes, elevation of serum glucagon-like peptide-1 and neuropeptide Y, decrease in orexin A, and upregulation of glucagon-like peptide-1 receptor mRNA [37].

**3.1.3. BBR Reduces Inflammatory Response in Diabetes Mellitus.** The anti-inflammatory activity of BBR has been observed in *in vitro* and *in vivo* studies. In immunocytes (macrophages) [26, 38], cultured metabolic cells (adipocytes and hepatocytes) [39, 40], or pancreatic  $\beta$  cells [41], BBR treatment reduces the production of TNF- $\alpha$ , IL-6, IL-1 $\beta$ , inducible nitric oxide synthase (iNOS), cyclooxygenase-2 (COX-2), matrix metalloproteinase 9 (MMP9), monocyte chemoattractant protein-1 (MCP-1), and CRP and haptoglobin (HP) increases the transcription of Nrf2-targeted antioxidative genes [*NADPH quinone oxidoreductase-1 (NQO-1)*, *heme oxygenase-1 (HO-1)*] [37–41]. The insulin-sensitizing effect of HepG2 cells is closely related to its anti-inflammatory activity. BBR administration significantly decreased serine phosphorylation and increased tyrosine phosphorylation of IRS in HepG2 cells, which improved insulin signaling and thus in turn ameliorated insulin resistance [40]. BBR inhibited inflammation, ameliorated insulin resistance, and reduced the production of proinflammatory cytokines such as IL-6, IL-17, TNF- $\alpha$ , and interferon- $\gamma$  (IFN $\gamma$ ) in NOD mice [42, 43]. Furthermore, BBR increased the ratios of anti-inflammatory/proinflammatory cytokines, such as IL-10/IL-6, IL-10/IL-1 $\beta$ , and IL-10/TNF- $\alpha$  [43].

**3.2. *M. charantia*.** *M. charantia*, also known as bitter melon, has been used for centuries in TCM as an antipyretic and alexipharmac herb. Recent studies have shown that *M. charantia* can ameliorate oxidative stress, hyperlipidemia

[44], inflammation [45], and apoptosis [46]. It also regulates glucose metabolism by acting as a “plant insulin” [47] and presents antidiabetic and antioxidant activities [48].

**3.2.1. Effect of *M. charantia* on Diabetes.** *Momordica charantia* (*M. charantia*) is a widely used traditional remedy for diabetes. It has been proven to be beneficial to insulin resistance, prediabetes, weight losing, and glycemic control in cultured cells, animal models, and human studies [49]. *M. charantia* can repair damaged beta cells, increase insulin levels, and also enhance insulin sensitivity. It inhibits the intestinal glucose absorption by inhibiting glucosidase and enterotoxin activities. It also stimulates the synthesis and release of thyroid hormones and adiponectin and enhances the activity of AMP-activated protein kinase (AMPK) [50]. A recent study showed that compared with metformin, the application of *M. charantia* in diabetes patients had lower probability of hypoglycemia although it is less effective than metformin in lowering blood glucose [51]. In addition, *M. charantia* has a superposition effect when taken with other hypoglycemic agents at the same time, and thus, patients may achieve better management of blood glucose [52]. *M. charantia* also reduces the obesity of rats fed with a high-fat diet [53, 54].

**3.2.2. *M. charantia* Changes Gut Microbiota.** The effect of *M. charantia* on intestinal flora and inflammation has been reported in obese rats fed with high-fat diets. A result showed that although the exact effect of *M. charantia* on intestinal flora was not yet known, the intestinal flora is considered to play an important role through which *M. charantia* improves obesity and metabolic diseases (including diabetes) and is worth the sustained attention [54]. It was reported that BLSP (a bitter melon formulation) treatment reduced the ratio of Firmicutes and Bacteroidetes in the intestinal microflora of diabetic rats, while the relative abundance of Ruminococcaceae, Bacteroides, and Ruminococcus was significantly lower in BLSP-treated rats than in diabetic rats. These demonstrate that BLSP can alter the proportion of specific intestinal microflora in diabetic rats [55].

**3.2.3. *M. charantia* Reduces Inflammatory Response in Diabetes Mellitus.** *M. charantia* possesses antioxidant activities; it enhances the activity of superoxide dismutase, catalase, and nonprotein sulfhydryls and decreases lipid peroxidation. Moreover, *M. charantia* can inhibit the expression of proinflammatory cytokines (TNF- $\alpha$ , IL-6, and IL-10), inflammatory markers (NO, inducible nitric oxide synthase, and myeloperoxidase), and apoptotic markers (BAX and caspase-3) and upregulate Bcl-2 expression [46]. By suppressing the activation of NF- $\kappa$ B by inhibiting NF- $\kappa$ B alpha ( $I\kappa$ B $\alpha$ ) degradation and phosphorylation of JNK/p38 mitogen-activated protein kinases (JNK/p38 MAPKs), *M. charantia* can inhibit inflammation and improve the insulin signaling pathway, thereby ameliorating insulin resistance [54]. *M. charantia* has been reported to inhibit inflammation and the development of diabetes mellitus in rats and mice [54, 56]. After weeks of treatment with *M. charantia*, fasting glucose, insulin, HOMA-IR index, serum lipid levels, fat cell size of epididymal adipose tissues, blood TNF- $\alpha$ , IL-6, and

IL-10 levels, and local endotoxin levels decreased in high-fat diet-induced obese rats [54]. Further studies have shown that *M. charantia* lowers mast cell recruitment in epididymal adipose tissues (EAT) and downregulates proinflammatory cytokines monocyte chemoattractant protein-1 (MCP-1), IL-6, and TNF- $\alpha$  in EAT [56].

**3.3. Curcumin.** Curcumin is the active component of rhizomes of *Curcuma longa*, a plant in the ginger family. The chemical structure of curcumin is (1E,6E)-1,7-bis(4-hydroxy-3-methoxyphenyl)hepta-1,6-diene-3,5-dione (Figure 2) [57]. Curcumin has been used as medicine for thousands of years. Recent years, extensive research on curcumin has found that curcumin has multiple biological activities, such as anticancer, anti-inflammation, antioxidation, antidiabetes, cardioprotective properties, and antiarthritis [58].

**3.3.1. Effect of Curcumin on Diabetes.** In different experimental animal models, such as rats with alloxan-, streptozotocin-(STZ-), or STZ-nicotinamide-induced diabetes [59], oral administration of curcumin resulted in a reduction in body weight, blood glucose, and glycosylated hemoglobin levels [60] and improvement of insulin sensitivity [61]. In diabetic patients, curcumin treatment lowered blood levels of glycated hemoglobin (HbA1c) and fasting plasma glucose (FPG) and improved the pancreatic  $\beta$  cell function, as indicated by homeostasis model assessment- $\beta$  (HOMA- $\beta$ ), C-peptide, and proinsulin/insulin ratio. Besides, curcumin can reduce the outcome of inflammatory cytokine [62] and improve relevant metabolic profiles in type 2 diabetic population [63].

**3.3.2. Effect of Curcumin on Gut Microbiota and Mucosal Immunity.** Curcumin changes the gut microbiota. Through high-throughput sequencing, at the phylum level, Spirochaetae, Tenericutes, and Elusimicrobia were decreased and Actinobacteria was increased after curcumin treatment. At the genus level, curcumin increased the abundance of *Collinsella*, *Streptococcus*, *Sutterella*, *Gemella*, *Thalassospira*, *Gordoniabacter*, and *Actinomyces* [64].

Curcumin treatment can increase the protein expression of occludin and zonula occluden-1 (ZO-1), which maintain intestinal tight junction and regulate the permeability of the intestinal epithelial barrier [16, 65]. Curcumin treatment also induces differentiation of naive CD4<sup>+</sup> T cells into CD4<sup>+</sup>CD25<sup>+</sup>Foxp3<sup>+</sup> Tregs and IL-10-producing Tr1 cells and increases the secretion of IL-10, TGF- $\beta$ , and retinoic acid in the intestinal lamina propria [66]. Curcumin can also stimulate the intestinal epithelial cells and innate lymphoid cells to increase the secretion of IL-25, IL-33, IL-22, and IL-17 and play a role in anti-inflammatory activity [67].

**3.3.3. Curcumin Reduces Inflammatory Response in Diabetes.** Curcumin suppresses inflammation through complex mechanisms and multiple targets, such as inflammatory cytokines, protein kinases, and transcription factors. Inflammatory cytokines affected by curcumin include interleukins, TNF, IFN, and COX-2. Protein kinases include Janus kinase 1/2 (JAK1/2), JNK, extracellular signal-regulated kinase 1/2 (ERK1/2), IKK, and MAPK. Transcription factors include NF- $\kappa$ B [58].

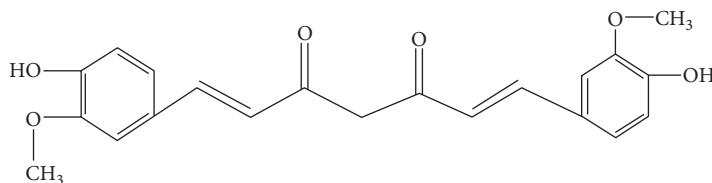


FIGURE 2: Molecular structure of curcumin.

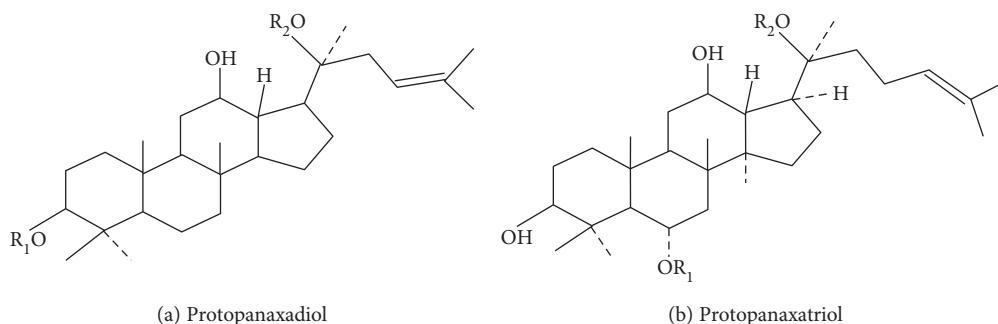


FIGURE 3: Molecular structure of ginsenoside.

Curcumin can reduce the production of inducible nitric oxide synthase (iNOS) and cyclooxygenase- (COX-) 2 by inhibiting LPS-induced iNOS and COX-2 gene expression [68]. iNOS, as an inflammatory signaling factor, mediated inflammation by multiple pathways. Excessive expression of iNOS in cells causes the inflammation and insulin resistance of metabolic organs [69]. COX-2 is a key enzyme in the synthesis of prostaglandins, which contributes to low-grade inflammation of tissues. It was found that curcumin exhibited anti-inflammatory activity by inhibiting the JNK/NF- $\kappa$ B activation and the gene expression of TNF- $\alpha$ , IL-10, and IL-6 [70].

**3.4. Ginsenoside.** *Panax ginseng* has been used for centuries in TCM as an herbal remedy. It is one of the best chosen medical plants to replenish vitality/energy, nourish body fluid, and calm the nerves [71]. The active components of ginseng have been identified as a group of saponins called ginsenosides. According to the chemical structure, ginsenosides can be divided into ginseng diol saponins, ginseng triol saponins, and oleanolic acid saponins (Figure 3). Recent studies have shown that *Panax ginseng* and its monomers have a variety of pharmacologic action such as antioxidation [72, 73], anti-tumor [74], anti-inflammation [75, 76], immune regulation [77], antidiabetes [78, 79], and myocardial protection [80, 81]. It can improve the immune system; inhibit inflammatory factors; protect cardiac function; lower blood glucose; inhibit rectal, liver, and breast cancers [74, 82, 83]; repair neurons; and delay the development of Parkinson's disease and Alzheimer's disease [84, 85].

**3.4.1. Benefits of Ginsenosides to Diabetes.** Studies have shown that ginsenoside Rg1 can improve glucose and lipid metabolisms and reduce blood glucose levels and insulin resistance indices in T2DM rats [86]. Ginsenoside Ge can improve hyperglycemia by improving cholinergic and

antioxidant systems in the brain of C57BL/6 mice and improve high-fat diet-induced insulin resistance, reducing triglycerides and cholesterol [72]. Peroxisome proliferator-activated receptors (PPARs) are transcription factors that play important roles in regulating glucose and lipid metabolisms and the development of atherosclerosis. A clinical study showed that ginsenosides could improve PPAR $\gamma$  expression and lipid metabolism, thereby reducing blood glucose [87]. Another study has shown that ginsenoside Rb1 activates the insulin signaling pathway, upregulates the expression and translocation of glucose transporters in adipose tissue, and thus increases glucose uptake in adipocytes, thereby reducing blood glucose levels and improving insulin resistance [88].

**3.4.2. Ginsenoside Reduces the Inflammatory Response in Diabetes Mellitus.** Studies have shown that inflammatory factors such as TNF- $\alpha$ , IL-6, and monocyte chemoattractant protein-1 (MCP-1) interfere with the insulin signal transduction pathway and cause insulin resistance. They can also directly damage pancreatic  $\beta$  cells [89–92]. It is reported that ginsenoside Rb1 reduces the expression of TNF- $\alpha$  and MCP-1 in 3T3-L1 cells through regulating the IKK/NF- $\kappa$ B signaling pathway [93, 94]. In addition, ginsenoside Rb1 suppresses lipid accumulation and increases the lipolysis in 3T3-L1 adipocytes induced by TNF- $\alpha$  [94, 95]. Ginsenoside Rb1 reduced free fatty acids in the blood and fat content, improved lipid metabolism and insulin resistance, and inhibited TNF- $\alpha$ , IL-6, and other inflammatory factors in obese mice [96–99].

**3.5. Mulberry Leaf Extract (MLE).** 1-Deoxyojirimycin (DNJ, Figure 4) and Kuwanon G (KWG, Figure 5) are the effective constituents of mulberry leaf, which belongs to the genus *Morus* of the Moraceae family. The chemical structure of DNJ is a glucose analogue with an NH group substituting for the oxygen atom of the pyranose ring

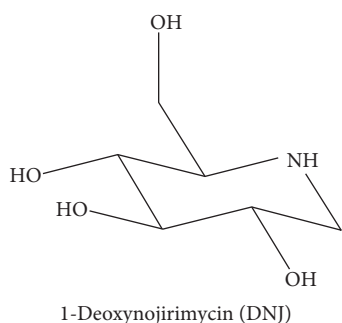


FIGURE 4: Molecular structure of DNJ.

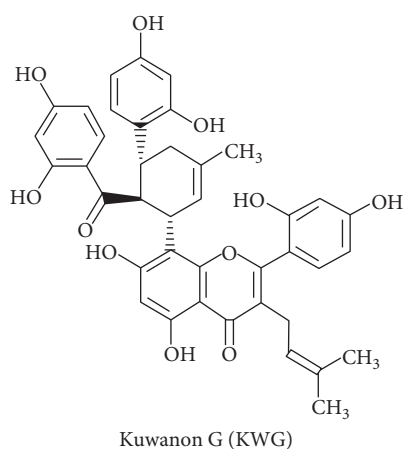


FIGURE 5: Molecular structure of KWG.

[100]. Mulberry leaf, as a traditional Chinese medicine, has been used to treat fever and inflammation for thousands of years. Recent research revealed that MLE has multiple biological activities, such as antidiabetes, antidyslipidemia, and anticancer [101].

**3.5.1. Benefits of MLE to Diabetes.** It is reported that 1-deoxynojirimycin (DNJ) is an important component of MLE that is beneficial to the diabetes. In rats with STZ- or alloxan-induced diabetes, DNJ treatment markedly reduced blood levels of glucose and glycosylated hemoglobin and prevented the dysfunction of pancreatic  $\beta$  cells [102, 103]. A large number of studies have shown that DNJ is a competitive  $\alpha$ -glucosidase inhibitor, which is present in the intestinal epithelial cells. The function of this enzyme is to hydrolyze the disaccharides to monosaccharides for absorption. DNJ inhibits the glucose absorption through competitive inhibition of  $\alpha$ -glucosidase [104]. In db/db mice, DNJ treatment improved insulin resistance via the activation of the insulin signaling PI3K/AKT pathway in skeletal muscle [100] and the activation of the PKB/GSK-3 $\beta$  signaling pathway in the liver [105].

**3.5.2. Effects of MLE on the Intestinal Epithelial Barrier and Inflammation.** Kuwanon G (KWG) which is essential in MLE is reported to protect the intestinal epithelial barrier. LPS can cause the disruption of the intestinal epithelial barrier and decrease the expression of intercellular

junction protein. KWG treatment can increase the protein expression levels of occludin and intercellular adhesion molecule-1 [106].

Mulberry leaf has been used to treat fever and inflammation for thousands of years, and its extract also has anti-inflammatory effects. A study showed that MLE inhibited the expression of inflammatory cytokines IL-1, IL-6, and TNF- $\alpha$  [107] and C-reactive protein (CRP) and MLE reduced the production of iNOS [108]. The decrease in inflammatory factors is indicative of reduced chronic inflammation and results in the improvement of insulin resistance.

**3.6. Other Herbal Monomers.** In addition to the five monomers described above, many other monomers are also found to be closely related to the BMID axis, including tetrandrine [109], notoginsenoside [110], *Lycium barbarum* polysaccharide [111], allicin [112], astragaloside IV [113, 114], quercetin [115], and resveratrol [116].

Among these monomers, astragaloside IV [117], quercetin [118], and resveratrol [119] affect gut microbiota, and notoginsenoside [120], *Lycium barbarum* polysaccharide [121], and allicin [122] affect the function of alleviating intestinal mucosal immunity; the anti-inflammatory monomers are tetrandrine [123], *Lycium barbarum* polysaccharide [124], allicin [125], astragaloside IV [126, 127], quercetin [128], resveratrol [116], and the effect and possible mechanism of these monomers are summarized in Table 1.

## 4. Formulae

A formula consists of multiple Chinese herbs, which are selected under the guidance of TCM theory. In the treatment of diabetes, a formula simultaneously affects multiple targets and regulates the homeostasis, and thus, the application of formulae attracted more focus. But the mechanism research of formulae is limited. The BMID axis will provide a new perspective and make it easier for further studies.

**4.1. Gegen Qinlian Decoction (GGQLD).** GGQLD has a very long history as a TCM formula, with the earliest record being found in the book *Treatise on Febrile and Miscellaneous Diseases* compiled by Zhongjing Zhang. GGQLD consists of extracts of Gegen (*Puerariae lobataeradix*), Huangqin (*Scutellariae radix*), Huanglian (*Coptidis rhizoma*), and Zhigancao (*Glycyrrhizae radix et Rhizoma Praeparata cum Melle*) [129]. In clinic, GGQLD is often used to treat ulcerative colitis and diabetes. Studies showed that GGQLD inhibits the inflammatory signaling pathway, enhances antioxidant effect, and thus improves ulcerative colitis. In addition, GGQLD improves glucose metabolism disorder, increases the insulin sensitivity index, and protects pancreatic  $\beta$  cells, playing a positive role in the treatment of diabetes [130–132].

**4.1.1. GGQLD Improves Diabetes.** In some clinical observations and animal trials, GGQLD has been reported to have beneficial effects on diabetes. For example, in STZ- and HFD-induced diabetic SD rats, GGQLD significantly reduced FBG, HbA1c, and insulin resistance index. In 3T3-L1 adipocytes, GGQLD at 4%, 8%, and 16% was found to

TABLE 1: Chinese herbal products based on the BMID axis.

Category	Chinese herbal products	“BMID” axis			
		Bacteria	Mucosal immunity	Inflammation	Diabetes
Monomers	Berberine	+	+	+	+
	<i>M. charantia</i> extract	+		+	+
	Curcumin	+	+	+	+
	Ginsenoside		+	+	+
	1-Deoxyojirimycin			+	+
	Kuwanon G		+		+
	Tetrandrine			+	+
	Notoginsenoside		+		+
	<i>Lycium barbarum</i> polysaccharide		+	+	+
	Allicin		+	+	+
	Astragaloside IV	+			+
	Quercetin	+		+	+
	Resveratrol	+		+	+
Formulae	GGQLD	+	+	+	+
	DGLHD		+	+	+
	HLWDD			+	+

“+” means positive effect while the “blank” means no effect. GGQLD: Gegen Qinlian Decoction; DGLHD: Danggui Liu Huang Decoction; HLWDD: Huanglian Wendan Decoction.

increase glucose consumption and decrease triglyceride in a dose-dependent manner [131]. In an observational study, T2DM patients treated with a high dose of modified GGQLD reduced blood HbA1c to 1.79% from the initial level of 9.2% [4]. Although limited, available information has demonstrated that GGQLD is beneficial to glucose metabolism and homeostasis.

**4.1.2. GGQLD Alters Gut Microbiota.** There is an established connection between an altered gut microbiota and metabolic disorders such as obesity and diabetes [133, 134]. After treatment with GGQLD, the relative abundance of intestinal beneficial bacteria such as *Lachnospiraceae incertae sedis*, *Gemmiger*, *Bifidobacterium*, and *Faecalibacterium* was significantly higher while harmful bacteria such as *F. prausnitzii*, *Alistipes*, *Pseudobutyrvibrio*, and *Parabacteroides* decreased. GGQLD increases butyrate production and protects the integrity of the mucosal barriers, thereby exerting anti-inflammatory effects which are beneficial to diabetes [135]. A study showed that GGQLD induces compositional changes in the intestinal microflora, increases beneficial bacteria, such as *Faecalibacterium* spp., and thus exerts an antidiabetic effect [135].

**4.2. Danggui Liu Huang Decoction (DGLHD).** DGLHD is an old Chinese herbal formula which comes from the book *Lan Shi Mi Cang* written by Gao Li 741 years ago. DGLHD prescription consists of Danggui (*Angelica sinensis*), Shengdihuang (*Radix rehmanniae preparata*), Huangqin (*Radix scutellariae*), Huanglian (*Rhizoma coptidis*), Huangbo (*Cortex phellodendri*), and Huangqi (*Radix astragali*). Researches indicate that DGLHD decreases FBG and HbA1c levels and protects pancreatic  $\beta$  cells [136].

Recent studies have demonstrated that DGLHD possesses antidiabetic and immunomodulatory effects. For instance, DGLHD enhances glucose uptake in HepG2 cells, inhibits T lymphocyte proliferation, and suppresses the function of dendritic cells. After 16 weeks of treatment, DGLHD promotes insulin secretion, increases insulin sensitivity, and decreases the range of lymphocyte infiltration to inhibit insulinitis as well as to protect pancreatic  $\beta$  cells in NOD mice [137].

DGLHD inhibited LPS-induced production of NO and IL-6 and the expression of iNOS and COX-2. Furthermore, DGLHD suppressed LPS-induced phosphorylation of ERK1/2 [138]. CD4<sup>+</sup>CD25<sup>+</sup>Foxp3<sup>+</sup> Tregs exhibit immune regulatory activity and protect against autoimmune diabetes development. With oral intake of DGLHD, forkhead box transcription factor (Foxp3) mRNA expression in the pancreas and spleen increased. Foxp3 is essential for the differentiation and function of Tregs; thus, DGLHD increases the percentage of CD4<sup>+</sup>CD25<sup>+</sup>Foxp3<sup>+</sup> Tregs in spleen lymphocytes, therefore inhibiting the low-grade inflammation in the pancreas. DGLHD also regulates the maturation and function of dendritic cells, increasing the expression of programmed death ligand-1 and decreasing the percentage of merocytic dendritic cell subset, which in turn decreases T cell-mediated inflammation and ameliorates diabetes [137].

**4.3. Huanglian Wendan Decoction (HLWDD).** HLWDD is a Chinese herbal formula recorded in the book *Liu Yin Tiao Bian* [139]. It consists of root and rhizome of *Coptis deltoidea* C. Y. Cheng & P. K. Hsiao (family: Ranunculaceae), cortex of *Bambusa textilis* McClure (family: Poaceae), caulis of *Pinellia ternata* (Thunb.) Makino (family: Araceae), fructus of *Citrus aurantium* L. (family: Rutaceae), pericarpium of *Citrus*



*reticulata* Blanco (family: Rutaceae), dried sclerotia of *Poria cocos* (Schw.) Wolf (family: Polyporaceae), root and rhizome of *Glycyrrhiza uralensis* Fisch (family: Leguminosae), and root and rhizome of *Zingiber officinale* Roscoe (family: Zingiberaceae). It has been used clinically to treat diabetes and its complications [140].

A recent study showed that treatment with HLWDD (6 g·kg<sup>-1</sup> body weight) for 30 days increased the body weight and decreased FBG, triglycerides, and cholesterol compared with the diabetic model group. HLWDD decreases the release of proinflammatory cytokines, such as TNF- $\alpha$ , IL-6, and IL-1 $\beta$ , and inhibits the phosphorylation of IRS1 at the Ser307 and JNK signal pathway. Through these mechanisms, HLWDD inhibits inflammatory responses and thus improves the insulin signaling pathway [141].

## 5. Conclusions

Diabetes and its complications seriously affect human health and impose increasingly a heavy burden on the health care in many countries. Chinese herbs are inexpensive, less toxic, and tolerable than drugs. Therefore, they have been attracting increased attention in the field of diabetic prevention and treatment. Although clinical efficacy of Chinese herbs or herbal formulae is supported by emerging evidence, the mechanism is still lacking.

Through the analysis of a large number of studies on diabetic pathogenesis and treatment, we proposed the “Bacteria-Mucosal Immunity-Inflammation-Diabetes” (BMID) axis through which we attempted to explain how herbal monomers and formulae improve diabetes. Evidence has demonstrated that monomers and formulae improve diabetes and insulin function via multiple targets. Moreover, the majority of the current studies of TCM on diabetes were focused on inflammation and limited gut microbiota and intestinal mucosal immunity. Furthermore, most studies were aimed to a single target.

Functional food and natural health products have been of great interest to patients, doctors, and researchers for over a decade. Chinese herbs and herbal products are critical and a rich resource of information for the development of health products and precision medicine. Although increasing scientific evidence has been generated from clinical, preclinical, and in vitro studies, the information is still limited and lacks systemic evaluation. The mechanisms of action are particularly a weak area that needs an increased attention. BMID is our first attempt to integrate information and results of various studies and inspire a focus of future direction at which future studies can be conducted to support and improve it. We hope that this review will provide new perspectives and strategies for future research on Chinese herbal products for the prevention and treatment of diabetes and further product development.

## Conflicts of Interest

The authors declare that they have no competing interests.

## Authors' Contributions

Ze Zheng Gao and Qingwei Li contributed equally to this work.

## References

- [1] Y. Zhang, X. Li, D. Zou et al., “Treatment of type 2 diabetes and dyslipidemia with the natural plant alkaloid berberine,” *The Journal of Clinical Endocrinology and Metabolism*, vol. 93, no. 7, pp. 2559–2565, 2008.
- [2] L. Ji, X. Tong, H. Wang et al., “Efficacy and safety of traditional Chinese medicine for diabetes: a double-blind, randomized, controlled trial,” *PLoS One*, vol. 8, no. 2, 2013.
- [3] X. L. Tong, S. T. Wu, F. M. Lian et al., “The safety and effectiveness of TM81, a Chinese herbal medicine, in the treatment of type 2 diabetes: a randomized double-blind placebo-controlled trial,” *Diabetes, Obesity & Metabolism*, vol. 15, no. 5, pp. 448–454, 2013.
- [4] X. L. Tong, L. H. Zhao, F. M. Lian et al., “Clinical observations on the dose-effect relationship of Gegen Qin Lian decoction on 54 out-patients with type 2 diabetes,” *Journal of Traditional Chinese Medicine*, vol. 31, no. 1, pp. 56–59, 2011.
- [5] B. Godman, R. E. Malmström, E. Diogene et al., “Are new models needed to optimize the utilization of new medicines to sustain healthcare systems?,” *Expert Review of Clinical Pharmacology*, vol. 8, no. 1, pp. 77–94, 2015.
- [6] J. E. Shaw, R. A. Sicree, and P. Z. Zimmet, “Global estimates of the prevalence of diabetes for 2010 and 2030,” *Diabetes Research and Clinical Practice*, vol. 87, no. 1, pp. 4–14, 2010.
- [7] H. Cai, G. Li, P. Zhang, D. Xu, and L. Chen, “Effect of exercise on the quality of life in type 2 diabetes mellitus: a systematic review,” *Quality of Life Research*, vol. 26, no. 3, pp. 515–530, 2017.
- [8] S. R. Gill, M. Pop, R. T. Deboy et al., “Metagenomic analysis of the human distal gut microbiome,” *Science*, vol. 312, no. 5778, pp. 1355–1359, 2006.
- [9] R. E. Ley, F. Bäckhed, P. Turnbaugh, C. A. Lozupone, R. D. Knight, and J. I. Gordon, “Obesity alters gut microbial ecology,” *Proceedings of the National Academy of Sciences of the United States of America*, vol. 102, no. 31, pp. 11070–11075, 2005.
- [10] P. D. Cani, A. M. Neyrinck, F. Fava et al., “Selective increases of bifidobacteria in gut microflora improve high-fat-diet-induced diabetes in mice through a mechanism associated with endotoxaemia,” *Diabetologia*, vol. 50, no. 11, pp. 2374–2383, 2007.
- [11] J. Qin, Y. Li, Z. Cai et al., “A metagenome-wide association study of gut microbiota in type 2 diabetes,” *Nature*, vol. 490, no. 7418, pp. 55–60, 2012.
- [12] E. Le Chatelier, T. Nielsen, J. Qin et al., “Richness of human gut microbiome correlates with metabolic markers,” *Nature*, vol. 500, no. 7464, pp. 541–546, 2013.
- [13] M. A. Odenwald and J. R. Turner, “The intestinal epithelial barrier: a therapeutic target?,” *Nature Reviews Gastroenterology & Hepatology*, vol. 14, no. 1, pp. 9–21, 2017.
- [14] J. Amar, C. Chabo, A. Waget et al., “Intestinal mucosal adherence and translocation of commensal bacteria at the early onset of type 2 diabetes: molecular mechanisms and probiotic treatment,” *EMBO Molecular Medicine*, vol. 3, no. 9, pp. 559–572, 2011.

- [15] P. D. Cani, J. Amar, M. A. Iglesias et al., "Metabolic endotoxemia initiates obesity and insulin resistance," *Diabetes*, vol. 56, no. 7, pp. 1761–1772, 2007.
- [16] P. D. Cani, R. Bibiloni, C. Knauf et al., "Changes in gut microbiota control metabolic endotoxemia-induced inflammation in high-fat diet-induced obesity and diabetes in mice," *Diabetes*, vol. 57, no. 6, pp. 1470–1481, 2008.
- [17] F. R. Costa, M. C. Franozo, G. G. de Oliveira et al., "Gut microbiota translocation to the pancreatic lymph nodes triggers NOD2 activation and contributes to T1D onset," *The Journal of Experimental Medicine*, vol. 213, no. 7, pp. 1223–1239, 2016.
- [18] S. Fukuda, H. Toh, K. Hase et al., "Bifidobacteria can protect from enteropathogenic infection through production of acetate," *Nature*, vol. 469, no. 7331, pp. 543–547, 2011.
- [19] C. L. Maynard, C. O. Elson, R. D. Hatton, and C. T. Weaver, "Reciprocal interactions of the intestinal microbiota and immune system," *Nature*, vol. 489, no. 7415, pp. 231–241, 2012.
- [20] L. Garidou, C. Pomi , P. Klopp et al., "The gut microbiota regulates intestinal CD4 T cells expressing ROR $\gamma$ t and controls metabolic disease," *Cell Metabolism*, vol. 22, no. 1, pp. 100–112, 2015.
- [21] M. Kassan, S. K. Choi, M. Gal n et al., "Enhanced NF- $\kappa$ B activity impairs vascular function through PARP-1-, SP-1-, and COX-2-dependent mechanisms in type 2 diabetes," *Diabetes*, vol. 62, no. 6, pp. 2078–2087, 2013.
- [22] I. Hameed, S. R. Masoodi, S. A. Mir, M. Nabi, K. Ghazanfar, and B. A. Ganai, "Type 2 diabetes mellitus: from a metabolic disorder to an inflammatory condition," *World Journal of Diabetes*, vol. 6, no. 4, pp. 598–612, 2015.
- [23] Z. T. Bloomgarden, "Inflammation and insulin resistance," *Diabetes Care*, vol. 26, no. 6, pp. 1922–6, 2003.
- [24] I. A. Zolotnik and T. Y. Figueroa, "Insulin receptor and IRS-1 co-immunoprecipitation with SOCS-3, and IKK $\alpha$ / $\beta$  phosphorylation are increased in obese Zucker rat skeletal muscle," *Life Sciences*, vol. 91, no. 15–16, p. 816, 2012.
- [25] X. Jin, X. Song, Y. B. Cao, Y. Y. Jiang, and Q. Y. Sun, "Research progress in structural modification and pharmacological activities of berberine," *Journal of Pharmacy Practice*, vol. 32, pp. 171–175, 2014.
- [26] H. Zhou, L. Feng, F. Xu et al., "Berberine inhibits palmitate-induced NLRP3 inflammasome activation by triggering autophagy in macrophages: a new mechanism linking berberine to insulin resistance improvement," *Biomedicine & Pharmacotherapy*, vol. 89, pp. 864–874, 2017.
- [27] L. M. Ortiz, P. Lombardi, M. Tillhon, and A. Scovassi, "Berberine, an epiphany against cancer," *Molecules*, vol. 19, pp. 12349–12367, 2014.
- [28] Y. Sun, K. Xun, Y. Wang, and X. Chen, "A systematic review of the anticancer properties of berberine: a natural product from Chinese herbs," *Anti-Cancer Drugs*, vol. 13, pp. 757–769, 2009.
- [29] J. Tang, Y. Feng, S. Tsao, N. Wang, R. Curtain, and Y. Wang, "Berberine and Coptidis rhizoma as novel antineoplastic agents: a review of traditional use and biomedical investigations," *Journal of Ethnopharmacology*, vol. 13, pp. 5–17, 2009.
- [30] M. Ming, J. Sinnett-Smith, J. Wang et al., "Dose-dependent AMPK-dependent and independent mechanisms of berberine and metformin inhibition of mTORC1, ERK, DNA synthesis and proliferation in pancreatic cancer cells," *PLoS One*, vol. 9, no. 12, 2014.
- [31] P. Jabbarzadeh Kaboli, A. Rahmat, P. Ismail, and K. H. Ling, "Targets and mechanisms of berberine, a natural drug with potential to treat cancer with special focus on breast cancer," *European Journal of Pharmacology*, vol. 740, pp. 584–595, 2014.
- [32] B. Vandanmagsar, Y. H. Youm, A. Ravussin et al., "The NLRP3 inflammasome instigates obesity-induced inflammation and insulin resistance," *Nature Medicine*, vol. 17, no. 2, pp. 179–188, 2011.
- [33] L. Ye, L. Shu, G. Chao et al., "Inhibition of M1 macrophage activation in adipose tissue by berberine improves insulin resistance," *Life Sciences*, vol. 166, pp. 82–91, 2016.
- [34] X. Wang, N. Ota, P. Manzanillo et al., "Interleukin-22 alleviates metabolic disorders and restores mucosal immunity in diabetes," *Nature*, vol. 514, no. 7521, pp. 237–241, 2014.
- [35] J. Gong, M. Hu, Z. Huang et al., "Berberine attenuates intestinal mucosal barrier dysfunction in type 2 diabetic rats," *Frontiers in Pharmacology*, vol. 3, no. 8, p. 42, 2017.
- [36] J. H. Xu, X. Z. Liu, W. Pan, and D. J. Zou, "Berberine protects against diet-induced obesity through regulating metabolic endotoxemia and gut hormone levels," *Molecular Medicine Reports*, vol. 15, no. 5, pp. 2765–2787, 2017.
- [37] H. Sun, N. Wang, C. Zhen et al., "Modulation of microbiota-gut-brain axis by berberine resulting in improved metabolic status in high-fat diet-fed rats," *Obesity Facts*, vol. 9, no. 6, p. 365, 2016.
- [38] C. Mo, L. Wang, J. Zhang et al., "The crosstalk between Nrf2 and AMPK signal pathways is important for the anti-inflammatory effect of berberine in LPS-stimulated macrophages and endotoxin-shocked mice," *Antioxidants & Redox Signaling*, vol. 20, no. 4, pp. 574–588, 2014.
- [39] B.-H. Choi, I.-S. Ahn, Y.-H. Kim et al., "Berberine reduces the expression of adipogenic enzymes and inflammatory molecules of 3T3-L1 adipocyte," *Experimental and Molecular Medicine*, vol. 38, no. 6, pp. 599–605, 2006.
- [40] T. Lou, Z. Zhang, Z. Xi et al., "Berberine inhibits inflammatory response and ameliorates insulin resistance in hepatocytes," *Inflammation*, vol. 34, no. 6, pp. 659–667, 2011.
- [41] Y. Wang, "Attenuation of berberine on lipopolysaccharide-induced inflammatory and apoptosis responses in  $\beta$ -cells via TLR4-independent JNK/NF- $\kappa$ B pathway," *Pharmaceutical Biology*, vol. 52, no. 4, 2013.
- [42] G. Cui, X. Qin, Y. Zhang, Z. Gong, B. Ge, and Y. Q. Zang, "Berberine differentially modulates the activities of ERK, p38 MAPK, and JNK to suppress Th17 and Th1 T cell differentiation in type 1 diabetic mice," *The Journal of Biological Chemistry*, vol. 284, no. 41, pp. 28420–28429, 2009.
- [43] W.-H. Chueh and J.-Y. Lin, "Protective effect of isoquinoline alkaloid berberine on spontaneous inflammation in the spleen, liver and kidney of non-obese diabetic mice through downregulating gene expression ratios of pro-/anti-inflammatory and Th1/Th2 cytokines," *Food Chemistry*, vol. 131, no. 4, pp. 1263–1271, 2012.
- [44] N. P. Fernandes, C. V. Lagishetty, V. S. Panda, and S. R. Naik, "An experimental evaluation of the antidiabetic and antilipidemic properties of a standardized Momordica charantia fruit extract," *BMC Complementary and Alternative Medicine*, vol. 7, p. 29, 2007.

- [45] J. S. Yu, J. H. Kim, S. Lee, K. Jung, K. H. Kim, and J. Y. Cho, "Src/Syk-targeted anti-inflammatory actions of triterpenoidal saponins from Gac (*Momordica cochinchinensis*) seeds," *The American Journal of Chinese Medicine*, vol. 2, pp. 1–15, 2017.
- [46] M. Raish, "Momordica charantia polysaccharides ameliorate oxidative stress, hyperlipidemia, inflammation, and apoptosis during myocardial infarction by inhibiting the NF- $\kappa$ B signaling pathway," *International Journal of Biological Macromolecules*, vol. 97, pp. 544–551, 2017.
- [47] P. Khanna, S. C. Jain, A. Panagariya, and V. P. Dixit, "Hypoglycemic activity of polypeptide-p from a plant source," *Journal of Natural Products*, vol. 44, pp. 648–655, 1981.
- [48] M. F. Mahmoud, F. E. El Ashry, N. N. El Maraghy, and A. Fahmy, "Studies on the antidiabetic activities of *Momordica charantia* fruit juice in streptozotocin-induced diabetic rats," *Pharmaceutical Biology*, vol. 55, no. 1, pp. 758–765, 2017.
- [49] M. B. Krawinkel and G. B. Keding, "Bitter melon (*Momordica charantia*): a dietary approach to hyperglycemia," *Nutrition Reviews*, vol. 64, pp. 331–337, 2006.
- [50] P. Chaturvedi, "Antidiabetic potentials of *Momordica charantia*: multiple mechanisms behind the effects," *Journal of Medicinal Food*, vol. 15, no. 2, p. 101, 2012.
- [51] A. Fuangchan, P. Sonthisombat, T. Seubnukarn et al., "Hypoglycemic effect of bitter melon compared with metformin in newly diagnosed type 2 diabetes patients," *Journal of Ethnopharmacology*, vol. 134, no. 2, pp. 422–428, 2011.
- [52] E. Basch, S. Gabardi, and C. Ulbricht, "Bitter melon (*Momordica charantia*): a review of efficacy and safety," *American Journal of Health-System Pharmacy*, vol. 60, pp. 356–359, 2003.
- [53] H. Hui, G. Tang, and V. L. W. Go, "Hypoglycemic herbs and their action mechanisms," *Chinese Medicine*, vol. 4, no. 1, p. 11, 2009.
- [54] J. Bai, Y. Zhu, and Y. Dong, "Response of gut microbiota and inflammatory status to bitter melon (*Momordica charantia* L.) in high fat diet induced obese rats," *Journal of Ethnopharmacology*, vol. 194, pp. 717–726, 2016.
- [55] Y. Zhu, J. Bai, Y. Zhang, X. Xiao, and Y. Dong, "Effects of bitter melon (*Momordica charantia* L.) on the gut microbiota in high fat diet and low dose streptozotocin-induced rats," *International Journal of Food Sciences & Nutrition*, vol. 67, no. 6, p. 686, 2016.
- [56] B. Bao, Y. G. Chen, L. Zhang et al., "*Momordica charantia* (bitter melon) reduces obesity-associated macrophage and mast cell infiltration as well as inflammatory cytokine expression in adipose tissues," *PLoS One*, vol. 8, no. 12, article e84075, 2013.
- [57] A. S. Pithadia, A. Bhunia, R. Sribalan, V. Padmini, C. A. Fierke, and A. Ramamoorthy, "Influence of a curcumin derivative on hIAPP aggregation in the absence and presence of lipid membranes," *Chemical Communications (Camb)*, vol. 52, no. 5, pp. 942–945, 2016.
- [58] S. Prasad, S. C. Gupta, A. K. Tyagi, and B. B. Aggarwal, "Curcumin, a component of golden spice: from bedside to bench and back," *Biotechnology Advances*, vol. 32, no. 6, pp. 1053–1064, 2014.
- [59] L. Pari and P. Murugan, "Tetrahydrocurcumin prevents brain lipid peroxidation in streptozotocin-induced diabetic rats," *Journal of Medicinal Food*, vol. 10, pp. 323–329, 2007.
- [60] N. Arun and N. Nalini, "Efficacy of turmeric on blood sugar and polyol pathway in diabetic albino rats," *Plant Foods for Human Nutrition*, vol. 57, pp. 41–52, 2002.
- [61] P. Murugan and L. Pari, "Influence of tetrahydrocurcumin on hepatic and renal functional markers and protein levels in experimental type 2 diabetic rats," *Basic & Clinical Pharmacology & Toxicology*, vol. 101, pp. 241–245, 2007.
- [62] S. Chuengsamarn, S. Rattanamongkolgul, R. Luechapudiporn, C. Phisalaphong, and S. Jirawatnotai, "Curcumin extract for prevention of type 2 diabetes," *Diabetes Care*, vol. 35, no. 11, pp. 2121–2127, 2012.
- [63] S. Chuengsamarn, S. Rattanamongkolgul, and B. Phonrat, "Reduction of atherogenic risk in patients with type 2 diabetes by curcuminoid extract: a randomized controlled trial," *The Journal of Nutritional Biochemistry*, vol. 25, pp. 144–150, 2014.
- [64] W. Feng, H. Wang, P. Zhang et al., "Modulation of gut microbiota contributes to curcumin-mediated attenuation of hepatic steatosis in rats," *Biochimica et Biophysica Acta*, vol. 1861, no. 7, pp. 1801–1812, 2017.
- [65] R. Al-Sadi, S. Guo, D. Ye, and T. Y. Ma, "TNF- $\alpha$  modulation of intestinal epithelial tight junction barrier is regulated by ERK1/2 activation of Elk-1," *The American Journal of Pathology*, vol. 183, pp. 1871–1884, 2013.
- [66] Y. Cong, L. Wang, A. Konrad, T. Schoeb, and C. O. Elson, "Curcumin induces the tolerogenic dendritic cell that promotes differentiation of intestine-protective regulatory T cells," *European Journal of Immunology*, vol. 39, no. 11, pp. 3134–3146, 2009.
- [67] J. Wang, S. S. Ghosh, and S. Ghosh, "Curcumin improves intestinal barrier function: modulation of intracellular signaling and 2 organization of tight junctions," *American Journal of Physiology - Cell Physiology*, vol. 312, no. 4, pp. C438–C445, 2017.
- [68] S. Gafner, S. K. Lee, M. Cuendet et al., "Biologic evaluation of curcumin and structural derivatives in cancer chemoprevention model systems," *Phytochemistry*, vol. 65, pp. 2849–2859, 2004.
- [69] K. M. Sakthivel and C. Guruvayoorappan, "Acacia ferruginea inhibits inflammation by regulating inflammatory iNOS and COX-2," *Journal of Immunotoxicology*, vol. 13, no. 1, pp. 127–135, 2016.
- [70] Y. Pan, Y. Wang, L. Cai et al., "Inhibition of high glucose-induced inflammatory response and macrophage infiltration by a novel curcumin derivative prevents renal injury in diabetic rats," *British Journal of Pharmacology*, vol. 166, no. 3, pp. 1169–1182, 2012.
- [71] J. Yin, H. Zhang, and J. Ye, "Traditional Chinese medicine in treatment of metabolic syndrome," *Endocrine Metabolic & Immune Disorders Drug Targets*, vol. 8, no. 2, p. 99, 2008.
- [72] J. M. Kim, C. H. Park, S. K. Park et al., "Ginsenoside Re ameliorates brain insulin resistance and cognitive dysfunction in high-fat diet-induced C57BL/6 mice," *Journal of Agricultural & Food Chemistry*, vol. 65, no. 13, pp. 2719–2729, 2017.
- [73] C. Lu, Z. Shi, L. Dong et al., "Exploring the effect of ginsenoside Rh1 in a sleep deprivation-induced mouse memory impairment model," *Phytotherapy Research (PTR)*, vol. 31, no. 5, pp. 763–770, 2017.
- [74] D. Dai, C. F. Zhang, S. Williams, C. S. Yuan, and C. Z. Wang, "Ginseng on cancer: potential role in modulating

- inflammation-mediated angiogenesis," *American Journal of Chinese Medicine*, vol. 45, no. 1, pp. 13–22, 2017.
- [75] I. S. Lee, I. J. Uh, K. S. Kim et al., "Anti-inflammatory effects of ginsenoside Rg3 via NF- $\kappa$ B pathway in A549 cells and human asthmatic lung tissue," *Journal of Immunology Research*, vol. 2016, Article ID 7521601, 11 pages, 2016.
- [76] S. Ahn, M. H. Siddiqi, V. C. Aceituno, S. Y. Simu, and D. C. Yang, "Suppression of MAPKs/NF- $\kappa$ B activation induces intestinal anti-inflammatory action of ginsenoside Rf in HT-29 and RAW264.7 cells," *Immunological Investigations*, vol. 45, no. 5, p. 439, 2016.
- [77] S. Bao, Z. Yun, W. Bing et al., "Ginsenoside Rg1 improves lipopolysaccharide-induced acute lung injury by inhibiting inflammatory responses and modulating infiltration of M2 macrophages," *International Immunopharmacology*, vol. 28, no. 1, pp. 429–434, 2015.
- [78] Q. T. Bu, W. Y. Zhang, Q. C. Chen et al., "Anti-diabetic effect of ginsenoside Rb(3) in alloxan-induced diabetic mice," *Medicinal Chemistry*, vol. 8, no. 5, pp. 934–941, 2012.
- [79] Y. C. Hwang, D. H. Oh, M. C. Choi et al., "Compound K attenuates glucose intolerance and hepatic steatosis through AMPK-dependent pathways in type 2 diabetic OLETF rats," *Korean Journal of Internal Medicine*, 2017.
- [80] Y. J. Zhang, X. L. Zhang, M. H. Li et al., "The ginsenoside Rg1 prevents transverse aortic constriction-induced left ventricular hypertrophy and cardiac dysfunction by inhibiting fibrosis and enhancing angiogenesis," *Journal of Cardiovascular Pharmacology*, vol. 62, no. 1, p. 50, 2013.
- [81] H. Yu, J. Zhen, Y. Yang, J. Gu, S. Wu, and Q. Liu, "Ginsenoside Rg1 ameliorates diabetic cardiomyopathy by inhibiting endoplasmic reticulum stress-induced apoptosis in a streptozotocin-induced diabetes rat model," *Journal of Cellular & Molecular Medicine*, vol. 20, no. 4, p. 623, 2016.
- [82] L. U. Ping, S. U. Wei, Z. H. Miao, H. R. Niu, J. Liu, and Q. L. Hua, "Effect and mechanism of ginsenoside Rg3 on postoperative life span of patients with non-small cell lung cancer," *Chinese Journal of Integrative Medicine*, vol. 14, no. 1, pp. 33–36, 2008.
- [83] Z. Yuan, H. Jiang, X. Zhu, X. Liu, and J. Li, "Ginsenoside Rg3 promotes cytotoxicity of paclitaxel through inhibiting NF- $\kappa$ B signaling and regulating Bax/Bcl-2 expression on triple-negative breast cancer," *Biomedicine & Pharmacotherapy*, vol. 89, pp. 227–232, 2017.
- [84] X. Zhang, Y. Wang, C. Ma et al., "Ginsenoside Rd and ginsenoside Re offer neuroprotection in a novel model of Parkinson's disease," *American Journal of Neurodegenerative Disease*, vol. 5, no. 1, p. 52, 2016.
- [85] F. Li, X. Wu, J. Li, and Q. Niu, "Ginsenoside Rg1 ameliorates hippocampal long-term potentiation and memory in an Alzheimer's disease model," *Molecular Medicine Reports*, vol. 13, no. 6, p. 4904, 2016.
- [86] W. Tian, L. Chen, L. Zhang et al., "Effects of ginsenoside Rg1 on glucose metabolism and liver injury in streptozotocin-induced type 2 diabetic rats," *Genetics & Molecular Research Gmr*, vol. 16, no. 1, 2017.
- [87] H. X. Ni, N. J. Yu, and X. H. Yang, "The study of ginsenoside on PPAR $\gamma$  expression of mononuclear macrophage in type 2 diabetes," *Molecular Biology Reports*, vol. 37, no. 6, p. 2975, 2010.
- [88] W. B. Shang, C. Guo, J. Zhao, X. Z. Yu, and H. Zhang, "Ginsenoside Rb1 upregulates expressions of GLUTs to promote glucose consumption in adipocytes," *Zhongguo Zhong Yao Za Zhi*, vol. 39, no. 22, p. 448, 2014.
- [89] K. Waugh, J. Snellbergeon, A. Michels et al., "Increased inflammation is associated with islet autoimmunity and type 1 diabetes in the Diabetes Autoimmunity Study in the Young (DAISY)," *PLoS One*, vol. 12, no. 4, article e0174840, 2017.
- [90] J. Z. Q. Luo, J. W. Kim, and L. Luo, "Effects of ginseng and its four purified ginsenosides (Rb2, Re, Rg1, Rd) on human pancreatic islet  $\beta$  cell in vitro," *European Journal Pharmaceutical & Medical Research*, vol. 3, no. 1, p. 110, 2016.
- [91] S. S. Kim, H. J. Jang, M. Y. Oh et al., "Ginsenoside Rg3 enhances islet cell function and attenuates apoptosis in mouse islets," *Transplantation Proceedings*, vol. 46, no. 4, pp. 1150–1155, 2014.
- [92] K. Eguchi and R. Nagai, "Islet inflammation in type 2 diabetes and physiology," *Journal of Clinical Investigation*, vol. 127, no. 1, p. 14, 2017.
- [93] W. Shang, Y. Yang, L. Zhou, B. Jiang, H. Jin, and M. Chen, "Ginsenoside Rb1 stimulates glucose uptake through insulin-like signaling pathway in 3T3-L1 adipocytes," *Journal of Endocrinology*, vol. 198, no. 3, p. 561, 2008.
- [94] Q. Mu, X. Fang, X. Li et al., "Ginsenoside Rb1 promotes browning through regulation of PPAR $\gamma$  in 3T3-L1 adipocytes," *Biochemical & Biophysical Research Communications*, vol. 466, no. 3, pp. 530–535, 2015.
- [95] Y. Gao, M. F. Yang, Y. P. Su et al., "Ginsenoside Re reduces insulin resistance through activation of PPAR- $\gamma$  pathway and inhibition of TNF- $\alpha$  production," *Journal of Ethnopharmacology*, vol. 147, no. 2, pp. 509–516, 2013.
- [96] L. Zhang, L. Zhang, X. Wang, and H. Si, "Anti-adipogenic effects and mechanisms of ginsenoside Rg3 in pre-adipocytes and obese mice," *Frontiers in Pharmacology*, vol. 8, p. 113, 2017.
- [97] Y. Wu, Y. Yu, A. Szabo, M. Han, and X. F. Huang, "Central inflammation and leptin resistance are attenuated by ginsenoside Rb1 treatment in obese mice fed a high-fat diet," *PLoS One*, vol. 9, no. 3, 2014.
- [98] X. M. Zhang, S. C. Qu, D. Y. Sui, X. F. Yu, and Z. Z. Lv, "Effects of ginsenoside-Rb on blood lipid metabolism and anti-oxidation in hyperlipidemia rats," *China Journal of Chinese Materia Medica*, vol. 29, no. 11, pp. 1085–1088, 2004.
- [99] S. Yu, X. Zhou, F. Li et al., "Microbial transformation of ginsenoside Rb1, Re and Rg1 and its contribution to the improved anti-inflammatory activity of ginseng," *Scientific Reports*, vol. 7, no. 1, p. 138, 2017.
- [100] Q. Liu, X. Li, C. Li, Y. Zheng, and G. Peng, "1-Deoxyojirimycin alleviates insulin resistance via activation of insulin signaling PI3K/AKT pathway in skeletal muscle of db/db mice," *Molecules*, vol. 20, no. 12, pp. 21700–21714, 2015.
- [101] Y. Liu, X. Li, C. Xie et al., "Prevention effects and possible molecular mechanism of mulberry leaf extract and its formulation on rats with insulin-insensitivity," *PLoS One*, vol. 11, no. 4, 2016.
- [102] V. Saini, "Molecular mechanisms of insulin resistance in type 2 diabetes mellitus," *World Journal of Diabetes*, vol. 1, no. 3, pp. 68–75, 2010.
- [103] A. Aziz and S. Wheatcroft, "Insulin resistance in type 2 diabetes and obesity: implications for endothelial function," *Expert Review of Cardiovascular Therapy*, vol. 9, no. 4, pp. 403–407, 2011.

- [104] A. Hatano, Y. Kanno, Y. Kondo et al., "Synthesis and characterization of novel, conjugated, fluorescent DNJ derivatives for  $\alpha$ -glucosidase recognition," *Bioorganic & Medicinal Chemistry*, vol. 25, no. 2, pp. 773–778, 2017.
- [105] Q. Liu, X. Li, C. Li et al., "1-Deoxynojirimycin alleviates liver injury and improves hepatic glucose metabolism in db/db mice," *Molecules*, vol. 21, no. 3, p. 279, 2016.
- [106] H. Guo, Y. Xu, W. Huang et al., "Kuwanon G preserves LPS-induced disruption of gut epithelial barrier in vitro," *Molecules*, vol. 21, no. 11, 2016.
- [107] H. N. Na, S. Park, H. J. Jeon, H. B. Kim, and J. H. Nam, "Reduction of adenovirus 36-induced obesity and inflammation by mulberry extract," *Microbiology and Immunology*, vol. 58, no. 5, pp. 303–306, 2014.
- [108] H. H. Lim, S. O. Lee, S. Y. Kim, S. J. Yang, and Y. Lim, "Anti-inflammatory and antiobesity effects of mulberry leaf and fruit extract on high fat diet-induced obesity," *Experimental Biology and Medicine (Maywood, N.J.)*, vol. 238, no. 10, pp. 1160–1169, 2013.
- [109] C. Song, Y. Ji, G. Zou, and C. Wan, "Tetrandrine down-regulates expression of miRNA-155 to inhibit signal-induced NF- $\kappa$ B activation in a rat model of diabetes mellitus," *International Journal of Clinical and Experimental Medicine*, vol. 8, no. 3, pp. 4024–4030, 2015.
- [110] E. Zhang, B. Gao, and L. Yang, "Notoginsenoside Ft1 promotes fibroblast proliferation via PI3K/Akt/mTOR signaling pathway and benefits wound healing in genetically diabetic mice," *The Journal of Pharmacology and Experimental Therapeutics*, vol. 356, no. 2, pp. 324–332, 2016.
- [111] M. Du, X. Hu, L. Kou, B. Zhang, and C. Zhang, "Lycium barbarum polysaccharide mediated the antidiabetic and antinephritic effects in diet-streptozotocin-induced diabetic Sprague Dawley rats via regulation of NF- $\kappa$ B," *BioMed Research International*, vol. 2016, Article ID 3140290, 9 pages, 2016.
- [112] A. Hosseini and H. Hosseinzadeh, "A review on the effects of *Allium sativum* (garlic) in metabolic syndrome," *Journal of Endocrinological Investigation*, vol. 38, no. 11, pp. 1147–1157, 2015.
- [113] R. Zhu, J. Zheng, L. Chen, B. Gu, and S. Huang, "Astragaloside IV facilitates glucose transport in C2C12 myotubes through the IRS1/AKT pathway and suppresses the palmitate-induced activation of the IKK/ $\text{I}\kappa\text{B}\alpha$  pathway," *International Journal of Molecular Medicine*, vol. 37, no. 6, pp. 1697–1705, 2016.
- [114] D. Gui, J. Huang, Y. Guo et al., "Astragaloside IV ameliorates renal injury in streptozotocin-induced diabetic rats through inhibiting NF- $\kappa$ B-mediated inflammatory genes expression," *Cytokine*, vol. 61, no. 3, pp. 970–979, 2013.
- [115] L. Du, M. Hao, C. Li et al., "Quercetin inhibited epithelial mesenchymal transition in diabetic rats, high-glucose-cultured lens, and SRA01/04 cells through transforming growth factor- $\beta$ 2/phosphoinositide 3-kinase/Akt pathway," *Molecular and Cellular Endocrinology*, vol. 452, pp. 44–56, 2017.
- [116] Y. Qiao, K. Gao, Y. Wang, X. Wang, and B. Cui, "Resveratrol ameliorates diabetic nephropathy in rats through negative regulation of the p38 MAPK/TGF- $\beta$ 1 pathway," *Experimental and Therapeutic Medicine*, vol. 13, no. 6, pp. 3223–3230, 2017.
- [117] Y. Jin, X. Guo, B. Yuan et al., "Disposition of astragaloside IV via enterohepatic circulation is affected by the activity of the intestinal microbiome," *Journal of Agricultural and Food Chemistry*, vol. 63, no. 26, pp. 6084–6093, 2015.
- [118] J. Firrman, L. Liu, L. Zhang et al., "The effect of quercetin on genetic expression of the commensal gut microbes *Bifidobacterium catenulatum*, *Enterococcus caccae* and *Ruminococcus gauvreauii*," *Anaerobe*, vol. 42, pp. 130–141, 2016.
- [119] M. M. Sung, T. T. Kim, E. Denou et al., "Improved glucose homeostasis in obese mice treated with resveratrol is associated with alterations in the gut microbiome," *Diabetes*, vol. 66, no. 2, pp. 418–425, 2017.
- [120] X. P. Zhang, J. Jiang, Q. H. Cheng et al., "Protective effects of Ligustrazine, Kakonein and Panax Notoginsenoside on the small intestine and immune organs of rats with severe acute pancreatitis," *Hepatobiliary & Pancreatic Diseases International*, vol. 10, no. 6, pp. 632–637, 2011.
- [121] L. Zhao, H. Wu, A. Zhao et al., "The in vivo and in vitro study of polysaccharides from a two-herb formula on ulcerative colitis and potential mechanism of action," *Journal of Ethnopharmacology*, vol. 153, no. 1, pp. 151–159, 2014.
- [122] A. Lang, M. Lahav, E. Sakhnini et al., "Allicin inhibits spontaneous and TNF-alpha induced secretion of proinflammatory cytokines and chemokines from intestinal epithelial cells," *Clinical Nutrition*, vol. 23, no. 5, pp. 1199–1208, 2004.
- [123] H. S. Choi, H. S. Kim, K. R. Min et al., "Anti-inflammatory effects of fangchinoline and tetrandrine," *Journal of Ethnopharmacology*, vol. 69, no. 2, pp. 173–179, 2000.
- [124] Y. C. Oh, W. K. Cho, G. Y. Im et al., "Anti-inflammatory effect of Lycium fruit water extract in lipopolysaccharide-stimulated RAW 264.7 macrophage cells," *International Immunopharmacology*, vol. 13, no. 2, pp. 181–189, 2012.
- [125] L. F. Cardozo, L. M. Pedruzzi, P. Stenvinkel et al., "Nutritional strategies to modulate inflammation and oxidative stress pathways via activation of the master antioxidant switch Nrf2," *Biochimie*, vol. 95, no. 8, pp. 1525–1533, 2013.
- [126] X. Zhou, X. Sun, X. Gong et al., "Astragaloside IV from *Astragalus membranaceus* ameliorates renal interstitial fibrosis by inhibiting inflammation via TLR4/NF- $\kappa$ B in vivo and in vitro," *International Immunopharmacology*, vol. 42, pp. 18–24, 2017.
- [127] Z. Cai, J. Liu, H. Bian, and J. Cai, "Astragaloside IV ameliorates necrotizing enterocolitis by attenuating oxidative stress and suppressing inflammation via the vitamin D3-upregulated protein 1/NF- $\kappa$ B signaling pathway," *Experimental and Therapeutic Medicine*, vol. 12, no. 4, pp. 2702–2708, 2016.
- [128] H. Iskender, E. Dokumacioglu, T. M. Sen, I. Ince, Y. Kanbay, and S. Saral, "The effect of hesperidin and quercetin on oxidative stress, NF- $\kappa$ B and SIRT1 levels in a STZ-induced experimental diabetes model," *Biomedicine & Pharmacotherapy*, vol. 90, pp. 500–508, 2017.
- [129] K. A. Kang, S. Chae, Y. S. Koh et al., "Protective effect of puerariae radix on oxidative stress induced by hydrogen peroxide and streptozotocin," *Biological and Pharmaceutical Bulletin*, vol. 28, pp. 1154–1160, 2005.
- [130] R. Li, Y. Chen, M. Shi et al., "Gegen Qinlian decoction alleviates experimental colitis via suppressing TLR4/NF- $\kappa$ B signaling and enhancing antioxidant effect," *Phytomedicine*, vol. 23, no. 10, pp. 1012–1020, 2016.
- [131] C. H. Zhang, G. L. Xu, Y. H. Liu et al., "Anti-diabetic activities of Gegen Qinlian decoction in high-fat diet combined with

- streptozotocin-induced diabetic rats and in 3T3-L1 adipocytes," *Phytomedicine*, vol. 20, no. 3-4, pp. 221–229, 2013.
- [132] Y. M. Li, X. M. Fan, Y. M. Wang, Q. L. Liang, and G. A. Luo, "Therapeutic effects of Gegen Qinlian decoction and its mechanism of action on type 2 diabetic rats," *Acta Pharmaceutica Sinica*, vol. 48, no. 9, p. 1415, 2013.
- [133] V. Tremaroli and F. Backhed, "Functional interactions between the gut microbiota and host metabolism," *Nature*, vol. 489, pp. 242–249, 2012.
- [134] P. J. Turnbaugh, R. E. Ley, M. A. Mahowald, V. Magrini, E. R. Mardis, and J. I. Gordon, "An obesity-associated gut microbiome with increased capacity for energy harvest," *Nature*, vol. 444, pp. 1027–1031, 2006.
- [135] J. Xu, F. Lian, L. Zhao et al., "Structural modulation of gut microbiota during alleviation of type 2 diabetes with a Chinese herbal formula," *ISME Journal*, vol. 9, no. 3, p. 552, 2015.
- [136] L. Zheng and Y. H. Quan, "Experience of treating side effects of antibiotic abuses by professor Quan Yihong's Danggui-liuhuang decoction," *Journal of Hubei University of Chinese Medicine*, vol. 16, pp. 107–109, 2014.
- [137] T. Liu, H. Cao, Y. Ji et al., "Interaction of dendritic cells and T lymphocytes for the therapeutic effect of Danggui-liuhuang decoction to autoimmune diabetes," *Scientific Reports*, vol. 5, 2015.
- [138] S. B. Kim, O. H. Kang, J. H. Keum et al., "Anti-inflammatory effects of Danggui Lihuang decoction in RAW 264.7 cells," *Chinese Journal of Integrative Medicine*, 2012.
- [139] G. Baorong and G. Liangqing, "Clinical observation of Huanglian Wendan Heji (Huanglian Wendan mixture) in treatment of damp-heat type of gerontic diabetes gastroparesis," *World Journal of Traditional Chinese Medicine*, vol. 2, p. 008, 2007.
- [140] L. Liu and Y. Sui, "The effect of Huanglianwendan decoction on insulin resistance and adipocytokines in metabolic syndrome rats," *Liaoning Journal of Traditional Chinese Medicine*, vol. 3, p. 002, 2011.
- [141] Y. B. Li, W. H. Zhang, H. D. Liu, Z. Liu, and S. P. Ma, "Protective effects of Huanglian Wendan decoction against cognitive deficits and neuronal damages in rats with diabetic encephalopathy by inhibiting the release of inflammatory cytokines and repairing insulin signaling pathway in hippocampus," *Chinese Journal of Natural Medicines*, vol. 14, no. 11, pp. 813–822, 2016.

## Research Article

# Protective Effects of *Ophiocordyceps lanpingensis* on Glycerol-Induced Acute Renal Failure in Mice

Yanyan Zhang,<sup>1</sup> Yaxi Du,<sup>2</sup> Hong Yu,<sup>3,4</sup> Yongchun Zhou,<sup>2</sup> and Feng Ge<sup>1,4</sup>

<sup>1</sup>Faculty of Life Science and Technology, Kunming University of Science and Technology, Kunming, Yunnan 650500, China

<sup>2</sup>Tumor Research Institute of Yunnan Province, The Third Affiliated Hospital of Kunming Medical University (Yunnan Tumor Hospital), Kunming, Yunnan 650118, China

<sup>3</sup>School of Life Sciences, Yunnan University, Kunming, Yunnan 650500, China

<sup>4</sup>The Research Center of Cordyceps Development and Utilization of Kunming, Kunming, Yunnan 650100, China

Correspondence should be addressed to Feng Ge; [panaxcordyceps@163.com](mailto:panaxcordyceps@163.com)

Received 15 June 2017; Accepted 9 August 2017; Published 12 October 2017

Academic Editor: Yong Tan

Copyright © 2017 Yanyan Zhang et al. This is an open access article distributed under the Creative Commons Attribution License, which permits unrestricted use, distribution, and reproduction in any medium, provided the original work is properly cited.

**Objective.** Oxidative stress and immune response are associated with acute renal failure (ARF). *Ophiocordyceps lanpingensis* (OL) might be an antioxidant and immunopotentiator. In this study, we explored the protective effects of OL on glycerol-induced ARF. **Methods.** Male mice were randomly divided into four groups, specifically, glycerol-induced ARF model group, low-dose OL-treated group (1.0 g/kg/d), high-dose OL-treated group (2.0 g/kg/d), and control group. Renal conditions were evaluated using kidney index, serum creatinine (Cr), blood urea nitrogen (BUN), and histological analysis. Rhabdomyolysis was monitored using creatine kinase (CK) level. Oxidative stress was determined using kidney tissue glutathione (GSH), malondialdehyde (MDA), and superoxide dismutase (SOD) levels. Immune status was evaluated using immune organ indices and immunoglobulin G (IgG) level. **Results.** OL could relieve renal pathological injury and decrease the abnormal levels of kidney index, serum Cr, CK, BUN, and MDA, as well as increase the immune organ indices and the levels of IgG, GSH, and SOD. Treatment with a high dose of OL had more positive therapeutic effects on ARF than using a low dose of OL. **Conclusion.** OL could ameliorate renal dysfunction in glycerol-induced ARF in mice by inhibiting oxidative stress and enhancing immune response.

## 1. Introduction

Acute renal failure (ARF) is a kind of acute urinary dysfunction of kidneys caused by various reasons in a short term, which usually leads to a serious disorder of the body's internal environment. ARF was characterized by acute elevations of serum creatinine (Cr) and blood urea nitrogen (BUN) in hours to days or weeks [1]. ARF has been widely concerned by the medical profession due to its complex pathogenesis and high mortality. Currently, early treatment of ARF focuses on treating the cause and correcting the imbalance of electrolyte and diuresis. Although these treatments can alleviate ARF to some extent, their therapeutic effect is not stable and durable, thus motivating medical researchers to explore new safe and effective medication.

Medicinal fungus in China is considered as one important category of traditional Chinese herbs. Increasing evidence

indicated that these fungi and their bioactive ingredients had been screened for antitumor, antiviral, antibacterial, and antithrombotic, and had been helping digestion, lowering blood pressure and sugar, relieving cough and asthma, nourishing the lung and kidney, regulating immunity and metabolism, and so on [2–9].

*Ophiocordyceps sinensis* (named *Cordyceps sinensis* before), commonly known as the Chinese caterpillar fungus [10], is the prime example of medicinal fungi, which has been widely used in traditional Chinese medicine for the treatments of renal failure, bronchitis, pneumonia, and asthma [11]. Clinical studies have shown that *O. sinensis* could cure or relieve several kidney diseases, but the mechanisms remained unclear [9–11]. The nephroprotective (acute and chronic) activity of *O. sinensis* may work through modulating the immune system and ameliorating renal functions and renal oxidative stress [12, 13].

Because of excessive collection and use, the wild resource of *O. sinensis* is decreasing rapidly and the large-scale artificial culture of *O. sinensis* is very hard. *Ophiocordyceps lanpingensis* (OL) has been identified as a new species of *Ophiocordyceps* genus, which belongs to the same genus of *O. sinensis* and they are close relatives [14]. *O. lanpingensis* has been used as an efficient herb treating the disease of urinary systems by the local ethnic people for a long time. Our previous study showed that the chemical composition of *O. lanpingensis* was similar to those of *O. sinensis*. Furthermore, *O. lanpingensis* is easy to be cultured artificially. Thus, it has the potential to be the alternative of *O. sinensis*.

In the present study, based on an ARF mouse model, the effects of OL on ARF were observed systematically using biochemical, immunological, and histopathological indicators. This study will contribute to better understand the mechanism of treating ARF by *Ophiocordyceps* medicinal fungi.

## 2. Materials and Methods

**2.1. Animals and Grouping.** Male mice with C57BL/6 background (6- to 8-week old; 20–25 g body weight) were obtained from Liaoning Changsheng Biotechnology Co. Ltd, China. The mice were maintained in a pathogen-free mouse facility; and clean food and water were supplied with free access. All experiments were performed according to the guidelines for the care of laboratory animals and were proved by the Ethics Committee Guide of Kunming University of Science and Technology.

**2.2. Drugs.** *Ophiocordyceps lanpingensis* (OL) powder was provided by Yunnan Yunbaicao Biotechnology Co. Ltd. which was suspended in 0.25% carboxymethyl cellulose sodium (CMC).

**2.3. Administration.** Mice were randomly divided into four groups, each comprising of 10 animals. The animals were allowed free access to food but deprived of drinking water for 24 hours before glycerol injection. Group 1 serves as normal control group. The animals were treated with saline (10.0 mL/kg/d, intragastric [i.g.]) for 7 days, deprived of drinking water for 24 hours on the sixth day, then were given saline (10.0 mL/kg intramuscular [i.m.]), divided equally among the hind legs. Group 2 is ARF model group. The animals were treated with saline (10.0 mL/kg/d, i.g.) for 7 days, deprived of drinking water for 24 hours on the sixth day, then were given 50% glycerol (10.0 mL/kg, i.m.), divided equally among the hind legs. Group 3 is low-dose OL-treated group. The animals were treated with OL (1.0 g/kg/d, i.g.) for 7 days, deprived of drinking water for 24 hours on the sixth day, then were given 50% glycerol (10.0 mL/kg, i.m.), divided equally among the hind legs. Group 4 is high-dose OL-treated group. The animals were treated with OL (2.0 g/kg/d, i.g.) for 7 days, deprived of drinking water for 24 hours on the sixth day, then were given 50% glycerol (10.0 mL/kg, i.m.), divided equally among the hind legs. The animals were allowed free access to food and water after the glycerol injection for 24 hours [15]. At the end of the treatment, animals were euthanized by CO<sub>2</sub>. The blood was obtained and

centrifuged (4000 ×g for 10 min at 4°C) to get serum which was then stored at –80°C until assay. The kidneys, thymus, and spleen were harvested and weighed. The left kidney was frozen at –80°C for subsequent evaluation, while the right kidney was fixed in 4% paraformaldehyde solution for histological sectioning.

**2.4. Renal Coefficient and Immune Organ Indices.** The weight of the mice was measured before death. Renal tissues, thymus tissue, and spleen tissue were collected from mice, washed by normal saline solution (0.9%), and then blotted them with paper. Renal index, thymus index, and spleen index were used to help evaluate renal and immune status.

$$\begin{aligned} \text{Renal index (mg/g)} &= \frac{\text{Renal weight}}{\text{Mice weight}}, \\ \text{Thymus index (mg/g)} &= \frac{\text{Thymus weight}}{\text{Mice weight}}, \\ \text{Spleen index (mg/g)} &= \frac{\text{Spleen weight}}{\text{Mice weight}}. \end{aligned} \quad (1)$$

**2.5. Serum Biochemical Analysis.** The level of serum IgG was detected using immunoglobulin G assay kit (Nanjing Jiancheng Bioengineering Institute, China) in the form of immunoturbidimetric assay. Serum biochemical parameters of BUN and serum Cr levels were measured using urea assay kit (Nanjing Jiancheng Bioengineering Institute, China) and creatinine assay kit (Nanjing Jiancheng Bioengineering Institute, China) in the form of urease method and picric acid colorimetric method, respectively. The activity of serum CK was detected using creatine kinase assay kit (Nanjing Jiancheng Bioengineering Institute, China) in the form of a colorimetric method.

**2.6. Antioxidant Indices.** Kidneys were homogenized in iced saline (0.9% sodium chloride). The homogenates were centrifuged at 800 ×g for 5 minutes at 4°C to separate the nuclear debris. The supernatant obtained was centrifuged at 10,500 ×g for 20 minutes at 4°C to get the postmitochondrial supernatant which was used to assay glutathione (GSH), malondialdehyde (MDA), and superoxide dismutase (SOD) levels. SOD activity was assayed in the form of hydroxylamine method by using SOD assay kit (Nanjing Jiancheng Bioengineering Institute, China), while GSH and MDA levels were assayed in the form of microplate test and thiobarbituric acid (TBA) method by using GSH assay kit (Nanjing Jiancheng Bioengineering Institute, China) and MDA assay kit (Nanjing Jiancheng Bioengineering Institute, China), respectively.

**2.7. Renal Histopathology.** Kidney tissues were embedded in paraffin and used for histopathological examination. Four-micrometer-thick sections were cut, deparaffinized, and hydrated. For light microscopic purpose, paraffin sections were stained with hematoxylin and eosin (H&E). The intact glomeruli, hemorrhage, capillary congestion, and vacuolization of the medullary tubular cells were evaluated.

**2.8. Statistical Analysis.** The results were reported as the mean ± SEM. All of the data were compared by one-way



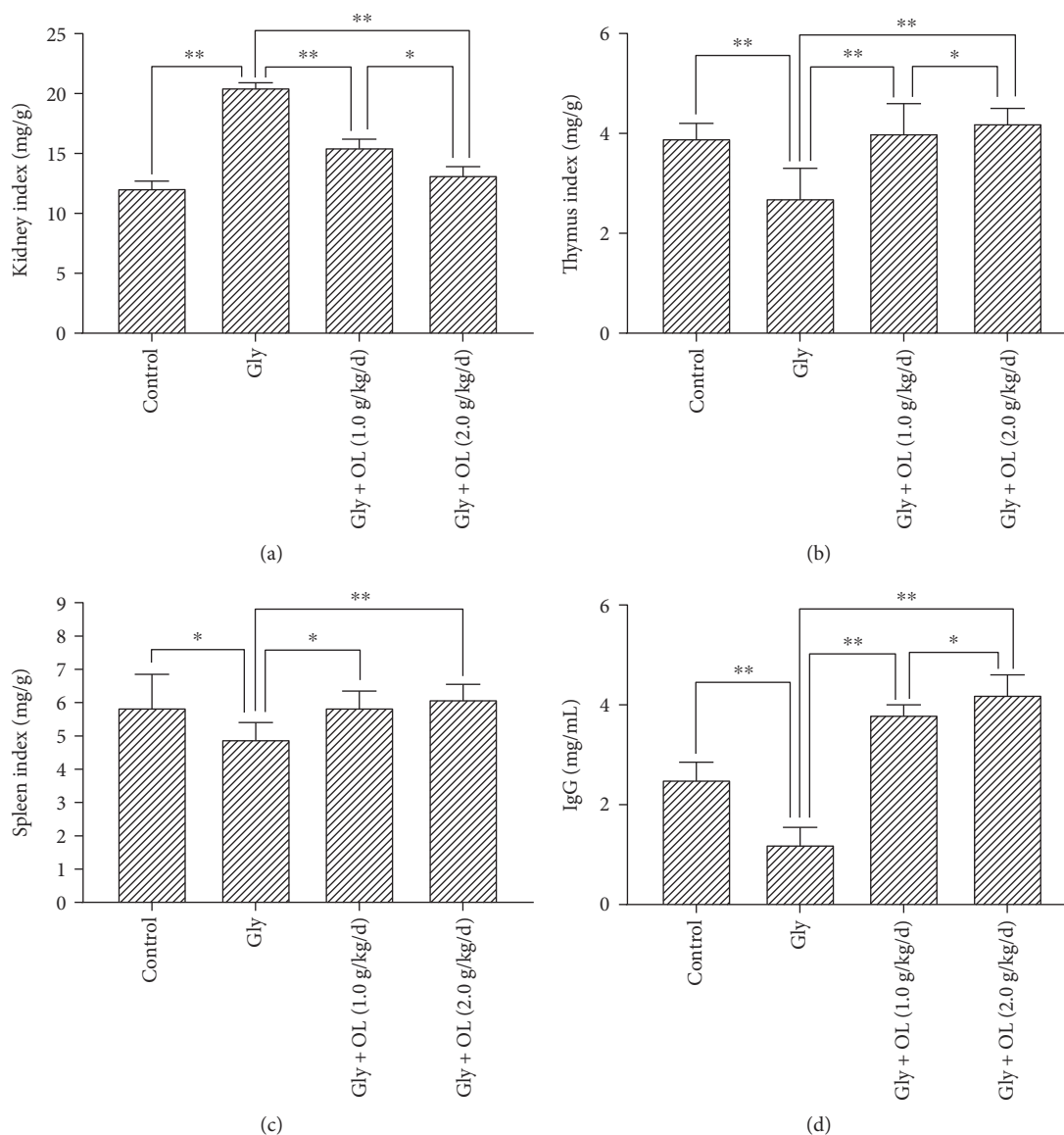


FIGURE 1: Kidney index, thymus index, spleen index, and serum IgG level. (a) The changes of kidney index in different groups. (b) The changes of thymus index in different groups. (c) The changes of spleen index in different groups. (d) The changes of serum IgG content in different groups. Notes: the statistical significance between the OL-treated groups, normal control group, and acute renal failure (ARF) model group was determined using Tukey's test. \* $P < 0.05$  and \*\* $P < 0.01$ . Gly: ARF induced by glycerol; OL: *Ophiocordyceps lanpingensis*; IgG: immunoglobulin G.

analysis of variance test (ANOVA) while Tukey's multiple comparison test was used to detect significance between all groups. For analysis, a  $P < 0.05$  was considered statistical significance. Statistical analysis was performed using SPSS® v.17.0 software.

### 3. Results

**3.1. Evaluation of a Mouse Model of ARF.** Comparing with the control group, ARF caused by glycerol injection in mice resulted in significant changes in immune organs and IgG. There were statistically significant decreases in thymus index ( $P < 0.01$ ), spleen index ( $P < 0.05$ ), and serum IgG ( $P < 0.01$ ) (Gly group in Figures 1(b), 1(c), and 1(d)). Levels of renal

GSH ( $P < 0.01$ ) and SOD ( $P < 0.01$ ) were also significantly reduced (Gly group in Figures 2(d) and 3(a)); meanwhile, the kidney index ( $P < 0.01$ ), levels of serum Cr ( $P < 0.01$ ), serum CK ( $P < 0.01$ ), BUN ( $P < 0.01$ ), and renal MDA ( $P < 0.01$ ) were enhanced much more (Gly group in Figures 1(a), 2(a), 2(b), 2(c), and 3(b)). Such results indicated that ARF induced severe failure in kidney functions and oxidative stress which suggested that the animal model of ARF was gotten definitely and efficiently.

**3.2. OL Improved Immunity of Mice in Glycerol-Induced ARF.** Intragastric administration of OL for 7 days in both doses of 1.0 g/kg/d and 2.0 g/kg/d resulted in significant improvement in immunity compared with ARF model group. A statistically

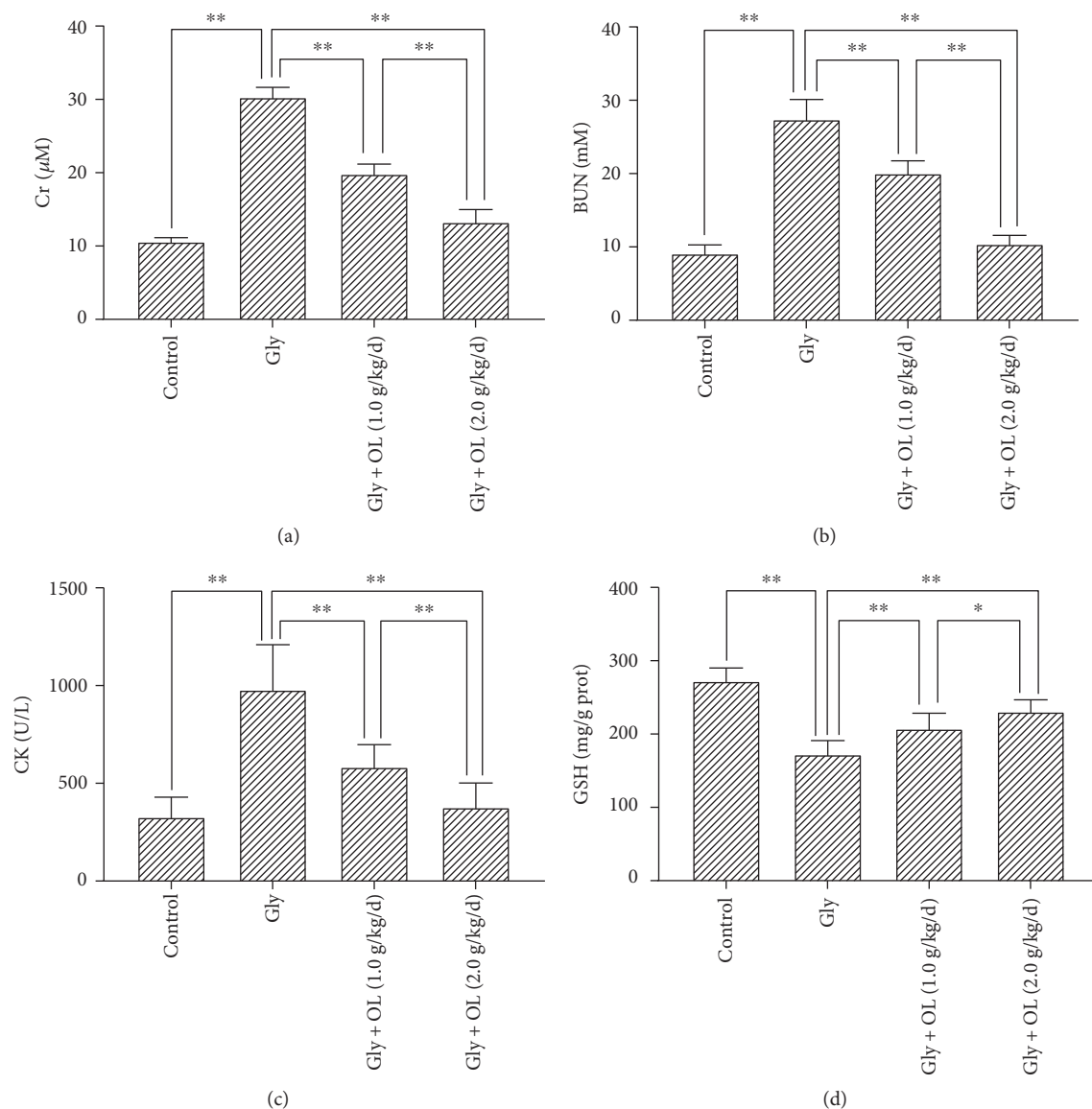


FIGURE 2: Serum Cr and BUN levels, serum CK activity and kidney tissue GSH level. (a) The effect of OL on glycerol-induced changes in serum Cr. (b) The effect of OL on glycerol-induced changes in BUN. (c) The effect of OL on glycerol-induced changes in serum CK. (d) The effect of OL on glycerol-induced changes in kidney tissue GSH. Notes: the statistical significance between the treated groups, normal control group, and acute renal failure (ARF) model group was determined using Tukey's test. \* $P < 0.05$  and \*\* $P < 0.01$ . OL: *Ophiocordyceps lanpingensis*; Gly: ARF induced by glycerol; Cr: creatinine; BUN: blood urea nitrogen; CK: creatine kinase; GSH: glutathione.

significant increase in thymus index ( $P < 0.01$ ), spleen index ( $P < 0.05$ ), and serum IgG level ( $P < 0.01$ ) were shown in Figures 1(b), 1(c), and 1(d). More efficient enhancement of related immunity parameters was observed in the group which received OL in a dose of 2.0 g/kg/d (Figures 1(b) and 1(d)). Such results indicated that the effects of OL in AFR may depend on the dose.

**3.3. OL Prevented Damage of Kidney Functions and Improved Oxidative Stress of Kidney in Glycerol-Induced ARF.** The serum Cr and BUN were analyzed in this study, which were two important biomarkers of renal function. In addition, chemical- or ischemia-induced renal failure is generally associated with a remarkable increase of MDA level and

decreases of GSH and SOD levels. Rhabdomyolysis was monitored by creatine kinase (CK) level, which was a representative symptom caused by glycerol. Treatments of OL in both doses of 1.0 g/kg/d and 2.0 g/kg/d showed significant improvements in kidney functions and oxidative stress compared with ARF model group. There were significant decreases in kidney index ( $P < 0.01$ ), serum Cr ( $P < 0.01$ ), serum CK ( $P < 0.01$ ), BUN ( $P < 0.01$ ), and renal MDA ( $P < 0.01$ ) (Figures 1(a), 2(a), 2(b), 2(c), and 3(b)), whereas enhancements in renal GSH ( $P < 0.01$ ) and SOD ( $P < 0.01$ ) were observed (Figures 2(d) and 3(a)). More prominent improvements in kidney functions and oxidative stress were shown in a dose of 2.0 g/kg/d OL group (Figures 1(a), 2(a), 2(b), 2(c), 2(d), and 3(a)).

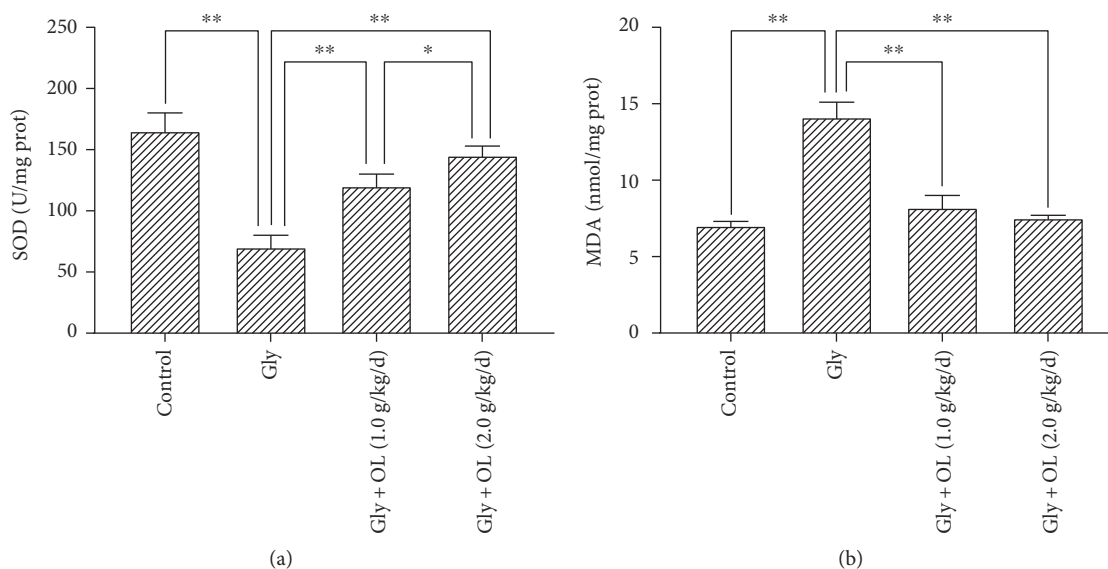


FIGURE 3: Kidney tissue SOD activity and MDA level. (a) The effect of OL on glycerol-induced changes in kidney tissue SOD. (b) The effect of OL on glycerol-induced changes in kidney tissue MDA. Notes: the statistical significance between the treated groups, normal control group, and acute renal failure (ARF) model group was determined using *Tukey's test*. \* $P < 0.05$  and \*\* $P < 0.01$ . OL: *Ophiocordyceps lanpingensis*; Gly: ARF induced by glycerol; SOD: superoxide dismutase; MDA: malondialdehyde.

**3.4. OL Administration Caused Regression of Renal Histopathological Changes.** The horizontal section of mouse kidney had no obvious pathological changes, showing normal structure of kidney tissue and integrality of cells in tubule epithelium in normal control group (Figure 4(a)). In ARF model group, many necrotic tubules with casts, tubular dilation, and vacuolation were seen (Figure 4(b)). Intra-gastric administration of OL in different doses resulted in significant regression of renal histopathological changes compared with ARF model group, especially when received OL in a dose of 2.0 g/kg/d (Figures 4(c) and 4(d)).

## 4. Discussion

ARF is a common clinical emergency with abrupt loss of kidney function, which may lead to a number of complications and even death. Studies have demonstrated that the pathogenesis of ARF was associated with the oxidative stress and a host of inflammatory mediators and cell-mediated immune responses [15–20]. A glycerol-induced mouse model can simulate ARF which is characterized by a significant increase of Cr, CK, and BUN in serum. CK is the most sensitive damage index for muscle cell damage and marks the occurrence of rhabdomyolysis [15]. In the animal model, significant structural changes of kidney including tubular dilatation, vacuolation, necrosis, and cellular debris could be observed [21–23].

The conventional treatments about ARF include the underlying causes and supportive care; furthermore, treatment with Chinese medicine has been applied widely in clinic. In recent years, herbs and their effective components are considered as promising therapeutic options for ARF and many studies indicated the potential role of them in reducing renal dysfunction after ARF [24–27].

As a famous traditional Chinese herb, the beneficial effects of *O. sinensis* or its water-soluble polysaccharide on various renal diseases have been proven [28]. So far, with the extreme lack of the natural resource of *O. sinensis*, the substitution of *O. sinensis* needs to be studied. *O. lanpingensis* (OL), a Chinese herb similar with *O. sinensis* which could protect against ARF, has been proven to contain bioactive constituents that may have pharmacological effects such as antioxidant, anti-inflammatory, and immune activation. In this study, we explored the protective effects of OL on glycerol-induced ARF in mice and firstly found that OL could enhance immunity, protect kidney functions, and relieve oxidative stress as well as renal pathological damage.

The possible explanation for the benefits in renal function recovery following administration of OL may be due to its role in increasing immunity as well as reducing oxidative stress. Oxidative stress is closely related to human health and plays an important role in the pathogenesis of glycerol-induced ARF. Normally, the production and elimination of oxygen free radicals in the human body are balanced. But when the body's antioxidant system is disordered, excessive oxygen free radicals will be produced; thus, the oxygen free radical metabolism in the body will be imbalanced, leading to cell damage and then even cause heart disease, cancer, or other serious problems [29, 30]. During physiological activities, the body produces reactive oxygen species (ROS) continuously. The biological activity of ROS is very strong, which plays a positive role in cell division, growth, anti-inflammation, and so on. Nevertheless, ROS is the most significant contributing factor to oxidative stress in complex systems and excessive ROS may cause cell aging, body damage, inflammation, immune disorders, and other diseases.

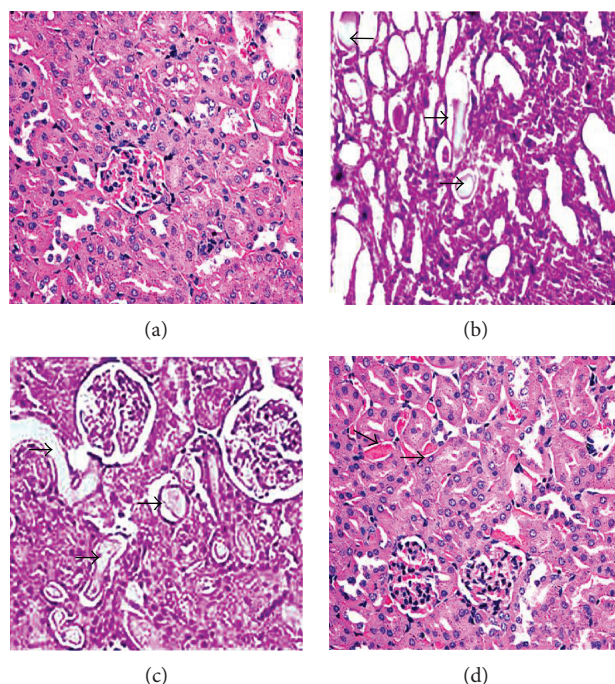


FIGURE 4: Hematoxylin and eosin results in mice's kidney tissues (magnification  $\times 400$ ). (a) Normal control group. (b) ARF model group. (c) 1.0 g/kg/d OL-treated group. (d) 2.0 g/kg/d OL-treated group. Notes: (a) normal architecture of kidney in the normal healthy group. (b) Many necrotic cortical tubules with casts (arrowheads), tubular dilation, and vacuolation were seen. (c) Severe necrotic tubules with some casts (arrowheads) were present. (d) Occasional necrotic tubules with casts (arrowheads) were seen. OL: *Ophiocordyceps lanpingensis*; ARF: acute renal failure.

In order to evaluate the antioxidant capacity of the body, the activity of SOD and the contents of renal GSH and MDA in the mice were measured in this study. SOD is one of the main free radical scavengers in the body, which plays an important role in the oxidation and antioxidation balance in the organism. SOD can remove excessive free radicals and reduce the negative effects of free radicals on biofilm and other tissues; meanwhile, GSH is another important free radical scavenger with strong protective effects [31–36]. High or low content of MDA in the tissues indirectly reflects the severity of the cells attacked by free radicals. The current study indicated that oral administration of OL caused significant increases in renal SOD and GSH while decreasing the renal MDA to normal condition compared with their levels in ARF model group. Moreover, the group received OL in a dose of 2.0 g/kg/d representing remarkable effects in all physiological parameters which were closed to those of normal group. The effects of renoprotection were dose dependent.

SOD and MDA are important in tissues and organs for their functions in the body's oxidative stress and immune protection. Correspondingly, the immune response of body can ameliorate oxidative stress and inflammation [37, 38]. Besides oxidative stress, another factor that plays a role in the pathogenesis of nephrotoxicity is the process of immunity. The occurrence of body damage is accompanied by an inflammatory response which regulates multiple physiological metabolisms. Such effects depend on the concentrations of cytokines, chemokines, and other inflammatory molecules. Very low levels of inflammatory molecules are enough

to induce immune responses. IgG is one of the critical substances in the immune system of the body, which is synthesized and secreted by plasma cells in spleen and lymph nodes. IgG plays an important role in the immune and physiological adjustment [39, 40]. As the main antibody composition in the serum, IgG is widely distributed in tissues, which possesses anti-infection function. The content of IgG is a crucial detection index of humoral immunity while the immune organ index is an important and intuitive parameter to reflect the immune status as well [17–19].

To explore the effects of immune role of OL in the present study, thymus index, spleen index, and IgG concentration were examined. The results showed that OL could significantly increase thymus index, spleen index, and the level of serum IgG in mice compared with those in the ARF model. When using the dose of 2.0 g/kg/d OL, the thymus and spleen indices in ARF mice were almost recovered to normal (control group), suggesting that the destroyed immune system might be established again.

## 5. Conclusion

In conclusion, this study showed that OL could relieve the renal injury caused by glycerol. OL ameliorated renal dysfunction of ARF by inhibiting oxidative stress and improving the body's immunity. In future studies, we will explore the definite bioactive components in OL and reveal the correlation between biological effects and these components, thus to provide strong evidence for application of OL.

## Conflicts of Interest

The authors declare that there is no conflict of interests regarding the publication of this paper.

## Authors' Contributions

Yanyan Zhang and Yaxi Du are co-first authors.

## Acknowledgments

This work was supported by Yunnan Yunbaicao Biotechnology Co. Ltd.

## References

- [1] A. R. Nissenson, "Acute renal failure: definition and pathogenesis," *Kidney International Supplements*, vol. 66, pp. S7–10, 1998.
- [2] Y. Y. Zhao, H. T. Li, Y. L. Feng, X. Bai, and R. C. Lin, "Urinary metabolomic study of the surface layer of *Poria cocos* as an effective treatment for chronic renal injury in rats," *Journal of Ethnopharmacology*, vol. 148, no. 2, pp. 403–410, 2013.
- [3] B. Joob and V. Wiwanitkit, "Linzhi (*Ganoderma lucidum*); evidence of its clinical usefulness in renal diseases," *Journal of Nephro pharmacology*, vol. 5, no. 1, pp. 9–10, 2015.
- [4] D. Zhong, H. Wang, M. Liu et al., "*Ganoderma lucidum* polysaccharide peptide prevents renal ischemia reperfusion injury via counteracting oxidative stress," *Scientific Reports*, vol. 5, no. 1, article 16910, 2015.
- [5] Y. Y. Zhao, Y. L. Feng, X. Bai, X. J. Tan, R. C. Lin, and Q. Mei, "Ultra performance liquid chromatography-based metabolomic study of therapeutic effect of the surface layer of *Poria cocos* on adenine-induced chronic kidney disease provides new insight into anti-fibrosis mechanism," *PLoS One*, vol. 8, no. 3, article e59617, 2013.
- [6] S. H. Yu, N. K. Dubey, W. S. Li et al., "*Cordyceps militaris* treatment preserves renal function in type 2 diabetic nephropathy mice," *PLoS One*, vol. 11, no. 11, article e0166342, 2016.
- [7] J. Song, Y. Wang, C. Liu et al., "*Cordyceps militaris* fruit body extract ameliorates membranous glomerulonephritis by attenuating oxidative stress and renal inflammation via the NF- $\kappa$ B pathway," *Food and Function*, vol. 7, no. 4, pp. 2006–2015, 2016.
- [8] F. Du, S. Li, T. Wang et al., "*Cordyceps sinensis* attenuates renal fibrosis and suppresses BAG3 induction in obstructed rat kidney," *American Journal of Translational Research*, vol. 7, no. 5, pp. 932–940, 2015.
- [9] C. H. Chiu, C. C. Chyau, C. C. Chen, C. H. Lin, C. H. Cheng, and M. C. Mong, "Polysaccharide extract of *Cordyceps sobolifera* attenuates renal injury in endotoxemic rats," *Food and Chemical Toxicology*, vol. 69, pp. 281–288, 2014.
- [10] G. H. Sung, N. L. Hywel-Jones, J. M. Sung, J. J. Luangsa-Ard, B. Shrestha, and J. W. Spatafora, "Phylogenetic classification of *Cordyceps* and the clavicipitaceous fungi," *Studies in Mycology*, vol. 57, no. 1, pp. 5–59, 2007.
- [11] J. S. Zhu, G. M. Halpern, and K. Jones, "The scientific rediscovery of an ancient Chinese herbal medicine: *Cordyceps sinensis*: part I," *Journal of Alternative and Complementary Medicine*, vol. 4, no. 3, pp. 289–303, 1998.
- [12] K. F. Hua, H. Y. Hsu, L. K. Chao et al., "Ganoderma lucidum polysaccharides enhance CD14 endocytosis of LPS and promote TLR4 signal transduction of cytokine expression," *Journal of Cellular Physiology*, vol. 212, no. 2, pp. 537–550, 2007.
- [13] J. Lin, Y. J. Chang, W. B. Yang, L. Y. Alice, and C. H. Wong, "The multifaceted effects of polysaccharides isolated from *Dendrobium huoshanense* on immune functions with the induction of interleukin-1 receptor antagonist (IL-1 ra) in monocytes," *PLoS One*, vol. 9, no. 4, article e94040, 2014.
- [14] Z. H. Chen, Y. D. Dai, H. Yu et al., "Systematic analyses of *Ophiocordyceps lanpingensis* sp. nov., a new species of *Ophiocordyceps* in China," *Microbiological Research*, vol. 168, no. 8, pp. 525–532, 2013.
- [15] E. Homsí, P. Janino, and J. B. Faria, "Role of caspases on cell death, inflammation, and cell cycle in glycerol-induced acute renal failure," *Kidney International*, vol. 69, no. 8, pp. 1385–1392, 2006.
- [16] N. Bank and H. S. Aynedjian, "Role of thromboxane in impaired renal vasodilatation response to acetylcholine in hypercholesterolemic rats," *Journal of Clinical Investigation*, vol. 89, no. 5, pp. 1636–1642, 1992.
- [17] A. Unis, "Açai berry extract attenuates glycerol-induced acute renal failure in rats," *Renal Failure*, vol. 37, no. 2, pp. 310–317, 2014.
- [18] A. P. Singh, A. Muthuraman, A. S. Jaggi et al., "Animal models of acute renal failure," *Pharmacological Reports*, vol. 64, no. 1, pp. 31–44, 2012.
- [19] A. K. A. Asmari, K. T. A. Sadoon, A. A. Obaid, D. Yesunayagam, and M. Tariq, "Protective effect of quinine against glycerol-induced acute kidney injury in rats," *BMC Nephrology*, vol. 18, no. 41, pp. 2–10, 2017.
- [20] K. Nishida, H. Watanabe, S. Ogaki et al., "Renoprotective effect of long acting thioredoxin by modulating oxidative stress and macrophage migration inhibitory factor against rhabdomyolysis-associated acute kidney injury," *Scientific Reports*, vol. 5, no. 1, pp. 14471–14485, 2015.
- [21] H. X. Gu, M. Yang, X. M. Zhao, B. Zhao, X. Sun, and X. Gao, "Pretreatment with hydrogen-rich saline reduces the damage caused by glycerol-induced rhabdomyolysis and acute kidney injury in rats," *Journal of Surgical Research*, vol. 188, no. 1, pp. 243–249, 2014.
- [22] F. Liano, E. Junco, and J. Pascual, "The spectrum of acute renal failure in the intensive care unit compared with that seen in other setting," *Kidney International Supplements*, vol. 66, pp. 16–24, 1998.
- [23] J. S. Cardinal, J. H. Zhan, Y. N. Wang et al., "Oral hydrogen water prevents chronic allograft nephropathy in rats," *Kidney International*, vol. 77, no. 2, pp. 101–109, 2010.
- [24] S. Ustundag, S. Sen, O. Yalcin, S. Ciftci, B. Demirkan, and M. Ture, "L-Carnitine ameliorates glycerol-induced myoglobinuric acute renal failure in rats," *Renal Failure*, vol. 31, no. 2, pp. 124–133, 2009.
- [25] C. J. Bowmer, M. G. Collis, and M. S. Yates, "Effect of the adenosine antagonist 8-phenyltheophylline on glycerol-induced acute renal failure in the rats," *British Journal of Pharmacology*, vol. 88, no. 1, pp. 205–212, 1986.
- [26] J. Zhou, H. A. Zhang, Y. Lin et al., "Protective effect of ginsenoside against acute renal failure via reduction of renal oxidative stress and enhanced expression of ChAT in the proximal convoluted tubule and ERK1/2 in the paraventricular nuclei," *Physiology Research*, vol. 63, no. 5, pp. 597–604, 2014.

- [27] Y. K. Lee, Y. W. Chin, and Y. H. Choi, "Effects of Korean red ginseng extract on acute renal failure induced by gentamicin and pharmacokinetic changes by metformin in rats," *Food and Chemical Toxicology*, vol. 59, pp. 153–159, 2013.
- [28] X. Jin, H. Ying, X. X. Chen, S.-C. Zheng, P. Chen, and M.-H. Mo, "The mechanisms of pharmacological activities of *Ophiocordyceps sinensis* fungi," *Phytotherapy Research*, vol. 30, no. 10, pp. 1572–1583, 2016.
- [29] D. G. Kang, H. Oh, E. J. Sohn et al., "Lithospermic acid B isolated from *Salvia miltiorrhiza* ameliorates ischemia/reperfusion-induced renal injury in rats," *Life Science*, vol. 75, no. 15, pp. 1801–1816, 2004.
- [30] K. W. K. Chan and W. S. Ho, "Anti-oxidative and hepatoprotective effects of lithospermic acid against carbon tetrachloride-induced liver oxidative damage in vitro and in vivo," *Oncology Reports*, vol. 34, no. 2, pp. 673–680, 2015.
- [31] L. F. Jia, Y. Yang, Q. Y. Li et al., "Antioxidant effect of glycoprotein from *Taraxacum mongolicum* in vitro and in vivo," *Acta Botanica Boreali-Occidentalia Sinica*, vol. 32, no. 12, pp. 2486–2491, 2012.
- [32] W. S. Yoon, Y. S. Chae, J. Hong, and Y. K. Park, "Antitumor therapeutic effects of a genetically engineered *Salmonella typhimurium* harboring TNF- $\alpha$  in mice," *Applied Microbiology and Biotechnology*, vol. 89, no. 6, pp. 1807–1819, 2011.
- [33] J. C. Zhong, Y. Zhang, Z. T. Ding, and Y. Ke, "Effect of polysaccharide extract from artificial *Cordyceps sinensis* on immune function of mouse," *Acta Scientiarum Naturalium Universitatis Sunyatseni*, vol. 50, no. 6, pp. 99–102, 2011.
- [34] F. Wang, C. J. Zhang, and L. Wang, "Empirical study progress about immune modulatory effect of extractive of artificial cultured *Cordyceps sinensis*," *Medical Recapitulate*, vol. 14, no. 6, pp. 933–993, 2008.
- [35] R. Manikandan, M. Beulaja, R. Thiagaraja et al., "Ameliorative effect of ferulic acid against renal injuries mediated by nuclear factor-kappaB during glycerol-induced nephrotoxicity in Wistar rats," *Renal Failure*, vol. 36, no. 2, pp. 154–165, 2004.
- [36] P. Vlahovic, T. Cvetkovic, V. Savic, and V. Stefanović, "Dietary curcumin does not protect kidney in glycerol induced acute failure," *Food and Chemical Toxicology*, vol. 45, no. 9, pp. 1777–1782, 2007.
- [37] T. Inoue, "M1 macrophage triggered by Mincle leads to a deterioration of acute kidney injury," *Kidney International*, vol. 91, no. 3, pp. 526–529, 2017.
- [38] L. L. Lv, P. M. Tang, C. J. Li et al., "The pattern recognition receptor, Mincle, is essential for maintaining the M1 macrophage phenotype in acute renal inflammation," *Kidney International*, vol. 91, no. 3, pp. 587–602, 2017.
- [39] J. C. Ciccirelli, N. A. Lemp, Y. Chang et al., "Renal transplant patients biopsied for cause and tested for C4d, DSA, and IgG subclasses and C1q: which humoral markers improve diagnosis and outcomes?," *Journal of Immunology Research*, vol. 2017, Article ID 1652931, 2017.
- [40] O. Kurtenkov and K. Klaamas, "Hidden IgG antibodies to the tumor-associated Thomsen-Friedenreich antigen in gastric cancer patients: lectin reactivity, avidity, and clinical relevance," *BioMed Research International*, vol. 2017, Article ID 6097647, 11 pages, 2017.

## Review Article

# Traditional Chinese Medicine Protects against Cytokine Production as the Potential Immunosuppressive Agents in Atherosclerosis

Yan Ren,<sup>1</sup> Wei Qiao,<sup>1</sup> Dongliang Fu,<sup>1</sup> Zhiwei Han,<sup>1</sup> Wei Liu,<sup>2</sup> Weijie Ye,<sup>2</sup> and Zunjing Liu<sup>2</sup>

<sup>1</sup>Department of Cardiology, China-Japan Friendship Hospital, Beijing 100029, China

<sup>2</sup>Department of Neurology, China-Japan Friendship Hospital, Beijing 100029, China

Correspondence should be addressed to Zunjing Liu; [liuzunjing@163.com](mailto:liuzunjing@163.com)

Received 20 April 2017; Accepted 10 July 2017; Published 6 September 2017

Academic Editor: Yong Tan

Copyright © 2017 Yan Ren et al. This is an open access article distributed under the Creative Commons Attribution License, which permits unrestricted use, distribution, and reproduction in any medium, provided the original work is properly cited.

Atherosclerosis is a chronic inflammatory disease caused by dyslipidemia and mediated by both innate and adaptive immune responses. Inflammation is a critical factor at all stages of atherosclerosis progression. Proinflammatory cytokines accelerate atherosclerosis progression, while anti-inflammatory cytokines ameliorate the disease. Accordingly, strategies to inhibit immune activation and impede immune responses towards anti-inflammatory activity are an alternative therapeutic strategy to conventional chemotherapy on cardiocerebrovascular outcomes. Since a number of Chinese medicinal plants have been used traditionally to prevent and treat atherosclerosis, it is reasonable to assume that the plants used for such disease may suppress the immune responses and the resultant inflammation. This review focuses on plants that have immunomodulatory effects on the production of inflammatory cytokine burst and are used in Chinese traditional medicine for the prevention and therapy of atherosclerosis.

## 1. Introduction

Atherosclerosis (AS), a chronic inflammatory disease characterized by dyslipidemia, is the most common type of cardiocerebrovascular disease and the leading cause of morbidity and mortality in the world nowadays [1, 2]. The characterization of atherosclerosis as an immune-mediated aberrance is based on evidence of immune activation and inflammatory signaling in human atherosclerotic lesions [3], the significance of inflammatory biomarkers as independent risk factors for cardiocerebrovascular events [4], as well as the ability of LDL particles and their contents to activate innate and adaptive immunity [5, 6]. Thus, strategies to inhibit immune activation and impede immune responses towards anti-inflammatory activity are an alternative therapeutic strategy to conventional chemotherapy on cardiocerebrovascular outcomes. In accordance with ancient Chinese pharmacopoeias, a large amount of medicinal plants has shown inhibitory potentials in immune responses and some of them have been used traditionally to

prevent and treat atherosclerosis. This is partly due to their safety and lower side effects and, in some ways, their more effectiveness. As inflammation is a critical factor at all stages of atherosclerosis progression, from attracting immune cells and atherosclerotic plaque formation to its rupture, cytokines are major mediators in all kinds of inflammation [7, 8]. In this review, we focus on plants that are used in traditional Chinese medicine (TCM) and have been reported to act as immunomodulatory agents of suppressive function on cytokine production in atherogenesis.

## 2. Role of Inflammatory Cytokines in the Pathogenesis of Atherosclerosis

The concept of atherosclerosis as an inflammatory disease is based on the evidence that inflammatory cells are abundant in atherosclerotic lesions, which are the major source of cytokine that was involved in all stages of atherosclerosis and have a profound impact on the pathogenesis of this disease [9]. Cytokines are protein mediators produced by

monocytes, macrophages, T cells, and platelets, as well as by ECs, smooth muscle cells (SMCs), and adipocytes, in answering to inflammation and other stimuli [10, 11].

Recently, emphasis has been placed on the role of cytokines and the way they act on a variety of objects exerting multiple effects and are largely responsible for the crosstalk among endothelial, smooth muscle cells, leukocytes, and other vascular residing cells having a potentially causative role in atherosclerosis. For example, cytokine-induced activation of ECs can induce endothelium dysfunction accompanied by upregulation of adhesion molecules and chemokines, such as intercellular adhesion molecule-1 (ICAM-1), vascular cell adhesion molecule-1 (VCAM-1), and monocyte chemoattractant protein-1 (MCP-1), which promotes migration of immune cells (monocytes, neutrophils, and lymphocytes) into the atherosclerosis lesion [12, 13]. Moreover, cytokines impress the function of SMCs by promoting their growth, proliferation, and migration. Studies by Cushing et al. demonstrated that minimally ox-LDLs, but not native LDLs, give rise to MCP-1 production in vascular wall cells such as endothelial cells and smooth muscle cells and MCP-1 functions in the recruitment of monocytes to atheroma [14]. Finally, at later stages of atherosclerosis, proinflammatory cytokines accelerate destabilization of atherosclerotic plaques, apoptosis of various cells, and matrix degradation, thereby accelerating plaque breakage and thrombus formation. For instance, TNF- $\alpha$  and IL-1 $\beta$  accelerate apoptosis of macrophages together with foam cells leading to the enlargement of the lipid core [15, 16]. Such cytokines also irritate apoptosis of SMCs leading to thinning of the fibrous cap. Further remodeling of the extracellular matrix (ECM) is controlled by a series of proteases, particularly matrix metalloproteinases (MMPs), and their inhibitors (tissue inhibitor of metalloproteinases (TIMPs)) produced by macrophages and other vascular cells [17]. The expression and/or activities of MMPs and TIMPs are adjusted by cytokines [18]. Vulnerable plaques have very few SMCs and high macrophage substance and are susceptible to rupture leading to thrombosis in the end [19]. What is more, key components involved in thrombosis are also the target of regulation by cytokines [20].

To date, atherosclerosis cannot be reversed by medical treatment, warranting the need for better understanding of this pathology in order to develop new strategies to struggle this deadly disease. Targeted intervention strategies on reducing proinflammatory cytokine expression may be of great help to improve current cardiovascular outcomes.

### 3. Immunosuppressive Role of Chinese Medicinal Plants on Inflammatory Cytokines Expression in Atherogenesis

Experimental endeavors to control atherosclerosis have included both wide-spectrum anti-inflammatory and immunomodulatory approaches, as well as specific targeting of mechanisms [21, 22]. Given traditional Chinese medicine is deeply rooted in the history and has been widely used to prevent and treat cardiocerebrovascular disease; it is

reasonable to assume that these plants used for such diseases may refrain the immune responses and the resultant inflammation. Furthermore, trying to describe the potential clinical predictive value of some TCMs on proinflammatory cytokine expression in the progression and complications of atherosclerosis may be of great help not only in understanding TCMs but also in determining the potential of cytokine-based therapies. In consideration of the variety of cells that participate in atherogenesis, the large number of cytokines that is expressed by each of them and the pleiotropic activity of each cytokine; it is almost impossible to describe minutely all interactions taking place during atherogenesis [23]. Herein, ICAM-1, VCAM-1, MCP-1, TNF- $\alpha$ , IL-1 $\beta$ , and MMPs-9, which participate in initial and later stages of atherosclerosis [24], will be more elaborately discussed.

*3.1. Intercellular Adhesion Molecule (ICAM-1) and Vascular Cell Adhesion Molecule (VCAM-1).* Inflammatory stimuli result in the upregulation of adhesion molecules, which is a critical feature in early atherosclerosis. ICAM-1 and VCAM-1 are the main adhesion molecules which are important for the firm adhesion of leukocytes to the endothelium. These adhesion molecules in turn enable the adhesion of mononuclear leukocytes to endothelial cells and also their transmigration into the intima, further leading to a series of inflammatory reactions, which finally aggravates plaque instability [25, 26]. Accordingly, inhibiting monocyte adhesion to the endothelium is considered a novel treatment strategy for atherosclerosis.

*Eucommia ulmoides* Oliver is the only known species of the genus *Eucommia*. Pharmacologically, researchers reported that long-term *Eucommia* leaf extract (ELE) intake can effectively improve vascular function by promoting plasma nitric oxide (NO) levels while suppressing the production of ICAM-1 and VCAM-1 [27]. Likewise, Hosoo et al. examined the effects of ELE administration on artery function and morphology in spontaneously hypertensive rats (SHRs) and found that ELE significantly perfected Ach-induced aortic endothelium-dependent relaxation as compared to animals taking a normal diet. Plasma NO levels and media thickness were significantly increased and decreased, respectively, in the ELE-treated SHRs, indicating that ELE may exert anti-endothelial dysfunction and antioxidant and antiatherogenic effects [28].

*Polygonum multiflorum* stilbene glycoside (PMS) is a water-soluble fraction of *Polygonum multiflorum* Thunb., one of the most famous tonic traditional Chinese medicines, that has protective effects on the cardiocerebrovascular system [29]. Yang et al. studied the function of PMS on macrophage-derived foam cell functions and found that PMS could reduce the high production of intercellular adhesion molecule- (ICAM-) 1 protein and the vascular endothelial growth factor (VEGF) protein levels in the medium induced by oxidized lipoprotein when analyzed by flow cytometry, suggesting that PMS is a powerful agent against atherosclerosis and that PMS action could possibly be through the inhibition of the production of ICAM-1 and VEGF in foam cells [30].



Genistein, a major isoflavone in soy and red clover, has won wide attention due to its potential beneficial impacts and various biological actions [31]. Recent human intervention researches using soy phytoestrogens proved their beneficial effect on atherosclerosis. For instance, studies by Jia et al. demonstrated that genistein at physiological concentrations ( $0.1\ \mu\text{M}$ – $5\ \mu\text{M}$ ) significantly restrained TNF- $\alpha$ -induced expression of adhesion molecules and chemokines such as ICAM-1 and VCAM-1, which play a critical role in the firm adhesion of monocytes to activated endothelial cells [32].

In light of the established pharmacological role of muscone, which is a pharmacologically active component isolated from musk, Wu et al. reported that the administration of muscone may reduce cardiac remodeling and improve cardiac function following MI, indicating a beneficial effect on the protection against the development of atherosclerotic lesions [33].

**3.2. Monocyte Chemoattractant Protein-1 (MCP-1).** MCP-1 and its receptor play key roles in monocyte recruitment during foam cell and fatty streak formation in atherogenesis. Studies prove that circulating blood monocytes are the precursors of foam cells that are made up of lipid-laden macrophages. Overexpression of MCP-1 in specific tissues induces a localized infiltration of monocyte/macrophages. Endothelial expression of MCP-1 is thought to cause the subendothelial migration of monocytes in early atherosclerotic lesions. Upon stimulation, macrophages are able to produce significant loss of MCP-1 in atherosclerotic lesions. Recent researches indicate that homocysteine stimulates MCP-1 expression in cultured endothelial cells, giving rise to enhanced monocyte adhesion to endothelial cells as well as increased chemotaxis. In addition to recruiting and accumulating monocyte into the inflammatory sites, such as atherosclerotic lesions, MCP-1 also mediates the development of medial thickening [34, 35].

Wogonin (Wog) is an active component isolated from *Scutellaria baicalensis* radix, possessing antioxidant and anti-inflammatory properties [36]. Chang et al. found the effect of Wog on phorbol myristate acetate- (PMA-) induced MCP-1 expression in human umbilical vein endothelial cells (HUVECs) and measured the MCP-1 mRNA levels and MCP-1 release in Wog-treated HUVECs and reported that Wog inhibits MCP-1 induction in HUVECs. Furthermore, this inhibition is mediated by suppressing AP-1 transcriptional activity via the attenuation of extracellular signal-regulated kinase1/2 (ERK1/2) and c-Jun N-terminal kinase (JNK) signal transduction pathways, indicating that Wog has the potential therapeutic advantage for use in anti-inflammatory and vascular disorders [37].

Tetramethylpyrazine (TMP), a pharmacologically active component isolated from the rhizome of the Chinese herb *Rhizoma Chuanxiong* (Chuanxiong), has been clinically used in China and Southeast Asian countries for the prevention and treatment of cardiocerebrovascular diseases for about fifty years [38]. Recently, the function of TMP on the critical components of atherogenesis has been intensively investigated. Wang et al. reported that TMP reduces MCP-1

levels in the plasma and inhibits lectin-like oxidized LDL receptor-1 (LOX-1) production in rabbit aortas. Likewise, in their in vitro study, they revealed that TMP inhibits the ox-LDL-induced activation of p-ERK, p-p38, and p-JNK mitogen-activated protein kinase (MAPK), proving that TMP protects the endothelium and prevents atherosclerosis via inhibition of immunological responses [39].

Curcumin, a major active component in turmeric, has anti-inflammatory, anti-oxidative, and anti-atherosclerotic properties [40]. Liu et al. studied the effect of curcumin on ox-LDL-induced MCP-1 production and cholesterol efflux in macrophages and revealed that curcumin significantly suppressed the MCP-1 production induced by ox-LDL and enhanced cholesterol efflux through the inhibition of JNK pathways, which suggest that the vascular protective effect of Curcumin is related to anti-inflammation and antiatherosclerosis [41].

Berberine is the main component of the traditional Chinese medicine umbellatine, which has a widespread property and was used to treat many diseases clinically [42]. Chen et al. investigated the function and the mechanism of action of berberine on the production and secretion of MCP-1 in vitro to identify new pharmacological actions of it and found that berberine may suppress the expression and secretion of the MCP-1 in macrophages stimulated by acetylated low-density lipoprotein (AcLDL), whereas the peroxisome proliferator-activated receptor (PPAR $\gamma$ ) inhibitor could recede this effect of berberine, which reveals that berberine may inhibit the production of MCP-1 in AcLDL-stimulated macrophages and, at least in part, be regulated through activation of PPAR $\gamma$  [43].

**3.3. Tumor Necrosis Factor- $\alpha$  (TNF- $\alpha$ ).** TNF- $\alpha$  is a proinflammatory molecule expressed by cellular components of early fatty streaks and late atherosclerotic lesions of humans. Moreover, TNF- $\alpha$  may be secreted by several cell types within atherosclerotic plaques, such as endothelial cells, SMCs, and macrophages. However, monocytes and macrophages are the main sources of TNF. Researches indicate that circulating levels of TNF- $\alpha$  are increased in advanced atherosclerosis and in patients symptomatic for acute stroke. In mice, TNF- $\alpha$  gene knockout on the ApoE $^{-/-}$  background results in significantly smaller atherosclerotic plaque areas [44, 45]. Together, these data indicate that TNF- $\alpha$  may represent a promising target to reduce atherosclerosis.

Paeonol is the main active component of Cortex Moutan, which has several effects in traditional Chinese medicine, possessing various pharmacological activities, particularly an antiatherosclerosis effect [46]. Li et al. studied the association of the therapeutic effect of paeonol on atherosclerotic rabbits with its anti-inflammatory function, and their histological analysis of rabbits on the high-fat diet with paeonol showed significant improvement in atherosclerosis plaque. Moreover, the blood levels of TNF- $\alpha$  and the translocation of NF- $\kappa$ B to the nucleus were significantly inhibited in paeonol groups, as was the suppression of lipid peroxidation, which indicates that the anti-inflammatory function of paeonol may contribute to its antiatherosclerosis effect [47].

Tanshinone IIA (Tan IIA) as a major component to exert therapeutic effects of danshen is a traditional Chinese medicine commonly used in Asia for the prevention and treatment of cardiocerebrovascular diseases, such as atherosclerosis [48]. Wang et al. investigated the putative protective function of Tan IIA on endothelial progenitor cells (EPCs) injured by tumor necrosis factor- $\alpha$  (TNF- $\alpha$ ) and showed that TNF- $\alpha$  impaired EPC proliferation, migration, adhesion capacity, and vasculogenesis ability in vitro as well as promoted EPC secretion of inflammatory cytokines. However, Tan IIA was able to reverse these effects, which revealed that Tan IIA may have the potential to protect EPCs against damage induced by TNF- $\alpha$ , offering evidence for the pharmacological basis of Tan IIA and its potential use in the prevention and treatment of early atherosclerosis associated with EPC and endothelial damage [49].

Catalpol, isolated from the roots of *Rehmannia glutinosa*, Chinese foxglove, is an iridoid glycoside with antioxidant, anti-inflammatory, and antihyperglycemic agent [50]. Liu et al. investigated the function of catalpol on diabetic atherosclerosis in alloxan-induced diabetic rabbits and showed that catalpol treatment ameliorated diabetic atherosclerosis in diabetic rabbits as revealed by significantly suppressed neointimal hyperplasia and macrophage recruitment. Catalpol treatment also increased the activities of superoxide dismutase and glutathione peroxidase and enhanced the plasma levels of total antioxidant status, meanwhile decreasing the levels of malondialdehyde, protein carbonyl groups, and advanced glycation end product. What is more, catalpol also reduced circulating levels of TNF- $\alpha$ . In a word, these data collectively indicated supporting evidence and important novel pharmacological function of catalpol, which may have potential therapeutic value for the treatment and/or prevention of atherosclerosis in diabetic patients [51].

**3.4. Interleukin-1 $\beta$  (IL-1 $\beta$ ).** IL-1 $\beta$ , as a gatekeeper of inflammation, is a proinflammatory cytokine produced by myeloid cells. Secretion of IL-1 $\beta$  cytokine and expression of their receptor are enhanced in atherosclerotic aortas. IL-1 $\beta$  is an essential factor of Th17 cell differentiation that can facilitate inflammation in the vascular wall. Experiments in mouse models confirmed the proatherogenic nature of IL-1 $\beta$  that is involved in the upregulation of adhesion molecule production by endothelial cells as well as macrophage activation. Therefore, strategies for the prevention of IL-1 $\beta$  burst resolves inflammation in consideration of how the cytokine is released from the cell or how the precursor is cleaved [52, 53].

*Toona sinensis* is well known as a traditional Chinese medicine; Yang et al. evaluated the protective function of noncytotoxic concentrations of aqueous leaf extracts of *Toona sinensis* (TS extracts) in human umbilical vein endothelial cells (HUVECs) and showed that HUVECs were preincubated with TS extracts which resulted in enhanced resistance to oxidative stress and cell viability in a dose-dependent manner. In addition, IL-1 $\beta$  was positively correlated with cytotoxicity and negatively with TS extract concentrations. Notably, TS extract treatment significantly restrained reactive oxygen species (ROS) generation in

HUVECs, which supported the traditional use of *Toona sinensis* in the treatment of free radical-related diseases and atherosclerosis [54].

Fistular onion stalk, derived from *A. fistulosum*, is used as a traditional herbal medicine, and its extract exhibits certain beneficial advantages on cardiocerebrovascular disorders [55]. He et al. examined the function of fistular onion stalk extract on the pathological features, circulating inflammatory cytokines in in vivo model of atherosclerosis, and reported that rats treated with fistular onion stalk extract showed a significant decrease in the pathological region compared with the vehicle-treated controls. Furthermore, the extract also restrained the levels of the local inflammatory cytokines IL-1 $\beta$  and IL-6, suggesting that fistular onion stalk extract may be helpful for the attenuation of atherosclerosis [56].

*Andrographis paniculata* (Burm.f.) Nees (*Acanthaceae*) is a long-established therapeutic herb. Recently, epidemiologic evidence has revealed significant associations between atherosclerosis and *Porphyromonas gingivalis* (Pg) [57]. Al Batran et al. examined the function of andrographolide (AND) on atherosclerosis induced by Pg in rabbits and found that rabbits treated with AND showed significant reduction in TC, TG, and LDL levels and significant promotion in HDL level in the serum. Moreover, the treated rabbits showed reductions in interleukins (IL-1 $\beta$  and IL-6) as compared to the atherogenic group, which could be attributed to the anti-inflammatory effect of AND, which was involved in the decrease of proinflammatory cytokines [58].

Scropolioside B isolated from *Scrophularia dentata* Royle ex Benth is used for antiviral and anti-inflammatory treatment [59]. Zhu et al. investigated whether scropolioside B exhibits anti-inflammatory function and further analyzed its underlying mechanism in human monocytes and showed that scropolioside B significantly diminished the production and secretion of IL-1 $\beta$  and IL-32; furthermore, their study also revealed that this is regulated by modulating NF- $\kappa$ B levels, which strengthen the previous notion of the anti-inflammatory effects of iridoids and highlight scropolioside B as a potential herb for the treatment of rheumatoid arthritis and atherosclerotic disease [60].

**3.5. Matrix Metalloproteinases (MMPs).** Atherosclerotic plaque rupture causes most myocardial infarctions. MMPs are involved in the development and the progression of atherosclerosis and are related to an enhanced factor of cardiocerebrovascular morbidity and mortality: an increased MMP expression has been detected in atherosclerotic plaques, and their activity may be responsible for plaque instability and rupture and for a strengthened platelet aggregation. MMPs, also named matrixins, are subdivided into at least five groups based on their structure and/or substrate specificities. MMP family members include collagenases (MMP-1, MMP-8, MMP-13, and MMP-18), gelatinases (MMP-2 and MMP-9), stromelysins (MMP-3, MMP-10, and MMP-11), matrilysins (MMP-7 and MMP-26), and membrane-type MMPs (MMP-14 and MMP-15). It has been demonstrated that specific matrix metalloproteinases (MMPs) such as MMP-1, MMP-2, MMP-3, MMP-9, and

MMP-14 have been proven to enhance angiogenesis, and in particular, an increase in MMP-9 plasma levels is related with higher all-cause mortality and cardiocerebrovascular mortality. Given MMPs have pleiotropic actions in atherosclerosis, strategy on a specific adverse effect of MMPs while leaving intact essential physiological functions, additionally, avoiding a narrow or nonexistent therapeutic window [61].

Red yeast rice (RYR) is a traditional Chinese medicinal agent prepared by using *Monascus purpureus* fermented with rice, which has been recorded in ancient Chinese pharmacopoeias since the Ming dynasty [62]. Red yeast rice extracts contain a mixture of starch, phytocholesterols, isoflavones, monounsaturated fatty acids, and polyketides called monacolins. Xie et al. used apolipoprotein E-deficient (ApoE<sup>-/-</sup>) male mice infused with angiotensin II to promote the development of atherosclerosis and showed that RYR extract significantly decreased atherosclerotic lesion areas in both the intima of aortic arches and cross sections of aortic roots. These functions were associated with reductions of serum total cholesterol, MMP-2, suggesting the potential interpretation that this traditional Chinese food herb may be used as a preventive treatment of atherosclerosis [63].

Alisma decoction (AD) is a classical traditional Chinese formula that was first prescribed in the Eastern Han dynasty, which composed of a combination of two herbs, including Alisma and Atractylodes [64]. Xue et al. examined the regulation of lipids and the anti-inflammatory function exerted by AD and evaluated the underlying molecular mechanisms using ox-LDL-stimulated foam cells derived from rat peritoneal macrophages and showed that AD markedly alleviated lipid deposition in foam cells as it inhibited the ox-LDL-induced expression of MMP-9. Collectively, their findings indicate that blocking lipid deposition and inhibiting inflammatory response may be one of the key mechanisms through which AD exerts its antiatherosclerotic effects [64].

Puerarin, a phytoestrogen derived from the Chinese medicinal herb radix puerariae, has been proven practical in the management of various cardiocerebrovascular diseases [65]. Li et al. examined the clinical significance of MMP-9 secreted by cultured monocyte-derived macrophages (HMDM) from patients with coronary heart disease (CHD) in vitro and evaluated the interventional function of puerarin on them and revealed that the levels of MMP-9 secreted in vitro by HMDM from CHD patients could be used as indexes for evaluating patient's condition of ACS. In addition, puerarin can restrain the production and the activity of MMP-9 secreted by HMDM, stabilize the plaque, and perfect the vulnerability of blood to a certain extent [66].

Artemisinin, derived from the sweet wormwood *Artemisia annua*, has been used in the treatment of malaria in China for over 2000 years. Recently, artemisinin and its derivatives have been proven to have pharmacological actions beyond their antimalarial effects; these other properties include immunosuppressive and anti-inflammatory properties [67]. Wang et al. examined whether artemisinin could reduce MMP-9 production in phorbol myristate acetate- (PMA-) induced macrophages by regulating the protein kinase (PK) Cd/JNK/p38/ERK pathway and revealed that artemisinin significantly inhibited the induction of MMP-9 at both the

transcriptional and translational levels in a dose-dependent manner in PMA-induced macrophages. In addition, artemisinin strongly blocked PKCd/JNK/p38/ERK MAPK phosphorylation, indicating that artemisinin may have a potential for use in the protection against the development of atherosclerotic lesions [68].

#### 4. Author's Comments: Challenges in Exerting Advantages of Chinese Herb in Antiatherosclerosis

The immunopathology of atherosclerosis emphasizes the active inflammatory, complex or multifactorial, and long-term property of the disease. Understanding the characteristic and interrelationship in atherosclerosis may offer new concepts with possible impact not only on early and accurate diagnosis but also on preventive programs and perhaps more effective therapeutic interventions. In accordance with ancient Chinese pharmacopoeias, a large amount of medicinal plants have shown inhibitory potentials in antiatherosclerosis from the formation of fatty streak to plaque complications, which have been widely used to prevent and treat atherosclerosis in China. Moreover, the evidence-based study of TCMs in treating atherosclerosis suggested that, in addition to anticytokine production, Chinese herb also exerts anti-endothelial dysfunction and antioxidant and antihyperlipidemic effects, thus having widespread properties.

Recently, the Nobel Prize-winning discoveries of Professor Tu related to artemisinin from the Chinese herb *Artemisia carvifolia* won global interest in TCM. The Chinese natural herbs outlined in this review are potential targets for an immunomodulatory cardiocerebrovascular prevention strategy mainly due to its anti-inflammatory property. Despite encouraging results from either clinical trials or experimental, researches show that TCMs and their components or derivatives have immunomodulatory effects and supplied the rationale for the therapeutic potential of targeting inflammation in atherosclerosis; data from randomized, controlled, and double-blind clinical trials to evaluate cardiocerebrovascular outcomes for specific monomer from these natural herbs are a few and far between. Thus, future researches are required to explore detailed immunomodulatory molecular mechanisms of these medicinal herbs to elucidate the precise function of active ingredients and perfect their therapeutic management in atherosclerosis, and further large randomized controlled trials (RCTs) will shed light on the guidelines to define the appropriate target population, treatment periods, outcomes, and prediction of potential adverse effects.

#### 5. Conclusions

The nature of atherosclerosis is chronic inflammation in the aortic, caused by dyslipidemia, innate and adaptive immune responses. Cytokines are elucidated to play a critical role in the interrelationship of atherosclerosis, such as in the initiation, progression, and even regression of atherosclerotic lesions. Given pro-inflammatory cytokines accelerate atherosclerosis progression, and anti-inflammatory cytokines

ameliorate the disease; the balance between pro- and anti-inflammatory cytokines is the major element that determines the stability of atherosclerotic plaque [69, 70]. The Chinese natural herbs outlined in this review possess a widespread property beyond anti-endothelial dysfunction, antioxidant and antihyperlipidemic property; anti-inflammatory property is the most important mechanism partly in the prevention and treatment of atherosclerosis. However, precise immunomodulatory molecular mechanisms of these medicinal herbs and their active ingredients or derivatives in the therapy of antiatherosclerosis are a few and far between. Thus, there is still a long but promising journey between these Chinese medicinal herbs and their appropriate therapeutic management in atherosclerosis.

### Conflicts of Interest

The authors declare that they have no conflict of interests regarding the publication of this paper.

### Authors' Contributions

Yan Ren and Wei Qiao contributed equally to this work.

### Acknowledgments

This work was supported by grants from the National Natural Science Foundation of China (no. 81173595 and no. 81373794), the Research Foundation of China-Japan Friendship Hospital (no. 2015-2-QN-34), and the China-Japan Friendship Hospital Youth Science and Technology Excellence Project (no. 2014-QNYC-A-04).

### References

- [1] P. Libby, P. M. Ridker, and G. K. Hansson, "Progress and challenges in translating the biology of atherosclerosis," *Nature*, vol. 473, no. 7347, pp. 317–325, 2011.
- [2] G. Fredman and M. Spite, "Recent advances in the role of immunity in atherosclerosis," *Circulation Research*, vol. 113, no. 12, pp. e111–e114, 2013.
- [3] J. Frostegard, "Immunity, atherosclerosis and cardiovascular disease," *BMC Medicine*, vol. 11, p. 117, 2013.
- [4] J. L. Witztum and A. H. Lichtman, "The influence of innate and adaptive immune responses on atherosclerosis," *Annual Review of Pathology*, vol. 9, pp. 73–102, 2014.
- [5] M. F. Lopes-Virella and G. Virella, "Pathogenic role of modified LDL antibodies and immune complexes in atherosclerosis," *Journal of Atherosclerosis and Thrombosis*, vol. 20, no. 10, pp. 743–754, 2013.
- [6] F. Akhter, M. S. Khan, A. A. Alatar, M. Faisal, and S. Ahmad, "Antigenic role of the adaptive immune response to d-ribose glycated LDL in diabetes, atherosclerosis and diabetes atherosclerotic patients," *Life Sciences*, vol. 151, pp. 139–146, 2016.
- [7] A. R. Fatkhullina, I. O. Peshkova, and E. K. Koltsova, "The role of cytokines in the development of atherosclerosis," *Biochemistry (Moscow)*, vol. 81, no. 11, pp. 1358–1370, 2016.
- [8] D. P. Ramji and T. S. Davies, "Cytokines in atherosclerosis: key players in all stages of disease and promising therapeutic targets," *Cytokine & Growth Factor Reviews*, vol. 26, no. 6, pp. 673–685, 2015.
- [9] A. Tedgui and Z. Mallat, "Cytokines in atherosclerosis: pathogenic and regulatory pathways," *Physiological Reviews*, vol. 86, no. 2, pp. 515–581, 2006.
- [10] D. Tousoulis, E. K. Economou, E. Oikonomou et al., "The role and predictive value of cytokines in atherosclerosis and coronary artery disease," *Current Medicinal Chemistry*, vol. 22, no. 22, pp. 2636–2650, 2015.
- [11] X. Blanchet, M. Langer, C. Weber, R. R. Koenen, and P. von Hundelshausen, "Touch of chemokines," *Frontiers in Immunology*, vol. 3, p. 175, 2012.
- [12] E. P. Schmidt, W. M. Kuebler, W. L. Lee, and G. P. Downey, "Adhesion molecules: master controllers of the circulatory system," *Comprehensive Physiology*, vol. 6, no. 2, pp. 945–973, 2016.
- [13] R. E. Gerszten, E. A. Garcia-Zepeda, Y. C. Lim et al., "MCP-1 and IL-8 trigger firm adhesion of monocytes to vascular endothelium under flow conditions," *Nature*, vol. 398, no. 6729, pp. 718–723, 1999.
- [14] S. D. Cushing, J. A. Berliner, A. J. Valente et al., "Minimally modified low density lipoprotein induces monocyte chemoattractant protein 1 in human endothelial cells and smooth muscle cells," *Proceedings of the National Academy of Sciences of the United States of America*, vol. 87, no. 13, pp. 5134–5138, 1990.
- [15] W. Cheng, Y. Zhao, S. Wang, and F. Jiang, "Tumor necrosis factor-related apoptosis-inducing ligand in vascular inflammation and atherosclerosis: a protector or culprit?," *Vascular Pharmacology*, vol. 63, no. 3, pp. 135–144, 2014.
- [16] A. Qamar and D. J. Rader, "Effect of interleukin 1 $\beta$  inhibition in cardiovascular disease," *Current Opinion in Lipidology*, vol. 23, no. 6, pp. 548–553, 2012.
- [17] S. Blankenberg, H. J. Rupprecht, O. Poirier et al., "Plasma concentrations and genetic variation of matrix metalloproteinase 9 and prognosis of patients with cardiovascular disease," *Circulation*, vol. 107, no. 12, pp. 1579–1585, 2003.
- [18] N. Kamaly, G. Fredman, J. J. Fojas et al., "Targeted interleukin-10 nanotherapeutics developed with a microfluidic chip enhance resolution of inflammation in advanced atherosclerosis," *ACS Nano*, vol. 10, no. 5, pp. 5280–5292, 2016.
- [19] L. L. Johnson, "Targeting activated macrophages to identify the vulnerable atherosclerotic plaque," *Journal of Nuclear Cardiology*, vol. 24, no. 3, pp. 872–875, 2017.
- [20] G. M. Grosse, W. J. Schulz-Schaeffer, O. E. Teebken et al., "Monocyte subsets and related chemokines in carotid artery stenosis and ischemic stroke," *International Journal of Molecular Sciences*, vol. 17, no. 4, p. 433, 2016.
- [21] M. Back and G. K. Hansson, "Anti-inflammatory therapies for atherosclerosis," *Nature Reviews Cardiology*, vol. 12, no. 4, pp. 199–211, 2015.
- [22] F. Roubille, E. A. Kritikou, C. Roubille, and J. C. Tardif, "Emerging anti-inflammatory therapies for atherosclerosis," *Current Pharmaceutical Design*, vol. 19, no. 33, pp. 5840–5849, 2013.
- [23] A. C. Foks and J. Kuiper, "Immune checkpoint proteins: exploring their therapeutic potential to regulate atherosclerosis," *British Journal of Pharmacology*, 2017.
- [24] N. Cichon, D. Lach, A. Dziedzic, M. Bijak, and J. Saluk, "The inflammatory processes in atherogenesis," *Polski Merkuriusz Lekarski*, vol. 42, no. 249, pp. 125–128, 2017.

- [25] M. J. Telen, "Role of adhesion molecules and vascular endothelium in the pathogenesis of sickle cell disease," *Hematology-American Society of Hematology Education Program*, vol. 2007, no. 1, pp. 84–90, 2007.
- [26] Y. Fan, Y. Wang, Z. Tang et al., "Suppression of pro-inflammatory adhesion molecules by PPAR- $\delta$  in human vascular endothelial cells," *Arteriosclerosis, Thrombosis, and Vascular Biology*, vol. 28, no. 2, pp. 315–321, 2008.
- [27] F. Greenway, Z. Liu, and Y. Yu, "A clinical trial testing the safety and efficacy of a standardized *Eucommia ulmoides* Oliver bark extract to treat hypertension," *Alternative Medicine Review*, vol. 16, no. 4, pp. 338–347, 2011.
- [28] S. Hosoo, M. Koyama, M. Kato et al., "The restorative effects of *Eucommia ulmoides* Oliver leaf extract on vascular function in spontaneously hypertensive rats," *Molecules*, vol. 20, no. 12, pp. 21971–21981, 2015.
- [29] M. Y. Um, W. H. Choi, J. Y. Aan, S. R. Kim, and T. Y. Ha, "Protective effect of *Polygonum multiflorum* Thunb on amyloid  $\beta$ -peptide 25-35 induced cognitive deficits in mice," *Journal of Ethnopharmacology*, vol. 104, no. 1-2, pp. 144–148, 2006.
- [30] P. Y. Yang, M. R. Almofti, L. Lu et al., "Reduction of atherosclerosis in cholesterol-fed rabbits and decrease of expressions of intracellular adhesion molecule-1 and vascular endothelial growth factor in foam cells by a water-soluble fraction of *Polygonum multiflorum*," *Journal of Pharmacological Sciences*, vol. 99, no. 3, pp. 294–300, 2005.
- [31] Q. Qiang, H. Adachi, Z. Huang et al., "Genistein, a natural product derived from soybeans, ameliorates polyglutamine-mediated motor neuron disease," *Journal of Neurochemistry*, vol. 126, no. 1, pp. 122–130, 2013.
- [32] Z. Jia, P. V. Babu, H. Si et al., "Genistein inhibits TNF- $\alpha$ -induced endothelial inflammation through the protein kinase pathway A and improves vascular inflammation in C57BL/6 mice," *International Journal of Cardiology*, vol. 168, no. 3, pp. 2637–2645, 2013.
- [33] Q. Wu, H. Li, Y. Wu et al., "Protective effects of muscone on ischemia-reperfusion injury in cardiac myocytes," *Journal of Ethnopharmacology*, vol. 138, no. 1, pp. 34–39, 2011.
- [34] J. Lin, V. Kakkar, and X. Lu, "Impact of MCP-1 in atherosclerosis," *Current Pharmaceutical Design*, vol. 20, no. 28, pp. 4580–4588, 2014.
- [35] M. M. Pirvulescu, A. M. Gan, D. Stan et al., "Subendothelial resistin enhances monocyte transmigration in a co-culture of human endothelial and smooth muscle cells by mechanisms involving fractalkine, MCP-1 and activation of TLR4 and Gi/o proteins signaling," *The International Journal of Biochemistry & Cell Biology*, vol. 50, pp. 29–37, 2014.
- [36] Y. S. Chi, B. S. Cheon, and H. P. Kim, "Effect of wogonin, a plant flavone from *Scutellaria radix*, on the suppression of cyclooxygenase-2 and the induction of inducible nitric oxide synthase in lipopolysaccharide-treated RAW 264.7 cells," *Biochemical Pharmacology*, vol. 61, no. 10, pp. 1195–1203, 2001.
- [37] Y. L. Chang, J. J. Shen, B. S. Wung, J. J. Cheng, and D. L. Wang, "Chinese herbal remedy wogonin inhibits monocyte chemoattractant protein-1 gene expression in human endothelial cells," *Molecular Pharmacology*, vol. 60, no. 3, pp. 507–513, 2001.
- [38] M. Guo, Y. Liu, and D. Shi, "Cardiovascular actions and therapeutic potential of tetramethylpyrazine (active component isolated from *Rhizoma Chuanxiong*): roles and mechanisms," *BioMed Research International*, vol. 2016, Article ID 2430329, 9 pages, 2016.
- [39] G. F. Wang, C. G. Shi, M. Z. Sun et al., "Tetramethylpyrazine attenuates atherosclerosis development and protects endothelial cells from ox-LDL," *Cardiovascular Drugs and Therapy*, vol. 27, no. 3, pp. 199–210, 2013.
- [40] H. S. Lee, M. J. Lee, H. Kim et al., "Curcumin inhibits TNF $\alpha$ -induced lectin-like oxidised LDL receptor-1 (LOX-1) expression and suppresses the inflammatory response in human umbilical vein endothelial cells (HUVECs) by an antioxidant mechanism," *Journal of Enzyme Inhibition and Medicinal Chemistry*, vol. 25, no. 5, pp. 720–729, 2010.
- [41] W. Liu, W. Guo, L. Guo et al., "Andrographolide sulfonate ameliorates experimental colitis in mice by inhibiting Th1/Th17 response," *International Immunopharmacology*, vol. 20, no. 2, pp. 337–345, 2014.
- [42] K. Zou, Z. Li, Y. Zhang et al., "Advances in the study of berberine and its derivatives: a focus on anti-inflammatory and anti-tumor effects in the digestive system," *Acta Pharmacologica Sinica*, vol. 38, no. 2, pp. 157–167, 2017.
- [43] F. L. Chen, Z. H. Yang, Y. Liu et al., "Berberine inhibits the expression of TNF $\alpha$ , MCP-1, and IL-6 in AcLDL-stimulated macrophages through PPAR $\gamma$  pathway," *Endocrine*, vol. 33, no. 3, pp. 331–337, 2008.
- [44] Y. Zhang, X. Yang, F. Bian et al., "TNF- $\alpha$  promotes early atherosclerosis by increasing transcytosis of LDL across endothelial cells: crosstalk between NF- $\kappa$ B and PPAR- $\gamma$ ," *Journal of Molecular and Cellular Cardiology*, vol. 72, pp. 85–94, 2014.
- [45] N. C. Olson, P. W. Callas, A. J. Hanley et al., "Circulating levels of TNF- $\alpha$  are associated with impaired glucose tolerance, increased insulin resistance, and ethnicity: the Insulin Resistance Atherosclerosis Study," *The Journal of Clinical Endocrinology and Metabolism*, vol. 97, no. 3, pp. 1032–1040, 2012.
- [46] W. L. Ma, C. Y. Yan, J. H. Zhu, G. Y. Duan, and R. M. Yu, "Biotransformation of paeonol and emodin by transgenic crown galls of *Panax quinquefolium*," *Applied Biochemistry and Biotechnology*, vol. 160, no. 5, pp. 1301–1308, 2010.
- [47] H. Li, M. Dai, and W. Jia, "Paeonol attenuates high-fat-diet-induced atherosclerosis in rabbits by anti-inflammatory activity," *Planta Medica*, vol. 75, no. 1, pp. 7–11, 2009.
- [48] S. Mao, X. Li, L. Wang, P. C. Yang, and M. Zhang, "Rationale and design of sodium tanshinone IIA sulfonate in left ventricular remodeling secondary to acute myocardial infarction (STAMP-REMODELING) trial: a randomized controlled study," *Cardiovascular Drugs and Therapy*, vol. 29, no. 6, pp. 535–542, 2015.
- [49] D. T. Wang, R. H. Huang, X. Cheng, Z. H. Zhang, Y. J. Yang, and X. Lin, "Tanshinone IIA attenuates renal fibrosis and inflammation via altering expression of TGF- $\beta$ /Smad and NF- $\kappa$ B signaling pathway in 5/6 nephrectomized rats," *International Immunopharmacology*, vol. 26, no. 1, pp. 4–12, 2015.
- [50] Y. F. Liu, Y. Zhao, X. S. Wen, and Q. T. Dong, "Advances in research on pharmacodynamics and chemical conversion of catalpol," *Zhongguo Zhong Yao Za Zhi*, vol. 32, no. 12, pp. 1128–1130, 2007.
- [51] J. Y. Liu, C. Z. Zheng, X. P. Hao, A. W. Mao, and P. Yuan, "Catalpol ameliorates diabetic atherosclerosis in diabetic rabbits," *American Journal of Translational Research*, vol. 8, no. 10, pp. 4278–4288, 2016.

- [52] D. J. Rader, "IL-1 and atherosclerosis: a murine twist to an evolving human story," *The Journal of Clinical Investigation*, vol. 122, no. 1, pp. 27–30, 2012.
- [53] V. Bhaskar, J. Yin, A. M. Mirza et al., "Monoclonal antibodies targeting IL-1 beta reduce biomarkers of atherosclerosis in vitro and inhibit atherosclerotic plaque formation in apolipoprotein E-deficient mice," *Atherosclerosis*, vol. 216, no. 2, pp. 313–320, 2011.
- [54] H. L. Yang, S. C. Chen, K. Y. Lin et al., "Antioxidant activities of aqueous leaf extracts of *Toona sinensis* on free radical-induced endothelial cell damage," *Journal of Ethnopharmacology*, vol. 137, no. 1, pp. 669–680, 2011.
- [55] Q. Fu, J. Liu, C. Zhang et al., "Separation and identification of flavonoids from fistular onion stalk (*Allium fistulosum* L. var. *Caespitosum* Makio)," *Journal of Huazhong University of Science and Technology - Medical Sciences*, vol. 30, no. 2, pp. 255–257, 2010.
- [56] B. He, J. Hao, W. Sheng et al., "Fistular onion stalk extract exhibits anti-atherosclerotic effects in rats," *Experimental and Therapeutic Medicine*, vol. 8, no. 3, pp. 785–792, 2014.
- [57] L. Wen, N. Xia, X. Chen et al., "Activity of antibacterial, antiviral, anti-inflammatory in compounds andrographolide salt," *European Journal of Pharmacology*, vol. 740, pp. 421–427, 2014.
- [58] R. Al Batran, F. Al-Bayaty, M. M. Al-Obaidi, and A. Ashrafi, "Insights into the antiatherogenic molecular mechanisms of andrographolide against *Porphyromonas gingivalis*-induced atherosclerosis in rabbits," *Naunyn-Schmiedeberg's Archives of Pharmacology*, vol. 387, no. 12, pp. 1141–1152, 2014.
- [59] T. Zhu, L. Zhang, S. Ling, F. Qian, Y. Li, and J. W. Xu, "Anti-inflammatory activity comparison among scropoliosides-catalpol derivatives with 6-O-substituted cinnamyl moieties," *Molecules*, vol. 20, no. 11, pp. 19823–19836, 2015.
- [60] T. Zhu, L. Zhang, S. Ling et al., "Scropolioside B inhibits IL-1 $\beta$  and cytokines expression through NF- $\kappa$ B and inflammasome NLRP3 pathways," *Mediators of Inflammation*, vol. 2014, Article ID 819053, 10 pages, 2014.
- [61] B. A. Brown, H. Williams, and S. J. George, "Evidence for the involvement of matrix-degrading metalloproteinases (MMPs) in atherosclerosis," *Progress in Molecular Biology and Translational Science*, vol. 147, pp. 197–237, 2017.
- [62] D. Heber, A. Lembertas, Q. Y. Lu, S. Bowerman, and V. L. Go, "An analysis of nine proprietary Chinese red yeast rice dietary supplements: implications of variability in chemical profile and contents," *Journal of Alternative and Complementary Medicine*, vol. 7, no. 2, pp. 133–139, 2001.
- [63] X. Xie, Y. Wang, S. Zhang et al., "Chinese red yeast rice attenuates the development of angiotensin II-induced abdominal aortic aneurysm and atherosclerosis," *The Journal of Nutritional Biochemistry*, vol. 23, no. 6, pp. 549–556, 2012.
- [64] X. Xue, T. Chen, W. Wei, X. Zhou, Z. Lin, and L. Chen, "Effects of Alisma Decoction on lipid metabolism and inflammatory response are mediated through the activation of the LXR $\alpha$  pathway in macrophage-derived foam cells," *International Journal of Molecular Medicine*, vol. 33, no. 4, pp. 971–977, 2014.
- [65] X. L. Lu, J. X. Liu, Q. Wu et al., "Protective effects of puerarin against Ass40-induced vascular dysfunction in zebrafish and human endothelial cells," *European Journal of Pharmacology*, vol. 732, pp. 76–85, 2014.
- [66] Y. Zhong, X. Zhang, X. Cai, K. Wang, Y. Chen, and Y. Deng, "Puerarin attenuated early diabetic kidney injury through down-regulation of matrix metalloproteinase 9 in streptozotocin-induced diabetic rats," *PLoS One*, vol. 9, no. 1, article e85690, 2014.
- [67] T. Weifeng, S. Feng, L. Xiangji et al., "Artemisinin inhibits in vitro and in vivo invasion and metastasis of human hepatocellular carcinoma cells," *Phytomedicine*, vol. 18, no. 2-3, pp. 158–162, 2011.
- [68] Y. Wang, Z. Q. Huang, C. Q. Wang et al., "Artemisinin inhibits extracellular matrix metalloproteinase inducer (EMMPRIN) and matrix metalloproteinase-9 expression via a protein kinase C $\delta$ /p38/extracellular signal-regulated kinase pathway in phorbol myristate acetate-induced THP-1 macrophages," *Clinical and Experimental Pharmacology & Physiology*, vol. 38, no. 1, pp. 11–18, 2011.
- [69] A. Mak, A. Johnston, and J. Uetrecht, "Effects of immunization and checkpoint inhibition on amodiaquine-induced liver injury," *Journal of Immunotoxicology*, vol. 14, no. 1, pp. 89–94, 2017.
- [70] S. Ederhy, A. L. Voisin, and S. Champiat, "Myocarditis with immune checkpoint blockade," *The New England Journal of Medicine*, vol. 376, no. 3, pp. 290–291, 2017.

## Research Article

# Chinese Herbal Formula, Modified Danggui Buxue Tang, Attenuates Apoptosis of Hematopoietic Stem Cells in Immune-Mediated Aplastic Anemia Mouse Model

Jingwei Zhou,<sup>1,2</sup> Xue Li,<sup>1</sup> Peiyong Deng,<sup>1</sup> Yi Wei,<sup>1</sup> Juan Liu,<sup>1</sup> Meng Chen,<sup>3</sup> Yamei Xu,<sup>4</sup> Dongmei Zhang,<sup>1</sup> Lingqun Zhu,<sup>1</sup> Lixia Lou,<sup>1</sup> Bin Dong,<sup>1</sup> Qiushuo Jin,<sup>1</sup> and Limin Chai<sup>1</sup>

<sup>1</sup>Key Laboratory of Chinese Internal Medicine of Ministry of Education and Beijing, Dongzhimen Hospital, Beijing University of Chinese Medicine, Beijing 100700, China

<sup>2</sup>Department of Rheumatology, Dongzhimen Hospital, Beijing University of Chinese Medicine, Beijing 100700, China

<sup>3</sup>School of Preclinical Medicine, Beijing University of Chinese Medicine, Beijing 100029, China

<sup>4</sup>Department of Hematology & Oncology, Dongzhimen Hospital, Beijing University of Chinese Medicine, Beijing 100700, China

Correspondence should be addressed to Limin Chai; [liminchai@hotmail.com](mailto:liminchai@hotmail.com)

Received 9 January 2017; Revised 1 June 2017; Accepted 12 July 2017; Published 16 August 2017

Academic Editor: Qingdong Guan

Copyright © 2017 Jingwei Zhou et al. This is an open access article distributed under the Creative Commons Attribution License, which permits unrestricted use, distribution, and reproduction in any medium, provided the original work is properly cited.

A derivative formula, DGBX, which is composed of three herbs (*Radix astragali*, *Radix Angelicae sinensis*, and *Coptis chinensis* Franch), is derived from a famous Chinese herbal formula, Danggui Buxue Tang (DBT) (*Radix astragali* and *Radix Angelicae sinensis*). We aimed to investigate the effects of DGBX on the regulation of the balance between proliferation and apoptosis of hematopoietic stem cells (HSCs) due to the aberrant immune response in a mouse model of aplastic anemia (AA). Cyclosporine (CsA), an immunosuppressor, was used as the positive control. Our results indicated that DGBX could downregulate the production of IFN $\gamma$  in bone marrow cells by interfering with the binding between SLAM and SAP and the expressions of Fyn and T-bet. This herbal formula can also inhibit the activation of Fas-mediated apoptosis, interferon regulatory factor-1-induced JAK/Stat, and eukaryotic initiation factor 2 signaling pathways and thereby induce proliferation and attenuate apoptosis of HSCs. In conclusion, DGBX can relieve the immune-mediated destruction of HSCs, repair hematopoietic failure, and recover the hematopoietic function of HSCs in hematogenesis. Therefore, DGBX can be used in traditional medicine against AA as a complementary and alternative immunosuppressive therapeutic formula.

## 1. Introduction

Aplastic anemia (AA) is a rare acquired bone marrow failure syndrome resulting from immune-mediated destruction of hematopoietic stem cells (HSCs), caused largely by many quantitative and qualitative defects in HSCs [1]. Allogeneic stem cell transplant can cure severe AA. Nevertheless, transplantation in patients who are old or lack family donors has many challenges [2]. The molecular basis of the aberrant immune response and deficiencies in HSC is now being defined genetically. Immunosuppression by antithymocyte globulins and cyclosporine A (CsA) is effective on restoring blood cell production in the majority of AA patients.

However, the incidence of relapse and evolution of clonal hematological diseases remain high [3].

Danggui Buxue Tang (DBT), one of the simplest traditional Chinese medicine (TCM) decoctions, has been used in the treatment of blood deficiency syndrome for more than 800 years in China. DBT is composed of two herbs, *Radix astragali* (Milkvetch Root) and *Radix Angelicae sinensis* (Chinese Angelica), boiled together at a 5 : 1 ratio. Pharmacological studies indicated that DBT has effects on bone development [4], blood enhancement [5], and immune stimulation [6]. Several studies have verified the hematopoietic function of DBT in a mouse model of bone marrow suppression. It can increase the production of peripheral blood and nucleated

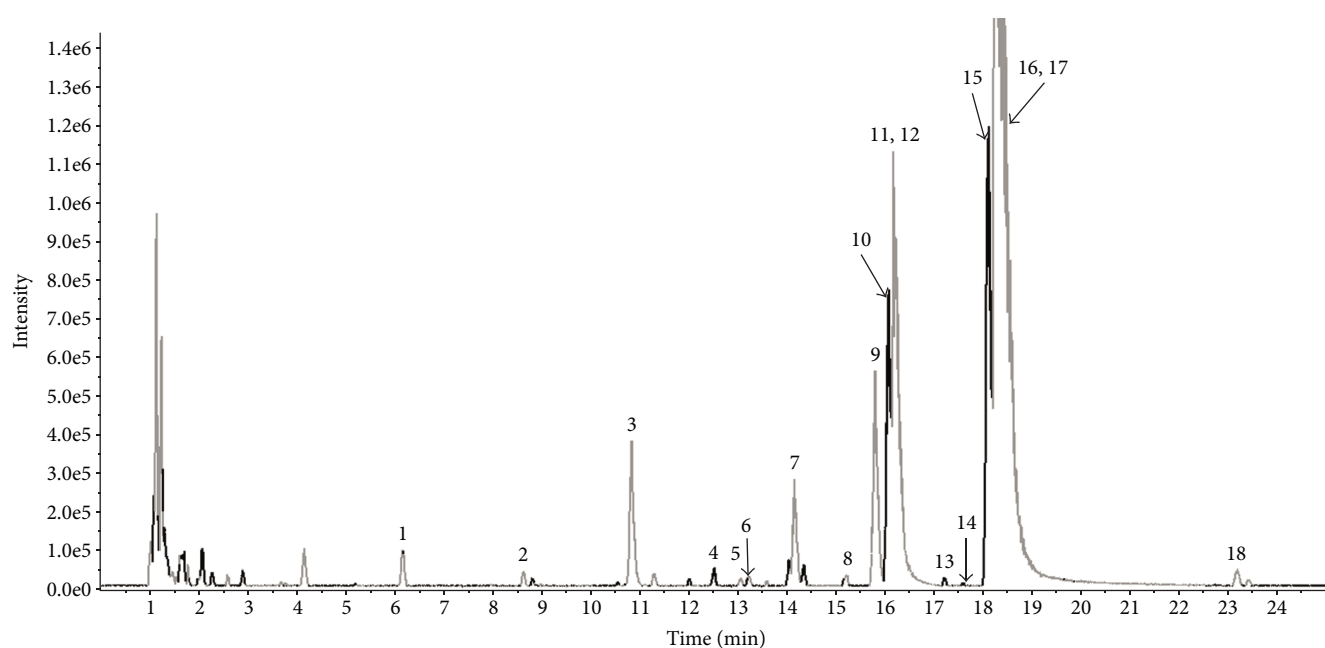


FIGURE 1: High-performance liquid chromatography-electrospray ionization/mass spectrometry ion chromatograms of lyophilized boiled aqueous extract of DGBX. Abscissa represents retention time, and ordinate represents chromatographic peak intensity.

bone marrow cells (BMCs) and the colony count of hematopoietic stem/progenitor cells (HSPCs) *in vitro*; regulate the expression of cytokines, such as erythropoietin, thrombopoietin, and granulocyte-macrophage colony-stimulating factor in bone marrow microenvironment; and contribute to cell cycle of HSPCs [7]. For the bone marrow failure syndrome resulting from immune-mediated destruction of HSC, we modified DBT to prepare a derivative herb formula (DGBX) by adding *Coptis chinensis* Franch (*Coptidis rhizoma*) for reinforcing the regulatory effect on aberrant immune response in the bone marrow of patients with AA. Pharmacological studies validated that *Coptis chinensis* Franch modulates immune responses and controls certain inflammation-related diseases [8]. The combination of these three herbs can contribute to multitargeting, multichannel immunosuppressive effects in AA treatment.

We investigated the possible mechanisms underlying the immunosuppressive and hematopoietic functions of DGBX in an immune-mediated AA mouse model. CsA was used as a positive control. The aim of this study was to identify the specific cellular targets involved in the immunosuppressive and hematopoietic functions of DGBX in AA treatment.

## 2. Materials and Methods

**2.1. Preparation of Herbal Composition of DGBX.** *Radix astragali*, *Radix Angelicae sinensis*, and *Coptis chinensis* Franch (total weight, 126 g; individual ratio, 5:1:1) were boiled together in 6× volume of water for 0.5 h. Then, residue from the first extraction was boiled in 8× volume of water for 25 min. Finally, the filtered solutions were combined and concentrated into aqueous extracts containing 0.9 g/mL of raw herbs.

**2.2. High-Performance Liquid Chromatography-Electrospray Ionization/Mass Spectrometry.** The herbal extracts were filtered using a 150 μm standard test sieve and maintained in desiccators at 4°C until use. Lyophilized flower (0.02 g) was extracted with 5 mL of methanol/water (*v/v*=1:1) in the sonicator for 20 min at room temperature. The extract was filtered through a 0.22 μm membrane. A 10 μL aliquot of the extract was injected into the analytical column for analysis. The compounds were separated on a Phenomenex Kinetex C18 (2.6 μm, 100 × 2.1 mm) operated at 35°C. The mobile phase (0.1% formic acid in water (A) and acetonitrile (B) as mobile phase) was delivered at a flow rate of 0.4 mL/min under a gradient program. The diode-array detector was set at 254 nm, and the online UV spectra were recorded in the scanning range of 190–400 nm.

The optimized parameters for negative and positive modes were as follows: the ion spray voltage was set at 5500 (positive ion mode) and –4500 V (negative ion mode); the turbo V spray temperature at 600°C, nebulizer gas (gas 1) at 50 psi, heater gas (gas 2) at 60 psi, collision gas at medium, the curtain gas at 30 psi, and the declustering potential at 80 (positive ion mode) and –80 V (negative ion mode). The collision energy was set at 35 (positive ion mode) and –35 V (negative ion mode), and the collision energy spread was set at 15 V for MS/MS experiments. The data was acquired with IDA (information-dependent acquisition) method and analyzed by Peak View Software™ 2.2 (SCIEX, Foster City, CA, USA).

**2.3. Mice.** BALB/c female mice (*n* = 6 per group, 7–8 weeks old) and DBA/2 female mice (7 to 8 weeks old) were purchased from HFK Bioscience Co. Ltd. (Beijing, China). Animal care and use were in accordance with the institutional guidelines. All animal experiments were approved by the Institutional



TABLE 1: Chemical components identified from DGBX by high-performance liquid chromatography-electrospray ionization/mass spectrometry.

Peak	$t_R$ (min)	Formula	Identification
1	6.14	$C_{11}H_{12}N_2O_2$	L-tryptophan
2	8.61	$C_{17}H_{20}O_9$	3-O-Feruloylquinic
3	10.82	$C_{20}H_{24}NO_4$	Magnoflorine
4	12.5	$C_{22}H_{22}NO_{10}$	Calycosin-7-O- $\beta$ -D-glucoside
5	13.04	$C_{10}H_{10}O_4$	Ferulic acid
6	13.2	$C_{12}H_{16}O_4$	Senkyunolide I
7	14.17	$C_{22}H_{24}NO_4^+Cl^-$	Tetradehydroscoulerine
8	15.22	$C_{22}H_{22}NO_{10}$	Calycosin-7-O- $\beta$ -D-glucoside-6''-O-malonate
9	15.81	$C_{20}H_{20}NO_4$	Jatrorrhizine
10	16.01	$C_{22}H_{22}O_9$	Ononin
11	16.08	$C_{20}H_{18}NO_4$	Epiberberine
12	16.21	$C_{19}H_{14}NO_4$	Coptisine
13	16.67	$C_{24}H_{26}O_{10}$	(6aR,-11aR)-3-Hydroxy-9,10-dimethoxypterotharpan-3-O- $\beta$ -D-glucoside
14	17.6	$C_{12}H_{12}O_2$	Z-Butylidenephthalide
15	18.12	$C_{21}H_{25}NO_4$	Palmatine
16	18.31	$C_{20}H_{18}NO_4$	Berberine
17	18.47	$C_{16}H_{12}O_5$	Calycosin
18	23.19	$C_{16}H_{12}O_4$	Formononetin

Animal Care and Use Committee of the National Institute of State Scientific and Technological Commission.

**2.4. Induction AA.** BALB/c mice, except mice in the normal group, received a sublethal total body irradiation dose of 3.5 Gy from Model 143  $^{137}$ Cesium  $\gamma$ -irradiator one hour before lymph node cell infusion. Inguinal, brachial, and axillary infusion of lymph node cells were obtained from female DBA/2 mice. Lymph cells ( $1 \times 10^6$ ) were injected into BALB/c mice through the tail vein for inducing AA [9].

**2.5. Drug Treatment.** The treatment was initiated after lymph node cell infusion and lasted for 28 days. Mice were randomly divided into four groups: normal group, mice were fed the control diet and orally administered sterile saline; model group, mice were fed the same as the normal group; cyclosporine (CsA) group, CsA (batch number H10960122, Zhongmei Huadong Pharmaceutical Co. Ltd., Hangzhou, China) mice were fed the same control diet and orally daily administered 25 mg/kg CsA daily for 28 days; and DGBX group, mice were fed the same control diet and orally administered 6.3 g/kg DGBX daily for 28 days. The mice were sacrificed on the 29th day after treatment. Mice were anesthetized by isoflurane anesthesia (2-3% isoflurane with oxygen supply). Peripheral blood samples were collected by removing eyeballs, and BMCs were obtained by femoral cavity flushing.

**2.6. Enzyme-Linked Immunosorbent Assay.** Twenty-four hours after the last administration, 0.8 mL of peripheral blood was collected from each mouse by eyeball extirpation. Sera were isolated by centrifuging at 3000 rpm and 4°C for 10 min. The concentrations of interferon  $\gamma$  (IFN $\gamma$ ), interleukin-2 (IL-2), and tumor necrosis factor  $\alpha$  (TNF $\alpha$ )

were measured using ELISA kits (eBioscience, San Diego, CA, USA), according to the instructions provided by the manufacturer.

**2.7. Fluorescence-Activated Cell Sorter Analysis.** BMCs were obtained by femoral cavity flushing and filtered through a 200-eye cell sieve mesh to obtain a single-cell suspension. To quantify the percentage of HSCs, CD117- and sac-1-positive cells were washed and stained with anti-mouse CD117 (c-Kit) FITC and anti-mouse Ly-6A/E (Sca-1) PE antibodies (eBioscience). For the detection of apoptosis in BMCs, an Annexin V-FITC Apoptosis Detection Kit (eBioscience) was used. BMCs were stained with FITC-conjugated annexin V and propidium iodide (PI). Flow cytometry was performed using a fluorescence-activated cell sorter Calibur cytometer and analyzed with CellQuest software (Beckman Coulter, Brea, CA, USA).

**2.8. Immunofluorescence.** To examine the expression and distribution of T-bet in BMCs, cells were fixed, permeabilized, and incubated with anti-human/mouse T-bet PE (1:100) (eBioscience). To identify changes in binding of signaling lymphocyte activation molecule (SLAM) and SLAM-associated protein (SAP), cells were stained with anti-mouse CD150/SLAM PE antibody (1:50) (eBioscience). After permeabilization, cells were incubated with SH2D1A/SAP antibody (FITC) (1:100) (EterLife, Birmingham, UK). Confocal fluorescence microscopy images were captured using a Leitz/Leica TCSSP2 microscope (Leica Lasertechnik GmbH, Heidelberg, Germany). The fluorescence intensity was quantified with ImageJ. At least 50 cells from 3 different areas of each chamber were measured.

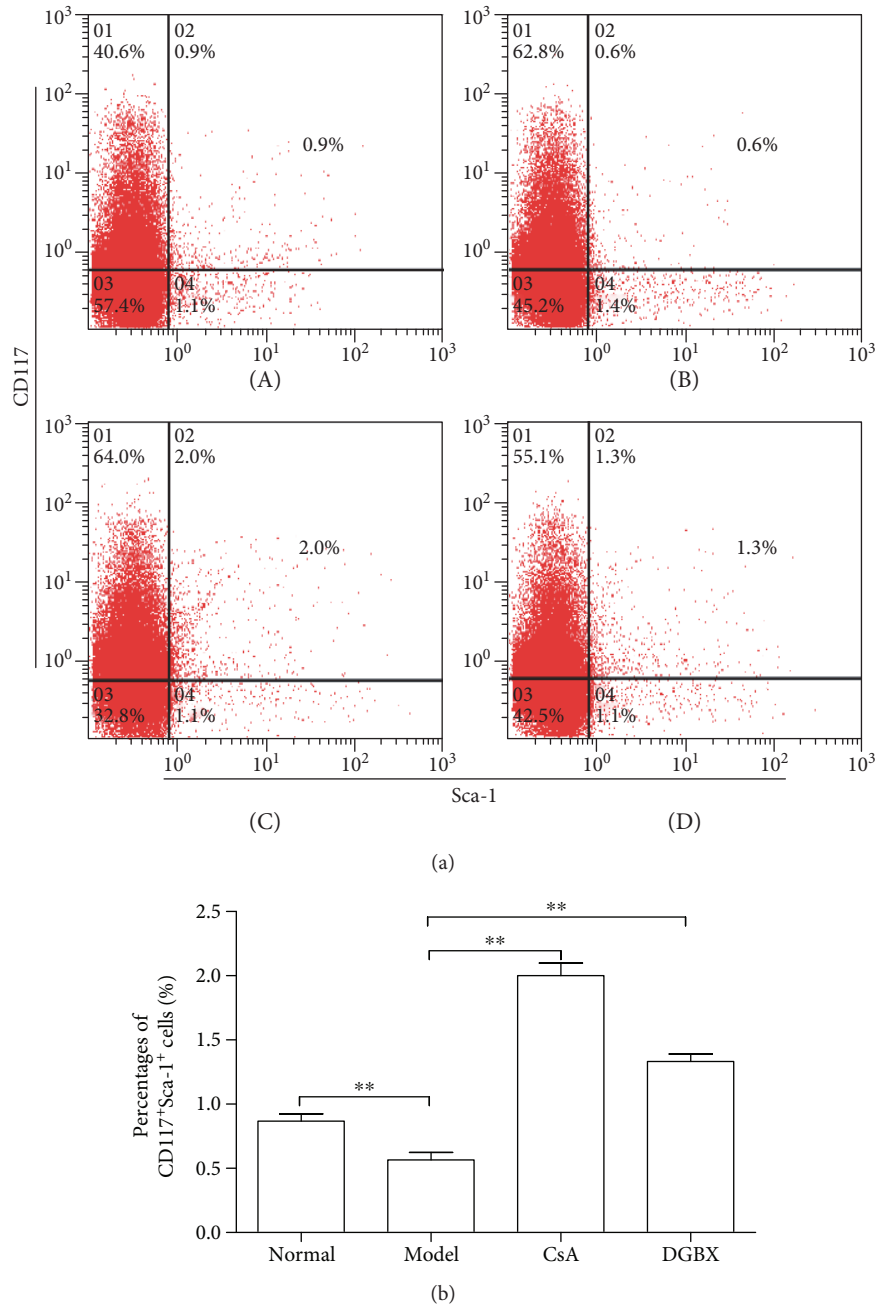


FIGURE 2: Effects of DGBX on proliferation of hematopoietic stem cells in bone marrow of mice with aplastic anemia (AA). (a) The percentage of CD117+Sca-1<sup>+</sup> hematopoietic stem cells in the bone marrow cells of mice after 4 weeks of treatment. A, normal group, B, model group, C, group treated with cyclosporine A, and D, group treated with DGBX. (b) Results are presented in the bar charts. Data are presented as mean  $\pm$  SD,  $n = 6$ . \*\* $P < 0.01$ .

2.9. *Western Blot Analysis.* BMCs ( $1 \times 10^7$ ) from each mouse were lysed in 0.5 mL of lysis buffer (Sigma, St. Louis, MO, USA). The extracts were cleared by centrifuging at 10,000g and 4°C for 15 min and diluted with the lysis buffer to achieve about 2 mg/mL protein concentration. Protein samples were separated on 10% SDS-PAGE and transferred onto nitrocellulose membranes (Amersham Pharmacia Biotech, Uppsala, Sweden). The membranes were incubated with primary

antibodies, including anti-T-bet/Tbx21 antibody (1:1000), anti-Fas antibody (1:1000) (Abcam, Cambridge, MA, USA), and anti-mouse-caspase-3, anti-mouse-cleaved caspase-3 antibody, anti-mouse-eukaryotic initiation factor 2 (eIF2)  $\alpha$  (D7D3), anti-mouse-phospho-eIF2 $\alpha$  (Ser51) (D9G8), anti-mouse-Fyn, anti-mouse interferon regulatory factor-1 (IRF-1), anti-mouse-signal transducer and activator of transcription (Stat) 1, and anti-mouse-Stat3 rabbit monoclonal

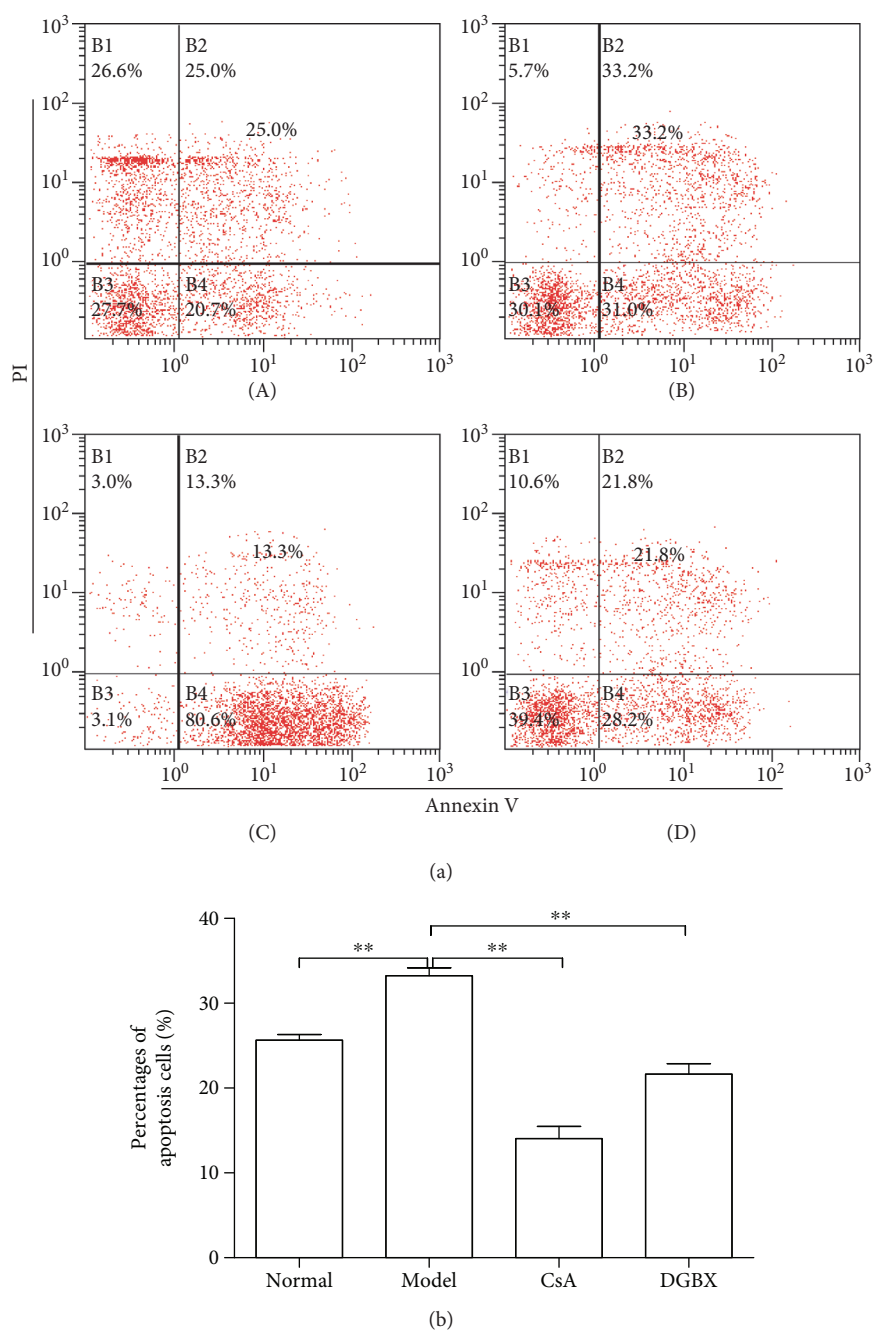


FIGURE 3: DGBX suppresses apoptosis of bone marrow cells in mice with aplastic anemia (AA). (a) The percentages of annexin V<sup>+</sup> PI<sup>+</sup> cells in bone marrow of mice after 4 weeks of treatment. A, normal group, B, model group, C, group treated with cyclosporin A, and D, group treated with DGBX. (b) Results are presented in the bar charts. Data are presented as mean  $\pm$  SD,  $n = 6$ . \*\* $P < 0.01$ .

antibodies (1:1000, CST, Boston, MA, USA) and incubated with horseradish peroxidase-conjugated secondary antibody (CST). All immunoreactive proteins were visualized with SuperSignal West Pico Chemiluminescent Substrate (Thermo Scientific, Rockford, IL, USA). Densitometry plots showing protein expression were normalized to GAPDH.

**2.10. Statistical Analysis.** All data were presented as mean  $\pm$  standard deviation (S.D.). The statistical analyses were performed using SPSS13.0 (SPSS Inc., Chicago, USA). One-way

analyses of variance (ANOVA) followed by the Tukey-Kramer test for multiple comparisons were used to compare the treatment groups. A  $P$  value of  $<0.05$  was considered statistically significant.

### 3. Results

**3.1. Characteristics of Pure Compounds from the Herbal Formula DGBX.** In this study, high-resolution MS was performed in negative and positive ion modes to obtain

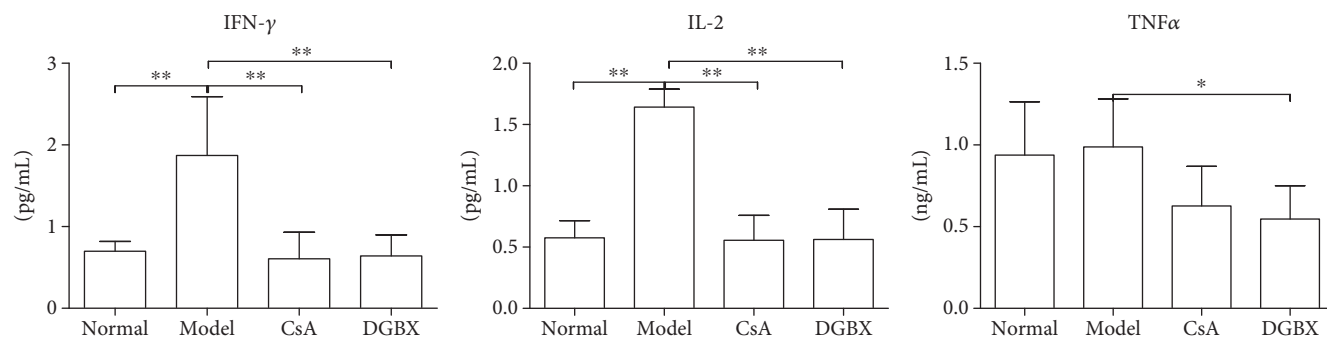


FIGURE 4: Evaluation of interferon  $\gamma$  (IFN $\gamma$ ), interleukin-2 (IL-2), and tumor necrosis factor  $\alpha$  (TNF $\alpha$ ) levels in sera of mice with aplastic anemia (AA) after treatment by using enzyme-linked immunosorbent assay. The results are presented in the bar chart. Data are presented as mean  $\pm$  SD,  $n = 6$ . \* $P < 0.05$ , \*\* $P < 0.01$ .

complete information about the chemical constitution of DGBX. The peak MS spectrum has been presented in Figure 1. Eighteen constituents were identified based on the accurate mass and relative ion abundance of the target peaks. The identified compounds are shown in Table 1.

**3.2. Effects of DGBX on Proliferation and Apoptosis of HSCs in AA Mouse Model.** Sca-1 and c-kit (CD117) are the major phenotypic markers for mouse HSPC subset [10]. Therefore, we quantified CD117<sup>+</sup>Sca-1<sup>+</sup> cells to assess the percentages of HSCs in total BMCs. As shown in Figure 2, the amount of HSCs in model group significantly decreased compared with that in normal group ( $P < 0.01$ ). HSC proliferation was significantly induced in DGBX group compared with that in the model group ( $P < 0.01$ ).

We also observed the percentage of apoptosis in BMCs by AnnexinV-PI staining using a flow cytometer. The apoptosis ratio of BMCs in model group was significantly higher than that in normal group ( $P < 0.01$ ). DGBX significantly inhibited the apoptosis of BMCs; apoptosis ratio in DGBX group significantly lower than that in model group ( $P < 0.01$ ) (Figure 3).

**3.3. Inhibition of IFN $\gamma$ , TNF $\alpha$ , and IL-2 Production in AA Mice by DGBX.** As shown in Figure 4, the levels of IFN $\gamma$  and IL-2 in model group were significantly higher than those in normal group ( $P < 0.01$ ), and there was no significant difference in TNF $\alpha$  levels between the groups. After treatment with CsA and DGBX, the abnormally high levels of IFN $\gamma$  and IL-2 significantly decreased ( $P < 0.01$ ) and the levels of TNF $\alpha$  also significantly decreased compared with that in the model group ( $P < 0.05$ ). These results indicated that DGBX treatment could inhibit the production of inflammatory factors and that the inhibitory effect of DGBX was equivalent to that of CsA.

**3.4. Effects of DGBX on Activation of SLAM/SAP Signaling Pathway.** The SLAM-SAP signaling is an important pathway in T cell activation when engaged with ligands of T cell receptor [11]. SAP/SLAM recruits Fyn (a member of the Src family of kinases) that inhibits the expression of IFN $\gamma$  [12]. As shown in Figure 5, immunofluorescence analysis showed that the SLAM/SAP double-stained cells in the bone marrow of

AA mice significantly decreased compared with that in normal group ( $P < 0.01$ ) and the decline was significantly inhibited by DGBX treatment ( $P < 0.01$ ) (Figure 5). However, DGBX treatment had no effect on the protein expression of Fyn.

**3.5. DGBX Interferes with T-bet Expression and Distribution in AA Mice.** T-bet, a transcription factor, binds to the IFN $\gamma$  promoter region and induces gene expression [13]. As shown in Figure 6, the T-bet<sup>+</sup>-stained cells significantly increased in bone marrow of AA mice ( $P < 0.01$ ) and T-bet expression significantly increased ( $P < 0.01$ ) compared with that in normal group. DGBX treatment significantly inhibited the levels of T-bet<sup>+</sup> cells and protein expression. Furthermore, the regulatory effect of DGBX was equivalent to CsA.

**3.6. Effects of DGBX on Activation of Eukaryotic Initiation Factor 2 $\alpha$  in BMCs of AA Mice.** Phosphorylation of the  $\alpha$ -subunit of eIF2 is a well-documented mechanism of downregulation of protein synthesis under various stress conditions. Western blot analysis demonstrated that eIF2 $\alpha$  expression in BMCs was not different between the groups. The phosphorylation level of total eIF2 $\alpha$  in DGBX group showed a decreasing trend compared with that in the model group ( $P < 0.05$ ) (Figure 7).

**3.7. DGBX Regulates Expression of Key Molecules of Fas-Mediated Apoptosis Signaling Pathway in BMCs of AA Mice.** As shown in Figure 8, the levels of Fas, caspase-3, and cleaved caspase-3 in model group were significantly higher than those in normal group ( $P < 0.01$ ). DGBX significantly down-regulated the expression of caspase-3 and cleaved caspase-3 compared with that in the model group ( $P < 0.05$  or  $P < 0.01$ ). Interestingly, the regulatory effects of DGBX were superior to those of CsA. However, DGBX did not exert a regulatory effect on the expression of Fas in BMCs of AA mice.

**3.8. DGBX Regulates Expression of Interferon Regulatory Factor 1 and Signal Transducer and Activator of Transcription 1 and 3 (Stat1 and Stat3) in BMC of AA Mice.** IRFs play an important role in the defense against pathogens, autoimmunity, lymphocyte development, cell growth, and susceptibility to transformation. Some effects of IFN $\gamma$  are mediated through IRF-1, which inhibits the transcription of

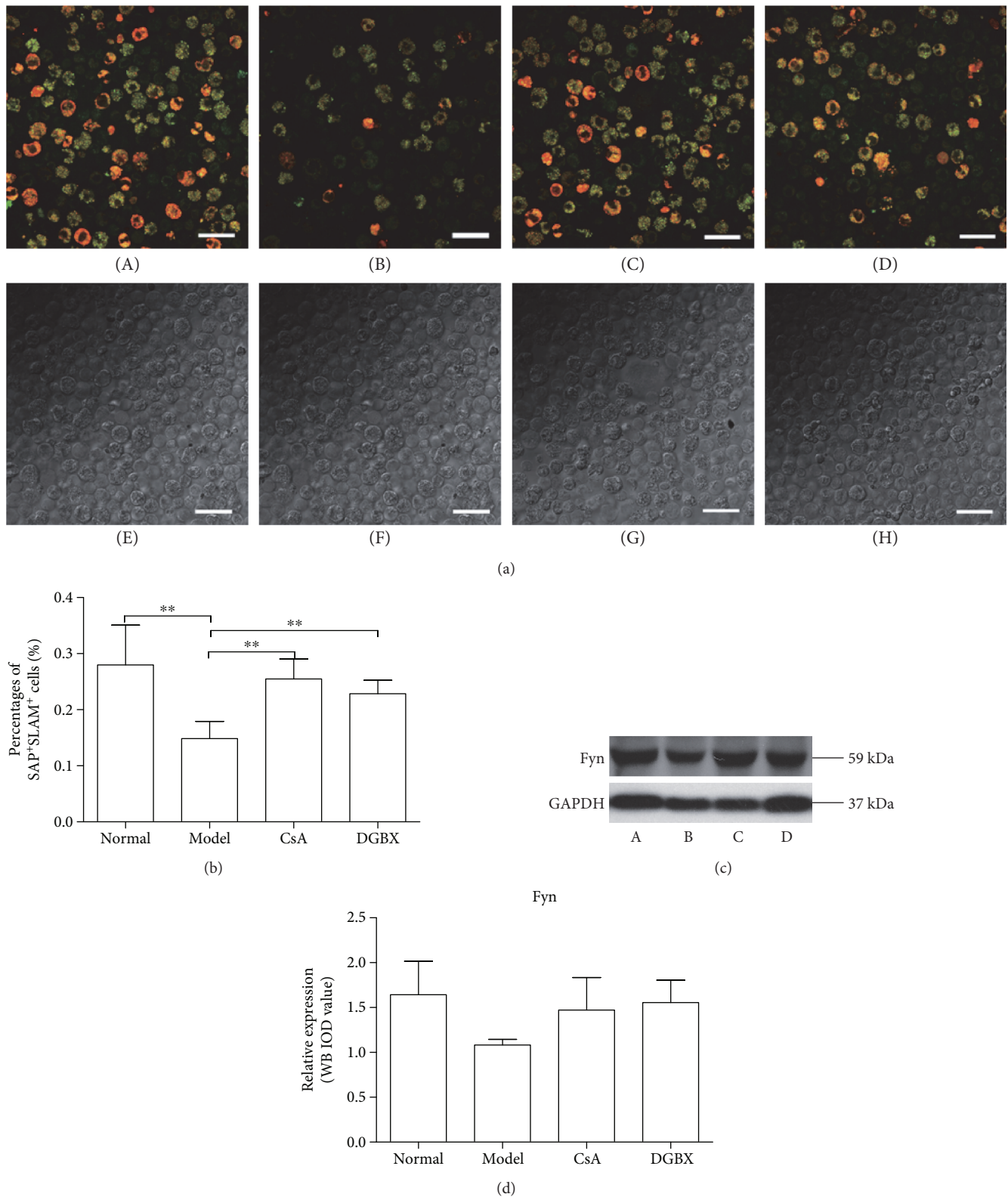
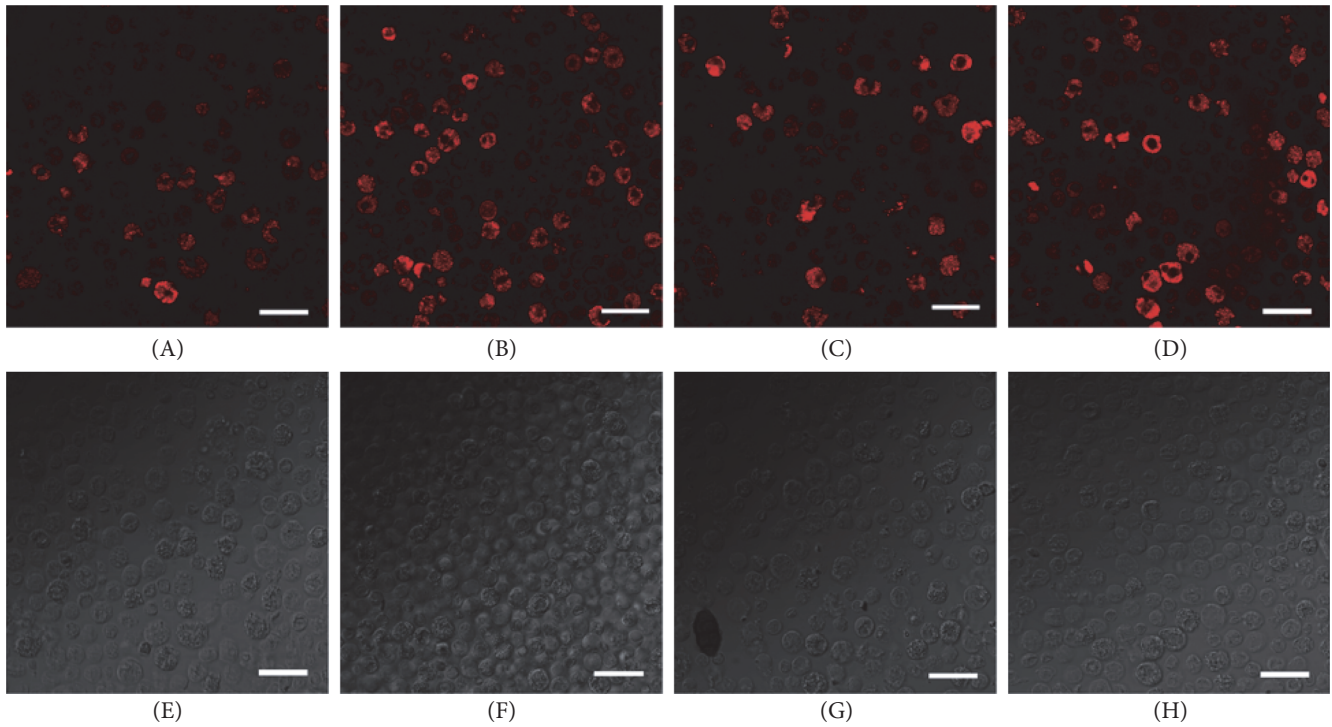
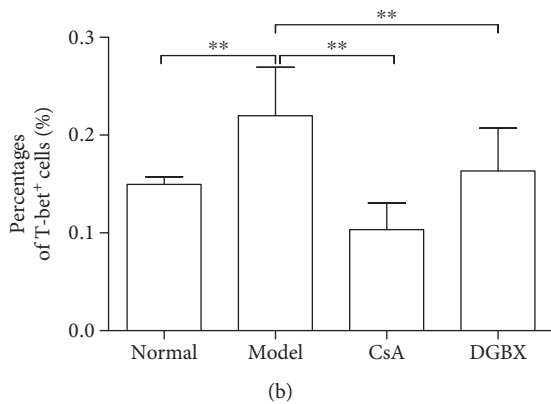


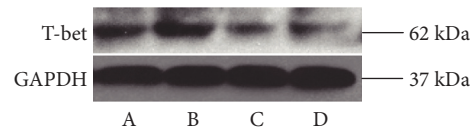
FIGURE 5: DGBX attenuates interferon  $\gamma$  (IFN $\gamma$ ) expression by regulating the activation of SLAM/SAP signal. (a) BMCs were stained for CD150/SLAM (red) and SH2D1A/SAP (green) antibodies and observed by confocal immunofluorescence microscopy. The bottom pictures were obtained in bright field. The double-stained cells (yellow) were quantified with ImageJ. (b) Results are presented in the bar charts. The scale bar corresponds to 100  $\mu$ m throughout. A, normal group, B, model group, C, group treated with cyclosporin A, and D, group treated with DGBX. (c) Fyn was assessed in whole BMC lysates by Western blot analysis. (d) The results are presented in the bar chart. GAPDH was used as an internal control. Data are presented as mean  $\pm$  SD,  $n = 6$ . \*\* $P < 0.01$ .



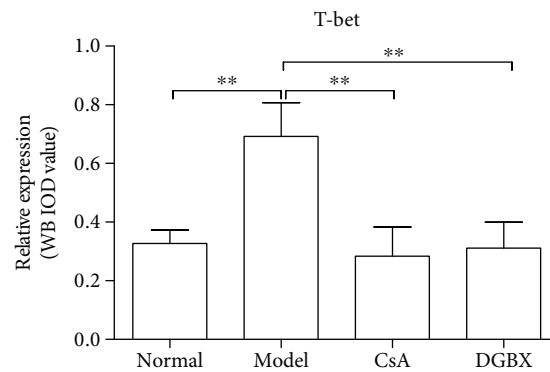
(a)



(b)



(c)



(d)

FIGURE 6: Expression and distribution of T-bet in bone marrow cells (BMCs) of mice with aplastic anemia (AA) after treatment. (a) Staining for T-bet (red) in BMCs was observed by confocal immunofluorescence microscopy. The bottom pictures were obtained in bright field. The stained cells (red) were quantitated with ImageJ. (b) Results are presented in the bar charts. The scale bar corresponds to 100  $\mu\text{m}$  throughout. A, normal group, B, model group, C, group treated with cyclosporin A, and D, group treated with DGBX. (c) The expression of T-bet was evaluated in whole BMC lysates by Western blot analysis. (d) The results are presented in the bar chart. Data are presented as mean  $\pm$  SD,  $n = 6$ . \*\* $P < 0.01$ .

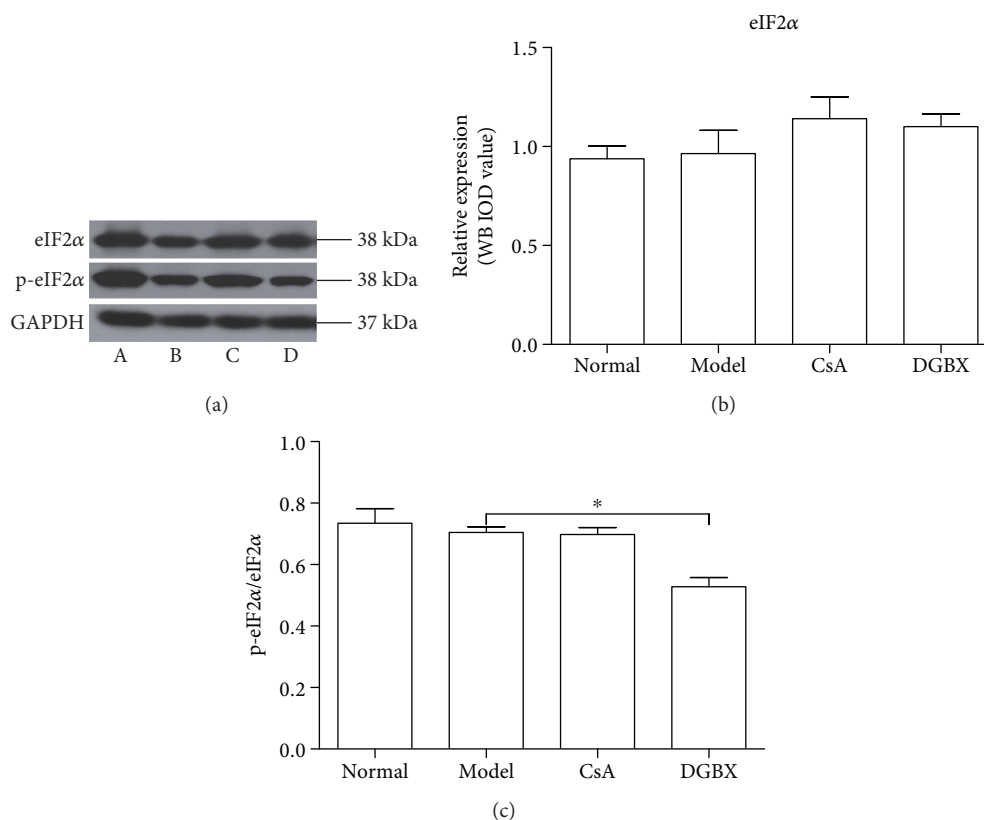


FIGURE 7: Effects of DGBX on phosphorylation of eIF2 $\alpha$  in bone marrow cells (BMCs) of mice with aplastic anemia (AA). (a) The expressive levels of eIF2 $\alpha$  and phospho-eIF2 $\alpha$  were estimated in whole BMC lysates by Western blot analysis. (b) Results are presented in the bar charts. A, normal group, B, model group, C, group treated with cyclosporin A, and D, group treated with DGBX. (c) The ratio of phospho-eIF2 $\alpha$  and total eIF2 $\alpha$  is presented in the bar chart. GAPDH was used as the internal control. Data are presented as mean  $\pm$  SD,  $n = 6$ . \* $P < 0.05$ .

cellular genes and entry into the cell cycle. Stat1 and Stat3 contribute to this function [12]. The protein levels of Stat1 in the model group were significantly higher than those in AA mice ( $P < 0.01$ ). DGBX downregulated the abnormally high expression of Stat1 ( $P < 0.05$ ), but had no regulatory effect on the expression of IRF-1 (Figure 9).

#### 4. Discussion

In TCM, combinatory therapeutic strategies based on patient symptoms and characteristics are often adopted to treat several diseases [14]. The Chinese herb formulae consist of several types of medicinal herbs or minerals, and multiple components could act on multiple targets and exert synergistic therapeutic efficacies [15]. Recently, LC-MS becomes an essential tool for analyzing the compounds of the herbal constituents in TCM complex formulae [16]. Eighteen constituents were identified by high-performance liquid chromatography-electrospray ionization/mass spectrometry from freeze-dried boiled aqueous extract of DGBX. The major components of DGBX-lyophilized powder were identified to be magnoflorine (3), tetradehydroscoulerine (7), jatrorrhizine (9), ononin (10), epiberberine (11), coptisine (12), palmatine (15), berberine (16), and calycosin (17) by Peak View Software analysis. Magnoflorine exhibits immunomodulatory effects on neutrophil and T cell-mediated

immunity [17]. Coptisine can inhibit IL-1 $\beta$ -induced inflammatory response by suppressing the nuclear factor-kappa B (NF- $\kappa$ B) signaling pathway [18]. Jatrorrhizine plays a critical cell-protective role in H<sub>2</sub>O<sub>2</sub>-induced cell apoptosis owing to its antioxidative property [19]. Palmatine plays an important role in osteoclast apoptosis by regulating the inducible nitric monoxide synthase (iNOS) system [20]. Berberine can also decrease cell apoptosis induced by LPS by suppressing iNOS protein expression [21]. Calycosin reduces oxidative stress by regulating the activation of the PI3K/Akt/GSK-3 $\beta$  signaling pathway and suppressing osteoclastogenesis through inhibition of MAPK and NF- $\kappa$ B activation [22]. AA is an acquired bone marrow failure syndrome resulting from immune-mediated destruction of HSC. Therefore, we suggest that the functions of these herbal constituents of DGBX contribute to interaction with multiple targets and exert synergistic therapeutic efficacy in immunosuppression and hematopoiesis against AA.

Dysregulation in HSC cycling contributes to AA by enhancing differentiation over self-renewal or inducing apoptosis of HSCs [23]. Acquired AA exhibits increased levels of circulating IFN $\gamma$ . IFNs have the pathogenic functions of impairing the proliferation of primitive HSPCs [24] and inducing apoptosis [25]. These evidences support that IFNs can impair hematopoiesis by attenuating HSC function. Antigen-presenting cells present antigens to T lymphocytes

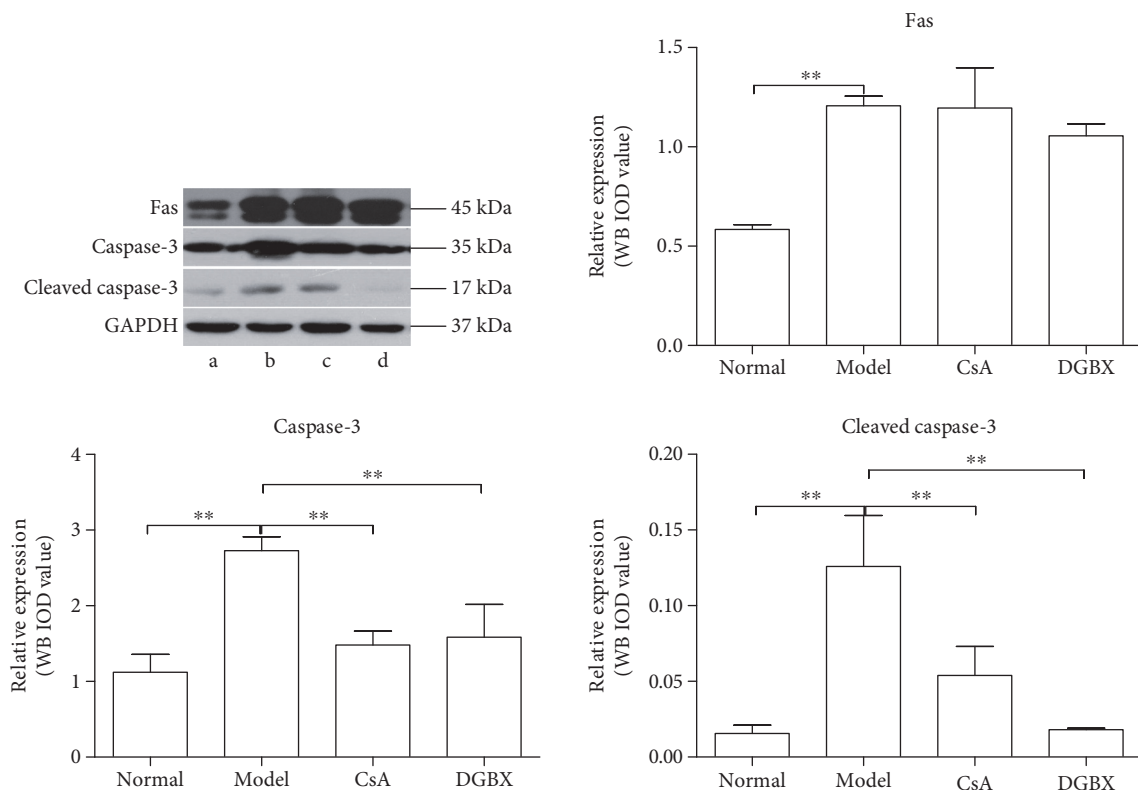


FIGURE 8: Effect of DGBX on the expressions of key molecule of Fas-dependent apoptosis pathway in AA mice. The protein levels of Fas, caspase-3, and cleave caspase-3 were estimated in whole BMC lysates by Western blot analysis. Results are presented in the bar charts. Data are presented as means  $\pm$  SD,  $n = 6$ . \*\* $P < 0.01$ .

and trigger T cells to proliferate. The prototypical Th1 transcription factor T-bet binds to the IFN $\gamma$  gene promoter region and induces gene expression [26]. CD150/SLAM is a prototypical member of glycoprotein receptors on hematopoietic cells. It is unique in its binding to the signaling molecule SAP [27]. The binding of SAP and Fyn modulates the SLAM function in IFN $\gamma$  expression and then decreases IFN $\gamma$  gene transcription [12]. Constitutive T-bet expression and low SAP levels are observed in AA. Activated T cells also produce proinflammatory cytokine at abnormal levels. Increased production of IL-2 leads to polyclonal expansion of T cells. These immune responses initiate the immune-mediated T cell destruction of BMCs. We observed that the levels of circulating IFN $\gamma$ , TNF $\alpha$ , and IL-2 in AA mice decreased to levels similar to those of normal group after treatment with DGBX. The quantity of SLAM/SAP double-stained cells significantly decreased, and the expression of Fyn was suppressed in BMCs by DGBX treatment. In addition, DGBX could inhibit the expression of T-bet, decreasing the level of T-bet-positive cells in the bone marrow. We believe that the immunosuppressive mechanisms of DGBX include SLAM-mediated T cell proliferation and IFN $\gamma$  production for attenuating the immune-mediated destruction of bone marrow.

In the pathogenesis of the immune destruction of hematopoiesis, aberrant immune response induced IFN $\gamma$  production as well as TNF $\alpha$  and IL-2. IFN $\gamma$  and TNF $\alpha$  activate the T cell cellular receptors and Fas receptor [28]. Trimerization

of Fas receptor interacts with Fas-associated death domain, activates caspase-3, and ultimately promotes HSC apoptosis [29]. IFN $\gamma$  can also activate the cell signaling cascade of IRF-1, contributing to the inhibition of the transcription of cellular genes and induction of eIF-2 phosphorylation for suppressing protein synthesis. IFN $\gamma$  induces IRF-1 binding to IFN-stimulated response elements, subsequently activating Stat1 and Stat3, inducing gene transcription associated with inflammation, and contributing to the immune-mediated destruction of the bone marrow [30]. This pathophysiology results in hematopoietic failure in AA. In this study, we found that the expression of phosphor-eIF2 $\alpha$ , Stat1, Stat3, and caspase-3 significantly decreased in AA mice treated with DGBX. There were no regulatory effects of DGBX on the expression of Fas and IRF-1. These results indicated that DGBX could inhibit the aberrant immune response and the apoptosis of HSCs by modulating the activation of Stat/JAK/IRF-1 pathway and Fas-dependent pathway.

CsA is a calcineurin inhibitor. It has selective effect on T cell functions by direct inhibition of the expression of nuclear regulatory proteins, contributing to reduction of T cell proliferation and activation. Severe AA can respond to CsA alone. Allogeneic bone transplantation and immunosuppressive treatment with antithymocyte globulin and CsA can significantly increase the 10-year survival rate in patients with severe AA [31]. In this study, we also assessed the significant



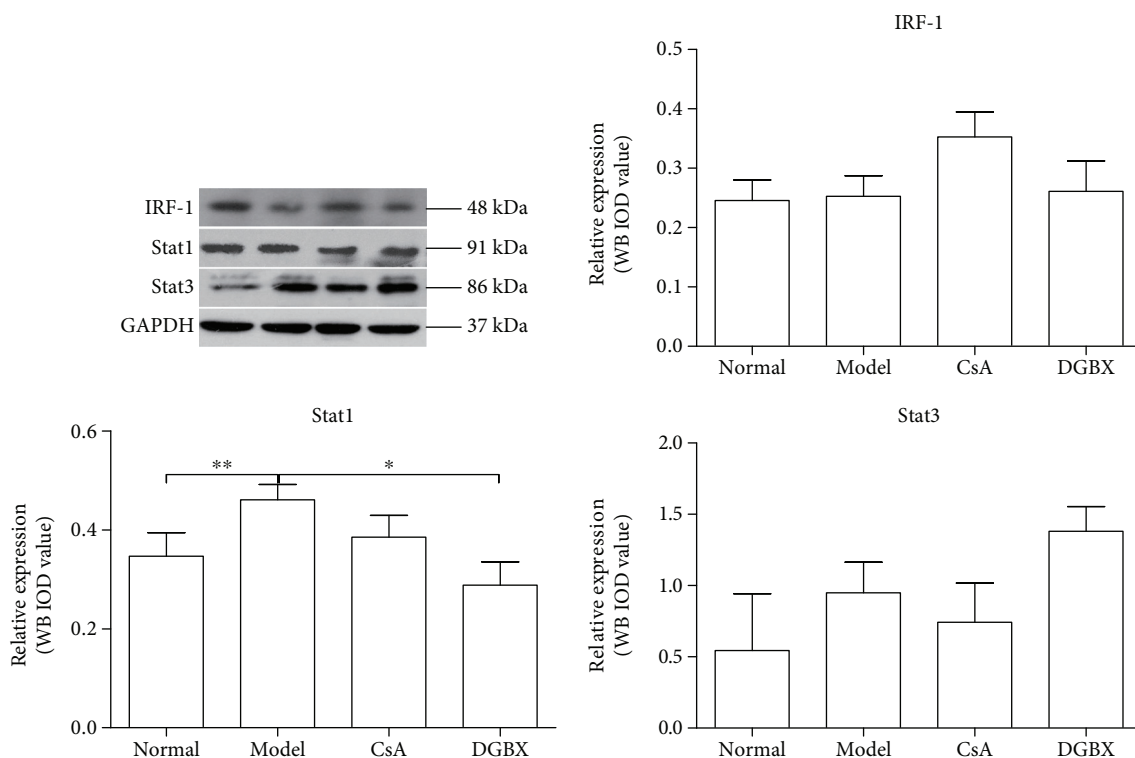


FIGURE 9: Effects of DGBX on regulation of expression of key molecules of interferon regulatory factor-1-mediated JAK/Stat signaling pathway in mice with aplastic anemia (AA). IRF-1, Stat1, and Stat3 expressions were estimated in whole BMC lysates by Western blot analysis. Data are presented as mean  $\pm$  SD,  $n = 6$ . \* $P < 0.05$ , \*\* $P < 0.01$ .

effects of CsA on the inhibition of proinflammatory cytokine and related protein expression, which participate in the immune response. CsA has many side effects, such as kidney damage and hepatotoxicity. These side effects can be managed by dose reduction [12]. Multiherbal formulas based on traditional medicine have been scientifically verified for use in complementary and alternative therapy for various diseases. Formulae composed of a mixture of natural products can target multiple sites. In our study, DGBX was verified as an effective medicine for AA treatment. It can also avoid kidney damage, hepatotoxicity, and other adverse reactions of drugs including CsA. Our results indicated that the immunosuppressive effects that aided recovery of the hematopoietic function of HSCs in hematogenesis in AA mice were equivalent or exceeded those of CsA.

## 5. Conclusions

Our data indicated that DGBX could attenuate  $\text{IFN}\gamma$  production by interfering in SLAM/SAP signaling and production and distribution of T-bet in T cells, exert immunosuppressive effects by modulating the activation of the Stat/JAK/IRF-1 pathway, restrain cell apoptosis by intervening in Fas-dependent pathway, and eventually attenuate immune-mediated destruction of HSCs, repair hematopoietic failure, and recover the hematopoietic function of HSCs in hematogenesis for AA therapy. DGBX can be used in traditional medicine against AA as a complementary and alternative immunosuppressive therapeutic formula.

## Conflicts of Interest

The authors declare that there is no potential conflict of interest.

## Authors' Contributions

Jingwei Zhou, Xue Li, Peiyong Deng, and Yi Wei contributed equally to this work.

## Acknowledgments

This work was supported by the National Natural Science Foundation of China (no. 81373583).

## References

- [1] A. M. Risitano, "Immunosuppressive therapies in the management of immune-mediated marrow failures in adults: where we stand and where we are going," *British Journal of Haematology*, vol. 152, no. 2, pp. 127–140, 2011.
- [2] M. M. Horowitz, "Current status of allogeneic bone marrow transplantation in acquired aplastic anemia," *Seminars in Hematology*, vol. 37, no. 1, pp. 30–42, 2000.
- [3] S. Rosenfeld, D. Follmann, O. Nunez, and N. S. Young, "Antithymocyte globulin and cyclosporine for severe aplastic anemia: association between hematologic response and long-term outcome," *Journal of the American Medical Association*, vol. 289, no. 9, pp. 1130–1135, 2003.

- [4] W. L. Wang, S. Y. Sheu, Y. S. Chen et al., "Enhanced bone tissue regeneration by porous gelatin composites loaded with the Chinese herbal decoction Danggui Buxue Tang," *PLoS One*, vol. 10, no. 6, article e0131999, 2015.
- [5] M. Yang, G. C. Chan, R. Deng et al., "An herbal decoction of Radix astragali and Radix angelicae sinensis promotes hematopoiesis and thrombopoiesis," *Journal of Ethnopharmacology*, vol. 124, no. 1, pp. 87–97, 2009.
- [6] Y. Liu, H. G. Zhang, and X. H. Li, "A Chinese herbal decoction, Danggui Buxue Tang, improves chronic fatigue syndrome induced by food restriction and forced swimming in rats," *Phytotherapy Research: PTR*, vol. 25, no. 12, pp. 1825–1832, 2011.
- [7] X. Yang, C. G. Huang, S. Y. Du et al., "Effect of Danggui Buxue Tang on immune-mediated aplastic anemia bone marrow proliferation mice," *Phytomedicine: International Journal of Phytotherapy and Phytopharmacology*, vol. 21, no. 5, pp. 640–646, 2014.
- [8] J. Wang, T. Zhang, L. Zhu, C. Ma, and S. Wang, "Anti-ulcerogenic effect of Zuojin pill against ethanol-induced acute gastric lesion in animal models," *Journal of Ethnopharmacology*, vol. 173, pp. 459–467, 2015.
- [9] J. Li, H. Chen, Y. B. Lv et al., "Intraperitoneal injection of multipotent pluripotent stem cells treatment on a mouse model with aplastic anemia," *Stem Cells International*, vol. 2016, Article ID 3279793, 6 pages, 2016.
- [10] S. E. Vazquez, M. A. Inlay, and T. Serwold, "CD201 and CD27 identify hematopoietic stem and progenitor cells across multiple murine strains independently of kit and Sca-1," *Experimental Hematology*, vol. 43, no. 7, pp. 578–585, 2015.
- [11] H. C. Chuang, J. D. Lay, W. C. Hsieh et al., "Epstein-Barr virus LMP1 inhibits the expression of SAP gene and upregulates Th1 cytokines in the pathogenesis of hemophagocytic syndrome," *Blood*, vol. 106, no. 9, pp. 3090–3096, 2005.
- [12] N. S. Young, "Current concepts in the pathophysiology and treatment of aplastic anemia," *Hematology/the Education Program of the American Society of Hematology American Society of Hematology Education Program*, vol. 2013, pp. 76–81, 2013.
- [13] C. L. Williams, M. M. Schilling, S. H. Cho et al., "STAT4 and T-bet are required for the plasticity of IFN-gamma expression across Th2 ontogeny and influence changes in Ifng promoter DNA methylation," *Journal of Immunology*, vol. 191, no. 2, pp. 678–687, 2013.
- [14] T. Liu, H. Cao, Y. Ji et al., "Interaction of dendritic cells and T lymphocytes for the therapeutic effect of Dangguihuang decoction to autoimmune diabetes," *Scientific Reports*, vol. 5, article 13982, 2015.
- [15] L. Wang, G. B. Zhou, P. Liu et al., "Dissection of mechanisms of Chinese medicinal formula Realgar-Indigo naturalis as an effective treatment for promyelocytic leukemia," *Proceedings of the National Academy of Sciences of the United States of America*, vol. 105, no. 12, pp. 4826–4831, 2008.
- [16] Q. Chen, S. Xiao, Z. Li, N. Ai, and X. Fan, "Chemical and metabolic profiling of Si-Ni decoction analogous formulae by high performance liquid chromatography-mass spectrometry," *Scientific Reports*, vol. 5, article 11638, 2015.
- [17] W. Ahmad, I. Jantan, E. Kumolosasi, and S. N. Bukhari, "Standardized extract of *Tinospora crispa* stimulates innate and adaptive immune responses in Balb/c mice," *Food & Function*, vol. 7, no. 3, pp. 1380–1389, 2016.
- [18] K. Zhou, L. Hu, W. Liao, D. Yin, and F. Rui, "Coptisine prevented IL-beta-induced expression of inflammatory mediators in chondrocytes," *Inflammation*, vol. 39, no. 4, pp. 1558–1565, 2016.
- [19] T. Luo, X. Shen, S. Li, T. Ouyang, and H. Wang, "The protective effect of jatrorrhizine against oxidative stress in primary rat cortical neurons," *CNS & Neurological Disorders Drug Targets*, vol. 15, 2016.
- [20] S. Ishikawa, M. Tamaki, Y. Ogawa et al., "Inductive effect of palmatine on apoptosis in RAW 264.7 cells," *Evidence-Based Complementary and Alternative Medicine: eCAM*, vol. 2016, Article ID 7262054, 9 pages, 2016.
- [21] J. S. Shin, H. E. Choi, S. Seo, J. H. Choi, N. I. Baek, and K. T. Lee, "Berberine decreased inducible nitric oxide synthase mRNA stability through negative regulation of human antigen R in lipopolysaccharide-induced macrophages," *The Journal of Pharmacology and Experimental Therapeutics*, vol. 358, no. 1, pp. 3–13, 2016.
- [22] G. H. Quan, H. Wang, J. Cao et al., "Calycosin suppresses RANKL-mediated osteoclastogenesis through inhibition of MAPKs and NF-kappaB," *International Journal of Molecular Sciences*, vol. 16, no. 12, pp. 29496–29507, 2015.
- [23] J. N. Smith, V. S. Kanwar, and K. C. MacNamara, "Hematopoietic stem cell regulation by type I and II interferons in the pathogenesis of acquired aplastic anemia," *Frontiers in Immunology*, vol. 7, p. 330, 2016.
- [24] A. M. de Bruin, O. Demirel, B. Hooibrink, C. H. Brandts, and M. A. Nolte, "Interferon-gamma impairs proliferation of hematopoietic stem cells in mice," *Blood*, vol. 121, no. 18, pp. 3578–3585, 2013.
- [25] E. M. Pietras, R. Lakshminarasimhan, J. M. Techner et al., "Re-entry into quiescence protects hematopoietic stem cells from the killing effect of chronic exposure to type I interferons," *The Journal of Experimental Medicine*, vol. 211, no. 2, pp. 245–262, 2014.
- [26] E. E. Solomou, K. Keyvanfar, and N. S. Young, "T-bet, a Th1 transcription factor, is up-regulated in T cells from patients with aplastic anemia," *Blood*, vol. 107, no. 10, pp. 3983–3991, 2006.
- [27] M. Morra, J. Lu, F. Poy et al., "Structural basis for the interaction of the free SH2 domain EAT-2 with SLAM receptors in hematopoietic cells," *The EMBO Journal*, vol. 20, no. 21, pp. 5840–5852, 2001.
- [28] J. Maciejewski, C. Sella, S. Anderson, and N. S. Young, "Fas antigen expression on CD34+ human marrow cells is induced by interferon gamma and tumor necrosis factor alpha and potentiates cytokine-mediated hematopoietic suppression in vitro," *Blood*, vol. 85, no. 11, pp. 3183–3190, 1995.
- [29] G. Kroemer, L. Galluzzi, and C. Brenner, "Mitochondrial membrane permeabilization in cell death," *Physiological Reviews*, vol. 87, no. 1, pp. 99–163, 2007.
- [30] M. S. Dickey, C. L. Hirota, N. J. Ronaghan et al., "Interferon-gamma suppresses intestinal epithelial aquaporin-1 expression via Janus kinase and STAT3 activation," *PLoS One*, vol. 10, no. 3, article e0118713, 2015.
- [31] M. Fuhrer, U. Rampf, I. Baumann et al., "Immunosuppressive therapy for aplastic anemia in children: a more severe disease predicts better survival," *Blood*, vol. 106, no. 6, pp. 2102–2104, 2005.

## Research Article

# Mahuang Fuzi Xixin Decoction Attenuates Th1 and Th2 Responses in the Treatment of Ovalbumin-Induced Allergic Inflammation in a Rat Model of Allergic Rhinitis

Mengyue Ren,<sup>1,2</sup> Qingfa Tang,<sup>1,2</sup> Feilong Chen,<sup>1,2</sup> Xuefeng Xing,<sup>1,2</sup> Yao Huang,<sup>1,2</sup> and Xiaomei Tan<sup>1,2</sup>

<sup>1</sup>School of Traditional Chinese Medicine, Southern Medical University, Guangzhou 510515, China

<sup>2</sup>Guangdong Provincial Key Laboratory of Chinese Medicine Pharmaceuticals, Southern Medical University, Guangzhou 510515, China

Correspondence should be addressed to Xiaomei Tan; [tanxm\\_smu@163.com](mailto:tanxm_smu@163.com)

Received 4 May 2017; Accepted 18 June 2017; Published 13 July 2017

Academic Editor: Yong Tan

Copyright © 2017 Mengyue Ren et al. This is an open access article distributed under the Creative Commons Attribution License, which permits unrestricted use, distribution, and reproduction in any medium, provided the original work is properly cited.

Allergic rhinitis (AR) is one of the most common allergic diseases, which adversely affect patients' quality of life. *Mahuang Fuzi Xixin* decoction (MFXD) has been widely used to treat AR in clinics in Asian countries. This study investigated the effect and possible therapeutic mechanisms of MFXD in the treatment of AR. A Wistar rat model of ovalbumin- (OVA-) induced AR was established and then treated with three doses of MFXD; AR symptoms, serum total immunoglobulin E, histamine, histopathological features, and release and expression of factors related to type 1 helper T (Th1) and type 2 helper T (Th2) responses were analyzed. Our study demonstrated that MFXD has a good therapeutic effect on OVA-induced allergic inflammation in an AR rat model as manifested in reduced frequencies of sneezing and nasal scratching and in reduced serum levels of total IgE and HIS. In addition, MFXD regulates imbalance in Th1/Th2 cells caused by AR by simultaneously attenuating Th1 and Th2 responses, such as by reducing the serum levels of IFN- $\gamma$  and IL-4 and mRNA expression levels of IFN- $\gamma$ , IL-4, GATA-3, and STAT-6. This study provided valuable information on the immunoregulatory effect of MFXD for the treatment of AR in future clinical studies.

## 1. Introduction

Allergic rhinitis (AR) is a type I allergic disease induced by an immunoglobulin E- (IgE-) mediated inflammation and characterized by paroxysmal nasal obstruction, rhinorrhea, nasal itching, and sneezing [1, 2]. As an extremely common disease, AR has affected more than 500 million people worldwide over the last 20 years [3]. AR is not a severe disease, but it significantly impacts patients' quality of life, school performance, and work productivity and is considered an economic burden; moreover, AR has multiple comorbidities, such as asthma, conjunctivitis, headache, nasal polyps, sinusitis, and otitis media [3, 4].

The allergic sensitization procedure for AR was well established in the 1970s. When persistently exposed to certain concentrations of allergens, an antigen-presenting cell

presents the allergens to CD4<sup>+</sup> T lymphocytes, which in turn release cytokines that stimulate B lymphocytes to differentiate into plasma cells; as a result, production of immunoglobulin E (IgE) is promoted. Individuals become sensitized when IgE antibodies bind to receptors on mast cells and eosinophils; when they are exposed to allergens once again, IgE-mediated inflammation is stimulated, resulting in AR symptoms [5–7].

The imbalance in type 1 helper T (Th1) cells and type 2 helper T (Th2) cells has been considered the main induction factor in IgE-mediated allergic inflammation [6, 8–11]. When infected with AR, the differentiated proportion into Th2 cells will increase significantly and interleukin-4 (IL-4) (mainly released by Th2 cells) secretion prominently increased to accelerate the production of IgE and simultaneously inhibit Th1 response such as the release of

interferon- $\gamma$  (IFN- $\gamma$ ), which is called the imbalance of Th1/Th2 [9, 12–14]. However, researchers have questioned the Th1/Th2 imbalance theory and the weakened immunological drive in the Th1 direction that leads to AR; Randolph et al. found that the Th1 response plays a dominant role in the early phase of ovalbumin- (OVA-) induced mouse airway inflammation [15].

The most popular medications currently used for AR are oral H1 antihistamines and intranasal corticosteroids, which are constantly combined with immunotherapy; these medications can control this allergic disease within either short or long term [5, 16]. However, a series of side effects, such as mild drowsiness, deep sleep, dizziness, lassitude, inability to concentrate, and arrhythmia, may occur during treatment [3]. Given these side effects, many patients have used complementary therapies, such as Chinese herbal medicine and acupuncture for the treatment of AR, and these therapies are used due to their few side effects and low toxicity [17–19].

*Mahuang Fuzi Xixin* decoction (MFXD) is an extract of a classical Chinese traditional formula consisting of *Ephedrae* (*Mahuang* in Chinese, dried herbaceous stems of *Ephedra sinica* Stapf), *Radix Aconiti Lateralis* (*Fuzi* in Chinese, dried lateral roots of *Aconitum carmichaelii* Debx), and *Asarum* (*Xixin* in Chinese, dried roots and rhizomes of *Asarum sieboldii* Miq.) at a dry weight ratio of 2:3:1; MFXD is used to treat common cold, migraine, asthma, rheumatoid arthritis, and AR [20, 21]. *Ephedrae* has been widely used in China to treat asthma and common cold, and alkaloids such as ephedrine and pseudoephedrine are its main effective constituents [22, 23]. Similarly, *Aconitum* alkaloids, especially lowly toxic monoester alkaloids, such as benzoylaconine, benzoylhypaconine, and benzoylmesaconine, have been identified as the main pharmacologic components of *Radix Aconiti Lateralis*, making it as an effective treatment against rheumatoid arthritis and asthma [24, 25]. *Asarum* has been generally used to treat common cold, migraine, and bronchitis, and its main effective components are the essential oils methyleugenol,  $\alpha$ -pinene, and safrole [26, 27]. MFXD is a traditional medicine used in China, Japan, and other Asian countries to treat AR; we previously demonstrated that MFXD is an effective treatment for allergic inflammation in a guinea pig model of AR [28]. However, the therapeutic mechanism of MFXD against allergic inflammation remains unclear.

In this study, a rat model of OVA-induced AR was used to investigate the effect of MFXD on allergic inflammation and Th1 and Th2 immune responses associated with AR were further examined to elucidate the possible therapeutic mechanisms of MFXD.

## 2. Materials and Methods

**2.1. Animal.** Specific pathogen-free (SPF) adult male Wistar rats ( $180 \pm 20$  g) were obtained from the Experimental Animal Center of Southern Medical University (number 44002100009161), and this study was approved by the Institutional Animal Care and Use Committee of Southern Medical University, Guangzhou, China (Approval number

L2016072). Rats were housed in the SPF Experimental Animal Center of Southern Medical University with a relative humidity of 40–70% and at a temperature of 20–24°C under lighting controls (12 h light/dark cycle). All rats had free access to standard food and water and were allowed to be acclimated for seven days before the experiment.

**2.2. Preparation of Herb Extract.** The preparation of MFXD was conducted as described in Treatise on Febrile Diseases, an ancient Chinese medical book. *Ephedrae* (60 g; Guangzhou Zhixin Chinese Medicine YinPian Co. Ltd., Guangzhou, China) was immersed in water (2700 mL) for 30 min and boiled for 20 min. *Radix Aconiti Lateralis* (90 g; Guangzhou Zhixin Chinese Medicine YinPian Co. Ltd., Guangzhou, China) and *Asarum* (30 g; Kangmei Pharmaceuticals Co. Ltd., Puning, China) were subsequently added and then simmered for another 90 min. Filtered water extract was concentrated to  $1.52 \text{ g}\cdot\text{mL}^{-1}$  under reduced pressure and then reconstituted in distilled water to achieve the required dose for all subsequent experiments.

**2.3. Fingerprint Analysis of MFXD through Ultra Performance Liquid Chromatography-Tandem Mass Spectrometry (UPLC-MS/MS).** UPLC-MS/MS was used to analyze the chemical composition of MFXD. Chromatographic analysis was performed on an Agilent 1290 Infinity LC system (Agilent Technologies, Wilmington, Delaware, USA) and on a 6410B Triple Quadrupole Mass Spectrometer (Agilent Technologies, USA). In brief, the analytes of MFXD were separated on a Zorbax SB-Aq column (100 mm  $\times$  2.1 mm, 3.5  $\mu\text{m}$ ; Agilent Technologies, USA) with a mobile phase consisting of acetonitrile (A) and 0.1% aqueous solution of formic acid (B); the following gradient program was used: 0% A at 0–2 min, 0% A–5% A at 2–5 min, 5% A at 5–8 min, 5% A–20% A at 8–15 min, 20% A–35% A at 15–28 min, 35% A–50% A at 28–31 min, 50% A–55% A at 31–36 min, 55% A–95% A at 36–45 min, and 95% A–100% A at 45–55 min. The injection volume was 1  $\mu\text{L}$ , the flow rate is 0.4 mL/min, and the column temperature was 25°C.

**2.4. Preparation of AR Rat Models and Drug Administration.** AR rat models were established as described previously [29] with minor modifications, as summarized in Figure 1. In brief, the rats were intraperitoneally sensitized with 0.3 mg of OVA (albumin egg, Sigma, MO, USA) and 30 mg of  $\text{Al}(\text{OH})_3$  (Damao Chemical Reagent Factory, China) dissolved in 1 mL of physiological saline once every other day for 2 weeks. The rats were subsequently challenged through nasal instillation with 50  $\mu\text{L}$  of OVA solution (5%, dissolved in physiological saline) into each nasal cavity once daily from day 15 to day 21. Forty AR rats were randomly divided into five groups (eight rats per group), namely, AR model, MFXD (1.9 g/kg), MFXD (3.8 g/kg), MFXD (7.6 g/kg), and loratadine (1 mg/kg, Aobang Pharmaceuticals Co. Ltd., Sichuan, China) groups. Rats in three MFXD groups were orally administered daily with three doses MFXD 1 h before nasal challenge for 10 days (day 22 to day 31) according to our preliminary study; rats in the loratadine and AR model groups were simultaneously treated intragastrically with loratadine

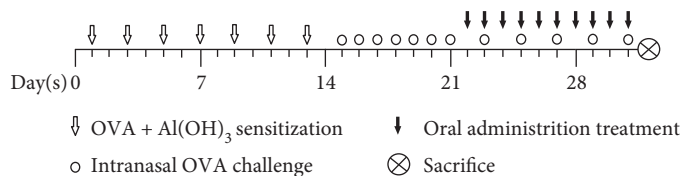


FIGURE 1: Schematic diagram of preparation of AR model rats and MFXD administration. Rats were intraperitoneally sensitized with OVA and Al(OH)<sub>3</sub> dissolved in physiological saline once every other day for 2 weeks and then challenged through nasal instillation with 5% OVA into each nasal cavity once daily from day 15 to day 21. Rats in MFXD, loratadine, and model groups were orally administered with three doses of MFXD, loratadine solution, and water once daily from day 22 to day 31, respectively, and were nasally instilled with OVA solution once every other day to maintain the nasal stimulation. Rats in the control group were sensitized with Al(OH)<sub>3</sub>, challenged with saline, and orally administered with water. All the rats were sacrificed on day 31.

solution (1 mg/kg) and filtered water, respectively. The rats in the control group were sensitized with Al(OH)<sub>3</sub>, challenged with saline, and orally administered with filtered water synchronously. During the period of oral administration, all of the AR rats were challenged through nasal instillation with 50  $\mu$ L of 5% OVA solution once every other day to maintain the nasal stimulation.

**2.5. Evaluation of Nasal Symptoms.** On the last day (day 31), the rats were placed in observation cages for approximately 10 min for acclimatization after oral administration. The frequencies of sneezing and nasal scratching in the rats were counted for 30 min immediately after the last challenge involving nasal instillation with 50  $\mu$ L of 5% OVA solution. After the evaluation of nasal symptoms, blood samples were collected from rats by using the abdominal aortic method under anesthesia; sera were obtained through centrifugation (3000 rpm) for 10 min and then stored at  $-80^{\circ}\text{C}$ . Nasal mucosa samples were removed for further histopathological and qRT-PCR analyses.

**2.6. Histopathological Examination.** Nasal mucosa samples were fixed in 4% paraformaldehyde (Biosharp, Hefei, Anhui, China) for 24 h and then embedded in paraffin. Paraffin-embedded tissue samples were cut into 4  $\mu$ m thick sections and stained with hematoxylin and eosin (HE) and toluidine blue (TB, for mast cells). Histopathological changes were evaluated and photographed using an orthorhombic optical photomicroscope (Eclipse Ci, Nikon, Japan).

**2.7. Detection of Total IgE, HIS, IFN- $\gamma$  (Th1 Cytokine), and IL-4 (Th2 Cytokine) in Rat Serum.** Serum levels of total IgE and HIS and those of IFN- $\gamma$  and IL-4 were measured via enzyme-linked immunosorbent assay (ELISA) according to the manuals of rat HIS and IgE Elisa Assay kits (Nanjing Jiancheng Bioengineering Institute, Nanjing, China) and rat IFN- $\gamma$  and IL-4 ELISA kits (CUSABIO, Wuhan, China), respectively. The minimum detection limits of IgE, HIS, IFN- $\gamma$ , and IL-4 were 0.05 U/mL, 0.5 ng/mL, 0.625 pg/mL, and 1.56 pg/mL, respectively.

**2.8. Detection of CD3<sup>+</sup>CD4<sup>+</sup>IFN- $\gamma$ <sup>+</sup> Th1 and CD3<sup>+</sup>CD4<sup>+</sup>IL-4<sup>+</sup> Th2 Cells through Flow Cytometry.** Peripheral blood mononuclear cells (PBMCs) of rats were separated from the blood sample according to the instruction provided in Rat Peripheral Blood Lymphocyte Separation Kit (Solarbio, Beijing, China) and placed in a tube containing RPMI 1640 (Gibco,

CA, USA). The PBMCs were stimulated with 81 ng/mL phorbol 12-myristate 13-acetate (eBioscience, CA, USA), 1.34  $\mu$ g/mL ionomycin (eBioscience, CA, USA), and 3.0  $\mu$ g/mL Brefeldin A (BFA) (eBioscience, CA, USA) for 6 h in 5% CO<sub>2</sub> humidified incubator (Thermo Fisher Scientific, Shanghai, China). Cells were subsequently surface-stained with fluorescein isothiocyanate- (FITC-) labeled anti-rat CD3 and allophycocyanin- (APC-) labeled anti-rat CD4 antibodies (BD Biosciences, CA, USA) at room temperature for 30 min in the dark and then fixed and permeabilized with intracellular fixation and permeabilization buffer (eBioscience, CA, USA), respectively, according to the manufacturer's instruction. After being washed in phosphate-buffered saline (PBS) and after centrifugation, the cells were divided equally and then incubated with phycoerythrin- (PE-) labeled anti-rat IFN- $\gamma$ , PE-labeled anti-rat IL-4, and PE-labeled anti-rat IgG1 antibodies (BD Biosciences, CA, USA) at room temperature for 15 min in the dark. The stained cells were washed once and detected by a FACSCalibur flow cytometer (BD Biosciences, San Jose, CA, USA), and the results were analyzed with CellQuest software (BD FACSDiva, USA).

**2.9. RNA Extraction and Quantitative Real-Time PCR (qRT-PCR) Analysis of the Nasal Mucosa.** Total RNA was isolated from the nasal mucosa by using a Total RNA Extraction Kit (Solarbio, Beijing, China). Complementary DNA (cDNA) was synthesized through reverse transcription reaction of the extracted RNA by using a Bestar<sup>TM</sup> qPCR RT Kit (DBI<sup>®</sup> Bioscience, Shanghai, China) according to the manufacturer's instruction under the following temperature conditions: 37 $^{\circ}\text{C}$  for 15 min and 98 $^{\circ}\text{C}$  for 5 min. qPCR was performed on an Applied Biosystems 7500 Real-Time PCR System (Life Technologies, USA) by using 10  $\mu$ L of qPCR MasterMix, 0.5  $\mu$ L of forward primer (10  $\mu$ M), 0.5  $\mu$ L of reverse primer (10  $\mu$ M), and 1  $\mu$ L of cDNA using Bestar<sup>®</sup> SYBR Green qPCR MasterMix Reagent (DBI Bioscience, Shanghai, China). The forward primer and reverse primer sequences of IFN- $\gamma$ , IL-4, T-bet, GATA-3, STAT-1, STAT-6, and  $\beta$ -actin (internal reference) are listed in Table 1. The conditions for PCR were as follows: initial denaturation at 95 $^{\circ}\text{C}$  for 5 min and then denaturation at 95 $^{\circ}\text{C}$  for 10 s, annealing at 55 $^{\circ}\text{C}$  for 30 s, and extension at 72 $^{\circ}\text{C}$  for 20 s for 40 cycles. The mRNA levels of the six target genes were normalized relative to  $\beta$ -actin by using cycle threshold (Ct) values.

TABLE 1: Primer sequences for quantitative real-time PCR.

Gene	Primer	Sequences (5'-3')
IFN- $\gamma$	Forward	CTGCTGATGGGAGGAGATGT
	Reverse	TTTGTCAATTCGGGTGTAGTCA
IL-4	Forward	GAGACTCTTTCGGGCTTTTCG
	Reverse	CAGGAAGTCTTTCAGTGATGTGG
T-bet	Forward	CAACAACCCCTTTGCCAAAG
	Reverse	TCC CCAAGCAGTTGACAGT
GATA-3	Forward	CTCGGCCATTCGTACATGGAA
	Reverse	GGATACCTCTGCACCGTAGC
STAT-1	Forward	TGACGAGGTGTCTCGGATAGT
	Reverse	GTAGCAGGAGGGAATCACAGA
STAT-6	Forward	CTGCCAAAGACCTGTCCATT
	Reverse	GGTAGGCATCTGGAGCTCTG
$\beta$ -Actin	Forward	ACCAACTGGGACGACATGGAGAA
	Reverse	GTGGTGGTGAAGCTGTAGCC

**2.10. Statistical Analysis.** The results of the four experiments were analyzed using SPSS for Windows version 16.0 (SPSS, Chicago, IL, USA) and expressed as mean  $\pm$  standard deviation (SD). Between-groups comparisons were performed using one-way ANOVA and analyzed by LSD *t*-test (when equal variances are assumed) or Tamhane's T2 test (nonparametric test; when equal variances are not assumed), and  $p < 0.05$  indicated statistical significance.

### 3. Results

**3.1. MFXD Fingerprint.** The components of 10 groups of MFXD consisting of different batches of *Mahuang*, *Fuzi*, and *Xixin* were analyzed by UPLC-MS/MS. Figure 2(a) shows the total ion chromatograms of the 10 groups of MFXD, which displayed a high degree of similarity. As shown in Figure 2(b), 25 peaks in the total ion chromatograms of MFXD were assigned as common peaks, and the relative standard deviations of the relative retention time (RRT) of these 25 common peaks were lower than 1.0%, indicating that the RRTs of the 25 components are comparatively stable. A total of 6, 4, and 5 peaks were found in *Mahuang*, *Fuzi*, and *Xixin*, respectively, and eight peaks were found in the three herbs. Nine compounds were detected based on the reference standards shown in Table 2. Peaks 2–6 derived from *Mahuang* were identified as norephedrine, norpseudoephedrine, ephedrine, pseudoephedrine, and methylephedrine, respectively. Peaks 10–12 derived from *Fuzi* were identified as benzoylmesaconine, benzoylaconine, and benzoylhypaconine, respectively. Peak 13 derived from *Xixin* was identified as 3,4,5-trimethoxytoluene.

**3.2. MFXD Relieved Nasal Symptoms in a Rat Model of AR.** The frequencies of sneezing and nasal scratching in rats were counted for 30 min to evaluate the therapeutic effect of MFXD after the last nasal challenge with OVA solution. As shown in Figure 3(a), the frequencies of sneezing and nasal scratching of rats in the AR model group significantly increased with an average of 17.38 and 44.00 times,

respectively, compared with those in the control group ( $p < 0.01$ ), wherein the rats did not show obvious sneezing and nasal scratching. After oral administration of MFXD, the nasal symptoms in rats of AR were relieved evidently. The frequencies of sneezing and nasal scratching in MFXD (3.8 g/kg) and MFXD (7.6 g/kg) groups significantly decreased compared with those in the AR model group ( $p < 0.05$  and  $p < 0.01$ , resp.). The frequencies of sneezing and nasal scratching in the MFXD (7.6 g/kg) group were 5.38 and 16.63, respectively, demonstrating the effective therapeutic effect of MFXD on the nasal symptoms in an AR rat model and that such effect is as good as that in the positive group.

**3.3. MFXD Reduced the Serum Levels of Total IgE and HIS in a Rat Model of AR.** AR is a type I allergic disease induced by IgE-mediated inflammation and characterized by the release of HIS [30]. As summarized in Figure 3(b), the total IgE levels in rats in MFXD (7.6 g/kg) and positive groups were 2.23 and 2.13 U/mL, respectively, which were significantly reduced compared with that of 2.86 U/mL in the AR model group ( $p < 0.01$ ;  $p < 0.01$ ). In addition, the concentrations of serum HIS in the high-dose MFXD group and positive group were 20.58 and 19.07 ng/mL, respectively, which were also significantly reduced compared with that in the AR model group ( $p < 0.05$ ;  $p < 0.05$ ).

**3.4. MFXD Relieved the Histopathological Injuries in the Nasal Mucosa in a Rat Model of AR.** HE and TB staining examinations were conducted to evaluate the effect of MFXD on the histopathological changes in the nasal mucosa. The HE (Figure 3(d)) and TB (Figure 3(e)) staining results show that rats in the control group displayed no obvious visible nasal lesions. However, nasal respiratory epithelium disruption, leucocyte and mast cell infiltration, and ciliated cell reduction were observed in the nasal mucosa sections of AR model rats. By contrast, compared with the model group, the groups administered with MFXD and positive agent, especially in MFXD (7.6 g/kg) and positive groups, showed significantly alleviated nasal mucosa injuries caused by AR.

**3.5. MFXD Reduced the Serum Levels of Th1 and Th2 Cytokines (IFN- $\gamma$  and IL-4).** IFN- $\gamma$  and IL-4 are the immune cytokines mainly released by Th1 and Th2 cells, respectively [9]. IFN- $\gamma$  and IL-4 measurements were performed to indirectly indicate the status of Th1 and Th2 responses. As depicted in Figure 4, the serum levels of IFN- $\gamma$  and IL-4 in AR model rats significantly increased compared with those in the control group. After oral administration of MFXD and loratadine, the serum levels of IFN- $\gamma$  and IL-4 significantly decreased (except in the low-dose MFXD group), especially in MFXD (7.6 g/kg) rats ( $p < 0.01$ ), compared with those in the model group. The serum IFN- $\gamma$  levels in control, AR model, and MFXD (7.6 g/kg) groups were 0.94, 1.34, and 1.15 pg/mL, respectively, and the corresponding serum IL-4 levels of these groups were 5.52, 15.21, and 8.19 pg/mL, respectively. To evaluate the status of Th1/Th2 balance, we calculated the IFN- $\gamma$ /IL-4 values in all groups (Figure 4). Compared with the IFN- $\gamma$ /IL-4 value of 0.17 in the control

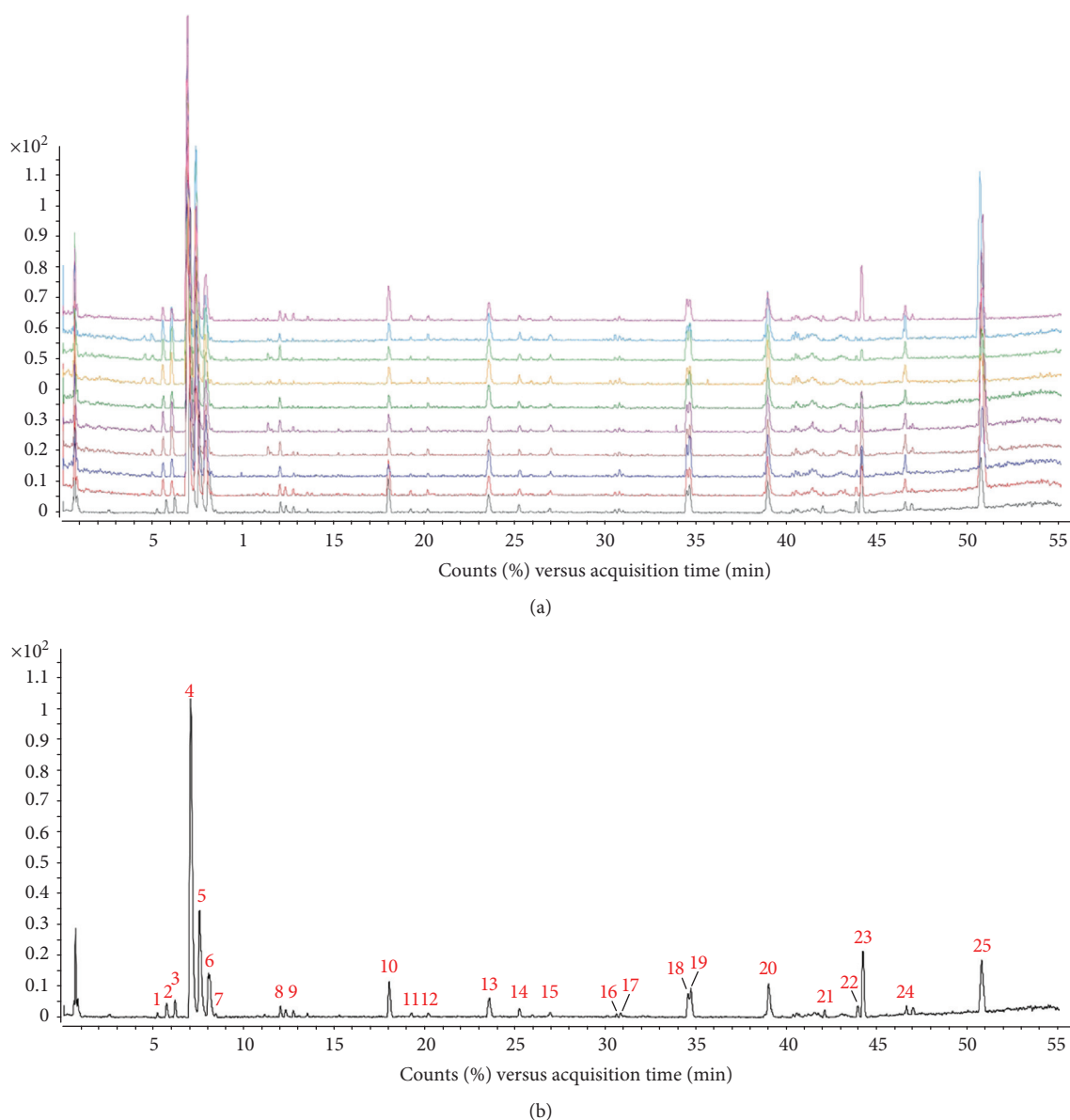


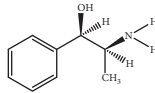
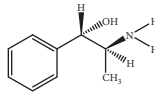
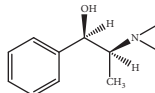
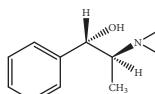
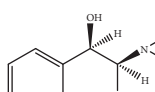
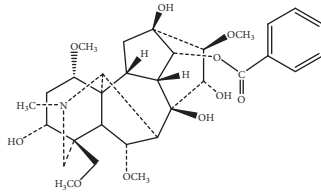
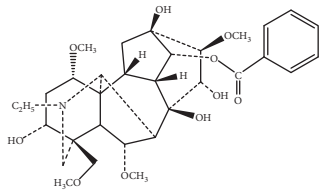
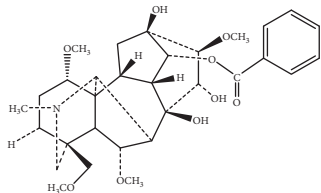
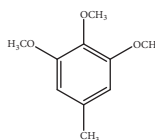
FIGURE 2: Total ion chromatograms of MFXD. 10 groups of MFXD consisting of different batches of *Mahuang*, *Fuzi*, and *Xixin* were diluted to 0.06 g/mL and precipitated with equal methanol. The supernatants were obtained by centrifugation (10000 rpm) for 10 min and analyzed by UPLC-MS/MS using a mobile phase consisting of acetonitrile (a) and 0.1% formic acid aqueous solution (b) with a gradient program. The injection volume was 1  $\mu$ L, the flow rate is 0.4 mL/min, and the column temperature was 25°C. (a) The total ion chromatograms of 10 groups of MFXD. (b) The MFXD fingerprint.

group, that in the AR model group significantly decreased to 0.09 ( $p < 0.01$ ). In addition, the IFN- $\gamma$ /IL-4 values in MFXD (3.9 g/kg), MFXD (7.6 g/kg), and positive groups significantly increased ( $p < 0.05$ ,  $p < 0.01$ , and  $p < 0.01$ , resp.) compared to that in the model group.

**3.6. Effect of MFXD on the Percentages of CD3<sup>+</sup>CD4<sup>+</sup>IFN- $\gamma$ <sup>+</sup> Th1 and CD3<sup>+</sup>CD4<sup>+</sup>IL-4<sup>+</sup> Th2 Cells in Peripheral Blood.** Th1 and Th2 cells differentiated from CD3<sup>+</sup>CD4<sup>+</sup> lymphocytes and the percentages of CD3<sup>+</sup>CD4<sup>+</sup>IFN- $\gamma$ <sup>+</sup> Th1 and CD3<sup>+</sup>CD4<sup>+</sup>IL-4<sup>+</sup> Th2 cells were analyzed and measured in PBMCs via flow cytometry. As shown in Figures 5(a) and 5(b), the percentage of CD3<sup>+</sup>CD4<sup>+</sup>IFN- $\gamma$ <sup>+</sup> Th1 cells was

significantly higher in the AR model group than in the normal control group ( $p < 0.01$ ), whereas no obvious changes were observed among the model, MFXD, and positive groups. As shown in Figures 5(a) and 5(c), the percentage of CD3<sup>+</sup>CD4<sup>+</sup>IL-4<sup>+</sup> Th2 cells in the AR model group was 5.16%, significantly higher than the 1.55% in the normal control group ( $p < 0.01$ ). However, the percentage of CD3<sup>+</sup>CD4<sup>+</sup>IL-4<sup>+</sup> Th2 cells significantly decreased after administration with MFXD and positive reagent ( $p < 0.01$ ), and the percentages in MFXD (7.6 g/kg) and positive groups were 2.47% and 2.53%, respectively. Moreover, the ratio of CD3<sup>+</sup>CD4<sup>+</sup>IFN- $\gamma$ <sup>+</sup> Th1 and CD3<sup>+</sup>CD4<sup>+</sup>IL-4<sup>+</sup> Th2 cells was calculated (Figure 5(d)), and the ratios in MFXD (7.6 g/kg)

TABLE 2: Identification of compounds of MFXD by UPLC-MS/MS.

Number	RRT/min*	Compound	Positive ion ( <i>m/z</i> )	Elemental composition	Chemical structures	Source
1	5.67	Norephedrine	152.1	C <sub>9</sub> H <sub>13</sub> NO		a
2	6.13	Norpseudoephedrine	152.1	C <sub>9</sub> H <sub>13</sub> NO		a
3	6.99	Ephedrine	166.1	C <sub>10</sub> H <sub>15</sub> NO		a
4	7.49	Pseudoephedrine	166.1	C <sub>10</sub> H <sub>15</sub> NO		a
5	7.97	Methylephedrine	180.1	C <sub>11</sub> H <sub>17</sub> NO		a
6	17.95	Benzoylmesaconine	590.3	C <sub>31</sub> H <sub>43</sub> NO <sub>10</sub>		b
7	19.17	Benzoylaconine	604.3	C <sub>32</sub> H <sub>45</sub> NO <sub>10</sub>		b
8	20.10	Benzoylhypaconine	574.3	C <sub>31</sub> H <sub>43</sub> NO <sub>9</sub>		b
9	23.47	3,4,5-Trimethoxytoluene	183.1	C <sub>10</sub> H <sub>14</sub> O <sub>3</sub>		c

\*RRT: relative retention time. <sup>a</sup>*Ephedrae*; <sup>b</sup>*Radix Aconiti Lateralis*; <sup>c</sup>*Asarum*.

and positive groups significantly increased compared with that in the AR model group ( $p < 0.01$ ) but did not significantly differ from that in the control group ( $p > 0.05$ ).

**3.7. Effect of MFXD on mRNA Expression Levels of IFN- $\gamma$ , IL-4, T-bet, GATA-3, STAT-1, and STAT-6 in the Nasal Mucosa.** T-bet and GATA-3 are important transcription factors that directly or indirectly regulate the differentiation and

development of Th1 and Th2 cells [31]. IFN- $\gamma$  activates the T-bet gene and induces the expression of T-bet through the Janus kinase/signal transducer and activator of transcription 1 signal transduction pathway [32, 33]. In addition, IL-4 increases the expression of GATA-3 by activating signal transducer and activator of transcription 6 (STAT-6) and then improves the development of Th2 cells [34]. As shown in Figures 6(a) and 6(b), the mRNA expression levels of



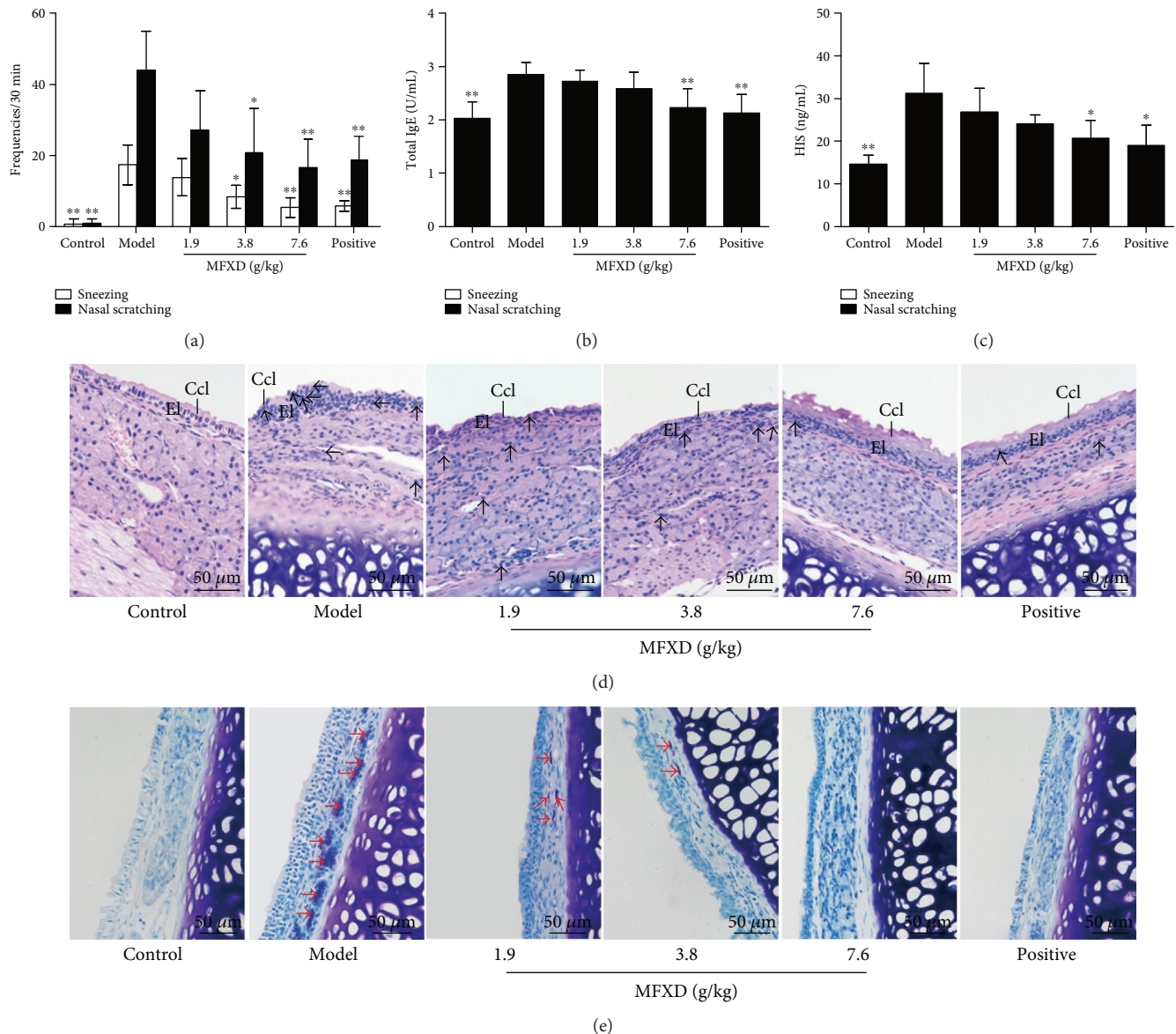


FIGURE 3: Effect of MFXD on OVA-induced allergic rhinitis in rat. (a) The frequencies of sneezing and nasal scratching of rats were counted for 30 min immediately after the last challenge by nasal instillation with OVA solution on day 31. Blood samples were collected and the serums were obtained by centrifugation. The total IgE (b) and HIS (c) levels in serum were detected by ELISA. The nasal mucosa samples were collected and stained with (d) hematoxylin and eosin (HE) and (e) toluidine blue (TB). Epithelial layer (El), ciliated cell layer (Ccl), leucocytes (represented by black arrows), and mast cells (represented by red arrows) were marked on the images. Data are expressed as mean  $\pm$  SD;  $N = 8$  rats; \* $p < 0.05$ , \*\* $p < 0.01$  versus model.

IFN- $\gamma$ , IL-4, T-bet, GATA-3, STAT-1, and STAT-6 in the nasal mucosa were significantly higher in the AR model group than in the control group. After intragastric administration of MFXD and positive drug, the expression levels of IFN- $\gamma$  and STAT-6 in all groups significantly decreased and the expression levels of IL-4 and GATA-3 in MFXD (7.6 g/kg) and positive groups significantly decreased compared with those in the AR model group. Figure 6(c) shows the IFN- $\gamma$ /IL-4, T-bet/GATA-3, and STAT-1/STAT-6 values, which were calculated to evaluate Th1 and Th2 responses. IFN- $\gamma$ /IL-4, T-bet/GATA-3, and STAT-1/STAT-6 values in the AR model group significantly decreased compared with

those in the control group, and T-bet/GATA-3 ratios were significantly higher in MFXD and positive groups than that in the model group. Moreover, compared with that in the AR model group, the STAT-1/STAT-6 values in MFXD (7.6 g/kg) and positive groups significantly increased and the IFN- $\gamma$ /IL-4 values in administered groups also tended to increase.

#### 4. Discussion

AR is one of the most common allergic diseases that do not only adversely affect patients' quality of life but also induce

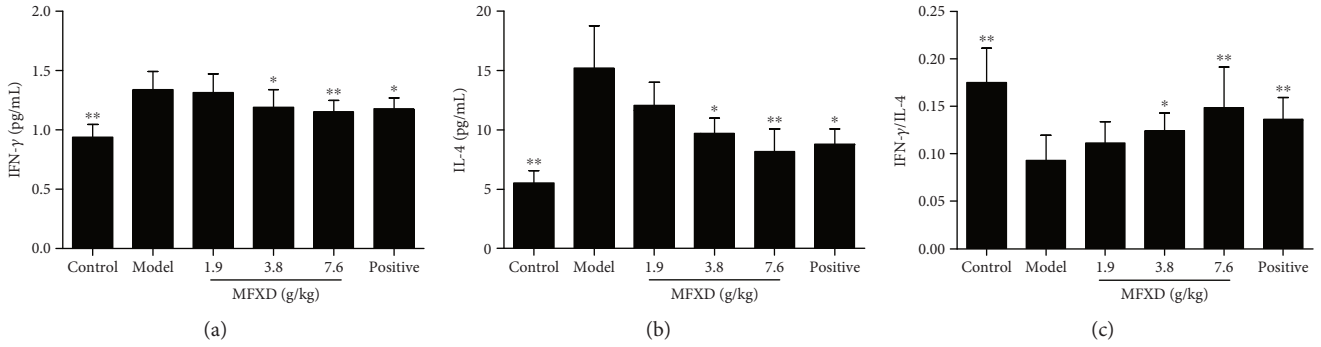


FIGURE 4: Effect of MFXD on serum IFN- $\gamma$  and IL-4 in OVA-induced rat of allergic rhinitis. Blood samples were collected after the last nasal challenge and the serums were obtained by centrifugation. The IFN- $\gamma$  (a) and IL-4 (b) levels in serum were detected by ELISA. (c) The IFN- $\gamma$ /IL-4 values in all groups were calculated. Data are expressed as mean  $\pm$  SD;  $N = 8$  rats; \* $p < 0.05$ , \*\* $p < 0.01$  versus model.

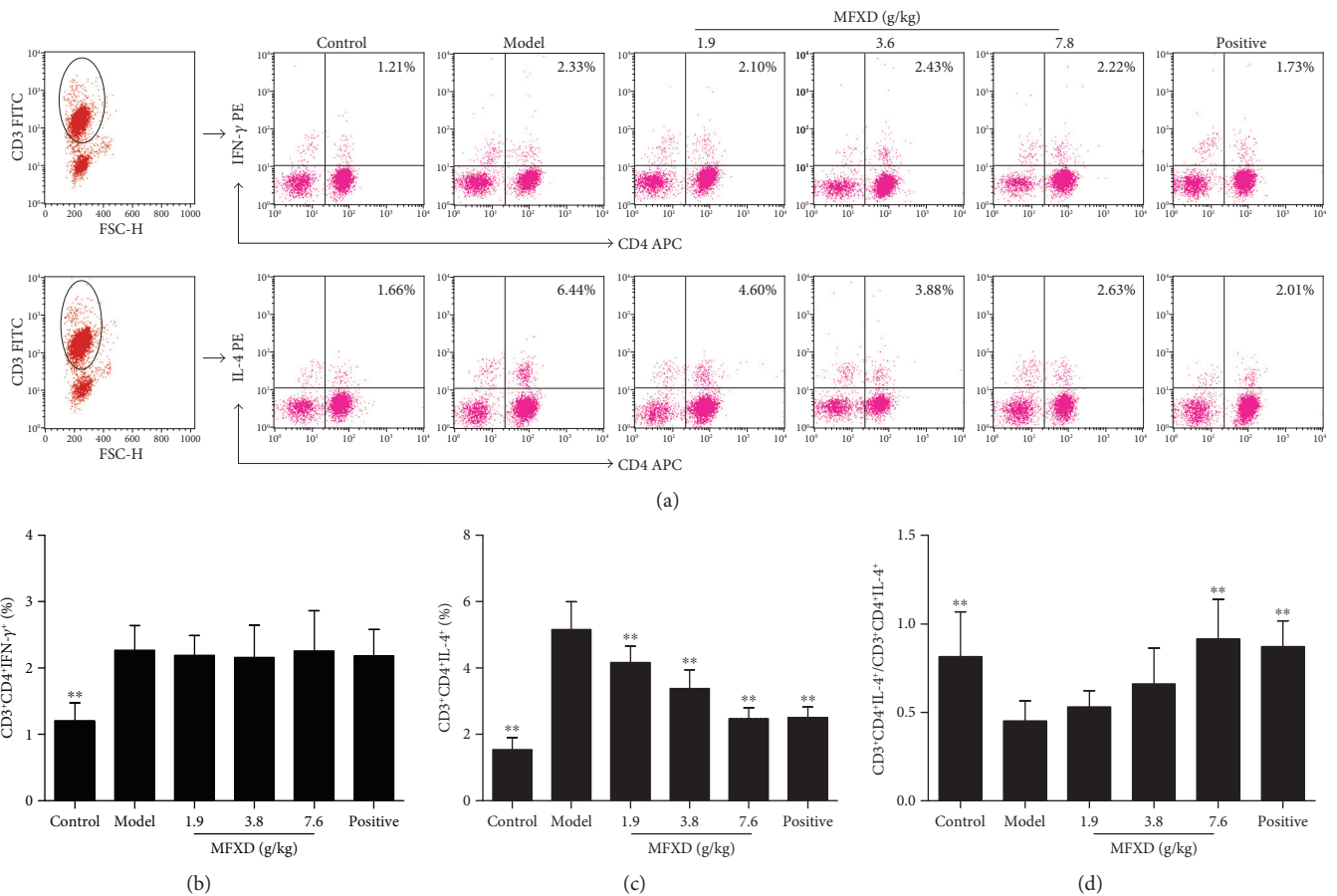


FIGURE 5: Effect of MFXD on the percentages of CD3<sup>+</sup>CD4<sup>+</sup>IFN- $\gamma$ <sup>+</sup> Th1 and CD3<sup>+</sup>CD4<sup>+</sup>IL-4<sup>+</sup> Th2 cells in peripheral blood mononuclear cells (PBMCs) of AR rats. PBMCs of rats were separated from anticoagulant blood sample, stained with fluorescently labeled anti-rat antibodies, and analyzed by flow cytometry. (a) Representative flow cytometry dot plots for each groups, and the plots in the upper right quadrant indicate the percentage of CD3<sup>+</sup>CD4<sup>+</sup>IFN- $\gamma$ <sup>+</sup> Th1 and CD3<sup>+</sup>CD4<sup>+</sup>IL-4<sup>+</sup> Th2 cells among PBMCs. Percentages of (b) CD3<sup>+</sup>CD4<sup>+</sup>IFN- $\gamma$ <sup>+</sup> Th1 cells and (c) CD3<sup>+</sup>CD4<sup>+</sup>IL-4<sup>+</sup> Th2 cells in each groups. (d) Ratios of CD3<sup>+</sup>CD4<sup>+</sup>IFN- $\gamma$ <sup>+</sup> Th1 and CD3<sup>+</sup>CD4<sup>+</sup>IL-4<sup>+</sup> Th2 cells were calculated. Data are expressed as mean  $\pm$  SD;  $N = 6$  rats; \*\* $p < 0.01$  versus model.

multiple relevant complications [4, 5]. Researchers have successfully established different animal models of AR by using OVA as an allergen and Al(OH)<sub>3</sub> as an adjuvant [35, 36]. In this study, a rat model of AR was successfully established through intraperitoneal injection of OVA and Al(OH)<sub>3</sub>

suspension and nasal instillation with 5% OVA solution. In the AR model group, the rats displayed extremely frequent sneezing and nasal scratching and significantly increased serum levels of total IgE and HIS; moreover, obvious epithelial disruption, leucocyte and mast cell

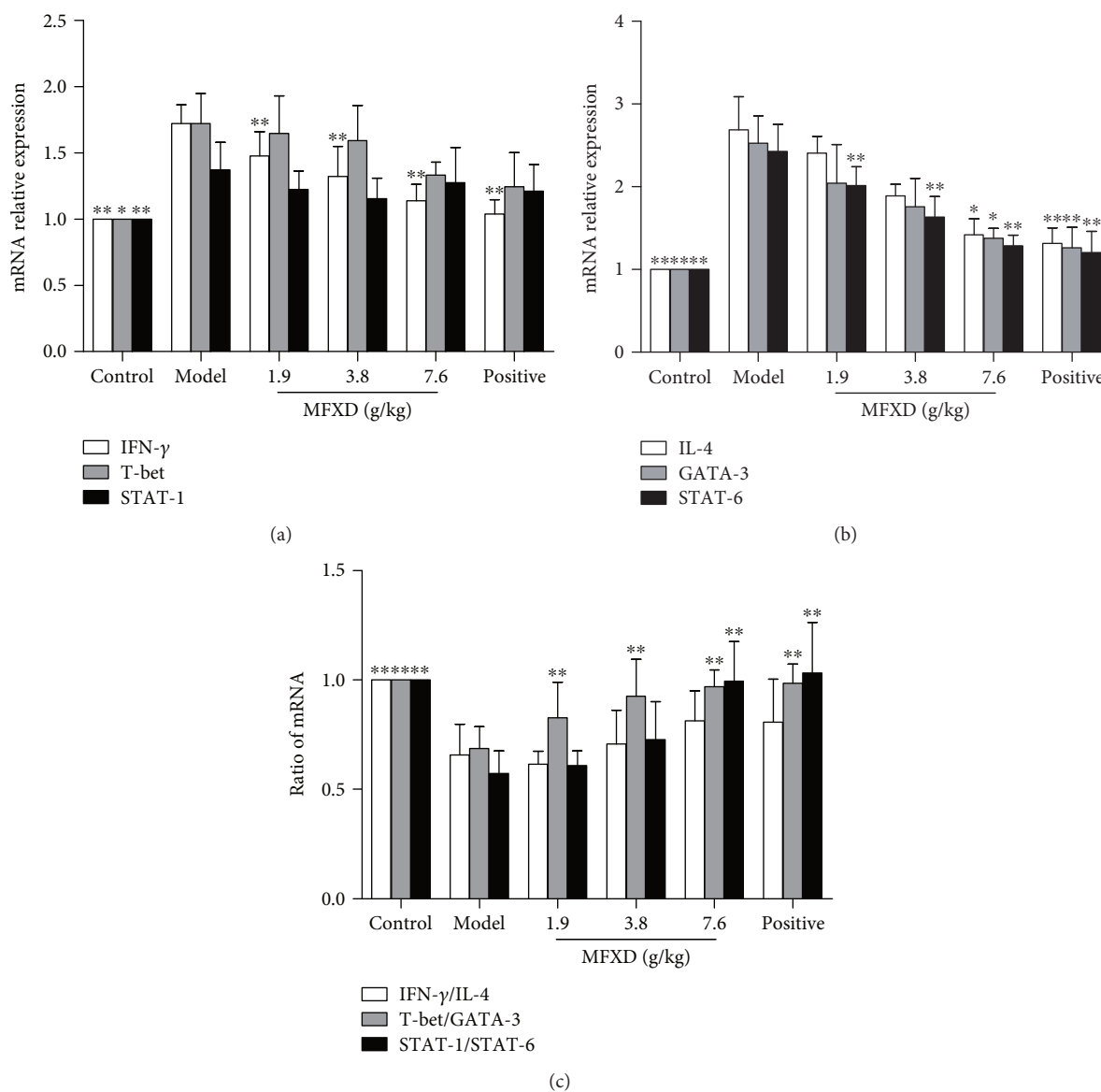


FIGURE 6: Effect of MFXD on the mRNA expression of IFN- $\gamma$ , IL-4, T-bet, GATA-3, STAT-1, and STAT-6 in the nasal mucosa. Nasal mucosa samples from rats in different groups were obtained after the last nasal challenge, and total RNA was isolated and analyzed with qRT-PCR. (a) The mRNA expression of IFN- $\gamma$ , T-bet, and STAT-1 in the nasal mucosa. (b) The mRNA expression of IL-4, GATA-3, and STAT-6 in the nasal mucosa. (c) The ratios of IFN- $\gamma$ /IL-4, T-bet/GATA-3, and STAT-1/STAT-6 are shown. Data are expressed as mean  $\pm$  SD;  $N = 6$  rats; \* $p < 0.05$ , \*\* $p < 0.01$  versus model.

infiltration, and cilia cell reduction were observed in nasal mucosa sections; these results indicated that the rat model of AR was successfully established and presented evident AR responses.

MFXD is a classical Chinese traditional formula that has been widely used in clinics to treat AR in Asian countries [20, 21]. In this study, three doses of MFXD were orally administrated to treat AR in rats. The frequencies of sneezing and nasal scratching in rats significantly decreased (except those in the low-dose MFXD group), and the serum levels of total IgE and HIS under high-dose MFXD treatment significantly decreased relative to those in the model group. In addition, MFXD significantly alleviated the nasal mucosa

injuries caused by AR. Therefore, MFXD obviously exerted therapeutic effect on a rat model of AR, especially under treatment with high dose of MFXD.

AR is a Th2-polarized allergic disease, and imbalance of Th1/Th2 cells is speculated to be an important factor that results in AR [8–11]. Differentiation from Th0 cell to Th2 cell is obviously enhanced in AR; as a result, the release of Th2 cytokines is increased, accelerating the expression of transcription factors and signal transducers and activators of transcription, such as GATA-3 and STAT6, which play important roles in Th2 immune response [31–33]. In addition, excessive Th2 cytokine inhibits the differentiation of Th0 cell into Th1 cell,

reducing the production of factors related to Th1 immune response, such as IFN- $\gamma$ , T-bet, and SATA-1, leading to the imbalance in Th1/Th2 cells [34]. Studies have reported that in animal models induced by OVA, Th1 response is inhibited [37, 38] or is not obviously affected [39, 40], whereas Th2 response is enhanced. However, the serum IFN- $\gamma$  content, the percentage of CD3<sup>+</sup>CD4<sup>+</sup>IFN- $\gamma$ <sup>+</sup> Th1 cells in PBMCs, and the mRNA expression levels of IFN- $\gamma$ , T-bet, and SATA-1 were all significantly increased compared with those in the normal control group; the same trend was observed for the serum IL-4 content, the percentage of CD3<sup>+</sup>CD4<sup>+</sup>IL-4<sup>+</sup> Th2 cells in PBMCs, and the mRNA expression levels of IL-4, GATA-3, and SATA-6. In this study, Th1 and Th2 responses were simultaneously enhanced in a rat model of AR, consistent with the results of Kim et al. who also used a mouse model of AR [41]. Two reasons are speculated to explain this phenomenon. First, although IgE-mediated AR is considered a disease primarily mediated by Th2, allergen-specific Th1 also plays an important role in allergic inflammation [42], especially in chronic allergic diseases, such as atopic dermatitis and chronic allergic asthma; moreover, the Th1 cytokine IFN- $\gamma$  promotes allergen penetration through the respiratory epithelium and aggravates allergic inflammation [43, 44]. Second, Th1 response possibly played different roles in different periods after AR has developed. As reported, the serum levels of the Th1 cytokine IFN- $\gamma$  in a rat model of OVA-induced AR obviously increased within 24 h after induction of AR and then decreased [45].

Although Th1 and Th2 responses were enhanced simultaneously in a rat model of AR, the imbalance in Th1/Th2 cells significantly changed. Compared with those in the control group, the following ratios significantly decreased in the AR model group: ratios of serum IFN- $\gamma$ /IL-4; CD3<sup>+</sup>CD4<sup>+</sup>IFN- $\gamma$ <sup>+</sup> Th1 (%) / CD3<sup>+</sup>CD4<sup>+</sup>IFN- $\gamma$ <sup>+</sup> Th1 (%) in PBMCs; and mRNA expression of IFN- $\gamma$ /IL-4, T-bet/GATA-3, and STAT-1/STAT-6. After oral administration of MFXD, all of the values tended to increase and high dose of MFXD significantly enhanced the values, consistent with the result for the positive reagent, indicating that MFXD can regulate the AR-induced imbalance in Th1/Th2 cells.

In conclusion, MFXD exerts a good therapeutic effect against OVA-induced allergic inflammation in a rat model of AR as seen in the reduced frequencies of sneezing and nasal scratching in rats and in the reduced serum levels of total IgE and HIS. MFXD regulates the AR-induced imbalance in Th1/Th2 cells by attenuating Th1 and Th2 responses simultaneously, such as reducing the serum levels of IFN- $\gamma$  and IL-4 and mRNA expression levels of IFN- $\gamma$ , IL-4, GATA-3, and STAT-6. This study provides some valuable information on the immunoregulatory effect of MFXD on the treatment of AR in future clinical studies.

## Conflicts of Interest

The authors declare that there are no competing interests.

## Authors' Contributions

Mengyue Ren conceived and obtained the data and drafted the first manuscript. Qingfa Tang conceived and revised the manuscript. Feilong Chen and Xuefeng Xing provided technical support for the experiment. Yao Huang participated in the analysis of data. Xiaomei Tan contributed to the conception of the study and provided economic support. All authors read the paper and approved the first submission. Mengyue Ren and Qingfa Tang contributed equally to this work.

## Acknowledgments

This work was supported by the Science and Technology Program of Guangzhou, China (Grant no. 201707010042).

## References

- [1] Y. M. Al Suleimani and M. J. Walker, "Allergic rhinitis and its pharmacology," *Pharmacology and Therapeutics*, vol. 114, no. 3, pp. 233–260, 2007.
- [2] A. Pipet, K. Botturi, D. Pinot, D. Vervloet, and A. Magnan, "Allergen-specific immunotherapy in allergic rhinitis and asthma. Mechanisms and proof of efficacy," *Respiratory Medicine*, vol. 103, no. 6, pp. 800–812, 2009.
- [3] J. Bousquet, P. van Cauwenberge, and N. Khaltaev, "Allergic rhinitis and its impact on asthma," *Journal of Allergy and Clinical Immunology*, vol. 108, no. 5, pp. S147–S336, 2001.
- [4] J. Bousquet, H. J. Schünemann, B. Samolinski et al., "Allergic rhinitis and its impact on asthma (ARIA): achievements in 10 years and future needs," *Journal of Allergy and Clinical Immunology*, vol. 130, no. 5, pp. 1049–1062, 2012.
- [5] D. I. Bernstein, G. Schwartz, and J. A. Bernstein, "Allergic rhinitis: mechanisms and treatment," *Immunology and Allergy Clinics North America*, vol. 36, no. 2, pp. 261–278, 2016.
- [6] F. Gomez, C. Rondon, M. Salas, and P. Campo, "Local allergic rhinitis: mechanisms, diagnosis and relevance for occupational rhinitis," *Current Opinion Allergy Clinical Immunology*, vol. 15, no. 2, pp. 111–116, 2015.
- [7] A. Tatar, M. Yayla, D. Kose, Z. Halici, O. Yoruk, and E. Polat, "The role of endothelin-1 and endothelin receptor antagonists in allergic rhinitis inflammation: ovalbumin-induced rat model," *Rhinology*, vol. 54, no. 3, pp. 266–272, 2016.
- [8] J. M. Smart, E. Horak, A. S. Kemp, C. F. Robertson, and M. L. K. Tang, "Polyclonal and allergen-induced cytokine responses in adults with asthma: resolution of asthma is associated with normalization of IFN- $\gamma$  responses," *Journal of Allergy and Clinical Immunology*, vol. 110, no. 3, pp. 450–456, 2002.
- [9] N. P. Jayasekera, T. P. Toma, A. Williams, and K. Rajakulasingam, "Mechanisms of immunotherapy in allergic rhinitis," *Biomedicine and Pharmacotherapy*, vol. 61, no. 1, pp. 29–33, 2007.
- [10] T. Hayashi and A. Murase, "Polarization toward Th1-type response in active, but not in inactive, lupus inhibits late allergic rhinitis in lupus-prone female NZBxNZWF<sub>1</sub> mice," *Inflammation*, vol. 35, no. 6, pp. 1753–1763, 2012.
- [11] P. A. Ricketti, S. Alandijani, C. H. Lin, and T. B. Casale, "Investigational new drugs for allergic rhinitis," *Expert Opinion Investigational Drugs*, vol. 26, no. 3, pp. 279–292, 2017.

- [12] Z. K. Liu, R. C. Wang, B. C. Han, Y. Yang, and J. P. Peng, "A novel role of IGFBP7 in mouse uterus: regulating uterine receptivity through Th1/Th2 lymphocyte balance and decidualization," *PloS One*, vol. 7, no. 9, 2012.
- [13] P. Pradhan, H. Qin, J. A. Leleux et al., "The effect of combined IL10 siRNA and CpG ODN as pathogen-mimicking microparticles on Th1/Th2 cytokine balance in dendritic cells and protective immunity against B cell lymphoma," *Biomaterials*, vol. 35, no. 21, pp. 5491–5504, 2014.
- [14] S. K. Ko, M. Jin, and M. Y. Pyo, "Inonotus obliquus extracts suppress antigen-specific IgE production through the modulation of Th1/Th2 cytokines in ovalbumin-sensitized mice," *Journal of Ethnopharmacology*, vol. 137, no. 3, pp. 1077–1082, 2011.
- [15] D. A. Randolph, R. Stephens, C. J. Carruthers, and D. D. Chaplin, "Cooperation between Th1 and Th2 cells in a murine model of eosinophilic airway inflammation," *Journal of Clinical Investigation*, vol. 104, no. 8, pp. 1021–1029, 1999.
- [16] V. Cardona, O. Luengo, and M. Labrador-Horrillo, "Immunotherapy in allergic rhinitis and lower airway outcomes," *Allergy*, vol. 72, no. 1, pp. 35–42, 2017.
- [17] J. Kern and L. Bielory, "Complementary and alternative therapy (CAM) in the treatment of allergic rhinitis," *Current Allergy and Asthma Reports*, vol. 14, no. 12, p. 479, 2014.
- [18] R. L. Guo, M. H. Pittler, and E. Ernst, "Herbal medicines for the treatment of allergic rhinitis: a systematic review," *Annals of Allergy Asthma and Immunology*, vol. 99, no. 6, pp. 483–495, 2007.
- [19] C. C. Xue, C. G. Li, H. M. Hügel, and D. F. Story, "Does acupuncture or Chinese herbal medicine have a role in the treatment of allergic rhinitis?," *Current Opinion Allergy and Clinical Immunology*, vol. 6, no. 3, pp. 175–179, 2006.
- [20] Y. X. Lv, "Clinical application of *Mahuang Fuzi Xixin* decoction," *Clinical Journal of Chinese Medicine*, vol. 3, no. 14, pp. 46–47, 2011.
- [21] P. Z. Xiong, X. M. Feng, and F. Wang, "Review on clinical application of *Mahuang Fuzi Xixin* decoction," *Journal of Practical Traditional Chinese Medicine*, vol. 32, no. 2, pp. 195–196, 2016.
- [22] X. Y. Yang, C. F. Xiao, K. Y. Zhang, and J. P. Chen, "Research progress on clinical application and pharmacological functions of *ephedra*," *Chinese Archives of Traditional Chinese Medicine*, vol. 33, no. 12, pp. 2874–2875, 2015.
- [23] L. C. Shi, C. Ye, and X. Li, "Research progress of *ephedra* alkaloids," *Guide of China Medicine*, vol. 10, no. 10, p. 74, 2012.
- [24] W. L. Guo and S. F. Shi, "Professor Suofang Shi using high-dose *Aconite* to treat asthma with cold symptoms," *Jilin Journal of Traditional Chinese Medicine*, vol. 31, no. 2, pp. 112–114, 2011.
- [25] Y. R. Gu and B. L. Tong, "30 cases of the treatment of rheumatoid arthritis with high-dose *Aconite*," *Journal of Anhui TCM College*, vol. 15, no. 3, p. 25, 1996.
- [26] L. Q. Rong, "Pharmacological activities and clinical applications of *asarum*," *Strait Pharmaceutical Journal*, vol. 23, no. 2, pp. 94–95, 2011.
- [27] X. L. Wang, L. J. Jin, F. X. Xu, Y. P. Xu, and X. Y. Li, "Research progress of Chinese herb-*asarum*," *Asia-Pacific Traditional Medicine*, vol. 9, no. 7, pp. 68–71, 2013.
- [28] W. F. Wang, X. M. Tan, S. Y. Liang, Y. L. Hu, M. M. Zhang, and T. Li, "Efficacy of *Mahuang Fuzi Xixin* decoction and Xiaoqinglong decoction on allergic rhinitis in guinea pigs," *Chinese Journal of Experimental Traditional Medical Formulae*, vol. 17, no. 7, pp. 176–178, 2011.
- [29] R. Long, Y. Zhou, J. Huang et al., "Bencycloquidum bromide inhibits nasal hypersecretion in a rat model of allergic rhinitis," *Inflammation Research*, vol. 64, no. 3–4, pp. 213–223, 2015.
- [30] K. Y. Kim, S. Y. Nam, T. Y. Shin, K. Y. Park, H. J. Jeong, and H. M. Kim, "Bamboo salt reduces allergic responses by modulating the caspase-1 activation in an OVA-induced allergic rhinitis mouse model," *Food and Chemical Toxicology*, vol. 50, no. 10, pp. 3480–3488, 2012.
- [31] Z. Wang, T. Chen, M. Long et al., "Electro-acupuncture at Acupoint ST36 ameliorates inflammation and regulates Th1/Th2 balance in delayed-type hypersensitivity," *Inflammation*, vol. 40, no. 2, pp. 422–434, 2017.
- [32] D. J. Kuter, "The biology of thrombopoietin and thrombopoietin receptor agonists," *International Journal of Hematology*, vol. 98, no. 1, pp. 10–23, 2013.
- [33] C. M. Horvath, "The Jak-STAT pathway stimulated by interferon gamma," *Science's STKE*, vol. 2004, no. 260, 2004.
- [34] E. G. Kim, H. J. Shin, C. G. Lee et al., "DNA methylation and not allelic variation regulates STAT6 expression in human T cells," *Clinical and Experimental Medicine*, vol. 10, no. 3, pp. 143–152, 2009.
- [35] S. H. Hong, S. R. Kim, H. S. Choi et al., "Effects of Hyeonggaeyeongyo-tang in ovalbumin-induced allergic rhinitis model," *Mediators of Inflammation*, vol. 2014, Article ID 418705, 9 pages, 2014.
- [36] M. Wang, W. Zhang, and J. Shang, "Immunomodulatory effects of IL-23 and IL-17 in a mouse model of allergic rhinitis," *Clinical and Experimental Allergy*, vol. 43, no. 8, pp. 956–966, 2013.
- [37] C. Ma, Z. Ma, X. L. Liao, J. Liu, Q. Fu, and S. Ma, "Immunoregulatory effects of glycyrrhizic acid exerts anti-asthmatic effects via modulation of Th1/Th2 cytokines and enhancement of CD4(+)CD25(+)Foxp3+ regulatory T cells in ovalbumin-sensitized mice," *Journal of Ethnopharmacology*, vol. 148, no. 3, pp. 755–762, 2013.
- [38] H. W. Guo, C. X. Yun, G. H. Hou et al., "Mangiferin attenuates Th1/Th2 cytokine imbalance in an ovalbumin-induced asthmatic mouse model," *PloS One*, vol. 9, no. 6, article e100394, 2014.
- [39] J. S. Lee, C. M. Lee, Y. I. Jeong et al., "D-Pinitol regulates Th1/Th2 balance via suppressing Th2 immune response in ovalbumin-induced asthma," *FEBS Letters*, vol. 581, no. 1, pp. 57–64, 2007.
- [40] H. S. Kumar, P. P. Singh, N. A. Qazi et al., "Development of novel lipidated analogs of picoside as vaccine adjuvants: acylated analogs of picoside-II elicit strong Th1 and Th2 response to ovalbumin in mice," *Vaccine*, vol. 28, no. 152, pp. 8327–8337, 2010.
- [41] E. H. Kim, J. H. Kim, R. Samivel et al., "Intralymphatic treatment of flagellin-ovalbumin mixture reduced allergic inflammation in murine model of allergic rhinitis," *Allergy*, vol. 71, no. 5, pp. 629–639, 2016.
- [42] G. Hansen, G. Berry, R. H. DeKruyff, and D. T. Umetsu, "Allergen-specific Th1 cells fail to counterbalance Th2 cell-

- induced airway hyperreactivity but cause severe airway inflammation,” *Journal of Clinical Investigation*, vol. 103, no. 2, pp. 175–183, 1999.
- [43] H. Yssel and H. Groux, “Characterization of T cell subpopulations involved in the pathogenesis of asthma and allergic diseases,” *International Archives of Allergy and Immunology*, vol. 121, no. 1, pp. 10–18, 2000.
- [44] T. Werfel, A. Morita, M. Grewe et al., “Allergen specificity of skin-infiltrating T cells is not restricted to a type-2 cytokine pattern in chronic skin lesions of atopic dermatitis,” *Journal of Investigative Dermatology*, vol. 107, no. 6, pp. 871–876, 1996.
- [45] J. Reisinger, A. Triendl, and E. Kuchler, “IFN-gamma-enhanced allergen penetration across respiratory epithelium augments allergic inflammation,” *Journal of Allergy and Clinical Immunology*, vol. 115, no. 5, pp. 973–981, 2005.

## Research Article

# Ethyl Caffeate Ameliorates Collagen-Induced Arthritis by Suppressing Th1 Immune Response

Shikui Xu,<sup>1,2</sup> Aixue Zuo,<sup>3</sup> Zengjun Guo,<sup>1</sup> and Chunping Wan<sup>4</sup>

<sup>1</sup>School of Pharmacy, Xi'an Jiaotong University, Xi'an 710061, China

<sup>2</sup>Yunnan Institute for Food and Drug Control, Kunming 650011, China

<sup>3</sup>School of Pharmacy, Yunnan University of Traditional Chinese Medicine, Kunming 650500, China

<sup>4</sup>Central Laboratory, The No.1 Affiliated Hospital of Yunnan University of Traditional Chinese Medicine, Kunming 650021, China

Correspondence should be addressed to Zengjun Guo; guozj@mail.xjtu.edu.cn and Chunping Wan; wanchunping1012@163.com

Received 22 January 2017; Accepted 26 March 2017; Published 15 June 2017

Academic Editor: Yong Tan

Copyright © 2017 Shikui Xu et al. This is an open access article distributed under the Creative Commons Attribution License, which permits unrestricted use, distribution, and reproduction in any medium, provided the original work is properly cited.

The present study was designed to assess the antiarthritic potential of ECF in collagen-induced arthritis (CIA) and explore its underlying mechanism. *Methods.* In vitro, lymphocyte proliferation assay was measured by CCK-8 kit. In vivo, the therapeutic potential of ECF on CIA was investigated; surface marker, Treg cell, and intracellular cytokines (IL-17A and IFN- $\gamma$ ) were detected by flow cytometry. Th1 cell differentiation assay was performed, and mRNA expression in interferon- $\gamma$ -related signaling was examined by q-PCR analysis. *Results.* In vitro, ECF markedly inhibited the proliferation of splenocytes in response to ConA and anti-CD3. In vivo, ECF treatment reduced the severity of CIA, inhibited IFN- $\gamma$  and IL-6 secretion, and decreased the proportion of CD11b+Gr-1+ splenic neutrophil. Meanwhile, ECF treatment significantly inhibited the IFN- $\gamma$  expression in CD4+T cell without obviously influencing the development of Th17 cells and T regulatory cells. In vitro, ECF suppressed the differentiation of naive CD4+ T cells into Th1. Furthermore, ECF intensely blocked the transcriptional expression in interferon- $\gamma$ -related signaling, including IFN- $\gamma$ , T-bet, STAT1, and STAT4. *Conclusion.* Our results indicated that ECF exerted antiarthritic potential in collagen-induced arthritis by suppressing Th1 immune response and interferon- $\gamma$ -related signaling.

## 1. Introduction

*Elephantopus scaber* L. (*E. scaber*) belonging to the Compositae family is a small herb that is present in many parts of the world with mild and warm climate [1]. In folk medicinal practices, *E. scaber* have been used in many countries for the treatment of a number of diseases. In traditional Chinese medicine, *E. scaber*, popularly known as “Didancao,” is widely used as a diuretic antifebrile, antiviral, and antibacterial agent in treating hepatitis, rheumatic arthritis, bronchitis, cough associated with pneumonia, and arthralgia [2, 3]. In a previous study, we isolated 15 compounds from the ethanolic extract of this plant and screened them for immunological activities in ConA-induced murine splenocyte proliferation assay and found that ethyl caffeate (ECF), which was isolated from this plant for the first time, exhibited significant

immunosuppressive activities [4]. Furthermore, it was determined that ECF markedly suppressed nitric oxide (NO) production and downregulated mRNA transcription of *iNOS*, *L-1 $\beta$* , and *IL-10* in LPS-treated RAW264.7 cells via suppressing the NF- $\kappa$ B pathway, suggesting that ECF also possesses potential anti-inflammatory capabilities useful for treating various autoimmune diseases [5].

Rheumatoid arthritis (RA) is a chronic and systemic autoimmune disease, the main symptoms of which include pain and stiffness of joints and the progressive destruction of which may lead to disability [6]. RA is the most frequent of the chronic inflammatory joint diseases, with a prevalence of 0.5–1% in the industrialized world [7]. Although the etiological mechanisms of RA have not been fully elucidated, abundant evidence indicates that T cells are required for the initiation and chronicity of RA in both human and mouse

models [8]. In light of the fact that there is an abundance of T cells in synovial tissues and fluids [9], recent studies showed that the imbalance of T cell subsets plays an important role in a variety of diseases, including RA [10]. Effector CD4<sup>+</sup> T cell could be divided into Th1, Th2, Th17, and Treg subsets according to its differentiation and function [11, 12] Th1 cells secrete a large number of IFN- $\gamma$ , which can promote cell-mediated immunity. Although the IFN- $\gamma$  prevalence in pathogenesis of RA is controversial [13–15], IFN- $\gamma$  was implicated as a major player in the pathogenesis of RA [16, 17].

Collagen-induced arthritis in DBA/1 mice is a well-established model of human RA [18–20]. The induction of severe chronic arthritis in naive mice requires type II collagen- (CII-) induced specific activation of T cells and B cells and is associated with Th1-polarized immune response. Moreover, IFN- $\gamma$  derived from Th1 cell predominates during the induction and acute phases of this disease [21]. Two signaling pathways are known to be involved in IFN- $\gamma$  production: IFN- $\gamma$ /signal transducer and activator of transcription 1 (STAT1)/(T-bet)/IFN- $\gamma$  signaling, and IL-12/STAT4/IFN- $\gamma$  signaling [22].

To date, both the therapeutic potential of ECF in CIA and its mechanism of action remain unclear. This study aims to investigate the antiarthritic potential of ECF in CIA and explore the potential underlying mechanism of ECF for the treatment of RA. Our data demonstrate that ECF ameliorates collagen-induced arthritis by suppressing Th1 response and IFN- $\gamma$  signaling pathway.

## 2. Materials and Methods

**2.1. Experimental Animals.** Female BALB/c and male DBA/1 mice (6–8 weeks old) were obtained from Shanghai Laboratory Animal Center of the Chinese Academy of Sciences and were housed in specific pathogen-free conditions (12 h light/12 h dark photoperiod, 22  $\pm$  1°C, and 55  $\pm$  5% relative humidity). All mice were allowed to acclimatize in our facility for 1 week before experiments. All experiments were carried out according to the institutional ethical guidelines on animal care and were approved by the Institute Animal Care and Usage Committee of the No. 1 Hospital Affiliated Yunnan University of Traditional Chinese Medicine.

**2.2. Isolation of Ethyl Caffate.** *E. scaber* was purchased from Juhachun medicine market of Yunnan province in 2010, and a voucher specimen (number DDC2010) was deposited at the herbarium of Yunnan University of TCM. Dried and powdered whole plants of *E. scaber* (10 kg) were extracted at room temperature with 100 L of 95% EtOH three times (100 L  $\times$  3). The extract was evaporated under reduced pressure to yield a dark brown residue (1.2 kg). The residue was then suspended in water and partitioned successively with 2.5 L of EtOAc to afford an EtOAc fraction (149 g). The EtOAc fraction was subjected to silica gel column chromatography (CC) eluted with CHCl<sub>3</sub> and a gradient of CHCl<sub>3</sub>-MeOH to yield five fractions (Fr. 1–Fr. 5). Fraction 4 (7.9 g) was loaded to silica gel CC, eluting with CHCl<sub>3</sub>-acetone (9:1–7:3) in a gradient mode to yield four subfractions

(Fr. 4a–Fr. 4d). Subfraction 4a was further separated with silica gel CC, eluted with CHCl<sub>3</sub>-acetone (8:2) to yield a residue, which was then recrystallized with MeOH to finally obtain the ethyl caffate (210 mg).

**2.3. Cell Preparation.** Mice were sacrificed and spleens were removed aseptically. Splenocyte suspension was prepared as previously described [23] and resuspended in RPMI 1640 media containing 10% FBS and supplemented with penicillin (100 U/ml) and streptomycin (100  $\mu$ g/ml).

**2.4. Proliferation Assay In Vitro.** The proliferation of splenocytes or T cells in response to ConA, LPS, and anti-CD3/28 was measured by CCK-8 Kit. Briefly, BALB/c splenocyte suspension (5  $\times$  10<sup>5</sup> cells/well) was cultured with ConA (5  $\mu$ g/ml), LPS (10  $\mu$ g/ml), and anti-CD3 (5  $\mu$ g/ml; 145-2C11, BD Pharmingen) in the presence of ECF at indicated concentrations. The cultures were incubated for 48 h, 20  $\mu$ l of CCK-8 was then added to each well before the end of culture, and OD value was read at 450 nm. The MTT method was used to measure the cytotoxicity of the sample. Splenocytes (5  $\times$  10<sup>5</sup> cells/well) were cultured in triplicates in the absence or presence of ECF in a 96-well flat-bottomed plate (Costar) for 48 h. MTT (5 mg/ml) was pulsed for 4 h prior to the end of the culture. Upon removal of MTT/medium, 150  $\mu$ l of DMSO was added to each well, and the plate was agitated on an oscillator for 5 min to dissolve the precipitate. The assay plate was read at 570 nm using a microplate reader. All experiments were performed in triplicates independently.

**2.5. Collagen-Induced Arthritis in DBA/1 Mice and Administration.** Collagen was dissolved in 0.1 M acetic acid at 4°C overnight. Male DBA/1 mice were immunized at the tail base with 125  $\mu$ g of collagen emulsified in complete Freund's adjuvant (CFA) containing *Mycobacterium tuberculosis* strain H37Rv. Each mouse was then boosted with the same amount of collagen plus CFA 21 days later (taken as day 0). Starting from day 9 for 10 consecutive days, the mice were administered daily with ECF (50 mg/kg) or methotrexate (2 mg/kg) by p.o.

**2.6. Evaluation of Severity of Arthritis.** The severity of arthritis were assessed daily and expressed as a clinical score according to the following scale: 0 = normal; 1 = erythema or swelling of one or several digits; 2 = erythema and moderate swelling extending from the ankle to the midfoot (tarsal); 3 = erythema and severe swelling extending from the ankle to the metatarsal joints; 4 = complete erythema and swelling encompassing the ankle, foot, and digits, resulting in deformity and/or ankylosis. The scores of four limbs were summed up, and maximum score for each animal was therefore 16.

**2.7. Splenocyte Proliferation Assay and Cytokines Production in CII-Immunized Mice.** Splenocytes (5  $\times$  10<sup>5</sup> cells/well) were obtained from CII-immunized mice with or without ECF treatment and cultured in vitro with 100  $\mu$ g/ml CII stimulation. After 72 h, splenocyte proliferation assay was performed by CCK-8 Kit. Culture supernatants were



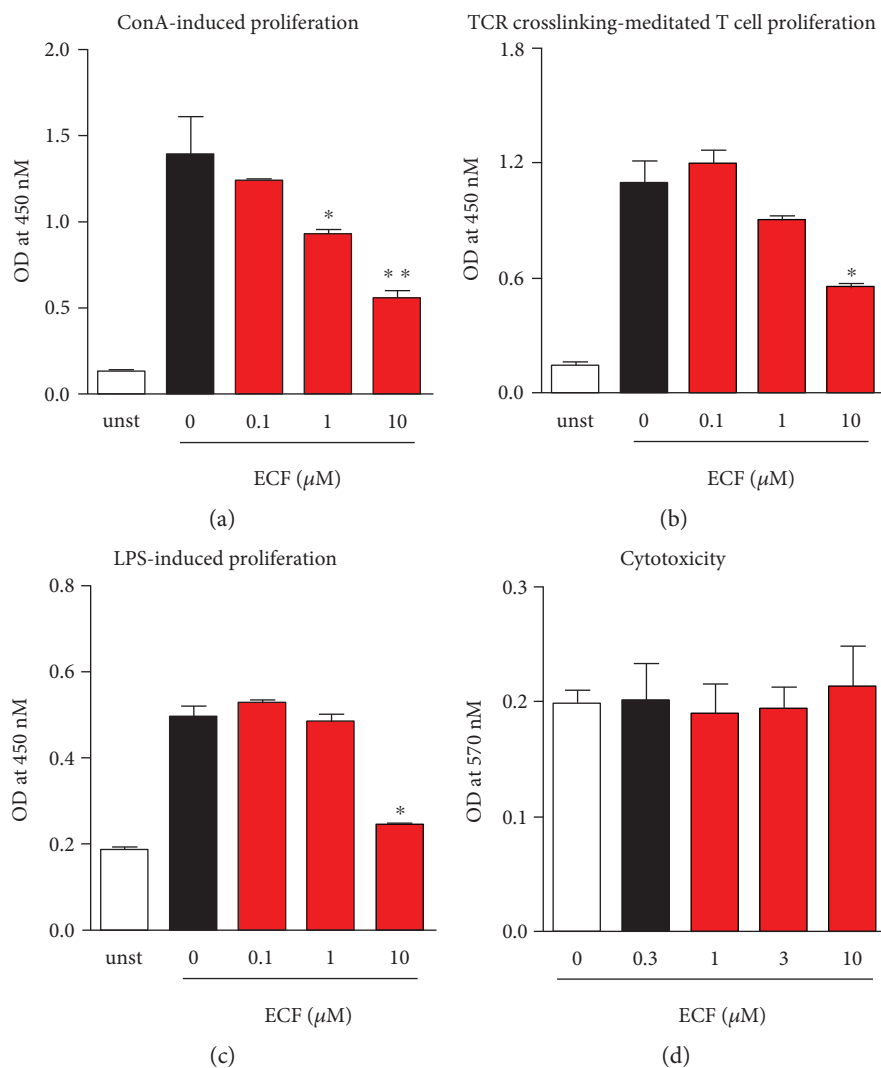


FIGURE 1: ECF inhibits lymphocyte proliferation in vitro. BALB/c splenocytes suspension ( $5 \times 10^5$  cells/well) or purified T cells ( $2 \times 10^5$  cells/well) were cultured with ConA ( $5 \mu\text{g/ml}$ ) (a), anti-CD3/CD28 (b), or LPS ( $10 \mu\text{g/ml}$ ) (c) in the presence of ECF at indicated concentrations for 48 h. The proliferation of lymphocytes was detected using CCK-8 Kit. The MTT method was used to measure the cytotoxicity of sample (d). Results presented are mean  $\pm$  s.e.m.,  $n = 3$ . \* $P < 0.05$ , \*\* $P < 0.01$  versus control group.

harvested at 48 h to measure IFN- $\gamma$ , TNF- $\alpha$ , IL-6, IL-17A, and IL-4 production by ELISA, in accordance with the manufacturer's instructions.

**2.8. Flow Cytometry.** Murine splenocytes were harvested and blocked with rat-anti-mouse CD16/CD32 (2.4G2, BD Pharmingen) and were then fluorescently labeled for 15 min at  $4^\circ\text{C}$  with the following mAbs diluted in PBS with 0.2% BSA: FITC-conjugated anti-mGr.1 (RB6-8C5, BD Pharmingen), PE-conjugated anti-mCD11b (M1/7), FITC-anti-mCD8a (53-6.7, BD Pharmingen), PE-conjugated anti-mB220 (RA3-682, BD Pharmingen), and PE-Cy7-conjugated anti-mCD4 (GK.1.5, BD Pharmingen).

Intracellular staining of cytokines was performed according to the method previously described [24, 25]. Briefly, splenocytes were restimulated for 4 h with PMA ( $50 \text{ ng/ml}$ ) and ionomycin ( $750 \text{ ng/ml}$ ) (Sigma-Aldrich) in the presence of Brefeldin A (Sigma-Aldrich). At the end of incubation,

cells were collected and blocked with rat-anti-mouse CD16/CD32, then those were stained with PE-Cy7-anti-mCD4 antibodies (GK.1.5, Biolegend); cells were fixed, permeabilized, and stained intracellularly with fluorochrome-conjugated anti-mIL-17A (TC11-18H10.1, Biolegend) and anti-mIFN- $\gamma$  (XMG1.2, Biolegend) using Foxp3 fixation/permeabilization reagents and protocols from eBioscience. Samples were acquired on a flow cytometer (FACSCanto™ II; BD Biosciences) and analyzed using FlowJo software (Tree Star).

**2.9. Th1 Cell Differentiation.** Purified  $\text{CD4}^+$  T cells were prepared using immunomagnetic negative selection (Miltenyi Biotec). Briefly, lymphocytes were allowed to react with  $\text{CD4}^+$  T cell biotin-antibody cocktail (biotin-conjugated monoclonal antibodies against CD8a, CD11b, CD11c, CD19, CD45R (B220), CD49b (DX5), CD105, anti-MHC class II, Ter-119, and TCR $\gamma/\delta$ ) and then incubated with antibiotin microbeads, followed by magnetic separation. The purity of

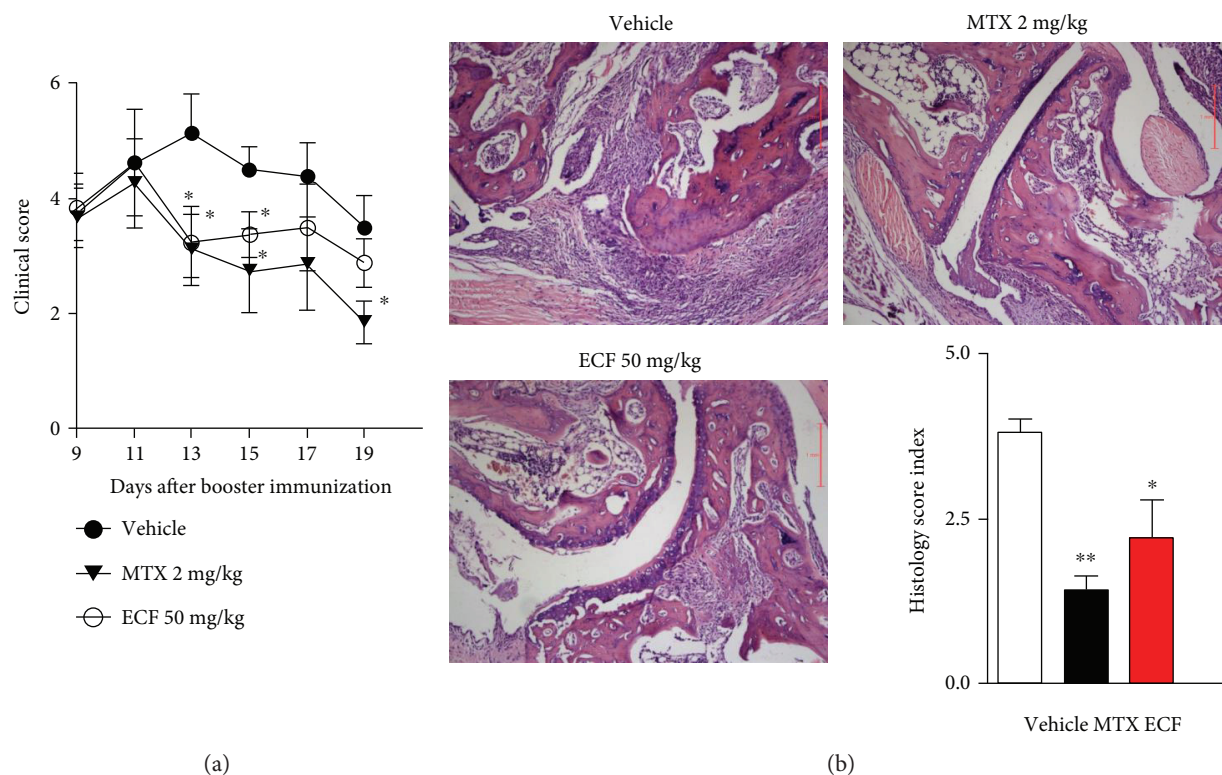


FIGURE 2: ECF attenuates collagen-induced arthritis in DBA/1 mice. Collagen-induced arthritis in DBA/1 mice was established via immunization twice with bovine collagen II in CFA. Mice were administered o.p. with vehicle, methotrexate (2 mg/kg), or ECF (50 mg/kg) once daily, starting from day 9 for 10 days. The severity of arthritis (a) and pathological changes to the joints (b) were evaluated using a clinical scoring system and H&E staining, respectively. Results presented are mean  $\pm$  s.e.m.,  $n = 7$ . \* $P < 0.05$ , \*\* $P < 0.01$  versus vehicle group. IFN- $\gamma$ , TNF- $\alpha$ , IL-6, IL-17A, and IL-4.

the resulting CD4<sup>+</sup> T cell populations was examined using flow cytometry, and was consistently above 95%.

T-helper cell differentiation was conducted as previously described [26]. Briefly, naive CD4 T cells ( $0.4 \times 10^6$ ) in 24-well plates (Costar) precoated with 5  $\mu$ g/ml of anti-CD3 (154-2C11, BioXcell) and 2  $\mu$ g/ml of anti-CD28 (37.51, BioXcell) were cultured in RPMI containing 10% FCS and polarizing cytokines at the various concentrations of ECF. The cytokines used were Th1, mIL-12 (10 ng/ml, Biologend), and anti-mIL-4 (11B11, 2  $\mu$ g/ml, BioXcell). Cells stimulated in “neutral” conditions (anti-mIL-4 and anti-mIFN- $\gamma$  without cytokines) were considered Th0 cells. The differentiated cells were harvested after 3 days and restimulated for 4 h with 50 ng/ml of PMA (Sigma-Aldrich) and 750 ng/ml of ionomycin (Sigma-Aldrich) in the presence or absence of Brefeldin A for flow cytometry.

**2.10. TCR Engagement-Mediated T Lymphocytes Activation and qPCR Analysis.** Purified CD4<sup>+</sup> T cells were cultured in 24-well flat-bottom plates coated with 5  $\mu$ g/ml of anti-CD3 (145-2C11, BD Pharmingen) and 2  $\mu$ g/ml anti-CD28 (37.51, BD Pharmingen) in the absence or presence of ECF at indicated concentrations. Total RNA was isolated 16h after stimulation with anti-CD3 and anti-CD28 using RNeasy Kit (Qiagen). 1  $\mu$ g of total RNA was used to synthesize cDNA using PrimeScript RT Master Mix Perfect

Real Time (TaKaRa). IFN- $\gamma$ , T-bet, STAT1, and STAT4 mRNA levels were detected by real-time quantitative PCR using SYBR Premix Ex Taq II kit (TaKaRa). Samples were assayed on Stratagene MX3000P Real-Time PCR machine (Agilent), and the relative expression level of the respective samples to  $\beta$ -actin was calculated with the delta-delta Ct. The gene-specific primers used were as follows:

IFN- $\gamma$ : (sense) 5'-ATGAACGCTACACACTGCATC-3'  
(Antisense) 5'-CCATCCTTTTGCCAGTTCCTC-3'  
T-bet: (sense) 5'-CCAGGAAGTTTCATTTGGGAAGC-3'  
(Antisense) 5'-ACGTGTTTAGAAGCACTG-3'  
STAT1: (sense) 5'-TCACAGTGGTTCGAGCTTCAG-3'  
(Antisense) 5'-CGAGACATCATAGGCAGCGTG-3'  
STAT4: (sense) 5'-GCAGCCAACATGCCTATCCA-3'  
(Antisense) 5'-TGGCAGACACTTTGTGTTCCA-3'  
 $\beta$ -Actin: (sense) 5'-GGCTGTATTCCCCTCCATCG-3'  
(Antisense) 5'-CCAGTTGGTAACAATGCCATGT-3'.

**2.11. Statistical Analysis.** Data are expressed as mean  $\pm$  s.e.m. of indicated experiments. Student's  $t$ -test was used to determine significance between two groups where appropriate.  $P < 0.05$  was considered to be statistically significant.

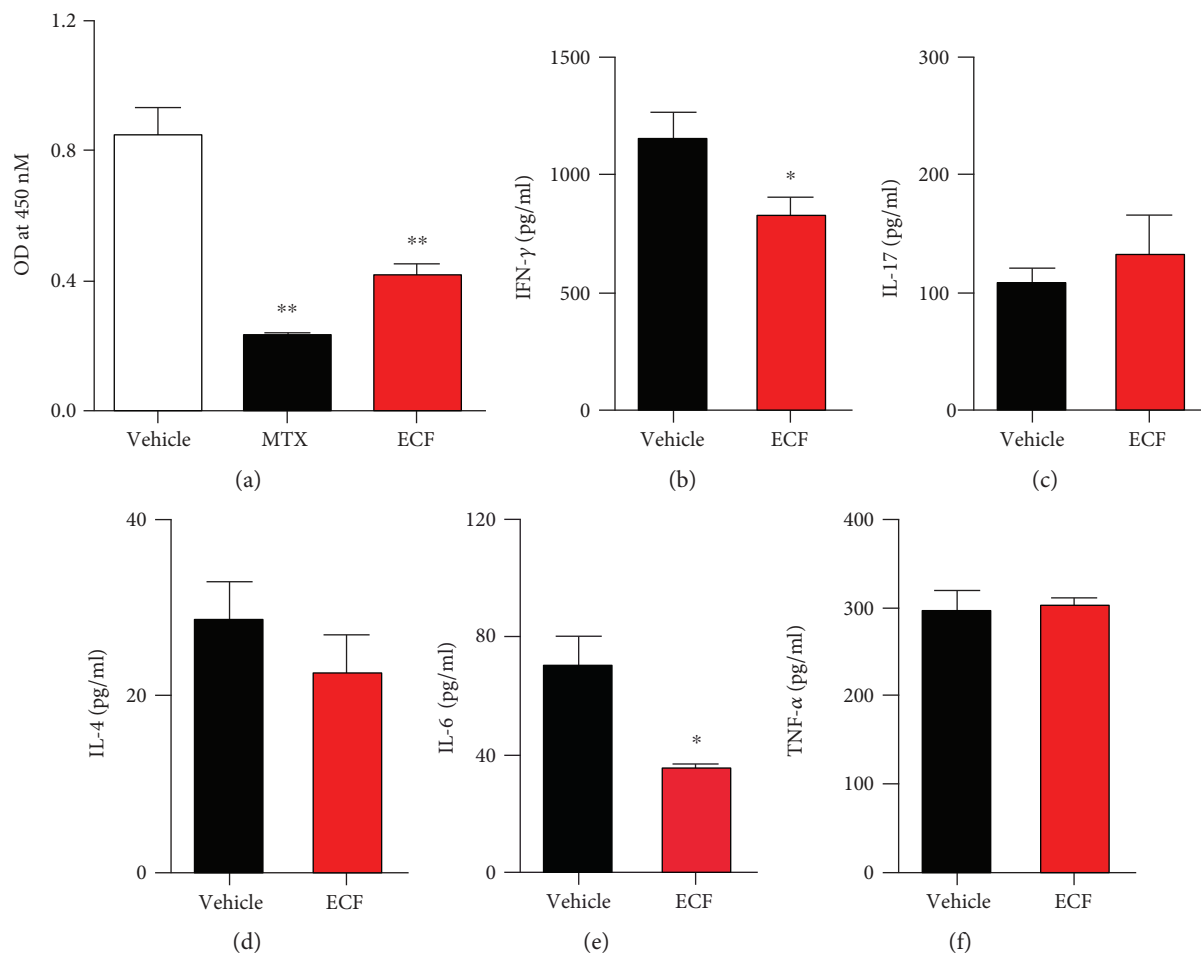


FIGURE 3: ECF inhibits CII-specific immune responses. Splenocytes ( $5 \times 10^5$  cells/well) from CIA mice were recalled with  $100 \mu\text{g/ml}$  CII. After 72 h, splenocyte proliferation assay was performed using CCK-8 Kit. Culture supernatants were harvested at 48 h, and IFN- $\gamma$ , TNF- $\alpha$ , IL-17A, and IL-4 levels were measured by ELISA. Results presented are mean  $\pm$  s.e.m.,  $n = 4$ . \* $P < 0.05$ , \*\* $P < 0.01$  versus vehicle group.

### 3. Results

#### 3.1. ECF Inhibits the Proliferation of Lymphocytes In Vitro.

To assess the immunosuppressive effect of ECF in vitro, lymphocyte proliferation assay was performed, in which in vitro stimulation of T cells with anti-CD3/28 serve to mimic the physiological crosslinking of TCR. ConA and LPS have been considered to be T and B cell mitogens, respectively. As shown in Figure 1, ECF significantly inhibits ConA-induced murine splenocyte proliferation (Figure 1(a)) as well as TCR crosslinking-mediated purified T cell proliferation (Figure 1(b)) in a concentration-dependent manner. ECF exerts immunosuppressive effects on LPS-induced B cell proliferation at the concentration of  $10 \mu\text{M}$  (Figure 1(c)). Importantly, ECF did not show obvious cell cytotoxicity on splenocytes at this concentration (Figure 1(d)). These data indicate that ECF can potentially serve as a promising therapeutic agent for treating autoimmune diseases.

3.2. ECF Attenuates Collagen-Induced Arthritis in DBA/1 Mice. To investigate the antiarthritic potential of ECF, we adopted a well-established murine model of human

rheumatoid arthritis, that is, collagen-induced arthritis in DBA/1 mice via immunization with bovine collagen II. The severity of the resulting arthritis in the presence or absence of ECF treatment was then evaluated using a clinical scoring system. We found that the clinical score for arthritis gradually increased in the vehicle group as the disease progressed and reached a peak at the day 13. In comparison, ECF treatment group exhibited significant reduction in clinical score from day 11 onwards, especially at the peak of arthritis progression (Figure 2(a)). The histopathological analysis of the joints by H&E staining indicated that the joints of CIA developed typical pathological changes, including severe cartilage and bone erosions, and infiltration of cells in the joints and synovial tissues and fluids. However, the number of infiltrated cells and the extent of bone destruction, as reflected by the histopathological score, show reduction in the ECF-treated group (Figure 2(b)). These data suggest that ECF possess therapeutic effects in treating arthritis.

3.3. ECF Inhibits Cytokine Production in CII-Specific Immune Responses. To assess the effects of ECF on cell-mediated immune responses against CII, we investigated the secretion of cytokine in CII-specific immune responses. Splenocytes

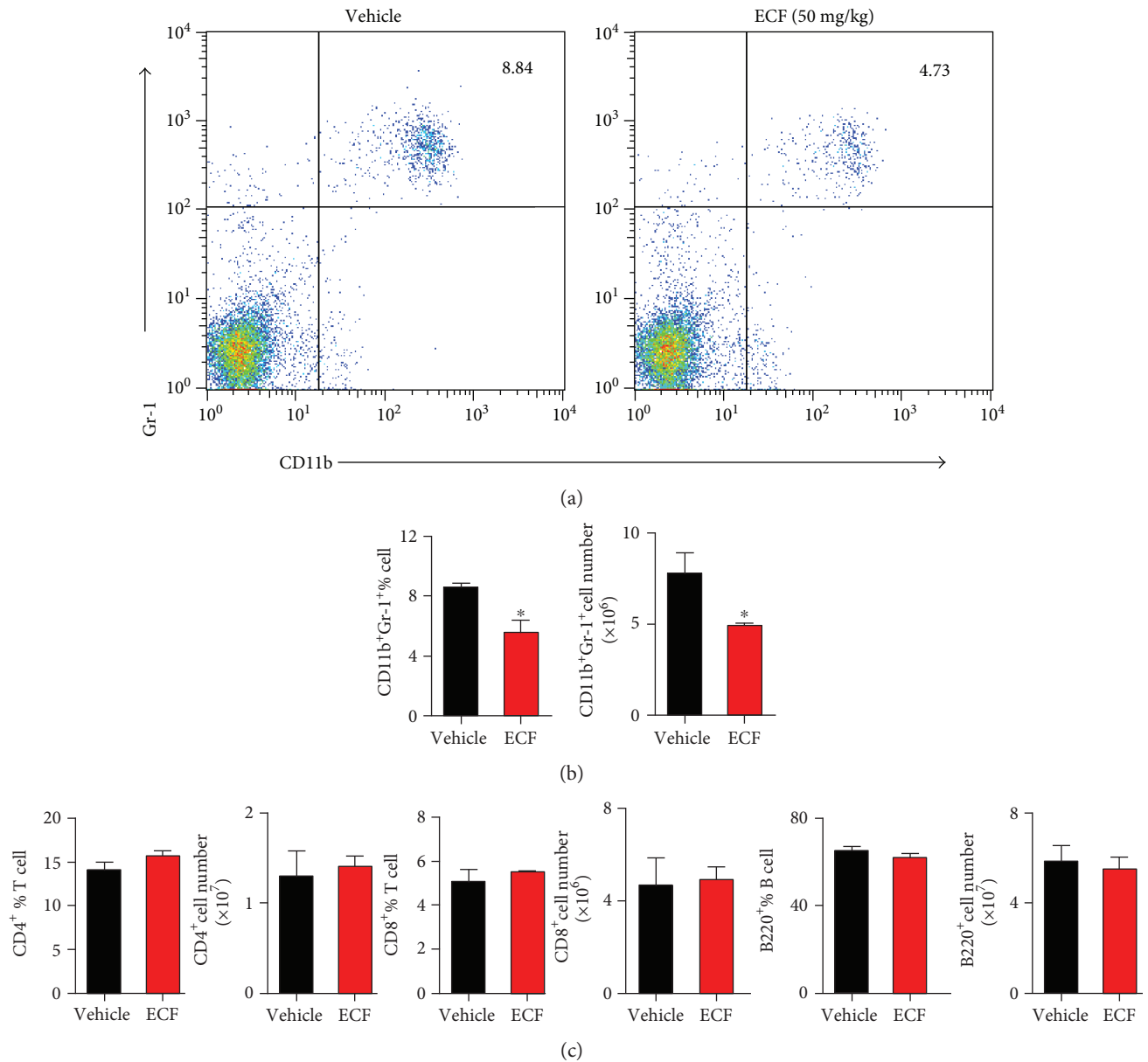


FIGURE 4: ECF treatment significantly reduces accumulation of neutrophils. Splenocytes from CIA mice were harvested and blocked with rat-anti-mouse CD16/CD32 and fluorescently labeled by incubation for 15 min at 4°C with the respective antibody. Samples were measured on flow cytometer and analyzed by FlowJo software. Results presented are mean ± s.e.m.,  $n = 4$ . \* $P < 0.05$ , \*\* $P < 0.01$  versus vehicle group.

from CIA mice were recalled with CII for 48 h or 72 h to induce the production of cytokines and detected splenocyte proliferation, respectively. IFN- $\gamma$ , IL-6, TNF- $\alpha$ , and IL-4 levels in the supernatants were determined by ELISA. As shown in Figure 3, ECF treatment significantly inhibited splenocyte proliferation (Figure 3(a)) and reduced the secretion of Th1-related cytokine (IFN- $\gamma$ ) in CII-induced specific immune response (Figure 3(b)). Since proinflammation cytokines such as IL-6 and TNF- $\alpha$  have a documented central role in the pathogenesis of arthritis, we further measured the levels of IL-6 and TNF- $\alpha$  under the same condition. ECF-treated CIA mice produced a lower level of IL-6 as compared to the vehicle group (Figure 3(d)), whereas no variation in TNF- $\alpha$  and IL-4

secretion levels were detected between them (Figures 3(c) and 3(e)). These data collectively indicated that treatment with ECF diminished the level of Th1 cytokine and some proinflammation cytokines.

**3.4. ECF Treatment Significantly Reduces Accumulation of Neutrophils.** Although the etiological mechanism of RA remains unclear, growing evidence indicates that T cells and B cells are involved in the pathogenesis of RA. Additionally, neutrophils are crucial for the pathogenesis of RA and other inflammatory conditions [27]. It has been reported that neutrophils in RA patients are highly activated in the circulation and synovial fluids and tissues [28]. In light of this, we analyzed the subset constitution of mouse spleens obtained

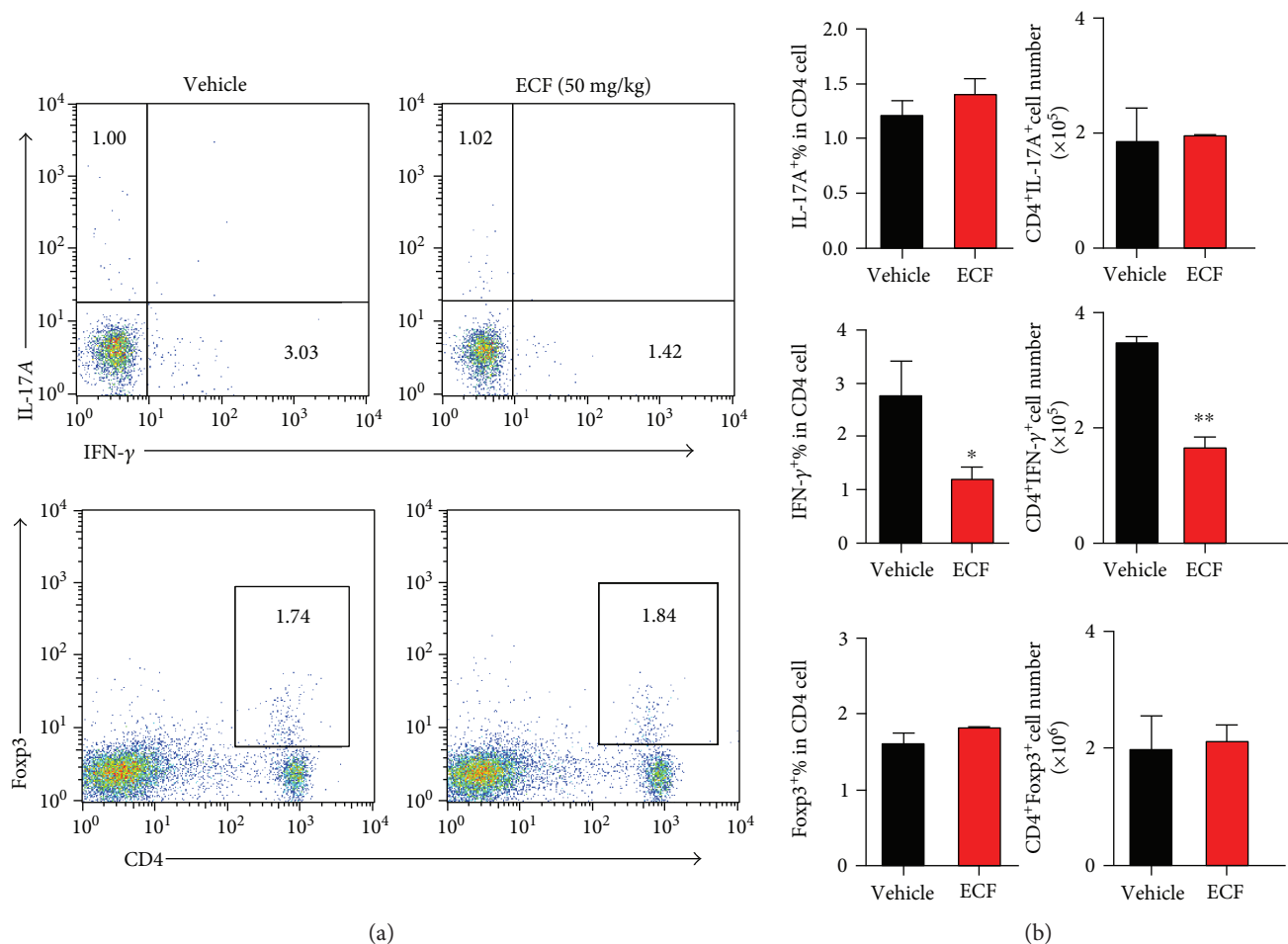


FIGURE 5: ECF treatment markedly suppresses Th1 cell response in CIA. Splenocytes from CIA mice were restimulated for 4 h with PMA and ionomycin in the presence of Brefeldin A. At the end of incubation, cells were collected and blocked with rat-anti-mouse CD16/CD32, and then those were stained with PE-Cy7-anti-mCD4 antibodies; cells were fixed, permeabilized, and stained intracellularly with fluorochrome-conjugated anti-mIL-17A, anti-mIFN- $\gamma$ . Samples were acquired on flow cytometer and analyzed by FlowJo software. Results presented are mean  $\pm$  s.e.m.,  $n = 4$ . \* $P < 0.05$ , \*\* $P < 0.01$  versus vehicle group.

from vehicle group mice and the ECF-treated group by flow cytometry (Figure 4). Surface marker staining indicated that compared with the vehicle group, spleens from ECF-treated mice showed lower percentage of CD11b<sup>+</sup>Gr-1<sup>+</sup> neutrophils but not CD4<sup>+</sup>, CD8<sup>+</sup>, or B220<sup>+</sup> cells.

**3.5. ECF Treatment Markedly Suppresses Th1 Cell Response in CIA.** T lymphocytes play a critical role in the pathogenesis of arthritis. Naive T cells could differentiate into pathogenic Th1 cells, proinflammatory T helper (Th17) cells, or tissue-protective induced T regulatory cells [29, 30]. To investigate whether ECF could regulate the development of Th1 and Th17 cells, we measured the intracellular cytokines expression in CD4<sup>+</sup> T cells from CIA mice by flow cytometry (Figure 5). Compared to vehicle group, ECF treatment significantly inhibited IFN- $\gamma$  expression in CD4<sup>+</sup> T cells; the development of Th17 cells and T regulatory cells, however, was not obviously impacted.

**3.6. ECF Inhibits Th1 Cell Differentiation.** In order to further investigate whether ECF could suppress Th1 differentiation,

we stimulated murine naive T cells to induce Th1 differentiation in the presence of Th1 polarized condition (mIL-12 plus anti-mIL-4) and treated these cells with ECF. Strikingly, ECF impaired Th1 cell differentiation (Figure 6), in agreement with *in vivo* results, implying that the inhibitory effect of ECF on Th1 differentiation may contribute to its antiarthritic potential for treating RA.

**3.7. ECF Suppresses IFN- $\gamma$ -Related Pathway in TCR-Engagement-Mediated T Lymphocyte Activation.** Given that considerable evidence points to a critical pathogenic role of IFN- $\gamma$  in both CIA model and patient, ECF significantly inhibits Th1 response and IFN- $\gamma$  production in CIA model as described above. In order to further explore the mechanistic pathways of ECF on IFN- $\gamma$  production, we measured the expression of IFN- $\gamma$ -related signature genes such as IFN- $\gamma$ , T-bet, STAT1, and STAT4 at the mRNA level upon TCR-engagement-mediated T lymphocyte activation (Figure 7). We found that transcriptional expression of IFN- $\gamma$ , T-bet, STAT1, and STAT4 was significantly downregulated in the presence of various concentrations of ECF, suggesting that

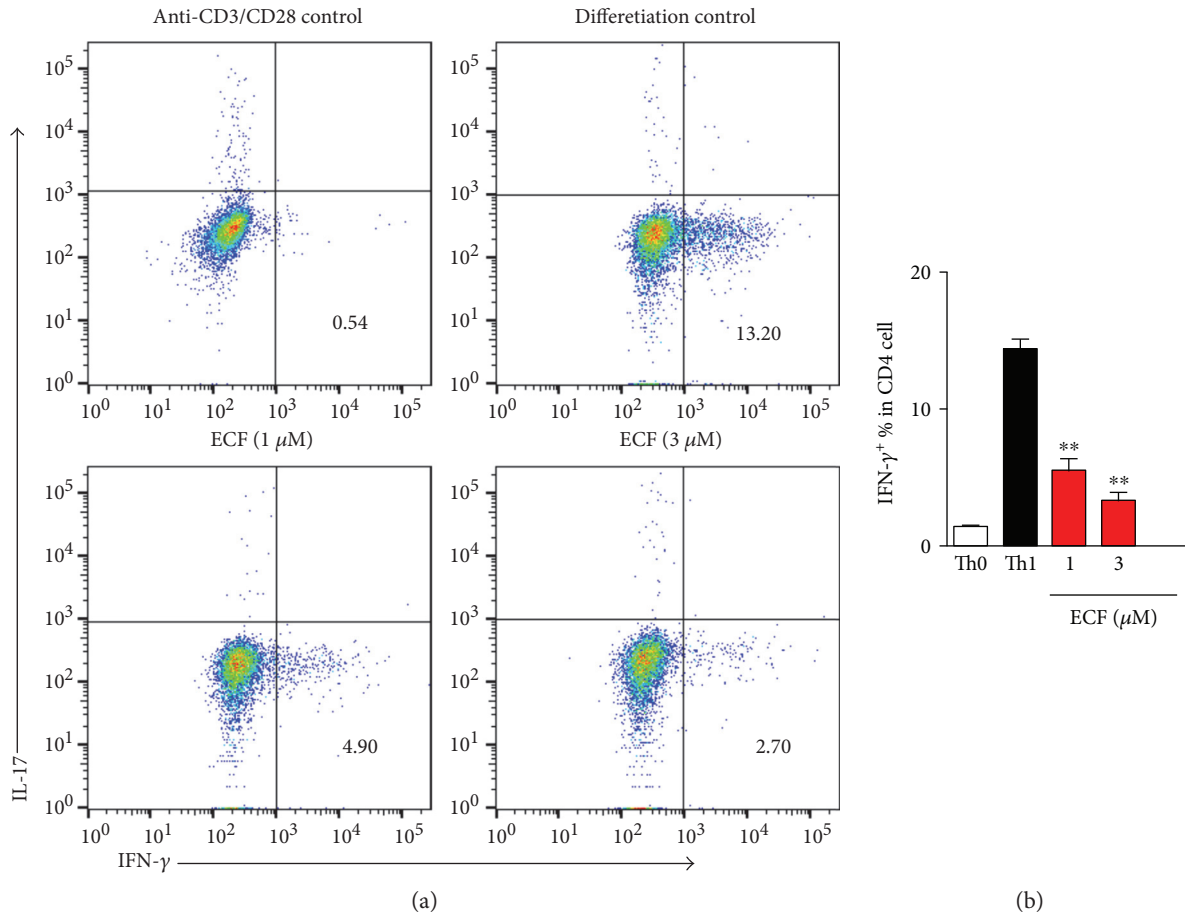


FIGURE 6: ECF inhibits Th1 cell differentiation. Naive CD4 T cells ( $4 \times 10^5$ ) in 24-well plates precoated with anti-CD3 and anti-CD28 were cultured in RPMI containing 10% FCS and polarizing cytokines at various concentrations of ECF. The differentiated cells were harvested after 3 days and were restimulated for 4 h with PMA and ionomycin in the presence or absence of Brefeldin A for flow cytometry. Data were analyzed by FlowJo software.

IFN- $\gamma$ -related pathways are possibly involved in the immunosuppressive effect of ECF on T cell activation.

#### 4. Discussions

It was reported that T lymphocytes play a pivotal role in the pathogenesis of cell-mediated autoimmune diseases and chronic inflammatory disorders [10]. Previous studies have indicated that ECF exhibits significant inhibitory effects on the proliferation of murine T lymphocytes induced by ConA, and the observed activities are not due to compound toxicity [4]. In vitro stimulation of T cells with anti-CD3/28 serves to mimic the physiological crosslinking of TCR. Importantly, ECF treatment markedly suppresses TCR-triggered T cell activation. The immunosuppressive activity of ECF on T cells revealed by the present study implies that ECF represents a potent therapeutic agent for the treatment of autoimmune diseases such as rheumatic arthritis. Moreover, collagen-induced arthritis (CIA) in DBA/1 mice is one of the many animal models used to study the pathogenic mechanisms of RA [31]. There is close resemblance in histopathology as well as in the production of inflammatory

mediators such as chemokines, cytokines, proteases, and autoantibodies [13]. Surprisingly, oral administration of ECF ameliorates collagen-induced arthritis, including reduction in clinical score and infiltration of cells in the joints and synovial tissues and fluids. Furthermore, bone destruction and histopathological score are also reduced upon ECF treatment.

Depending on functions and cytokines produced, CD4 $^+$  T cells can be classified into four subsets, including T helper 1 (Th1), Th2, Th17, and CD4 $^+$  CD25 $^+$  T regulatory (Treg) cells. The imbalance of cytokine production by Th1/Th2/Th17 lymphocytes doubtlessly plays a crucial role in RA pathogenesis [10]. As Th1 cells mainly secrete interferon gamma (IFN- $\gamma$ ) and IL-2, Th1 cytokines are generally defined as cytokines that promote cell-mediated immune responses as well as activation of macrophage and neutrophils, leading to amplified production of proinflammatory cytokines [32]. Many studies have also provided evidence for the predominance of Th1 cytokine production in the synovial fluid from RA patients [33]. Intracellular cytokine staining reveals that ECF treatment inhibits the expression of IFN- $\gamma$ -producing T cells compared to vehicle group when

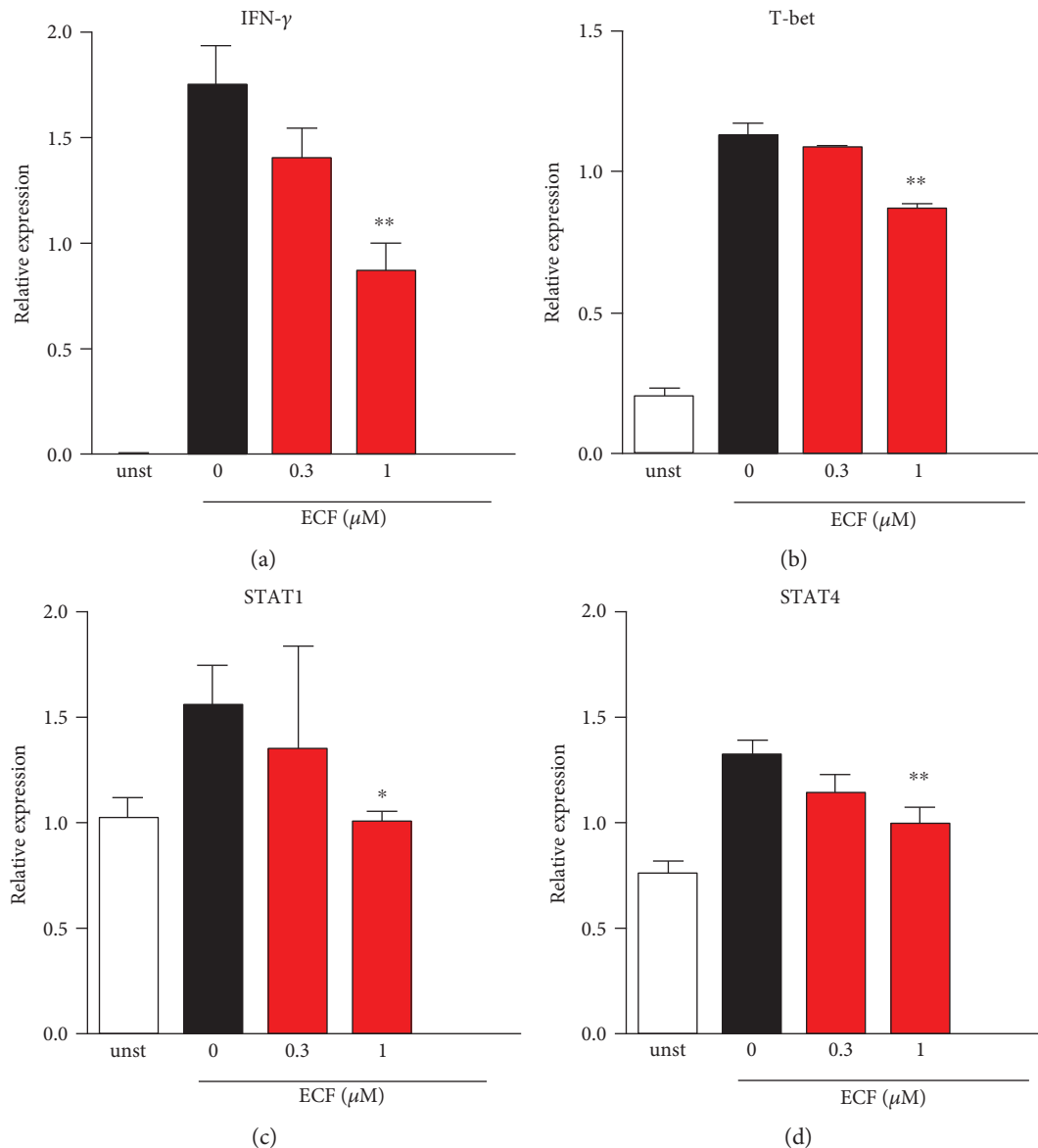


FIGURE 7: ECF suppresses IFN- $\gamma$ -related pathway in TCR engagement-mediated T lymphocyte activation. Purified CD4<sup>+</sup> T cells were stimulated with anti-CD3 (5  $\mu$ g/ml) and anti-CD28 (2  $\mu$ g/ml) for 16 h. Total RNA was isolated using RNeasy kits, and 1  $\mu$ g of total RNA was used to synthesis cDNA. Real-time quantitative PCR assay was carried out using SYBR Premix Ex Taq II kit, and relative quantification of mRNA expression was calculated as the fold increase using the delta-delta Ct; the housekeeping gene is  $\beta$ -actin. Results presented are mean  $\pm$  s.e.m.,  $n = 3$ . \* $P < 0.05$ , \*\* $P < 0.01$  versus vehicle group.

analyzed immediately ex vivo, whereas no difference was observed in Th17 cells or T regulatory cell response. This is consistent with the finding that IFN- $\gamma$  production from T cells following restimulation with CII ex vivo was significantly reduced in ECF-treated mice. This response was antigen-specific and accompanied by reduced production of some inflammatory cytokines in the ECF-treated group, including reduction in the accumulation of neutrophils and the production of proinflammatory cytokines IL-6, which is mainly produced by activated macrophages and fibroblast-like synoviocytes (FLS). In RA, the level of IL-6 is also found to be elevated and correlates with radiological joint destruction. These results revealed that the inhibition of

Th1-mediated immune response by ECF, especially the downregulation of IFN- $\gamma$  expression, consequently limits the proinflammatory response and activation of neutrophils, which may contribute to the protective effect of ECF on CIA.

In adaptive immune response, IFN- $\gamma$  is secreted by CD8<sup>+</sup> T cells in control of infection, and by CD4<sup>+</sup> T helper1(Th1) subset, which promotes inflammatory response, clearance of intracellular pathogens, and class-switching to IgG 2a, IgG 2b, and IgG [34]. Differentiation of CD4<sup>+</sup> T cells to the Th1 subset is driven primarily by IL-12 in the absence of IL-4 and TGF- $\beta$ , which signal via factors such as signal transducer and activator of transcription 1 (STAT1),

T-bet (also known as Tbx21), and STAT4 [35, 36]. Considerable evidence has indicated that pathogenic Th1-mediated immune response plays a crucial role in the pathogenesis of RA [33]. In vivo, ECF treatment markedly reduced the expression of IFN- $\gamma$ -producing T cells compared to the vehicle group. Consistent with in vivo results, ECF also impaired Th1 cell differentiation and IFN- $\gamma$  production in vitro, confirming that the inhibitory effect of ECF on Th1 differentiation is responsible for its antiarthritic potential.

The role of IFN- $\gamma$  in the pathogenesis of RA is controversial, as both disease-limiting and disease-promoting activities of IFN- $\gamma$  in the pathogenesis have been reported in the past decade [13]. Till now, there exists no satisfactory explanation for such dual effects in RA. It is reported that IFN- $\gamma$ -deficient mice lead to disease exacerbation in CIA via IFN-mediated suppression of IL-17 [37]. Moreover, IFN- $\gamma$  inhibits differentiation of monocyte/macrophage in osteoclasts through ubiquitin-proteasome-mediated degradation of TRAF6 [38]. Meanwhile, considerable evidence has revealed that IFN- $\gamma$  may exacerbate RA: clinically, increased expression of IFN- $\gamma$  has been detected in synovial tissues and fluids of RA patients [39–41], and for a small group of patients, intramuscular injection of anti-IFN antibodies appeared to be beneficial [42]. Administration of IFN- $\gamma$  at the initial phase accelerated the onset and increased the incidence of arthritis [43, 44]. Furthermore, susceptible mice lacking IFN- $\gamma$  or IFN- $\gamma$  R exhibited decreased incidence and severity of CIA [45]. Many studies also suggested that the role of IFN- $\gamma$  in RA may be associated with the disease stage and the use of CFA [46]. There are two signaling pathways involved in IFN- $\gamma$  production: IFN- $\gamma$ /signal transducer and activator of transcription 1 (STAT1)/(T-bet)/IFN- $\gamma$ , signaling, and IL-12/STAT4/IFN- $\gamma$  signaling [22]. PCR results indicated that ECF treatment downregulated the mRNA transcription of IFN- $\gamma$ , STAT1, T-bet, and STAT4, providing molecular basis for its suppression of IFN- $\gamma$  and the therapeutic effect of ECF in CIA.

Collectively, our results showed that ECF have antiarthritic effect in CIA mice, and its mechanism of action is tightly related to the blockade of IFN- $\gamma$  signaling pathway. ECF may therefore present a promising agent for treating RA and other autoimmune diseases.

## Conflicts of Interest

The authors disclose no conflict of interests regarding this study.

## Authors' Contributions

Shikui Xu and Aixue Zuo contributed equally to this work.

## Acknowledgments

This work was funded by the Natural Science Foundation of China (Grant no. 81460624) and the Applied Basic Research Program of Yunnan Province, China (Grant no. 2015FB199).

## References

- [1] S. Singh, V. Krishna, K. Mankani, B. K. Manjunatha, S. M. Vidya, and Y. N. Manohara, "Wound healing activity of the leaf extracts and deoxyelephantopin isolated from *Elephantopus scaber* Linn," *Indian Journal of Pharmacology*, vol. 37, no. 4, pp. 238–242, 2005.
- [2] C. C. Huang, K. J. Lin, Y. W. Cheng, C. A. Hsu, S. S. Yang, and L. F. Shyur, "Hepatoprotective effect and mechanistic insights of deoxyelephantopin, a phyto-sesquiterpene lactone, against fulminant hepatitis," *The Journal of Nutritional Biochemistry*, vol. 24, no. 3, pp. 516–530, 2013.
- [3] M. Su, H. Y. Chung, and Y. Li, "Deoxyelephantopin from *Elephantopus scaber* L. Induces cell-cycle arrest and apoptosis in the human nasopharyngeal cancer CNE cells," *Biochemical and Biophysical Research Communications*, vol. 411, no. 2, pp. 342–347, 2011.
- [4] A.-X. Zuo, C.-P. Wan, X. Zheng, and G. X. Rao, "Chemical constituents of *Elephantopus scaber*," *Chemistry of Natural Compounds*, vol. 52, no. 3, pp. 484–486, 2016.
- [5] Y. W. Mao, H. W. Tseng, W. L. Liang, I. S. Chen, S. T. Chen, and M. H. Lee, "Anti-inflammatory and free radical scavenging activities of the constituents isolated from *Machilus zuihoensis*," *Molecules (Basel, Switzerland)*, vol. 16, no. 11, pp. 9451–9466, 2011.
- [6] I. B. McInnes and G. Schett, "The pathogenesis of rheumatoid arthritis," *New England Journal of Medicine*, vol. 365, no. 23, pp. 2205–2219, 2011.
- [7] C. Selmi, E. Generali, M. Massarotti, G. Bianchi, and C. A. Scir , "New treatments for inflammatory rheumatic disease," *Immunologic Research*, vol. 60, no. 2-3, pp. 277–288, 2014.
- [8] D. L. Perkins, "T-cell activation in autoimmune and inflammatory diseases," *Current Opinion in Nephrology and Hypertension*, vol. 7, no. 3, pp. 297–303, 1998.
- [9] F. M. Brennan and I. B. McInnes, "Evidence that cytokines play a role in rheumatoid arthritis," *The Journal of Clinical Investigation*, vol. 118, no. 11, pp. 3537–3545, 2008.
- [10] E. Brzustewicz and E. Bryl, "The role of cytokines in the pathogenesis of rheumatoid arthritis—practical and potential application of cytokines as biomarkers and targets of personalized therapy," *Cytokine*, vol. 76, no. 2, pp. 527–536, 2015.
- [11] L. Zhou, M. M. W. Chong, and D. R. Littman, "Plasticity of CD4+ T cell lineage differentiation," *Immunity*, vol. 30, no. 5, pp. 646–655, 2009.
- [12] A. Kosmaczewska, J. Swierkot, L. Cizak, and P. Wiland, "The role of Th1, Th17, and Treg cells in the pathogenesis of rheumatoid arthritis including anti-inflammatory action of Th1 cytokines," *Postępy Higieny i Medycyny Doświadczalnej (Online)*, vol. 65, pp. 397–403, 2011.
- [13] E. Schurgers, A. Billiau, and P. Matthys, "Collagen-induced arthritis as an animal model for rheumatoid arthritis: focus on interferon- $\gamma$ ," *Journal of Interferon & Cytokine Research*, vol. 31, no. 12, pp. 917–926, 2011.
- [14] S. Tukaj, A. Kotlarz, A. Jozwik et al., "Cytokines of the Th1 and Th2 type in sera of rheumatoid arthritis patients; correlations with anti-hsp40 immune response and diagnostic markers," *Acta Biochimica Polonica*, vol. 57, no. 3, pp. 327–332, 2010.
- [15] J. Miao, K. Zhang, M. Lv et al., "Circulating Th17 and Th1 cells expressing CD161 are associated with disease activity in rheumatoid arthritis," *Scandinavian Journal of Rheumatology*, vol. 43, no. 3, pp. 194–201, 2014.



- [16] R. Zhou, W. Tang, Y. X. Ren et al., "(5 $\alpha$ )-5-hydroxytryptolide attenuated collagen-induced arthritis in DBA/1 mice via suppressing interferon-gamma production and its related signaling," *The Journal of Pharmacology and Experimental Therapeutics*, vol. 318, no. 1, pp. 35–44, 2006.
- [17] R. Baccala, D. H. Kono, and A. N. Theofilopoulos, "Interferons as pathogenic effectors in autoimmunity," *Immunological Reviews*, vol. 204, no. 1, pp. 9–26, 2005.
- [18] L. K. Myers, E. F. Rosloniec, M. A. Cremer, and A. H. Kang, "Collagen-induced arthritis, an animal model of autoimmunity," *Life Sciences*, vol. 61, no. 19, pp. 1861–1878, 1997.
- [19] D. E. Trentham, A. S. Townes, and A. H. Kang, "Autoimmunity to type II collagen an experimental model of arthritis," *The Journal of Experimental Medicine*, vol. 146, no. 3, pp. 857–868, 1977.
- [20] D. D. Brand, A. H. Kang, and E. F. Rosloniec, "Immunopathogenesis of collagen arthritis," *Springer Seminars in Immunopathology*, vol. 25, no. 1, pp. 3–18, 2003.
- [21] E. H. Choy and G. S. Panayi, "Cytokine pathways and joint inflammation in rheumatoid arthritis," *The New England Journal of Medicine*, vol. 344, no. 12, pp. 907–916, 2001.
- [22] J. L. Grogan and R. M. Locksley, "T helper cell differentiation: on again, off again," *Current Opinion in Immunology*, vol. 14, no. 3, pp. 366–372, 2002.
- [23] C. P. Wan, L. X. Gao, L. F. Hou et al., "Astragaloside II triggers T cell activation through regulation of CD45 protein tyrosine phosphatase activity," *Acta Pharmacologica Sinica*, vol. 34, no. 4, pp. 522–530, 2013.
- [24] L. F. Hou, S. J. He, X. Li et al., "Oral administration of artemisinin analog SM934 ameliorates lupus syndromes in MRL/lpr mice by inhibiting Th1 and Th17 cell responses," *Arthritis and Rheumatism*, vol. 63, no. 8, pp. 2445–2455, 2011.
- [25] L. F. Hou, S. J. He, X. Li et al., "SM934 treated lupus-prone NZB x NZW F1 mice by enhancing macrophage interleukin-10 production and suppressing pathogenic t cell development," *PLoS One*, vol. 7, no. 2, article e32424, 2012.
- [26] L. Hou, J. Cooley, R. Swanson et al., "The protease cathepsin I regulates Th17 cell differentiation," *Journal of Autoimmunity*, vol. 65, pp. 56–63, 2015.
- [27] M. A. Shelef, S. Tauzin, and A. Huttenlocher, "Neutrophil migration: moving from zebrafish models to human autoimmunity," *Immunological Reviews*, vol. 256, no. 1, pp. 269–281, 2013.
- [28] H. L. Wright, R. J. Moots, and S. W. Edwards, "The multifactorial role of neutrophils in rheumatoid arthritis," *Nature Reviews. Rheumatology*, vol. 10, no. 10, pp. 593–601, 2014.
- [29] T. Korn, E. Bettelli, M. Oukka, and V. K. Kuchroo, "IL-17 and Th17 cells," *Annual Review of Immunology*, vol. 27, pp. 485–517, 2009.
- [30] C. Dong, "Th17 cells in development: an updated view of their molecular identity and genetic programming," *Nature Reviews. Immunology*, vol. 8, no. 5, pp. 337–348, 2008.
- [31] J. S. Courtenay, M. J. Dallman, A. D. Dayan, A. Martin, and B. Mosedale, "Immunisation against heterologous type II collagen induces arthritis in mice," *Nature*, vol. 283, no. 5748, pp. 666–668, 1980.
- [32] P. Miossec and W. van den Berg, "Th1/Th2 cytokine balance in arthritis," *Arthritis and Rheumatism*, vol. 40, no. 12, pp. 2105–2115, 1997.
- [33] R. Gerli, O. Bistoni, A. Russano et al., "In vivo activated T cells in rheumatoid synovitis. Analysis of Th1- and Th2-type cytokine production at clonal level in different stages of disease," *Clinical and Experimental Immunology*, vol. 129, no. 3, pp. 549–555, 2002.
- [34] K. M. Beima, M. M. Miazgowicz, M. D. Lewis, P. S. Yan, T. H. Huang, and A. S. Weinmann, "T-bet binding to newly identified target gene promoters is cell type-independent but results in variable context-dependent functional effects," *The Journal of Biological Chemistry*, vol. 281, no. 17, pp. 11992–12000, 2006.
- [35] J. Zhu, H. Yamane, and W. E. Paul, "Differentiation of effector CD4 T cell populations," *Annual Review of Immunology*, vol. 28, pp. 445–489, 2010.
- [36] K. M. Murphy and B. Stockinger, "Effector T cell plasticity: flexibility in the face of changing circumstances," *Nature Immunology*, vol. 11, no. 8, pp. 674–680, 2010.
- [37] C. Q. Chu, D. Swart, D. Alcorn, J. Tocker, and K. B. Elkon, "Interferon-gamma regulates susceptibility to collagen-induced arthritis through suppression of interleukin-17," *Arthritis and Rheumatism*, vol. 56, no. 4, pp. 1145–1151, 2007.
- [38] N. Takahashi, G. R. Mundy, and G. D. Roodman, "Recombinant human interferon-gamma inhibits formation of human osteoclast-like cells," *Journal of Immunology (Baltimore, Md.: 1950)*, vol. 137, no. 11, pp. 3544–3549, 1986.
- [39] R. J. Dolhain, N. T. ter Haar, S. Hoefakker et al., "Increased expression of interferon (IFN)-gamma together with IFN-gamma receptor in the rheumatoid synovial membrane compared with synovium of patients with osteoarthritis," *British Journal of Rheumatology*, vol. 35, no. 1, pp. 24–32, 1996.
- [40] G. Steiner, M. Tohidast-Akrad, G. Witzmann et al., "Cytokine production by synovial T cells in rheumatoid arthritis," *Rheumatology (Oxford, England)*, vol. 38, no. 3, pp. 202–213, 1999.
- [41] Z. Yin, S. Siegert, L. Neure et al., "The elevated ratio of interferon gamma-/interleukin-4-positive T cells found in synovial fluid and synovial membrane of rheumatoid arthritis patients can be changed by interleukin-4 but not by interleukin-10 or transforming growth factor beta," *Rheumatology (Oxford, England)*, vol. 38, no. 11, pp. 1058–1067, 1999.
- [42] Y. A. Sigidin, G. V. Loukina, B. Skurkovich, and S. Skurkovich, "Randomized, double-blind trial of anti-interferon-gamma antibodies in rheumatoid arthritis," *Scandinavian Journal of Rheumatology*, vol. 30, no. 4, pp. 203–207, 2001.
- [43] S. M. Cooper, S. Sriram, and G. E. Ranges, "Suppression of murine collagen-induced arthritis with monoclonal anti-Ia antibodies and augmentation with IFN-gamma," *Journal of Immunology (Baltimore, Md.: 1950)*, vol. 141, no. 6, pp. 1958–1962, 1988.
- [44] N. J. Mauritz, R. Holmdahl, R. Jonsson, P. H. Van der Meide, A. Scheynius, and L. Klareskog, "Treatment with gamma-interferon triggers the onset of collagen arthritis in mice," *Arthritis and Rheumatism*, vol. 31, no. 10, pp. 1297–1304, 1988.
- [45] Y. Kageyama, Y. Koide, A. Yoshida et al., "Reduced susceptibility to collagen-induced arthritis in mice deficient in IFN-gamma receptor," *Journal of Immunology (Baltimore, Md.: 1950)*, vol. 161, no. 3, pp. 1542–1548, 1998.
- [46] D. K. Dalton, L. Haynes, C. Q. Chu, S. L. Swain, and S. Wittmer, "Interferon gamma eliminates responding CD4 T cells during mycobacterial infection by inducing apoptosis of activated CD4 T cells," *The Journal of Experimental Medicine*, vol. 192, no. 1, pp. 117–122, 2000.